ABSTRACT

Total Syntheses of (±)-Dracephalone A and (±)-Dracocequinones A and B, Progress Towards a Total Synthesis of Cassiabudanols A and B, and Synthetic Studies Towards Total Synthesis of *N*-Oxy-Diketopiperazine Containing Natural Products

Taehwan Hwang, Ph.D.

Mentor: John L. Wood, Ph.D.

In 2022 we reported the first total syntheses of 20-*nor*-abietanoids (±)-dracocephalone A and (±)-dracocequinones A and B. Our synthesis originally involved an isobenzofuran intramolecular Diels-Alder, a strategy that eventually evolved into a Lewis acid-mediated spirocyclization in a highly diastereoselective fashion. Subsequent *trans*-decalin formation and a late-stage Suárez oxidation constructed the [3.2.1] oxabicylic core that led to the completion of (±)-dracocephalone A in 10 steps and 8% overall yield from known materials. Brønsted acid-promoted aromatization of a late-stage intermediate, followed by careful oxidations, allowed for the rearrangement to the [2.2.2] oxabicyclic core poised for conversion to (±)-dracocequinones A and B in 13 and 15 steps, respectively, from known materials.

An asymmetric synthesis of the cyclopentane portion of Cassiabudanol A and B is described, wherein stereoselective ring contraction under Favorskii conditions was used as the key step from (*R*)-14-hydroxycarvone derivative. Initial challenges were associated with the scalable preparation of (*R*)-14-hydroxycarvone. Screening of cyclobutane

fragmentation revealed $SnCl_4$ as the most reliable Lewis acid in various scales. Subsequent manipulation of (*R*)-14-hydroxycarvone set the stage for Favorskii rearrangement albeit mixture of diastereomers. Further functional group interconversions not only allowed for the separation of diastereomers but set the stage for the future strategy that includes intramolecular furan Diels-Alder.

In 2021 we completed the asymmetric total synthesis of (+)-raistrickindole A in 9 steps and overall 2% yield from known materials, featuring a diastereoselective intermolecular nitroso Diels-Alder (NDA) cycloaddition as the key step in constructing the oxazine core. In utilizing (+)-raistrickindole A as a late-stage intermediate to target (-)-haenamindole, optimization efforts of the route, especially Mukaiyama hydration and diketopiperazine (DKP) formation steps, are discussed to achieve overall 13% yield.

An asymmetric synthesis of the tricyclic core of [2.2.3]-Epidithiodiketopiperazines is described. The key step features a diastereoselective intramolecular NDA reaction of the cyclopentadiene adduct intermediate derived from (-)-quinic acid. Attempts to install the tertiary alcohol via a diastereoselective epoxidation from the NDA cycloadduct, as well as a proposed synthetic plan, are discussed.

Total Syntheses of (±)-Dracocephalone A and (±)-Dracocequinones A and B, Progress Towards a Total Synthesis of Cassiabudanols A and B, and Synthetic Studies Towards Total Synthesis of *N*-Oxy-Diketopiperazine Containing Natural Products.

by

Taehwan Hwang, B.S.

A Dissertation

Approved by the Department of Chemistry and Biochemistry

_____

John L. Wood, Ph.D., Chairperson

Submitted to the Graduate Faculty of Baylor University in Partial Fulfillment of the Requirements for the Degree of

Doctor of Philosophy

Approved by the Dissertation Committee

_____

John L. Wood, Ph.D., Chairperson

_____

Daniel Romo, Ph.D.

_____

Kevin G. Pinney, Ph.D.

_____

Caleb D. Martin, Ph.D.

_____

William Hockaday, Ph.D.

Accepted by the Graduate School

August 2023

_____

J. Larry Lyon, Ph.D., Dean

Page bearing signatures is kept on file in the Graduate School.

TABLE OF CONTENTS

LIST OF FIGURES

LIST OF SCHEMES

LIST OF TABLES

LIST OF ABBREVIATIONS

Ac	acetate
AIBN	azobisisobutyronitrile
API	active pharmaceutical ingredient
aq.	aqueous
Boc	*tert*-butoxycarbonyl
CAN	cerium (IV) ammonium nitrate
$CDCl_3$	deuterated chloroform
CDI	1,1'-carbonyldiimidazole
C–C	carbon–carbon
C–H	carbon–hydrogen
C–O	carbon–oxygen
DBU	1,8-diazabicyclo[5.4.0]undec-7-ene
DCC	dicyclohexylcarbodiimide
DDQ	2,3-dichloro-5,6-dicyano-1,4-benzoquinone
DFT	density functional theory
DHP	dihydropyran
DIBAL-H	diisobutylaluminum hydride
DKP	2,5-diketopiperazine
DMB	3,4-dimethoxybenzyl
DMAP	4-(dimethylamino)pyridine
DMDO	dimethyldioxirane
DMSO	dimethyl sulfoxide
DMP	Dess-Martin periodinane
ECD	electron capture detector
EDCI	1-ethyl-3-(3-dimethylaminopropyl)carbodiimide
EEDQ	2-ethoxy-1-ethoxycarbonyl-1,2-dihydroquinoline
ETP	epidithiodiketopiperazine
FTIR	Fourier-transform infrared spectroscopy
HATU	hexafluorophosphate azabenzotriazole tetramethyl uronium
HIV	human immunodeficiency virus
HMPA	hexamethylphosphoramide
HRMS	high-resolution mass spectrometry
HPLC	high-pressure liquid chromatography
LAH	lithium aluminum hydride
HMDS	hexamethyldisilazide
m-CPBA	*meta*-chloroperoxybenzoic acid
MLCs	minimum lethal concentrations
MM2	molecular mechanics
MOM	methoxymethyl
MP	melting point

MPLC	medium-pressure liquid chromatography
Ms	mesyl
NBS	*N*-bromosuccinimide
NCS	*N*-chlorosuccinimide
NDA	nitroso Diels-Alder
NHS	*N*-hydroxysuccinimide
NMR	nuclear magnetic resonance
n-BuLi	*normal*-butyllithium
OTf	triflate
o-tol	*ortho*-tolyl
PIDA	(diacetoxyiodo)benzene
PMB	*para*-methoxybenzyl
ppm	parts per million
PPTS	pyridinium *p*-toluene sulfonate
PTSA	*para*-toluenesulfonic acid
R_f	retention factor
sat.	saturated
S_N1	unimolecular nucleophilic substitution
S_N2	bimolecular nucleophilic substitution
s-BuLi	*sec*-butyllithium
TBAF	*tetra*-butylammonium fluoride
TBS	*tert*-butyldimethylsilyl
TDDFT	time-dependent density functional theory
THF	tetrahydrofuran
THP	tetrahydropyran
TIPS	triisopropylsilyl
TLC	thin-layer chromatography
TMEDA	tetramethylethylenediamine
TMS	trimethylsilyl
t-BuLi	*tert*-butyllithium
UPLC	ultra-performance liquid chromatography
μM	micromolar
W	watt

ACKNOWLEDGMENTS

Throughout my graduate I owe a great deal to many people for supporting me throughout my chemistry career. First and foremost, I thank God for His guidance and direction under his providence that paved the way and allowed me to find what I really enjoy as my career.

To my wife Yerim, I cannot say enough how much it means to me that you have always been my side from the happiest to the saddest moments of our life together. I am very grateful to have such a cheerful and supporting wife that makes me feel rejuvenated on daily basis. Thank you for being the most significant part of my life and for making my future exciting as can be.

I thank Professor John L. Wood for his sincere guidance not only as a chemist, but also as a mentor. I truly enjoyed working with you over the last four years and I could not have asked for a more enthusiastic and committed advisor than you are. Your creativity and passion have challenged me to become a better problem solver and chemist, and your advice and leadership have taught me to grow as a person.

I would like to thank my entire family: my wife, my parents, my brother, my parents-in-law, and my cats Zion and Haon for being the shelter during difficult times and always supporting me in various ways. You all are what keeps me going forward to become a better husband, son, brother, son-in-law, and dad.

I thank my committee members: Professor John L. Wood, Professor Daniel Romo, Professor Kevin G. Pinney, Professor Caleb D. Martin, Professor William Hockaday, and Dr. Brian Lindley for playing important roles throughout my journey of graduate studies.

I would not have been able to start my journey as a chemist without Professor David Sarlah; I would like to thank you for letting me develop a true passion in chemistry. Thank you for taking me in even when I had nothing to offer and supporting me when I needed the most help. I also thank Dr. Jola Pospech, Dr. Chris Bemis, Dr. Chad Ungarean, and Dan Holycross for taking time to teach me patiently. I am very grateful for all things, from strong work ethics to small lab tricks, that I learned from you all. These skills ended up being extremely useful throughout my graduate studies.

I feel extremely fortunate to have met a number of great chemists at Gilead Sciences that helped me affirm my decisions for career. I thank Dr. Jonathan Medley, Dr. Scott Lazerwith, and Dr. William Watkins for being great supervisors during my times at Gilead. I was able to grow, become a more mature chemist, and develop passion in pharmaceutical research. I thank Paulo Machicao and David Gutierrez for being great colleagues and friends. I will never forget our daily and humble conversations to become better chemists, which founded my passion for continuous learning and helped me pursue graduate studies.

I thank the Wood group members, past and present, for building a culture that is full of excitement and joy in learning and sharing chemistry. I am highly grateful to the ones that really dedicated their time and efforts to make things happen in the lab with resilience and tenacity, which has created the reputation that their younger siblings can be a part of.

To my family

CHAPTER ONE

Total Synthesis of (±)-Dracocephalone A and (±)-Dracocequinones A and B

1.1 Background

1.1.1 C^{20}-Norabietane and Icetexane Diterpenoids

Originally found in the West Tien Shan mountain system in Uzbekistan, *Dracocephalum komarovi* Lipsky (Labiatae), a perennial semishrub also known as 'buzbosh,' was used by the local people to cure various diseases, such as inflammation and hypertony by consuming the aerial parts in a tea.[1] Uchiyama *et al*., while searching for trypanocidal compounds in medicinal plants in Uzbekistan, noticed that there had been no previous reports on the constituents of this plant. In 2003, preliminary studies by Uchiyama *et al*. with the extracts from *D. komarovi* showed strong *in vitro* trypanocidal activity against epimastigotes of *Trypanosoma cruzi*, the protozoan parasite that transmits Chagas disease.[1] Inspired by these findings, further studies on the isolation of natural products led them to disclose a unique C^{20}-norabietane diterpenoid, (+)-dracocephalone A (**1.01**, Figure 1.1), and two novel icetexane diterpenoids(-)-cyclocoulterone (**1.02**), and (+)-komaroviquinone (**1.03**). In addition, it was revealed that **1.01**, **1.02**, and **1.03** display minimum lethal concentrations (MLCs) of 200, 20, and 0.4 μM, respectively towards trypanodical activity.[1] Several years later, Uchiyama *et al*. discovered two new structurally related C^{20}-norabietane diterpenoids, (+)-dracocequinone A (**1.04**, Figure 1.1) and (-)-dracocequinone B (**1.05**), as well as a new abietane diterpenoid: (+)-komarovinone (**1.06**)

from *D. komarovi*. The former two (**1.04** and **1.05**) were found to exhibit trypanocidal activity with MLC values of 12.5 and 25 μM.[2]

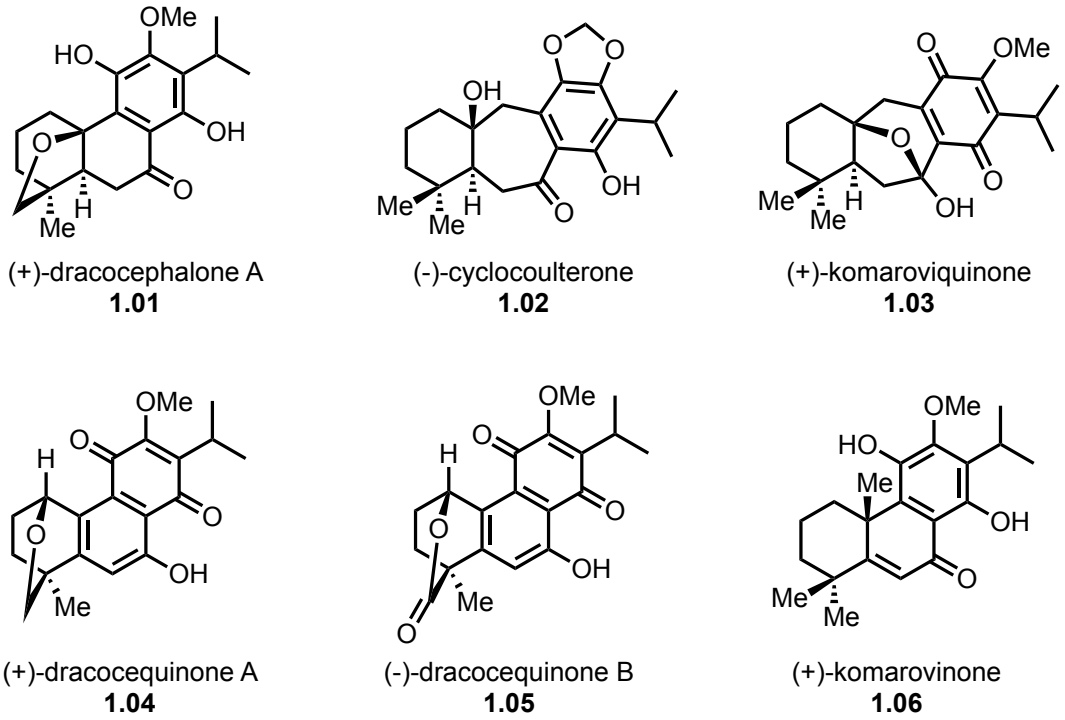

Figure 1.1. Representative diterpenoids from *Dracocephalum komarovi*.

1.1.2 Previous Syntheses of Icetexane Diterpenoids

Due to their potent biological activity towards Chagas disease and their structural architecture, icetexane diterpenoids, **1.02** and **1.03**, have captured the attention of the synthetic community. To date, numerous completed syntheses have been reported, including: three *de novo* total synthesis, two formal synthesis of **1.03**, and one semisynthesis of **1.02** and **1.03**.[3] The first total synthesis of **1.03** was reported by Sengupta and coworkers in 2005.[3a] As illustrated in scheme 1.1, the synthesis commenced with an allylation, followed by decarboalkoxylation of enone **1.07** under Krapcho conditions to deliver **1.08**. Subsequent methylation using Gilman's reagent proceeded in 1,4-fashion,

thereby setting the stage for a subsequent 1,2-arylation at the ketone. In the event, conversion of **1.09** to the corresponding organolithium, followed by addition to ketone **1.08** furnished tertiary alcohol **1.10** in a modest yield. In an attempt to brominate the electron-rich aryl moiety using NBS, an undesired dibromination was observed. The latter event necessitated a regioselectively debrominate using zinc and acetic acid. Subsequent intramolecular Heck cyclization afforded the tricycle **1.11**. With tricycle **1.11** in hand, two-step oxidative cleavage delivered ketone **1.12** and aryl oxidation using silver (II) oxide and dilute nitric acid completed the racemic synthesis of **1.03**.

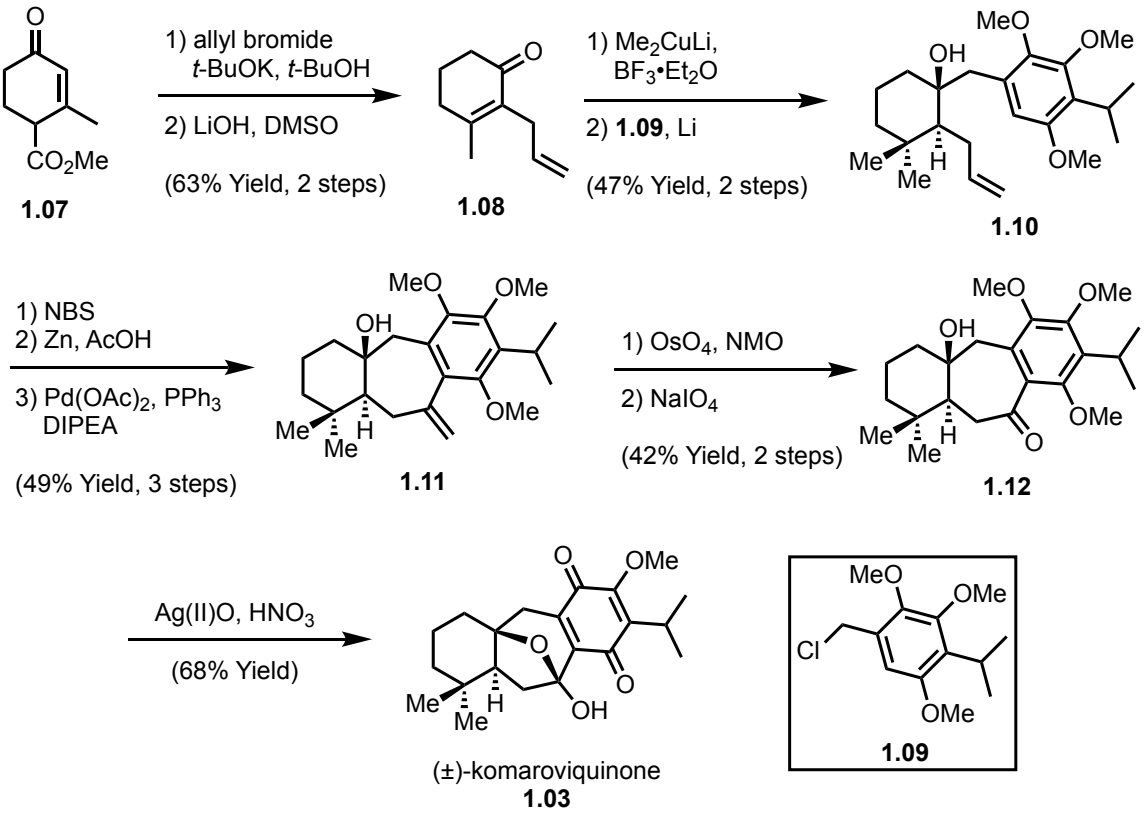

Scheme 1.1. Sengupta's first total synthesis of (±)-komaroviquinone.

In 2007, Majetich *et al*. reported their synthetic approach to **1.03**.[3b] Similar to Sengupta, Majetich utilized a convergent approach wherein arylation of 1,3-diketone **1.13** and pentasubstituted arene **1.14** was followed by treatment with vinylithium to give enone **1.15** (Scheme 1.2). Having accessed enone **1.15**, the stage was set for the preparation of ketone **1.12** via a series of functional group interconversions. To this end, construction of the tricycle **1.16** via Lewis acid-mediated cyclization, followed by reduction of the enone to a secondary alcohol with L-Selectride and subsequent acetate protection using acetic anhydride, furnished **1.16**. Benzylic oxidation in the presence of copper sulfate followed by Jones oxidation installed the benzylic ketone, and elimination of the *O*-acetate using KOH and thionyl chloride afforded olefin **1.17**. To install the tertiary alcohol found in **1.12**, the trisubstituted olefin was converted into the corresponding bromohydrin, followed by radical debromination. Lastly, utilization of the same conditions reported by Sengupta and coworkers resulted in the desired aryl oxidation to give **1.03** as a racemic mixture.

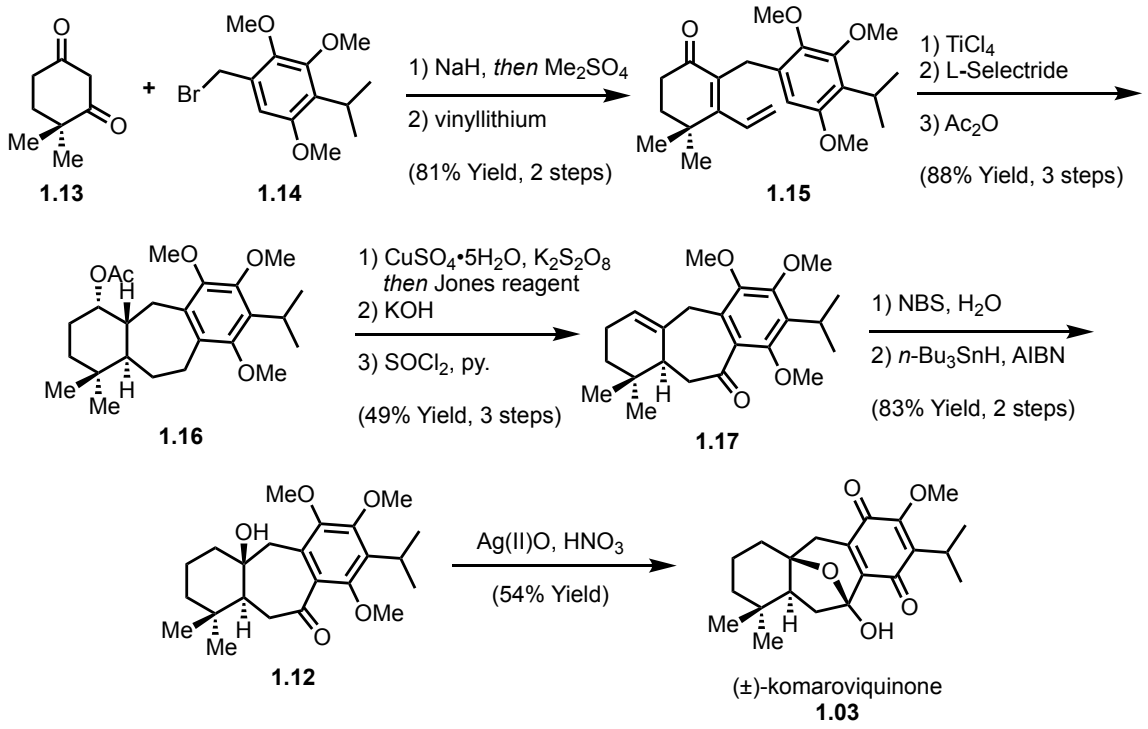

Scheme 1.2. Majetich's total synthesis of (±)-komaroviquinone.

While the former two syntheses provided **1.03** as a racemic mixture, it was not until 2010 that the first asymmetric synthesis of **1.03** was realized by Suto and coworkers. Similar to the previous racemic synthesis, Suto and coworkers envisioned accessing **1.03** in a convergent manner by combining enantioenriched vinyl iodide **1.18** and the known arene **1.14**. As demonstrated in Scheme 1.3, **1.18** and **1.14** were combined under the standard Negishi coupling conditions and subsequent lactonization under aqueous HCl generated lactone **1.19** in good yields.[3c] Iodination and cyclization gave the same penultimate intermediate employed by Sengupta and Majetich. Accordingly the previously reported aryl oxidation conditions were then employed to complete (+)-**1.03**.

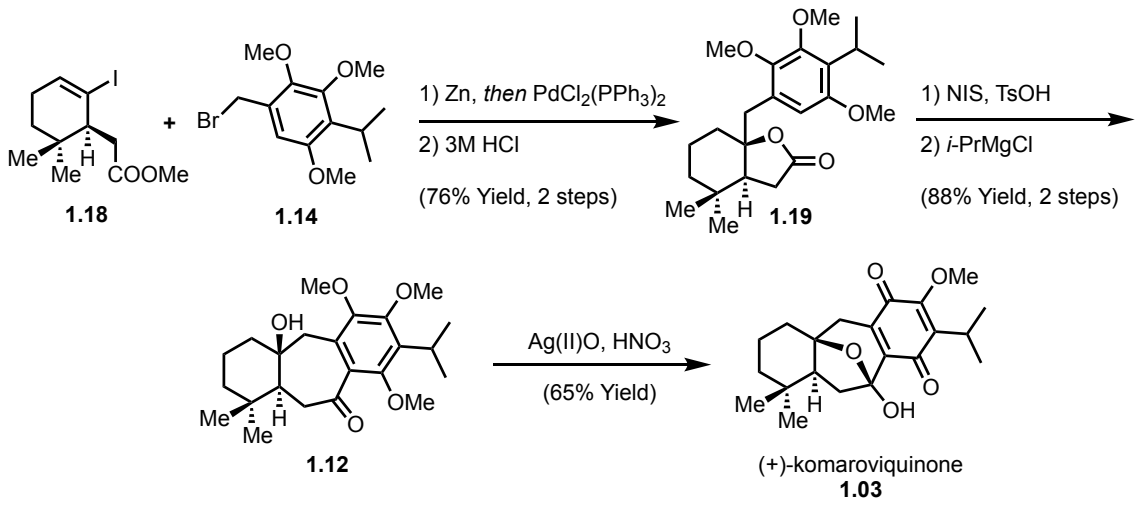

Scheme 1.3. Suto's total synthesis of (+)-komaroviquinone.

In 2016, two groups separately reported synthetic access to **1.03**. First, Thommen *et al*. reported the semisynthetic route to both (-)-**1.02** and (+)-**1.03** from trimethylated carnosic acid **1.20** (Scheme 1.4).[3d] Reduction of the methyl ester, followed by mesylation promoted a ring expansion. Subsequent treatment with *m*-CPBA and L-Selectride afforded tertiary alcohol **1.21**. To oxidize the benzylic methylene, they opted to protect the phenol with an acetate. Exposure of the derived acetate to oxidation conditions then forged the benzylic ketone. Subsequent removal of the acetate and aryl oxidation delivered **1.03** as a single enantiomer. When **1.03** was exposed to sunlight at low temperature (4 °C), it was proportionally converted to **1.02** and komarovispirone (**1.22**).

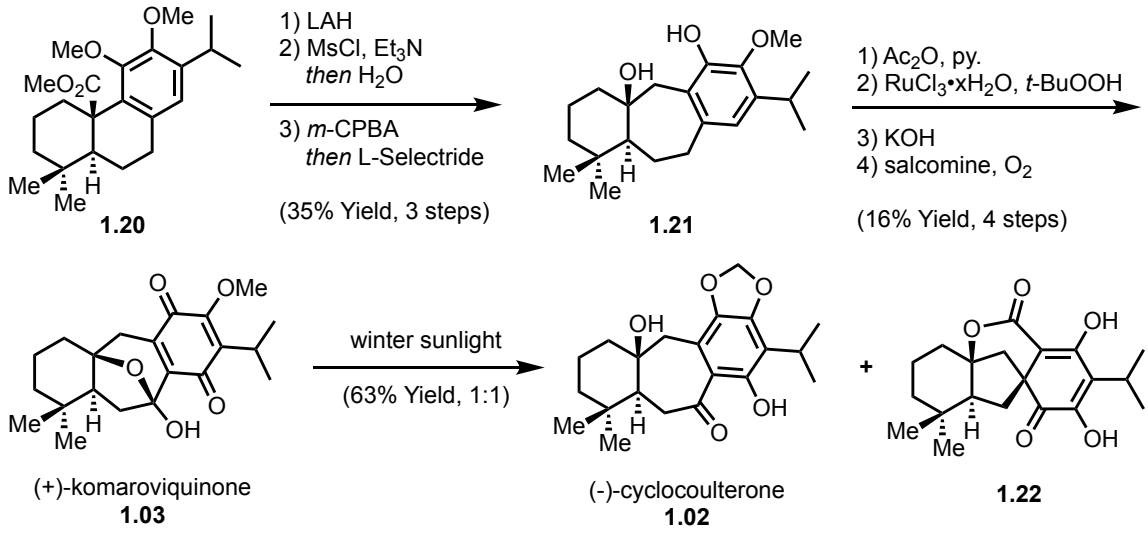

Scheme 1.4. Thommen's semisynthesis of (+)-komaroviquinone and (-)-cyclocoulterone.

As illustrated in Scheme 1.5, a formal synthesis of **1.03** was reported in 2016 by Oh *et al*.[3e] After combining alkyne **1.23** and aryl bromide **1.24** via Sonogashira coupling to afford aldehyde **1.25**, Pt-mediated [5+2] cycloaddition delivered the tricycle **1.26** as a mixture of diastereomers. Redox manipulation of **1.26**, followed by Lewis acid-mediated isomerization gave the known ketone **1.17** an intermediate that had previously been prepared by Majetich.

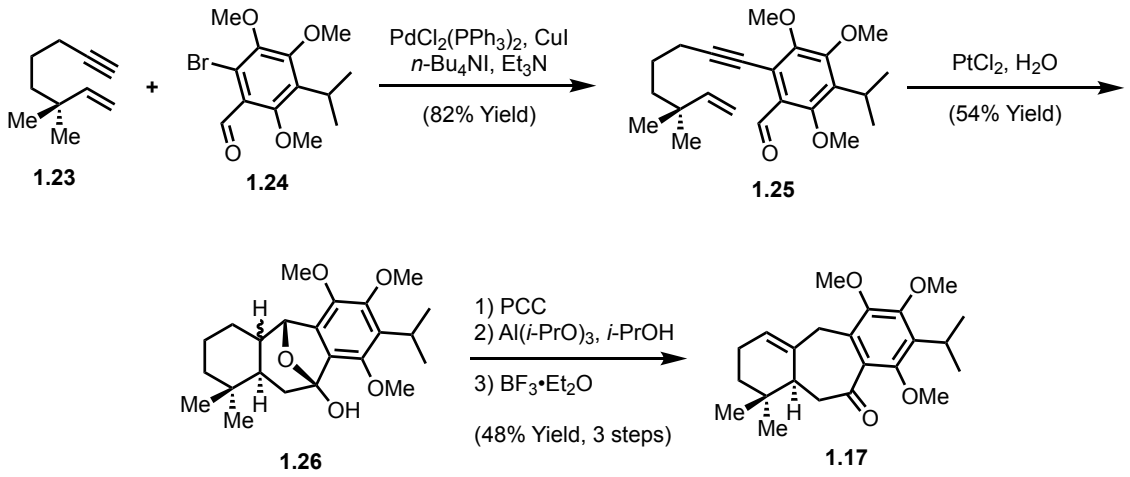

Scheme 1.5. Oh's formal synthesis of (±)-komaroviquinone.

In 2019, another formal synthesis of **1.03** was reported by Ahmed *et al*. (Scheme 1.6).[3f] In this study, epoxide **1.27** was subjected to cross-electrophile coupling with aryl bromide **1.28**. The resulting lactol was then oxidized to the corresponding lactone under Fetizon oxidation conditions to yield the known lactone **1.19** reported by Suto.

Though there are a number of synthetic approaches that have been developed for accessing **1.03**, its corresponding C^{20}-norabietane congeners (**1.01**, **1.04**, and **1.05**) have not been prepared by total synthesis. The scarcity of available methods for preparing C^{20}-norabietane diterpenoids, coupled with their potential ability to become new lead compounds towards targeting Chagas disease led us to develop a new synthetic strategy towards these natural products.

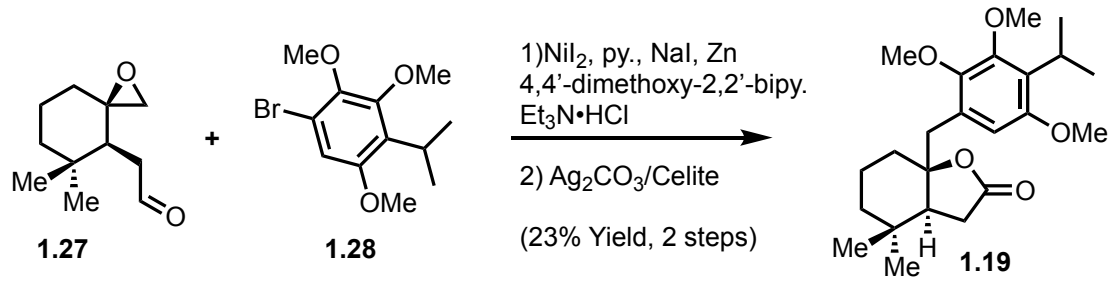

Scheme 1.6. Ahmad's formal synthesis of (±)-komaroviquinone.

1.2 Total Synthesis of (±)-Dracocephalone A

1.2.1 Retrosynthetic Analysis

In devising a retrosynthetic strategy towards **1.01**, we envisioned that a late-stage Suárez oxidation, followed by an oxidation/reduction of the arene from [3.2.1] oxabicycle **1.29** would secure the formation of **1.01** (Scheme 1.7). We suspected that ketone in **1.29** could be generated by silyl ketal fragmentation and decarboalkoxylation of the [2.2.1] oxabicycle **1.30**. In constructing the carbon skeleton, we were inspired by the previous syntheses of **1.03**, in which trimethoxyarene and alkyl chain fragments were combined in a convergent manner and subsequent cyclization furnished the carbon framework. Similarly, we envisioned a fragment coupling approach, followed by cyclization as providing a viable means of accessing the carbon skeleton. Specifically, we suspected that an intramolecular Diels-Alder reaction with a 2-siloxyisobenzofuran (**1.31**), which could be prepared *in situ* from lactone **1.32**, would afford **1.30** wherein the trans decalin core would be selectively furnished via a presumed preference the endo orientation of the carboxyethyl group in the transition state leading to cyclization. In order to prepare the Diels-Alder precursor **1.32**, we envisioned that aldehyde **1.33** and benzamide **1.34** could

be combined via a Snieckus directed *ortho*-metalation/nucleophilic addition sequence and subsequent acid-catalyzed lactonization.[4]

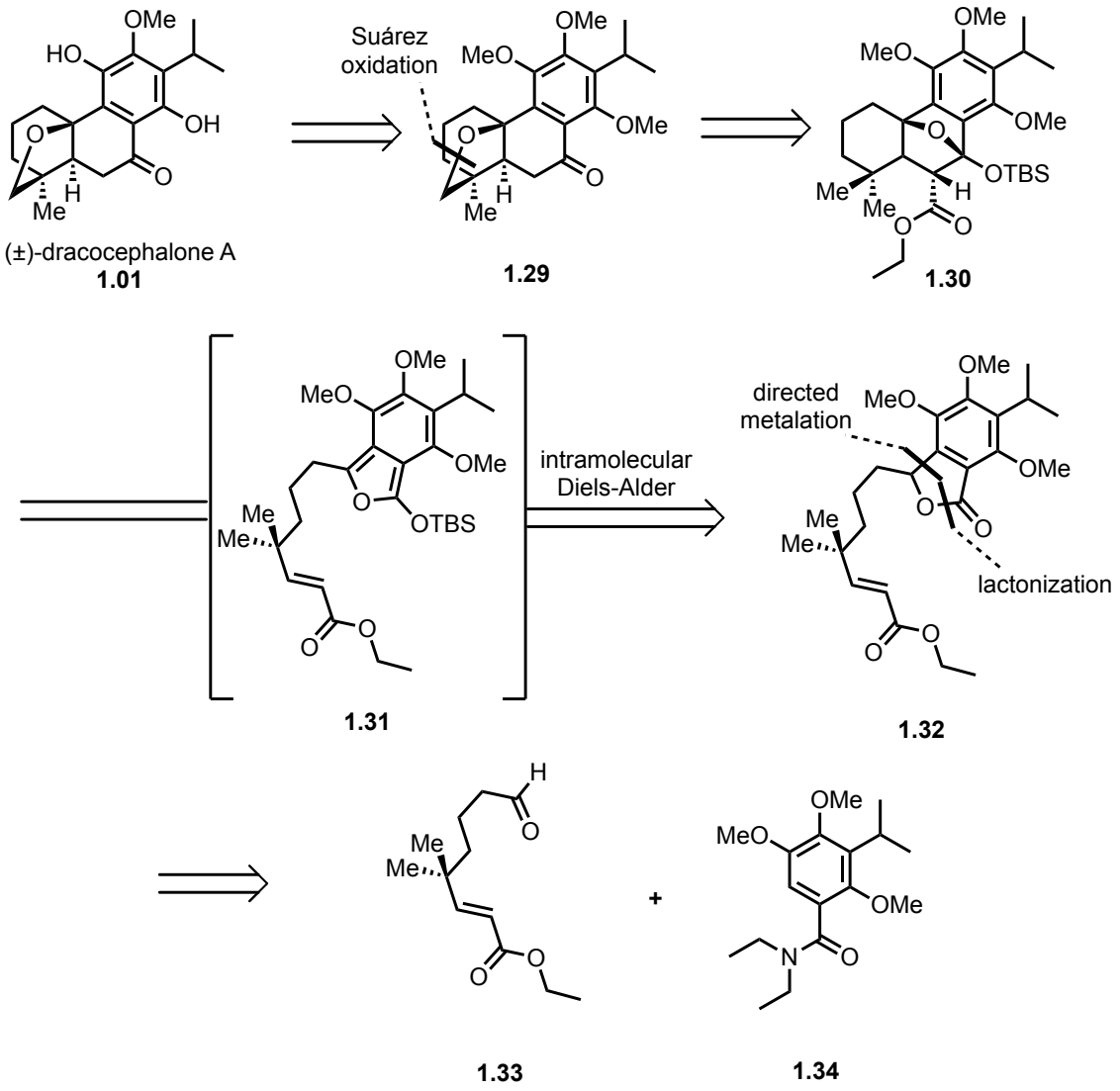

Scheme 1.7. Initial retrosynthetic analysis of (±)-dracocephalone A (**1.01**).

1.2.2 Intramolecular Diels-Alder Cycloaddition

In the forward sense, we first focused on the preparation of **1.33** from known aldehyde **1.38** as depicted in Scheme 1.8. Following the procedure reported by Frontier and coworkers, tetrahydrofuran **1.35** was subjected to ring-opening event in the presence

of TBSCl and sodium iodide to furnish alkyl iodide **1.36**.[5] Subsequent displacement of **1.36** with lithiated isobutyronitrile delivered nitrile **1.37** and reduction of the nitrile secured the formation of **1.38**. With **1.38** in hand, Horner-Wadsworth-Emmons olefination, desilylation with TBAF, and Dess-Martin oxidation delivered **1.33**.

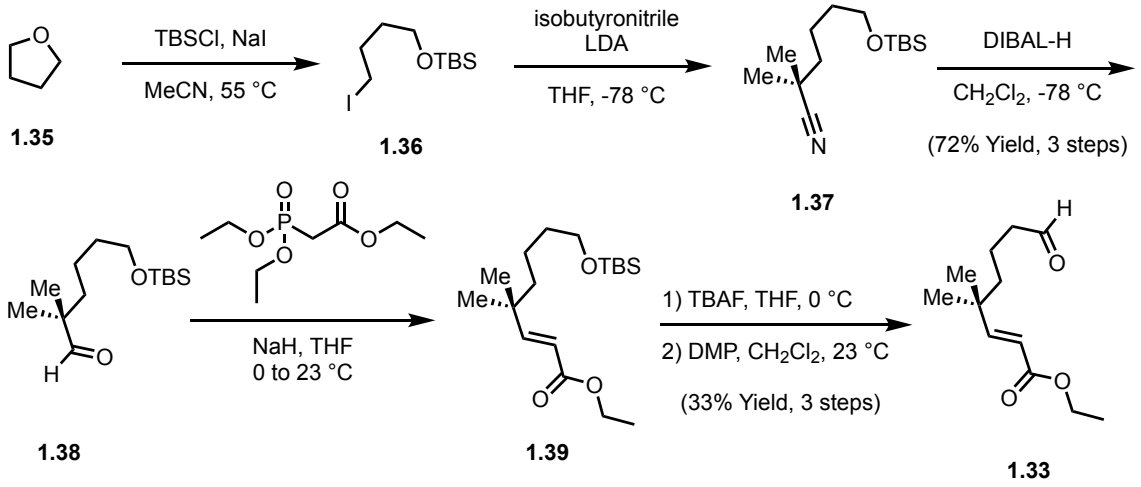

Scheme 1.8. Synthesis of aldehyde **1.33**.

Having prepared the requisite electrophile, we turned our attention to the nucleophile, **1.34**. Our initial efforts were focused on the preparation of known bromide **1.43**. Treatment of commercially available 1,2,4-trimethoxybenzene **1.40** with *n*-BuLi generated the transient lithiated arene intermediate. (Scheme 1.9).[6] Subsequent addition of methyl chloroformate followed by excess methyl magnesium bromide secured the formation of tertiary alcohol **1.41**. Next, **1.41** was subjected to deoxygenation conditions of which elimination of tertiary alcohol facilitated by sulfuric acid and hydrogenation of the resulting alkene delivered arene **1.42**.[6] Regioselective bromination of **1.42** using NBS gave **1.43** in excellent yield, and lithium-halogen exchange, followed by addition of the resultant organolithium to *N*,*N*-diethylcarbamoyl chloride forged **1.34**.[7]

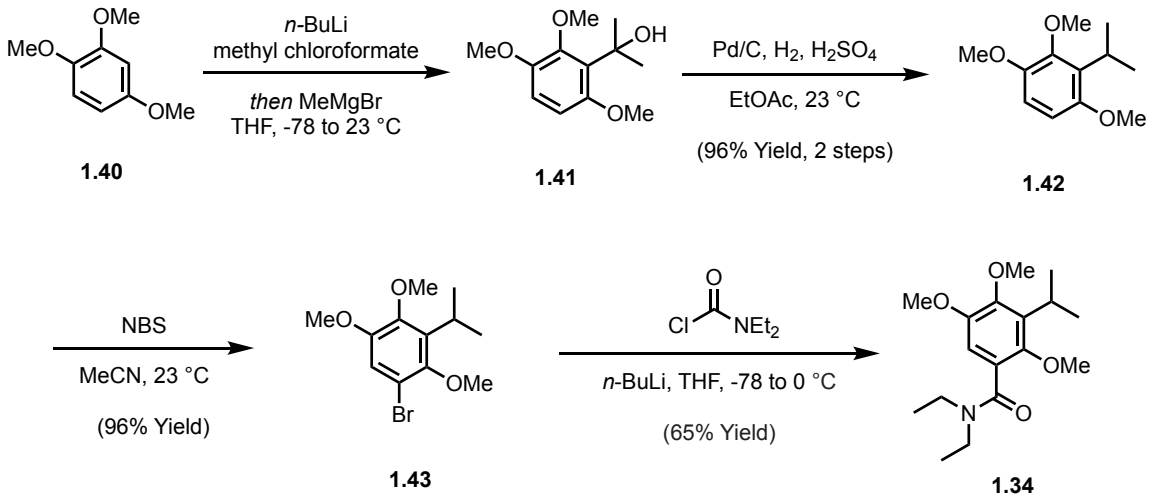

Scheme 1.9. Synthesis of benzamide **1.34**.

With the both coupling fragments in hand, we turned to the directed *ortho*-metalation reaction. To this end, exposure of **1.34** to conditions developed by Snieckus produced an intermediate anion which, upon exposure to aldehyde **1.33** (Scheme 1.10) and standard work-up,[4] furnished intermediate alcohol **1.44**. Exposure of the crude alcohol to catalytic PTSA then afforded lactone **1.32** in modest yield. After preparation of **1.32**, we focused on the generation of transient 2-siloxyisobenzofuran to effect intramolecular Diels-Alder. Upon treatment of **1.32** with LiHMDS and TBSCl, **1.32** was converted to the corresponding **1.31** which, upon warming to room temperature, smoothly underwent the desired Diels-Alder cycloaddition to generate the sensitive [2.2.1] oxabicycle **1.30** as the only isolable product (Scheme 1.11).[8]

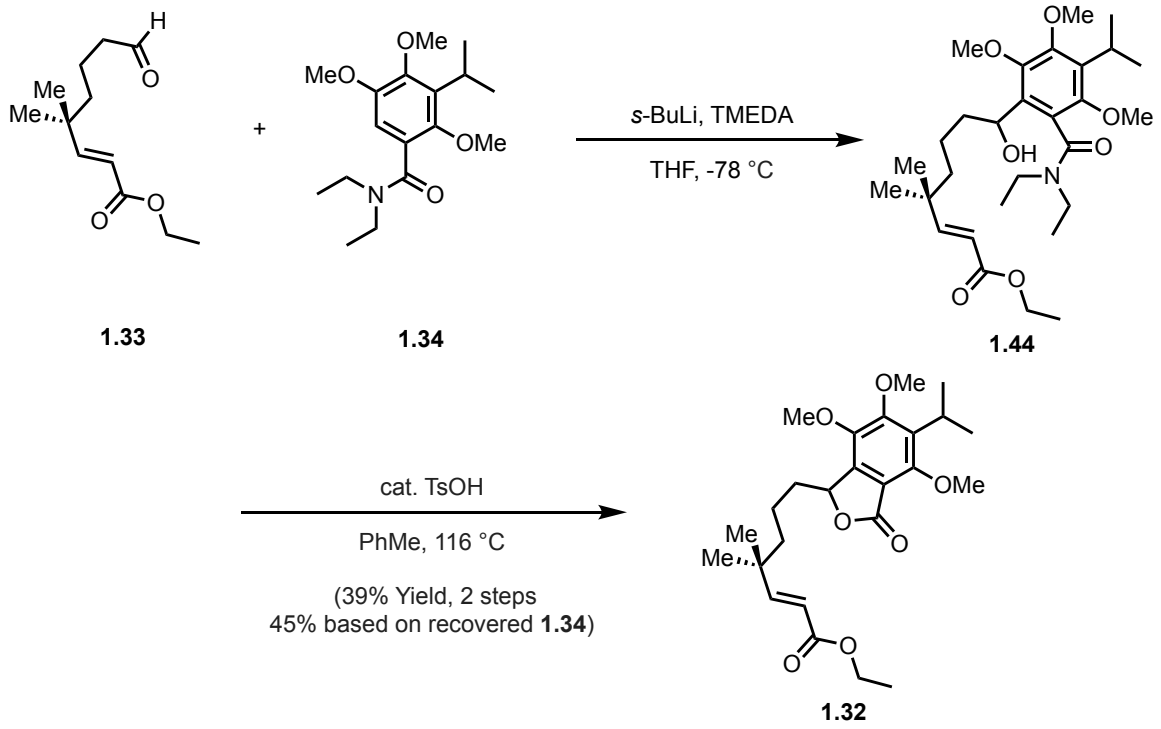

Scheme 1.10. Synthesis of lactone **1.32**.

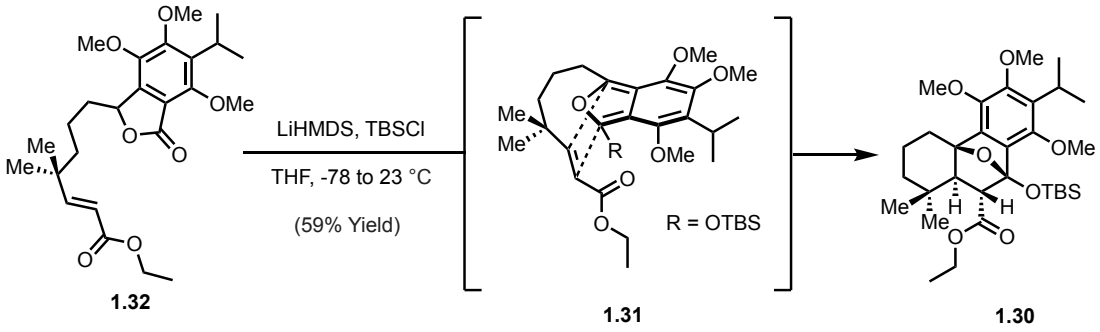

Scheme 1.11. Intramolecular Diels-Alder cycloaddition.

1.2.3 Undesired retro-*Dieckmann Cyclization*

We envisioned that the initial stages of transforming of **1.30** to **1.29** would involve the careful removal of the silyl group, followed by fragmentation of the C–O bond, to yield beta-ketoester **1.46**. To this end, we first subjected **1.30** to acidic conditions in hope of

effecting the desired ring opening. To our dismay, we observed cleavage of the C–C bond via a *retro*-Dieckmann cyclization (**1.47**) instead of the desired C–O bond (**1.45**) to furnish spirolactone **1.48** (Scheme 1.12), a structure that was unambiguously assigned by X-ray analysis. We hypothesized that PPTS could catalyze the fragmentation of the C–C bond due to the Lewis basicity of the ester.

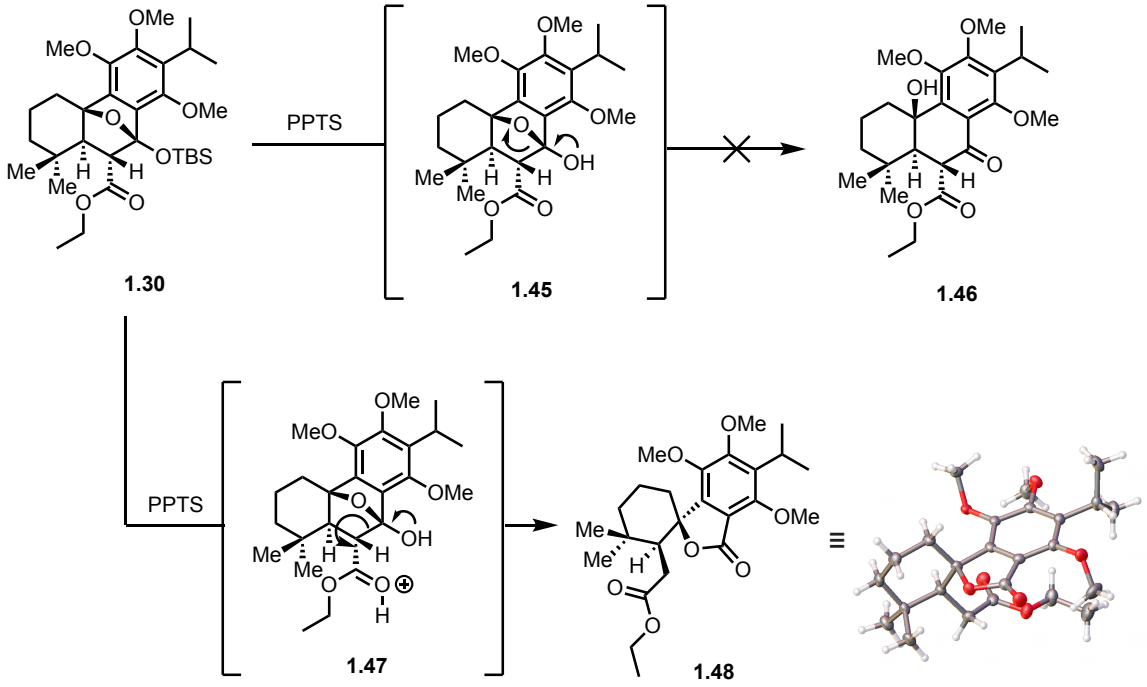

Scheme 1.12. Undesired formation of spirolactone **1.48** under acidic conditions.

Thus, we decided to attempt removing the silyl group of **1.30** by employing TBAF which, based on the well-known affinity of the fluoride ion for silicon, was expected to result in removal of the silyl group and formation of the corresponding alkoxyanion intermediate **1.49**. The expectation was that the intermediate oxy-anion would undergo ring opening via fragmentation of the C–O bond (Scheme 1.13). Unfortunately, we again only observed the formation of the undesired retro-Dieckmann product (**1.48**).

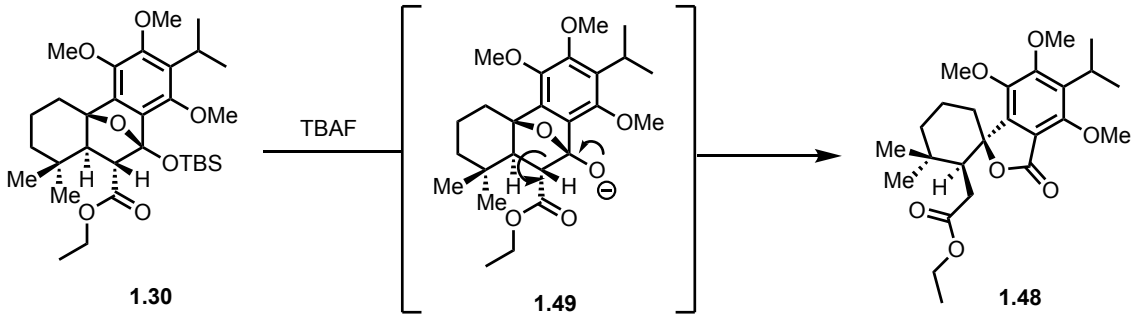

Scheme 1.13. Undesired formation of spirolactone **1.48** with TBAF.

After the observing the propensity of **1.30** to undergo *retro*-Dieckmann cyclization in lieu of C–O bond fragmentation under both acidic and basic conditions, we realized the need to alter the ethyl ester so as to prevent it from stabilizing the resulting carbanion. Our thought was to saponify the ester to the corresponding lithium carboxylate **1.50** using LiOH (Scheme 1.14). We hypothesized that the presence of the carboxylic acid would result in formation of a dianion upon *retro*-Dieckmann and thereby promote reaction via rupture of the C–O bond (i.e., **1.50**). Additionally, the derived beta-keto carboxylate (**1.51**) was expected to undergo spontaneous loss of CO_2 to furnish the desired ketone (**1.52**). Unfortunately, all efforts to effect saponification of, **1.30** resulted in the formation of **1.48** as the only observed and isolable product.

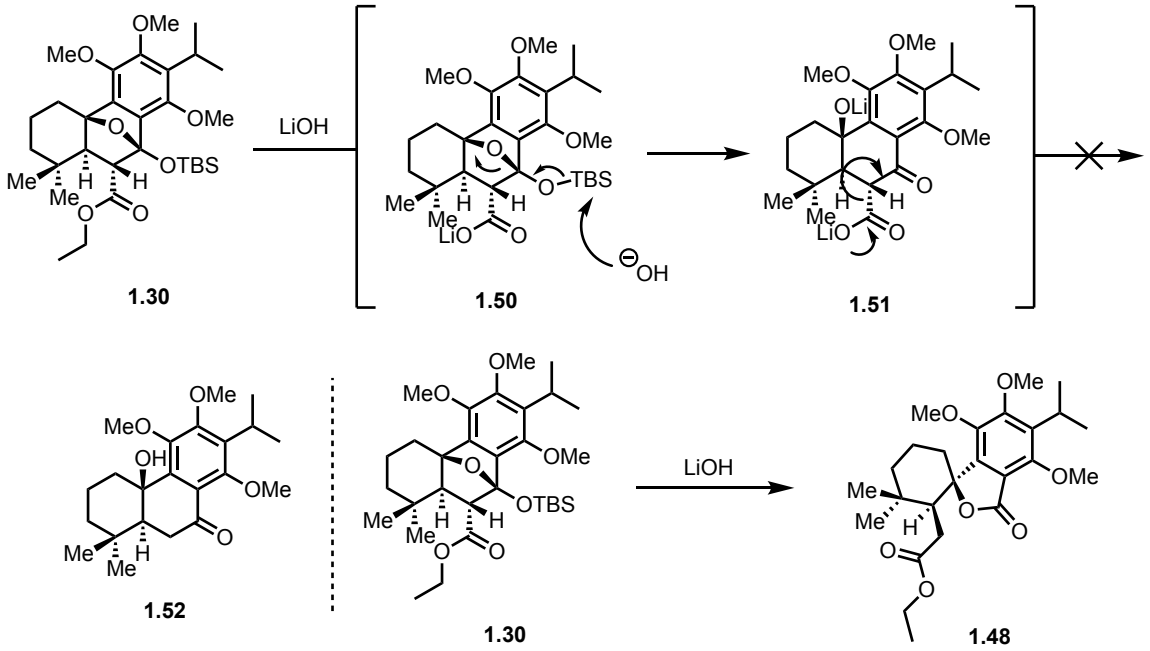

Scheme 1.14 Undesired formation of spirolactone **1.48** with lithium hydroxide.

After realizing the difficulty of fragmenting the C–O bond in the presence of the ethyl ester in **1.30**, we opted to reduce the ester to its corresponding alcohol. After extensive screening of reducing conditions, a number of hydride sources such as: DIBAL-H, LAH, lithium triethyl borohydride, and Red-Al, the desired transformation could not be achieved. In addition, treatment of **1.30** with lithium borohydride led to the formation of **1.48** (Scheme 1.15).

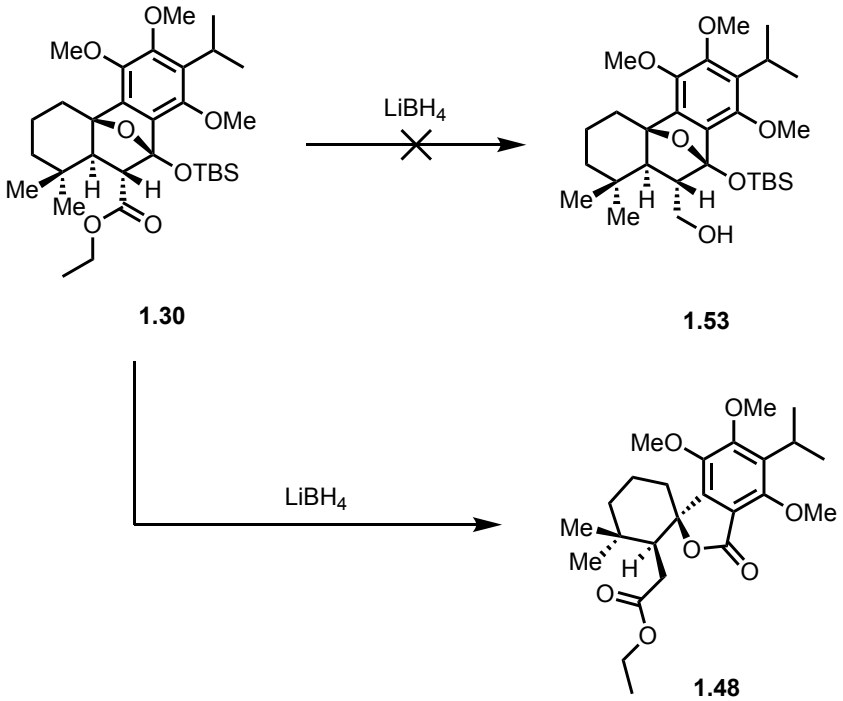

Scheme 1.15 Undesired formation of spirolactone **1.48** with lithium borohydride.

1.2.4 Revising the Retrosynthetic Analysis

Given the sensitivity of the silyl acetal moiety of **1.30**, coupled with its propensity to undergo a *retro*-Dieckmann reaction under acidic, basic, and reductive conditions, it was clear that an alternative strategy was needed. As illustrated in Scheme 1.16, we still envisioned that the late-stage Suárez oxidation to be a viable approach in constructing the [3.2.1] oxabicycle (**1.29**) from tertiary alcohol **1.52**. The first major change involves forming the decalin moiety found in **1.52** via an intramolecular nucleophilic acyl substitution of the alkyl iodide **1.54** into the lactone. The iodide **1.54** would be assembled from the acid **1.55** via decarboxylative Hunsdiecker iodination. Given its accessibility, **1.48** was seen as an attractive intermediate for formation of **1.55**.

Based on this revised plan, preliminary studies were conducted to convert **1.48** into its corresponding carboxylic acid **1.55**. Unfortunately, all attempts to selectively hydrolyze

the ethyl ester moiety failed. Accordingly, we opted to prepare a more malleable allyl ester (**1.56**). In constructing ester **1.56**, we planned to parallel the previous sequence and employ an intramolecular Diels-Alder reaction/*retro*-Dieckmann sequence to advance lactone **1.57** to **1.56**. Preparation of **1.57** would require modified aldehyde **1.58** and the previously employed benzamide **1.34** as substrates for the directed *ortho*-metalation/lactonization cascade leading to **1.57**.

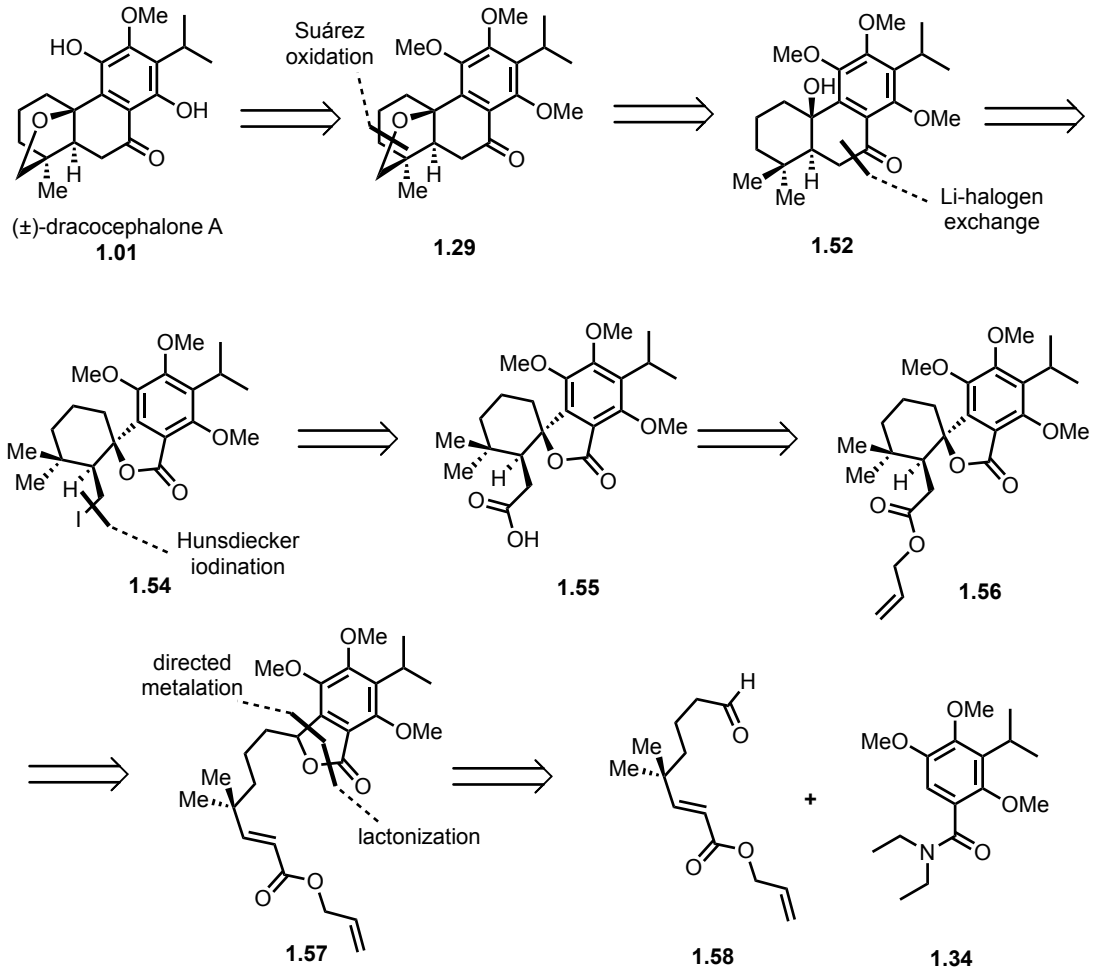

Scheme 1.16. Revised retrosynthetic analysis.

*1.2.6 Synthesis of Allyl Spirolactone **1.56***

Given that the steps leading to aldehyde **1.58** had been defined in our previous ethyl ester series, these latter efforts were accompanied with optimization studies. Accordingly, our efforts commenced with the subjection of aldehyde **1.38** to Masamune-Roush modified Horner-Wadsworth-Emmons olefination conditions (Scheme 1.17). Subsequent aqueous HCl-mediated cleavage of the silyl group and Dess-Martin oxidation furnished **1.58** in a greatly improved yield relative to that observed for **1.33**. Turning our attention to the fragment coupling, we were delighted to find that the *ortho*-metalation/lactonization sequence can be significantly improved by employing an additive, lanthanum(III) chloride bis-lithium chloride complex, and performing the lactonization by direct exposure to PTSA in the same reaction pot (Scheme 1.18).[9] Under these conditions, **1.57** was delivered in 68% yield. In further optimization efforts designed to bypass the intermediate [2.2.1] oxabicycle derived from intramolecular Diels-Alder reaction, we discovered that exposure of **1.57** to LiHMDS and catalytic amount of $Cu(OTf)_2$ and no added silyl chloride, resulted in excellent yields of **1.56** as a single diastereomer. The structure of **1.56** was confirmed by X-ray analysis.

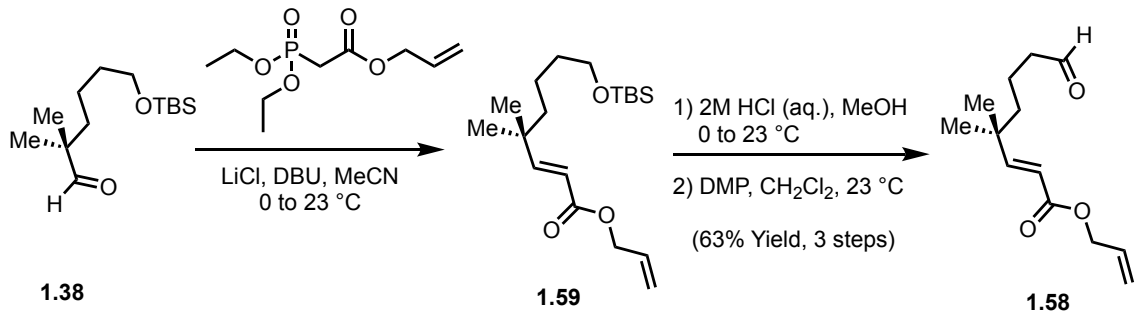

Scheme 1.17. Synthesis of aldehyde **1.58**.

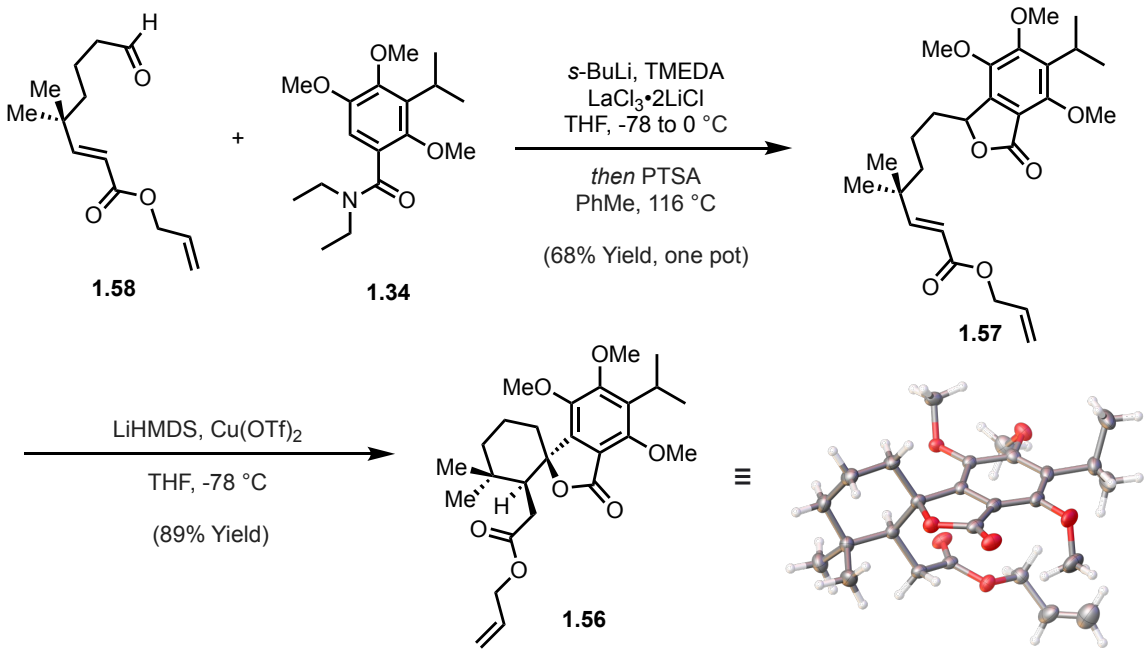

Scheme 1.18. Synthesis of spirolactone **1.56**.

1.2.6 Mechanistic Aspects of Diastereoseletive Spirocyclization

The highly diastereoselective spirocyclization could arise via two distinct mechanistic pathways: (1) anionic Diels-Alder/*retro*-Dieckmann cascade and (2) an intramolecular Michael cyclization (Scheme 1.19).[10] Given that the sense and extent of diastereoselectivity very closely matched the outcome of the *endo*-selective 2-siloxyisobenzofuran Diels-Alder, we hypothesize that the former is at play. Furthermore, examples of anion-assisted furanone Diels-Alder reaction in the literature support the feasibility of such a process.[11] On the other hand, we acknowledge the possibility the observed diastereomer could selectivity arise via equilibrium through a Michael/*retro*-Michael process, arriving at the more thermodynamically stable diastereomer. In order to further explore the latter possibility, we employed DFT calculations to estimate the ground-state energies of the respective diastereomers. These efforts revealed that the two differ by

6 kcal/mol with the unobserved diastereomer **1.63** having the higher energy. This led to the conclusion that both mechanistic pathways are viable possibilities.

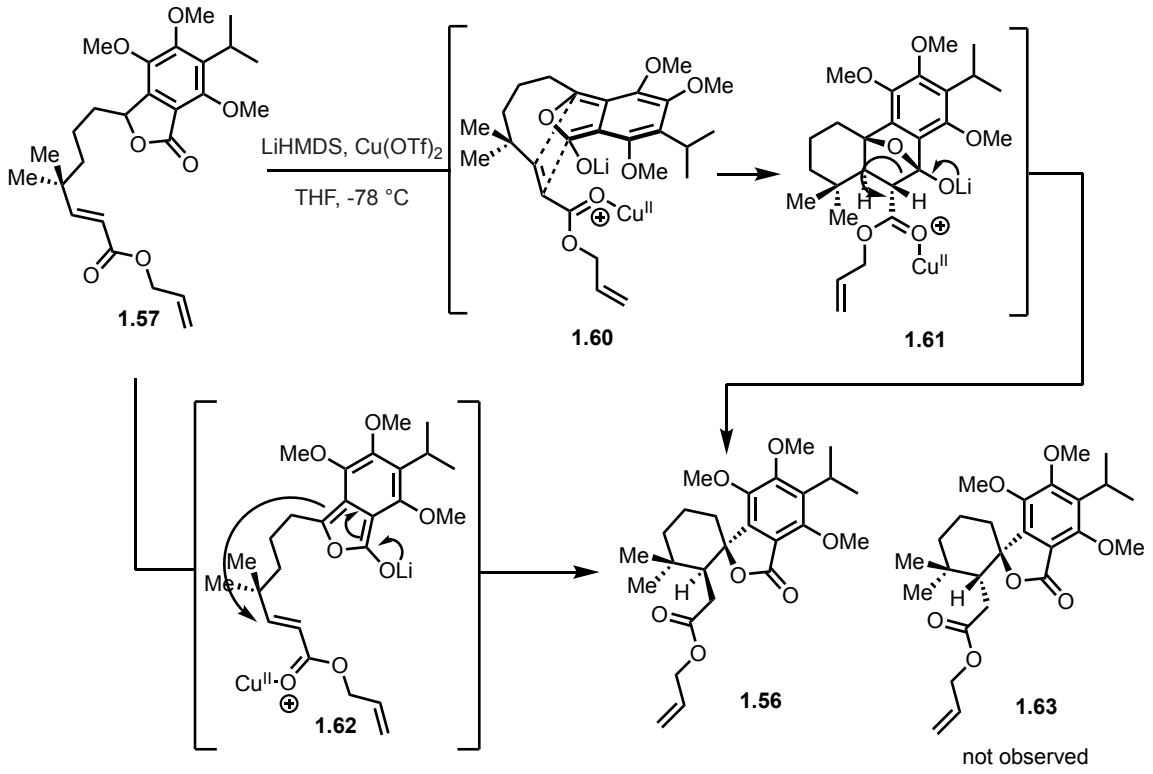

Scheme 1.19. Two potential mechanistic pathways.

1.2.7 Completion of (±)-Dracocephalone A

With **1.56** in hand, we were poised for the completion of synthesis. Subjecting **1.56** to palladium-mediated deallylation in the presence of morpholine furnished the corresponding carboxylic acid **1.55** (Scheme 1.20). Subsequent exposure of **1.55** to modified Husdiecker conditions smoothly induced decarboxylative iodination to obtain alkyl iodide **1.54**.[12] Metal-halogen exchange using *t*-BuLi then initiated a rapid intramolecular nucleophilic acyl substitution reaction that produced tertiary alcohol **1.52** which, upon treatment with phenyl iodide diacetate (PIDA) and I_2 under Suárez conditions,

undergoes a diastereotopic group selective transannular oxidation of the *syn*-methyl group to furnish [3.2.1] oxabicycle **1.29**.[13,14] At this point, all that remained was a regioselective double demethylation to the hydroquinone, a transformation that in practice proved to be a considerable challenge due to the lability of **1.29** under acidic conditions as precedented.[3a-c] After considerable experimentation, it was eventually determined that cerium (IV) ammonium nitrate (CAN) can be employed to convert **1.29** to a transient *para*-quinone intermediate which, upon reduction with aqueous sodium dithionite as a work-up, gives rise to (±)-dracocephalone A (**1.01**).[3d,15] Notably, this efficient synthetic approach provided quantities sufficient for crystallization of **1.01** and further structural confirmation via single crystal X-ray analysis.

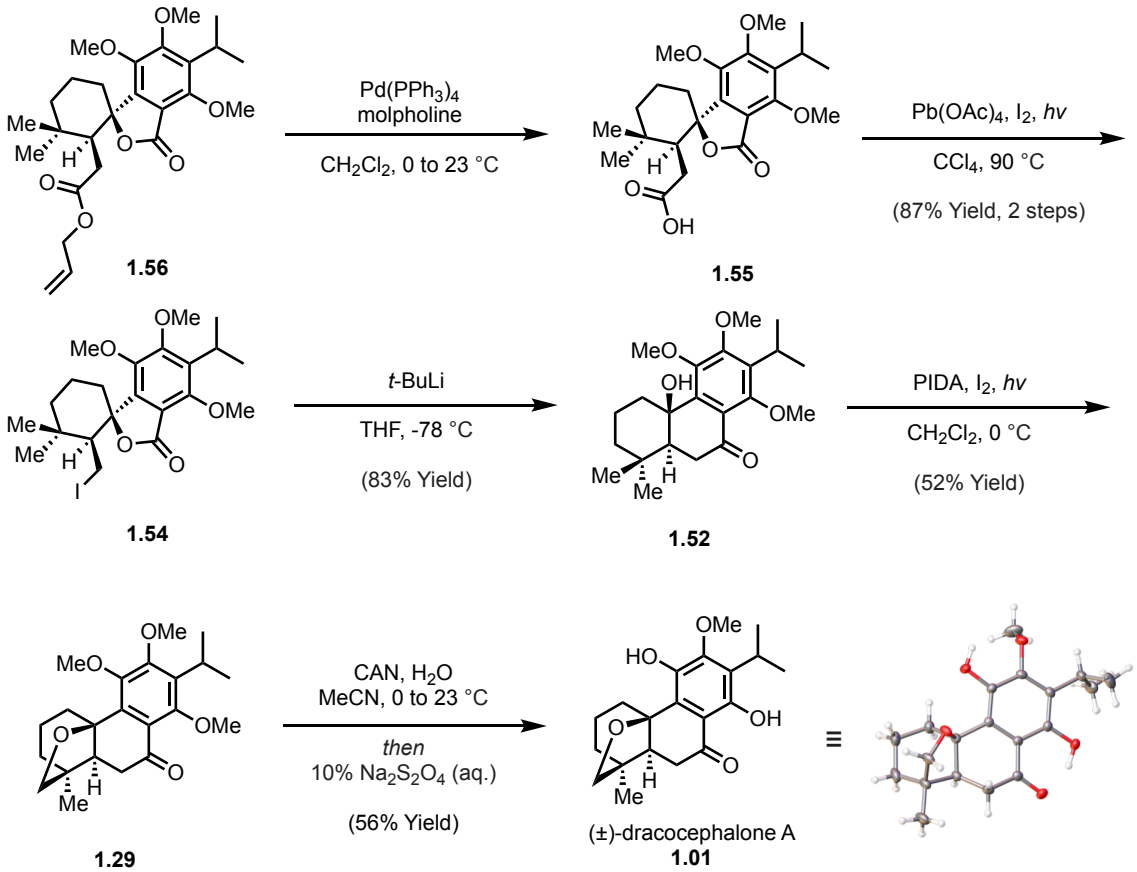

Scheme 1.20. Completed synthesis of (±)-dracocephalone A (**1.01**).

1.3 Total Synthesis of (±)-Dracocequinones A and B

1.3.1 Retrosynthetic Analysis

Having accessed (±)-dracocephalone A (**1.01**), we sought to extend this strategy to the aromatized and further oxidized congeners (±)-dracocequinone A (**1.04**) and (±)-dracocequinone B (**1.05**). As illustrated retrosynthetically in Scheme 1.21, our plan envisioned **1.05** as arising from a regio-and chemoselective C–H oxidation of **1.04**. Preparation of the quinone would involve an oxidative double demethylation akin to that used in the total synthesis of **1.01**. Thus arene **1.64** was seen as the precursor the requisite *para*-quinone (**1.04**). In order to construct the [2.2.2] oxabicycle in **1.64**, we planned to subject [3.2.1] oxabicycle **1.29** to aromative elimination to **1.66** which, upon subsequent oxidation to the corresponding *para*-quinone methide (**1.65**) would set the stage for a transannular *oxa*-1,6-addition and result in the formation of **1.64**.

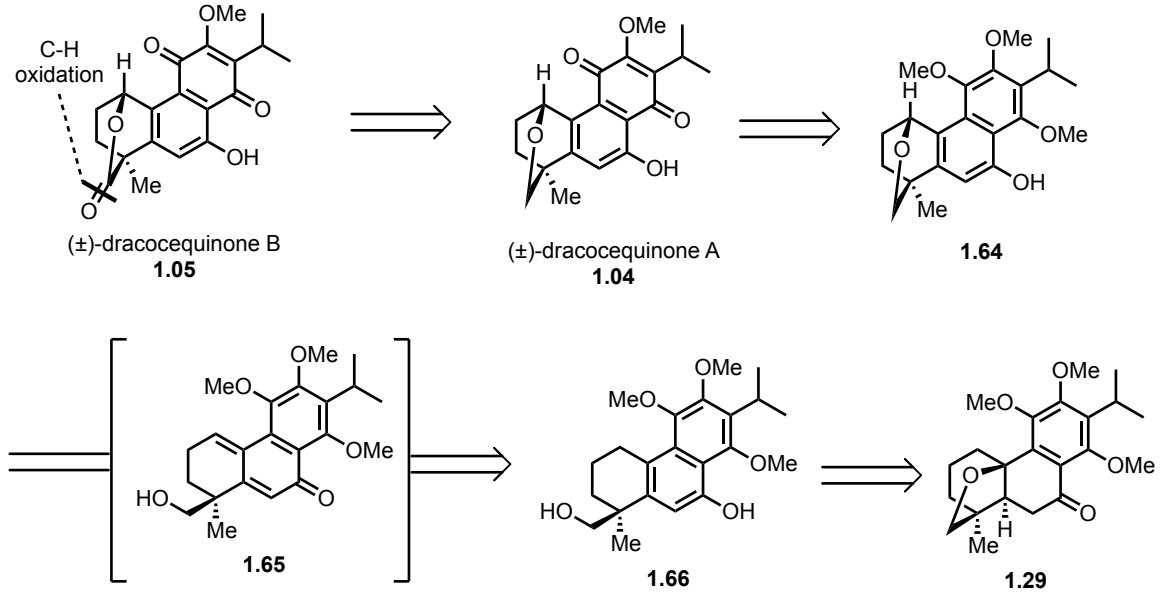

Scheme 1.21. Retrosynthesis of (±)-dracocequinone A (**1.04**) and (±)-dracocequinone B (**1.05**).

1.3.2 Aryl Oxidation vs. Phenolic Oxidation

Based on the retrosynthetic plan, our efforts toward **1.04** began with aromatization of the central ring of **1.29**, a transformation found to be most efficiently accomplished by treating **1.29** with catalytic PTSA in refluxing benzene (Scheme 1.22). A number of oxidants were then screened in hope of transforming the derived naphthol (**1.66**) to its corresponding *para*-quinone methide (**1.65**) from which transannular etherification would deliver **1.64**. Although these efforts revealed DDQ-mediated oxidations to be most promising, they were initially found to be poorly reproducible. In anhydrous methylene chloride, trapping the aryl oxidation intermediate was found to deliver phenolic oxidation product **1.67** as the predominant event; only traces of the desired [2.2.2] oxabicycle **1.64** were observed. Switching the solvent to 1,4-dioxane gave improved but variable yields of **1.64** along with **1.67**. Eventually, we discovered the course of this reaction to be reliant on water content of the solvent. Interestingly, the addition of superstoichiometric water was found to completely suppress formation of **1.67**, thereby enabling isolation of **1.64** in good yield (Scheme 1.23).

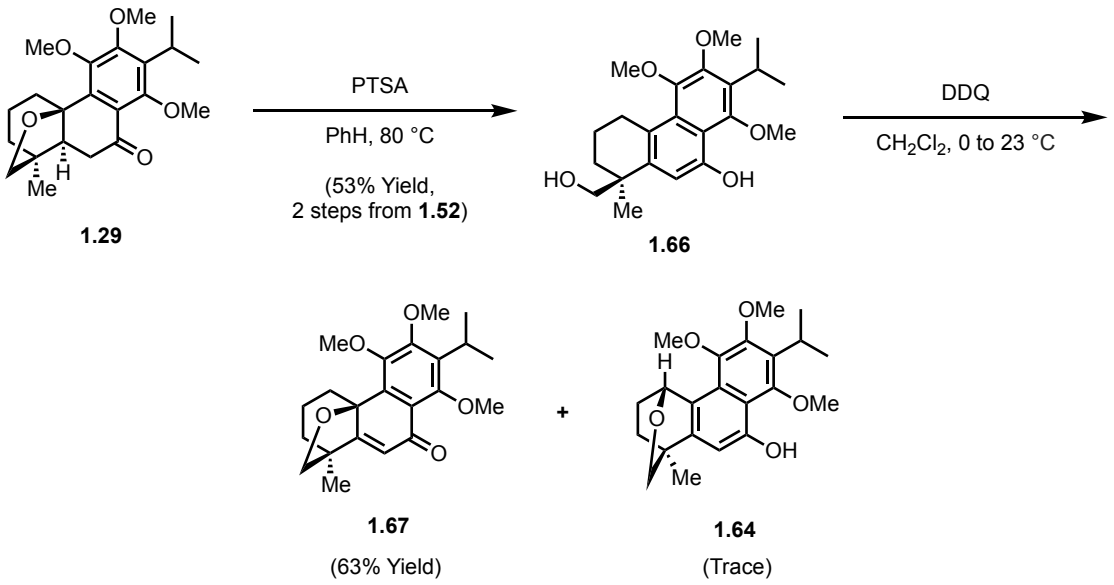

Scheme 1.22. Undesired phenolic oxidation of **1.66**.

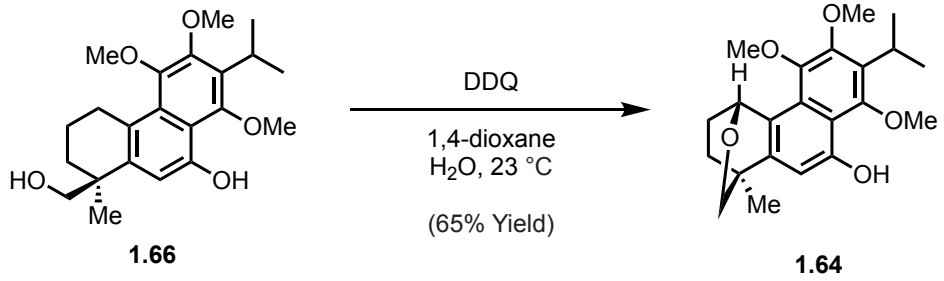

Scheme 1.23. Successful transannular etherification.

1.3.3 Completion of (±)-Dracocequinone A

At this stage, to complete the syntheses of **1.04** and **1.05**, we hoped to apply oxidative demethylation conditions to **1.64** akin to those which had proven effective in the completion of **1.01**. Unfortunately, under the previously developed conditions, direct aryl oxidation proved ineffective in producing **1.04** (Scheme 1.24). Suspecting that the free phenol in **1.64** was the culprit in these failed attempts we opted to mask **1.64** as its corresponding acetate. To this end, acylation of **1.64** with acetic anhydride gave the crystalline naphthol acetate **1.68**; the structure of which was confirmed via single crystal

X-ray analysis. Fortunately, with the masked substrate oxidation of the trimethoxyarene **1.68** using CAN proved successful in furnishing the corresponding *para*-quinone which, upon *in situ* removal of the naphthol acetate, produced (±)-dracocequinone A (**1.04**).

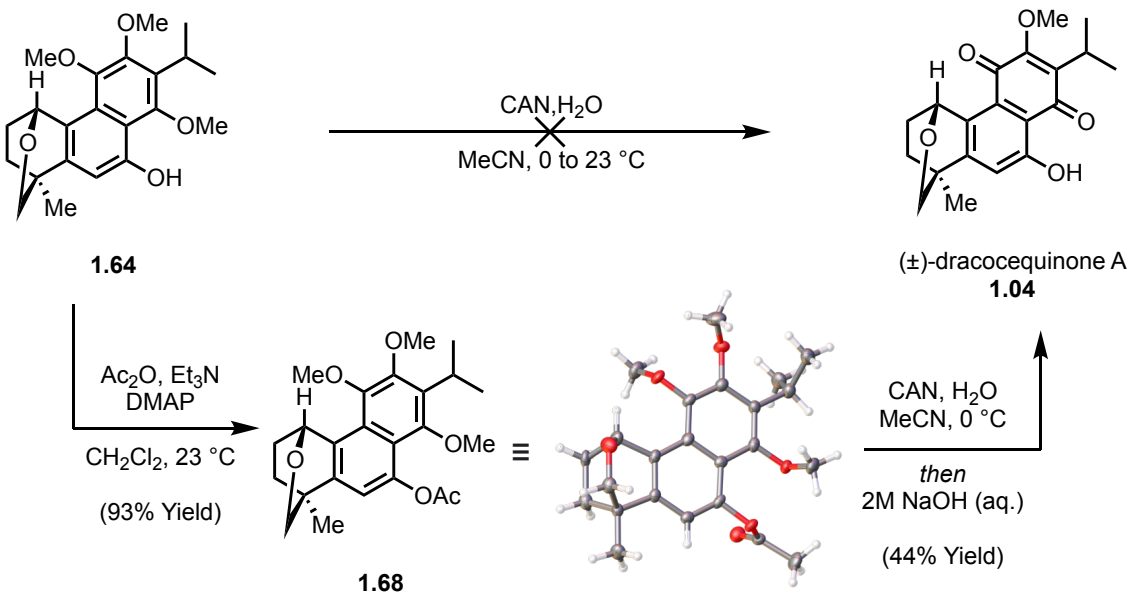

Scheme 1.24. Completed synthesis of (±)-dracocequinone A.

1.3.3 Completion of (±)-Dracocequinone B

Turning to the completion of (±)-dracocequinone B (**1.05**), we envisioned that a direct oxidation of tetrahydropyran in **1.04** to its corresponding lactone could secure formation of **1.05**. To our dismay, direct oxidation conditions, such as exposure to the White-Chen catalyst (**1.69**) or *in situ* generated ruthenium tetroxide, led to the formation of complex mixtures (Scheme 1.25). In order to install the desired oxidation state in **1.05**, a slight modified course of events was required. Specifically, selective protection of the naphthol **1.66** as the corresponding acetate using sodium hydride and acetyl chloride was required since the free hydroxyl group was found to preclude selective oxidation of the

primary alcohol (Scheme 1.26). Subsequent Dess-Martin oxidation of the intermediate acetate proceeded to give aldehyde **1.70** in excellent yield over the two steps. Oxidation of **1.70** under standard Pinnick conditions resulted in smooth conversion to carboxylic acid **1.71**. Much to our chagrin, efforts to advance **1.71** via the previously developed DDQ/water-mediated protocol failed and returned only starting material. Fortunately, we found that the desired lactone **1.72** could be prepared under Wohl-Ziegler bromination conditions, presumably via an S_N1-type displacement of the transient benzylic bromide. Finally, CAN-mediated oxidation and subsequent removal of the naphthol acetate in the same pot secured access to (±)-dracocequinone B (**1.05**).

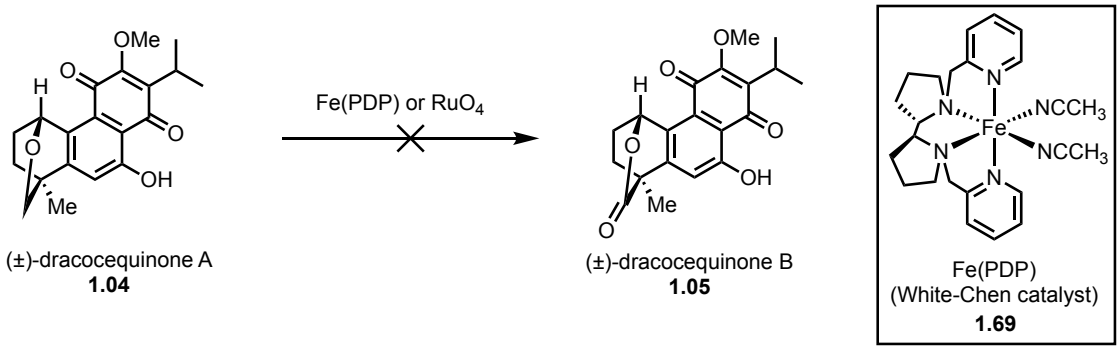

(±)-dracocequinone A
1.04

(±)-dracocequinone B
1.05

Fe(PDP)
(White-Chen catalyst)
1.69

Scheme 1.25. Failed direct C–H oxidation.

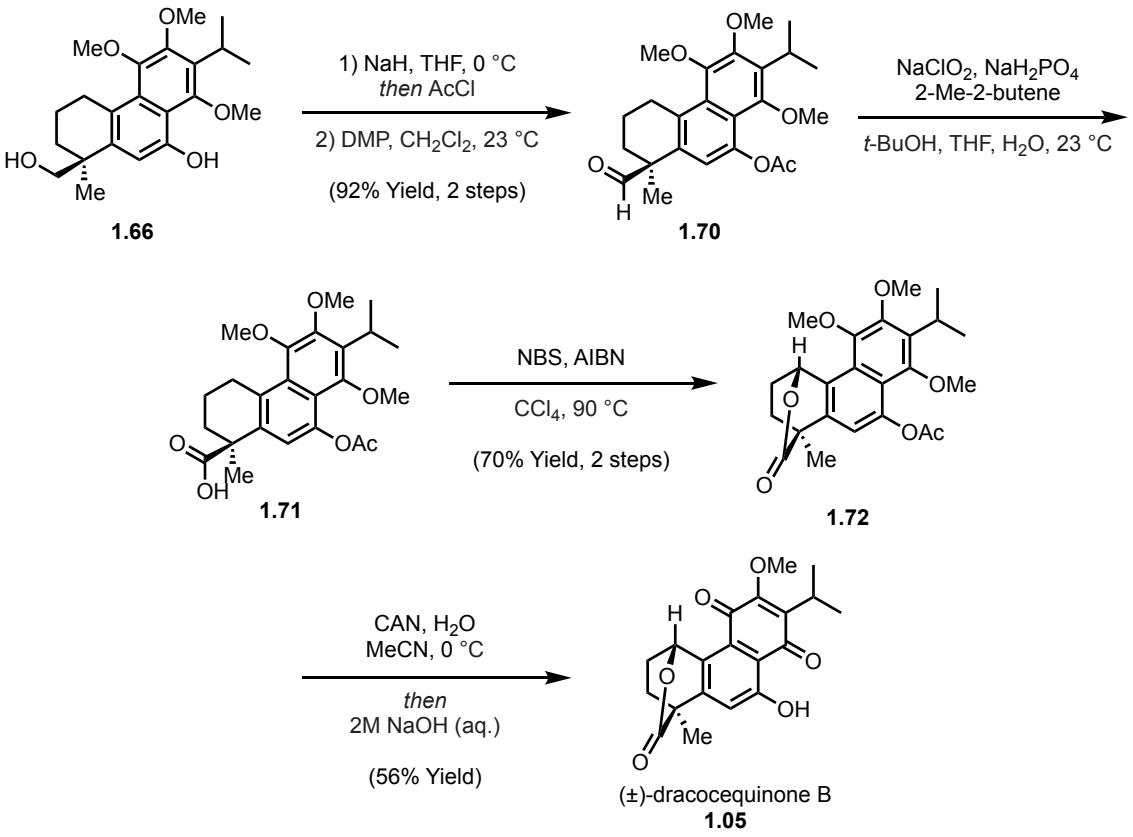

Scheme 1.26. Completed synthesis of (±)-dracocequinone B.

1.4 Conclusion

In conclusion, the first total synthesis of (±)-dracocephalone A (**1.01**) was accomplished in 10-steps and 8% overall yield from known materials. The developed synthetic strategy was successfully extended to the first total syntheses of (±)-dracocequinones A (**1.04**) and B (**1.05**), in 13 and 15 steps, respectively, from known materials. These also represent the first total syntheses of C^{20}-norabietane natural products to date. The most notable features of the synthetic route include: a highly diastereoselective Lewis acid-promoted spirocyclization strategy that evolved from an intramolecular Diels-Alder reaction, a late-stage Suárez oxidation that produced a [3.2.1] oxabicycle embedded in **1.01**. A Brønsted acid-mediated aromatization was followed by a series of carefully

choreographed oxidations that allowed for rearrangement of an intermediate [3.2.1] oxabicycle to a [2.2.2] oxabicycle suited for conversion to **1.04** and **1.05**. It is expected that the efficiency of the approach, coupled with our demonstrated ability to prepare intermediates on gram scale, will provide access to other C^{20}-norabietane natural products and facilitate investigations into novel analogues that may possess trypanocidal activity.

1.5 Experimental

1.5.1 General

Unless otherwise noted, all reactions were carried out in flame- or oven-dried glassware under a nitrogen (N_2) atmosphere. Anhydrous THF, benzene, CH_2Cl_2, toluene, Et_2O, and MeCN were obtained from a solvent purification system manufactured by SG Water U.S.A., LLC maintained under a positive pressure of argon. All reactions were monitored for completion by normal-phase thin layer chromatography (TLC) using Millipore glass-backed 60 Å silica gel plates (indicator F-254, 250 μM) or Fluka Analytical glass-backed 60 Å basic alumina plates (indicator F-254, 250 μM). Flash column chromatography purifications were carried out using the indicated solvent systems (ACS-grade solvents) utilizing Silicycle SiliaFlash P60® (230-400 mesh) silica gel or Sigma-Aldrich Brockmann I (58 Å pore size) basic alumina as the stationary phase. Medium-pressure liquid chromatography (MPLC) purifications were carried out using the indicated solvent systems and flow rate on a Teledyne CombiFlash NextGen 300+ RF system using either Teledyne RediSep® Rf normal-phase or Biotage Sfär® normal-phase column of the indicated size. ^1H and ^{13}C NMR spectra were recorded on either a Bruker Avance 300, Bruker AscendTM 400 autosampler or a Bruker AscendTM 600 autosampler. ^1H chemical shifts (δ) are reported in parts per million (ppm) relative to the residual solvent resonance

of $CHCl_3$ (7.26 ppm), ^{13}C chemical shifts (δ) are reported in ppm relative to the central resonance of $CDCl_3$ (77.16 ppm), and coupling constants (*J*) are reported in hertz (Hz). NMR peak pattern abbreviations are as follows: s = singlet, d = doublet, dd = doublet of doublets, ddd = doublet of doublet of doublets, t = triplet, dt = doublet of triplets, q = quartet, m = multiplet, dtd= doublet of triplet of doublets, dq = doublet of quartets, qt = quartet of triplets, sept = septet, br = broad. High Resolution mass spectra (HRMS) were obtained in the Baylor University Mass Spectrometry Center on a Thermo Scientific Orbitrap Q-Exactive mass spectrometer using electrospray ionization (+ESI) and reported for the molecular ion ($[M+H]^+$ or $[M+Na]^+$). Infrared (IR) spectra were recorded on a Bruker Platinum-ATR IR spectrometer using a diamond window. Single crystal X-ray diffraction data were collected on a Bruker Apex IV-CCD detector using Mo-K_α radiation (λ = 0.71073 Å). Crystals were selected under Paratone® oil, placed on MiTeGen MicroMounts™, then immediately positioned under an N_2 cold stream at 150 K. Structures were solved and refined using APEX IV and SHELXTL software. Crystal graphics were generated using either SHELXTL and OLEX 2 software.

*1.5.2 Preparation of known aldehyde **1.38***

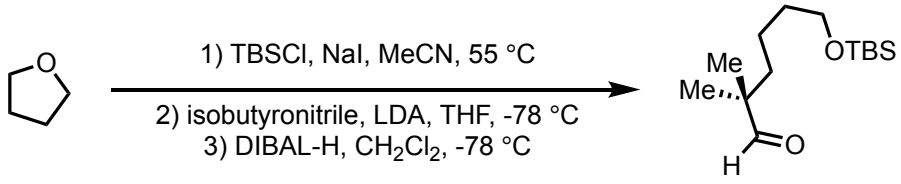

1.35 **1.38**

To a solution containing anhydrous THF **1.35** (53 mL, 645 mmol) in anhydrous MeCN (600 mL, 0.5 M with respect to TBSCl) was added TBSCl (46.1 g, 300 mmol) and NaI (89.9 g, 600 mmol) successively in one portion at 23 °C. The resulting clear and

colorless mixture was then lowered into a preheated heating mantle maintained at 55 °C, and the mixture was stirred at this temperature for 18 h during which the solution turned yellow-orange and turbid. The mixture was then cooled to 23 °C and poured into a separatory funnel containing 1L of H_2O. The mixture was extracted with Et_2O (3 x 600 mL), washed with sat. aq. $Na_2S_2O_3$ (1 x 500 mL) and brine (1 x 500 mL), dried over anhydrous $MgSO_4$, filtered, and concentrated to afford the crude iodide as a red oil. The crude material was used directly in the following step without any further purification. To a stirred solution of diisopropylamine (85 mL, 600 mmol) in THF (1.0 L) maintained at 0 °C, *n*-BuLi (168 mL, 2.5 M in hexanes, 420 mmol) was added dropwise *via* addition funnel over the course of 30 minutes. The mixture was allowed to stir at 0 °C for 1 h, and the mixture was cooled to -78 °C and isobutyronitrile (38 mL, 420 mmol) was introduced *via* syringe dropwise over the course of 10 minutes, and the mixture was stirred at -78 °C for 1 h. The crude iodide (ca. 300 mmol) in THF (100 mL) was added slowly *via* syringe over the course of 10 minutes. The mixture was allowed to stir at -78 °C for 2 h and then was allowed to warm to 23 °C over the course of 1 h. The mixture was then carefully quenched with sat. aq. NH_4Cl (500 mL) and extracted with Et_2O (3 x 500 mL). The combined organic layers were dried over anhydrous $MgSO_4$, filtered, and concentrated to afford the crude nitrile as a yellow oil. The crude material was used directly in the following step without any further purification. The crude nitrile was taken up in CH_2Cl_2 (1 L, ca. 0.3 M) and cooled to -78 °C. DIBAL-H (70 mL, 392 mmol) was then added dropwise *via* syringe over the course of 30 minutes (*Caution: addition of neat DIBAL-H initially results in vigorous gas evolution, precautions must be taken to make sure the vessel is properly ventilated.*) The mixture was allowed to stir at -78 °C for 2 h, upon which the reaction was carefully

quenched with sat. aq. potassium sodium tartrate (1 L), and allowed to warm to 23 °C. The biphasic mixture was then filtered through a short bed of Celite, the layers were separated, and aqueous layer was extracted with CH_2Cl_2 (2 x 500 mL). The combined organic layers were washed with brine (1 x 500 mL), dried over anhydrous $MgSO_4$, filtered, and concentrated to afford the crude aldehyde. Purification *via* flash column chromatography (silica gel, 10% EtOAc/hexanes) afforded aldehyde **1.38** (56.0 g, 72% yield, 3 steps). **^{1}H NMR** (400 MHz, $CDCl_3$): δ 9.45 (s, 1H), 3.59 (t, *J* = 6.4 Hz, 2H), 1.57 – 1.41 (m, 5H), 1.32 – 1.18 (m, 2H), 1.04 (s, 6H), 0.88 (s, 9H), 0.04 (s, 6H). **^{13}C NMR** (101 MHz, $CDCl_3$): δ 206.6, 62.9, 46.0, 37.2, 33.4, 26.1, 21.4, 20.7, 18.5, -5.1. **FTIR** (neat): 2930, 2857, 2802, 2693, 1728, 1471, 1254, 1100, 834, 773 cm^{-1}. **HRMS** (ESI+) *m/z* Calc'd. for $C_{14}H_{30}O_2SiNa$ $[M+Na]^+$: 281.1907, found: 281.1906. $\mathbf{R}_f$ = 0.38 (5% EtOAc/hexanes).

*1.5.3 Preparation of ethyl ester **1.39***

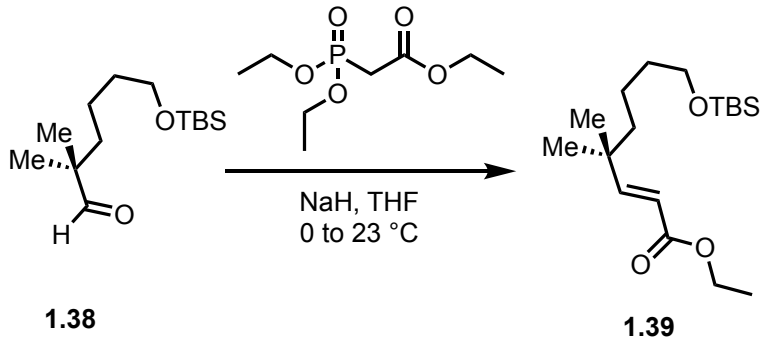

1.38 **1.39**

To a flamed-dried round bottom flask equipped with a magnetic stir bar was added triethyl phosphonoacetate (31.0 mL, 156 mmol) and anhydrous THF (110 mL ca. 1.18 M with respect to aldehyde **1.38**). The resulting solution was cooled to 0 °C and NaH (7.30 g, 60% dispersion in mineral oil, 182 mmol) was added portion-wise over 10 min (*Caution: addition of NaH results in vigorous gas evolution)*. After 30 min, a solution of aldehyde **12** (33.7 g, 130 mmol) in dry THF (110 mL, ca. 1.18 M) was added dropwise *via* cannula. The

resulting mixture was stirred 24 h as it was allowed to warm to 23 °C. Next, sat. aq. NH_4Cl (400 mL) and EtOAc (200 mL) were added. The layers were separated and the aqueous layer was extracted with EtOAc (2 x 200 mL). The combined organic layers were washed with brine (1 x 400 mL), dried over anhydrous Na_2SO_4, filtered, and concentrated to afford the crude ethyl ester **1.39** as a pale, yellow oil. The crude material was used directly in the following step without any further purification. **Purification for characterization purposes**: Flash column chromatography (silica gel, 10% EtOAc/hexanes) **^{1}H NMR** (400 MHz, $CDCl_3$): δ 6.91 (d, *J* = 15.9 Hz, 1H), 5.71 (d, *J* = 15.9 Hz, 1H), 4.19 (q, *J* = 7.1 Hz, 2H), 3.58 (t, *J* = 6.5 Hz, 2H), 1.53 – 1.41 (m, 2H), 1.40 – 1.32 (m, 2H), 1.29 (t, *J* = 7.1 Hz, 3H), 1.27 – 1.19 (m, 2H), 1.04 (s, 6H), 0.88 (s, 9H), 0.04 (s, 6H). **^{13}C NMR** (151 MHz, $CDCl_3$): δ 167.4, 158.5, 117.9, 63.1, 60.3, 42.2, 36.9, 33.5, 26.5, 26.1, 21.0, 18.5, 14.4, -5.1. **FTIR** (neat): 2930, 2858, 1721, 1650, 1471, 1298, 1254, 1165, 1100, 991, 834, 774 cm^{-1}. **HRMS** (ESI+) *m/z* Calc'd. for $C_{22}H_{30}O_5Na$ $[M+Na]^+$: 351.2326, found: 351.2295. $\mathbf{R_f}$ = 0.49 (10% EtOAc/hexanes).

*1.5.4 Preparation of alcohol **1.73***

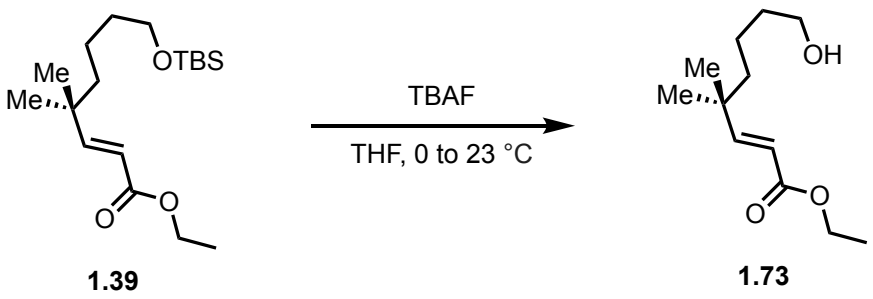

1.39 **1.73**

To a round bottom flask equipped with a magnetic stir bar was added ethyl ester **1.39** (8.9 g, 27.0 mmol) and anhydrous THF (90 mL ca. 0.3 M). The resulting solution was cooled to 0 °C and a solution of TBAF (30.0 mL, 1.0 M in THF, 30.0 mmol) was added dropwise *via* syringe. The resulting mixture was stirred 12 h as it was allowed to warm to 23 °C. Next, water (200 mL) and EtOAc (100 mL) were added. The layers were separated and the aqueous layer was extracted with EtOAc (2 x 100 mL). The combined organic layers were washed with brine (1 x 200 mL), dried over anhydrous Na_2SO_4, filtered, and concentrated to afford the crude alcohol. Purification *via* flash column chromatography (silica gel, 20% EtOAc/hexanes) afforded alcohol **1.73** as a pale, yellow oil (2.1 g, 37% yield, 2 steps). **^{1}H NMR** (400 MHz, $CDCl_3$): δ 6.90 (d, J = 15.9 Hz, 1H), 5.71 (d, J = 15.9 Hz, 1H), 4.18 (q, J = 7.1 Hz, 2H), 3.63 (t, J = 6.5 Hz, 2H), 1.52 (p, J = 6.8 Hz, 2H), 1.44 – 1.35 (m, 2H), 1.32 – 1.24 (m, 5H), 1.05 (s, 6H). **^{13}C NMR** (151 MHz, $CDCl_3$): δ 167.3, 158.3, 118.0, 63.0, 60.4, 42.3, 36.9, 33.5, 26.5, 21.1, 14.4. **FTIR** (neat): 3390, 2935, 1715, 1647, 1366, 1308, 1168, 1035, 992, 863 cm^{-1}. **HRMS** (ESI+) *m*/*z* Calc'd. for $C_{14}H_{31}O_2Si$ $[M+H]^+$: 215.1642, found: 215.1694. $\mathbf{R}_f$ = 0.24 (20% EtOAc/hexanes).

*1.5.5 Preparation of aldehyde **1.33***

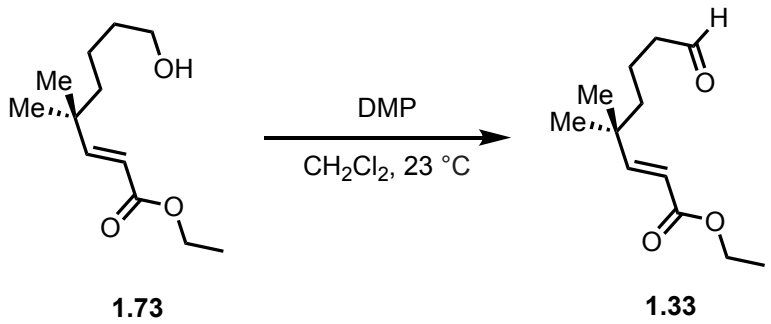

1.73 **1.33**

To a round bottom flask equipped with a magnetic stir bar was added alcohol **1.73** (460 mg, 2.16 mmol) and anhydrous CH_2Cl_2 (20 mL ca. 0.11 M). To the resulting solution was added Dess-Martin periodinane (1.0 g, 2.37 mmol) in one portion. The resulting mixture was stirred 2 h at 23 °C. Next, sat. aq. $Na_2S_2O_3$ (10 mL) and sat. aq. $NaHCO_3$ (10 mL) were added and stirred 30 min. The layers were separated and the aqueous layer was extracted with CH_2Cl_2 (2 x 50 mL). The combined organic layers were washed with brine (1 x 100 mL), dried over anhydrous $MgSO_4$, filtered, and concentrated to afford the crude aldehyde. Purification *via* flash column chromatography (silica gel, 10% EtOAc/hexanes) afforded aldehyde **1.33** (410 mg, 89% yield) as a colorless oil. **^{1}H NMR** (600 MHz, $CDCl_3$): δ 9.75 (s, 1H), 6.89 (d, J = 16.0 Hz, 1H), 5.73 (d, J = 16.0 Hz, 1H), 4.19 (q, J = 7.1 Hz, 2H), 2.41 (td, J = 7.3, 1.6 Hz, 2H), 1.60 – 1.50 (m, 2H), 1.43 – 1.33 (m, 2H), 1.30 (d, J = 7.2 Hz, 3H), 1.07 (s, 6H). **^{13}C NMR** (151 MHz, $CDCl_3$): δ 202.0, 166.8, 157.3, 118.2, 60.1, 44.1, 41.5, 36.6, 26.2, 17.2, 14.2. **FTIR** (neat): 2961, 1713, 1648, 1366, 1308, 1167, 1035, 991, 863 cm^{-1}. **HRMS** (ESI+) *m/z* Calc'd. for $C_{12}H_{20}O_3Na$ $[M+Na]^+$: 235.1305, found: 235.1293. $\mathbf{R}_f$ = 0.30 (10% EtOAc/hexanes).

*1.5.6 Preparation of benzamide **1.33***

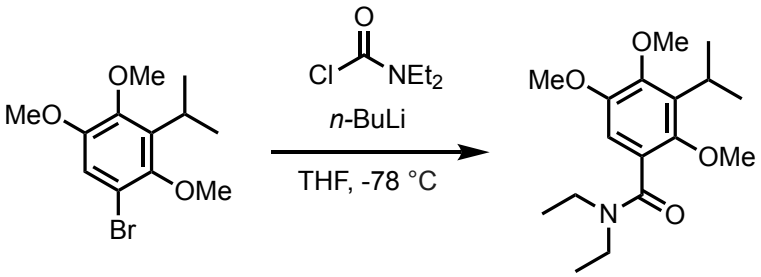

1.43 **1.34**

To a flame-dried round bottom flask with a magnetic stir bar was added aryl bromide **1.43** (48 g, 166 mmol) and THF (830 mL, 0.2 M). The resulting solution was cooled to -78 °C and *n*-BuLi (80 mL, 2.5 M in hexanes, 199 mmol) was added dropwise over the course of 30 minutes *via* addition funnel. After stirring for 15 minutes, *N,N*-diethylcarbamoyl chloride (32 mL, 247.5 mmol) was added dropwise over the course of 15 minutes *via* syringe. The reaction mixture was continued stirring for 1 hour, warmed to 0 °C, and stirred for an additional hour. The reaction was then quenched with sat. aq. NH_4Cl (500 mL) and was extracted with EtOAc (3 x 500 mL). The combined organic layers were washed with brine (1 x 500 mL), dried over anhydrous Na_2SO_4, filtered, and concentrated to afford a crude orange oil. Purification *via* flash column chromatography (silica gel, 50% EtOAc/hexanes) afforded benzamide **1.34** (33 g, 65% yield), as a white amorphous solid. **^{1}H NMR** (600 MHz, $CDCl_3$): δ 6.63 (s, 1H), 3.83 (s, 3H), 3.81 (s, 3H), 3.72 (s, 3H), 3.42 (sept, J = 7.1 Hz, 1H), 3.34 – 3.07 (m, 3H), 1.32 (dd, J = 12.1, 7.1 Hz, 6H), 1.26 (t, J = 7.1 Hz, 4H), 1.04 (t, J = 7.1 Hz, 3H). **^{13}C NMR** (151 MHz, $CDCl_3$): δ 169.2, 149.7, 149.0, 148.0, 135.6, 126.5, 108.7, 62.7, 61.0, 56.0, 43.1, 39.1, 25.9, 22.0, 21.9, 14.1, 12.9. **FTIR** (neat): 2960, 2871, 1625, 1592, 1441, 1337, 1223, 1032, 997 cm^{-1}. **HRMS** (ESI+) *m/z*

Calc'd. for $C_{17}H_{27}NO_4Na$ $[M+Na]^+$: 332.1832, found: 332.1815. $\mathbf{R_f}$ = 0.23 (50% EtOAc/hexanes).

*1.5.7 Preparation of lactone **1.32***

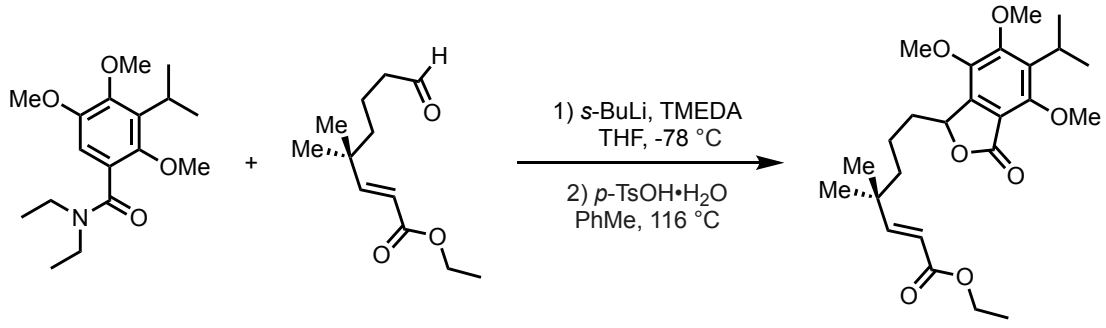

1.34 **1.33** **1.32**

To a flame-dried round bottom flask equipped with a magnetic stir bar was added benzamide **1.34** (1.2 g, 3.9 mmol) and anhydrous THF (10.0 mL, ca. 0.4 M with respect to benzamide **1.34**), followed by TMEDA (0.70 mL, 4.7 mmol). The resulting mixture was cooled to -78 °C and *s*-BuLi (2.8 mL, 1.4 M in cyclohexane, 3.9 mmol) was added dropwise *via* syringe. After stirring 1 h, a solution of aldehyde **1.33** (1.7 g, 7.8 mmol) in anhydrous THF (4.0 mL) was added dropwise *via* syringe to the reaction mixture and stirred 5 h. The reaction was quenched by addition of sat. aq. NH_4Cl (10.0 mL) and was allowed to warm to 23 °C. EtOAc (10.0 mL) was added, and the layers were separated. The aqueous layer was extracted with EtOAc (1 x 10 mL). Combined organic layers were dried over anhydrous Na_2SO_4, filtered, and concentrated to afford the crude alcohol. The crude material was used directly in the following step without any further purification. To a round bottom flask equipped with a magnetic stir bar was added the crude alcohol and *p*-TsOH•H_2O (5.5 mg, 0.026 mmol, 0.01 equiv.), followed by anhydrous toluene (8.8 mL, ca. 0.3 M). The resulting mixture was heated to reflux and stirred 24 h. The reaction mixture

was cooled to 23 °C and loaded directly to column and purified *via* flash column chromatography (silica gel 10% EtOAc/hexanes) to afford lactone **1.32** (675 mg, 39% yield, 45% yield based on recovered **11**, 2 steps) as a colorless oil. **^{1}H NMR** (400 MHz, $CDCl_3$): δ 6.88 (d, *J* = 16.0 Hz, 1H), 5.70 (d, *J* = 15.9 Hz, 1H), 5.33 (dd, *J* = 8.9, 2.8 Hz, 1H), 4.17 (q, *J* = 7.1 Hz, 2H), 3.99 (s, 3H), 3.89 (s, 3H), 3.83 (s, 3H), 3.52 (sept, *J* = 7.1 Hz, 1H), 2.18 – 2.08 (m, 1H), 1.66 – 1.53 (m, 1H), 1.50 – 1.34 (m, 4H), 1.33 – 1.31 (m, 3H), 1.31 – 1.25 (m, 6H), 1.04 (d, *J* = 4.1 Hz, 6H). **^{13}C NMR** (151 MHz, $CDCl_3$): δ 168.0, 167.2, 158.0, 157.7, 154.4, 143.3, 141.7, 136.9, 118.2, 113.5, 79.1, 63.1, 60.8, 60.4, 60.4, 42.1, 36.9, 34.5, 26.5, 26.3, 25.7, 21.8, 20.8, 14.4. **FTIR** (thin film): 2957, 1759, 1715, 1648, 1596, 1473,1334, 1267, 1118, 1028, 955 cm^{-1}. **HRMS** (ESI+) *m/z* Calc'd. for $C_{25}H_{36}O_7Na$ $[M+Na]^+$: 471.2353, found: 471.2354. $\mathbf{R}_f$ = 0.72 (50% EtOAc/hexanes).

*1.5.8 Preparation of silyl acetal **1.30***

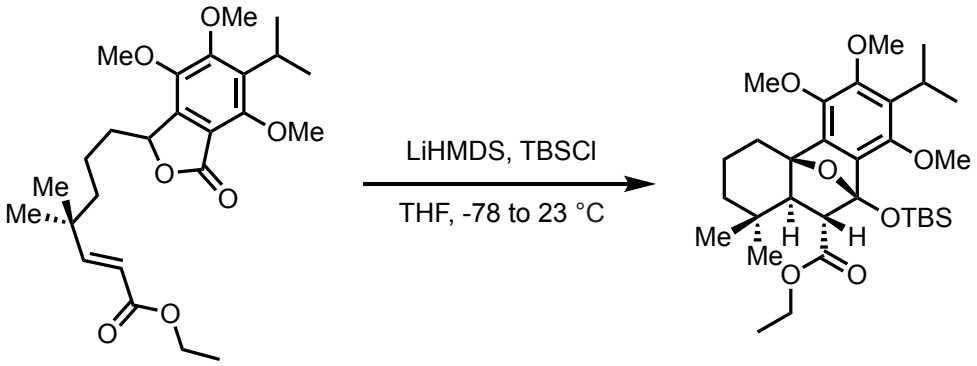

1.32 **1.30**

To a flame-dried round bottom flask equipped with a magnetic stir bar was added lactone **1.32** (415 mg, 0.925 mmol) and anhydrous THF (9.3 mL, ca. 0.1 M). The resulting mixture was cooled to -78 °C and LiHMDS (1.1 mL, 1.0 M in THF, 1.1 mmol) was added dropwise *via* syringe. After stirring 1 h, TBSCl (167 mg, 1.1 mmol) was added in one

portion to the reaction mixture and stirred 2 h. The cold bath was removed and stirred 24 h at 23 °C. EtOAc (10.0 mL) and sat. aq. $NaHCO_3$ (20.0 mL) were added and the layers were separated. The aqueous layer was extracted with EtOAc (1 x 10 mL). Combined organic layers were dried over anhydrous Na_2SO_4, filtered, and concentrated to afford the crude cycloadduct. Purification *via* flash column chromatography (basic alumina, 5% EtOAc/hexanes) afforded the silyl acetal **1.30** (310 mg, 59% yield) as a white solid. **^{1}H NMR** (600 MHz, $CDCl_3$): δ 3.97 (s, 3H), 3.91 (s, 3H), 3.84 (s, 3H), 3.66 (q, *J* = 7.0 Hz, 2H), 3.49 (sept, *J* = 7.1 Hz, 1H), 3.30 (d, *J* = 10.0 Hz, 1H), 2.94 (d, *J* = 10.4 Hz, 1H), 2.19 (td, *J* = 13.7, 4.3 Hz, 1H), 1.89 (qt, *J* = 11.0, 3.0 Hz, 1H), 1.67 (d, *J* = 13.8 Hz, 1H), 1.63 – 1.54 (m, 3H), 1.45 (td, *J* = 13.3, 3.2 Hz, 1H), 1.30 (d, *J* = 7.7 Hz, 6H), 1.10 (t, *J* = 7.0 Hz, 3H), 1.02 (s, 3H), 0.92 (s, 3H), 0.80 (s, 9H), -0.05 (s, 3H), -0.25 (s, 3H). **^{13}C NMR** ^{13}C NMR (151 MHz, $CDCl_3$): δ 168.0, 157.4, 154.1, 153.6, 146.6, 143.4, 136.1, 114.3, 88.9, 79.0, 62.9, 62.0, 60.4, 60.2, 46.6, 40.7, 36.1, 35.2, 32.3, 25.7, 25.6, 22.1, 21.9, 19.1, 18.0, 15.1. **FTIR** (thin film): 2932, 1754, 1671, 1593, 1472, 1327, 1217, 1046, 950, 840, 783 cm^{-1}. **HRMS** (ESI+) *m*/*z* Calc'd. for $C_{31}H_{51}O_7Si$ $[M+H]^+$: 563.3399, found: 563.3377. $\mathbf{R_f}$ = 0.58 (10% EtOAc/hexanes), basic alumina TLC plate.

*1.5.9 Preparation of spirolactone **1.48***

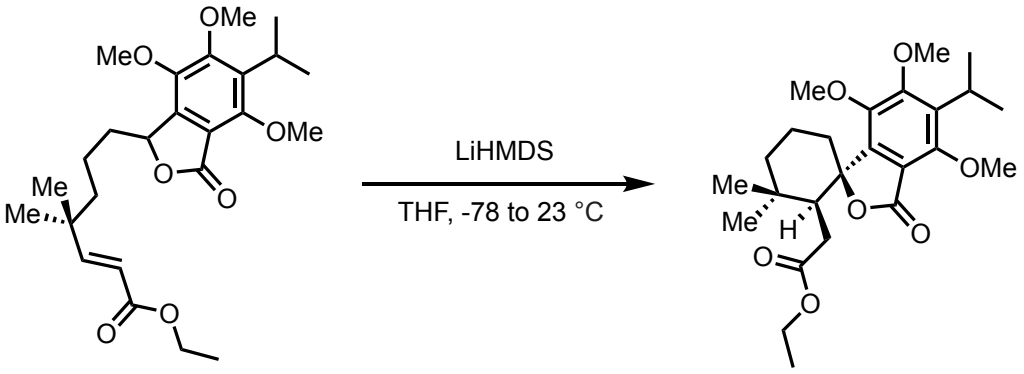

1.32 **1.48**

To a flame-dried round bottom flask with a magnetic stir bar was added lactone **1.32** (137 mg, 0.306 mmol) and anhydrous THF (3.0 mL, 0.1 M). The resulting solution was cooled to -78 °C and LiHMDS (0.35 mL, 1.0 M in THF, 0.35 mmol) was added dropwise *via* syringe. After 2 min, the reaction mixture was warmed to 23 °C and continued stirring for 12 h. The reaction was diluted with EtOAc (10.0 mL) and quenched by addition of sat. aq. NH_4Cl (10.0 mL). The two layers were separated and the aqueous layer was extracted with EtOAc (1 x 5.0 mL). The combined organic layers were dried over anhydrous Na_2SO_4, filtered, and concentrated. Purification *via* flash column chromatography (10% EtOAc/hexanes) afforded spirolactone **1.48** (91 mg, 66% yield) as a crystalline solid. **^{1}H NMR** (400 MHz, $CDCl_3$): δ 4.00 (s, 3H), 3.93 (s, 3H), 3.92 – 3.80 (m, 4H), 3.63 – 3.43 (m, 2H), 2.68 (qt, *J* = 13.1, 3.1 Hz, 1H), 2.30 – 2.17 (m, 2H), 1.92 (qt, *J* = 13.5 Hz, 1H), 1.82 (dd, *J* = 16.8, 7.4 Hz, 1H), 1.70 (dq, *J* = 13.8, 2.4 Hz, 1H), 1.66 – 1.46 (m, 3H), 1.31 (s, 3H), 1.29 (s, 3H), 1.09 – 1.01 (m, 6H), 0.99 (s, 3H). **^{13}C NMR** (101 MHz, $CDCl_3$): δ 173.3, 167.6, 157.6, 153.8, 144.1, 143.9, 137.0, 114.0, 87.6, 63.1, 60.4, 60.4, 60.2, 46.2, 41.1, 36.1, 34.4, 31.8, 30.6, 25.6, 21.9, 21.8, 21.8, 18.9, 14.2. **FTIR** (thin film): 1935, 2872, 1753, 1733, 1592, 1472, 1460, 1327, 1277, 1111, 1020, 945 cm^{-1}.

HRMS (ESI+) *m/z* Calc'd. for $C_{25}H_{36}O_7Na$ $[M+Na]^+$: 471.2353, found: 471.2334. $\mathbf{R_f}$ = 0.24 (10% EtOAc/hexanes). **MP** = 101-103 °C.

*1.5.10 Preparation of allyl ester **1.59***

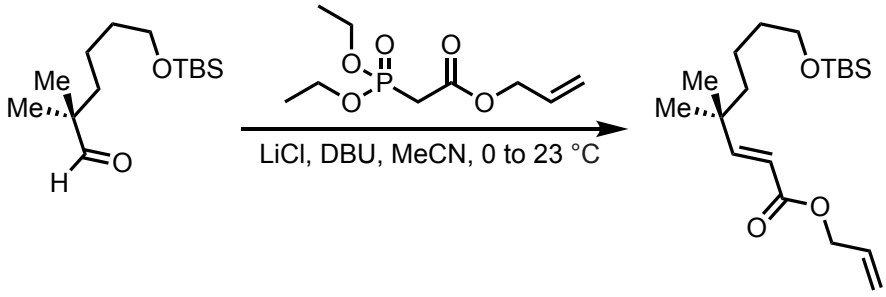

1.38 **1.59**

Allyl diethylphosphonoacetate[17] (60.3 g, 255 mmol) was taken up in anhydrous MeCN (430 mL, 0.5 M with respect to aldehyde) in a 1L round bottom flask. Then, LiCl (13.5 g, 319 mmol) was added in one portion, followed by the addition of DBU (48 mL, 319 mmol) dropwise over the course of 20 min *via* addition funnel, upon which the turbid, colorless mixture turned to a clear yellow mixture. The mixture was stirred for 10 min at 23 °C, upon which it was cooled to 0 °C, and aldehyde **1.38** (55 g, 213 mmol) was introduced dropwise *via* addition funnel over the course of 10 minutes. The mixture was stirred and allowed to naturally warm to room temperature over the course of 3 hours, upon which the reaction was diluted with water (500 mL) and extracted with Et_2O (3 x 500 mL). The combined organic layers were washed with brine (1 x 500 mL), dried over anhydrous $MgSO_4$, filtered, and concentrated to afford a crude yellow oil. The crude material was purified *via* flash column chromatography (10% EtOAc/hexanes) to afford of allyl ester **1.59** (61.3 g, 85% yield) as a colorless oil. **^{1}H NMR** (600 MHz, $CDCl_3$): δ 6.94 (d, J = 16.0 Hz, 1H), 6.01 – 5.91 (m, 1H), 5.74 (d, J = 16.0 Hz, 1H), 5.34 (dq, J = 17.2, 1.6 Hz, 1H), 5.25 (dq, J = 10.4, 1.3 Hz, 1H), 4.66 – 4.62 (m, 2H), 3.58 (t, J = 6.5 Hz, 2H), 1.51 – 1.41

(m, 2H), 1.39 – 1.33 (m, 2H), 1.28 – 1.19 (m, 2H), 1.04 (s, 6H), 0.88 (s, 9H), 0.04 (s, 6H). **^{13}C NMR** (101 MHz, $CDCl_3$): δ 166.9, 159.0, 132.5, 118.3, 117.6, 65.1, 63.1, 42.2, 37.0, 33.5, 26.4, 26.1, 21.0, 18.5, -5.1. **FTIR** (neat): 2930, 2858, 1721, 1650, 1471, 1165, 1100, 834, 774 cm^{-1}. **HRMS** (ESI+) *m/z* Calc'd. for $C_{19}H_{36}O_3SiNa$ $[M+Na]^+$: 363.2326, found: 363.2326. $\mathbf{R}_f$ = 0.18 (10% EtOAc/hexanes).

*1.5.11 Preparation of alcohol **1.74***

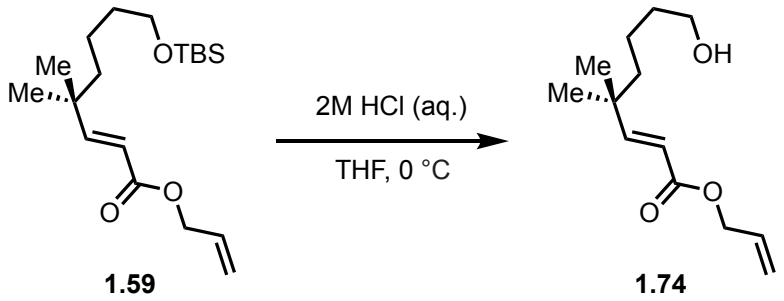

1.59 **1.74**

To a solution of allyl ester **1.59** (16.8 g, 49.3 mmol) in THF (200 mL, 0.25 M) maintained at 0 °C was added aq. 2M HCl (125 mL, 250 mmol) dropwise over the course of 20 minutes *via* addition funnel. Upon completion of addition, the mixture was stirred for an additional hour at 0 °C. The solution was then transferred to a separatory funnel, extracted with CH_2Cl_2 (3 x 100 mL). The combined organic layers were washed with sat. aq. $NaHCO_3$ (1 x 100 mL) followed by brine (1 x 100 mL), dried over anhydrous $MgSO_4$, filtered, and concentrated to afford a crude yellow oil. The crude material was purified *via* flash column chromatography (30% EtOAc/hexanes) to afford alcohol **1.74** (9.8 g, 88% yield) as a pale, yellow oil. **^{1}H NMR** (400 MHz, $CDCl_3$): δ 6.95 (d, *J* = 16.1 Hz, 1H), 5.96 (dddd, *J* = 17.0, 10.4, 5.8, 0.7 Hz, 1H), 5.75 (d, *J* = 15.9 Hz, 1H), 5.34 (ddd, *J* = 17.1, 2.4, 1.1 Hz, 1H), 5.25 (d, *J* = 10.2 Hz, 1H), 4.64 (dt, *J* = 5.8, 1.6 Hz, 2H), 3.63 (q, *J* = 6.2 Hz, 2H), 1.64 – 1.47 (m, 3H), 1.43 – 1.20 (m, 4H), 1.05 (s, 6H). **^{13}C NMR** (101 MHz, $CDCl_3$):

δ 166.8, 158.8, 132.3, 118.1, 117.4, 64.9, 62.4, 42.1, 36.8, 33.2, 26.2, 20.8. **FTIR** (thin film): 3435, 1936, 2868, 1717, 1649, 1364, 1297, 1241, 1165, 1044, 990, 931 cm^{-1}. **HRMS** (ESI+) *m*/*z* Calc'd for $C_{13}H_{22}O_3Na$ $[M+Na]^+$: 249.1461, found: 241.1460. $\mathbf{R}_f$ = 0.26 (30% EtOAc/hexanes).

*1.5.12 Preparation of aldehyde **1.58***

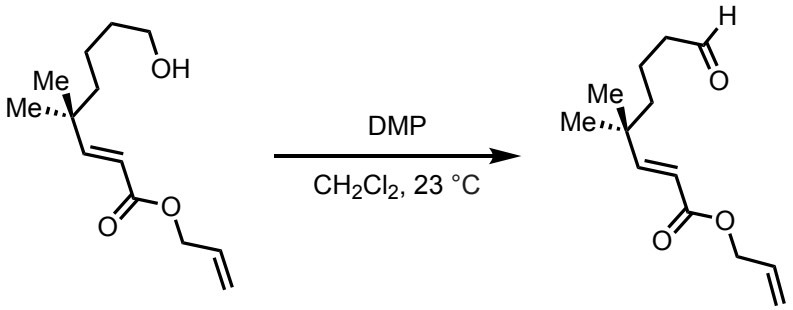

1.74 **1.58**

To a solution of alcohol **1.74** (9.8 g, 43.3 mmol) and anhydrous CH_2Cl_2 (200 mL, 0.22 M) was added DMP (20.4 g, 48 mmol) in one portion at 23 °C. The resulting mixture was stirred 2 h at 23 °C. After this time, the reaction was quenched with sat. aq. $Na_2S_2O_3$ (100 mL) and sat. aq. $NaHCO_3$ (100 mL) and stirred vigorously for 30 minutes upon which both layers became clear. The layers were separated and the aqueous layer was further extracted with CH_2Cl_2 (2 x 100 mL). The combined organic layers were washed with brine (1 x 100 mL), dried over anhydrous $MgSO_4$, filtered, and concentrated to afford a crude yellow oil. Purification *via* flash column chromatography (silica gel, 10% EtOAc/hexanes) afforded aldehyde **1.58** (8.1 g, 83% yield) as a colorless oil. **^{1}H NMR** (400 MHz, $CDCl_3$): δ 9.74 (s, 1H), 6.92 (d, *J* = 15.9 Hz, 1H), 6.02 – 5.88 (m, 1H), 5.76 (d, *J* = 15.9 Hz, 1H), 5.33 (dq, *J* = 17.2, 1.5 Hz, 1H), 5.24 (dq, *J* = 10.5, 1.3 Hz, 1H), 4.63 (dt, *J* = 5.8, 1.4 Hz, 2H), 2.40 (td, *J* = 7.2, 1.6 Hz, 2H), 1.60 – 1.48 (m, 2H), 1.41 – 1.33 (m, 2H), 1.06 (s, 6H). **^{13}C NMR** (101 MHz, $CDCl_3$): δ 202.3, 166.8, 158.1, 132.4, 118.4, 118.1, 65.2, 44.4, 41.7,

37.0, 26.3, 17.4. **FTIR** (neat): 2959, 1716, 1649, 1459, 1363, 1294, 1164, 990, 930, 646 cm^{-1}. **HRMS** (ESI+) *m/z* Calc'd for $C_{13}H_{20}O_3Na$ $[M+Na]^+$: 247.1305, found: 247.1305. $\mathbf{R_f}$ = 0.19 (10% EtOAc/hexanes).

*1.5.13 Preparation of lactone **1.57***

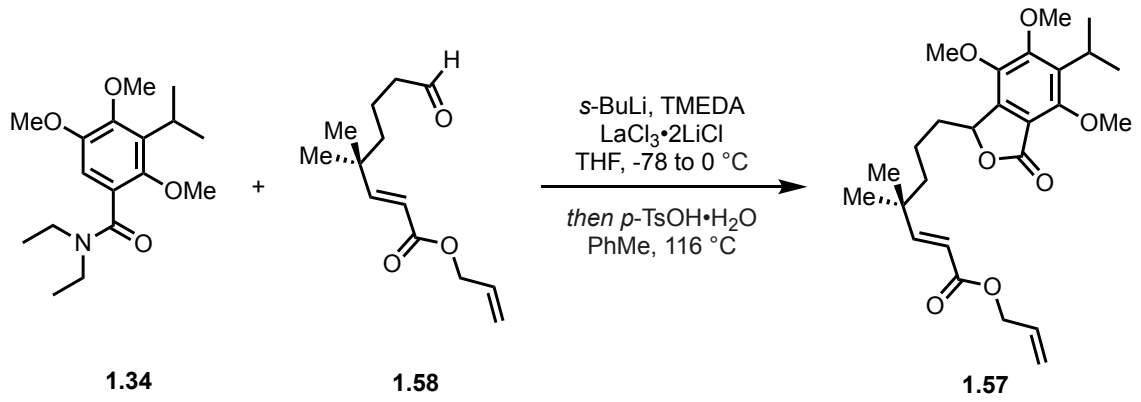

1.34 **1.58** **1.57**

A solution of benzamide **1.34** (12.6 g, 40.7 mmol) in anhydrous THF (200 mL, 0.2 M with respect to benzamide **1.34**) was cooled to -78 °C and TMEDA (8.1 mL, 54 mmol) was added in one portion, followed by *s*-BuLi (29 mL, 1.4 M in cyclohexane, 40.7 mmol) dropwise over the course of 10 minutes *via* syringe. The mixture was allowed to stir at -78 °C for 1 hour at this temperature. Meanwhile, to a solution of aldehyde **1.58** (8.7 g, 38.8 mmol) in anhydrous THF (100 mL) was added $LaCl_3$•2LiCl solution (68 mL, 0.6 M in THF, 40.7 mmol) in one portion at 23 °C. The mixture was stirred at this temperature for 15 minutes, upon which it was cooled to 0 °C and the freshly-prepared organolithium solution was introduced *via* cannula over the course of 15 minutes. Upon completion of the transfer, the mixture was stirred for a further 30 minutes at 0 °C. The reaction was then quenched by addition of *p*-TsOH•H_2O (38 g, 200 mmol) and the solvent was concentrated under reduced pressure. The resulting white solid was then suspended in PhMe (200 mL, 0.2 M), the flask was fitted with a reflux condenser, and the suspension was heated to reflux

(sand bath temp. = 120 °C) for 4 hours. The reaction mixture was cooled to 23 °C, diluted in CH_2Cl_2 (500 mL) and the suspended solids were removed by filtration. Concentration and direct purification *via* flash column chromatography (10% EtOAc/hexanes) afforded lactone **1.57** (12.2 g, 68% yield) as a pale, yellow oil. **^{1}H NMR** (600 MHz, $CDCl_3$): δ 6.92 (dd, *J* = 15.9, 1.9 Hz, 1H), 6.00 – 5.90 (m, 1H), 5.73 (dd, *J* = 15.9, 1.9 Hz, 1H), 5.37 – 5.30 (m, 2H), 5.24 (dp, *J* = 10.4, 1.3 Hz, 1H), 4.63 (dt, *J* = 5.8, 1.6 Hz, 2H), 3.99 (s, 3H), 3.89 (s, 3H), 3.83 (s, 3H), 3.52 (sept, *J* = 8.0, 6.2 Hz, 1H), 2.18 – 2.08 (m, 1H), 1.65 – 1.56 (m, 1H), 1.48 – 1.34 (m, 4H), 1.31 (d, *J* = 7.1 Hz, 6H), 1.04 (d, *J* = 6.7 Hz, 6H). **^{13}C NMR** (151 MHz, $CDCl_3$): δ 168.0, 166.8, 158.5, 157.7, 154.4, 143.3, 141.7, 136.9, 132.5, 118.4, 117.8, 113.5, 79.1, 65.1, 63.1, 60.8, 60.4, 42.1, 37.0, 34.5, 26.5, 26.3, 25.7, 21.8, 20.8. **FTIR** (thin film): 2956, 2873, 1758, 1717, 1649, 1596, 1473, 1334, 1266, 1167, 1119, 989 cm^{-1}. **HRMS** (ESI+) *m*/*z* Calc'd for $C_{26}H_{36}O_7Na$ $[M+Na]^+$: 483.2353, found: 483.2332. $\mathbf{R_f}$ = 0.17 (10% EtOAc/hexanes).

*1.5.14 Preparation of spirolactone **1.56***

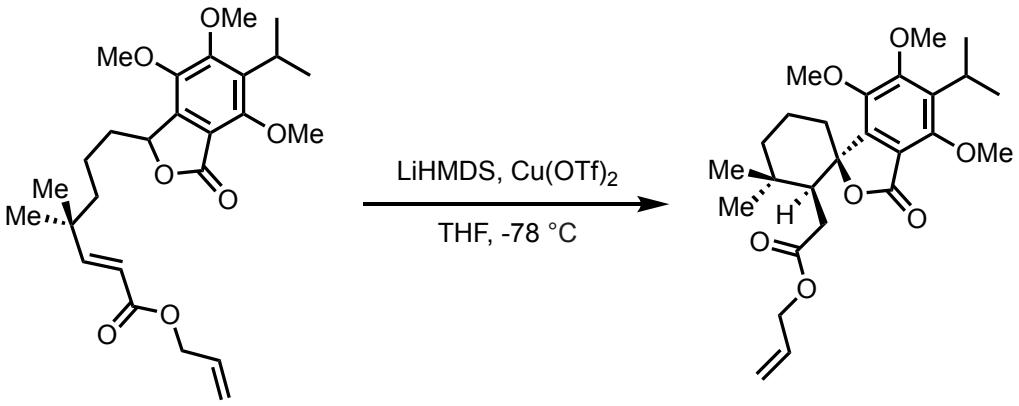

1.57 **1.56**

To a solution of lactone **1.57** (11.8 g, 25.6 mmol) in anhydrous THF (260 mL, 0.1 M) maintained at -78 °C was added $Cu(OTf)_2$ (930 mg, 2.56 mmol) and LiHMDS (75 mL, 1.0 M in THF, 75 mmol) was added dropwise over the course of 30 minutes *via* addition funnel. The reaction mixture turned from pale yellow to dark brown upon addition of LiHMDS and the mixture was stirred as such for an additional hour at -78 °C. The reaction was then quenched with sat. aq. NH_4Cl (200 mL) and warmed to 23 °C. The aqueous layer was extracted with Et_2O (3 x 200 mL) and the combined organic layers were washed with brine (1 x 200 mL), dried over anhydrous $MgSO_4$, filtered, and concentrated to afford a crude yellow oil. Purification *via* flash column chromatography (10% EtOAc/hexanes) afforded spirolactone **1.56** (10.5 g, 89% yield) as a white solid. Crystals suitable for X-Ray analysis were grown *via* slow evaporation from a hexanes/CH_2Cl_2 solution (*ca.* 5:1 v/v) to afford colorless blocks. **^{1}H NMR** (400 MHz, $CDCl_3$): δ 5.68 (ddt, *J* = 17.3, 10.5, 5.7 Hz, 1H), 5.19 – 5.08 (m, 2H), 4.33 (ddt, *J* = 13.3, 5.7, 1.5 Hz, 1H), 4.01 (ddt, *J* = 13.3, 5.6, 1.5 Hz, 1H), 3.98 (s, 3H), 3.92 (s, 3H), 3.87 (s, 3H), 3.50 (sept, *J* = 7.1 Hz, 1H), 2.69 (dd, *J* = 7.3, 4.0 Hz, 1H), 2.24 (td, *J* = 17.2, 4.1 Hz, 2H), 1.99 – 1.89 (m, 1H), 1.85 (dd, *J* = 16.9, 7.3 Hz, 1H), 1.74 – 1.67 (m, 1H), 1.66 – 1.48 (m, 3H), 1.31 (s, 3H), 1.29 (s, 3H), 1.04 (s,

3H), 0.98 (s, 3H). **^{13}C NMR** (101 MHz, $CDCl_3$): δ 172.9, 167.5, 157.6, 153.9, 144.1, 143.8, 137.0, 131.9, 118.2, 114.0, 87.6, 65.0, 63.1, 60.4, 46.2, 41.0, 36.1, 34.4, 31.8, 30.5, 25.6, 21.9, 21.8, 21.8, 18.8. **FTIR** (thin film): 2933, 2872, 1756, 1734, 1591, 1459, 1409, 1280, 1079, 1020, 938 cm^{-1}. **HRMS** (ESI+) *m/z* Calc'd for $C_{26}H_{36}O_7Na$ $[M+Na]^+$: 483.2353, found: 483.2354. **R_f** = 0.24 (10% EtOAc/hexanes). **MP** = 108-111 °C.

*1.5.15 Preparation of carboxylic acid **1.55***

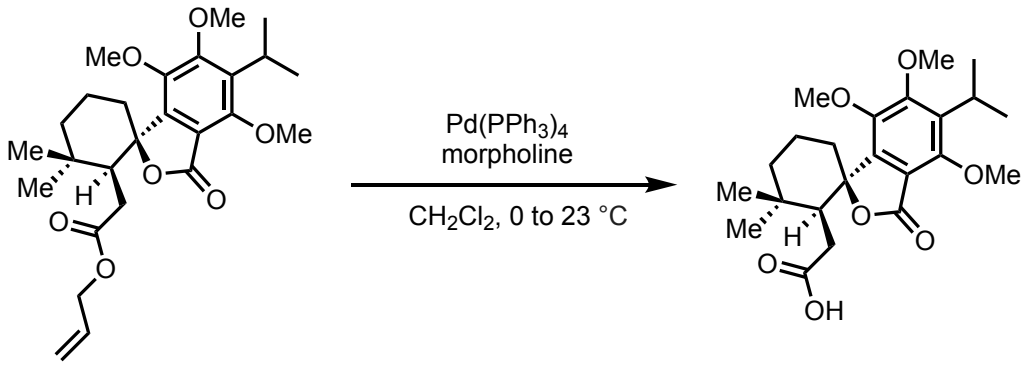

1.56 **1.55**

To a solution of spirolactone **1.56** (10.0 g, 21.74 mmol) in anhydrous CH_2Cl_2 (110 mL, 0.2 M) was added morpholine (11 mL, 130 mmol) and $Pd(PPh_3)_4$ (1.26 g, 1.087 mmol) successively in one portion at 0 °C. The reaction was allowed to warm naturally to room temperature over the course of 12 hours upon which the mixture was diluted in 2M HCl (aq.) (200 mL), and the layers were separated. The aqueous layer was further extracted with CH_2Cl_2 (2 x 200 mL) and the combined organic layers were washed with brine (1 x 200 mL), dried over anhydrous $MgSO_4$, filtered, and concentrated to afford a crude orange residue. Purification *via* flash column chromatography (30% EtOAc/hexanes) afforded acid **1.55** (8.7 g, 95% yield) as a white amorphous solid. **^{1}H NMR** (400 MHz, $CDCl_3$): δ 3.93 (s, 3H), 3.85 (s, 3H), 3.74 (s, 3H), 3.45 (sept, *J* = 7.1 Hz, 1H), 2.55 (dd, *J* = 7.0, 4.3

Hz, 1H), 2.19 (dd, J = 15.7, 4.1 Hz, 2H), 1.95 – 1.82 (m, 1H), 1.79 – 1.66 (m, 2H), 1.58 (dt, J = 12.8, 3.1 Hz, 2H), 1.53 – 1.43 (m, 1H), 1.32 – 1.16 (m, 6H), 1.02 (s, 3H), 0.95 (s, 3H). **^{13}C NMR** (101 MHz, $CDCl_3$): δ 179.5, 167.5, 157.6, 154.0, 143.8, 143.6, 137.6, 114.1, 87.4, 63.0, 60.3, 60.1, 46.6, 41.0, 35.8, 34.5, 31.8, 30.7, 29.8, 25.6, 21.7, 21.7, 18.7. **FTIR** (neat): 2961, 1754, 1698, 1591, 1473, 1406, 1309, 1287, 1114, 1006, 942 cm^{-1}. **HRMS** (ESI+) *m*/*z* Calc'd for $C_{23}H_{32}O_7Na$ $[M+Na]^+$: 443.2040, found: 443.2040. $\mathbf{R}_f$ = 0.54 (50% EtOAc/hexanes).

*1.5.16 Preparation of iodide **1.54***

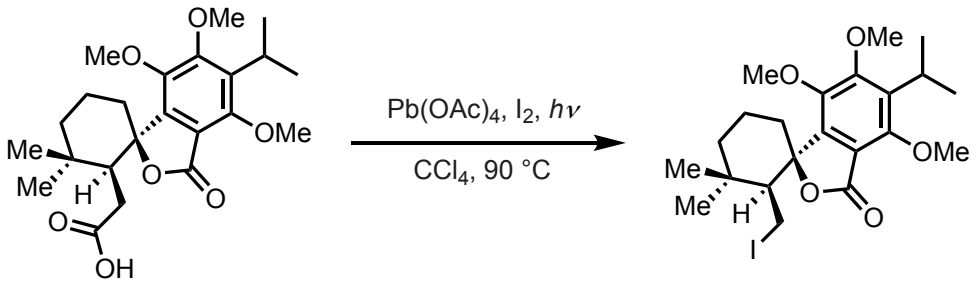

1.55 **1.54**

To a 400 mL pressure tube equipped with a magnetic stir bar was added acid **1.55** (8.6 g, 20.5 mmol) and anhydrous CCl_4 (200 mL, 0.1 M). $Pb(OAc)_4$ (19.1 g, 43 mmol) and I_2 (10.4 g, 40.9 mmol) were added successively in one portion. The vessel was sealed and the mixture was heated to 90 °C and irradiated with a 300W tungsten lamp in an oil bath. After 30 min, the reaction mixture was removed from the oil bath and was cooled to 23 °C. The reaction mixture was filtered through a short bed of celite and the filter cake was washed with CH_2Cl_2 (2 x 50 mL). The filtrate was then washed with sat. aq. $Na_2S_2O_3$ solution (1 x 50 mL) and brine (1 x 50 mL). The organic layer was then dried over anhydrous $MgSO_4$, filtered, and concentrated to afford a crude yellow foam. The resulting

residue was purified *via* MPLC (100 g column, 5-10% EtOAc/hexanes, step gradient, 110 mL/min) to afford iodide **1.54** (9.5 g, 92% yield) as a white foam. **^{1}H NMR** (600 MHz, $CDCl_3$): δ 4.01 (s, 3H), 3.97 (s, 3H), 3.88 (s, 3H), 3.53 (hept, *J* = 7.1 Hz, 1H), 3.17 – 3.11 (m, 1H), 2.53 (m, 2H), 2.18 (td, *J* = 13.8, 4.3 Hz, 1H), 1.90 (qt, *J* = 14.3, 3.6 Hz, 1H), 1.70 (dq, *J* = 13.8, 2.6 Hz, 1H), 1.63 – 1.55 (m, 2H), 1.47 (td, *J* = 13.8, 13.2, 3.9 Hz, 1H), 1.33 (dd, *J* = 7.1, 4.9 Hz, 6H), 1.15 (s, 3H), 1.03 (s, 3H). **^{13}C NMR** (151 MHz, $CDCl_3$): δ 167.7, 157.5, 154.5, 144.2, 143.6, 137.8, 113.6, 86.5, 63.2, 60.3, 60.1, 53.3, 41.6, 36.6, 36.3, 31.9, 25.7, 21.9, 21.9, 20.9, 18.5, -3.1. **FTIR** (thin film): 2953, 1758, 1593, 1472, 1408, 1359, 1124, 951 cm^{-1}. **HRMS** (ESI+) *m/z* Calc'd for $C_{22}H_{33}IO_5$ $[M+H]^+$: 503.1294, found: 503.1292. $\mathbf{R}_f$ = 0.78 (50% EtOAc/hexanes).

*1.5.17 Preparation of ketone **1.52***

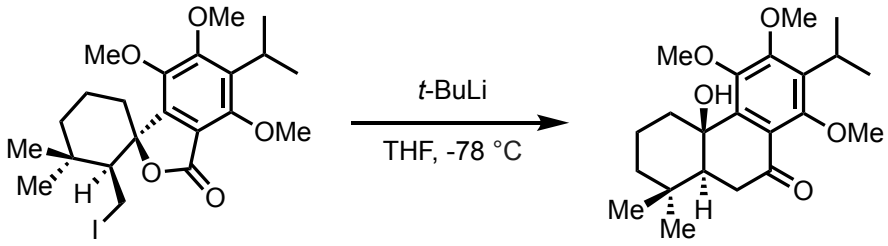

1.54 **1.52**

A solution of iodide **1.54** (4.2 g, 8.36 mmol) in anhydrous THF (170 mL, 0.05 M) was cooled to -78 °C. Then, *t*-BuLi (9.8 mL, 1.7 M in pentane, 16.7 mmol) was carefully added dropwise over the course of 20 minutes down the cooled side of the round bottom flask *via* syringe. Following completion of the addition, the resulting mixture was stirred for 30 minutes at -78 °C. The reaction mixture was quenched with sat. aq. NH_4Cl solution (50 mL) and warmed to 23 °C. The aqueous layer was extracted with CH_2Cl_2 (3 x 50 mL), dried over anhydrous $MgSO_4$, filtered, and concentrated to afford a crude yellow oil.

Purification *via* flash column chromatography (10-15% EtOAc/hexanes) afforded ketone **1.52** (2.62 g, 83% yield) as a white foam. *Note: Failure to carefully control the slow addition of* t-*BuLi results in varying amounts of an inseparable, unidentified byproduct. Careful temperature control and adherence to the described protocol consistently and entirely suppresses formation of this byproduct which can be identified by a diagnostic singlet in the* ^{1}*H NMR spectrum (*δ *= 5.07 ppm).* **^{1}H NMR** (600 MHz, $CDCl_3$): δ 3.88 (s, 3H), 3.82 (s, 3H), 3.79 (s, 3H), 3.50 (sept, 1H), 2.95 – 2.89 (m, 1H), 2.79 (t, *J* = 14.5 Hz, 1H), 2.45 (dd, *J* = 14.7, 2.3 Hz, 1H), 2.27 (d, *J* = 1.3 Hz, 1H), 2.09 – 1.98 (m, 1H), 1.77 (d, *J* = 14.2 Hz, 1H), 1.59 – 1.53 (m, 2H), 1.49 (dd, *J* = 13.2, 4.0 Hz, 1H), 1.31 (d, *J* = 7.1 Hz, 3H), 1.30 (d, *J* = 7.1 Hz, 3H), 1.08 (s, 3H), 0.96 (s, 3H). **^{13}C NMR** (151 MHz, $CDCl_3$): δ 197.0, 157.7, 156.0, 148.0, 140.4, 136.4, 121.2, 74.3, 63.3, 60.4, 48.6, 41.0, 37.7, 36.9, 33.6, 32.3, 25.4, 21.9, 21.9, 21.7, 18.7. **FTIR** (neat): 3499, 2936, 1759, 1681, 1556, 1451, 1404, 1365, 1305, 1280, 1113, 1024 cm^{-1}. **HRMS** (ESI+) *m/z* Calc'd for $C_{22}H_{32}O_5Na$ $[M+Na]^+$: 399.2147, found: 399.2278. $\mathbf{R}_f$ = 0.13 (10% EtOAc/hexanes).

1.5.18 Preparation of tetrahydrofuran ***1.29***

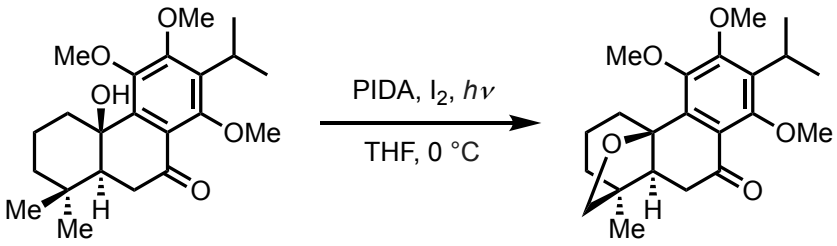

1.52 **1.29**

To a solution of ketone **1.52** (210 mg, 0.56 mmol) in anhydrous CH_2Cl_2 (11 mL, 0.05 M). I_2 (142 mg, 0.56 mmol) and PIDA (359 mg, 1.12 mmol) were added to the solution successively and the mixture was cooled to 0 °C in a clear glass bowl. The purple mixture

was then irradiated using a 300W tungsten lamp for 1 h at this temperature. The lamp was turned off, the mixture was warmed to 23 °C, and quenched by the addition of sat. aq. $Na_2S_2O_3$ solution (10 mL) and sat. aq. $NaHCO_3$ (10 mL). The two layers were separated and the aqueous layer was further extracted with CH_2Cl_2 (2 x 20 mL). The organic layers were combined, washed with brine (1 x 20 mL), dried over anhydrous $MgSO_4$, filtered, and concentrated. Purification *via* flash column chromatography (10% EtOAc/hexanes) afforded tetrahydrofuran **1.29** (165 mg) as a 2:1 mixture with an unknown byproduct favoring the desired compound as a white foam (52% yield by ^{1}H NMR). For characterization purposes, the major component can be isolated in suitable purity on small scale by repeated preparative TLC (5% EtOAc/hexanes, 5 mg aliquot, 4-5 developments on a 10 x 10 cm TLC plate). **^{1}H NMR** (600 MHz, $CDCl_3$): δ 3.96 (d, *J* = 8.0 Hz, 1H), 3.89 (s, 3H), 3.87 – 3.84 (m, 4H), 3.75 (s, 3H), 3.50 (sept, *J* = 7.1 Hz, 1H), 2.86 (dd, *J* = 13.0, 6.0 Hz, 1H), 2.60 (dd, *J* = 14.6, 12.3 Hz, 1H), 2.44 (dd, *J* = 12.3, 3.9 Hz, 1H), 2.19 (dd, *J* = 14.6, 3.9 Hz, 1H), 2.16 – 2.06 (m, 1H), 1.81 – 1.73 (m, 1H), 1.65 (dd, *J* = 13.2, 6.2 Hz, 1H), 1.59 (dtd, *J* = 13.2, 7.5, 6.6, 2.0 Hz, 1H), 1.44 (td, *J* = 12.9, 5.5 Hz, 1H), 1.32 (d, *J* = 7.1 Hz, 3H), 1.29 (d, *J* = 7.1 Hz, 3H), 0.99 (s, 3H). **^{13}C NMR** (151 MHz, $CDCl_3$): δ 198.4, 149.4, 137.0, 135.6, 122.6, 83.5, 77.9, 63.4, 60.8, 60.3, 54.3, 43.8, 39.1, 39.0, 36.4, 25.5, 21.9, 21.8, 20.6, 19.0. **FTIR** (thin film): 2980, 1696, 1563, 1455, 1381, 1339, 1143, 1010, 953 cm^{-1}. **HRMS** (ESI+) *m/z* Calc'd for $C_{22}H_{30}O_5Na$ $[M+Na]^+$: 397.1985, found: 397.1986. **R_f** = 0.23 (10% EtOAc/hexanes).

1.5.19 Preparation of (±)-dracocephalone A ***1.01***

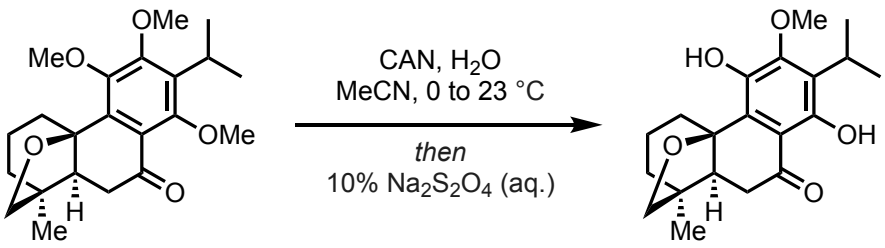

1.29 **1.01**

A solution of tetrahydrofuran **1.29** (6.0 mg, 16 μmol) in MeCN (1.6 mL, 0.01 M) was cooled to 0 °C and a solution of CAN (35 mg, 64 μmol) in H_2O (0.8 mL, 0.02 M) was added dropwise over the course of 5 minutes. The ice bath was removed and the resulting yellow solution was allowed to stir at 23 °C for 16 hours upon which the reaction mixture was diluted in water (5 mL) and extracted with Et_2O (3 x 5 mL) and the combined organic layers were added to a 10% aq. $Na_2S_2O_4$ solution (5 mL) and the biphasic mixture was shaken vigorously for 5 minutes. The layers were separated, and the organic layer was dried over anhydrous $MgSO_4$, filtered, and concentrated to afford a crude yellow oil. Purification *via* flash column chromatography (20% EtOAc/hexanes) afforded dracocephalone A (**1.01**) (3.1 mg, 56% yield) as a white, crystalline solid. Crystals suitable for X-Ray analysis were obtained by slow evaporation from a CH_2Cl_2/hexanes solution to give colorless blocks. **^{1}H NMR** (600 MHz, $CDCl_3$): δ 12.16 (s, 1H), 5.86 (s, 1H), 4.02 (d, J = 8.1 Hz, 1H), 3.90 (dd, J = 8.2, 2.2 Hz, 1H), 3.88 (s, 3H), 3.43 (sept, J = 6.8 Hz, 1H), 2.86 (dd, J = 13.6, 6.0 Hz, 1H), 2.56 – 2.49 (m, 2H), 2.20 (dd, J = 12.2, 6.5 Hz, 1H), 2.15 – 2.04 (m, 1H), 1.81 (m, 1H), 1.68 (dd, J = 13.2, 6.2 Hz, 1H), 1.61 (tdd, J = 13.1, 5.8, 2.1 Hz, 1H), 1.43 (td, J = 13.2, 5.6 Hz, 1H), 1.35 (d, J = 7.1 Hz, 6H), 1.03 (s, 3H). **^{13}C NMR** (101 MHz, $CDCl_3$): δ 203.2, 156.0, 154.3, 140.8, 129.0, 124.6, 111.8, 83.1, 78.3, 61.8,

52.0, 43.8, 39.2, 36.5, 35.6, 25.6, 20.6, 20.6, 20.4, 18.7. **FTIR** (thin film): 3342, 2932, 2870, 1622, 1460, 1416, 1337, 1259, 1170, 1088, 1054, 1028, 952, 906, 876, 806, 621 cm^{-1}. **HRMS** (ESI+) *m/z* Calc'd for $C_{20}H_{28}O_5$ $[M+H]^+$: 347.1858, found: 347.1951. $\mathbf{R_f}$ = 0.51 (40% EtOAc/hexanes). **MP** = 170-172 °C.

*1.5.20 Preparation of naphthol **1.66***

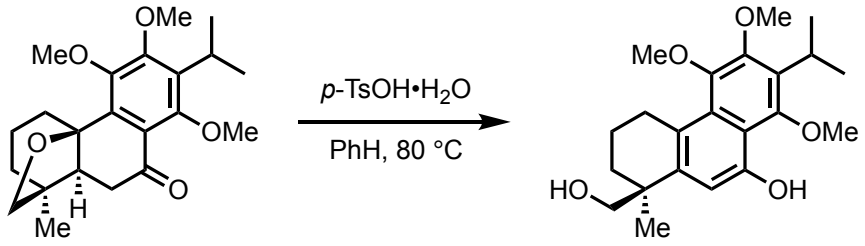

1.29 **1.66**

To a dry 20 mL scintillation vial was added tetrahydrofuran **1.29** (490 mg, ~1.31 mmol, 2:1 mixture with unidentified impurity), benzene (10 mL, 0.13 M), and *p*-TsOH•H_2O (75 mg, 0.39 mmol, 0.3 equiv). The vial was sealed under an argon atmosphere and the vial was lowered into a heating block maintained at 80 °C. The mixture was stirred at this temperature for 5 hours, upon which the mixture was cooled to 23 °C, the solvent level was concentrated *in vacuo* to approximately half volume, and the solution obtained was loaded directly onto a 25 g MPLC column eluting with 20% EtOAc/hexanes isocratic (60 mL/min) to afford naphthol **1.66** (332 mg, 53% yield, two steps) as a tan solid. **^{1}H NMR** (400 MHz, $CDCl_3$): δ 9.71 (s, 1H), 6.78 (s, 1H), 3.97 (s, 3H), 3.86 (d, *J* = 11.1 Hz, 1H), 3.83 (s, 3H), 3.74 (s, 3H), 3.59 – 3.47 (m, 2H), 3.36 (dt, *J* = 17.5, 5.1 Hz, 1H), 3.19 (ddd, *J* = 17.4, 9.4, 5.4 Hz, 1H), 2.10 – 2.01 (m, 1H), 1.94 – 1.82 (m, 1H), 1.77 – 1.67 (m, 1H), 1.56 – 1.52 (m, 1H), 1.42 (d, *J* = 2.4 Hz, 3H), 1.40 (d, *J* = 2.5 Hz, 4H), 1.28 (s, 3H).

^{13}C NMR (101 MHz, $CDCl_3$): δ 152.3, 151.5, 148.8, 148.2, 140.0, 131.8, 129.7, 125.5, 114.5, 108.5, 72.1, 64.0, 60.7, 60.5, 40.6, 32.9, 29.8, 26.7, 25.9, 22.1, 22.0, 20.4. **FTIR** (thin film): 3344, 2931, 2870, 1629, 1591, 1367, 1104, 1073, 1028, 951, 733 cm^{-1}. **HRMS** (ESI+) *m/z* Calc'd for $C_{22}H_{30}O_5Na$ $[M+Na]^+$: 397.1991, found: 397.1968. $\mathbf{R}_f$ = 0.24 (20% EtOAc/hexanes).

*1.5.21 Preparation of phenolic oxidation product **1.67***

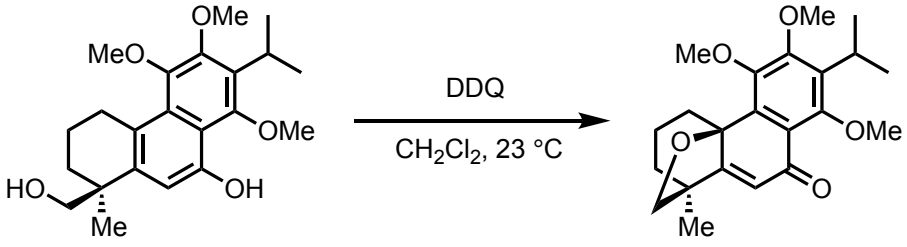

1.66 **1.67**

To a solution of naphthol **1.66** (35 mg, 0.09 mmol) in anhydrous CH_2Cl_2 (2 mL, 0.05 M) under an argon atmosphere was added DDQ (23 mg, 0.099 mmol) in one portion at 23 °C. The reaction was allowed to stir for 30 minutes at this temperature upon which the mixture was diluted in H_2O (5 mL) and extracted with CH_2Cl_2 (3 x 5 mL). The combined organic layers were washed with brine (1 x 5 mL), dried over anhydrous $MgSO_4$, filtered, and concentrated to afford a crude orange residue. The crude residue obtained was purified *via* flash column chromatography to afford phenolic oxidation product **1.67** (22 mg, 63% yield) as an orange amorphous solid. *Note: As described in the text, the yield and selectivity of this reaction depend both on the solvent employed (CH_2Cl_2 vs. 1,4-dioxane) and the water content of the reaction. As such, the reproducibility of this protocol and the yield obtained depend strongly on the ability to maintain anhydrous conditions. Otherwise, the desired benzylic oxidation product predominates* (vide infra). **^{1}H NMR** (600 MHz,

$CDCl_3$): δ 5.98 (s, 1H), 4.16 (d, *J* = 7.6 Hz, 1H), 3.92 (s, 3H), 3.88 (s, 3H), 3.76 – 3.71 (m, 4H), 3.57 (sept, *J* = 7.1 Hz, 1H), 2.62 (dd, *J* = 13.4, 5.6 Hz, 1H), 2.17 (ddt, *J* = 19.0, 12.7, 6.4 Hz, 1H), 1.88 (dd, *J* = 13.0, 6.0 Hz, 1H), 1.74 (dt, *J* = 13.9, 5.6 Hz, 1H), 1.67 (td, *J* = 13.0, 5.7 Hz, 1H), 1.50 (td, *J* = 13.0, 5.6 Hz, 1H), 1.33 (d, *J* = 7.1 Hz, 3H), 1.31 (d, *J* = 7.1 Hz, 3H), 1.21 (s, 3H). **^{13}C NMR** (151 MHz, $CDCl_3$): δ 184.8, 168.1, 157.3, 155.6, 148.1, 137.1, 136.1, 119.4, 115.4, 79.2, 78.3, 62.5, 60.9, 60.3, 43.3, 42.0, 40.1, 25.4, 21.9, 21.9, 19.7, 18.2. **FTIR** (thin film): 2958, 2933, 1693, 1656, 1566, 1455, 1410, 1311, 1214, 1114, 1037, 955 cm^{-1}. **HRMS** (ESI+) *m/z* Calc'd for $C_{22}H_{30}O_5Na$ $[M+Na]^+$: 395.1829, found: 395.1797. $\mathbf{R_f}$ = 0.20 (10% EtOAc/hexanes).

*1.5.22 Preparation of tetrahydropyran **1.64***

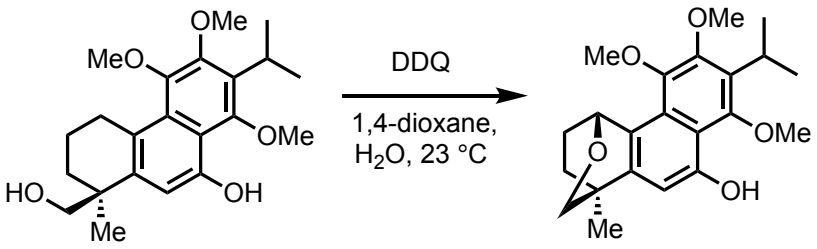

1.66 **1.64**

To a solution of naphthol **1.66** (110 mg, 0.29 mmol) in 1,4-dioxane (5.8 mL, 0.05 M) was added H_2O (52 µL, 2.9 mmol) and DDQ (72 mg, 0.32 mmol) at 23 °C and the pale, yellow solution became turbid and red. The resulting mixture was stirred for 15 minutes at 23 °C upon which the reaction was quenched with sat. aq. $NaHCO_3$ (10 mL) and extracted with CH_2Cl_2 (3 x 10 mL). The combined organic layers were washed with brine (1 x 10 mL), dried over anhydrous $MgSO_4$, filtered, and concentrated to afford a crude brown oil. Purification *via* MPLC (10 g column, 10% EtOAc/hexanes isocratic, 30 mL/min) afforded tetrahydropyran **1.64** (70 mg, 65% yield) as a white foam. **^{1}H NMR** (400 MHz, $CDCl_3$): δ

9.71 (s, 1H), 6.78 (s, 1H), 3.97 (s, 3H), 3.86 (d, J = 11.1 Hz, 1H), 3.83 (s, 3H), 3.74 (s, 3H), 3.59 – 3.47 (m, 2H), 3.36 (dt, J = 17.5, 5.1 Hz, 1H), 3.19 (ddd, J = 17.4, 9.4, 5.4 Hz, 1H), 2.10 – 2.01 (m, 1H), 1.94 – 1.82 (m, 1H), 1.77 – 1.67 (m, 1H), 1.56 – 1.52 (m, 1H), 1.42 (d, J = 2.4 Hz, 3H), 1.40 (d, J = 2.5 Hz, 4H), 1.28 (s, 3H). **^{13}C NMR** (101 MHz, $CDCl_3$): δ 152.3, 151.5, 148.8, 148.2, 140.0, 131.8, 129.7, 125.5, 114.5, 108.5, 72.1, 64.0, 60.7, 60.5, 40.6, 32.9, 29.8, 26.7, 25.9, 22.1, 22.0, 20.4. **FTIR** (thin film): 3332, 2956, 2853, 1620, 1594, 1507, 1383, 1202, 1102, 1029, 732 cm^{-1}. **HRMS** (ESI+) *m/z* Calc'd for $C_{22}H_{30}O_5Na$ $[M+Na]^+$: 395.1829, found: 395.1830. $\mathbf{R}_f$ = 0.25 (10% EtOAc/hexanes).

*1.5.23 Preparation of acetate **1.68***

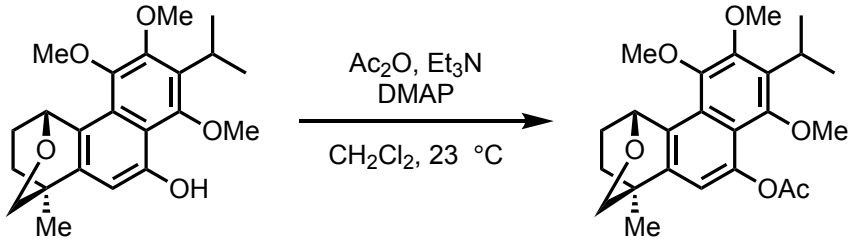

1.64 **1.68**

To a solution of tetrahydropyran **1.64** (10 mg, 26 μmol) in anhydrous CH_2Cl_2 (0.5 mL, 0.05 M) was added Ac_2O (30 μL, 0.26 mmol), Et_3N (70 μL, 0.52 mmol), and DMAP (1 mg) at 23 °C for 17 hours, upon which the reaction mixture was concentrated *in vacuo* and purified directly *via* flash column chromatography (10% EtOAc/hexanes) and afforded acetate **1.68** (10 mg, 93% yield) as a white, crystalline solid. Crystals suitable for X-Ray analysis were grown *via* slow evaporation from a hexanes/Et_2O solution (*ca.* 5:1 v/v) in a loosely-capped vial overnight. **^{1}H NMR** (600 MHz, $CDCl_3$): δ 7.03 (s, 1H), 6.49 (dd, J = 4.1, 1.8 Hz, 1H), 3.98 (s, 3H), 3.85 (s, 3H), 3.78 (d, J = 7.4 Hz, 1H), 3.71 (s, 3H), 3.65 (sept, J = 7.2 Hz, 1H), 3.11 (dd, J = 7.5, 3.3 Hz, 1H), 2.47 – 2.33 (m, 4H), 1.75 (ddd, J =

13.1, 10.2, 3.5 Hz, 1H), 1.69 – 1.60 (m, 1H), 1.39 (6, 9H). **^{13}C NMR** (151 MHz, $CDCl_3$): δ 169.9, 151.9, 148.6, 145.9, 145.3, 141.7, 134.0, 133.7, 125.1, 118.0, 113.7, 72.1, 66.7, 63.1, 60.7, 60.3, 35.3, 29.8, 27.4, 25.9, 22.2, 22.1, 21.1, 19.2. **FTIR** (thin film): 2932, 2855, 1767, 1587, 1448, 1365, 1342, 1203, 1112, 1030, 733 cm^{-1}. **HRMS** (ESI+) *m/z* Calc'd for $C_{24}H_{30}O_6Na$ $[M+Na]^+$: 437.1940, found: 437.1912. $\mathbf{R_f}$ = 0.15 (5% EtOAc/hexanes). **MP** = 178-180 °C.

*1.5.24 Preparation of (±)-dracocequinone A **1.04***

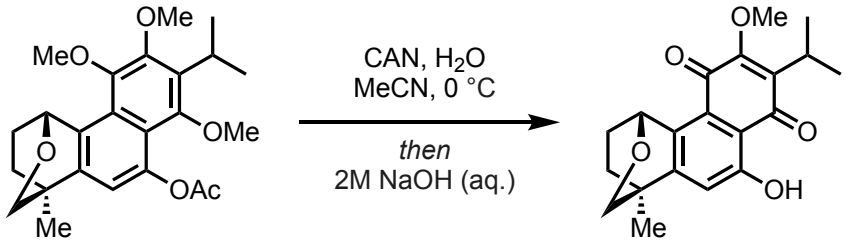

1.68 **1.04**

To a solution of acetate **1.68** (5.4 mg, 13 μmol) in MeCN (1.3 mL, 0.01 M) was added a solution of CAN (15 mg, 27.3 μmol) in H_2O (0.52 mL, 0.025 M) dropwise over the course of 1 minute at 0 °C. The bright yellow solution was stirred at this temperature for 1 h, upon which the mixture was diluted in MeOH (1.3 mL) and 2M NaOH (aq.) (0.2 mL, 0.4 mmol) was added in one portion. The ice bath was removed and the mixture was allowed to stir for 30 minutes at 23 °C. The mixture was poured into 1M HCl (aq.) (10 mL), and extracted with CH_2Cl_2 (3 x 10 mL). The combined organic layers were washed with brine (1 x 10 mL), dried over anhydrous $MgSO_4$, filtered, and concentrated to afford a crude red oil. Purification *via* preparative TLC (10 x 10 cm, 20% EtOAc/hexanes) afforded dracocequinone A (**1.04**) (2.0 mg, 44% yield) as an orange oil. **^{1}H NMR** (600

MHz, $CDCl_3$): δ 12.97 (s, 1H), 7.12 (s, 1H), 6.09 (m, 1H), 4.05 (s, 3H), 3.80 (d, *J* = 7.9 Hz, 1H), 3.42 (sept, *J* = 6.9 Hz, 1H), 3.20 (dd, *J* = 7.9, 3.3 Hz, 1H), 2.40 (m, 1H), 1.80 (ddd, *J* = 13.9, 10.7, 3.5 Hz, 1H), 1.64 (t, *J* = 13.3 Hz, 1H), 1.33 (s, 3H), 1.29 (d, *J* = 7.1 Hz, 3H), 1.27 (d, *J* = 7.3 Hz, 3H). **^{13}C NMR** (151 MHz, $CDCl_3$): δ 191.5, 183.5, 161.6, 159.4, 153.8, 138.7, 134.7, 124.6, 117.5, 112.6, 71.8, 64.9, 61.0, 35.5, 30.2, 26.0, 24.4, 20.6, 20.4, 18.7. **FTIR** (thin film): 2928, 2864, 1756, 1668, 1631, 1509, 1452, 1394, 1302, 1199, 1138, 835, 777, 690, 616 cm^{-1}. **HRMS** (ESI+) *m/z* Calc'd for $C_{20}H_{22}O_5Na$ $[M+Na]^+$: 363.1359, found: 363.1360. $\mathbf{R}_f$ = 0.48 (20% EtOAc/hexanes).

*1.5.25 Preparation of naphthol acetate **1.75***

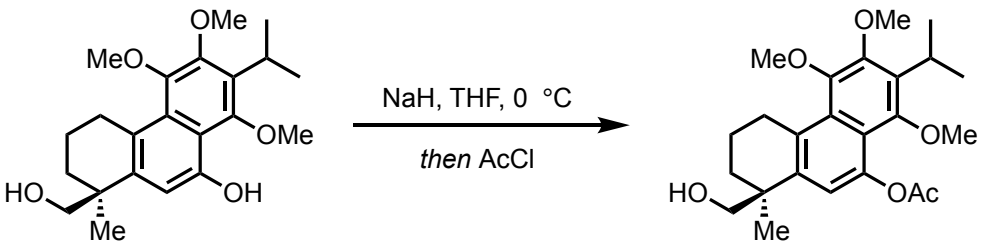

1.66 **1.75**

To a solution of naphthol **1.66** (140 mg, 0.374 mmol) in anhydrous THF (7 mL, 0.05 M) and NaH (17 mg, 60% dispersion in mineral oil, 0.41 mmol) at 0 °C for 30 minutes, and then AcCl (30 μL, 0.41 mmol) was added dropwise over the course of 1 minute. The ice bath was removed and stirred at 23 °C for 2 hours. The reaction was then quenched with sat. aq. NH_4Cl (15 mL) and extracted with CH_2Cl_2 (3 x 15 mL). The combined organic layers were washed with brine (1 x 15 mL), dried over anhydrous $MgSO_4$, filtered, and concentrated to afford a pale, brown crude residue. Purification *via* MPLC (10 g column, 10% EtOAc/hexanes isocratic, 30 mL/min) afforded naphthol acetate **1.75** (147 mg, 94%

yield) as a pale, yellow foam. **^{1}H NMR** (600 MHz, $CDCl_3$): δ 6.95 (s, 1H), 3.94 (s, 3H), 3.79 (d, *J* = 11.2 Hz, 1H), 3.75 (s, 3H), 3.70 (s, 3H), 3.61 (sept, *J* = 7.1 Hz, 1H), 3.55 (d, *J* = 11.2 Hz, 1H), 3.42 (dt, *J* = 17.8, 5.3 Hz, 1H), 3.29 (ddd, *J* = 17.7, 8.9, 5.4 Hz, 1H), 2.35 (s, 3H), 2.07 – 1.99 (m, 1H), 1.92 – 1.83 (m, 1H), 1.77 – 1.67 (m, 1H), 1.60 – 1.53 (m, 1H), 1.37 (d, *J* = 7.1 Hz, 6H), 1.28 (s, 3H). **^{13}C NMR** (151 MHz, $CDCl_3$): δ 170.0, 152.6, 148.3, 147.5, 143.8, 138.6, 134.4, 133.2, 130.1, 118.0, 117.9, 71.9, 63.0, 60.6, 60.5, 40.4, 32.6, 30.4, 26.6, 25.8, 22.2, 22.1, 21.1, 20.2. **FTIR** (thin film): 3337, 2930, 1755, 1621, 1580, 1354, 1197, 1068, 1011, 721 cm^{-1}. **HRMS** (ESI+) *m/z* Calc'd for $C_{24}H_{32}O_5Na$ $[M+Na]^+$: 439.2097, found: 439.2069. $\mathbf{R}_f$ = 0.24 (20% EtOAc/hexanes).

*1.5.26 Preparation of aldehyde **1.70***

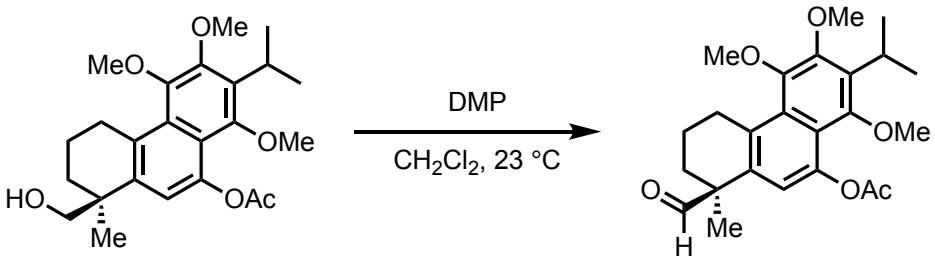

1.75 **1.70**

To a solution of naphthol acetate **1.75** (145 mg, 0.348 mmol) in CH_2Cl_2 (7 mL, 0.05 M) was added DMP (162 mg, 0.383 mmol) in one portion at 23 °C. The cloudy white mixture was stirred at this temperature for 2 hours upon which the reaction was quenched with sat. aq. $Na_2S_2O_3$ (5 mL) and sat. aq. $NaHCO_3$ (5 mL) and stirred vigorously for 10 minutes, upon which the biphasic mixture became clear. The layers were separated, and the aqueous layer was extracted with CH_2Cl_2 (2 x 10 mL). The combined organic layers were dried over anhydrous $MgSO_4$, filtered, and concentrated to afford a crude yellow residue. The resulting residue was purified *via* MPLC (10 g column, 20% EtOAc/hexanes

isocratic, 30 mL/min) to afford aldehyde **1.70** (142 mg, 98% yield) as a colorless oil that solidified to a white, amorphous solid upon standing. **^{1}H NMR** (400 MHz, $CDCl_3$): δ 9.53 (s, 1H), 6.68 (s, 1H), 3.96 (s, 3H), 3.79 (s, 3H), 3.70 (s, 3H), 3.63 (sept, *J* = 7.1 Hz, 1H), 3.52 (dt, *J* = 18.1, 5.5 Hz, 1H), 3.36 (ddd, *J* = 18.1, 8.5, 5.6 Hz, 1H), 2.34 (s, 3H), 2.08 (ddd, *J* = 13.5, 10.1, 3.2 Hz, 1H), 1.95 – 1.71 (m, 1H), 1.66 (ddd, *J* = 13.0, 7.5, 2.7 Hz, 1H), 1.47 (s, 3H), 1.38 (dd, *J* = 7.1, 2.1 Hz, 6H). **^{13}C NMR** (101 MHz, $CDCl_3$): δ 202.7, 169.7, 152.7, 148.4, 147.5, 143.9, 135.0, 133.2, 132.8, 130.1, 119.2, 118.5, 63.1, 60.6, 60.5, 51.5, 30.2, 29.7, 25.8, 23.7, 22.1, 22.1, 20.9, 19.7. **FTIR** (thin film): 2934, 1767, 1722, 1615, 1585, 1385. 1362, 1347, 1202, 1113, 1031, 755 cm^{-1}. **HRMS** (ESI+) *m/z* Calc'd for $C_{24}H_{30}O_6Na$ $[M+Na]^+$: 437.1940, found: 437.1912. $\mathbf{R}_f$ = 0.29 (20% EtOAc/hexanes).

*1.5.27 Preparation of carboxylic acid **1.71***

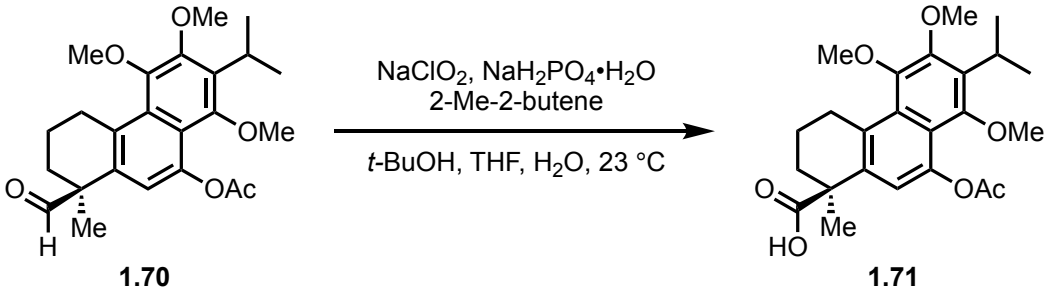

1.70 **1.71**

Aldehyde **1.70** (60 mg, 0.145 mmol) was taken up in THF (1 mL, 0.15 M) and *t*-BuOH/H_2O (3:2 v/v, 1 mL, 0.15 M), and 2-methyl-2-butene (0.15 mL, 1.45 mmol), NaH_2PO_4•H_2O (40 mg, 0.29 mmol), and $NaClO_2$ (66 mg, 0.725 mmol) were added in sequence at 23 °C with vigorous stirring (*ca.* 800 rpm). After stirring for 1 hour at this temperature, the mixture was diluted with 1M HCl (aq.) (10 mL) and extracted with CH_2Cl_2 (3 x 10 mL). The combined organic layers were washed with brine (1 x10 mL), dried over anhydrous $MgSO_4$, filtered, and concentrated to afford crude acid **1.71** (73 mg, *ca.* 0.145

mmol) as a pale, yellow foam, which was used directly in the next step without further purification.

*1.5.28 Preparation of carboxylic acid **1.72***

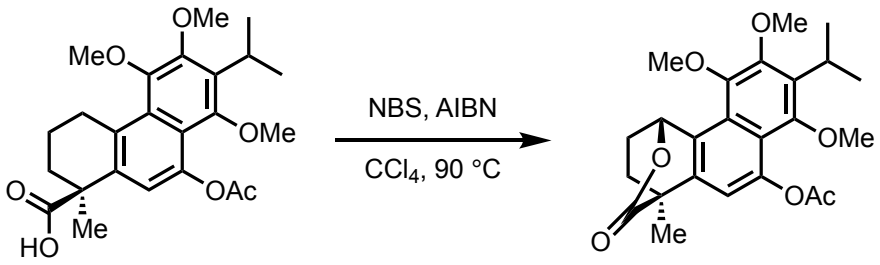

1.71 **1.72**

A solution of crude acid **1.71** (73 mg, *ca.* 0.145 mmol), NBS (52 mg, 0.29 mmol), and AIBN (5 mg, 0.029 mmol) in CCl_4 (3 mL, 0.05 M) was sealed in a scintillation vial under argon and heated to 80 °C upon which the solution turned from colorless to bright orange. The mixture was stirred at this temperature for 30 minutes, upon which the mixture was cooled to 23 °C, and concentrated under reduced pressure to afford a crude yellow residue. The resulting residue was purified *via* flash column chromatography (10%→20%→30% EtOAc/hexanes step gradient) to afford (44 mg, 70% yield, 2 steps) to give lactone **1.72** as a white foam. **^{1}H NMR** (600 MHz, $CDCl_3$): δ 7.22 (dd, *J* = 4.2, 1.5 Hz, 1H), 7.02 (s, 1H), 3.99 (s, 3H), 3.89 (s, 3H), 3.71 (s, 3H), 3.64 (sept, *J* = 7.1 Hz, 1H), 2.51 (dddd, *J* = 14.0, 9.9, 5.5, 4.1 Hz, 1H), 2.38 (s, 3H), 2.01 (ddd, *J* = 13.1, 10.0, 3.3 Hz, 1H), 1.91 (dddd, *J* = 12.9, 11.1, 3.4, 1.6 Hz, 1H), 1.75 (s, 3H), 1.57 (1, 3H), 1.39 (d, *J* = 7.1 Hz, 3H), 1.37 (d, *J* = 7.1 Hz, 3H). **^{13}C NMR** (151 MHz, $CDCl_3$): δ 176.3, 169.7, 152.5, 148.9, 146.3, 145.3, 138.8, 135.2, 130.6, 125.2, 118.3, 113.8, 75.4, 63.2, 60.7, 60.4, 44.7, 28.7, 27.1, 26.0, 22.1, 22.1, 21.0, 16.7. **FTIR** (thin film): 2931, 2864, 1754, 1655, 1560,

1448, 1349, 1179, 990, 775 cm^{-1}. **HRMS** (ESI+) *m/z* Calc'd for $C_{22}H_{26}O_6Na$ $[M+Na]^+$: 409.1622, found: 409.1620. $\mathbf{R}_f$ = 0.13 (10% EtOAc/hexanes).

*1.5.29 Preparation of (±)-dracocequinone B **1.05***

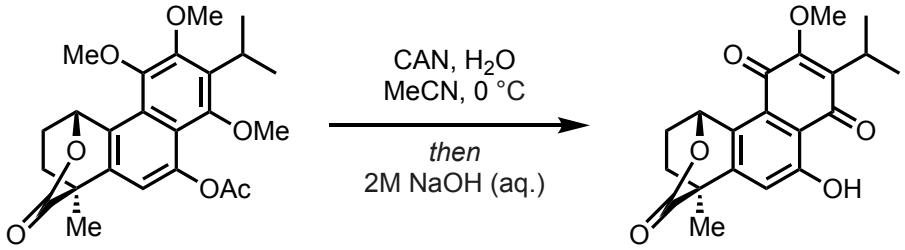

1.72 **1.05**

To a solution of lactone **1.72** (49 mg, 0.114 mmol) in MeCN (5 mL, 0.025 M) was added a solution of CAN (250 mg, 0.456 mmol) in H_2O (2.5 mL, 0.05 M) dropwise over the course of 5 minutes at 0 °C. The bright yellow solution was stirred at this temperature for 1 h, upon which the mixture was diluted in MeOH (5 mL) and 2M NaOH (aq.) (2.2 mL, 4.4 mmol) was added in one portion. The ice bath was removed and the mixture was allowed to stir for 30 minutes at 23 °C. The mixture was poured into 1M HCl (aq.) (15 mL), and extracted with CH_2Cl_2 (3 x 15 mL). The combined organic layers were washed with brine (1 x 15 mL), dried over anhydrous $MgSO_4$, filtered, and concentrated to afford a crude red oil. Purification *via* flash column chromatography (10→20% EtOAc/hexanes) afforded dracocequinone B (**1.05**) (18.6 mg, 46% yield) as an orange oil. **^{1}H NMR** (600 MHz, $CDCl_3$): δ 12.92 (s, 1H), 7.16 (s, 1H), 6.87 (d, *J* = 3.1 Hz, 1H), 4.09 (s, 3H), 3.42 (sept, *J* = 7.1 Hz, 1H), 2.49 (dddd, *J* = 14.6, 10.1, 5.0, 2.8 Hz, 1H), 2.04 (ddd, *J* = 13.0, 10.5, 3.4 Hz, 1H), 1.87 (t, *J* = 12.6 Hz, 1H), 1.68 (s, 3H), 1.60 (td, *J* = 12.8, 5.5 Hz, 1H), 1.29 (d, *J* = 7.1 Hz, 3H), 1.27 (d, *J* = 7.1 Hz, 3H). **^{13}C NMR** (151 MHz, $CDCl_3$): δ 191.1, 183.0, 174.4, 162.1, 159.2, 149.4, 139.3, 130.4, 125.8, 118.3, 113.1, 73.3, 61.2, 45.2, 29.3,

26.0, 24.6, 20.5, 20.3, 16.2. **FTIR** (thin film): 2928, 2864, 1756, 1668, 1631, 1509, 1452, 1394, 1302, 1181, 1138, 835, 777, 690, 616 cm^{-1}. **HRMS** (ESI+) *m/z* Calc'd for $C_{20}H_{20}O_6Na$ $[M+Na]^+$: 379.1152, found: 379.1131. $\mathbf{R_f}$ = 0.41 (20% EtOAc/hexanes).

1.6 References and Notes

[1] Uchiyama, N.; Kiuchi, F.; Ito, M.; Honda, G.; Takeda, Y.; Khodzhimatov, O. K.; Ashurmetov, O. A. *J. Nat. Prod.* **2003**, *66*, 1, 128-131.

[2] Uchiyama, N.; Kiuchi, F.; Ito, M.; Honda, G.; Takeda, Y.; Khodzhimatov, O. K.; Ashurmetov, O. A. *Tetrahedron* **2006**, *62*, 18, 4355-4359.

[3] Previous total syntheses of komaroviquinone and cyclocoulterone:
(a) Sengupta, S.; Drew, M. G. B.; Mukhopadhyay, R.; Achari, B.; Banerjee, A. K. *J. Org. Chem.* **2005**, *70*, 7694-7700.
(b) Majetich, G.; Li, Y.; Zou, G. *Heterocycles*, **2007**, *73*, 217-225.
(c) Suto, Y.; Kaneko, K.; Yamagiwa, N.; Iwasaki, G. *Tetrahedron Lett.* **2010**, *51*, 6329-6330.
(d) Thommen, C.; Neuburger, M.; Gademann, K. *Chem. Eur. J.* **2016**, *22*, 1-9.
(e) Oh, C. H.; Piao, L.; Jung, J.; Kim, J. *Asian J. Org. Chem.* **2016**, *5*, 1237-1241.
(f) Ahmad, A.; Burtoloso, A. C. B. *Org. Lett.* **2019**, *21*, 6079-6083.

[4] Mills, R. J.; Snieckus, V. *J. Org. Chem.* **1989**, *54*, 4386-4390.

[5] Ciesielski, J.; Canterbury, D. P.; Frontier, A. J. *Org. Lett.* **2009**, *11*, 4374-4377.

[6] Carreño, M. C.; Ruano, J. L. G.; Toledo, M. A.; Urbano, A. *Tetrahedon: Asymmetry.* **1997**, *8*, 913-921.

[7] Maier, M. E.; Bayer A. *Eur. J. Org. Chem*. **2006**, 4034-4043.

[8] Schneider, F.; Samarin, K.; Zanella, S.; Gaich, T. *Science,* **2020**, *367*, 676-681.

[9] Krasovskiy, A.; Kopp, F.; Knochel, P. *Angew. Chem. Int. Ed.* **2006**, *118*, 511-515.

[10] Ihara, M.; Toyota, M.; Abe, M.; Ishida, Y.; Fukumoto, K.; Kametani, T. *J. Chem. Soc. Perkin Trans. 1.* **1986**, 1543-1549.

[11] Caine, D.; Collison, R. F. *Synlett*, **1995**, 503-504.

[12] Nakhla, M. C.; Wood, J. L. *J. Am. Chem. Soc.* **2017**, *139*, 18504-18507.

[13] Beemelmanns, C.; Gross, S.; Reissig, H.-U. *Chem. Eur. J.* **2013**, *19*, 17801-17808.

[14] Haider, M.; Sennari, G.; Eggert, A.; Sarpong, R. *J. Am. Chem. Soc.* **2021**, *143*, 2710-2715.

[15] Deng, J.; Zhou, S.; Zhang, W.; Li, J.; Li, R.; Li, A. *J. Am. Chem. Soc.* **2014**, *136*, 8185-8188.

[16] Ramadayl, F. D.; Kiemle, D. J. LaLonde, R. T. *J. Org. Chem.* **1999**, *64*, 4607-4609.

[17] Hardman, C.; Ho, S.; Shimizu, A.; Luu-Nguyen, Q.; Sloane, J.L.; Soliman, M. S. A.; Marsden,
M. D.; Zack, J. A.; Wender, P. A. *Nature Communications* **2020**, *11* (1879), 1-11.

CHAPTER TWO

Progress Towards a Total Synthesis of Cassiabudanols A and B

2.1 Isolation and Background

2.1.1 The Cassiabudane Diterpenoids

Cassiabudanols A (**2.01**, Figure 2.1) and B (**2.02**) were isolated in 2019 by Zhou and coworkers from the dried immature fruits of *Cinnamomum cassia*, also known as cassia buds, which are widely used not only as food spice and flavoring ingredients, but also as a traditional Chinese medicine to treat cardiothoracic pains, cold pain in the stomach and abdomen, nausea, vomiting, belch, hiccup, cough, and dyspnea.[1] In the isolation, 5 kg of the immature fruits of *C. cassia* were powdered and extracted by soaking in 95% ethanol four times at 45 °C and evaporating the resultant filtrates. The crude residue was extracted by soaking with petroleum ether and ethyl acetate three times at 40 °C and the ethyl acetate extract was fractionated via silica gel column chromatography and then further purified several times by MPLC and HPLC, eventually giving 4.8 mg of **2.01** and 16 mg of **2.02**.

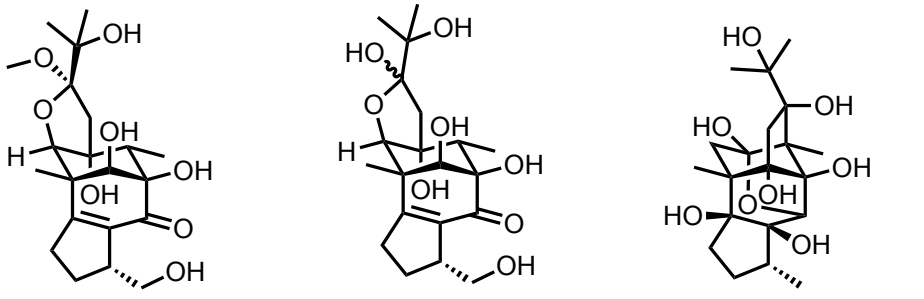

Figure 2.1. Representative diterpenoids from *Cinnamomum cassia*.

The cassiabudane diterpenoids **2.01** and **2.02** possess an unprecedented oxatetracyclo [6.6.1.$0^{2,6}$.$0^{10,14}$] pentadecane carbon skeleton which is proposed to be derived from 18-hydroxyperseanol **2.03** (Scheme 2.1).[1] As illustrated in Scheme 2.1 this transformation is believed to arrive via opening of the hemiketal moiety in **2.03** to its corresponding hydroxyketone **2.04** followed by a *retro*-aldol reaction to generate dione **2.05**. Reclosure via an alternative tans annular aldol reaction then forges [2.2.1] bicyclic intermediate **2.06** which, upon yet another *retro*-aldol and subsequent oxidation results in two hydroxyl groups that eventually engage to form a mixture of hemiacetal diastereomers that constitute the oxatetracyclo [6.6.1.$0^{2,6}$.$0^{10,14}$] pentadecane carbon skeleton that is present in **2.01** and **2.02**. The syn-vicinal diol found in **2.09** is converted to the corresponding tetrasubstituted olefin and subsequent oxidation of the allylic alcohol furnishes enone **2.10**. Lastly, diastereoselective reduction of the ketone generates **2.02**. From the diastereomeric mixture of **2.02**, methylation of the hemiketal moiety converges the two diastereomers into **2.01**.

Biologically, both **2.01** and **2.02** exhibit immunostimulative activity in the nanomolar range via a mode of action that is believed to involve enhancement of the rate of both B and T cell proliferation. Importantly, neither compound was found to exhibit general cytotoxicity up to a 25 μM concentration.[1] Moreover, *in vitro* studies support higher rates of both B and T cell proliferation compared to thymopentin, an API which is currently used to treat HIV.[1] The intricated details of **2.01** and **2.02's** biological mechanism of action of remain unknown and there have been no reported total syntheses of the cassiabudane diterpenoids.

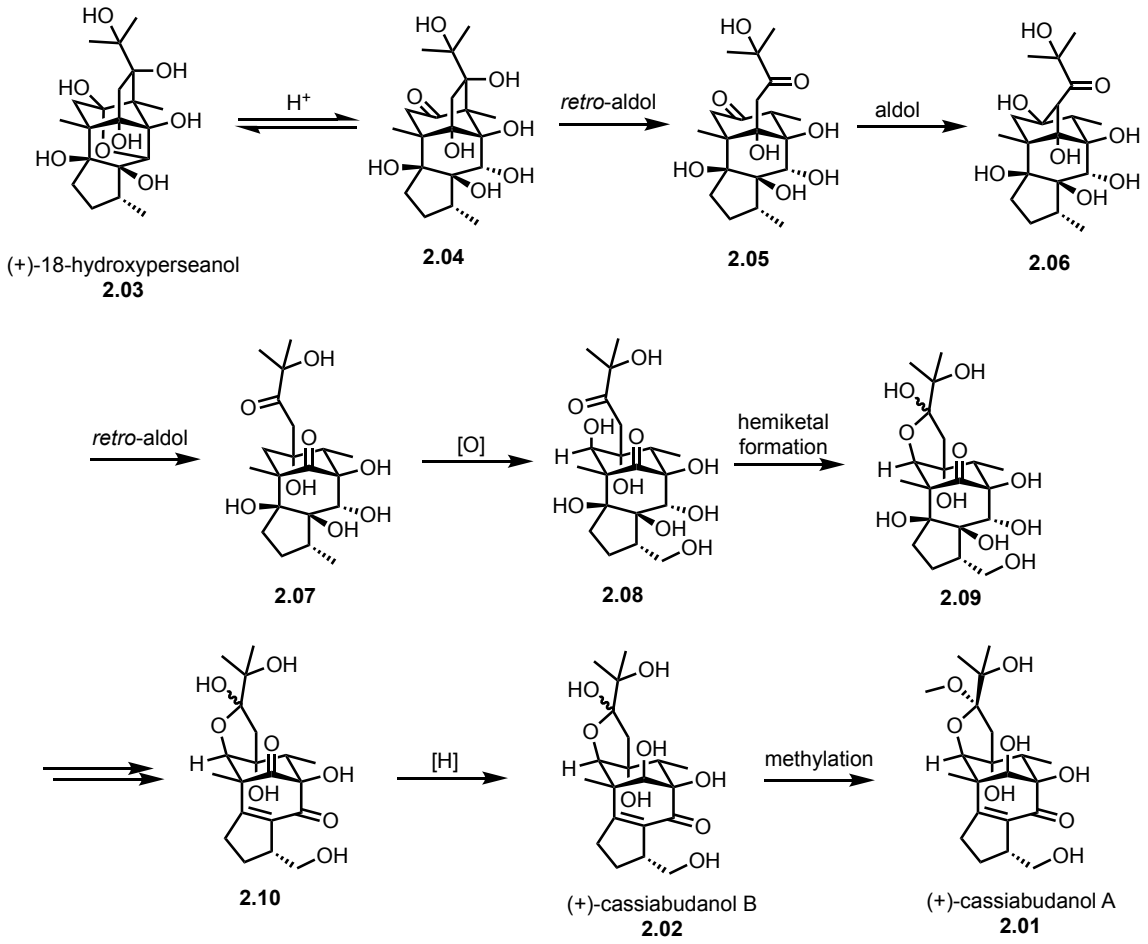

Scheme 2.1. Proposed biosynthesis of cassiabudanols A and B.

2.2 Synthetic Studies toward Cassisbudanols A and B

2.2.1 Retrosynthetic Analysis

Our synthetic strategy was initially focused on constructing the acetal and hemiacetal moieties found in **2.01** and **2.02**, respectively (Scheme 2.2). We envisioned the alkylsilane in **2.04** serving as precursor for a late-stage anionic fragmentation of the 1,3-dioxane to furnish an intermediate enol ether which, upon subsequent quenching with either methanol or water could result in the formation of **2.01** and **2.02**, respectively. The 1,3-dioxane moiety found in **2.04** was seen as arising from condensation of the

corresponding ketone and the requisite diaxial 1,3-diol **2.05**. The enone moiety present in **2.05** would be prepared via 1,4-oxidation from the corresponding ketone **2.06**. In order to install 4-hydroxyketone, we envisioned that removal of the TIPS group in **2.07** would furnish an intermediate oxyanion which would intern rupture the bridging C–O bond of the [2.2.1] oxabicycle. The secondary and tertiary alcohols in **2.07** were seen as arising by two different events: the former deriving from Baeyer-Villiger oxidation of the aldehyde in **2.08** followed by diacylation of the resultant formate and the latter arising from **2.09** via hydration of the tetrasubstituted. Intermediate **2.09** would be produced via an intramolecular furan Diels-Alder of enal **2.10**. The enal moiety found in the Diels-Alder precursor **2.10** could be directly installed from 1,1-disubstituted alkene **2.11** via cross-metathesis with an acrolein surrogate. Although 2-siloxyfurans like that present in **2.11** are often produced by enolization and trapping of a butenolide precursor, we planned to introduce the furan intact via nucleophilic acyl substitution of Weinreb Amide **2.12** with a lithiated furan. The amid would arise from the corresponding ester (**2.13**) which, in turn, would be produced from chloroketone **2.14** via modification of a known ring contraction procedure applied to (*R*)-7-hydroxycarvone **2.15**.[2]

As illustrated in Scheme 2.3, anionic fragmentation can occur via two different mechanistic pathways. We envisioned that the alkyl anion **2.16** can be formed from **2.14** via removal of the corresponding alkyl TMS using TBAF. In pathway 1, the alkyl anion fragments the C–O bond to form an oxyanion adjacent to the ketone (**2.17**). By addition of a Lewis acid, such as BF_3•Et_2O, the ketone can be activated to promote an intramolecular Mukaiyama-type aldol reaction to generate an oxocarbenium **2.19** embedded in a [3.2.2] oxabicycle. Having a secondary alcohol in a close proximity to the electrophilic carbon,

isomerization to the fused oxocarbenium **2.20** would furnish the carbon skeleton of **1.01** and **1.02**. Lastly, quenching with either methanol or water could secure the formation of **2.01** and **2.02**, respectively.

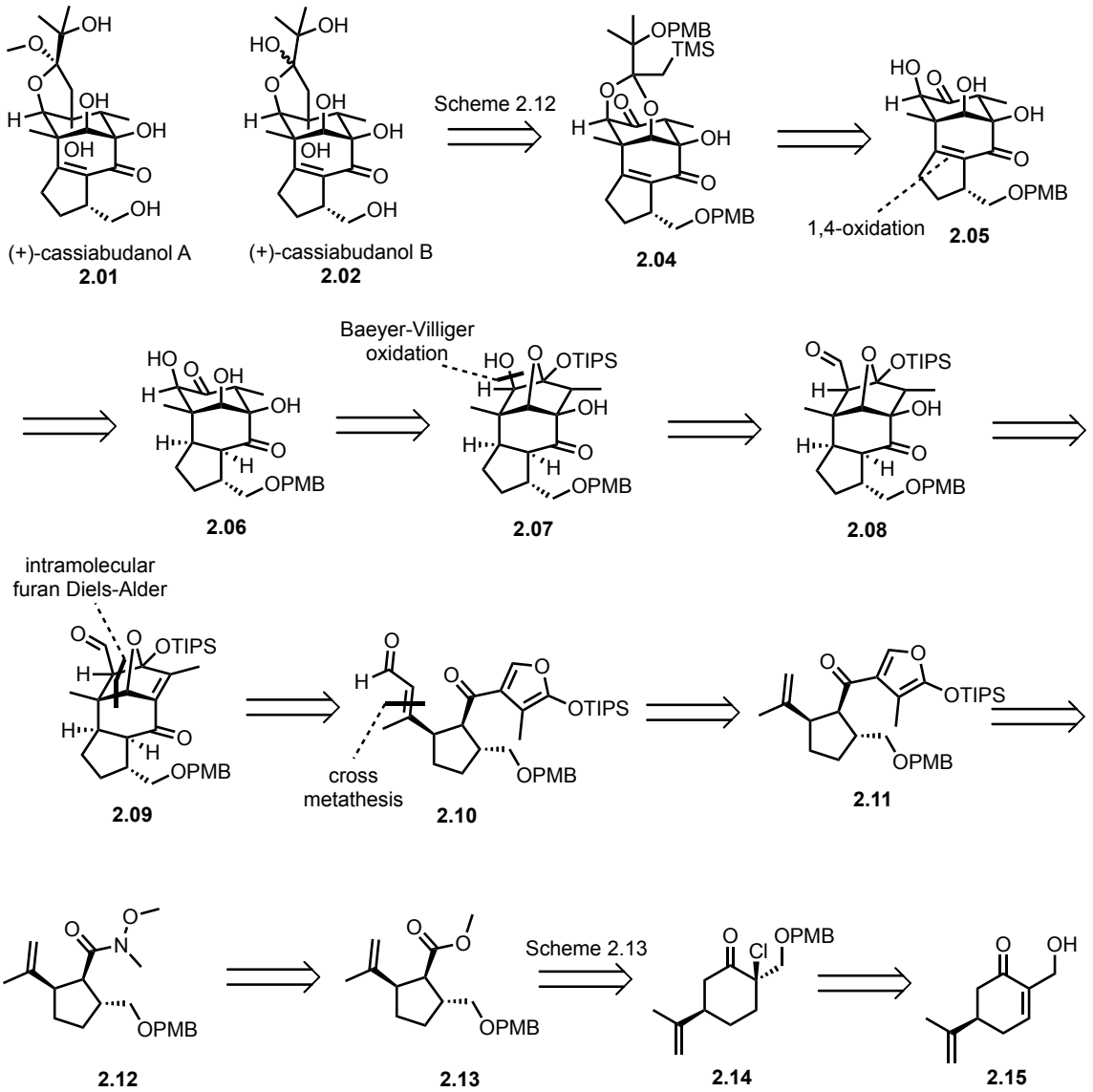

Scheme 2.2. Retrosynthetic analysis of cassiabudanols A (**2.01**) and B (**2.02**).

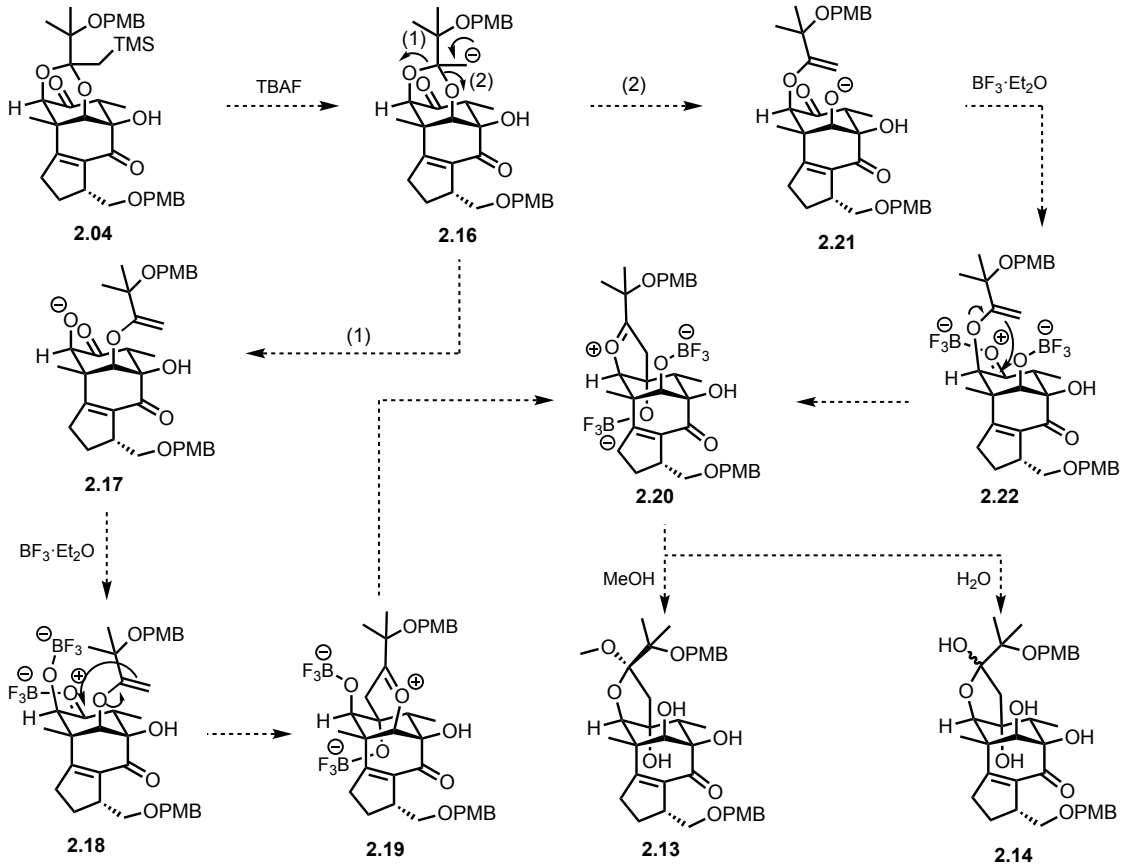

Scheme 2.3. Potential mechanistic pathways of the proposed anionic fragmentation of **2.04**.

In an alternative pathway, cleavage of the C–O illustrated in pathway 2 converts **2.16** to the distal oxyanion (**2.21**). In a fashion similar to that described above, BF_3•Et_2O can initiate an intramolecular Mukaiyama-type aldol reaction, which can directly lead to the formation of **2.20**. This mechanistic hypothesis supports that both pathways with C–O bond fragmentations could converge to the formation of the desired carbon skeleton.

As eluded to above, the stereoselective Favorskii rearrangement was based on literature precedent and inspired by the work of Lee and coworkers (Scheme 2.4).[2] Specifically, in their synthetic efforts toward (+)-dihydronepetalactone and (+)-iridomyrmecin, the Lee Group developed a diastereoselective ring-contraction strategy

wherein functionalized (-)-carvone (**2.23**) was subjected to diastereoselective Weitz-Scheffer epoxidation to furnish epoxide **2.24**. Treating of **2.24** with TMSCl promoted opening of the epoxide with concomitant delivery of chloride from to the more substituted carbon. Subsequent protection of the resulting secondary alcohol with DHP in the presence of catalytic acid produced the corresponding THP acetal (**2.25**). Subjecting **2.25** to standard Favorskii Rearrangement conditions led to formation of methyl ester **2.28** as the only isolable product, presumably through opening of cyclopronanone **2.26** via anionic intermediate **2.27**. The observed selectivity was noted and experimentally proven by Lee. Notably, Favorskii rearrangement on substrates lacking the OTHP moiety resulted in the formation of undesired products (Scheme 2.5). We hypothesized that we could leverage Lee's ring contraction strategy in our synthetic plan since **2.14** also bears a PMB ether albeit on a different beta-carbon.

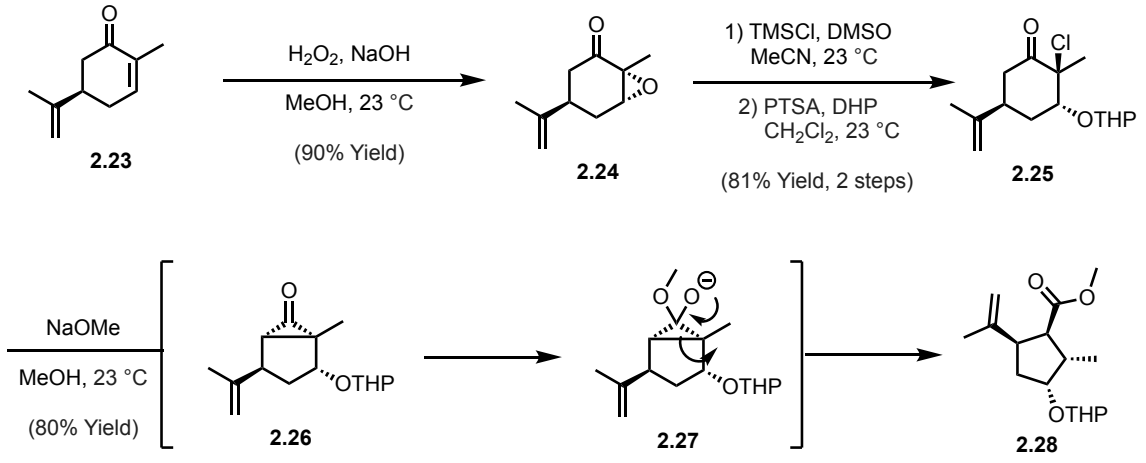

Scheme 2.4. Lee's ring contraction of functionalized carvone via Favorskii rearrangement.

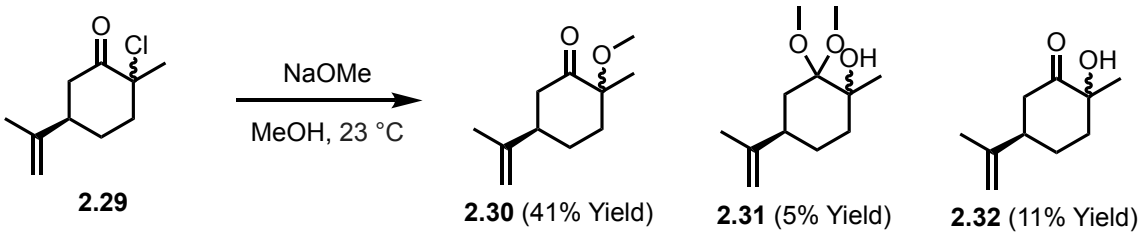

Scheme 2.5. Lee's failed ring-contraction without the OTHP group.

2.2.2 Synthesis of Known Beta-Hydroxycarvone

Our synthetic efforts commenced with attempts to deliver multi-gram quantities of known (*R*)-7-hydroxycarvone **2.15** by reproducing the work by Lakshmi and coworkers.[3] To this end, photooxygenation of (-)-α-pinene (**2.33**), followed by Swern oxidation of the derived epoxy-alcohol (**2.34**), afforded the desired epoxy-ketone (**2.34**) in excellent overall yield (Scheme 2.6). Unfortunately, attempts to complete the preparation of **2.15** via the reported BF_3•Et_2O induced epoxide/cyclobutane ring opening were met with consistently low yields (<10%). Usuki and coworkers reported similar difficulties in reproducing Lakshmi's work and eventually found that $Cu(OTf)_2$ promoted the ring opening with improved and more consistent yields (55%) even on a large scale.[4] Much to our chagrin, our attempts to employ these latter conditions resulted in only trace amounts of **2.15**. Thus, we decided to screen a variety of other Lewis acids (Table 2.1).

As depicted in Table 2.10, efforts to optimize the Lewis acid-mediated ring opening resulted in 40% yield of **2.15** using $Sc(OTf)_3$, a result similar to that reported by Usuki. Unfortunately, under these conditions the yields for reactions performed on gram-scale were very inconsistent. Upon further screening of different Lewis acids, such as $AlCl_3$, $ZnBr_2$, ZnI_2, and $AlMe_3$, we only observed either complex mixture or trace amounts of

2.15. Ultimately, we found that reproducibility was greatly improved on larger scales when $SnCl_4$ is employed as the Lewis acid.

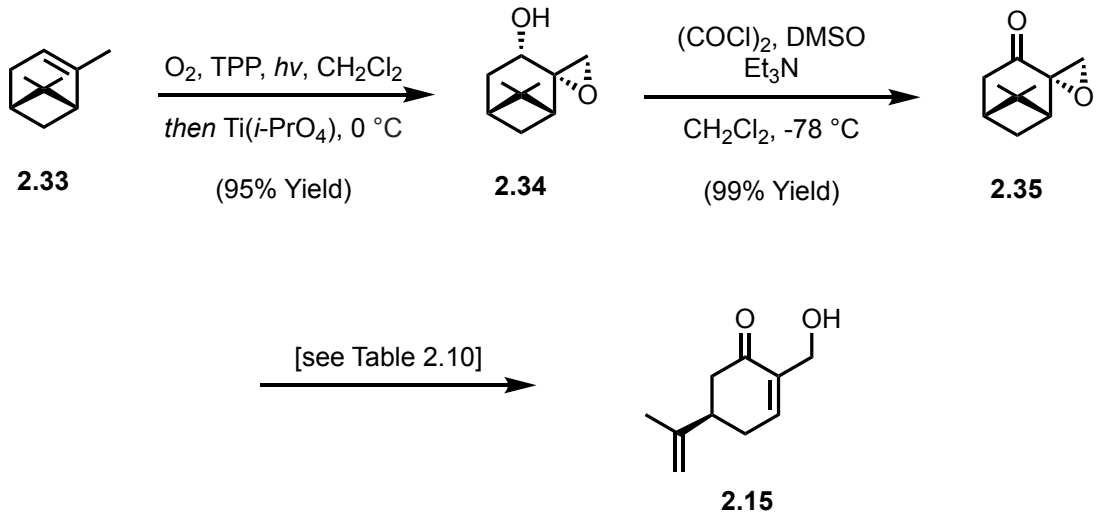

Scheme 2.6. Synthesis of (*R*)-7-hydroxycarvone **2.15**.

However, under the latter conditions **2.15** is produced in rather low yield (23%) and accompanied by chloride **2.36** as the major product.

Given the relative difficulty with larger scale ring openings, we also investigated the palladium-catalyzed direct acetoxylation of **2.23**, an effort inspired by recent reports from Xing and coworkers (Table 2.2).[5] Subjecting **2.23** to the reported conditions resulted in the desired allyl acetoxylation to afford **2.37**, albeit in a low yield (20%) as a 5:1 mixture with minor regioisomer **2.38**. Initial optimization efforts involved lowering the catalyst loading (Entry 1–5). Interestingly, upon decreasing the catalyst loading to 10 mol%, the ratio of the desired regioisomer decreased, but the overall yield increased. However, further decreasing the catalyst loading resulted in decreasing the ratio and the overall yield. Longer reaction time only led to slight decrease in both the ratio and the overall yield. Further optimization efforts focused on changing the atmosphere of the reaction. We first placed

the reaction under nitrogen and observed that the ratio did not change, but the yield was increased by 13%. Inspired by this finding, we degassed the reaction mixture with nitrogen and we were delighted to see the best yield of our optimization effort. Further screening with different additives proved to result only in diminished yields. Ultimately, the cost of $Pd(OAc)_2$, coupled with the inefficient access to **2.37**, even after the optimization efforts, led us stop pursuing the direct allylic acetoxylation strategy.

Table 2.1 Optimization of Lewis acid-mediated ring opening of **2.15**.

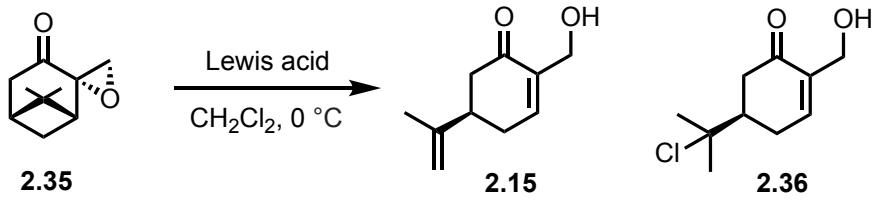

2.35 **2.15** **2.36**

Entry	Lewis acid	Time	Result
1	$BF_3 \cdot Et_2O$	4 h	10% Yield (**2.15**)*
2	$Cu(OTf)_2$	2 h	Trace (**2.15**)
3	$Sc(OTf)_3$	1 h	40% Yield (**2.15**)*
4	$AlCl_3$	4 h	Complex mixture
5	$ZnBr_2$	4 h	Trace (**2.15**)
6	ZnI_2	4 h	Trace (**2.15**)
7	$AlMe_3$	4 h	Trace (**2.15**)
8	$SnCl_4$	1.5 h	23% (**2.15**), 56% Yield (**2.36**)

* Yield decreases on gram-scale.

Turning our attention back to the former strategy, we focused on improving the sequence by salvaging chloride **2.36**. To this end, we explored the conversion of **2.36** to **2.15** by a base promoted dehydrohalogenation. To this end, attempting elimination with bases, such as DBU and potassium *tert*-butoxide, as well as several silver(I)-mediated conditions (e.g., AgOAc and AgOTf), only led to complex mixtures (Scheme 2.7). Speculating that the free alcohol could be the problem, we opted to install a protecting group. Initial attempts with PMBCl and PMB-trichloroacetimidate only led to complex mixtures. After some experimentation it was found that a modification of Dudley's protocol furnished excellent yields of the PMB-protected tertiary chloride **2.38**.[6] Exposure of **2.38** to sodium acetate in hot acetic acid for twelve hours resulted in conversion to enone **2.39**.

Table 2.2. Optimization efforts toward allylic acetoxylation.

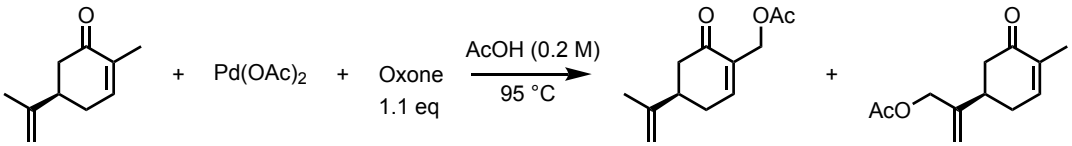

2.23
100 mg

2.37

2.38

Entry	Cat. Loading	Time	Yield (Yield of 2.37)	2.37:2.38 Ratio	Conditions
1	20 mol%	16 h	24% (20%)	5.0 : 1	–
2	10 mol%	16 h	38% (31%)	4.35 : 1	–
3	5 mol%	16 h	37% (28%)	2.94 : 1	–
4	1 mol%	16 h	33% (17%)	1.11 : 1	–
5	0.5 mol%	16 h	< 10% (< 3.5%)	0.53 : 1	–
6	5 mol%	41 h	34% (25%)	2.86 : 1	–
7	20 mol%	16 h	40% (33%)	5.0 : 1	Under N_2
8	5 mol%	16 h	48% (36%)	3.15 : 1	Degassed w/ N_2
9	5 mol%	16 h	20% (13%)	2.0 : 1	2.2 eq. oxone
10	5 mol%	16 h	39% (25%)	1.7 : 1	Degassed w/ O_2
11	5 mol%	16 h	29% (23%)	3.5 : 1	Added 2 drops of water
12	5 mol%	16 h	28% (19%)	2.2 : 1	$Mn(OAc)_2$ 1.1 eq.
13	5 mol%	16 h	23% (16%)	2.4 : 1	NaOAc 1.1 eq.
14	5 mol%	16 h	31% (25%)	3.8 : 1	500 mg of **2.23**

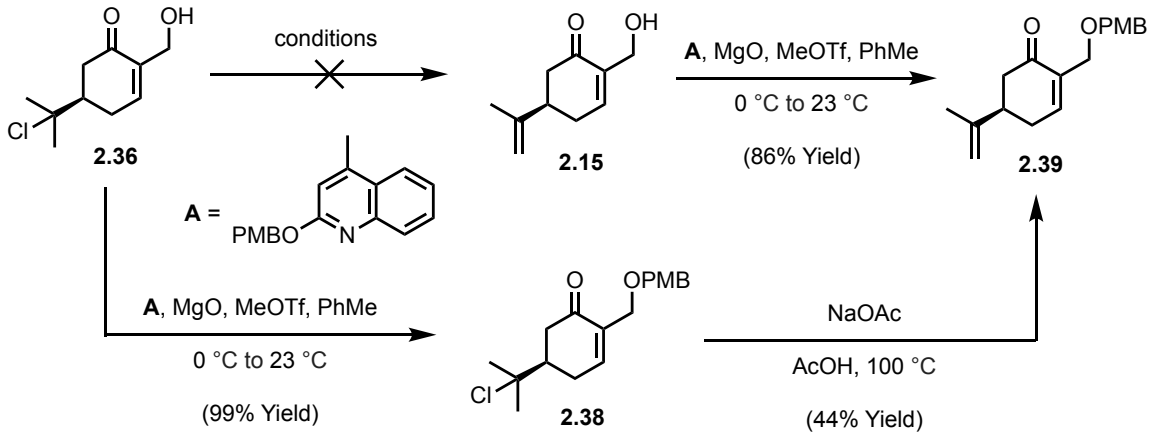

Scheme 2.7. Salvaging chloride **2.36**.

2.2.3 Favorskii Rearrangement

Having devised a reasonably efficient means for reproducibly accessing **2.39**, we turned our attention to setting the stage for ring contraction. Our efforts began with 1,4-reduction and installation of chlorine (Scheme 2.8). By exposing **2.39** to L-Selectride at -78 °C resulted in smooth reduction to an intermediate enolate which, upon subsequent introduction of NCS, initially provided **2.14** and **2.40** as an inseparable 1:1 mixture of diastereomers.[7] We hypothesized that the stereoelectronic preferences for cyclohexanone enolates (**2.41** vs. **2.42**) could be at play in the diastereomeric outcome. In hope of promoting reaction via the "chair-like" transition state we lowered the reaction temperature to -100 °C. Indeed, the diastereomeric ratio was improved to 2:1 in favor of the desired diastereomer **2.14**.

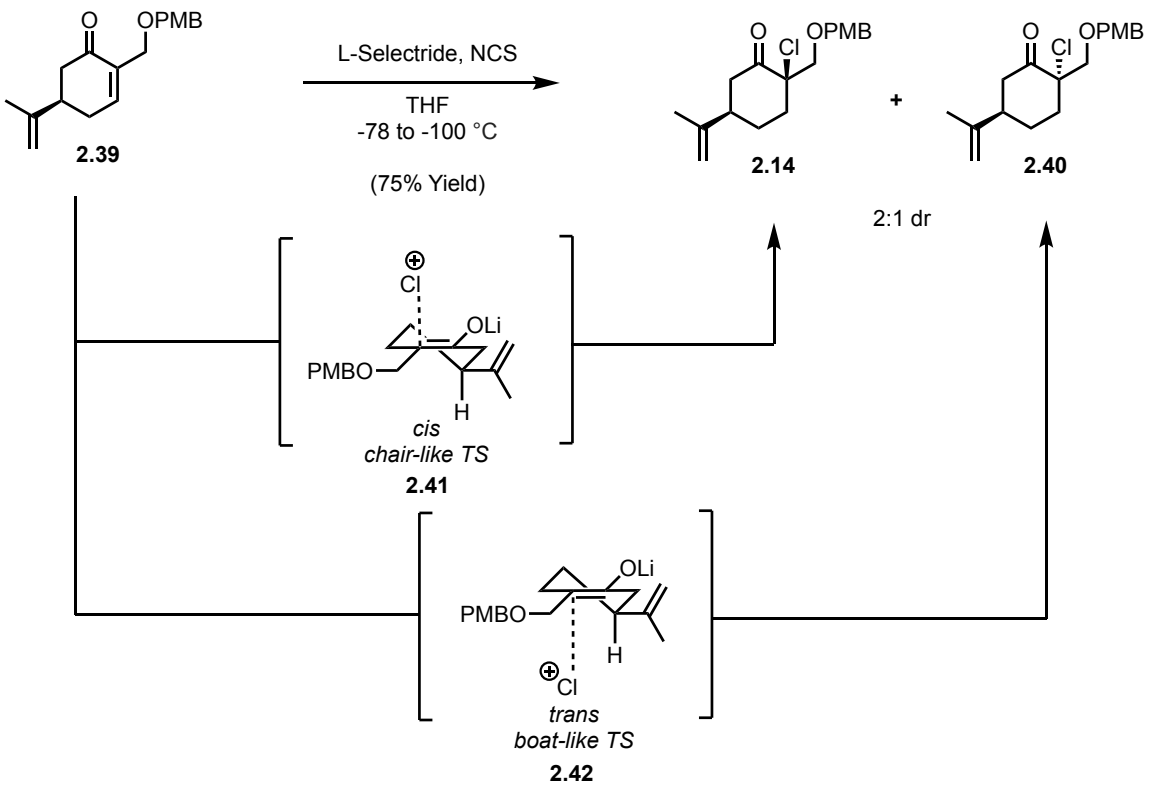

Scheme 2.8. Diastereoselective chlorination.

At this stage, the mixture of diastereomers **2.14** and **2.40** was subjected to Favorskii rearrangement under Lee's conditions (Scheme 2.9).[2] To our delight, the reaction proceeded smoothly to furnish methyl esters **2.13** and **2.43** in the same ratio as the ketone progenitor. In accord with our synthetic plan we next converted **2.13** and **2.43** to their corresponding Weinreb amides **2.12** and **2.44** by exposure to *N*,*O*-dimethyl hydroxylamine hydrochloride and *n*-BuLi. Not surprisingly, under these strongly basic conditions we observed a slight change in diastereomeric ratio (from 2:1 to 1.8:1). Less basic conditions, such as $AlMe_3$, only resulted in recovered starting material.

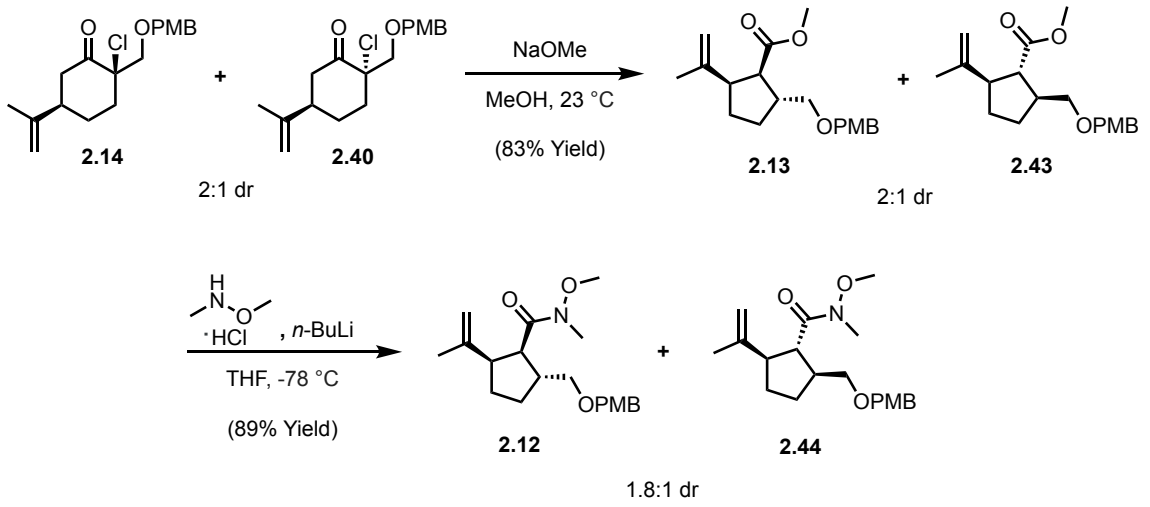

Scheme 2.9. Ring contraction via Favorskii rearrangement and Weinreb amide synthesis.

2.2.4 Failed Nucleophilic Acyl Substitution

At this point, we turned to introducing a functionalized furan via a nucleophilic acyl substitution into Weinreb amides **2.12** and **2.44**. After preparing known 3-bromofuran **2.45**, we subjected it to metal-halogen exchange with *t*-BuLi and then introduced the amides **2.12** and **2.44**.[8] Initially, we noticed that there was almost no conversion after stirring for 6 hours at -78 °C (Table 2.3). Further, any prolonged stirring (12 hours) did not improve the result. In efforts to improve conversion, we increased the temperature of the reaction gradually from -78 °C to -30 °C. Indeed, the warmer temperatures resulted in consumption of starting material. To our dismay, under these conditions we also observed a full migration of the 3-lithiated furan to the more stable 2-lithiated variant prior to nucleophilic addition. Given that our initial attempts were unsuccessful we sought to delay installing the furan moiety and turned toward functionalizing the isopropenyl group.

Table 2.3. Attempted nucleophilic acyl substitution with furan **2.45**.

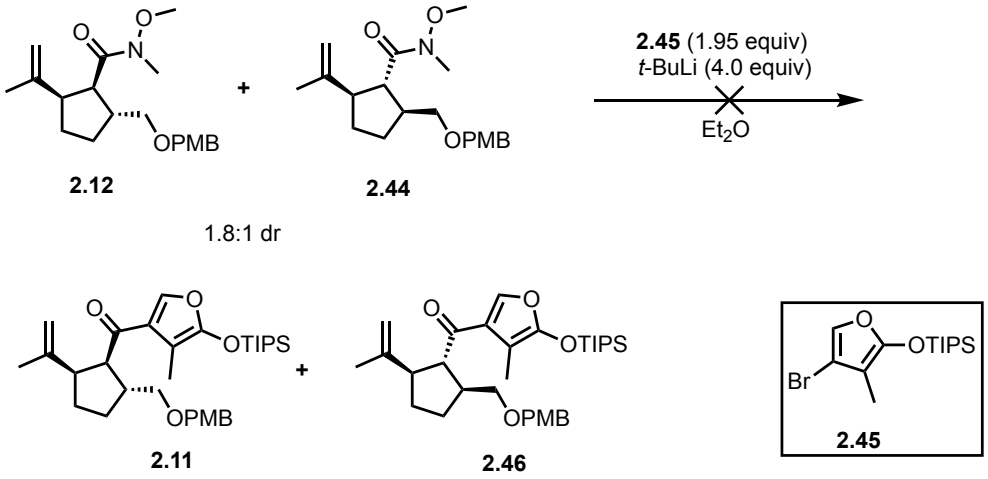

Entry	Temperature	Time	Result
1	-78 °C	6 h	trace conversion
2	-78 °C	12 h	trace conversion
3	-78 to -30 °C	12 h	C2 addition of **2.45**

2.2.5 Failed Cross-Metathesis Approach

As illustrated in our retrosynthetic plan (Scheme 2.2) we envisioned that a cross-metathesis reaction would allow for advancing the isopropenyl group to the requisite conjugated carbonyl, a structural element that would in turn serve as the dienophile in the proposed intramolecular Diels-Alder reaction. For our initial investigations of the metathesis, we utilized more accessible **2.13** and **2.43** as the substrates. In screening acrolein surrogates as the cross-metathesis partner, initial attempt with crotonaldehyde and second-generation Grubbs catalyst in refluxing CH_2Cl_2 only led to recovered starting material (Table 2.4). We then opted to change the cross-metathesis partner to 2-vinyl-1,3-

dioxolane. Under the same conditions as Entry 1, however, we again observed only returned starting material. Further optimization attempts were initiated that involved increasing the reaction temperature. Even after prolonged heating at 90 °C in toluene, we did not observe the consumption of **2.13** and **2.43**. Additionally, attempts with methacrylate as the cross-metathesis partner proved unsuccessful.

Table 2.4. Attempted cross-metathesis conditions.

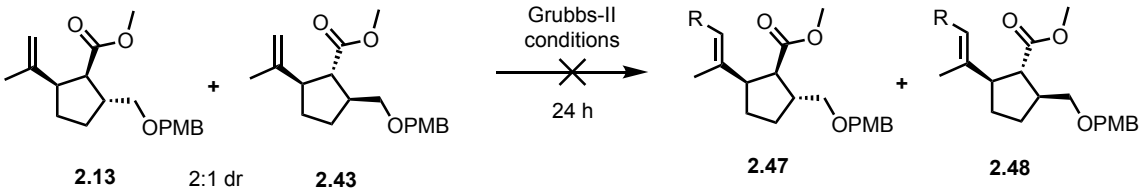

2.13 2:1 dr **2.43** **2.47** **2.48**

Entry	Substrate	R =	Solvent	Temperature	Result
1	crotonaldehyde	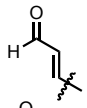	CH_2Cl_2	40 °C	recovered S.M.
2	2-vinyl-1,3-dioxolane	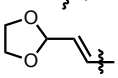	CH_2Cl_2	40 °C	recovered S.M.
3	2-vinyl-1,3-dioxolane	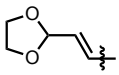	PhMe	90 °C	recovered S.M.
4	methacrylate	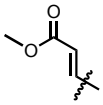	PhMe	90 °C	recovered S.M.

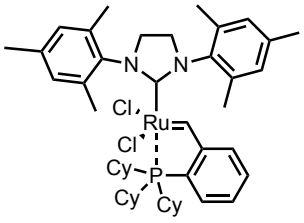

Grubbs-II

2.2.6 Separation of Diastereomers

To aid in the interpretation of the data we were obtaining in our optimization studies, it was decided that we should make a concerted effort to separate the

diastereomeric mixture. Up to this point, none of the diastereomeric mixtures we had prepared proved amenable to easy separation. However, we found that exchanging the hydroxy protecting group from PMB to TIPS produced a mixture that could be readily separated by standard column chromatography. As illustrated in Scheme 2.10, this protecting group interchange was performed by removal of the PMB group under oxidative conditions using DDQ to furnish alcohols **2.49** and **2.50**. Subsequent treatment of **2.49** and **2.50** TIPSOTf and Et_3N converted them to their corresponding silyl ethers **2.51** and **2.52**.

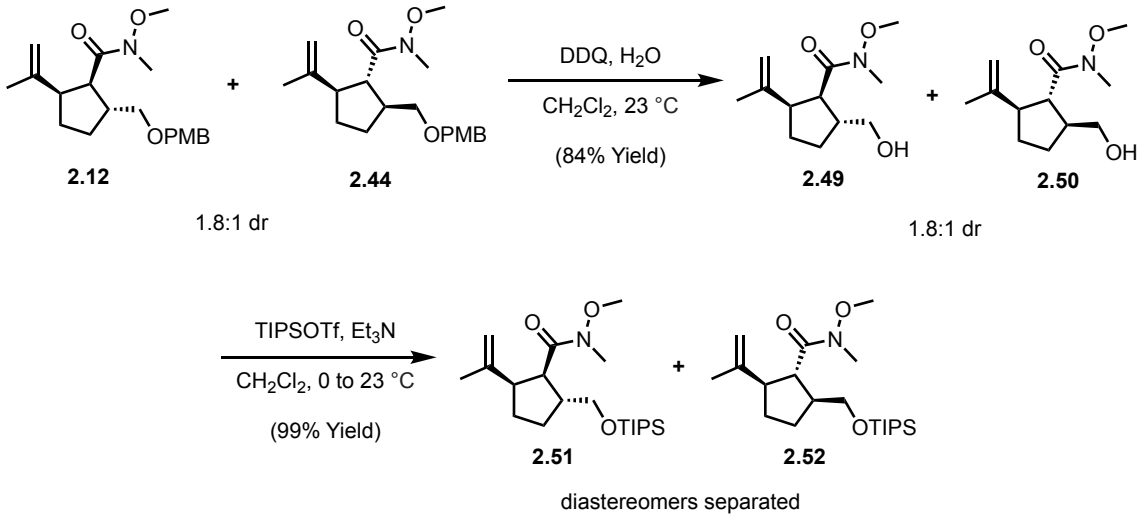

Scheme 2.10. Separation of diastereomeric mixture.

2.3 Future Work

Having established means of accessing a functionalized cyclopentane system, we envision accessing furan **2.53** via nucleophilic acyl substitution with lithiated **2.45** under optimized conditions (Scheme 2.11). With diastereomerically pure **2.53** in hand, we plan to construct the [3.3.1] bicyclic core present in **2.55** by tandem vinyl-nitration of the isopropenyl group to afford **2.54** using conditions developed by Maity and coworkers[9],

followed by an intramolecular Diels-Alder cycloaddition. The olefin resulting from the Diels-Alder reaction will be subjected to a Markovnikov hydration under conditions developed by Mukaiyama. Following diastereoselective installation of the requisite tertiary alcohol (**2.56**) we will introduce secondary alcohol (**2.57**) via Nef reaction/reduction sequence. Subsequently, we expect the more sensitive silyl acetal will undergo selective desilylation to promote a C–O ring opening to **2.59** via the intermediacy of **2.58**. At this point, the stage will be set for the formation of acetal **2.61** via condensation with bis(trimethylsilyl)ketone **2.60**. Finally, we will induce the anionic ring-opening by desilylation of the trimethylsilyl group to furnish **2.01** and **2.02** by addition of either methanol or water, respectively.

2.4 Conclusion

In conclusion, we have established access to asymmetric cyclopentane intermediate **2.12** in seven linear steps from commercially available of (-)-α-pinene **2.33**. The developed route features a diastereoselective chlorination and Favorskii rearrangement. As subsequent protecting group exchange was found to be required so as to allow separation of the diastereomeric mixture that was produced in the chlorination step. Access to diastereomerically pure advanced intermediates has enabled investigation into the end-game strategy.

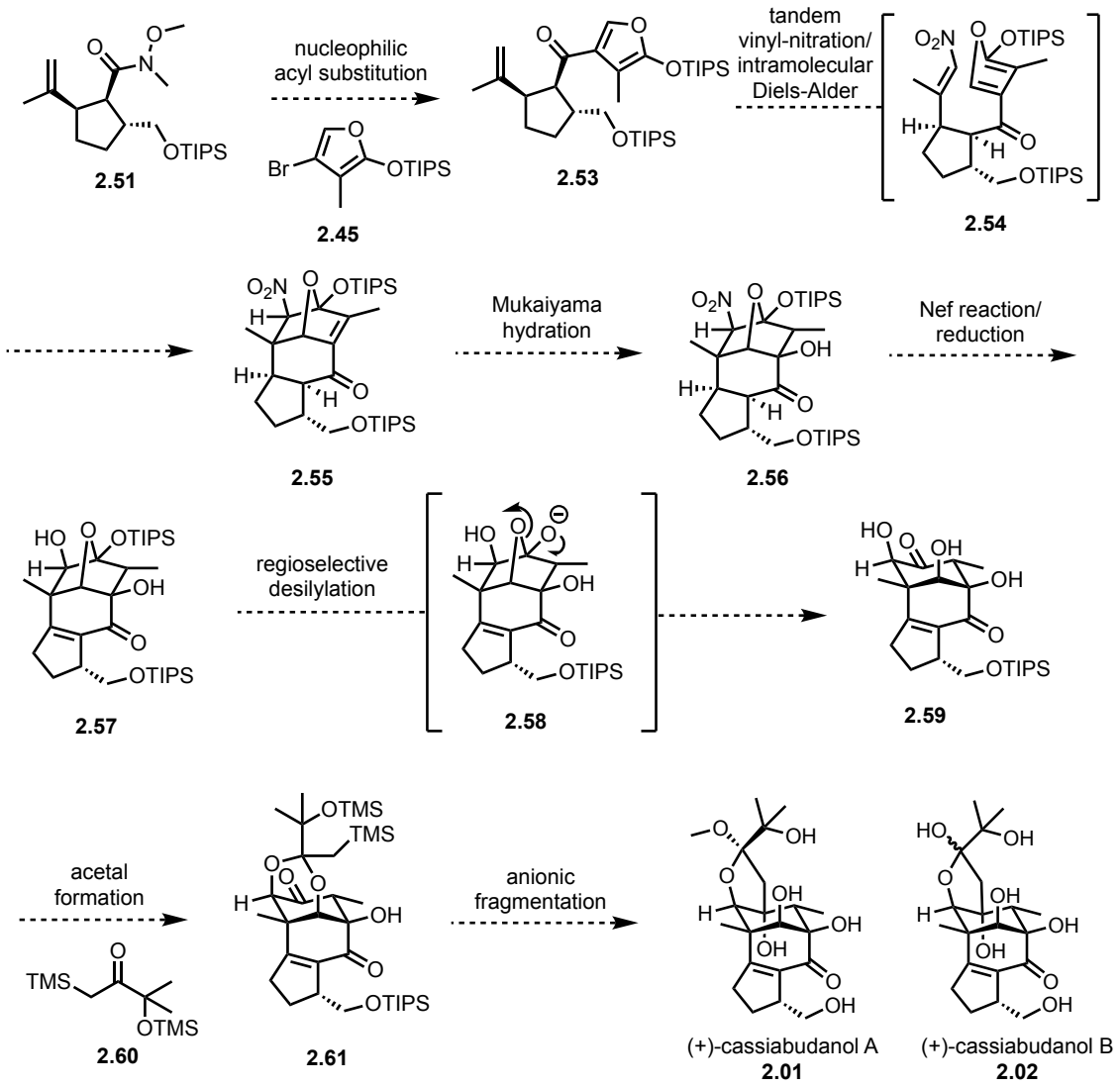

Scheme 2.11. Endgame strategy.

2.5 Experimental

2.5.1 General

Unless otherwise stated, all reactions were performed in flame- dried glassware under a nitrogen atmosphere, using reagents as received from the manufacturers. The reactions were monitored, and analytical samples purified by normal phase thin-layer

chromatography (TLC) using Millipore glass-backed 60 Å plates (indicator F-254, 250 μM). Tetrahydrofuran, dichloromethane, and toluene were dried using a solvent purification system manufactured by SG Water U.S.A., LLC. Methanol was dried over 3 Å molecular sieves purchased from Sigma-Aldrich. Manual flash chromatography was performed using the indicated solvent systems with Silicycle SiliaFlash® P60 (230–400 mesh) silica gel as the stationary phase. ^{1}H and ^{13}C NMR spectra were recorded on a Bruker Ascend^{TM} 400 MHz fitted with an autosampler or a Bruker Ascend^{TM} 600 MHz fitted with an autosampler. Chemical shifts (δ) are reported in parts per million (ppm) relative to the residual solvent resonance ($CHCl_3$ = 7.26 ppm (^{1}H NMR)/ 77.16 ppm (^{13}C NMR)) and coupling constants (*J*) are reported in Hertz (Hz). Coupling pattern abbreviations are as follows: s = singlet, d = doublet, dd = doublet of doublets, m = multiplet. The IR spectra were obtained using a Bruker Platinum-ATR IR spectrometer equipped with a diamond window. High Resolution mass spectra (HRMS) were obtained in the Baylor University Mass Spectrometry Center on a Thermo Scientific LTQ Orbitrap Discovery spectrometer using +ESI and reported for the molecular ion ($[M+H]^+$ & $[M+Na]^+$). Optical rotations were obtained using a Rudolph Research Analytical Autopol IV Automatic Polarimeter with samples prepared in Chloroform purchased from Fisher Chemical (HPLC grade; approx. 0.75% Ethanol as preservative).

*2.5.2 Preparation of tertiary chloride **2.36***

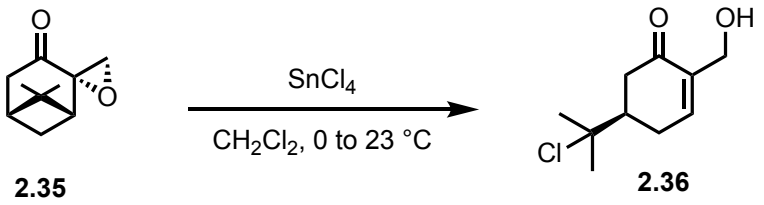

2.35 **2.36**

To a flame-dried round bottom flask equipped with a stir bar was added epoxy-ketone **2.53**[3] (11.0 g, 66.4 mmol 1.0 equiv) and dry CH_2Cl_2 (330 mL, 0.2 M). The flask was capped with a rubber septum, flushed with N_2 solution and then cooled to 0 °C in an ice bath. To the solution was added $SnCl_4$ (100.0 mL, 1.0 M in CH_2Cl_2, 100.0 mmol, 1.5 equiv) dropwise and the resulting solution was warmed to 23 °C. After stirring for 1.5 h, the reaction mixture was quenched with saturated aqueous $NaHCO_3$ solution (300 mL) and stirred for 5 min. The mixture was then transferred to a separatory funnel and diluted with CH_2Cl_2 (200 mL) and water (200 mL). The layers were partitioned, and the aqueous layer was extracted with CH_2Cl_2 (3 x 200 mL). The combined organic layer was dried over anhydrous sodium sulfate, filtered, and concentrated under reduced pressure. The residue was purified via flash column chromatography: silica gel, 33% ethyl acetate in hexanes. This yielded 7.6 g (56% yield) of tertiary chloride **2.36** as a yellow oil. **^{1}H NMR** (400 MHz, $CDCl_3$) δ 6.95 (d, J = 7.0 Hz, 1H), 4.24 (s, 2H), 2.75 – 2.57 (m, 2H), 2.51 – 2.37 (m, 2H), 2.32 – 2.19 (m, 1H), 1.59 (s, 3H), 1.57 (s, 3H). **^{13}C NMR** (151 MHz, $CDCl_3$) δ 199.9, 145.8, 137.9, 72.0, 61.4, 46.9, 40.2, 30.6, 30.4, 27.7. **FTIR** (Neat) 3413, 2976, 2932, 1663, 1454, 1431, 1389, 1372, 1305, 1250, 1208, 1184, 1148, 1110, 1059, 1009, 992, 909, 887, 806, 730, 690, 647, 603, 562, 481 cm^{-1}. **HRMS** (ESI+) m/z: calc'd for $[M+Na]^+$ $C_{10}H_{15}O_2ClNa^+$ = 225.0653, found $C_{10}H_{15}O_2ClNa^+$ = 225.0653. $\mathbf{R_f}$ = 0.40 (50% EtOAc/hexanes). $[\boldsymbol{\alpha}]_D^{24.1}$: (c = 1.36, $CHCl_3$), -12.6°.

This reaction also produced 2.5 g (23% yield) of (*R*)-7-hydroxycarvone **2.15** as a yellow oil.[3]

*2.5.3 Preparation of (R)-7-para-methoxybenzyloxycarvone **2.39***

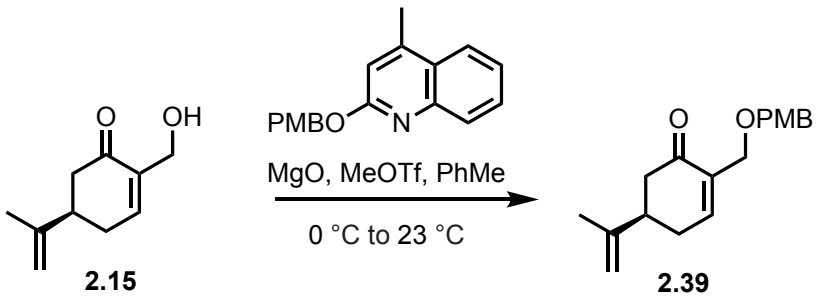

To a flame-dried round bottom flask equipped with a stir bar was added (*R*)-7-hydroxycarvone **2.15** (2.5 g, 15.0 mmol, 1.0 equiv) followed by 2-PMBO-lepidine (8.4 g, 30.1 mmol, 2.0 equiv), and dry toluene (111 mL, 0.135 M). The resultant solution was treated with MgO (1.2 g, 30.1 mmol, 2.0 equiv) and then cooled to 0 °C in an ice bath. The cooled suspension was treated with MeOTf (3.3 mL, 30.1 mmol, 2.0 equiv, added dropwise) and then warmed to 23 °C. After stirring for 12 h, the reaction mixture was filtered through a pad of Celite® and the filtercake was rinsed with ethyl acetate (100 mL). The organic layer was washed with brine (200 mL), dried over anhydrous sodium sulfate, filtered, and concentrated under reduced pressure. The residue was purified via flash column chromatography: silica gel, 20% ethyl acetate in hexanes. This yielded 3.7 g (86% yield) of (*R*)-7-*para*-methoxybenzyloxycarvone **2.39** as a pale, yellow oil. **^{1}H NMR** (400 MHz, $CDCl_3$) δ 7.30 – 7.24 (m, 2H), 7.05 – 7.03 (m, 1H), 6.91 – 6.84 (m, 2H), 4.84 – 4.79 (m, 1H), 4.76 (s, 1H), 4.50 (s, 2H), 4.17 (d, *J* = 1.2 Hz, 2H), 3.79 (s, 3H), 2.75 – 2.63 (m, 1H), 2.57 – 2.45 (m, 2H), 2.42 – 2.25 (m, 2H), 1.75 (s, 3H). **^{13}C NMR** (151 MHz, $CDCl_3$)

δ 198.6, 159.3, 146.6, 145.6, 136.2, 130.4, 129.4, 113.9, 110.7, 72.8, 66.5, 55.3, 43.2, 42.1, 31.0, 20.6. **FTIR** (neat) 2888, 1891, 1785, 1670, 1511, 1453, 1351, 1247, 1173, 1101, 959, 889, 834, 704, 513 cm^{-1}. **HRMS** (ESI+) m/z: calc'd for $[M+Na]^+$ $C_{18}H_{22}O_3Na$ = 309.1461, found $C_{18}H_{22}O_3Na$ = 309.1469. $\mathbf{R_f}$ = 0.78 (50% EtOAc/hexanes). $[\boldsymbol{\alpha}]_D^{22.7}$: (*c* = 5.19, $CHCl_3$), -13.3°.

*2.5.4 Preparation of tertiary chloride **2.38***

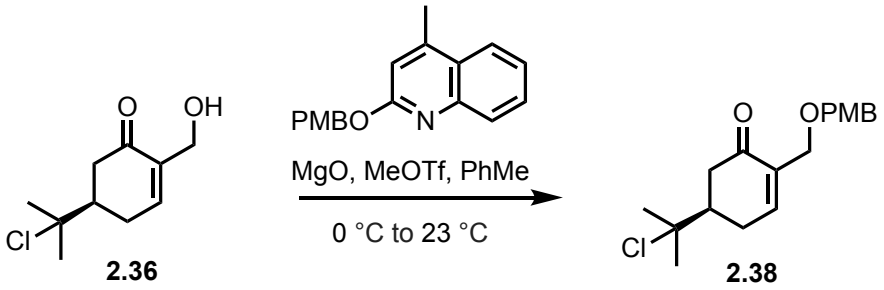

To a flame-dried round bottom flask equipped with a stir bar was added tertiary chloride **2.36** (7.6 g, 37.5 mmol, 1.0 equiv) followed by 2-PMBO-lepidine (21.0 g, 75.0 mmol, 2.0 equiv), and dry toluene (278 mL, 0.135 M). The resultant solution was treated with MgO (3.0 g, 75.0 mmol, 2.0 equiv) then cooled to 0 °C in an ice bath. The cooled suspension treated with MeOTf (8.2 mL, 75.0 mmol, 2.0 equiv, added dropwise) and then warmed to 23 °C. After stirring for 12 h, the reaction mixture was filtered through a pad of Celite® and the filtercake was rinsed with ethyl acetate (250 mL). The organic layer was washed with brine (500 mL), dried over anhydrous sodium sulfate, filtered, and concentrated under reduced pressure. The residue was purified via flash column chromatography: silica gel, 20% ethyl acetate in hexanes. This yielded 12.0 g (99% yield) of tertiary chloride **2.38** as a clear oil. **^{1}H NMR** (400 MHz, $CDCl_3$) δ 7.32 – 7.23 (m, 2H), 7.08 – 7.01 (m, 1H), 6.94 – 6.84 (m, 2H), 4.50 (s, 2H), 4.18 – 4.15 (m, 2H), 3.80 (s, 3H), 2.78 – 2.56 (m, 2H), 2.49 – 2.35 (m, 2H), 2.29 – 2.20 (m, 1H), 1.60 (s, 3H), 1.58 (s, 3H).

^{13}C NMR (151 MHz, $CDCl_3$) δ 198.2, 159.4, 145.4, 136.2, 130.4, 129.5, 113.9, 72.9, 72.1, 66.4, 55.4, 47.0, 40.3, 30.7, 30.4, 27.8. **FTIR** (neat) 2857, 1668, 1611, 1511, 1455, 1372, 1301, 1244, 1173, 1112, 1077, 1031, 908, 817 cm^{-1}. **HRMS** (ESI+) m/z: calc'd for $[M+Na]^+$ $C_{18}H_{23}O_3ClNa$ = 345.1228, found $C_{18}H_{23}O_3ClNa$ = 345.1237. $\mathbf{R}_f$ = 0.70 (50% EtOAc/hexanes). $[\boldsymbol{\alpha}]_D^{23.8}$: (*c* = 0.65, $CHCl_3$), -14.8°.

*2.5.5 Preparation of (R)-7-para-methoxybenzyloxycarvone **2.39***

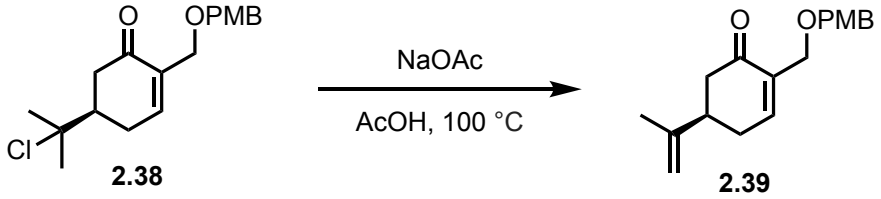

To a round bottom flask equipped with a stir bar was added tertiary chloride **2.38** (3.4 g, 10.6 mmol, 1.0 equiv), NaOAc (8.7 g, 105.9 mmol, 10.0 equiv), and AcOH (35 mL, 0.3 M). The resulting mixture was heated to 100 °C and stirred for 14 h. The flask was then removed from the heat and cooled to 23 °C. The reaction mixture was diluted with CH_2Cl_2 (150 mL) and water (200 mL). The aqueous layer was extracted with CH_2Cl_2 (3 x 100 mL). The combined organic layers were washed with saturated aqueous $NaHCO_3$ solution until gas evolution ceased and then washed with brine (150 mL). The organic layer was dried over anhydrous sodium sulfate, filtered, and concentrated under reduced pressure. The residue was purified via flash column chromatography: silica gel, 20% ethyl acetate in hexanes. This yielded 1.3 g (44% yield) of (*R*)-7-*para*-methoxybenzyloxycarvone **2.39** as a pale, yellow oil.

Spectral data matched the previous report (see *2.5.3*).

*2.5.6 Preparation of chloroketone **2.14***

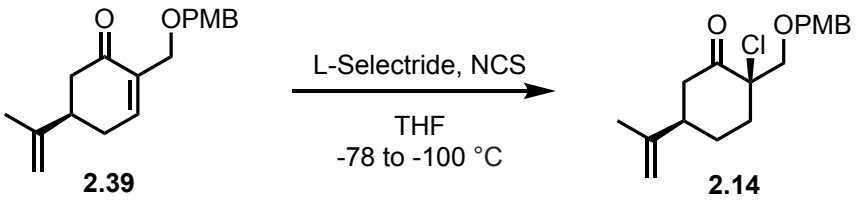

2.39 **2.14**

To a flame-dried flask equipped with a stir bar was added (*R*)-7-*para*-methoxybenzyloxycarvone **2.39** (2.6 g, 9.1 mmol, 1.0 equiv) and dry THF (90 ml, 0.1 M). The flask was flushed with argon, cooled to -78 ˚C and treated with the dropwise addition of L-Selectride (11 mL, 1.0 M in THF, 11.0 mmol, 1.2 equiv). After stirring for 2 h, the reaction mixture was cooled to -100 ºC using a dry ice/liquid nitrogen/acetone bath and then a suspension of NCS (7.3 g, 54.5 mmol, 6.0 equiv) in dry THF (90 mL) was added by syringe. After stirring for 3 h, the reaction was quenched by the addition of water (150 mL) and warmed to 23 ˚C. The reaction mixture was diluted with ethyl acetate (100 mL) poured into a separatory funnel and washed with water (4 x 100 mL). The organic layer was washed with brine (200 mL), dried over anhydrous sodium sulfate, filtered, and concentrated under reduced pressure. The residue was purified via flash column chromatography: silica gel, 10% ethyl acetate in hexanes. This yielded 2.2 g (75% yield) of chloroketone **2.14** as a clear oil (2:1 diastereomeric mixture). **^{1}H NMR** (400 MHz, $CDCl_3$) δ 7.30 – 7.20 (m, 2H), 6.92 – 6.83 (m, 2H), 4.85 – 4.83 (m, 0.4H), 4.80 – 4.77 (m, 0.6H), 4.76 (s, 0.6H), 4.63 (s, 0.4H), 4.60 – 4.52 (m, 1.6H), 4.49 (d, *J* = 11.7 Hz, 0.4H), 3.88 (d, *J* = 10.3 Hz, 0.6H), 3.83 (d, *J* = 10.4 Hz, 0.5H), 3.81 – 3.78 (m, 3H), 3.76 (d, *J* = 10.4 Hz, 0.4H), 3.65 (d, *J* = 10.3 Hz, 0.6H), 3.02 – 2.88 (m, 1H), 2.68 – 2.60 (m, 0.4H), 2.53 – 2.47 (m, 0.4H), 2.42 – 2.26 (m, 2H), 2.19 – 2.06 (m, 1.5H), 2.05 – 1.93 (m, 0.6H), 1.88 – 1.77 (m, 1H), 1.75 (s, 1.8H), 1.70 (s, 1.2H). **^{13}C NMR** (101 MHz, $CDCl_3$) δ 203.6,

203.4, 159.41, 159.39, 147.0, 146.0, 130.1, 129.9, 129.48, 129.46, 113.90, 113.88, 112.2, 110.0, 73.50, 73.45, 72.9, 72.5, 69.9, 55.4, 45.6, 42.9, 42.2, 42.0, 36.2, 34.3, 25.9, 24.5, 21.7, 20.4. **FTIR** (neat) 2938, 1717, 1645, 1612, 1512, 1453, 1360, 1302, 1245, 1172, 1086, 1034, 895, 818, 736, 637, 575, 514 cm^{-1}. **HRMS (**ESI+) m/z: calc'd for $[M+Na]^+$ $C_{18}H_{23}O_3ClNa$ = 345.1228, found $C_{18}H_{23}O_3ClNa$ = 345.1234. $\mathbf{R_f}$ = 0.38 (10% EtOAc/hexanes). $[\boldsymbol{\alpha}]_D^{22.8}$: (c = 1.76, $CHCl_3$), +31.7°.

*2.5.7 Preparation of methyl ester **2.13***

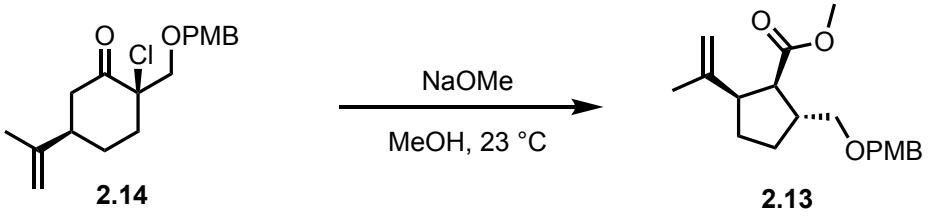

2.14 **2.13**

To a flame-dried round bottom flask equipped with a stir bar was added chloroketone **2.14** (2.2 g, 6.5 mmol, 1.0 equiv) and dry MeOH (14.0 mL, 0.5 M). Following this was added a solution of NaOMe (2.0 mL, 30% in MeOH, 10.2 mmol, 1.5 equiv) at 23 °C. After stirring for 10 min, the reaction mixture was quenched with water (10 mL) and saturated aqueous NH_4Cl solution (20 mL). The aqueous layer was extracted with CH_2Cl_2 (3 x 20 mL). The combined organic layer was dried over anhydrous sodium sulfate, filtered, and concentrated under reduced pressure. The residue was purified via flash column chromatography: silica gel, 10% ethyl acetate in hexanes. This yielded 1.8 g (83% yield) of methyl ester **2.13** as a clear oil (2:1 diastereomeric mixture). **^{1}H NMR** (400 MHz, $CDCl_3$) δ 7.30 – 7.18 (m, 2H), 6.92 – 6.83 (m, 2H), 4.78 – 4.73 (m, 1H), 4.70 (d, *J* = 1.5 Hz, 1H), 4.48 – 4.38 (m, 2H), 3.82 – 3.78 (m, 3H), 3.61 (s, 1H), 3.57 (s, 1.6H), 3.51 – 3.28 (m, 2H), 3.17 (s, 0.2H), 2.93 (dd, *J* = 8.6, 4.8 Hz, 0.6H), 2.88 – 2.77 (m, 0.4H), 2.77 – 2.62

(m, 1.3H), 2.61 – 2.52 (m, 0.5H), 2.46 (dd, J = 10.5, 9.0 Hz, 0.4H), 2.10 – 2.08 (m, 0.2H), 2.06 – 1.82 (m, 2H), 1.78 – 1.68 (m, 4H), 1.59 – 1.46 (m, 1H), 4.85 – 1.28 (m, 0.6H). **^{13}C NMR** (101 MHz, $CDCl_3$) δ 176.2, 175.3, 159.23, 159.19, 145.9, 145.2, 130.8, 129.6, 129.23, 129.21, 113.9, 113.8, 110.7, 110.6, 73.4, 73.1, 72.7, 72.6, 55.4, 52.44, 52.36, 51.7, 51.3, 50.9, 50.0, 44.5, 42.3, 30.6, 29.3, 28.2, 27.9, 23.1, 20.1. (one methoxy peak is either missing or overlapping with other peaks). **FTIR** (neat) 2949, 2858, 1730, 1677, 1646, 1612, 1586, 1512, 1435, 1373, 1362, 1301, 1245, 1194, 1171, 1089, 1034, 891, 819, 516 cm^{-1}. **HRMS (**ESI+) m/z: calc'd for $[M+Na]^+$ $C_{19}H_{26}O_4Na$ = 341.1723, found $C_{19}H_{26}O_4Na$ = 341.1741. $\mathbf{R}_f$ = 0.28 (10% EtOAc/hexanes). $[\boldsymbol{\alpha}]_D^{22.9}$: (c = 1.01, $CHCl_3$), -0.66°.

*2.5.8 Preparation of amide **2.12***

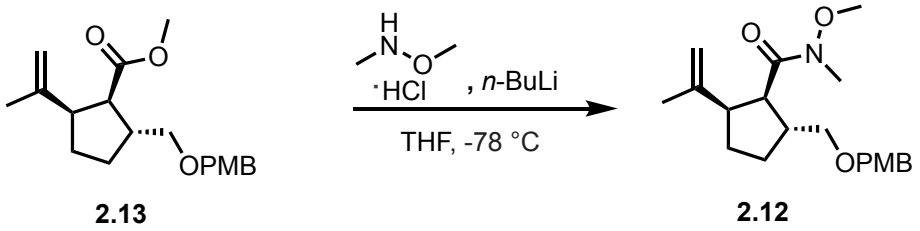

2.13 **2.12**

To a flame-dried round bottom flask equipped with a stir bar was added *N,O*-dimethylhydroxylamine hydrochloride (1.7 g, 17.0 mmol, 3.0 equiv) and dry THF (30 mL, 0.19 M). The flask was flushed with argon and then the suspension was cooled to -78 °C. The cooled suspension was added *n*-BuLi (13.6 mL, 34.0 mmol, 2.5 M in hexane, 6.0 equiv) dropwise. After stirring for 30 min, the ice bath was removed, and the reaction allowed to warm to 23 °C. After stirring for another 30 min at 23 °C, the reaction mixture was re-cooled to -78 °C. The cool reaction was treated by the dropwise addition of methyl ester **2.13** (1.8 g, 5.7 mmol, 1.0 equiv) in dry THF (10 mL). After stirring for 2 h, the mixture was quenched with saturated NH_4Cl aqueous solution (50 mL). The aqueous layer

was extracted with ethyl acetate (3 x 30 mL). The combined organic layer was dried over anhydrous sodium sulfate, filtered, and concentrated under reduced pressure. The residue was purified via flash column chromatography: silica gel, 10% ethyl acetate in hexanes. This yielded 1.7 g (89% yield) of amide **2.12** as a clear oil (1.8:1 diastereomeric mixture). **^{1}H NMR** (400 MHz, $CDCl_3$) δ 7.25 – 7.20 (m, 2H), 6.89 – 6.82 (m, 2H), 4.79 – 4.65 (m, 2H), 4.47 – 4.65 (m, 2H), 3.80 (s, 3H), 3.63 – 3.56 (m, 3H), 3.45 – 3.33 (m, 2H), 3.16 (d, *J* = 20.8 Hz, 1H), 3.10 (s, 2H), 2.97 – 2.56 (m, 2H), 2.09 – 1.82 (m, 2H), 1.82 – 1.74 (m, 1H), 1.74 – 1.69 (m, 3H), 1.67 – 1.51 (m, 1H), 1.44 – 1.23 (m, 1H). **^{13}C NMR** (151 MHz, $CDCl_3$) δ 176.8, 175.8, 159.14, 159.12, 146.5, 145.7, 130.8, 130.75, 129.3, 129.2, 113.74, 113.70, 111.3, 110.6, 73.5, 72.9, 72.54, 72.51, 61.31, 61.27, 60.5, 60.3, 55.3, 52.6, 49.8, 46.7, 44.7, 42.7, 30.4, 30.1, 28.4, 28.3, 22.7, 21.4, 20.1, 14.3. **FTIR** (neat) 2938, 2858, 1654, 1612, 1586, 1512, 1460, 1442, 1420, 1385, 1374, 1362, 1301, 1245, 1173, 1087, 1033, 888, 819 cm^{-1}. **HRMS (**ESI+) m/z: calc'd for $[M+Na]^+$ $C_{20}H_{29}NO_4Na$ = 370.1989, found $C_{20}H_{29}NO_4Na$ = 370.2006. $\mathbf{R_f}$ = 0.11 (10% EtOAc/hexanes). $[\boldsymbol{\alpha}]_D^{24.6}$: (c = 0.34, $CHCl_3$), -9.41°.

*2.5.9 Preparation of alcohol **2.49***

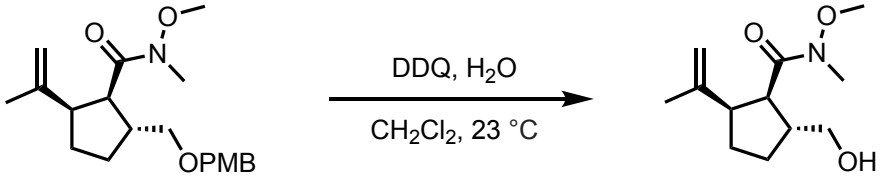

2.12 **2.49**

To a round bottom flask equipped with a stir bar was added amide **2.12** (1.7 g, 4.9 mmol, 1.0 equiv), CH_2Cl_2 (49 mL, 0.1 M), water (2.7 mL), and then was DDQ (1.7 g, 7.4 mmol, 1.5 equiv). After stirring for 12 h at 23 °C the reaction mixture was quenched with

saturated $NaHCO_3$ aqueous solution (50 mL). The aqueous layer was extracted with CH_2Cl_2 (3 x 30 mL). The combined organic layer was washed with saturated $NaHCO_3$ aqueous solution (50 mL) and brine (50 mL). The organic layer was then dried over anhydrous sodium sulfate, filtered, and concentrated under reduced pressure. The residue was purified via flash column chromatography: silica gel, 60% ethyl acetate in hexanes. This yielded 0.94 g (84% yield) of alcohol **2.49** as a clear oil (1.8:1 diastereomeric mixture). **^{1}H NMR** (400 MHz, $CDCl_3$) δ 4.76 – 4.64 (m, 2H), 3.67 (s, 3H), 3.64 – 3.54 (m, 1H), 3.51 – 3.38 (m, 1H), 3.19 – 3.07 (m, 3H), 2.98 – 2.83 (m, 2H), 2.67 – 2.55 (m, 0.6H), 2.48 – 2.36 (m, 1.4H), 2.01 – 1.73 (m, 2.6H), 1.68 (s, 3H), 1.65 – 1.42 (m, 1H), 1.33 – 1.19 (m, 0.5H). **^{13}C NMR** (101 MHz, $CDCl_3$) δ 176.8, 175.9, 146.3, 145.8, 111.5, 110.5, 66.5, 65.6, 61.5, 61.3, 52.2, 49.6, 48.3, 48.1, 47.7, 45.0, 32.5, 32.3, 30.1, 30.0, 28.0, 27.7, 22.3, 20.1. **FTIR** (neat) 3421, 2941, 2869, 1737, 1635, 1440, 1387, 1375, 1240, 1178, 996, 889, 732, 440 cm^{-1}. **HRMS** (ESI+) m/z: calc'd for $[M+Na]^+$ $C_{12}H_{21}NO_3Na$ = 250.1414, found $C_{12}H_{21}NO_3Na$ = 250.1430. $\mathbf{R_f}$ = 0.075 (50% EtOAc/hexanes). $[\boldsymbol{\alpha}]_D^{25.3}$: (c = 0.16, $CHCl_3$), -22.8°.

*2.5.10 Preparation of silyl ether **2.51***

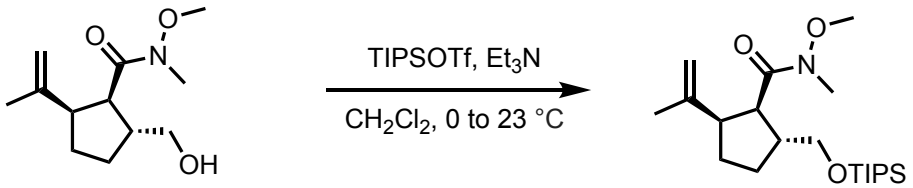

2.49 **2.51**

To a flame-dried round bottom flask equipped with a stir bar was added alcohol **2.49** (710 mg, 3.1 mmol, 1.0 equiv) and dry CH_2Cl_2 (16 mL, 0.2 M). The flask was flushed with argon and then the solution was cooled to 0 °C. After cooling the reaction mixture

was treated sequentially with Et_3N (0.66 mL, 4.7 mmol, 1.5 equiv) and TIPSOTf (0.88 mL, 3.3 mmol, 1.05 equiv) and then the resultant mixture was warmed to 23 ˚C. After stirring for 1 h, the reaction mixture was quenched with water (20 mL). The aqueous layer was extracted with CH_2Cl_2 (2 x 10 mL). The combined organic layer was washed with brine (20 mL), dried over anhydrous sodium sulfate, filtered, and concentrated under reduced pressure. The residue was purified via flash column chromatography: silica gel, 5% ethyl acetate in hexanes. This yielded 0.76 g (64% yield) of silyl ether **2.51**. **^{1}H NMR** (400 MHz, $CDCl_3$) δ 4.75 (s, 2H), 3.69 – 3.61 (m, 5H), 3.40 (s, 1H), 3.11 (s, 3H), 2.89 – 2.78 (m, 1H), 2.66 – 2.55 (m, 1H), 2.03 – 1.90 (m, 2H), 1.82 – 1.71 (m, 4H), 1.56 – 1.42 (m, 1H), 1.15 – 1.00 (m, 21H). **^{13}C NMR** (101 MHz, $CDCl_3$) δ 176.2, 146.1, 111.1, 66.0, 61.3, 50.0, 46.2, 45.2, 30.3, 27.7, 22.8, 18.2, 17.9, 12.4, 12.1. **FTIR** (neat) 2941, 2892, 2865, 1663, 1461, 1414, 1381, 1247, 1175, 1102, 1068, 998, 882, 782, 679 cm^{-1}. **HRMS** (ESI+) m/z: calc'd for $[M+H]^+$ $C_{21}H_{42}NO_3Si$ = 384.2928, found $C_{21}H_{42}NO_3Si$ = 384.2944. $\mathbf{R_f}$ = 0.25 (10% EtOAc/hexanes). $[\boldsymbol{\alpha}]_D^{25.2}$: (c = 0.21, $CHCl_3$), -13.1°.

This reaction also produced 0.42 g (35% yield) of silyl ether **2.52**. **^{1}H NMR** (400 MHz, $CDCl_3$) δ 4.77 (s, 1H), 4.71 – 4.65 (m, 1H), 3.71 – 3.61 (m, 5H), 3.18 (s, 3H), 3.10 (s, 1H), 2.99 – 2.87 (m, 1H), 2.53 – 2.39 (m, 1H), 1.93 – 1.80 (m, 2H), 1.72 (s, 3H), 1.70 – 1.58 (m, 2H), 1.12 – 1.00 (m, 21H). **^{13}C NMR** (151 MHz, $CDCl_3$) δ 177.1, 146.8, 110.5, 65.6, 61.4, 52.8, 47.4, 47.0, 32.4, 30.8, 28.2, 20.1, 18.2, 12.2. **FTIR** (neat) 2942, 2892, 2865, 1661, 1462, 1415, 1382, 1247, 1173, 1113, 1090, 1067, 1003, 882, 782, 680, 658 cm^{-1}. **HRMS** (ESI+) m/z: calc'd for $[M+H]^+$ $C_{21}H_{42}NO_3Si$ = 384.2928, found $C_{21}H_{42}NO_3Si$ = 384.2935. $\mathbf{R_f}$ = 0.24 (10% EtOAc/hexanes). $[\boldsymbol{\alpha}]_D^{24.7}$: (c = 0.09, $CHCl_3$), +4.4°.

2.6 References

[1] Zhou, H.; Guoruoluo, Y.; Tuo, Y.; Zhou, J.; Zhang, H.; Wang, W.; Xiang, M.; Aisa, H. A.; Yao, G. *Org. Lett.* **2019**, *21*, 549-553.

[2] Lee, E.; Yoon, C. H. *J. Chem. Soc., Chem. Commun*, **1994**, 479-481.

[3] Lakshmi, R.; Bateman, T. D.; McIntosh, M. C. *J. Org. Chem.* **2005**, *70*, 5313-5315.

[4] Egoshi, Y.; Kondo, R.; Yoshimoto, Y.; Sugiyama, Usuki, T. *Tetrahedron Lett.* **2013**, *54*, 7029-7030.

[5] Xing, X.; O'Connor, N. R.; Stoltz, B. M. *Angew. Chem. Ent. Ed.* **2015**, *54*, 11186-11190.

[6] Nwoye, E. O.; Dudley, G. B. *Chem. Commun.* **2007**, 1436-1437.

[7] Reisman, S. E.; Ready, J. M.; Weiss, M. M.; Hasuoka, A.; Hirata, M.; Tamaki, K.; Ovaska, T. V.; Smith, C. J.; Wood, J. L. *J. Am. Chem. Soc.* **2008**, *130*, 2087-2100.

[8] Boukouvalas, J.; Albert, V. *Tetrahedron Lett.* **2012**, *53*, 3027-3029.

[9] Maity, S.; Manna, S.; Rana, S.; Naveen, T.; Mallick, A.; Maiti, D. *J. Am. Chem. Soc.* **2013**, *135*, 3355-3358.

CHAPTER THREE

Synthetic Studies toward Total Synthesis of *N*-Oxy-Diketopiperazine Containing Natural Products

Part 1: Scalable Total Synthesis of (+)-Raistrickindole A and Progress Towards a Total Synthesis of (-)-Haenamindole

3.1 Background and Significance

3.1.1 N-oxy-2,5-diketopiperazines

2,5-Diketopiperazines (DKP) are the smallest cyclodipeptides found in numerous natural products isolated from fungi, bacteria, plants, and mammals.[1] The natural products with these interesting scaffolds also exhibit a variety of biological activities that have attracted and inspired synthetic chemists for drug discovery since they are small, conformationally constrained heterocycle in which diverse and stereoselective functionalization is possible.[1] A unique subclass of DKP is *N*-oxy-DKP that features an *N*-*O* bond that introduces a synthetic challenge, such as chemical sensitivity, especially under reductive, relatively acidic, and basic conditions.

3.1.2 Isolation of (-)-Haenamindole

In 2015 (-)-haenamindole (**3.01**) was first isolated by Kim and coworkers from a marine-derived *Penicillium* sp. KCB12F005 found in Haenam, Korea (Figure 3.1).[2a] One year later, Song and coworkers isolated **3.01** from *Penicillium citrinum* (MF006) found in the deep South China Sea.[2b] Song and coworkers claimed that the stereochemical assignment of **3.01** was incorrect based on their ROESY analysis. In the same year (2016)

Hwang and coworkers isolated **3.01** from another *Penicillium* species, *Penicillium lanosum*.[2c] In their isolation studies, they were able to determine the relative stereochemistry by an X-Ray analysis, disputing the previous assignments by Kim and Song. Furthermore, biological evaluation of **3.01** revealed modest antiinsectan activity by reducing the growth rate of 40% against the fall armyworm, *Spodoptera grugiperda*, which causes a major crop damage across the globe.

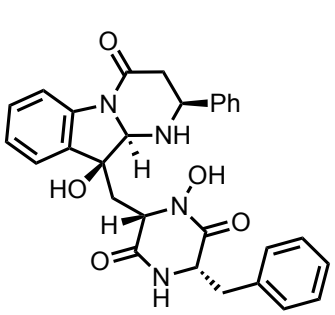

(-)-haenamindole
3.01

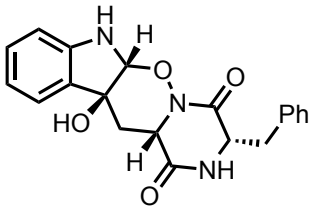

(+)-raistrickindole A
3.02

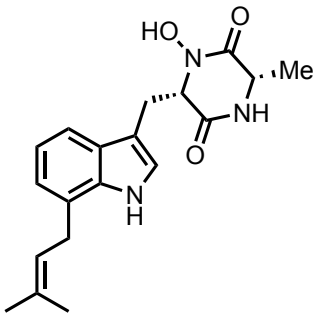

(+)-14-hydroxyterezine D
3.03

Figure 3.1. Structures of Representative *N*-oxy-diketopiperazines.

3.1.3 (+)-Raistrickindole A Background

In 2019 (+)-raistrickindole A (**3.02**, Figure 3.1) was isolated by Li and coworkers from the marine-derived fungus *Penicillium raistricki* IMB17-034, and the structure was originally elucidated by extensive spectroscopic analyses and TDDFT calculations of the NMR and ECD data.[3] Biologically, it showed a modest anti-hepatitis C properties with an EC_{50} value of 5.7 μM. Li and coworkers also isolated **3.01** from *Penicillium raistricki* IMB17-034. In their proposed biosynthesis, L-tryptophan (**3.04**) and L-phenylalanine (**3.05**) undergo two condensation events to furnish DKP (**3.06**). A subsequent oxidation of amide installs *N*-hydroxy DKP (**3.07**) that sets the stage for an equilibrium between epoxide (**3.08**) and 3*H*-indole (**3.09**) upon epoxidation of the indole in **3.07**. Intramolecular

opening of the epoxide with *N*-hydroxy DKP constructs the tetrahydro-1,2-oxazine core and affords **3.02**. On the other hand, addition of β-phenylalanine (**3.10**) to the imine of (**3.09**) can generate aminal (**3.11**) and subsequent amidation affords **3.01**.

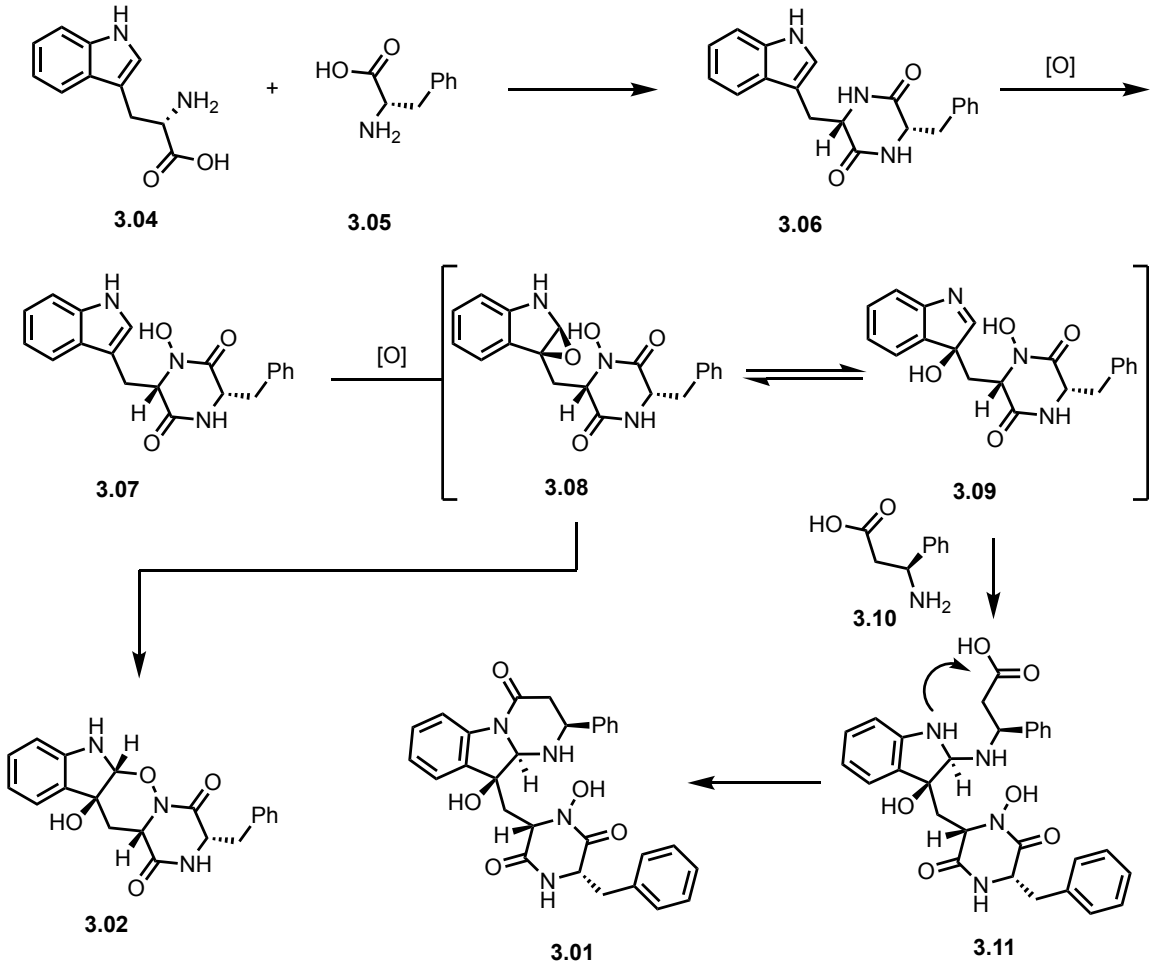

Scheme 3.1. Li's proposed biosynthetic relationship between **3.01** and **3.02**.

3.1.4 Pham's Total Synthesis of (+)-Raistrickindole

In 2022, Pham and coworkers disclosed their synthetic efforts towards the completion of **3.02** (Scheme 3.2).[4] Nucleophilic opening of an enantioenrich epoxide (**3.13**) with indole (**3.12**) in the presence of ytterbium (III) trifluoromethansulfonate furnished

alcohol (**3.14**). Subsequent silylation and saponification afforded carboxylic acid **3.15**. Peptide coupling with L-phenylalanine methyl ester with EDCI installs the dipeptide needed for the formation of DKP. Another saponification using LiOH, followed by amidation using HATU with silyl-protected hydroxylamine delivered bis-silylated intermediate (**3.18**) that was desilylated under acidic conditions to afford hydroxamic acid (**3.19**). Stereoinvertive intramolecular displacement of the secondary alcohol under Mitsunobu conditions installed the *N*-hydroxy DKP (**3.20**) that was subjected to *m*-CPBA-mediated epoxidation to afford **3.02**.

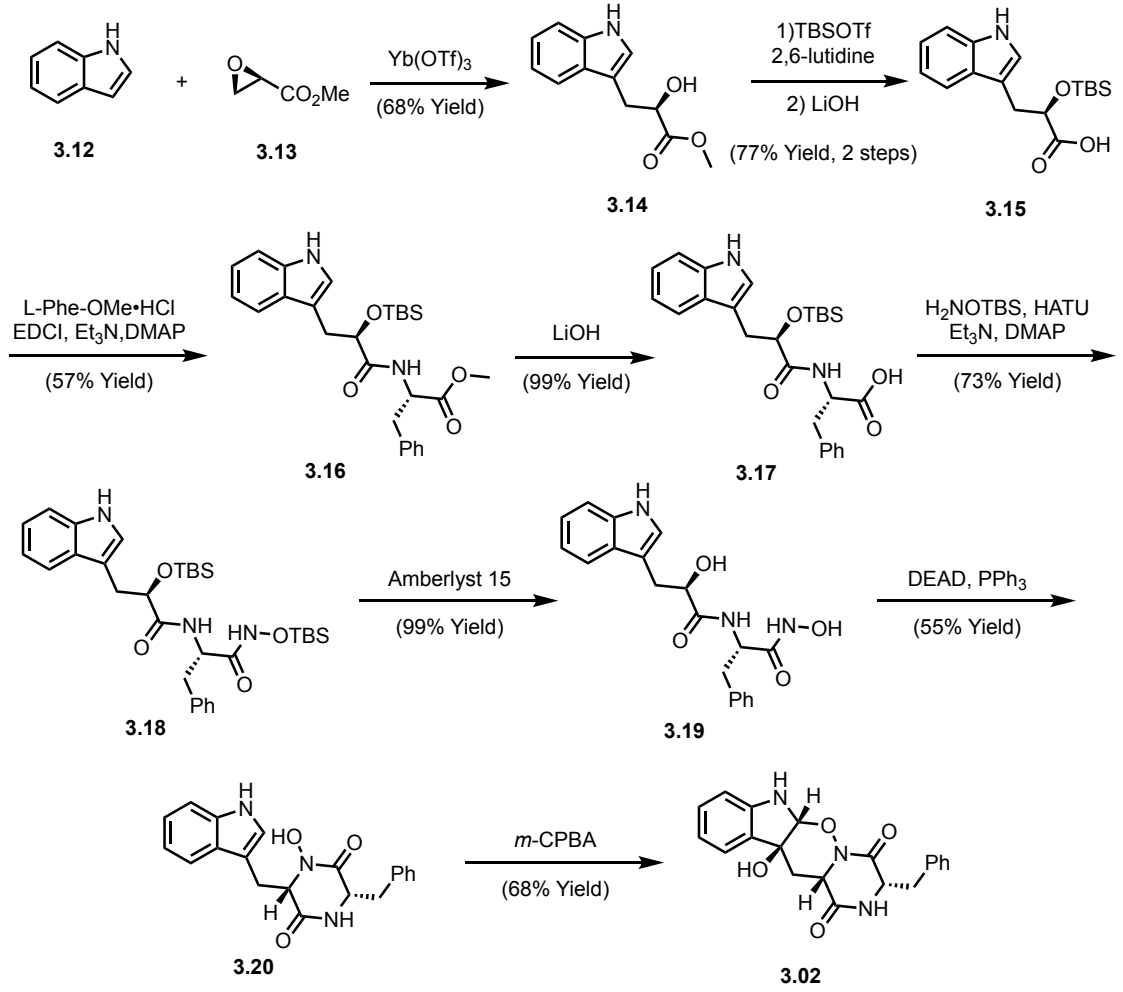

Scheme 3.2. Pham's total synthesis of (+)-raistrickindole A (**3.02**).

3.2.1 Our Total Synthesis of (+)-Raistrickindole A

In 2021, we completed the total synthesis of **3.02**. Initially, *N*-nosyl-indole-3-carboxylaldehyde (**3.21**) was subjected to Masamune-Roush modified Horner-Wadsworth-Emmons olefination in the presence of triethyl phosphonoacetate to afford enoate (**3.22**, Scheme 3.3). Subsequent reduction of **3.22** using DIBAL-H furnished allylic alcohol (**3.23**) that was protected as its corresponding silyl ether (**3.24**) in excellent yields over the two steps. The construction of 1,2-oxazine core was accomplished via intermolecular NDA with *in situ* generation of acyl nitroso compound from *N*-Boc-protected L-phenylalanine hydroxamic acid in the presence of PIDA.[5] High diastereoselectivity of the intermolecular NDA cycloaddition can be rationalized by Vogt and coworkers' hypothesis of a six-membered intramolecular hydrogen bonding adopted by acyl nitroso compound, as well as an *endo*-selective transition state shown in **3.27**.[6]

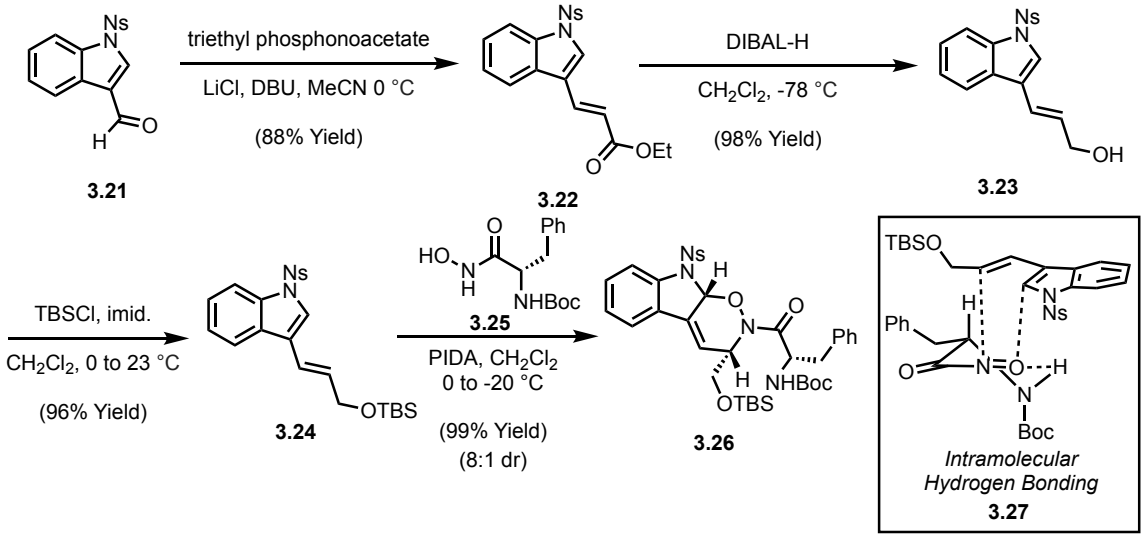

Scheme 3.3. Diastereoselective intermolecular NDA.

With **3.26** in hand, we turned our attention to the diastereoselective installation of the tertiary alcohol. Oxymercuration/demercuration or epoxidation/reduction did not prove to be fruitful. Eventually, we were delighted to obtain the desired tertiary alcohol (**3.28**) as a single diastereomer under Mukaiyama hydration conditions albeit low and inconsistent yield (Scheme 3.4). Nonetheless, subsequent one-pot desilylation and oxidation under Jones conditions afforded crude carboxylic acid (**3.29**) that was subjected to ethereal HCl. Upon removal of the Boc-protecting group, the formation of hydrochloride salt resulted in precipitation to obtain amino acid (**3.30**) in 81% yield over the two steps.

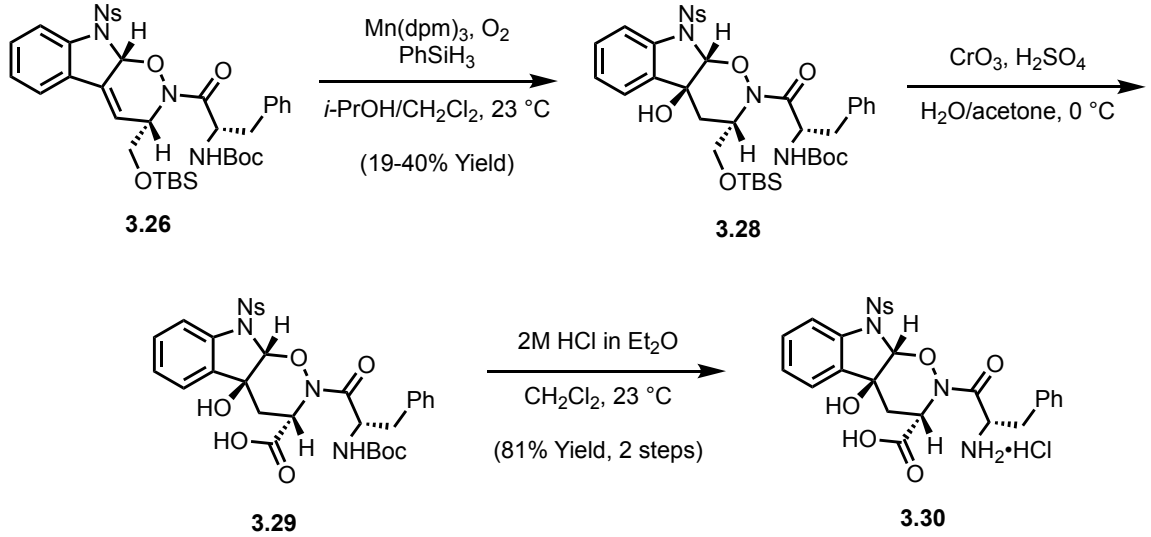

Scheme 3.4. Synthesis of amino acid (**3.30**).

In order to construct the tetracyclic core in **3.02**, intramolecular peptide coupling of **3.30** using CDI gave rise to DKP (**3.31**) in a modest yield (Scheme 3.5). Lastly, removal of the nosyl protecting group using thiophenol and cesium carbonate gave rise to **3.02**. With the current route, we were able to produce 10.5 milligrams of **3.02** in one pass with overall 2% yield.

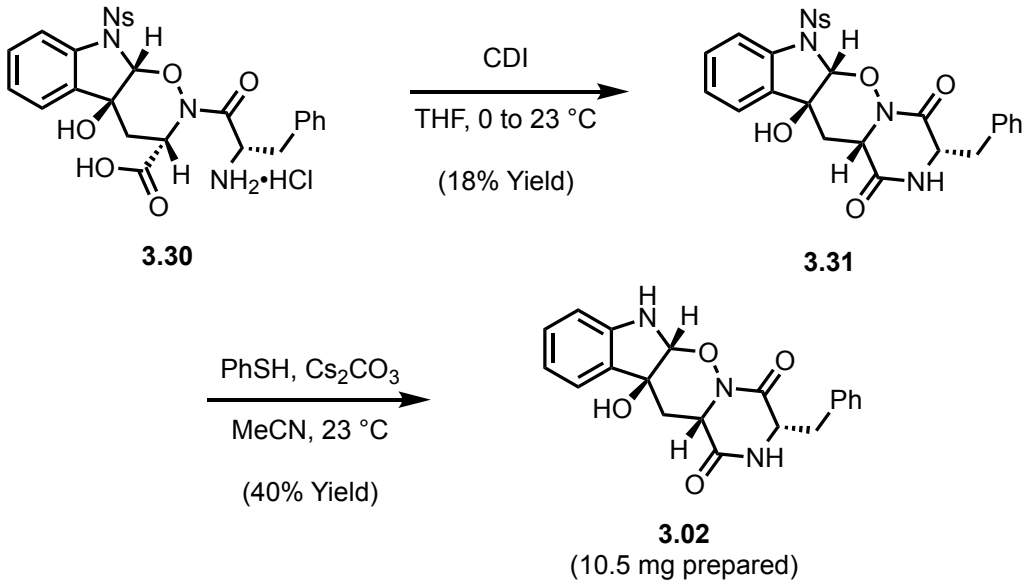

Scheme 3.5. Total synthesis of (+)-raistrickindole A (**3.02**).

3.3 Optimized Total Synthesis of (+)-Raistrickindole A

3.3.1 Retrosynthetic Analysis of (-)-Haenamindole

After securing access to **3.02**, we now turned our attention to the preparation of **3.01**. Inspired by Li and coworkers' proposed biosynthesis, we envisioned that **3.01** could be accessed from **3.02** (Scheme 3.6).[3] The aminal of **3.01** was seen as arising from cleavage of the C–O bond in *N*,*O*-acetal (**3.33**) under acidic conditions to deliver a transient iminium ion (**3.32**). We expected that the removal of the Boc group in the same pot would expose the primary amine shown in **3.32** to capture the iminium ion and deliver **3.01**. We envisioned that **3.33** would be delivered by amidation of **3.02** with Boc-protected β-phenylalanine (**3.34**).

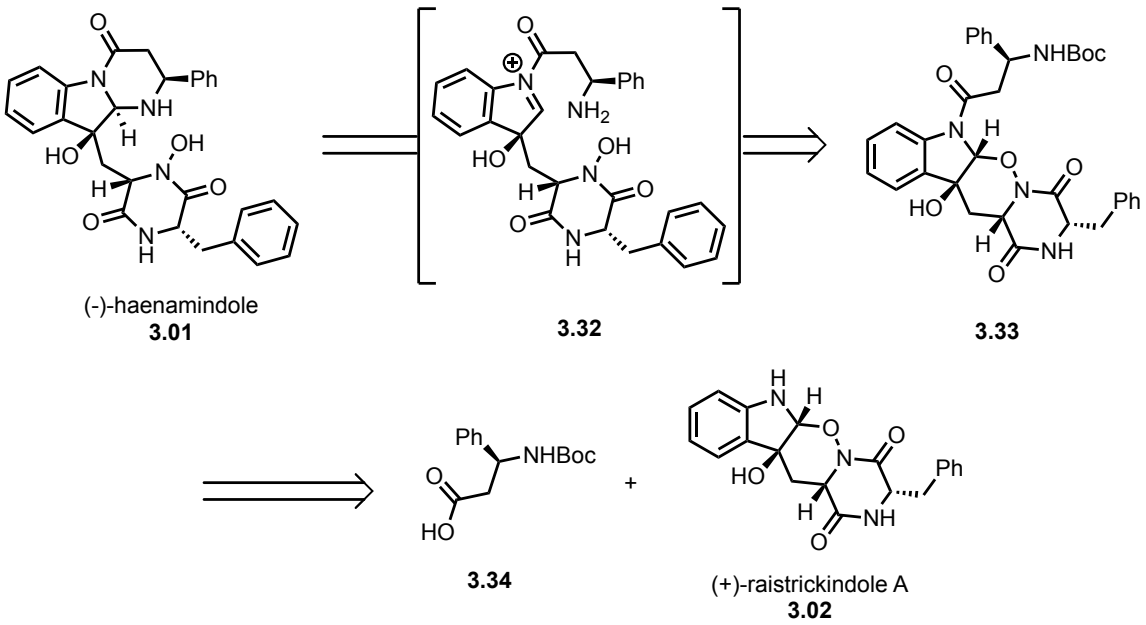

Scheme 3.6. Retrosynthetic analysis of (-)-haenamindole (**3.01**).

3.3.2 Optimization of Mukaiyama Hydration

Prior to executing the forward synthesis towards **3.01**, we opted to optimize the route to **3.02**, especially Mukaiyama hydration and DKP formation steps due to their low yields. First, we revisited Mukaiyama hydration as we faced with difficulties in inconsistent yields, especially on gram-scale (19-40% yield, Scheme 3.4). Since these conditions were the results from the initial optimization, there was a necessity to attempt changes in conditions. After a literature survey, we found Mukaiyama hydration conditions used by Miloserdov and coworkers in which they utilized sodium borohydride as a reducing agent in ethanol and using air as the oxygen source.[7] Initially, we subjected **3.26** to their original conditions albeit mixture of 1:1 ethanol and CH_2Cl_2 due to the insolubility in only EtOH. To our dismay, we obtained 7% yield of **3.28** (Table 3.1). Since over-reduction outcompeted the formation of **3.28**, we first increased the concentration of oxygen by changing the source to O_2 balloon from air. Gratifyingly, the yield became

comparable to the one before optimization. In screening solvent, isopropanol only produced a trace amount of **3.28** due to the insolubility of sodium borohydride. We also suspected that over-reduction could be compromised by lowering the concentration of sodium borohydride. Thus, we attempted to lower the temperature of the reaction to 0 °C. To our delight, we observed increased yield to 49%. Further decreasing the reaction temperature to -78 °C did not yield **3.28**. On the other hand, slowly warming the reaction mixture from -40 °C to 23 °C gave us 56% yield of **3.28**. Ultimately, further cooling the mixture to -78 °C gave us the highest yield (65%) of **3.28** to date.

Table 3.1. Optimization of Mukaiyama hydration.

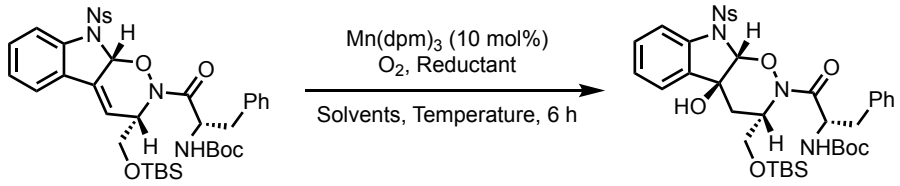

3.26 **3.28**

Reductant	Solvent	Temperature	O_2 source	Yield
$PhSiH_3$	*i*-PrOH/CH_2Cl_2	23 °C	O_2 balloon	19 - 40 %
$NaBH_4$	EtOH/CH_2Cl_2	23 °C	Air	7%
	EtOH/CH_2Cl_2	23 °C	O_2 balloon	24 - 39%
	i-PrOH/CH_2Cl_2	23 °C	O_2 balloon	trace
	EtOH/CH_2Cl_2	0 °C	O_2 balloon	49%
	EtOH/CH_2Cl_2	-78 °C	O_2 balloon	N.R.
	EtOH/CH_2Cl_2	-40 to 23 °C	O_2 balloon	56%
	EtOH/CH_2Cl_2	-78 to 23 °C	O_2 balloon	65%

3.3.3 Optimization of Diketopiperazine Formation

After optimization of Mukaiyama hydration, we turned our attention to the DKP formation. Prior to CDI, we initially attempted to prepare a mixed anhydride transiently to promote a cyclization (Table 3.2). Unfortunately, upon subjecting **3.30** to isobutyl chloroformate or trifluoroacetic anhydride, we only recovered **3.30**. Further attempts to promote the DKP formation using carbodiimide as the coupling reagent only led to recovered **3.30**. To our delight, CDI gave rise to **3.31** albeit as an inseparable 2:1 mixture with spiro-*N*,*O*-acetal **3.34**. We suspected that having imidazole as a side product might promote a base-mediated cleavage of the N–O bond. Therefore, in order to keep the conditions neutral, we envisioned $TMSCHN_2$-mediated methylation of **3.30** and subsequent intramolecular nucleophilic acyl substitution to form **3.31**. Much to our chagrin, we only observed the formation of **3.34**, proposing the lability of the N–O bond under thermolysis. Eventually, we found that EEDQ furnished **3.31** without the formation of **3.34** with the highest yield (43%) to data and allowed to furnish **3.02** with 72% yield from **3.31** (Scheme 3.7).[8]

Table 3.2. Optimization of intramolecular amidation.

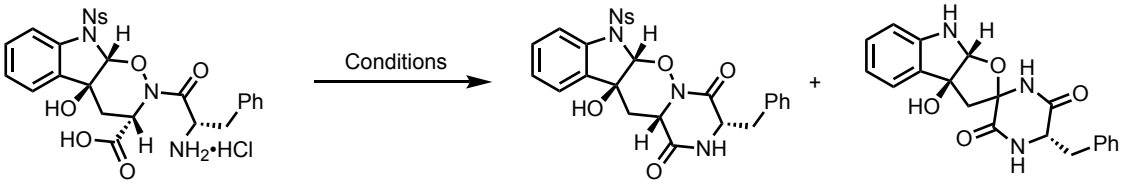

3.30 **3.31** **3.34**

Reagents	Solvent	Temperature	Result
isobutyl chloroformate	CH_2Cl_2	23 °C	recovered **3.30**
TFAA	CH_2Cl_2	0 °C	recovered **3.30**
DCC, Et_3N DMAP	CH_2Cl_2	23 °C	recovered **3.30**
CDI	THF	23 °C	27% Yield 2:1 (**3.31**:**3.34**)
$TMSCHN_2$	MeOH, PhH	80 °C	23% Yield (**3.34**)
EEDQ	EtOH	23 °C	43% Yield (**3.31**)

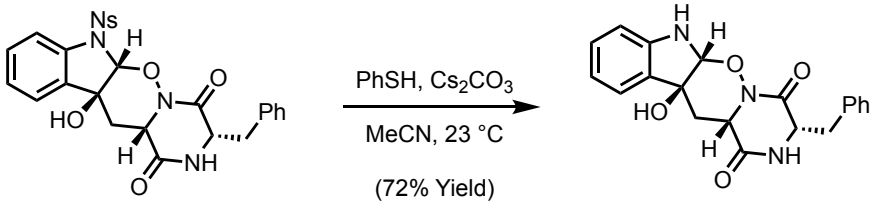

3.31

3.02
(450 mg prepared)

Scheme 3.7. Scalable preparation of (+)-raistrickindole A (**3.02**).

3.4 Future Work

With practical quantities of **3.02** in hand, we plan to execute the forward synthesis towards **3.01** via screening *N*-acylation conditions to furnish amide (**3.33**, Scheme 3.8). Upon subjecting **3.33** to acidic conditions, we envision a transient formation of the *N*-acyl

iminium ion (**3.32**) that would be capture by the amine to effect cyclic aminal formation and afford **3.01**.

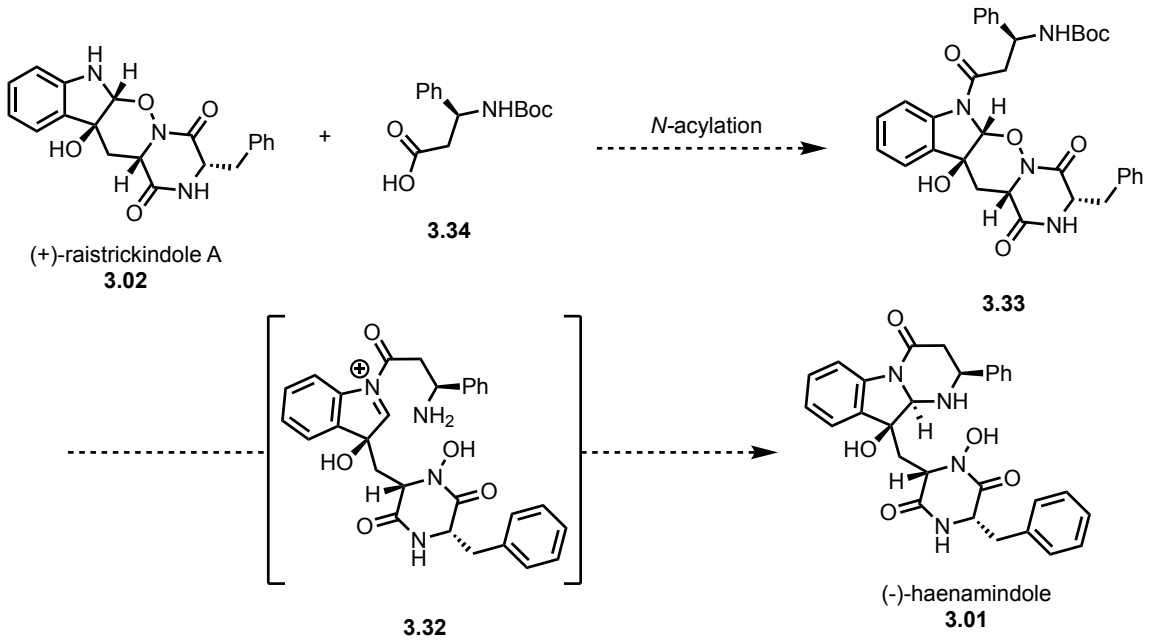

Scheme 3.8. Endgame strategy.

3.5 Conclusion

In conclusion, we reported a scalable total synthesis of (+)-raistrickindole A (**3.02**) in 9 steps from known materials featuring a diastereoselective intermolecular nitroso Diels-Alder cycloaddition as the key step. Original conditions involved modest yields in Mukaiyama hydration, DKP formation, and denosylation steps that resulted in overall 2% yield of **3.02**. Extensive optimization efforts successfully improved the yields of aforementioned steps and increased the overall yield to 13%. This set the stage for a more practical preparation of **3.02** which will serve as the key intermediate towards the total synthesis of (-)-haenamindole (**3.01**).

3.6 Experimental

3.6.1 General

Unless otherwise stated, all reactions were performed in flame-dried glassware under a nitrogen atmosphere, using reagents as received from the manufacturers. The reactions were monitored, and analytical samples purified by normal phase thin-layer chromatography (TLC) using Millipore glass-backed 60 Å plates (indicator F-254, 250 μM). Dichloromethane was dried using a solvent purification system manufactured by SG Water U.S.A., LLC. Ethanol was dried over 3 Å molecular sieves purchased from Sigma-Aldrich. Manual flash chromatography was performed using the indicated solvent systems with Silicycle SiliaFlash® P60 (230–400 mesh) silica gel as the stationary phase.

*3.6.2 Preparation of tertiary alcohol **3.28***

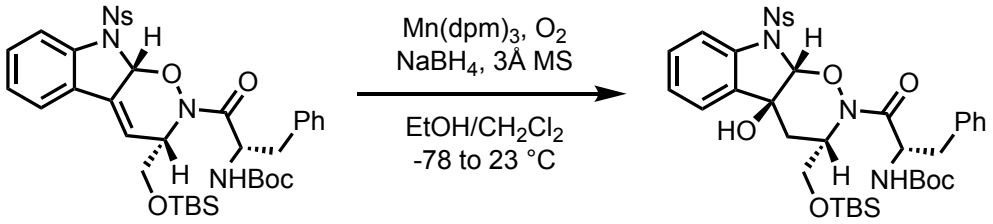

3.26 **3.28**

To a flame-dried round bottom flask with a magnetic stir bar was added cycloadduct **3.26** (200 mg, 0.27 mmol) and anhydrous EtOH/CH_2Cl_2 (9.0 mL, 1:1/v:v, ca. 0.03 M). To the resulting solution was added activated 3Å molecular sieves (205 mg) and oxygen was bubbled via balloon for 15 min at 23 °C. To the resulting mixture was added $Mn(dpm)_3$ (13 mg, 0.027 mmol) and stirred 0.5 h. The reaction was cooled to -78 °C and then granular $NaBH_4$ (51.1 mg, 1.35 mmol) was added in one portion. The resulting mixture was stirred 6 hours while slowly warming to 23 °C. Next, water (1 mL) was added to the reaction

mixture and was dried over Na_2SO_4. The resulting mixture was then filtered through a short pad of Celite eluting with CH_2Cl_2 and concentrated to afford the crude tertiary alcohol **3.28**. Purification *via* flash column chromatography (20% EtOAc in hexanes then 25% EtOAc in hexanes) afford tertiary alcohol **3.28** alcohol (136 mg, 65% yield) as a pale, yellow foam.

For spectral data, see section 3.5.28 of ACJ dissertation.

*3.6.3 Preparation of diketopiperazine **3.31***

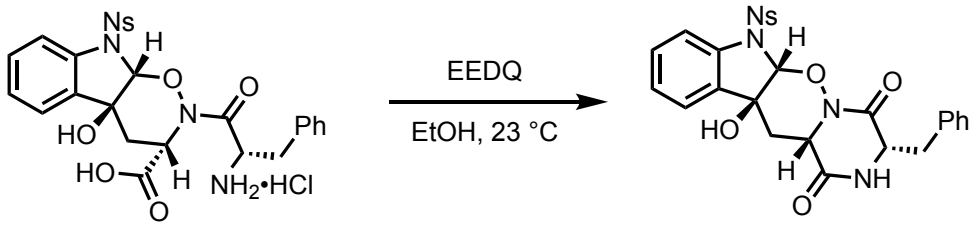

3.30 **3.31**

To a flame-dried round bottom flask with a magnetic stir bar was added amino acid **3.30** (866 mg, 1.43 mmol) and anhydrous EtOH (29.0 mL, ca. 0.05 M). To the resulting solution was added EEDQ (425 mg, 1.72 mmol) as a single portion. The reaction mixture was stirred 24 h at 23 °C and concentrated to afford the crude DKP. Purification *via* flash column chromatography (silica gel, 50% EtOAc in hexanse then 90% EtOAc in hexanes) afforded DKP **3.31** (342 mg, 43% yield) as a pale, brown solid.

For spectral data, see section 3.5.31 of ACJ dissertation.

3.7 References

[1] Borthwick, A. D. *Chem. Rev.* **2012**, *112*, 3641-3716.

[2] Isolation of (-)-haenamindole :
(a) Kim, J. W.; Ko, S.-K.; Son, S.; Shin, K.-S.; Ryoo, I.-J. Hong, Y.-S.; Oh, H.; Hwang, B. Y.;
Hirota, H.; Takahashi, S.; Kim, B. Y.; Osada, H.; Jang, J.-H.; Ahn, J. S. *Bioorg. Med. Chem. Lett*.
2015, *25*, 5398-5401.
(b) Song, F.; He, H.; Ma, R.; Xiao, X.; Wei, Q.; Wang, Q.; Ji, Z.; Dai, H.; Zhang, L.; Capon, R.
J. *Tetrahedron Lett.* **2016**, *57*, 3851-3852.
(c) Hwang, I. H., Che, Y.; Swenson, D. C.; Gloer, J. B.; Wicklow, D. T.; Peterson, S. W.; Dowd,
P. F. *J. Antibiot*, **2016**, *69*, 631-636.

[3] Li, J.; Hu, Y.; Hao, X.; Tan, J.; Li, F.; Qiao, X.; Chen, S.; Xiao, C.; Chen, M.; Peng, Z.; Gan, M. *J. Nat. Prod.* **2019**, *82*, 1391-1395.

[4] Pham, T. L.; Sae-Lao, P.; Toh, H. H. M.; Csókás, D.; Bates, R. W. *J. Org. Chem.* **2022**, *87*, 16111-16114.

[5] Shimizu, H.; Yoshimura, A.; Noguchi, K.; Nemekin, V. N.; Zhdankin, V. V.; Saito, A. *Beilstein. J. Org. Chem.* **2018**, *14*, 531-536.

[6] Vogt, P. F.; Miller, M. J. *Tetrahedron* **1998**, *54*, 1317-1348.

[7] Miloserdov, F. M.; Kirillova, M. S.; Muratore, M. E.; Echavarren, A. M. *J. Am. Chem. Soc.* **2018**, *140*, 5393-5400.

[8] Zacharie, B.; Connolly, T. P.; Penney, C. L. *J. Org. Chem.* **1995**, *60*, 7072-7074.

CHAPTER FOUR

Synthetic Studies toward Total Synthesis of *N*-Oxy-Diketopiperazine Containing Natural Products

Part 2: Progress towards Total Synthesis of [2.2.3]-Epidithiodiketopiperazines

4.1 Background and Significance

4.1.1 [2.2.3]-Epidithiodiketopiperazines

Epidithiodiketopiperazines (ETPs) are a class of natural products that possess a characteristic structural core consisting of a disulfide bridged DKP. Two major subclasses of ETPs are 3,6-ETPs and [2.2.3]-ETPs. 3,6-ETPs, the more common group, structurally feature a [2.2.2]-disulfide bridged DKP as depicted in hyalodendrin (**4.01**, Figure 4.1). On the other hand, [2.2.3]-ETPs (e.g., **4.02**-**4.04**) exhibit a unique combination of an *N*-oxy-DKP and a rearranged disulfide bridge that constitutes the [2.2.3] bicyclic core.

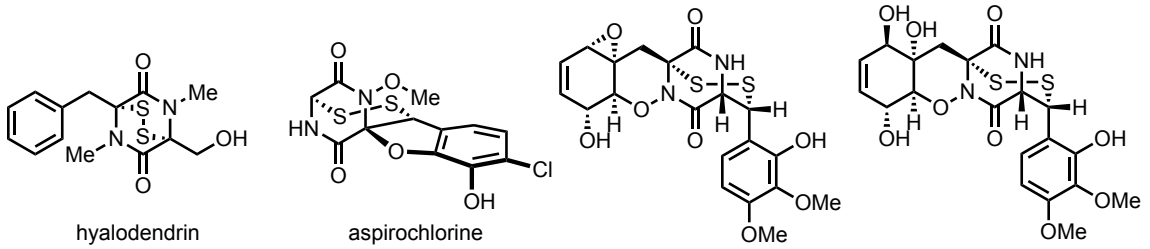

Figure 4.1. Representative epidithiodiketopiperazines.

4.1.2 Isolation and Biosyntheses of Aspirochlorine, (-)-Gliovirin, and (-)-Pretrichodermamide A

In 1976, aspirochlorine (**4.02**, Figure 4.1), originally named A30641, was isolated from *Aspergillus tamari* and represents the first member of the [2.2.3]-ETP family.[1] It exhibits various biological activities, such as antifungal, antibacterial, and antiviral.[2] Biosynthetically it is believed that dimerization of L-phenylalanine, mediated by non-ribosomal peptide synthetase, generates the DKP (**4.05**, scheme 4.1).[2] Subsequent oxidation events: thiolations and disulfide bridge formation, two benzylic hydroxylations and an aryl hydroxylation then furnish triol (**4.06**). Acylation of the benzylic alcohol adjacent to phenol furnishes **4.07** which, following a histidine-mediated deprotonation and dearomative elimination of the acetate, results in the formation of *ortho*-quinone methide (**4.08**). Initiated by a cysteine residue, cleavage of the disulfide bridge promotes an intramolecular *thia*-Michael addition that affords episulfide (**4.09**). To furnish the rearranged [2.2.3] core, fragmentation of the *N,S*-acetal reconstructs the disulfide bridge by displacement of the cysteine residue and addition of the phenoxide to the iminium (**4.10**) results in the formation of the spirocyclic *N,O*-acetal (**4.11**). Further oxidations install both phenol and *N*-hydroxyl group on the nitrogen of the spirocyclic *N,O*-acetal and methyltransferase delivers methyl group on the *N*-hydroxyl group to generate the *N*-methoxy group shown in **4.13**. Lastly, a *retro*-aldol reaction releases benzaldehyde and subsequent halogenase-mediated aryl chlorination generates **4.02**.

The structurally more complex [2.2.3]-ETPs, (-)-gliovirin (**4.03**) and (-)-pretrichodermamide A (**4.04**), were isolated in 1982 and 2006, respectively (Figure 4.10).[3,4] As one might imagine, the biosyntheses of **4.03** and **4.04** were proposed to proceed

via dimerized L-phenylalanine (**4.05**), which was postulated to undergo a series of events similar to those of **4.02** to deliver spirocyclic *N,O*-acetal (**4.15**, Scheme 4.2).[5] Oxidation of **4.15** to the corresponding *N*-hydroxy-DKP (**4.16)**, is followed by dearomative epoxidation to deliver **4.17**. Intramolecular nucleophilic opening of the derived epoxide delivers the tricyclic core shown in **4.18**. Subsequent aryl oxidation, followed by two methylation events, sets the stage for reduction of the spirocyclic *N,O*-acetal to afford phenol **4.21**. Subsequent regioselective epoxidation generates **4.03** and transformation of the epoxide to the corresponding *trans*-1,2-diol furnishes **4.04**.

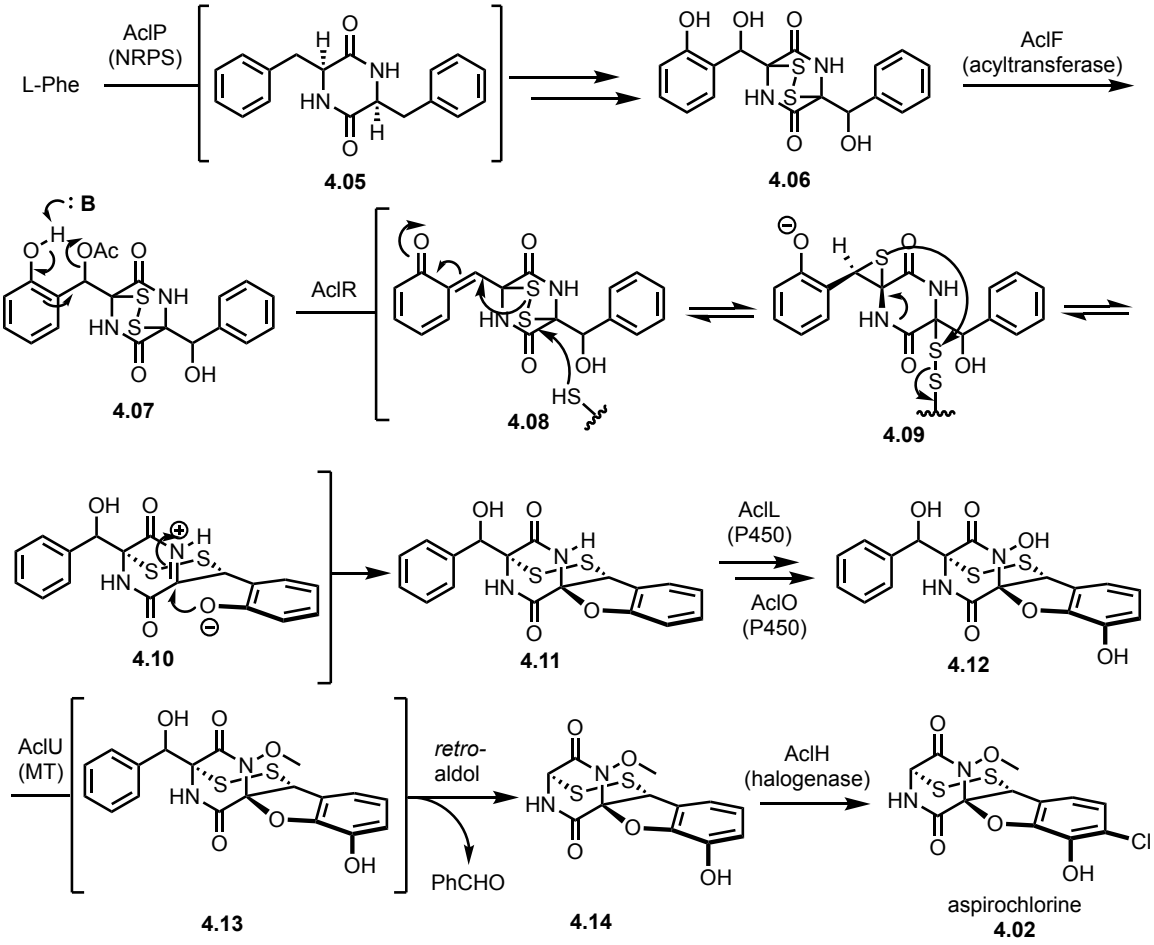

Scheme 4.1. Proposed biosynthetic pathway of aspirochlorine (**4.02**).

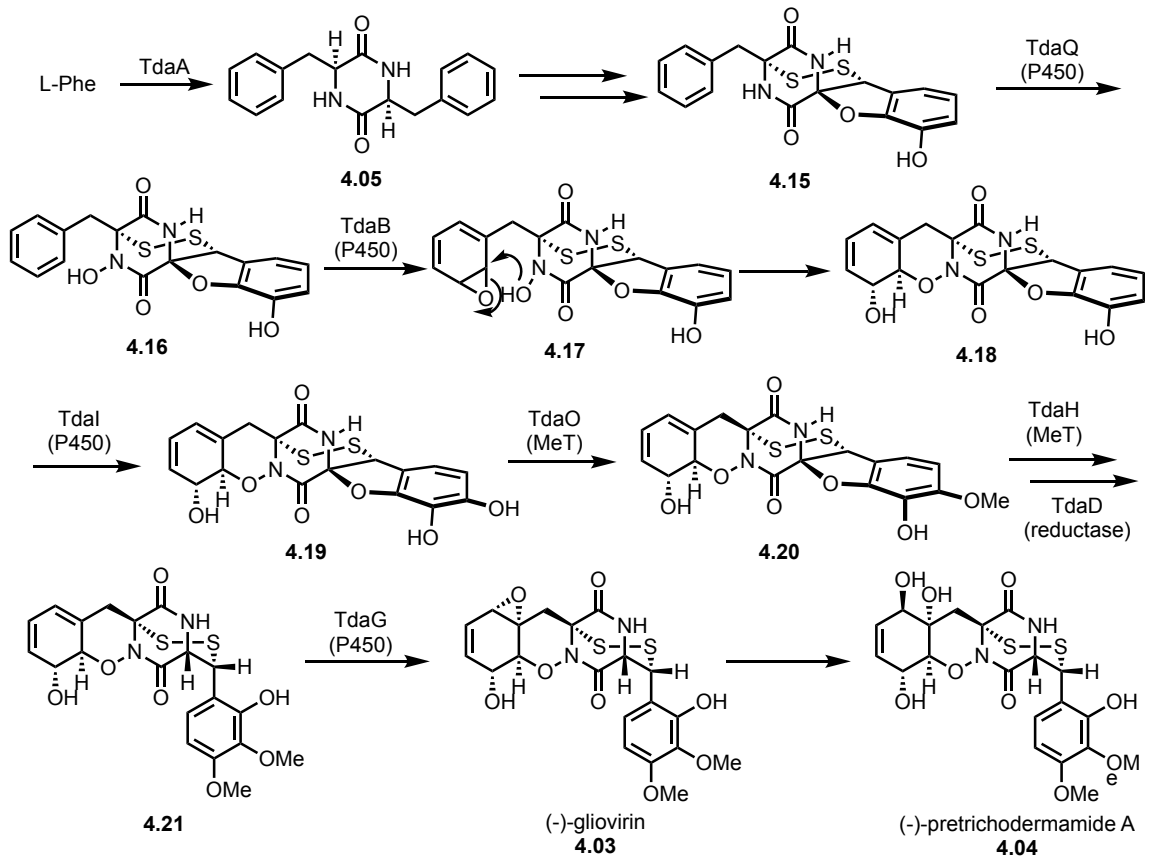

Scheme 4.2. Proposed biosynthesis of (-)-gliovirin (**4.03**) and (-)-pretrichodermamide A (**4.04**).

4.1.3 Previous Syntheses of [2.2.3]-ETPs

Since the isolation of aspirochlorine (**4.02**), many other [2.2.3]-ETPs have been isolated (Figure 4.2), and found to exhibit a broad range of activities, rendering them attractive synthetic targets in the context of drug discovery.[6-9] Nevertheless, **4.02** stands as the sole example of a [2.2.3]-ETPs to be prepared by total synthesis to date.

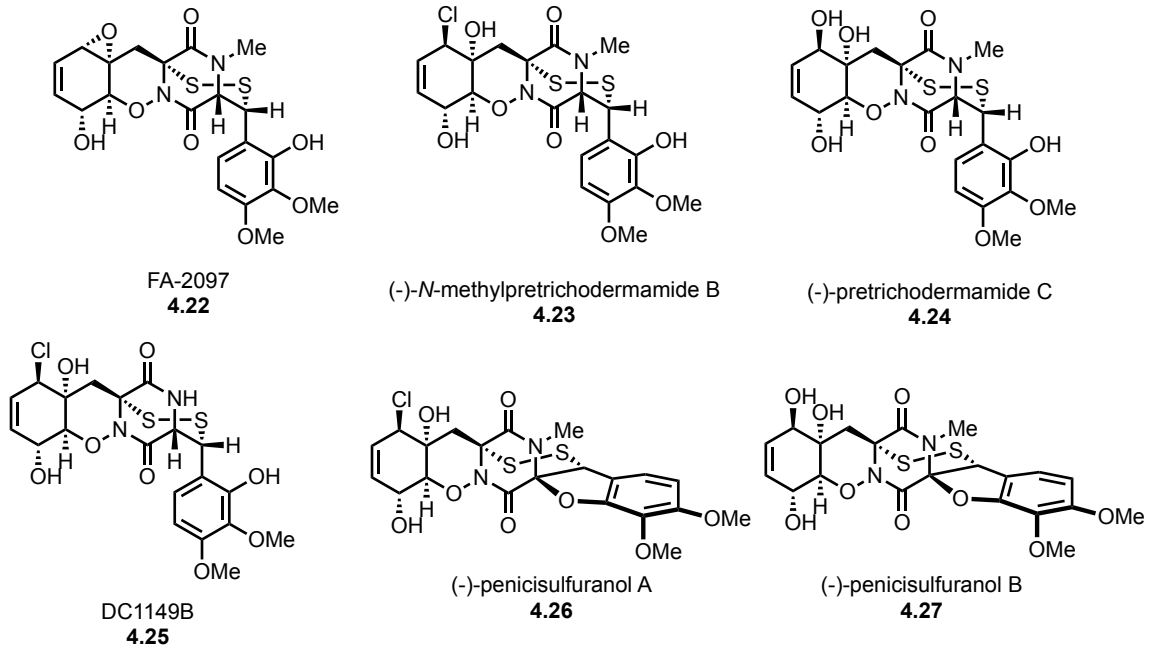

Figure 4.2. Other examples of [2.2.3]-ETPs.

In 1993, Miknis and coworkers reported a total synthesis of (±)-**4.02**.[1] Initially, 4-chlororesorcinol was subjected to a Gatterman formylation using zinc(II) cyanide and HCl (Scheme 4.3). Subsequent regioselective MOM protection in the presence of triethylamine and treating the resulting intermediate with diethyl bromomalonate and potassium carbonate, followed by hydrolysis gave coumarillic acid derivative (**4.29**) in a modest yield. Amide coupling of **4.29** with *o*-nitrobenzyl-protected glycine ethyl ester under Schotten-Baumann conditions using oxalyl chloride and sodium bicarbonate, followed by protecting group interchange to the corresponding acetate, set the stage for nucleophilic acyl substitution to install hydroxamic methyl ester (**4.30**) in 58% yield over three steps. Treating **4.30** with NBS smoothly promoted spirocyclization to furnish and intermediate benzylic bromide which upon treatment with silver in the presence of methanol underwent smooth conversion to the corresponding ether (not shown). Subsequent *N*-deprotection by photolysis of *o*-nitrobenzyl group gave *N,O*-spiroacetal (**4.31**). In order to install an

oxidation of the DKP core, *tert*-butyl hypochlorite was used to chlorinate the N-H and sodium methoxide-mediated elimination and addition to the resulting iminium, followed by diacylation of phenol under nucleophilic conditions using sodium ethoxide, delivered *N,O*-acetal (**4.32**). To complete the synthesis, efforts were turned to installation of the sulfur moieties. In the presence of BF_3•Et_2O and thioacetic acid, double displacement of the methoxy groups furnished the penultimate compound **4.33** and double diacylation under aminolysis, followed by aerobic oxidation secured the access to **4.02**.

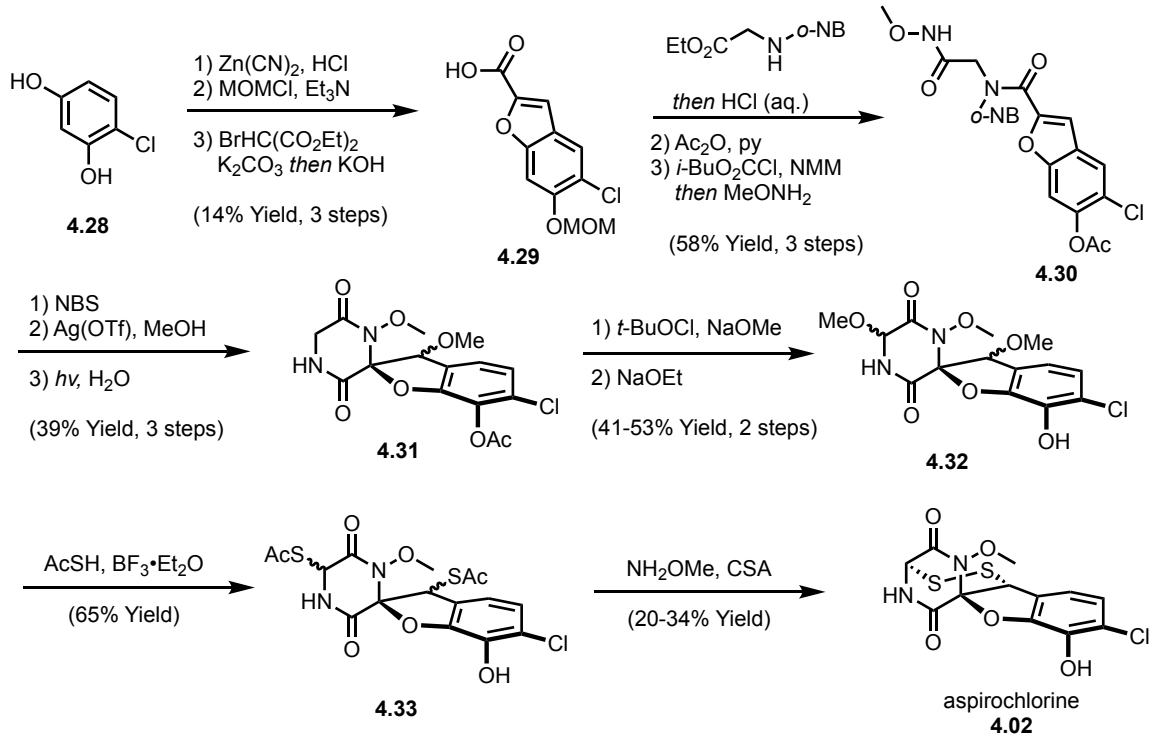

Scheme 4.3. Williams' total synthesis of (±)-aspirochlorine (**4.02**).

While the work by Miknis remains the only successful total synthesis of [2.2.3]-ETP to date, Wu and coworkers accomplished an alternative approach towards the [2.2.3]-ETP core by rearranging the disulfide bridge of a 3,6-ETP.[10] As illustrated in Scheme 4.4, starting from protected 3,6-ETP **4.34**, stoichiometric deprotonation under strongly basic conditions and subsequent addition of functionalized benzaldehyde smoothly produced the aldol product **4.35**. Treating **4.35** with triflic acid was found to promote cleavage of both MOM groups to furnish an intermediate which, upon protonation of the benzylic alcohol and subsequent elimination of water, delivered *ortho*-quinone methide (**4.37**). This highly electrophilic moiety could undergoes a 1,2-sulfur migration and cyclization to construct the [2.2.3]-ETP core. Lastly, *m*-CPBA-mediated oxidation to the corresponding monosulfoxide and subsequent treatment with dimethyl perchloric acid cleanly converted **4.38** to disulfide **4.39**.

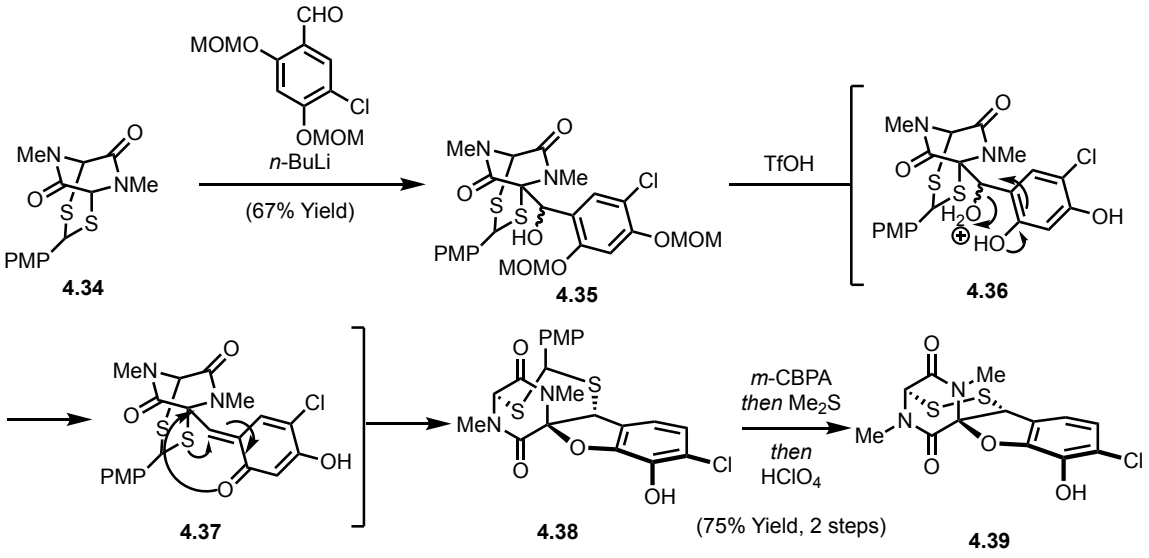

Scheme 4.4. Danishefsky's synthetic access to [2.2.3]-ETP from 3,6-ETP.

More recently, Cowper and coworkers reported a synthetic progress towards (-)-gliovirin (**4.03**).[11] In their attempts to construct the tricyclic core of **4.03**, silylated oxime (**4.40**) was prepared in two steps from glyoxylic acid monohydrate and subjected to enantioselective copper-catalyzed propargylation using allenyl boronate to afford alkyne **4.41** in 87% yield and 95% enantiomeric excess (Scheme 4.5). After protection of the secondary amine to its corresponding *N*-benzoyl group, enyne metathesis with 1,5-cyclooctadiene delivered 1,3-cyclohexadiene **4.42** in excellent yield over two steps. Cleavage of the silyl group in **4.42** using mesic acid set the stage for radical-mediated 6-*endo*-trig cyclization in the presence of a copper catalyst. The resulting radical was trapped by molecular oxygen and a subsequent Kornblum-DeLaMare sequence resulted in formation of the corresponding enone **4.43**. Although not detailed rationale was provided it is notable that the overall transformation resulted in a predominance of the desired diastereomer. Following construction of the bicyclic core, a series of events: nucleophilic epoxidation, modified Saegusa-Ito oxidation, and a second nucleophilic epoxidation smoothly forged *bis*-epoxide **4.44** in 44% yield over three steps. To install the vinyl epoxide present in **4.03**, 4.44 was exposed to anhydrous hydrazine and catalytic benzoic acid to promote a Wharton rearrangement which, following silyl protection, gave **4.45**. Lastly, removal of the benzoyl group using zirconium provided a secondary amine (**4.46**) that can serve as the initial point for the amino acid moiety needed for installation of the DKP.

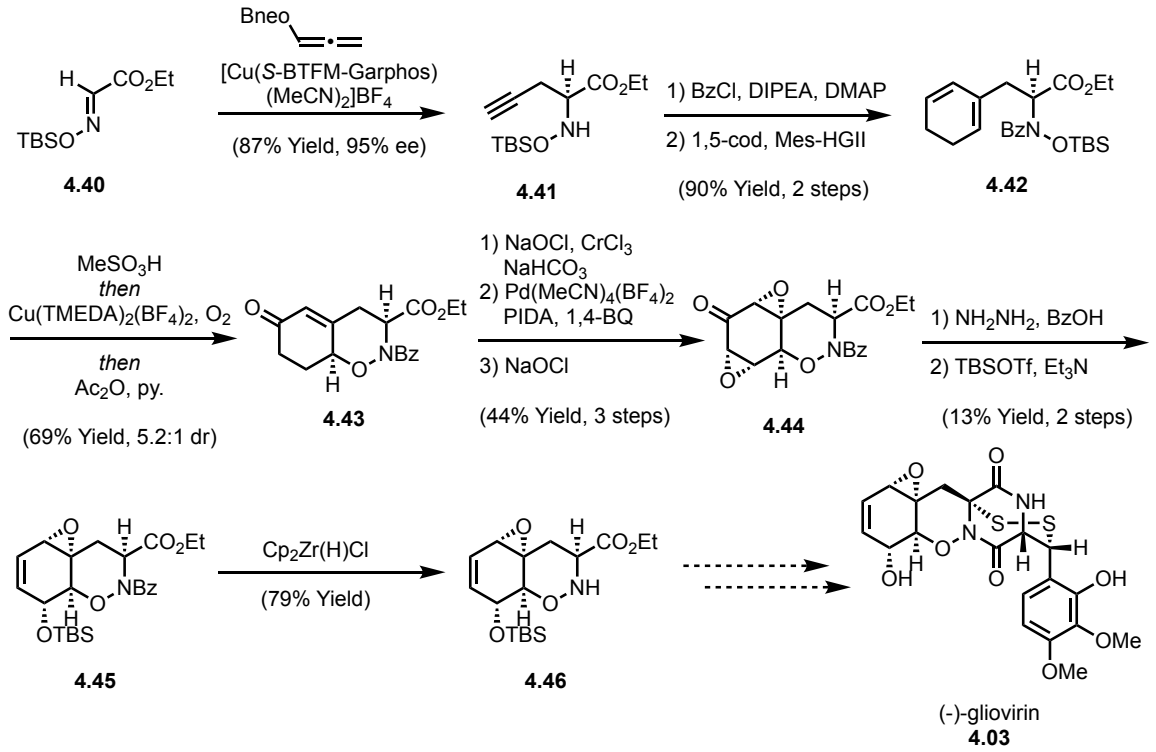

Scheme 4.5. Reisman's synthetic efforts toward (-)-gliovirin (**4.03**).

Recently our group reported a highly efficient approach towards **4.27** (Scheme 4.15).[12] In this approach, a benzaldehyde derivative (**4.47**) was condensed with symmetrical DKP **4.48** under basic conditions to furnish an intermediate enamine (**4.49**) which had undergone diacylation at the amine proximal to the newly introduced aryl ring. Subsequent *N*-methylation transiently gave DKP **4.50** which, upon addition of another benzaldehyde derivative (**4.51**), completed the single pot preparation of DKP **4.52**. *N*-oxidation of **4.52** was accomplished using BSA and MoO_5(HMPA) and the intermediate *N*-hydroxy-DKP (**4.53**) was silylated using TBSOTf to furnish **4.54** the most advanced intermediate reached in this effort towards **4.27**.

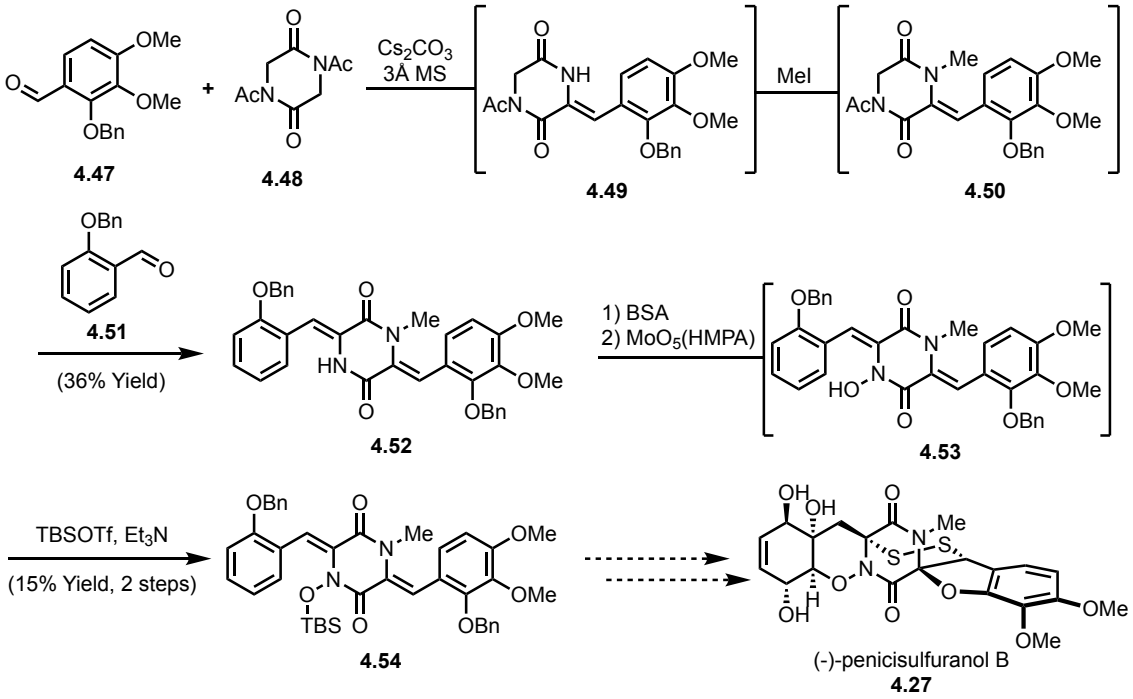

Scheme 4.6. Wood's synthetic efforts toward (-)-penicisulfuranol B (**4.27**).

4.2 Synthetic Studies toward [2.2.3]-ETPs

4.2.1 Retrosynthetic Analysis

In devising a retrosynthetic plan, we envisioned a highly divergent approach wherein late-stage functionalization allow access to a number of [2.2.3]-ETPs. Inspired by the NDA approach used in the previous chapter, we planned to incorporate a similar strategy in constructing a versatile tricyclic DKP-core. In contrast to the intermolecular NDA approach that had proven successful in our previous studies, we envisioned an intramolecular variant akin to that recently reported by Sheradsky and involving an intermediate cyclopentadienyl cycloadduct (**4.57**) as a acyl nitroso precursor (Scheme 4.7).[13] To this end, preparation of **4.57** began with the coupling of NHS-ester **4.55** and L-proline, followed by NHS-esterification to give activated ester **4.56**. Nucleophilic acyl

substitution with hydroxylamine hydrochloride delivered the corresponding hydroxamic acid and subsequent oxidation using tetraethylammonium periodate in the presence of cyclopentadiene resulted in the formation of the cyclopentadiene adduct (**4.57**), the desired precursor to acyl nitroso compound **4.58**. Upon thermolytic release of cyclopentadiene via *retro*-Diels-Alder reaction the intermediate **4.58** underwent subsequent intramolecular NDA to furnished *N*-oxy-DKP **4.59**. The necessity for masking **4.58** as its corresponding cyclopentadiene adduct derives from its thermal instability in the presence of the reagents employed and byproducts produced during hydroxamic acid oxidation, such as tetraethylammonium periodate. Although the acyl nitroso compounds are quite reactive as dienophiles, this particular substrate, which possesses and electron poor diene, requires heating in toluene.

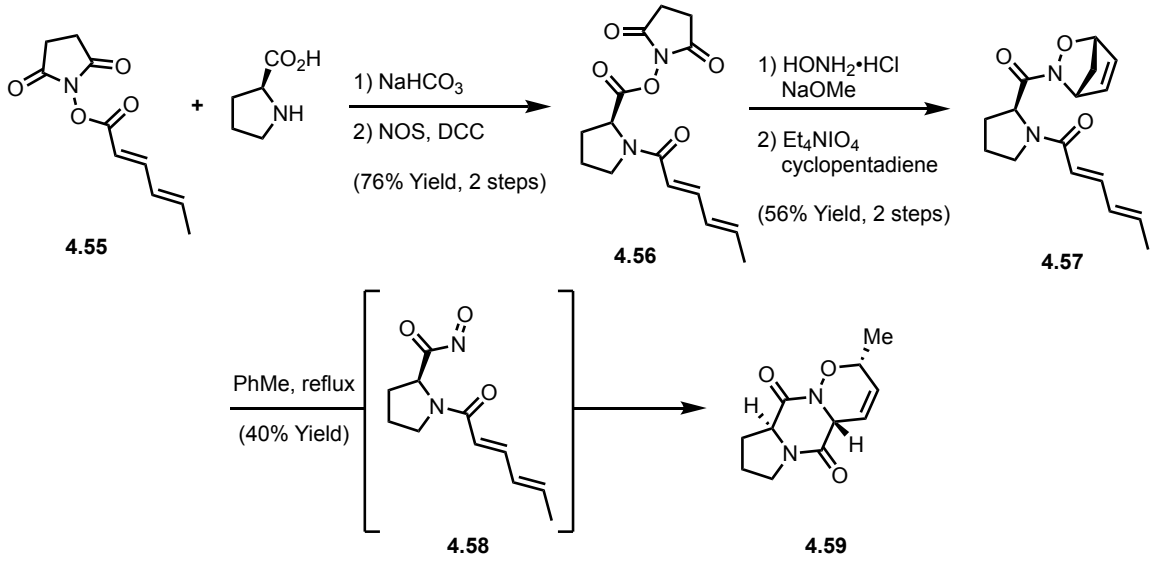

Scheme 4.7. Sheradsky's intramolecular NDA approach to *N*-oxy-DKP (**4.59**).

Clearly, the intent to employ NDA chemistry dictated that we take an approach calling for installation of the disulfide bridge and the requisite components later in the

synthesis. Thus as illustrated in Scheme 4.8, we envisioned that **4.22** derive from oxidation of a dithioxide (**4.60**) which, in turn, would arise from global deprotection of thioacetate **4.61**. The thioacetates in **4.61** would be introduced by functionalization of **4.62** at the *N,O*-acetal and benzylic alcohol positions via acid-mediated iminium formation and *thia*-Mitsunobu reaction, respectively. The highly functionalized aryl group could be attached to the tricycle (**4.64**) via aldol reaction with aldehyde **4.63**. The vinyl epoxide in **4.64** was seen as arising by displacement of the allylic alcohol by the neighboring tertiary alcohol in **4.65**. We envisioned that **4.65** would be derive from acetonide **4.66** via a sequence involving beta-elimination, benzoylation, and 1,2-reduction of the resulting enone. Removal of the silyl group in **4.67** and subsequent oxidation would secure the formation of ketone **4.66**. In order to install the tertiary alcohol shown in **4.67**, we hoped to effect diastereoselective epoxidation of the alkene **4.70** to afford **4.69**. Opening of the derived epoxide via beta-elimination would produce the requisite allylic alcohol (**4.68**) and, following methoxylation, a corresponding *N,O*-acetal that would serve as a synthetic handle for eventual installation of the *N,S*-acetal. In a manner analogous to that illustrated in Scheme 4.15, we envisioned that alkene (**4.70**) would arise from an intramolecular NDA reaction wherein the acyl nitroso dienophile (**4.71**) would be produced from hydroxamic acid **4.73** via a sequence involving intermolecular NDA, *retro*-Diels-Alder, and intramolecular NDA. Hydroxamic acid **4.73** would be directly formed by nucleophilic acyl substitution from the corresponding methyl ester (**4.74**) which would derive from peptide coupling between carboxylic acid **4.75** and sarcosine. Carboxylic acid **4.75** could arise from hydrolysis of enoate (**4.76**) which, in turn, would be produced from a known iodide[14] (**4.77**) via an intermolecular Heck reaction with methyl acrylate.

As illustrated in Scheme 4.9 in order to target both **4.23** and **4.24**, we envisioned that the key intermediate **4.64** could be diverged into either chloride (**4.78**) or acetate (**4.79**) via nucleophilic opening of the epoxide in **4.64** with a chloride source or a acetate source, respectively. Chloride **4.78** and acetate **4.79** would be respectively converted to **4.23** and **4.24** via an approach similar to that shown in Scheme 4.8.

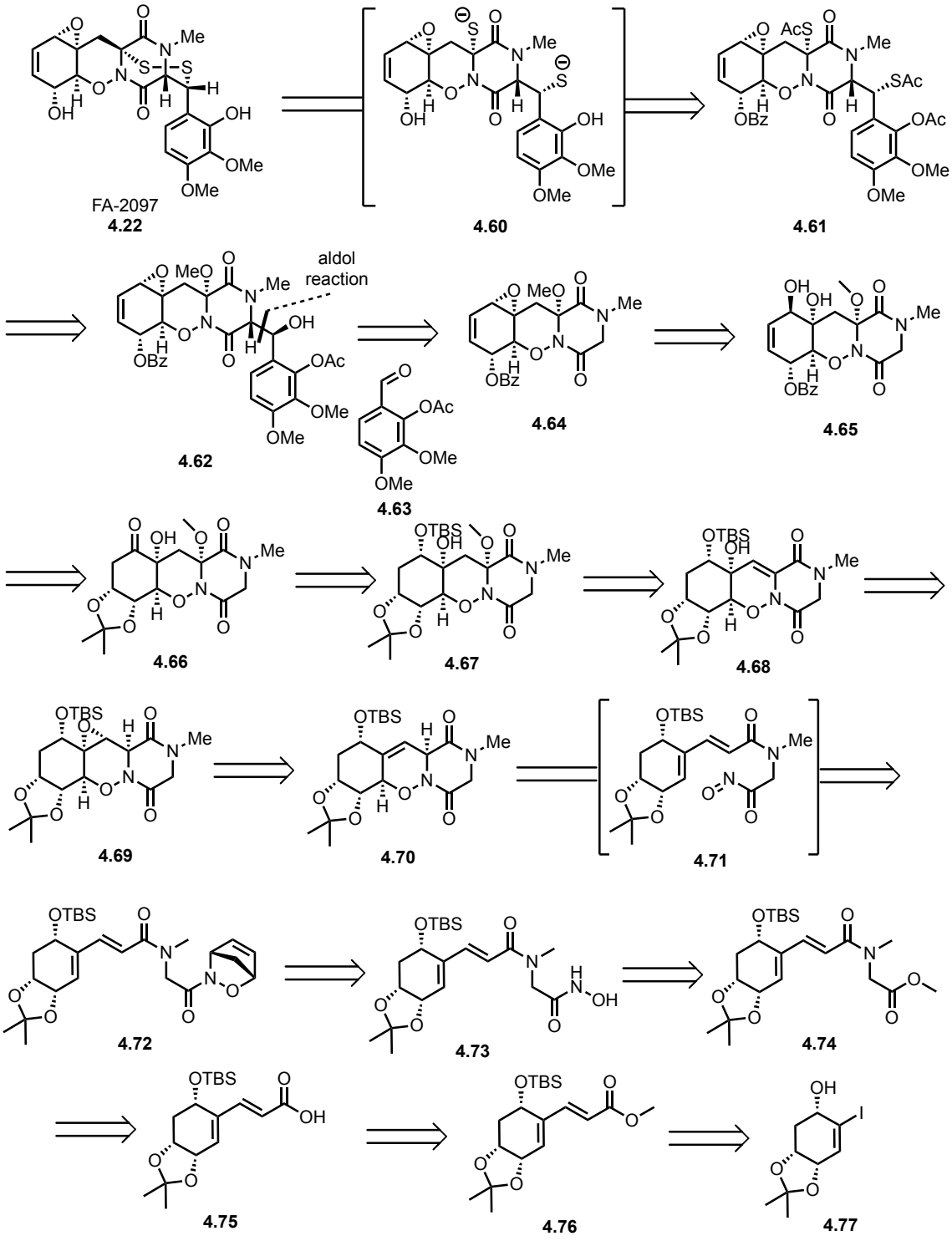

Scheme 4.8. Retrosynthetic analysis of FA-2097 (**4.22**).

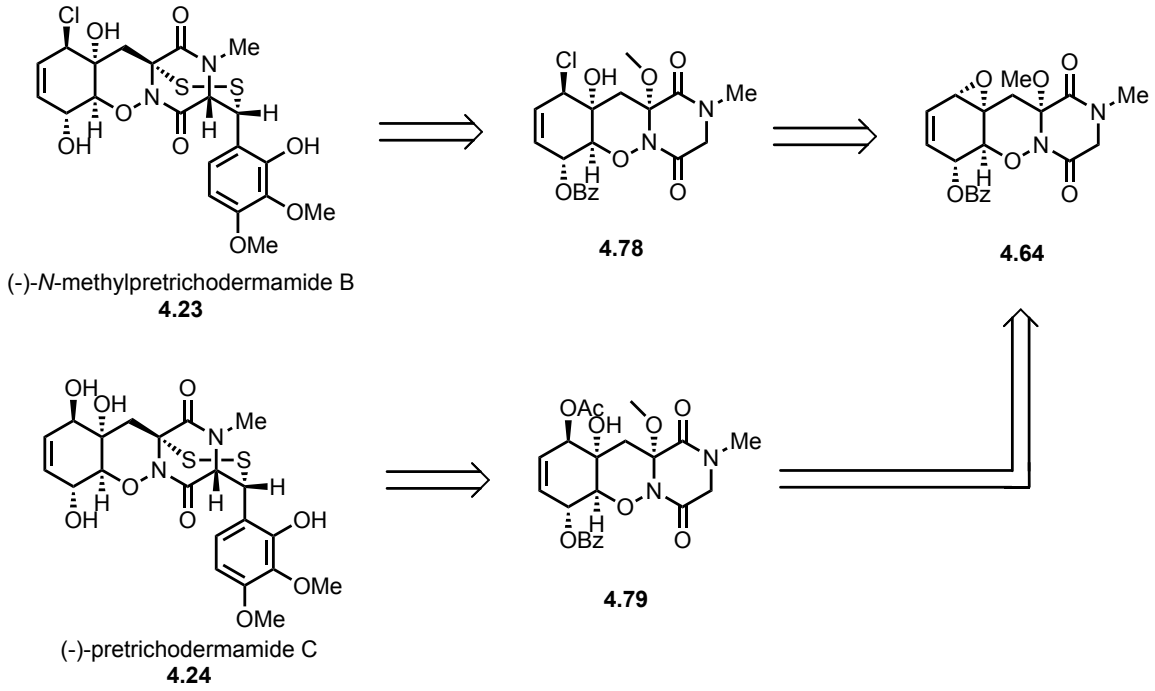

Scheme 4.9. Retrosynthetic analysis of (-)-*N*-methylpretrichodermamide B (**4.23**) and (-)-pretrichodermamide C (**4.24**).

In order to further extend this strategy to [2.2.3]-ETPs that lack an *N*-methylated DKP, such as **4.03**, **4.04**, and **4.25**, we envisioned substituting the methyl group with a protecting group (e.g., 3,4-dimethoxybenzyl group) that could be removed at a late-stage to expose the secondary amide present in **4.03**, **4.04**, and **4.25** (Scheme 4.10). As illustrated we expected the point of divergence would be epoxide **4.81**.

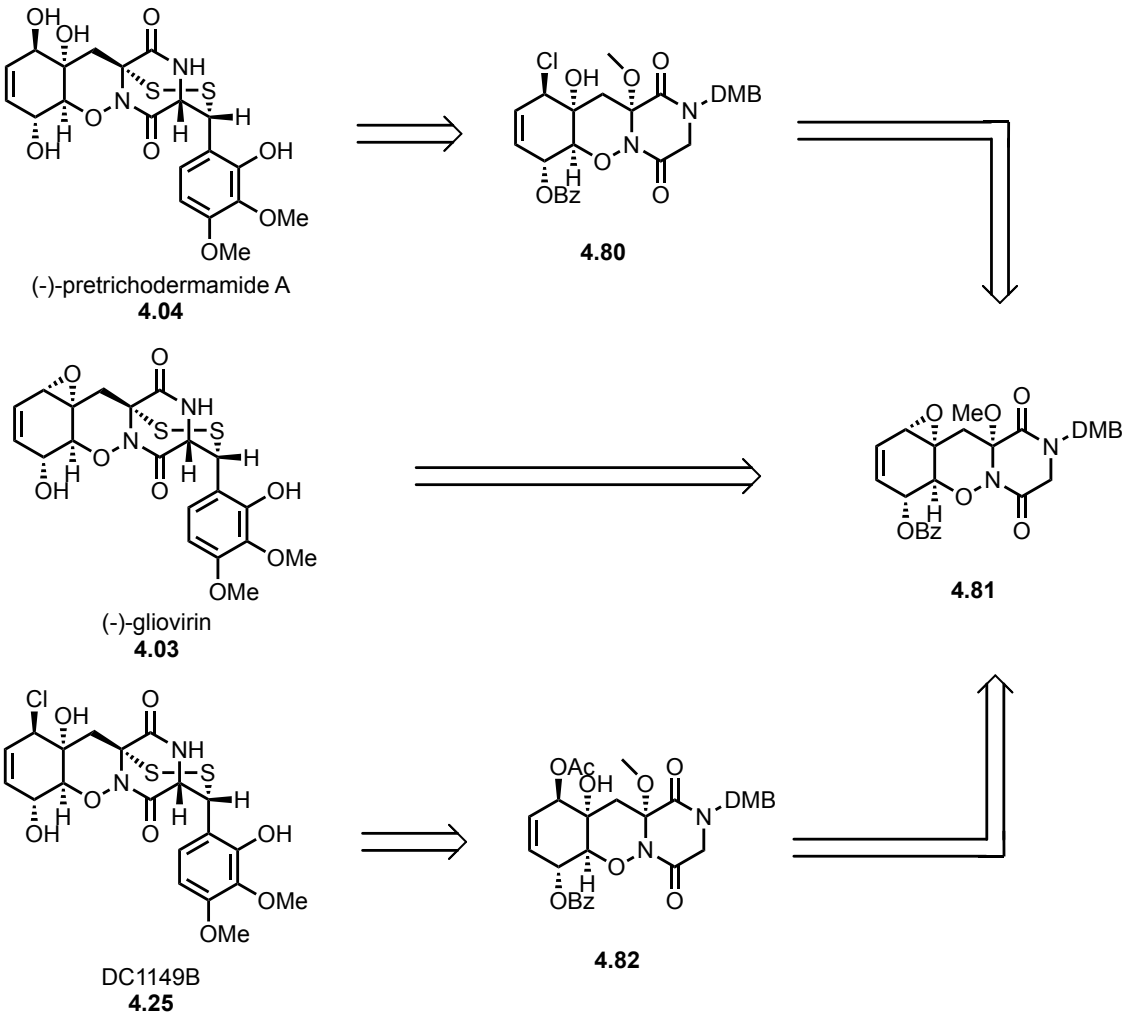

Scheme 4.10. Retrosynthetic analysis of (-)-pretrichodermamide A (**4.04**), (-)-gliovirin (**4.03**), and DC1149B (**4.25**).

In addition to the pretrichodermamides, there are [2.2.3]-ETPs, such as **4.26** and **4.27**, that possess spiro *N,O*-acetals and are thus at a higher overall oxidation level. As illustrated in Scheme 4.11, we envisioned accessing these congeners by condensing **4.78** with aldehyde 4.88 to afford an intermediate alkene (**4.87**) which, upon dihydroxylation would furnish hemiaminal (**4.86**). Subjecting **4.86** to acidic conditions is expected to initiate cleavage of the TBS group and result in formation of an intermediate iminium ion (**4.85**) which will then undergo spirocyclization to install the spiro *N,O*-acetal present in

4.26. Analogous to the retrosynthesis of the pretrichodermamides, dithialation, followed by global deprotection and subsequent disulfide bridge formation, would secure access to **4.26**. Furthermore, this strategy could also be applied in accessing **4.27** from **4.79** (Scheme 4.12).

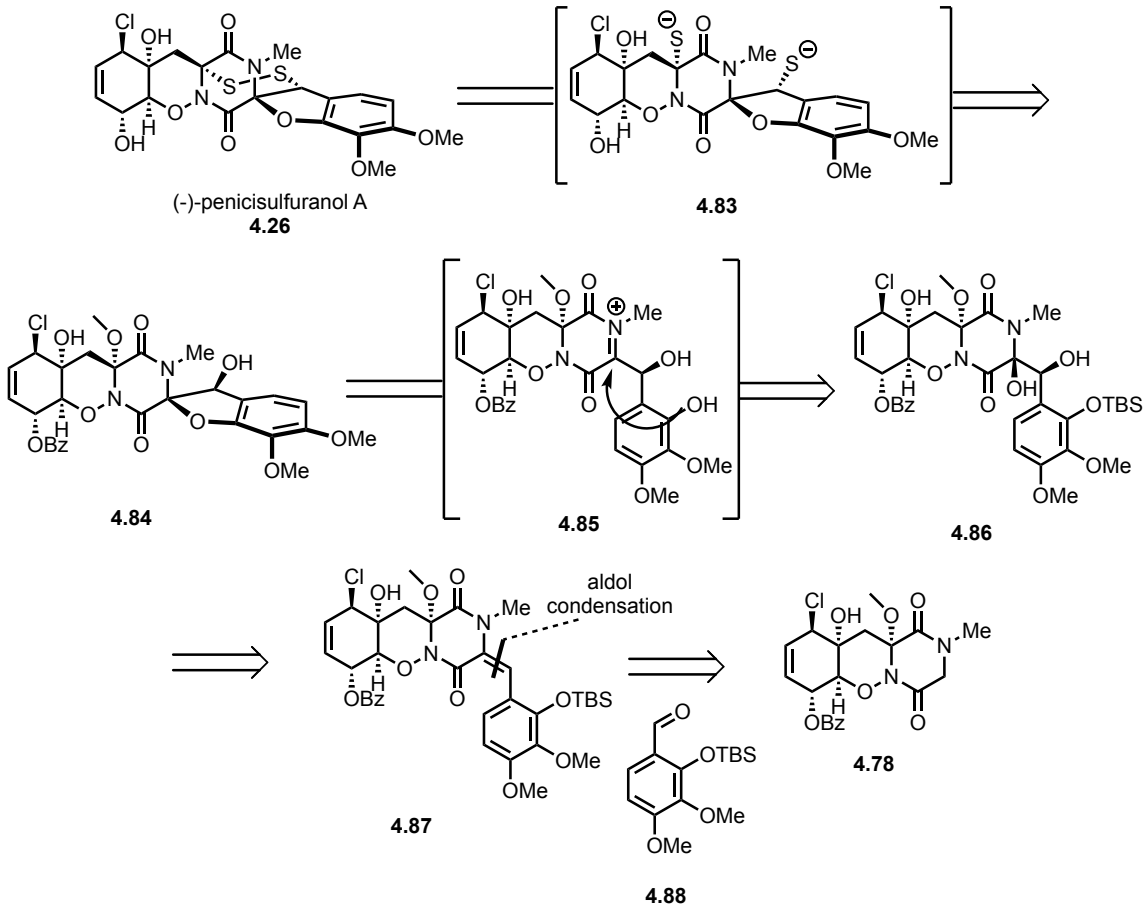

Scheme 4.11. Retrosynthetic analysis of (-)-penicisulfuranol A (**4.26**).

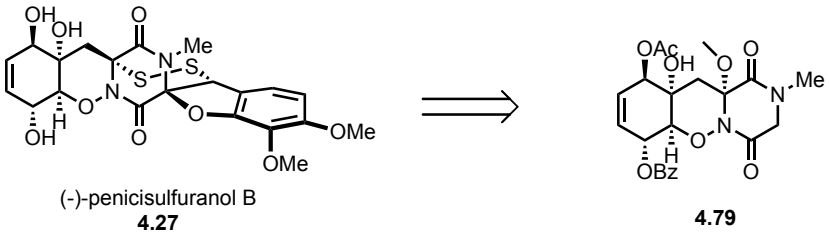

Scheme 4.12. Retrosynthetic analysis of (-)-penicisulfuranol B (**4.27**).

4.2.2 Forward Synthesis: Accessing the Tricyclic Core

Having devised a unified approach, we initially focused on reproducing the work by Hong and coworkers in obtaining enantiomerically pure iodide (**4.77**, Scheme 4.13).[14] Commercially available (-)-quinic acid (**4.89**) was converted to ketone **4.90** via a series of transformations that included: protection of the *syn*-1,2-diol as its corresponding acetonide, intramolecular lactonization, reduction with excess sodium borohydride, and oxidative cleavage to afford the ketone. The hydroxyl group in **4.90** was eliminated by initial mesylation and subsequent treatment with Et_3N. The derived enone was then converted to vinyl iodide **4.77** by employing standard iodination conditions followed by a diastereoselective Luche reduction.

With **4.77** in hand, silylation of the allylic alcohol and subsequent Heck coupling with the derived iodide (**4.91**) and methyl acylate gave enoate **4.76** in near quantitative yield over the two steps (Scheme 4.14). Saponification of **4.76** to its corresponding carboxylic acid (**4.92**) set the stage for peptide coupling with sarcosine to generate amide **4.74**. Nucleophilic acyl substitution with deprotonated hydroxylamine smoothly converted **4.74** to hydroxamic acid (**4.73**) which was converted to the cyclopentadiene adduct (**4.72**) in the presence of PIDA.[15] Isolation of the cycloadduct to remove any remaining oxidant and reaction by products was then followed by heating **4.72** to reflux in toluene to induce a *retro*-Diels-Alder reaction and reveal an acyl nitroso intermediate that undergoes intramolecular NDA to give tricyclic core (**4.70**) and its diastereomer (**4.93**) in a 5:1 ratio (Scheme 4.15).[13]

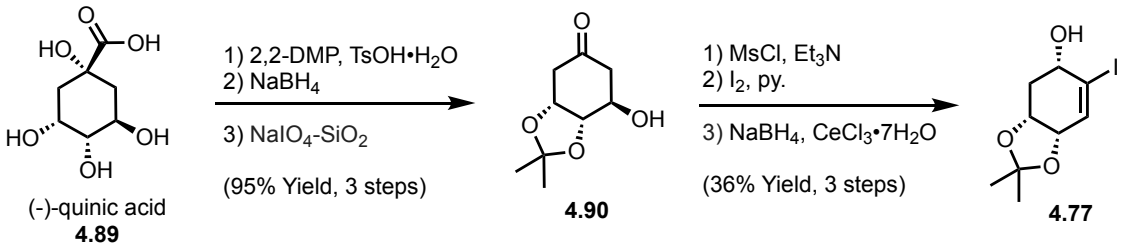

Scheme 4.13. Accessing iodide (**4.77**).

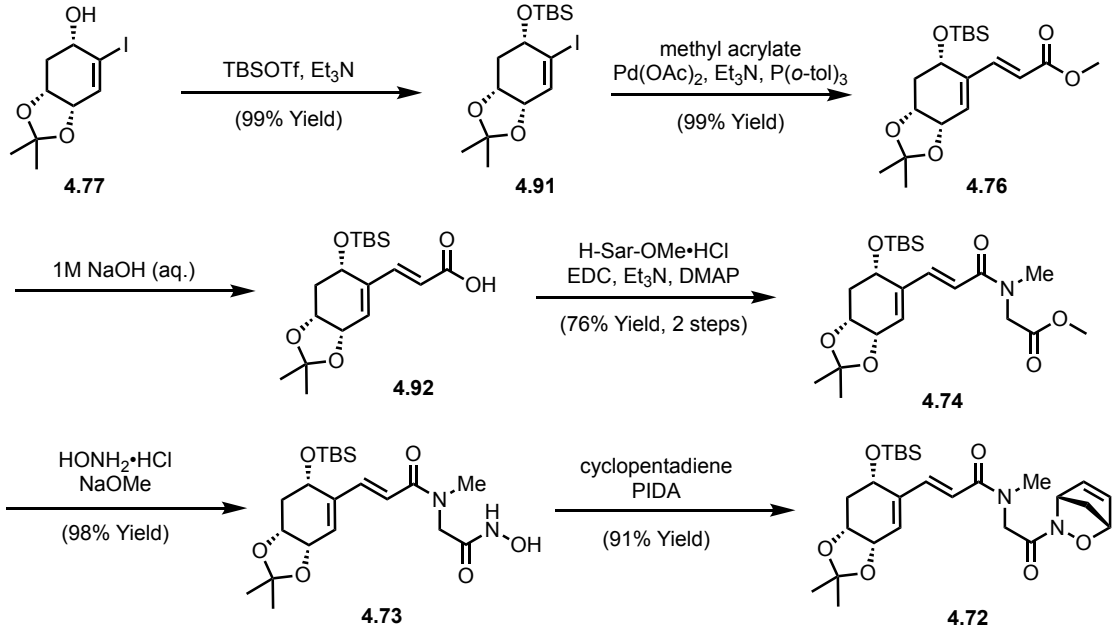

Scheme 4.14. Accessing intramolecular NDA precursor (**4.72**).

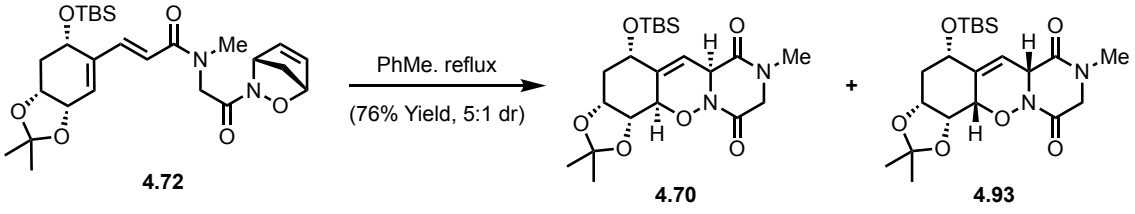

Scheme 4.15. Intramolecular NDA in accessing the tricyclic core (**4.70**).

4.2.3 Forward Synthesis: Undesired Stereochemical Outcome of Epoxidation

After accessing the tricyclic core, we turned our attention to completing the functionalization of the middle ring. As noted above shown in Scheme 4.8, we envisioned that these latter transformations would proceed via diastereoselective epoxidation of the alkene and subsequent elimination of the resulting epoxide. Accordingly, **4.70** was subjected to *m*-CPBA-mediated epoxidation (Scheme 4.16). To our initial delight, we observed formation of a single diastereomer from the epoxidation. In order to assign the correct stereochemistry of **4.94**, we attempted to prepare an analytically pure sample of **4.94**. Unfortunately, it was found that **4.94** was unstable under chromatographic purification. Therefore, we opted to move forward until a more stable intermediate could be prepared for analytical purpose. Unstable epoxide **4.94** was treated with DBU and the resulting allylic alcohol (**4.95**) proved even more unstable than **4.94**. Therefore, after a brief work-up, **4.95** was immediately treated with NBS in the presence of methanol to give yet, another unstable bromohydrin (**4.96**).[16] Lastly, radical dehalogenation with tributyltin hydride and triethylborane in the air, followed by quenching with TBAF, resulted in the removal of the silyl group, and the formation of a stable diol **4.97** as a single diastereomer.[17] To our dismay, X-Ray analysis of **4.97** revealed the undesired stereochemistry of the tertiary alcohol. Although the result was in contrast to expectations based on the analysis of simple molecular models, subsequent MM2 calculations clearly indicated that the thermodynamically preferred product (2.0 kcal/mol) to be **4.94**. Since we were not expecting product stability to have an overriding effect on the outcome we decided to continue exploring this approach by reducing the steric environment encompassing the

alpha face of the molecule. To this latter end, we decided to remove the sterically bulky OTBS and acetonide protecting groups and reattempt the epoxidation.

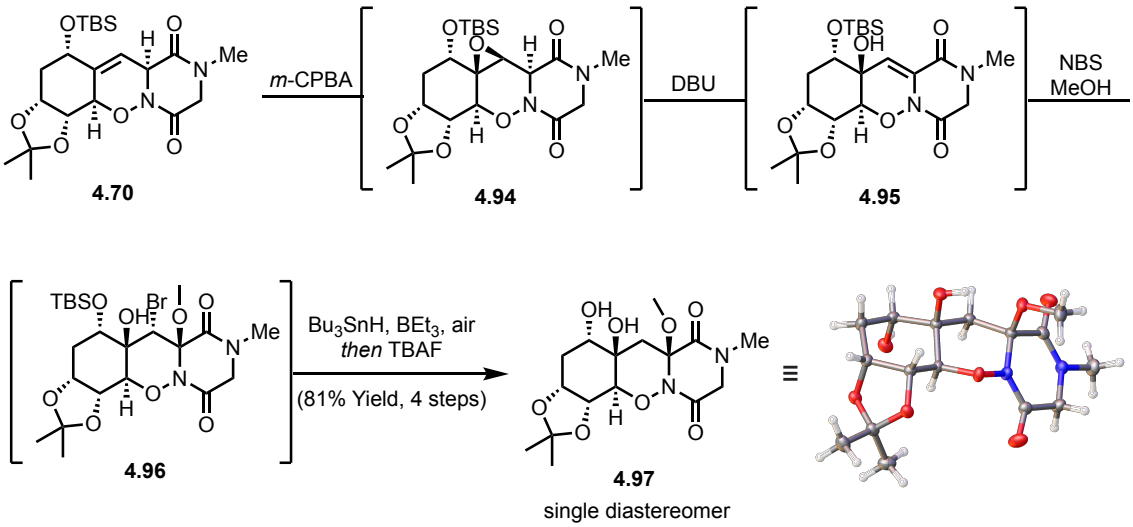

Scheme 4.16. Undesired stereochemical outcome in diol (**4.97**).

As illustrated in Scheme 4.17, we were delighted to observe the smooth conversion of **4.70** to protecting group-free triol (**4.98**) in excellent yield by simply treating with HCl. The structure was confirmed by an X-ray analysis (Scheme 4.17). Based on this latter analysis we had high hopes that epoxidation would now give the desired stereochemical outcome based on two factors: (1) the axial alcohol at the allylic position is directing epoxidation with *m*-CPBA; (2) *m*-CPBA approaching from the more sterically accessible convex face as opposed to the concave. Upon treating with *m*-CPBA, **4.98** was converted to epoxide (**4.99**) with a complete diastereoselectivity. In order to confirm the stereochemical outcome of the epoxidation, we opted to subject **4.99** to the same series of transformation that gave **4.97** and eventually compare the NMR data to that obtained for material derived from **4.99**. As observed previously, it was challenging to prepare an

analytically pure sample. Therefore, *Syn*-1,2-diol in **4.99** was carefully protected as its corresponding acetonide (**4.100**) and the alcohol was protected with a benzoyl group. Elimination of epoxide (**4.101**) with DBU and converting allylic alcohol (**4.102**) to bromohydrin (**4.103**) in the presence of NBS and methanol.[16] Subsequently, radical dehalogenation and removal of the benzoyl group under methanolysis gave **4.97**, thus proving that unfortunately the epoxidation of **4.98** had provided the undesired stereochemistry.[17]

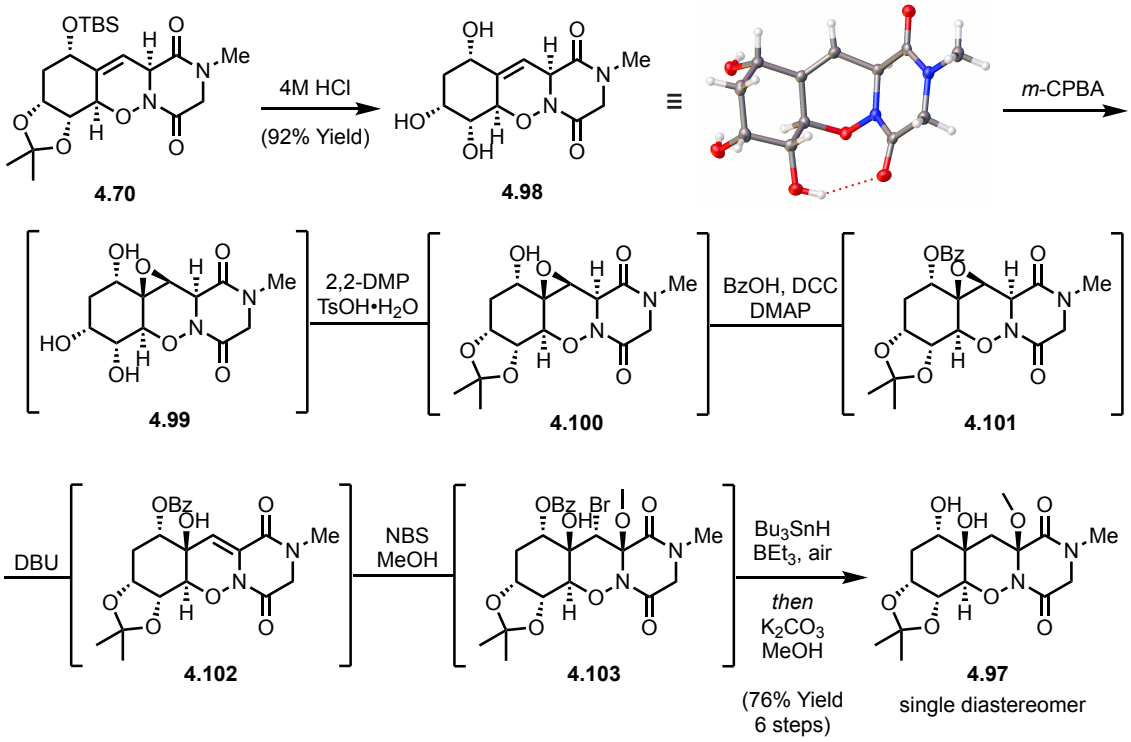

Scheme 4.17. Unsuccessful installation of the tertiary alcohol with desired stereochemistry.

4.3 Future Work

Although not described above, further attempts to perform a directed epoxidation under different conditions, such as $VO(acac)_2$/*t*BuOOH or DMDO, failed. Thus, we decided to slightly modify our synthetic plan. In efforts to advance **4.98** via methods other than epoxidation, we found out that after protection of the *syn*-1,2-diol as its corresponding acetonide (**4.103**), facile mesylation, followed by elimination of the resulting allylic mesylate delivered diene (**4.104**) reliably with excellent yield (Scheme 4.18).

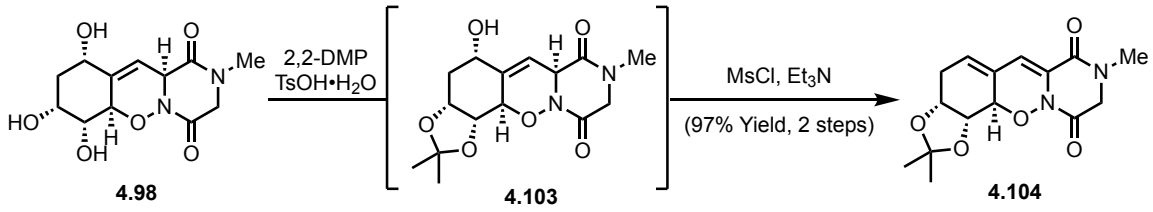

Scheme 4.18. Synthesis of diene (**4.104**).

With **4.104** in hand, we suspected that elimination of the acetonide could furnish *cis*-1,3-diene shown in **4.105**, which would set the stage for cycloaddition singlet oxygen to afford peroxybicycle (**4.106**, Scheme 4.19). Upon treating **4.106** with triphenylphosphine, cleavage of the peroxide from the less hinder side, followed by a tertiary oxyanion (**4.107**), would promote an intramolecular S_N2' to generate vinyl epoxide (**4.108**). Methoxylation of the enamine and benzoyl protection would furnish **4.64** to return to the originally proposed plan.

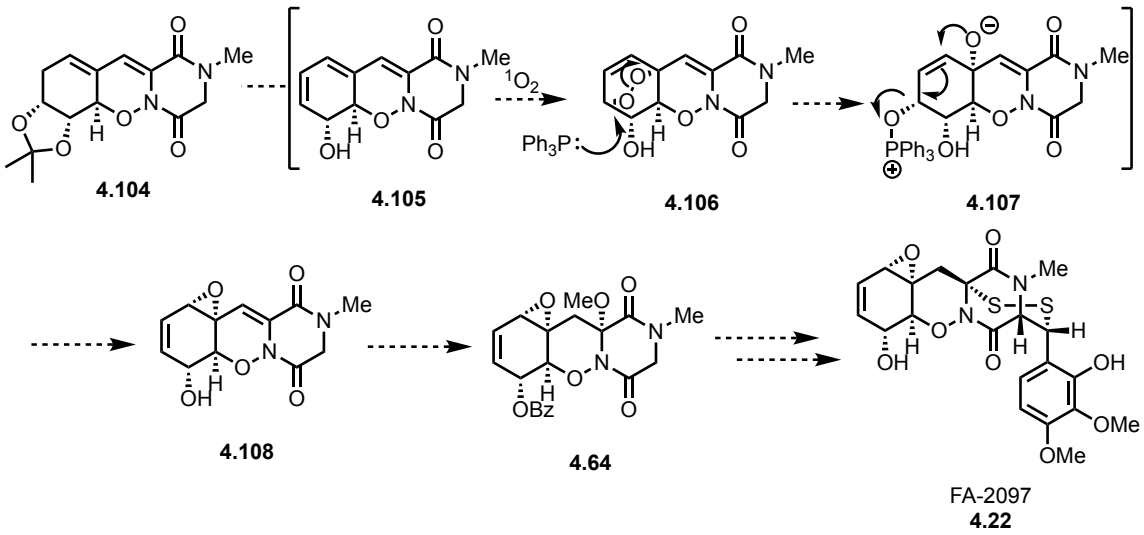

Scheme 4.19. Proposed synthesis of FA-2097 (**4.22**).

4.4 Conclusion

In conclusion, we have established asymmetric access to the tricyclic core of [2.2.3]-ETPs, which has not been reported to date, with appropriate oxidation patterns around the core for subsequent functionalization to target various [2.2.3]-ETPs. This highly efficient approach features diastereoselective intramolecular NDA as the key step to construct not only the tricyclic but also *N*-oxy-DKP. With this divergent strategy, this synthetic route can lead to a number of [2.2.3]-ETPs.

4.5 Experimental

4.5.1 General

Unless otherwise noted, all reactions were carried out in flame- or oven-dried glassware under a nitrogen (N_2) atmosphere. Anhydrous THF, benzene, CH_2Cl_2, toluene, Et_2O, and MeCN were obtained from a solvent purification system manufactured by SG

Water U.S.A., LLC maintained under a positive pressure of argon. Methanol and ethanol were dried over 3 Å molecular sieves purchased from Sigma-Aldrich. Acetone was dried over 4 Å molecular sieves purchased from Sigma-Aldrich. Anhydrous 1,4-dioxane was purchased from Sigma-Aldrich. All reactions were monitored for completion by normal-phase thin layer chromatography (TLC) using Millipore glass-backed 60 Å silica gel plates (indicator F-254, 250 μM). Flash column chromatography purifications were carried out using the indicated solvent systems (ACS-grade solvents) utilizing Silicycle SiliaFlash P60® (230-400 mesh) silica gel or Sigma-Aldrich Brockmann I (58 Å pore size) basic alumina as the stationary phase. Medium-pressure liquid chromatography (MPLC) purifications were carried out using the indicated solvent systems and flow rate on a Teledyne CombiFlash NextGen 300+ RF system using either Teledyne RediSep® Rf normal-phase or Biotage Sfär® normal-phase column of the indicated size. ^{1}H and ^{13}C NMR spectra were recorded on either a Bruker AscendTM 400 autosampler, Varian INOVA 500 or a Bruker AscendTM 600 autosampler. ^{1}H chemical shifts (δ) are reported in parts per million (ppm) relative to the residual solvent resonance of $CHCl_3$ (7.26 ppm), ^{13}C chemical shifts (δ) are reported in ppm relative to the central resonance of $CDCl_3$ (77.16 ppm), and coupling constants (*J*) are reported in hertz (Hz). NMR peak pattern abbreviations are as follows: s = singlet, d = doublet, dd = doublet of doublets, ddd = doublet of doublet of doublets, t = triplet, dt = doublet of triplets, q = quartet, m = multiplet, dtd= doublet of triplet of doublets, dq = doublet of quartets, qt = quartet of triplets, sept = septet, br = broad. High Resolution mass spectra (HRMS) were obtained in the Baylor University Mass Spectrometry Center on a Thermo Scientific Orbitrap Q-Exactive mass spectrometer using electrospray ionization (+ESI) and reported for the molecular ion

([M+H]$^+$ or [M+Na]$^+$). Infrared (IR) spectra were recorded on a Bruker Platinum-ATR IR spectrometer using a diamond window. Single crystal X-ray diffraction data were collected on a Bruker Apex IV-CCD detector using Mo-K_α radiation (λ = 0.71073 Å). Crystals were selected under Paratone® oil, placed on MiTeGen MicroMounts^{TM}, then immediately positioned under an N_2 cold stream at 150 K. Structures were solved and refined using APEX IV and SHELXTL software. Crystal graphics were generated using either SHELXTL and OLEX 2 software.

*4.5.2 Preparation of iodide **4.91***

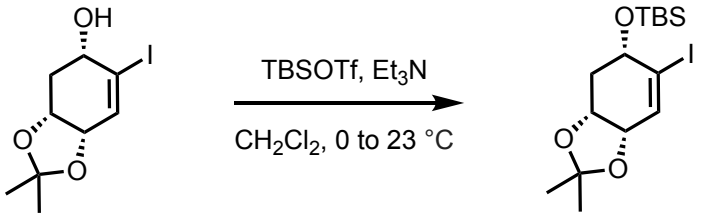

4.77 **4.91**

To a round bottom flask equipped with a magnetic stir bar was added alcohol **4.77** (21.1 g, 71.3 mmol) and anhydrous CH_2Cl_2 (710 mL, ca. 0.1 M). The resulting solution was cooled to 0 °C and Et_3N (13.0 mL, 92.6 mmol), followed by TBSOTf (18.0 mL, 78.4 mmol) was added *via* syringe. The resulting mixture was allowed to warm to 23 °C and stirred 2 h. Next, sat. aq. NH_4Cl (500 mL) was added and the aqueous layer was extracted with CH_2Cl_2 (1 x 400 mL). The combined organic layers were dried over anhydrous Na_2SO_4, filtered, and concentrated to afford the crude iodide **4.91** as a pale, yellow oil. Purification *via* flash column chromatography (silica gel, 17% EtOAc/hexanes) afforded iodide **4.91** (29.0 g, 99% yield) as a colorless oil. **^{1}H NMR** (600 MHz, $CDCl_3$) δ 6.59 – 6.55 (m, 1H), 4.33 – 4.26 (m, 2H), 4.12 – 4.08 (m, 1H), 2.21 – 2.15 (m, 1H), 1.91 – 1.82 (m, 1H), 1.47 (s, 3H), 1.35 (s, 3H), 0.94 (s, 9H), 0.19 (s, 3H), 0.12 (s, 3H). **^{13}C NMR** (151

MHz, $CDCl_3$) δ 134.2, 114.3, 110.4, 73.2, 71.9, 70.0, 36.7, 28.4, 26.4, 26.0, 18.3, -4.1, -4.3. **FTIR** (neat): 3336, 2954, 2929, 2857, 1621, 1508, 1461, 1369, 1330, 1308, 1248, 1215, 1162, 1113, 1052, 983, 944, 883, 834, 774, 719, 670, 594, 512, 482, 456, 426 cm^{-1}. **HRMS** (ESI+) *m/z* Calc'd. for $C_{15}H_{27}IO_3SiNa$ $[M+Na]^+$: 433.0666, found: 433.0658. $\mathbf{R_f}$ = 0.41 (17% EtOAc/hexanes). $[\boldsymbol{\alpha}]_D^{21.8}$: (c = 0.27, $CHCl_3$), +7.4°.

*4.5.3 Preparation of methyl ester **4.76***

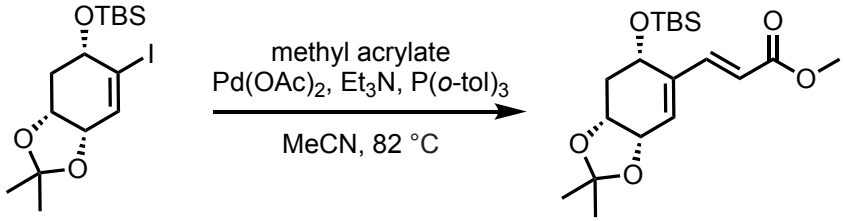

4.91 **4.76**

To a round bottom flask equipped with a magnetic stir bar was added iodide **4.77** (29.0 g, 70.7 mmol) and anhydrous MeCN (710 mL, ca. 0.1 M). To the resulting solution was added methyl acrylate (26.0 mL, 283 mmol), Et_3N (30.0 mL, 212 mmol), P(*o*-tol)$_3$ (2.2 g, 7.1 mmol) and $Pd(OAc)_2$ (0.4 g, 1.8 mmol), sequentially. The resulting mixture was heated to 82 °C using a heating mantle and stirred 4 h. The flask was then removed from the heat and cooled to 23 °C. The reaction mixture was quenched by addition of water (500 mL) and was extracted with CH_2Cl_2 (2 x 400 mL). The combined organic layers were dried over anhydrous Na_2SO_4, filtered, and concentrated to afford the crude methyl ester **4.91** as a yellow oil. Purification *via* flash column chromatography (silica gel, 17% EtOAc/hexanes) afforded methyl ester **4.76** (26.0 g, 99% yield) as a colorless oil. **^{1}H NMR** (600 MHz, $CDCl_3$) δ 7.37 (d, *J* = 16.0 Hz, 1H), 6.15 – 6.08 (m, 2H), 4.53 (t, *J* = 5.0 Hz, 1H), 4.39 – 4.34 (m, 1H), 4.30 (ddd, *J* = 9.1, 6.2, 4.6 Hz, 1H), 3.75 (s, 3H), 2.08 (dt, *J* = 13.0, 4.6 Hz, 1H), 1.95 – 1.87 (m, 1H), 1.46 (s, 3H), 1.37 (s, 3H), 0.89 (s, 9H), 0.13 (s,

3H), 0.13 (s, 3H). **^{13}C NMR** (151 MHz, $CDCl_3$) δ 167.3, 143.5, 142.0, 127.0, 119.8, 110.0, 71.9, 71.5, 65.9, 51.8, 35.9, 28.3, 26.3, 25.9, 18.2, -3.7, -4.7. **FTIR** (neat): 2984, 2931, 2887, 2857, 1720, 1640, 1624, 1472, 1462, 1435, 1369, 1308, 1273, 1250, 1215, 1192, 1164, 1103, 1078, 1045, 1018, 981, 939, 891, 835, 773, 670, 594, 513, 469, 419 cm^{-1}. **HRMS** (ESI+) *m/z* Calc'd. for $C_{19}H_{32}O_5SiNa$ $[M+Na]^+$: 391.1911, found: 391.1900. $\mathbf{R}_f$ = 0.75 (100% EtOAc). $[\boldsymbol{\alpha}]_D^{22.6}$: (c = 0.35, $CHCl_3$), +18.9°.

*4.5.4 Preparation of carboxylic acid **4.92***

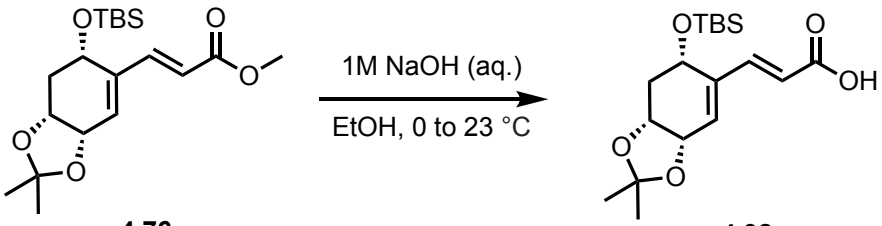

4.76 **4.92**

To a round bottom flask equipped with a magnetic stir bar was added methyl ester **4.76** (26.0 g, 70.6 mmol) and EtOH (350 mL, ca. 0.2 M). The resulting solution was cooled to 0 °C and 1 M aq. NaOH solution (180 mL, 180 mmol) was added slowly. The resulting mixture was allowed to warm to 23 °C and stirred 14 h. Next, 1 M aq. HCl solution (180 mL) was added to neutralize the reaction mixture and the aqueous layer was extracted with CH_2Cl_2 (2 x 400 mL) (if the aqueous layer contains product at this point, more 1 M aq. HCl was added). The combined organic layers were washed with brine (1 x 400 mL), dried over anhydrous Na_2SO_4, filtered, and concentrated to afford the crude carboxylic acid **4.92** (25.0 g, quantitative yield) as a yellow oil that solidifies upon standing. The crude material was sufficiently clean to be used in the next step without further purification. **^{1}H NMR** (600 MHz, $CDCl_3$) δ 7.44 (d, *J* = 16.0 Hz, 1H), 6.14 (d, *J* = 3.8 Hz, 1H), 6.12 (d, *J* = 15.9 Hz, 1H), 4.57 – 4.52 (m, 1H), 4.40 – 4.36 (m, 1H), 4.32 (ddd, *J* = 9.0, 6.1, 4.5 Hz, 1H), 2.09

(dt, J = 13.0, 4.6 Hz, 1H), 1.93 (ddd, J = 13.0, 9.0, 7.9 Hz, 1H), 1.46 (s, 3H), 1.37 (s, 3H), 0.89 (s, 9H), 0.14 (s, 3H), 0.13 (s, 3H). **^{13}C NMR** (151 MHz, $CDCl_3$) δ 171.6, 145.6, 141.8, 128.2, 119.3, 110.1, 71.8, 71.5, 65.7, 35.8, 28.3, 26.3, 25.9, 18.2, -3.7, -4.7. **FTIR** (neat): 2928, 2853, 1698, 1594, 1409, 1380, 1368, 1330, 1281, 1234, 1185, 1160, 1114, 1073, 1043, 1012, 993, 978, 942, 851, 834, 810, 772, 717, 670, 583, 513, 422 cm^{-1}. **HRMS** (ESI+) *m*/*z* Calc'd. for $C_{18}H_{30}O_5SiNa$ $[M+Na]^+$: 377.1755, found: 377.1755. $\mathbf{R}_f$ = 0.69 (100% EtOAc). $[\boldsymbol{\alpha}]_D^{20.6}$: (c = 0.12, $CHCl_3$), +20.3°.

*4.5.5 Preparation of amide **4.74***

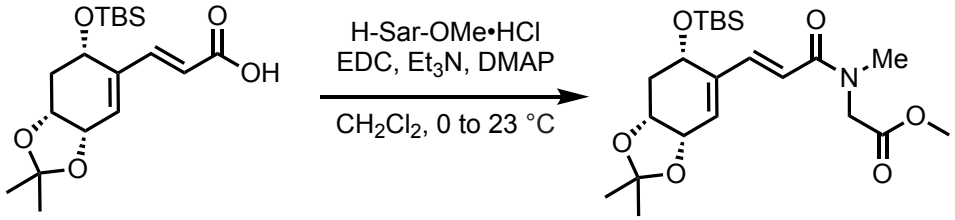

4.92 **4.74**

To a round bottom flask equipped with a magnetic stir bar was added carboxylic acid **4.92** (19.3 g, 54.4 mmol) and anhydrous CH_2Cl_2 (360 mL, ca. 0.15 M). To the resulting solution was added sarcosine hydrochloride (11.4 g, 81.5 mmol), DMAP (660 mg, 5.44 mmol), Et_3N (23.0 mL, 163 mmol), and EDC•HCl (12.5 g, 65.2 mmol), sequentially. The resulting mixture was stirred 24 h at 23 °C. Next, 1 M aq. HCl solution (300 mL) was added to the reaction mixture and the aqueous layer was extracted with CH_2Cl_2 (2 x 300 mL). The combined organic layers were washed with brine (1 x 300 mL), dried over anhydrous Na_2SO_4, filtered, and concentrated to afford the crude amide **4.74** as a yellow oil. Purification *via* flash column chromatography (silica gel, 33% EtOAc/hexanes) afforded amide **4.76** (18.5 g, 77% yield) as a pale, yellow oil. **^{1}H NMR** (600 MHz, $CDCl_3$) δ 7.35 (d, J = 14.9 Hz, 1H), 6.61 (d, J = 15.4 Hz, 1H), 6.09 (d, J = 4.0 Hz, 1H), 4.56 – 4.52

(m, 1H), 4.43 – 4.38 (m, 1H), 4.33 – 4.28 (m, 1H), 4.26 – 4.15 (m, 2H), 3.73 (s, 3H), 3.16 (s, 3H), 2.08 (dt, *J* = 12.9, 4.6 Hz, 1H), 1.97 – 1.86 (m, 1H), 1.46 (s, 3H), 1.37 (s, 3H), 0.89 (s, 9H), 0.14 (s, 3H), 0.13 (s, 3H). **^{13}C NMR** (151 MHz, $CDCl_3$) δ 166.5, 163.6, 139.6, 139.0, 122.3, 115.0, 106.6, 68.6, 68.1, 62.8, 48.9, 46.5, 33.3, 32.6, 25.0, 22.9, 22.5, 14.8, 7.9, 7.1. **FTIR** (neat): 2953, 2931, 2890, 2857, 1749, 1653, 1628, 1607, 1472, 1462, 1437, 1397, 1380, 1368, 1251, 1209, 1182, 1164, 1106, 1075, 1046, 1016, 980, 891, 835, 809, 774, 722, 670, 594, 511 cm^{-1}. **HRMS** (ESI+) *m/z* Calc'd. for $C_{22}H_{37}NO_6SiNa$ $[M+Na]^+$: 462.2282, found: 462.2270. $\mathbf{R}_f$ = 0.66 (100% EtOAc). $[\boldsymbol{\alpha}]_D^{20.7}$: (c = 0.41, $CHCl_3$), -11.7°.

*4.5.6 Preparation of hydroxamic acid **4.73***

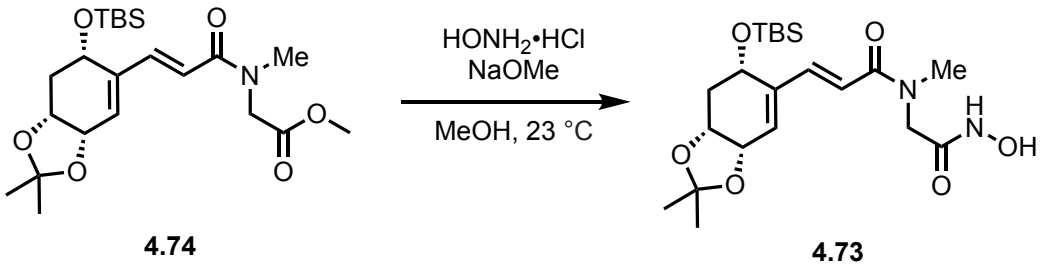

4.74 **4.73**

To a round bottom flask equipped with a magnetic stir bar was added amide **4.74** (18.5 g, 42.1 mmol) and anhydrous MeOH (170 mL, ca. 0.25 M). To the resulting solution was added hydroxylamine hydrochloride (11.7 g, 168 mmol), followed by NaOMe (48.0 mL, 252 mmol, 30% in MeOH) dropwise. The resulting mixture was stirred 2 h at 23 °C. Next, sat. aq. NH_4Cl solution (300 mL) was added to the reaction mixture and the aqueous layer was extracted with EtOAc (2 x 200 mL). The combined organic layers were washed with brine (1 x 300 mL), dried over anhydrous Na_2SO_4, filtered, and concentrated to afford the crude hydroxamic acid **4.73** (18.2 g, 98% yield) as a pale, yellow, foamy oil. The crude material was sufficiently clean to be used in the next step without further purification. **^{1}H NMR** (600 MHz, $CDCl_3$) δ 7.35 (d, *J* = 15.3 Hz, 1H), 6.56 (d, *J* = 15.3 Hz, 1H), 6.10 (d, *J*

= 3.9 Hz, 1H), 4.54 (br t, *J* = 5.1 Hz, 1H), 4.41 – 4.36 (m, 1H), 4.33 – 4.28 (m, 1H), 4.06 (d, *J* = 15.1 Hz, 1H), 4.01 (d, *J* = 15.0 Hz, 1H), 3.22 (s, 3H), 2.08 (dt, *J* = 13.0, 4.6 Hz, 1H), 1.95 – 1.86 (m, 1H), 1.46 (s, 3H), 1.37 (s, 3H), 0.88 (s, 9H), 0.12 (s, 6H). **^{13}C NMR** (151 MHz, $CDCl_3$) δ 167.9, 166.8, 143.3, 142.7, 126.5, 117.7, 110.0, 71.9, 71.4, 66.2, 50.6, 37.5, 35.9, 28.3, 26.3, 25.9, 18.2, 3.7, 4.5. **FTIR** (neat): 3215, 2984, 2953, 2930, 2887, 2857, 1649, 1626, 1596, 1472, 1462, 1402, 1379, 1369, 1251, 1215, 1162, 1116, 1077, 1046, 1017, 975, 907, 893, 835, 774, 729, 670, 646, 511 cm^{-1}. **HRMS** (ESI+) *m*/*z* Calc'd. for $C_{21}H_{36}N_2O_6SiNa$ $[M+Na]^+$: 463.2235, found: 463.2234. $\mathbf{R_f}$ = 0.13 (100% EtOAc). $[\boldsymbol{\alpha}]_D^{20.9}$: (c = 0.46, $CHCl_3$), -9.0°.

*4.5.7 Preparation of cyclopentadiene adduct **4.72***

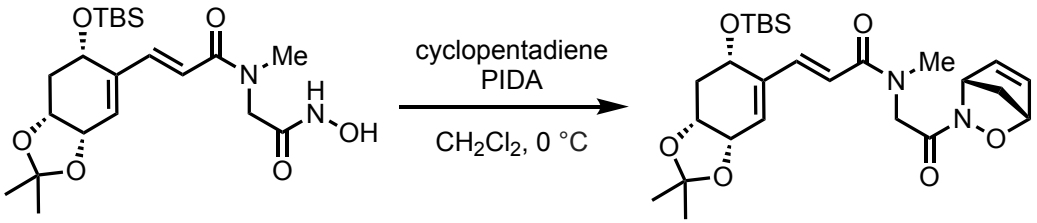

4.73 **4.72**

To a round bottom flask equipped with a magnetic stir bar was added hydroxamic acid **4.73** (18.2 g, 41.3 mmol) and anhydrous CH_2Cl_2 (410 mL, ca. 0.1 M). The resulting solution was cooled to 0 °C and freshly distilled cyclopentadiene (7.0 mL, 82.6 mmol), immediately followed by PIDA (14.6 g, 45.4 mmol), was added as a single portion. The resulting mixture was stirred 1 h at 0 °C. Next, sat. aq. $NaHCO_3$ solution (200 mL) and sat. aq. $Na_2S_2O_3$ solution (200 mL) were added to the reaction mixture and the aqueous layer was extracted with CH_2Cl_2 (2 x 200 mL). The combined organic layers were washed with brine (1 x 300 mL), dried over anhydrous Na_2SO_4, filtered, and concentrated to afford the crude cyclopentadiene adduct **4.72** as a yellow oil. Purification *via* flash column

chromatography (silica gel, 40% EtOAc/hexanes, then 60% EtOAc/hexanes) afforded cyclopentadiene adduct **4.72** (19.0 g, 91% yield) as a pale, yellow oil that solidifies upon standing. **^{1}H NMR** (600 MHz, $CDCl_3$) δ 7.31 – 7.19 (m, 1H), 6.62 – 6.46 (m, 2H), 6.41 – 6.19 (m, 1H), 6.05 – 5.92 (m, 1H), 5.35 – 5.22 (m, 2H), 4.49 (br s, 1H), 4.40 – 4.22 (m, 2H), 4.14 – 3.85 (m, 2H), 3.11 – 2.92 (m, 3H), 2.01 – 1.80 (m, 4H), 1.41 (br s, 3H), 1.32 (br s, 3H), 0.84 (br s, 9H), 0.08 (br s, 6H). **^{13}C NMR** (151 MHz, $CDCl_3$) δ 173.1, 172.2, 167.2, 166.8, 142.8, 142.0, 140.8, 140.7, 136.8, 136.4, 132.9, 126.0, 125.8, 123.9, 123.4, 119.0, 118.6, 109.8, 84.9, 84.5, 71.94, 71.85, 71.5, 71.3, 66.5, 66.3, 65.9, 62.8, 60.4, 52.7, 51.1, 48.6, 48.4, 36.6, 36.2, 35.8, 35.5, 28.3, 26.3, 26.2, 25.9, 18.14, 18.12, 14.3, 4.6, 4.5, 4.0, 3.8. **FTIR** (neat): 2954, 2930, 2887, 2856, 1681, 1652, 1629, 1607, 1472, 1462, 1393, 1379, 1369, 1329, 1284, 1249, 1214, 1176, 1163, 1112, 1077, 1045, 1017, 978, 920, 893, 835, 800, 774, 728, 677, 646, 574, 511, 462, 420 cm^{-1}. **HRMS** (ESI+) *m/z* Calc'd. for $C_{26}H_{40}N_2O_6SiNa$ $[M+Na]^+$: 527.2548, found: 527.2547. $\mathbf{R_f}$ = 0.45 (100% EtOAc). $[\boldsymbol{\alpha}]_D^{22.9}$: (c = 0.39, $CHCl_3$), -9.5°.

*4.5.8 Preparation of NDA cycloadducts **4.70** and **4.93***

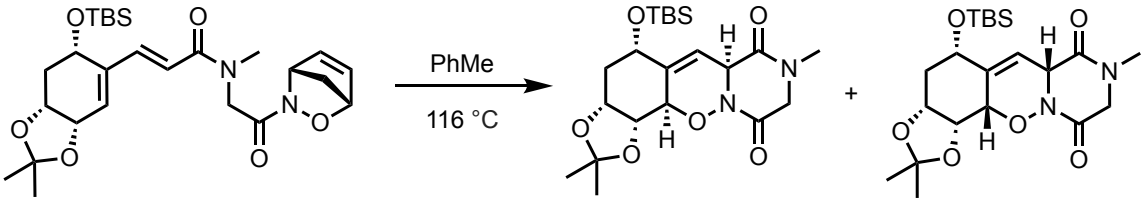

4.72 **4.70** **4.93**

To a round bottom flask equipped with a magnetic stir bar was added cyclopentadiene adduct **4.72** (19.0 g, 37.7 mmol) and anhydrous PhMe (870 mL, ca. 0.043 M). The resulting mixture was heated to 116 °C and stirred 12 h. The flask was then removed from the heat and cooled to 23 °C. Next, the reaction mixture was concentrated

to afford the crude NDA cycloadducts **4.70** and **4.93** as a yellow oil. Purification *via* flash column chromatography (silica gel, 75% EtOAc/hexanes) afforded NDA cycloadduct **4.70** (10.0 g, 61% yield) as a white solid. **^{1}H NMR** (500 MHz, $CDCl_3$) δ 6.18 (s, 1H), 4.92 – 4.87 (m, 2H), 4.46 (br t, *J* = 3.3 Hz, 1H), 4.37 – 4.31 (m, 1H), 4.18 – 4.10 (m, 2H), 3.96 (d, *J* = 17.6 Hz, 1H), 2.99 (s, 3H), 2.36 (dt, *J* = 15.7, 2.3 Hz, 1H), 1.82 (br dt, *J* = 15.6, 4.6 Hz, 1H), 1.55 (s, 3H), 1.35 (s, 3H), 0.89 (s, 9H), 0.09 (s, 3H), 0.05 (s, 3H). **^{13}C NMR** (126 MHz, $CDCl_3$) δ 162.7, 159.4, 139.2, 116.5, 109.5, 80.1, 77.9, 73.8, 70.7, 56.4, 51.2, 35.9, 33.7, 28.7, 25.9, 25.7, 18.0, -4.7, -4.9. **FTIR** (thin film): 2984, 2953, 2929, 2886, 2857, 1670, 1503, 1472, 1462, 1437, 1406, 1381, 1369, 1332, 1303, 1240, 1214, 1169, 1092, 1051, 1027, 1004, 976, 944, 921, 891, 853, 834, 808, 775, 669, 647, 629, 590, 555, 511, 486, 406 cm^{-1}. **HRMS** (ESI+) *m/z* Calc'd. for $C_{21}H_{34}N_2O_6SiNa$ $[M+Na]^+$: 461.2078, found: 461. 2079. $\mathbf{R}_f$ = 0.18 (100% EtOAc, $KMnO_4$ stain). $[\boldsymbol{\alpha}]_D^{23.1}$: (c = 0.39, $CHCl_3$), -2.4°.

Purification *via* flash column chromatography (silica gel, 75% EtOAc/hexanes) afforded NDA cycloadduct **4.93** (2.0 g, 12% yield) as a clear oil. **^{1}H NMR** (500 MHz, $CDCl_3$) δ 6.35 – 6.33(m, 1H), 4.97 (br s, 1H), 4.58 (br t, *J* = 4.2 Hz, 1H), 4.44 – 4.39 (m, 1H), 4.30 – 4.23 (m, 1H), 4.18 – 4.09 (m, 1H), 4.01 (d, *J* = 17.3 Hz, 1H), 3.89 (d, *J* = 17.2 Hz, 1H), 2.98 (s, 3H), 2.18 – 2.09 (m, 1H), 1.66 – 1.55 (m, 1H), 1.36 (s, 3H), 1.30 (s, 3H), 0.92 (s, 9H), 0.10 (s, 3H), 0.07 (s, 3H).**^{13}C NMR** (126 MHz, $CDCl_3$) δ 162.8, 157.8, 137.2, 115.0, 110.9, 76.8, 75.5, 73.0, 67.4, 57.1, 51.1, 40.1, 33.6, 28.3, 26.1, 25.9, 18.4, -4.7, -4.8. **FTIR** (neat): 2954, 2931, 2894, 2857, 1672, 1503, 1471, 1461, 1438, 1404, 1380, 1370, 1329, 1305, 1251, 1243, 1217, 1167, 1153, 1119, 1088, 1065, 1045, 1023, 989, 962, 945, 919, 904, 890, 875, 835, 806, 776, 732, 702, 669, 648, 628, 573, 552, 514, 488, 409 cm^{-1}. **HRMS**

(ESI+) *m/z* Calc'd. for $C_{21}H_{34}N_2O_6SiNa$ $[M+Na]^+$: 461.2078, found: 461. 2079. $\mathbf{R}_f$ = 0.15 (100% EtOAc). $[\boldsymbol{\alpha}]_D^{21.6}$: (c = 0.28, $CHCl_3$), -115.4°.

*4.5.9 Preparation of epoxide **4.94***

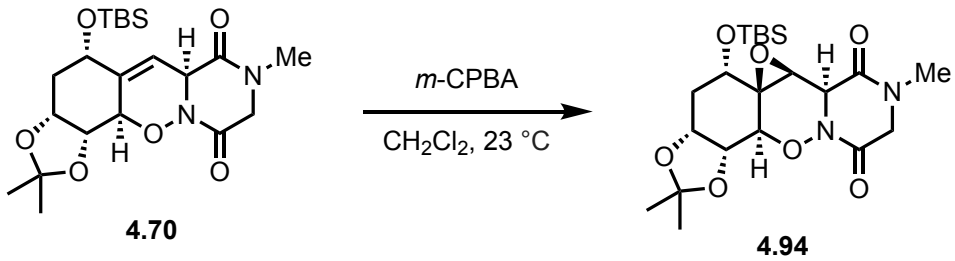

4.70 **4.94**

To a round bottom flask equipped with a magnetic stir bar was added NDA cycloadduct **4.70** (440 mg, 1.01 mmol) and CH_2Cl_2 (10 mL, ca. 0.1 M). To the resulting solution was added *m*-CPBA (1.16 g, 5.05 mmol, 75% weight) in a single portion. The resulting mixture was stirred 5 days at 23 °C. Next, sat. aq. $NaHCO_3$ solution (10 mL) and sat. aq. $Na_2S_2O_3$ solution (10 mL) were added to the reaction mixture and the aqueous layer was extracted with CH_2Cl_2 (2 x 10 mL). The combined organic layers were washed with sat. aq. $NaHCO_3$ solution (1 x 10 mL), dried over anhydrous Na_2SO_4, filtered, and concentrated to afford the crude epoxide **4.94** (460 mg, assumed quantitative yield) as a yellow foamy oil, which was used immediately in the next step.

*4.5.10 Preparation of allylic alcohol **4.95***

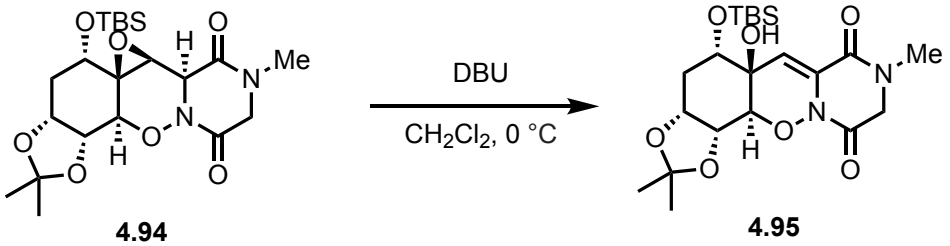

4.94 **4.95**

To a round bottom flask equipped with a magnetic stir bar was added crude epoxide **4.94** (460 mg, 1.01 mmol) and anhydrous CH_2Cl_2 (10 mL, ca. 0.1 M). The resulting

solution was cooled to 0 °C and added DBU (0.16 mL, 1.06 mmol) dropwise by syringe. The resulting mixture was stirred 10 min at 0 °C. Next, sat. aq. NH_4Cl solution (10 mL) was added to the reaction mixture and the aqueous layer was extracted with CH_2Cl_2 (2 x 10 mL). The combined organic layers were dried over anhydrous Na_2SO_4, filtered, and concentrated to afford the crude allylic alcohol **4.95** (460 mg, assumed quantitative yield) as a dark brown foamy oil, which was used immediately in the next step.

*4.5.11 Preparation of bromohydrin **4.96***

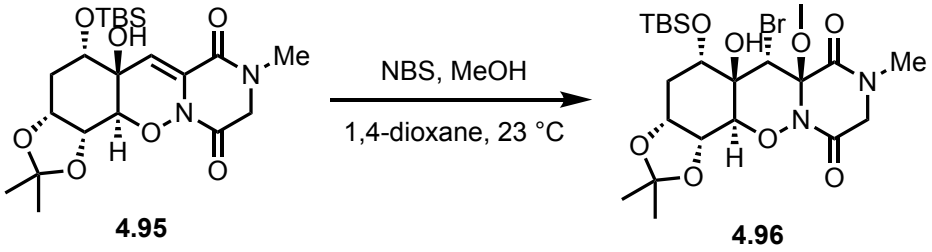

4.95 **4.96**

To a round bottom flask equipped with a magnetic stir bar was added crude allylic alcohol **4.95** (460 mg, 1.01 mmol), anhydrous MeOH (2.0 mL, ca. 0.5 M), and anhydrous 1,4-dioxane (1.0 mL, ca. 1.0 M). To the resulting solution was added NBS (1.16 g, 1.06 mmol) in a single portion. The resulting mixture was stirred 4 h at 23 °C. Next, the reaction mixture was concentrated to afford the crude bromohydrin **4.96** (570 mg, assumed quantitative yield) as a yellow foamy oil, which was used immediately in the next step.

*4.5.12 Preparation of diol **4.97***

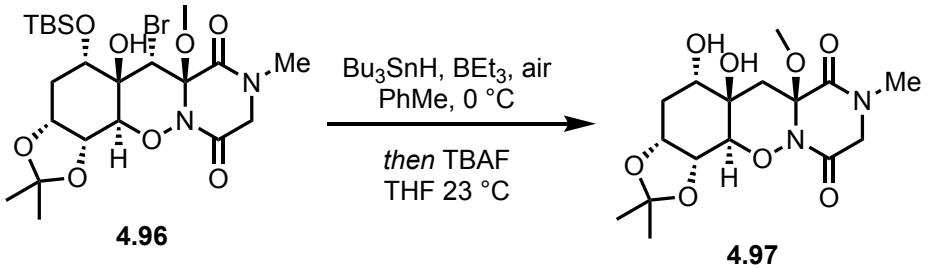

4.96 **4.97**

To a round bottom flask equipped with a magnetic stir bar was added crude bromohydrin **4.96** (550 mg, 1.01 mmol) and PhMe (19.0 mL, ca. 0.052 M). The resulting solution was left uncapped and Bu_3SnH (0.29 mL, 1.06 mmol), immediately followed by BEt_3 (0.4 mL, 0.4 mmol, 1.0 M in hexanes). The resulting mixture was stirred 10 min at 0 °C and was concentrated. The crude mixture was redissolved in THF (10.0 mL, ca. 0.1 M) and TBAF (1.1 mL, 1.1 mmol, 1.0 M in THF) was added. The reaction mixture was stirred 24 h at 23 °C and was concentrated to afford the crude diol **4.97**. Purification *via* flash column chromatography (silica gel, 100% EtOAc, then 10% MeOH in CH_2Cl_2) afforded diol **4.97** (280 mg, 75% yield over four steps) as a clear crystalline solid. **^{1}H NMR** (500 MHz, $CDCl_3$) δ 4.43 (br t, *J* = 3.8 Hz, 1H), 4.26 (dd, *J* = 8.0, 4.9 Hz, 1H), 4.21 (d, *J* = 8.0 Hz, 1H), 4.15 (d, *J* = 18.0 Hz, 1H), 4.05 – 3.98 (m, 2H), 3.64 (br t, *J* = 3.1 Hz, 1H), 3.46 (s, 1H), 3.30 (s, 3H), 3.01 (s, 3H), 2.44 (dt, *J* = 16.0, 4.0 Hz, 1H), 2.31 (d, *J* = 14.4 Hz, 1H), 2.25 (d, *J* = 14.4 Hz, 1H), 2.19 (dt, *J* = 16.0, 2.2 Hz, 1H), 1.54 (s, 3H), 1.35 (s, 3H).**^{13}C NMR** (126 MHz, $CDCl_3$) δ 162.2, 159.8, 109.2, 89.8, 83.6, 75.0, 74.5, 71.8, 71.6, 52.3, 50.9, 39.2, 33.8, 28.5, 27.7, 26.2. **FTIR** (neat): 3515, 2986, 2923, 2854, 1697, 1671, 1508, 1461, 1434, 1404, 1386, 1376, 1367, 1343, 1312, 1272, 1256, 1238, 1227, 1210, 1167, 1148, 1097, 1086, 1045, 1021, 1001, 974, 953, 937, 927, 912, 859, 851, 838, 817, 777, 755, 704, 678, 658, 609, 585, 562, 539, 513, 490, 462, 442 cm^{-1}. **HRMS** (ESI+) *m*/*z* Calc'd. for $C_{16}H_{24}N_2O_8Na$ $[M+Na]^+$: 395.1425, found: 395. 1422. $\mathbf{R}_f$ = 0.05 (100% EtOAc). $[\boldsymbol{\alpha}]_D^{21.4}$: (c = 0.57, $CHCl_3$), -80.1°. **MP** = 209-213 °C (decomposed).

*4.5.13 Preparation of triol **4.98***

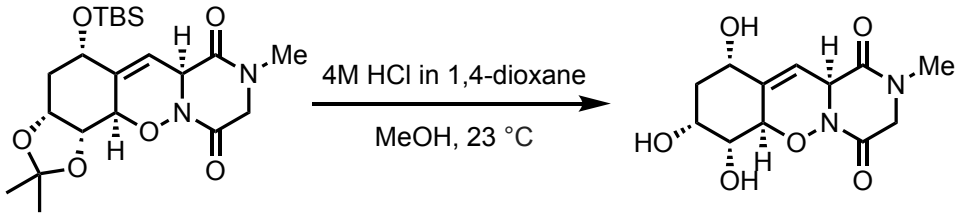

4.70 **4.98**

To a round bottom flask equipped with a magnetic stir bar was added NDA cycloadduct **4.70** (1.0 g, 2.3 mmol) and anhydrous MeOH (23 mL, ca. 0.1 M). *Of note, **4.70** needs to be completely dissolved in MeOH for the best result during precipitation.* To the resulting solution was added HCl (2.9 mL, 11.4 mmol, 4.0 M in 1,4-dioxane) via syringe. After 10 min, precipitation was observed and Et_2O (10 mL) was added to accelerate the rate of precipitation. After 20 min, the reaction mixture was sealed and place in a freezer (-20 °C) for 12 h. After warming to 23 °C the resulting precipitate was filtered and rinsed with Et_2O (10 mL). The first crop was collected. Next, the mother liquor was collected and concentrated. The crude residue was dissolved in MeOH/Et_2O (15 mL, 2:1, v:v) sealed, and place in a freezer (-20 °C) for 12 h. After warming to 23 °C the resulting precipitate was filtered and rinsed with Et_2O (10 mL) and the second crop was collected to afford triol **4.98** (600 mg, 92% yield) as a clear crystalline solid. **^{1}H NMR** (600 MHz, DMSO) δ 5.94 (t, *J* = 1.7 Hz, 1H), 5.08 – 5.00 (m, 2H), 4.71 (dt, *J* = 9.8, 2.1 Hz, 1H), 4.50 (d, *J* = 4.7 Hz, 1H), 4.35 (br s, 1H), 4.13 (dd, *J* = 17.3, 1.6 Hz, 1H), 4.03 (br s, 1H), 3.98 (dd, *J* = 17.3, 1.5 Hz, 1H), 3.50 – 3.44 (m, 1H), 2.82 (s, 3H), 1.99 (dt, *J* = 14.8, 2.8 Hz, 1H), 1.52 (dt, *J* = 14.8, 3.2 Hz, 1H). **^{13}C NMR** (151 MHz, DMSO) δ 162.2, 160.3, 140.0, 115.8, 78.3, 72.9, 71.0, 70.5, 56.4, 50.2, 37.1, 32.7. **FTIR** (thin film): 2984, 2953, 2929, 2886, 2857, 1670, 1503, 1472, 1462, 1437, 1406, 1381, 1369, 1332, 1303, 1240, 1214,

1169, 1092, 1051, 1027, 1004, 976, 944, 921, 891, 853, 834, 808, 775, 669, 647, 629, 590, 555, 511, 486, 406 cm^{-1}. **HRMS** (ESI+) *m/z* Calc'd. for $C_{21}H_{34}N_2O_6SiNa$ $[M+Na]^+$: 307.0901, found: 307. 0901. $\mathbf{R}_f = 0.53$ (20% MeOH in CH_2Cl_2). $[\boldsymbol{\alpha}]_D^{20.3}$: (c = 0.48, DMSO), -6.1°.

*4.5.14 Preparation of epoxide **4.99***

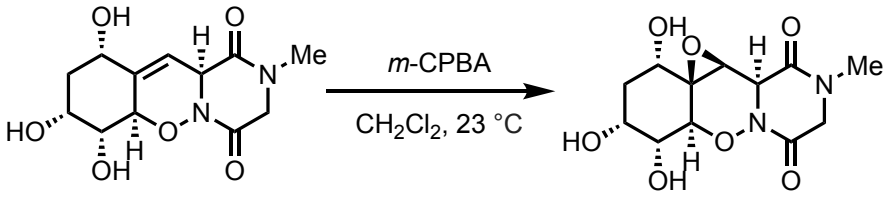

4.98 **4.99**

To a round bottom flask equipped with a magnetic stir bar was added triol **4.98** (730 mg, 2.57 mmol) and CH_2Cl_2 (26 mL, ca. 0.1 M). To the resulting suspension was added *m*-CPBA (3.0 g, 12.9 mmol, 75% weight) in a single portion. The resulting mixture was stirred 5 days at 23 °C. Next, the white suspension was filtered and rinsed with EtOAc (5 x 10 mL) or until no more filtercake was washed away. The remaining filtercake was dried under reduced pressure to afford the crude epoxide **4.99** (650 mg, 84% yield) as a white solid, which was used immediately in the next step.

*4.5.15 Preparation of acetonide **4.100***

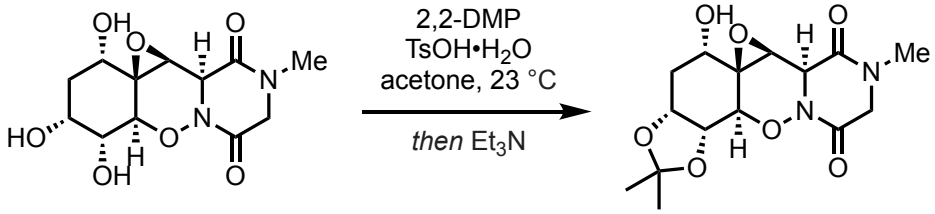

4.99 **4.100**

To a round bottom flask equipped with a magnetic stir bar was added crude epoxide **4.99** (650 mg, 2.17 mmol) and anhydrous acetone (22 mL, ca. 0.1 M). To the resulting

suspension was added 2,2-dimethoxypropane (1.2 mL, 9.6 mmol) and TsOH•H_2O (41 mg, 0.22 mmol), respectively. The resulting suspension was stirred 2 h at 23 °C, which eventually became a homogenous mixture. Next, Et_3N (30 μL, 0.22 mmol) was added to the reaction mixture and concentrated to afford the crude acetonide **4.100** (740 mg, assumed quantitative yield) as a white foamy oil, which was used immediately in the next step.

*4.5.16 Preparation of benzoate **4.101***

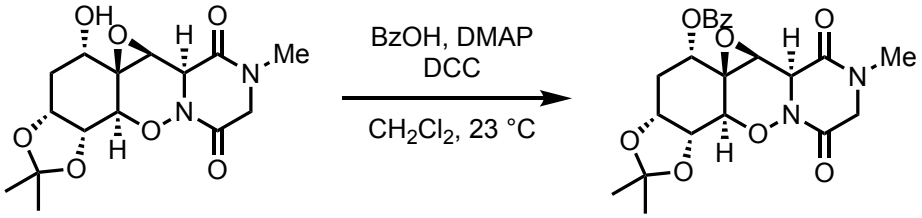

4.100 **4.101**

To a vial equipped with a magnetic stir bar was added crude acetonide **4.100** (10 mg, 0.029 mmol), anhydrous CH_2Cl_2 (0.3 mL, ca. 0.1 M). To the resulting solution was added BzOH (4.0 mg, 0.032 mmol), DMAP (0.4 mg, 2.9 μmol), and DCC (7.0 mg, 0.032 mmol), respectively. The resulting mixture was stirred 12 h at 23 °C. Next, the reaction mixture was concentrated to afford the crude benzoate **4.101** (13 mg, assumed quantitative yield) as a white solid, which was used immediately in the next step.

*4.5.17 Preparation of allylic alcohol **4.102***

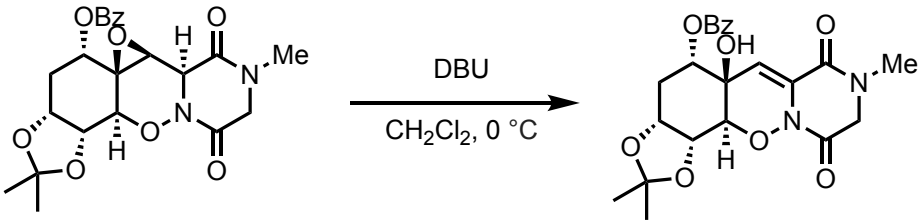

4.101 **4.102**

To a vial equipped with a magnetic stir bar was added crude acetonide **4.101** (13 mg, 0.029 mmol) and anhydrous CH_2Cl_2 (0.3 mL, ca. 0.1 M). The resulting solution was cooled to 0 °C and added DBU (5.0 μL, 0.031 mmol) by syringe. The resulting mixture was stirred 10 min at 0 °C. Next, CH_2Cl_2 (5 mL) and sat. aq. NH_4Cl solution (5 mL) were added to the reaction mixture and the aqueous layer was extracted with CH_2Cl_2 (2 x 5 mL). The combined organic layers were dried over anhydrous Na_2SO_4, filtered, and concentrated to afford the crude allylic alcohol **4.102** (13 mg, assumed quantitative yield) as a white solid, which was used immediately in the next step.

*4.5.18 Preparation of bromohydrin **4.103***

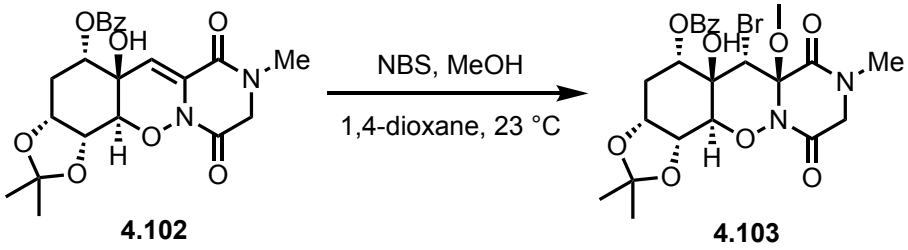

4.102 **4.103**

To a vial equipped with a magnetic stir bar was added crude allylic alcohol **4.102** (13 mg, 0.029 mmol), anhydrous MeOH (60 μL, ca. 0.5 M), and anhydrous 1,4-dioxane (30 μL, ca. 1.0 M). To the resulting solution was added NBS (5.5 mg, 0.031 mmol) in a single portion. The resulting mixture was stirred 4 h at 23 °C. Next, the reaction mixture was concentrated to afford the crude bromohydrin **4.103** (16 mg, assumed quantitative yield) as a yellow solid, which was used immediately in the next step.

*4.5.19 Preparation of diol **4.97***

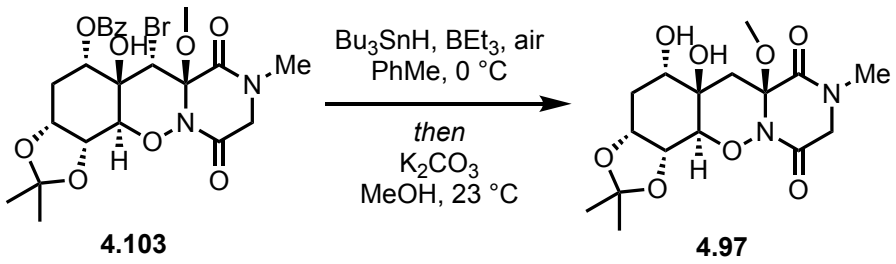

4.103 **4.97**

To a vial equipped with a magnetic stir bar was added crude bromohydrin **4.103** (16 mg, 0.029 mmol) and PhMe (0.6 mL, ca. 0.052 M). The resulting solution was left uncapped and Bu_3SnH (8.0 µL, 0.031 mmol), immediately followed by BEt_3 (12 µL, 0.012 mmol, 1.0 M in hexanes). The resulting mixture was stirred 10 min at 0 °C and was concentrated. The crude mixture was redissolved in anhydrous MeOH (0.3 mL, ca. 0.1 M) and K_2CO_3 (20.0 mg, 0.15 mmol) was added. The reaction mixture was stirred 1 h at 23 °C and was concentrated to afford the crude diol **4.97**. Purification *via* flash column chromatography (silica gel, 100% EtOAc, then 10% MeOH in CH_2Cl_2) afforded diol **4.97** (10 mg, 91% yield over six steps) as a clear crystalline solid. *Spectral data matched the previous report (see 4.5.12).*

*4.5.20 Preparation of acetonide **4.104***

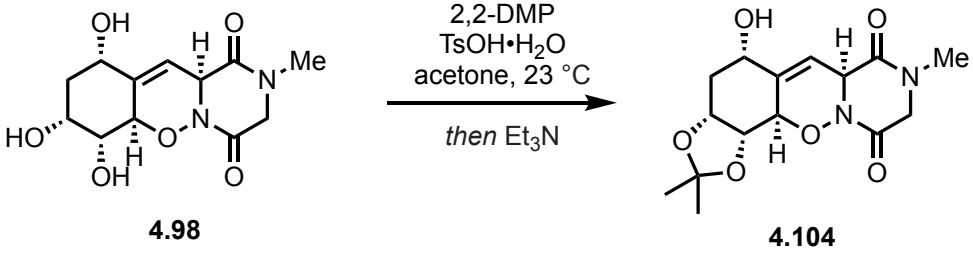

4.98 **4.104**

To a round bottom flask equipped with a magnetic stir bar was added triol **4.98** (620 mg, 2.17 mmol) and anhydrous acetone (22 mL, ca. 0.1 M). To the resulting suspension was added 2,2-dimethoxypropane (1.2 mL, 9.6 mmol) and $TsOH•H_2O$ (41 mg, 0.22 mmol),

respectively. The resulting suspension was stirred 2 h at 23 °C, which eventually became a homogenous mixture. Next, Et_3N (30 μL, 0.22 mmol) was added to the reaction mixture and concentrated to afford the crude acetonide **4.104** (700 mg, assumed quantitative yield) as a white foam, which was used immediately in the next step.

*4.5.21 Preparation of diene **4.105***

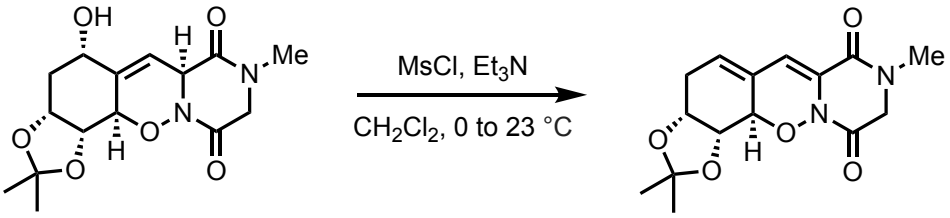

4.104 **4.105**

To a round bottom flask equipped with a magnetic stir bar was added acetonide **4.104** (700 mg, 2.17 mmol) and anhydrous CH_2Cl_2 (12 mL, ca. 0.18 M). The resulting solution was cooled to 0 °C and Et_3N (0.9 mL, 6.5 mmol), followed by MsCl (14.6 g, 45.4 mmol), was added dropwise via syringe. The resulting mixture was allowed to warm to 23 °C and stirred 2 h. Next, CH_2Cl_2 (5 mL) and sat. aq. NH_4Cl solution (10 mL) were added to the reaction mixture and the aqueous layer was extracted with CH_2Cl_2 (2 x 5 mL). The combined organic layers were dried over anhydrous Na_2SO_4, filtered, and concentrated to afford the crude diene **4.102** Purification *via* flash column chromatography (silica gel, 75% EtOAc in hexanes) afforded diene **4.105** (640 mg, 97% yield) as a pale yellow foamy solid. **^{1}H NMR** (500 MHz, $CDCl_3$) δ 6.72 (s, 1H), 5.95 – 5.90 (m, 1H), 4.50 (br s, 1H), 4.36 (q, J = 6.5 Hz, 1H), 4.29 – 4.23 (m, 1H), 4.18 (d, J = 17.9 Hz, 1H), 4.11 (d, J = 17.8 Hz, 1H), 3.05 (s, 3H), 2.85 (dt, J = 18.4, 6.6 Hz, 1H), 2.40 (d, J = 18.5 Hz, 1H), 1.51 (s, 3H), 1.40 (s, 3H). **^{13}C NMR** (151 MHz, $CDCl_3$) δ 156.8, 155.3, 127.8, 1126.3, 125.7, 111.4, 109.3, 80.0, 75.5, 70.9, 51.6, 33.8, 29.7, 27.8, 25.4. **FTIR** (thin film): 3579, 3496,

2987, 2932, 1694, 1613, 1497, 1456, 1425, 1397, 1360, 1320, 1245, 1212, 1160, 1054, 966, 901, 858, 828, 735, 647, 620, 576, 548, 513, 410 cm^{-1}. **HRMS** (ESI+) *m*/*z* Calc'd. for $C_{15}H_{18}N_2O_5Na$ $[M+Na]^+$: 329.1108, found: 329. 1102. $\mathbf{R_f}$ = 0.24 (100% EtOAc). $[\boldsymbol{\alpha}]_D^{21.7}$: (c = 0.44, $CHCl_3$), +30.9°.

4.6 References

[1] Miknis, G. F.; Williams, R. M. *J. Am. Chem. Soc.* **1993**, *115*, 536-547.

[2] Tsunematsu, Y.; Maeda, N.; Sato, M.; Hara, K.; Hashimoto, H.; Watanabe, K.; Hertweck, C. *J. Am. Chem. Soc.* **2021**, *143*, 206-213.

[3] Stipanovic, R. D.; Howell, C. R. *J. Antiobiot.* **1982**, 1326-1330.

[4] Seephonkai, P.; Kongsaeree, P.; Prabpai, S.; Isaka, M.; Thebtaranonth, Y. *Org. Lett.* **2006**, *8*, 3073-3075.

[5] Fan, J.; Ran, H.; Wei, P.-L. Li, Y.; Liu, H.; Li, S.-M.; Hu, Y.; Yin, W.-B. *Angew. Chem. Int. Ed.* **2023**, *62*, e202217212.

[6] Miyamoto, C.; Yokose, K.; Furumai, T.; Maruyama, H. B. *J. Antiobiot.* **1982**, 1326-1330.

[7] Isolation of *N*-methylpretrichodermamide B and pretrichodermamide C:
(a) Orfali, R. S.; Aly, A. H.; Ebrahim, W.; Abdel-Aziz, M. S.; Müller, W. E. G.; Lin, W.; Daletos, G.; Proksch, P. *Phytochem. Lett.* **2015**, *11*, 168-172.
(b) Liu, Y.; Li, X.-M.; Meng, L.-H.; Jiang, W.-L., Xu, G.-M.; Huang, C.-G.; Wang, B.-G. *J. Nat. Prod.* **2015**, *78*, 1294-1299.

[8] Nakano, H.; Hara, M.; Meshiro, T.; Ando, K.; Saito, Y.; Morimoto, S. Japan Patent Kokai 1990–218686 (1990.08.31).

[9] Krasovskiy, A.; Kopp, F.; Knochel, P. *Angew. Chem. Int. Ed.* **2006**, *118*, 511-515.

[10] Wu, Z.; Williams, L. J.; Danishefsky, S. J. *Angew. Chem. Int. Ed.* **2000**, *39*, 3866-3868.

[11] Cowper, N. G. W.; Hesse, M. J.; Chan, K. M.; Reisman, S. E. *Chem. Sci.* **2020**, *11*, 11897-11901.

[12] Gayler, K. M.; Lambert, K. M.; Wood, J. L. *Tetrahedron* **2019**, *75*, 3154-3159.

[13] Sheradsky, T.; Silcoff, E. R. *Molecules* **1998**, *3*, 80-87.

[14] Hong, A.-W.; Cheng, T.-H.; Raghukumar, V.; Sha, C.-K. *J. Org. Chem.* **2008**, *73*, 7580-7585.

[15] Shimizu, H.; Yoshimura, A.; Noguchi, K.; Nemykin, V. N.; Zhdankin, V. V.; Saito, A. *Beilstein J. Org. Chem.* **2018**, *14*, 531-536.

[16] Hodges, T. R.; Benjamin, N. M.; Martin, S. F. *Tetrahedron* **2018**, *74*, 3329-3338.

[17] Roush, W. R.; Bennett, C. E. *J. Am. Chem. Soc.* **2000**, *122*, 6124-6125.

APPENDICES

APPENDIX A

Spectral Data for Chapter One

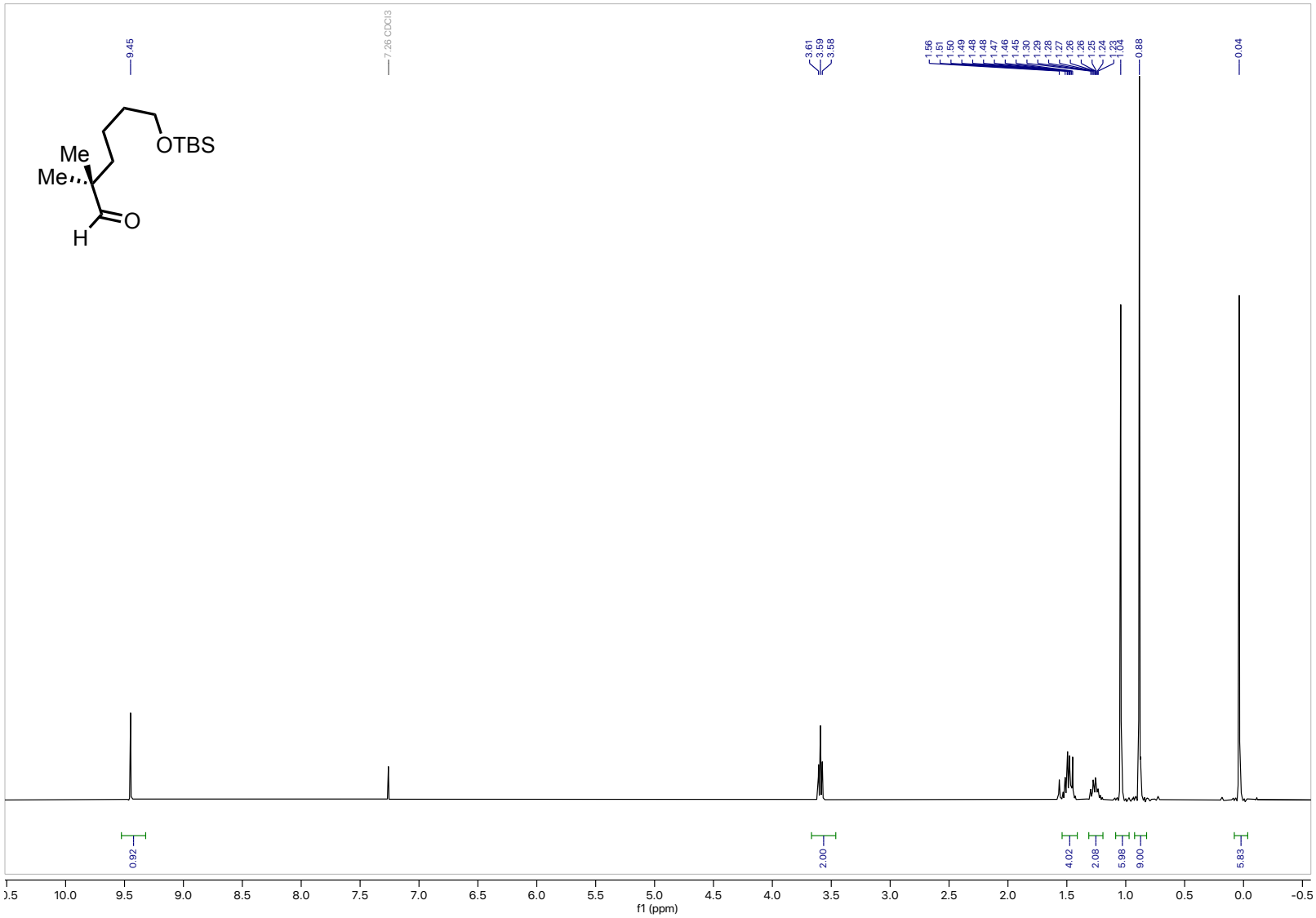

Figure A.01. ^{1}H NMR (400 MHz, $CDCl_3$) known aldehyde **1.38**

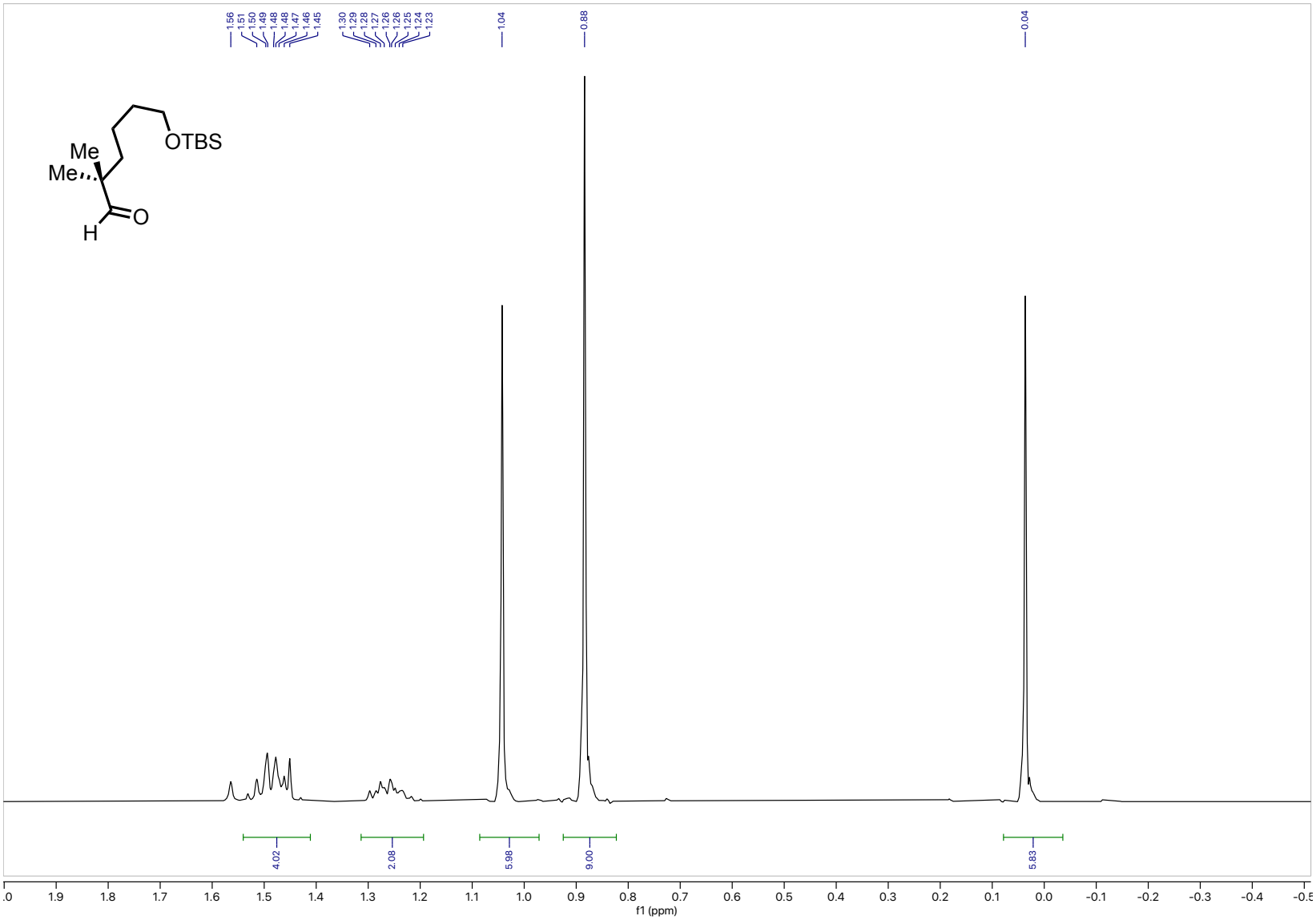

Figure A.02. ^{1}H NMR (400 MHz, $CDCl_3$) known aldehyde **1.38** (2.0 – -0.5 ppm inset)

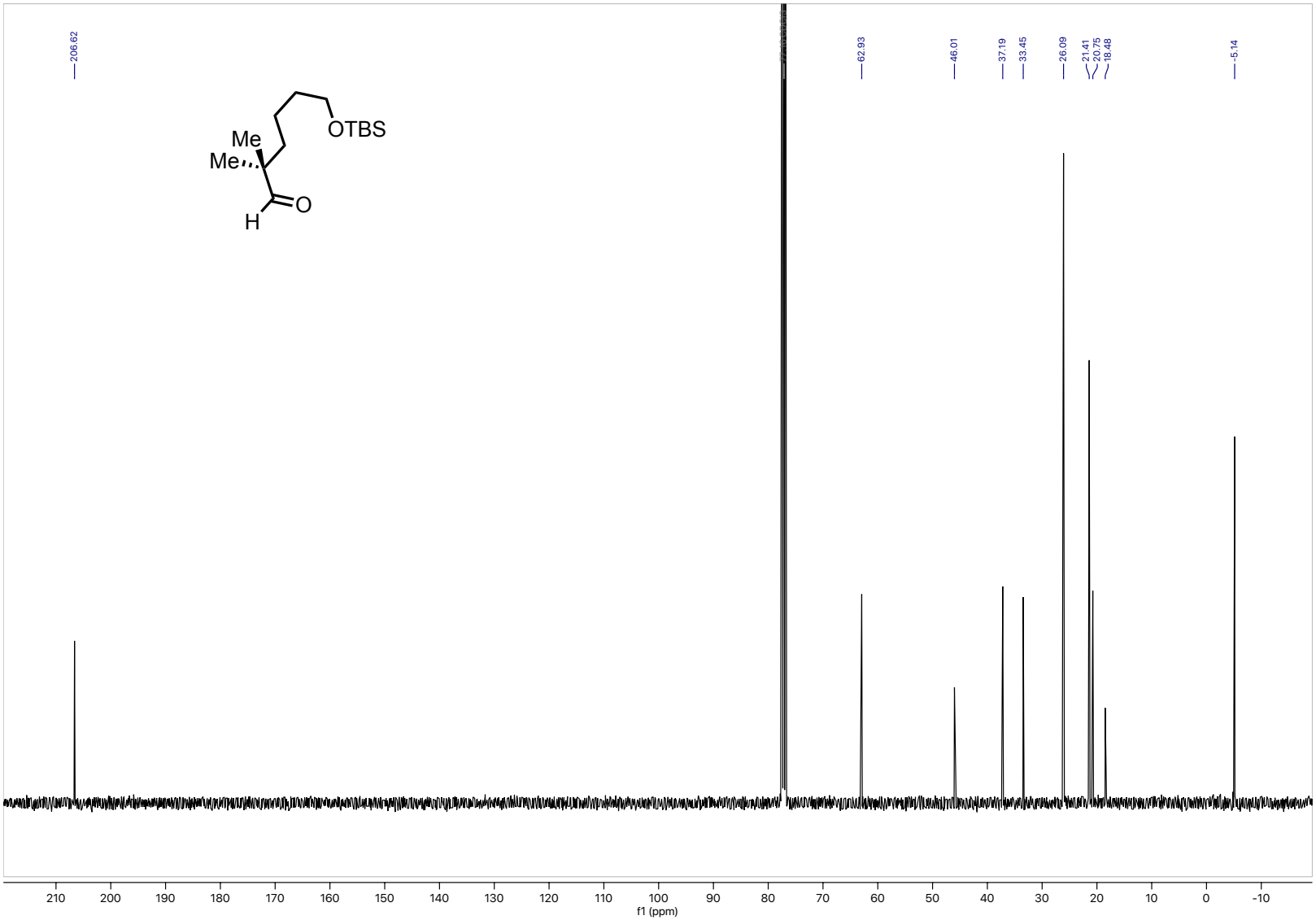

Figure A.03. ^{13}C NMR (101 MHz, $CDCl_3$) known aldehyde **1.38**

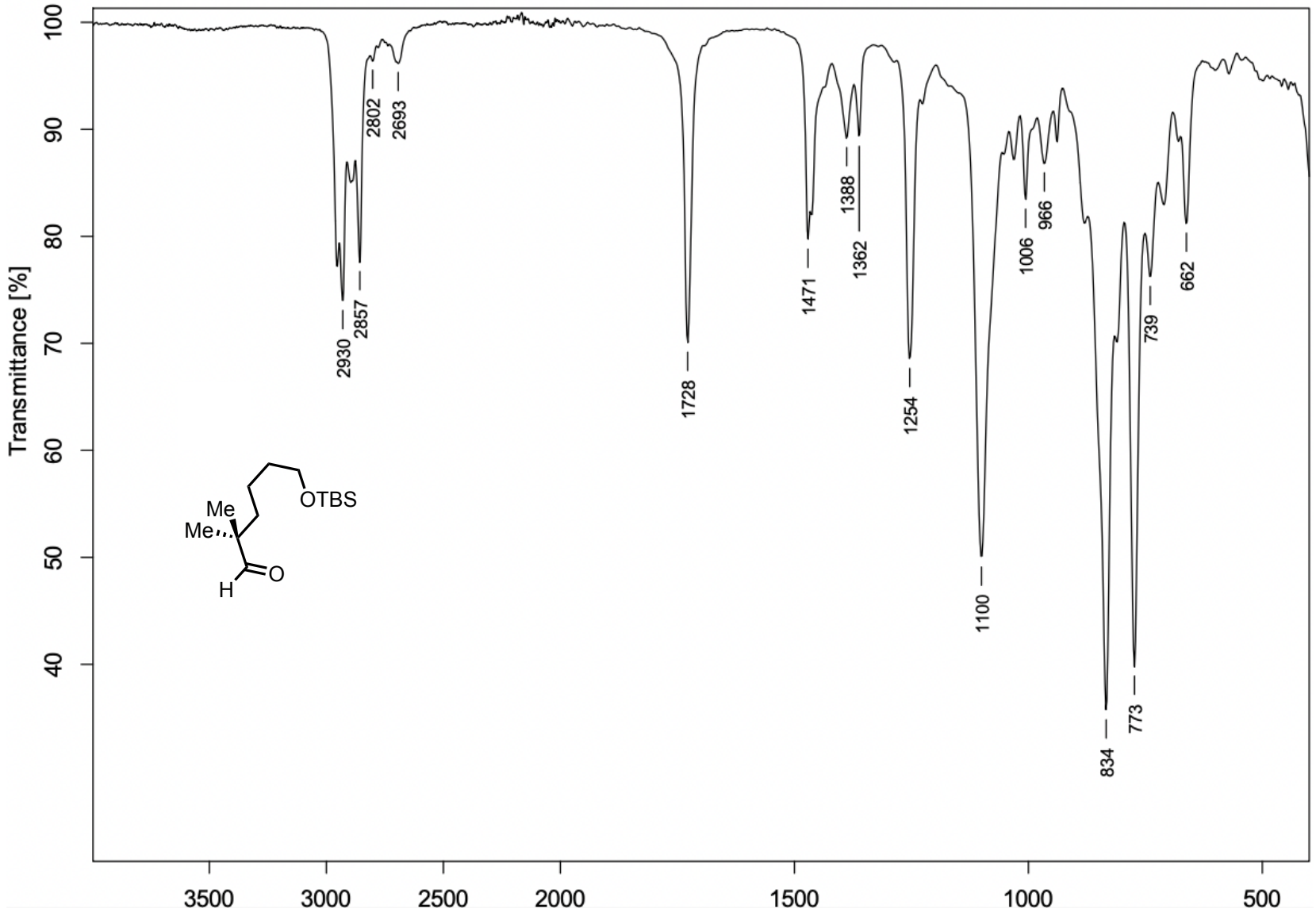

Figure A.04. FTIR (neat) known aldehyde **1.38**

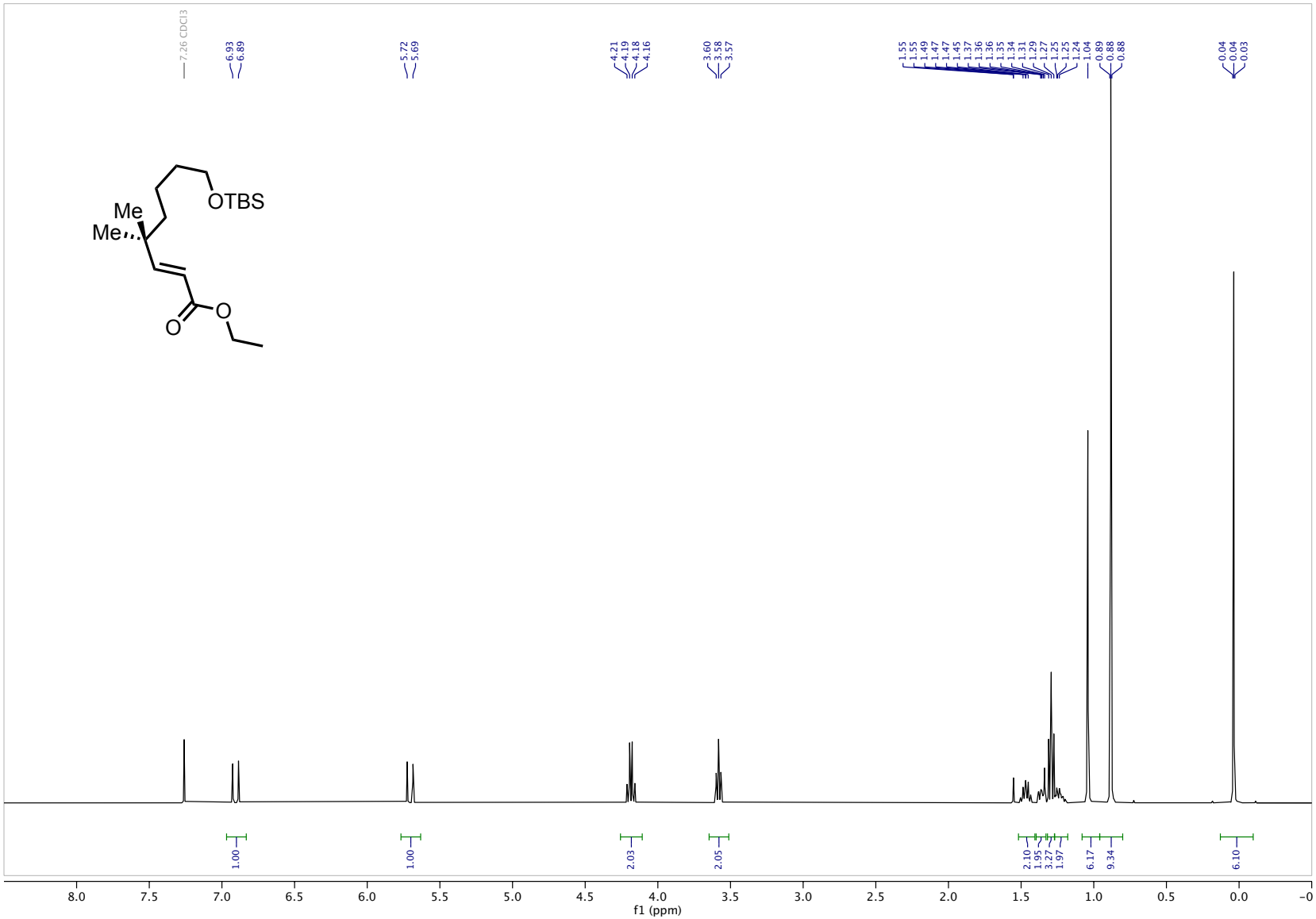

Figure A.05. ^{1}H NMR (400 MHz, $CDCl_3$) ethyl ester **1.39**

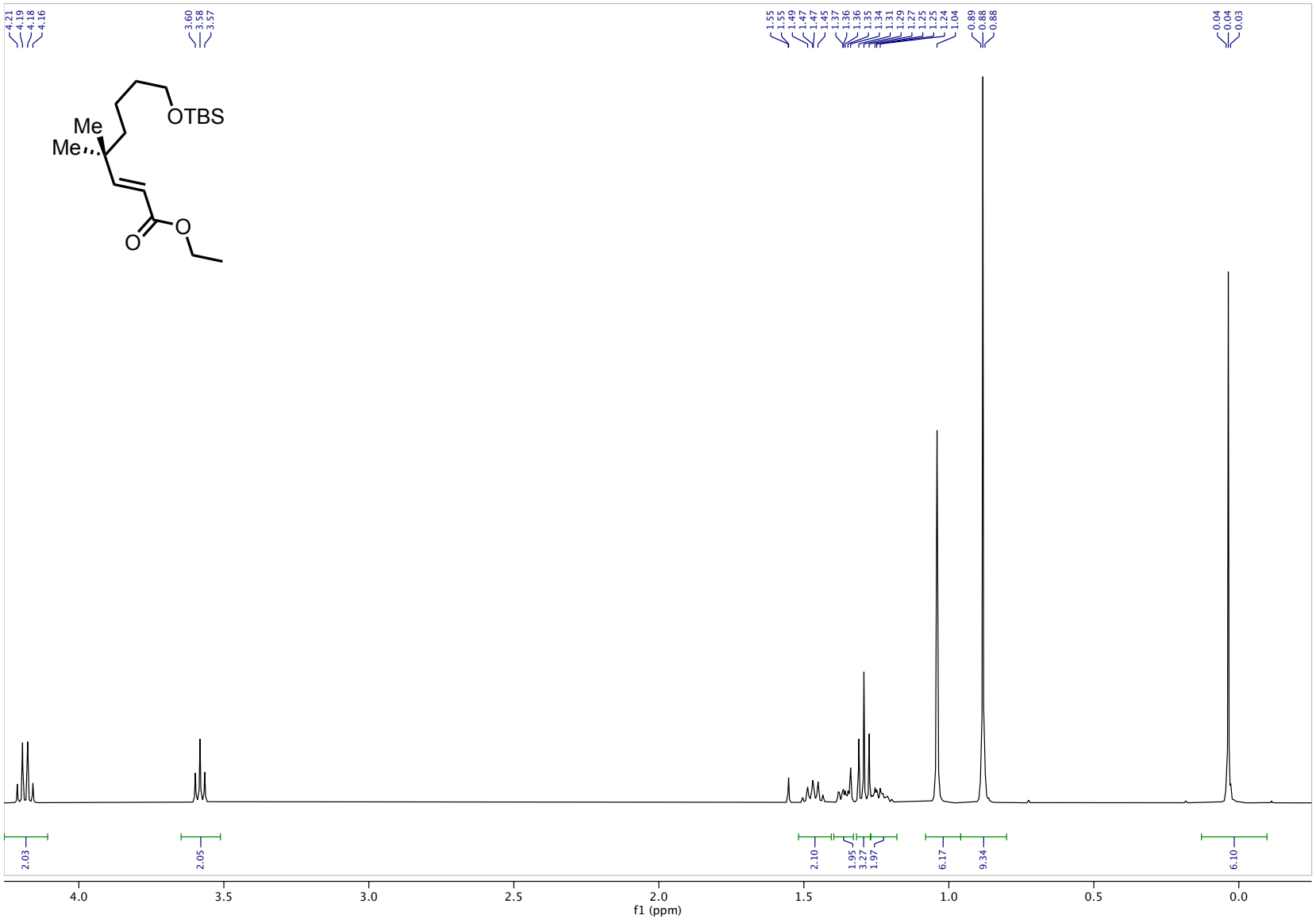

Figure A.06. ^{1}H NMR (400 MHz, $CDCl_3$) ethyl ester **1.39** (4.25 – -0.5 ppm inset)

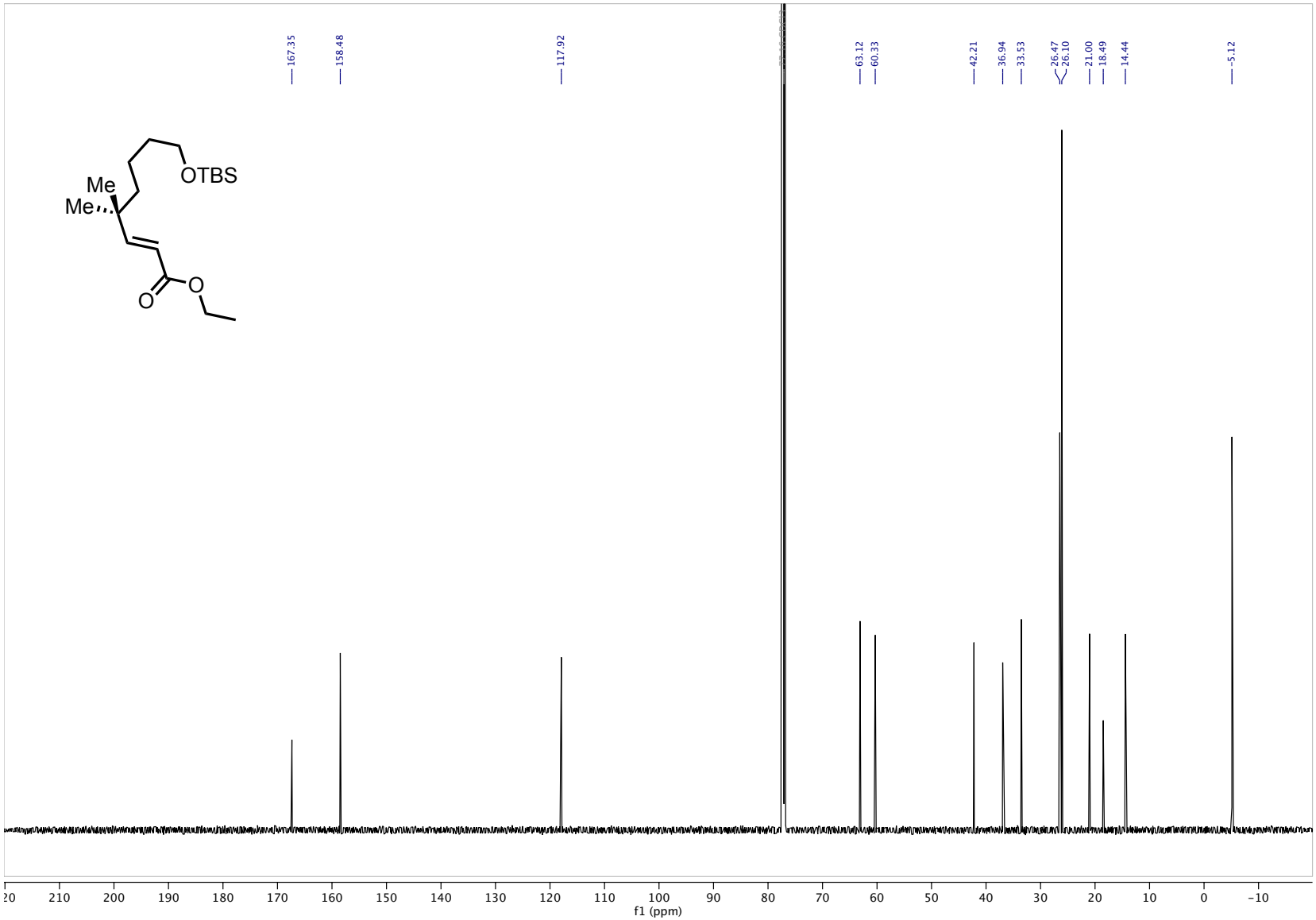

Figure A.07. ^{13}C NMR (151 MHz, $CDCl_3$) ethyl ester **1.39**

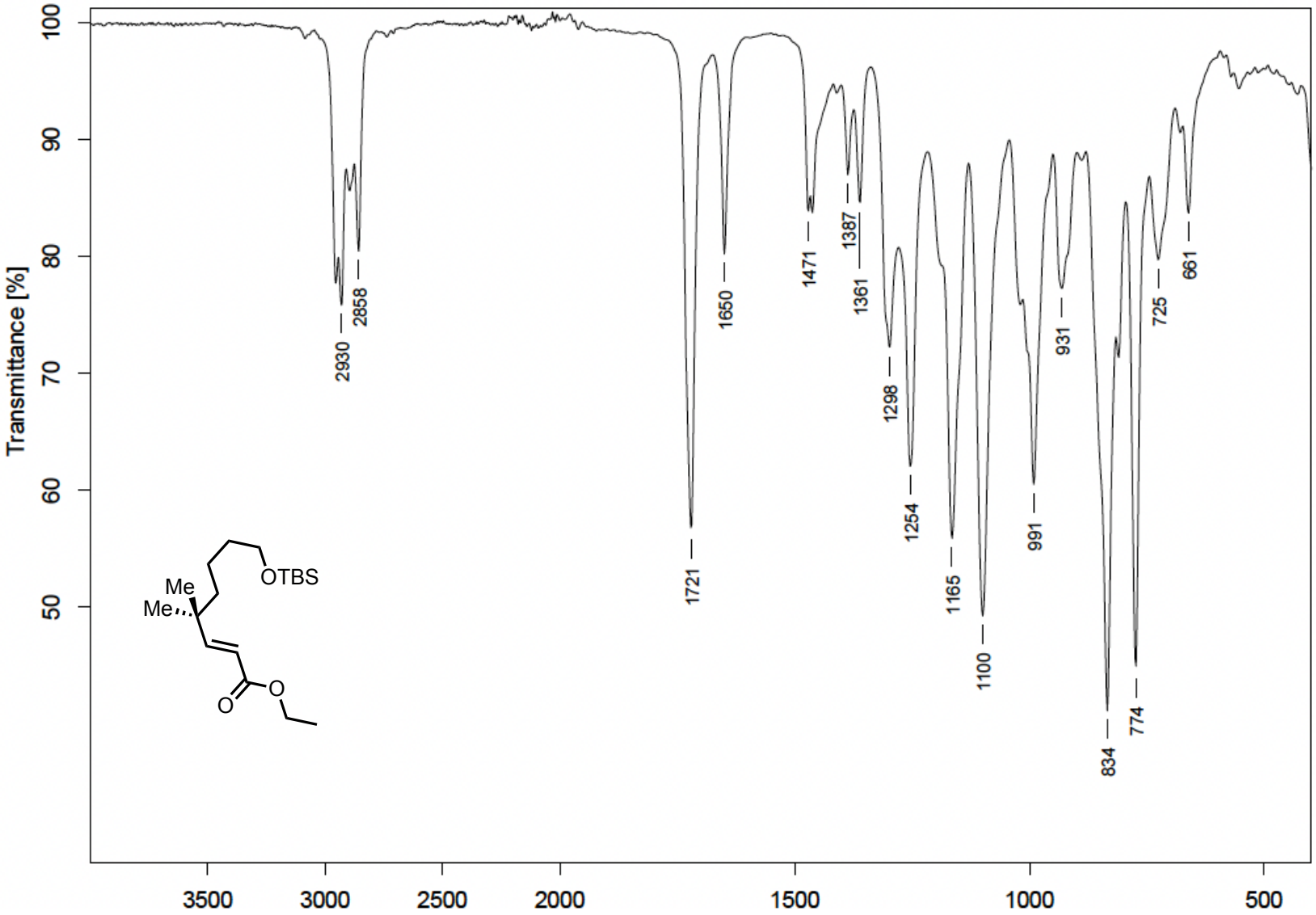

Figure A.08. FTIR (neat) ethyl ester **1.39**

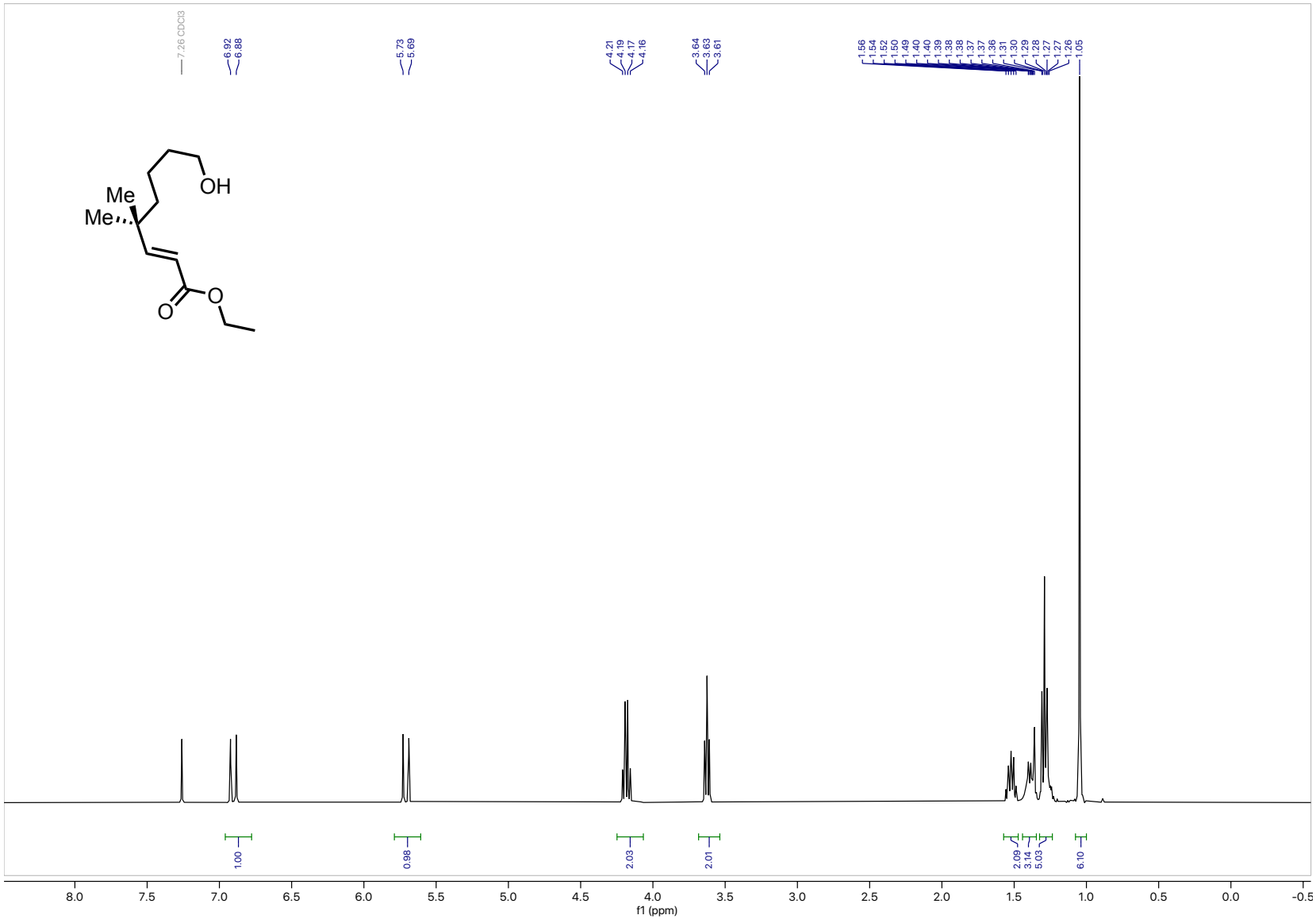

Figure A.09. ^{1}H NMR (400 MHz, $CDCl_3$) alcohol **1.73**

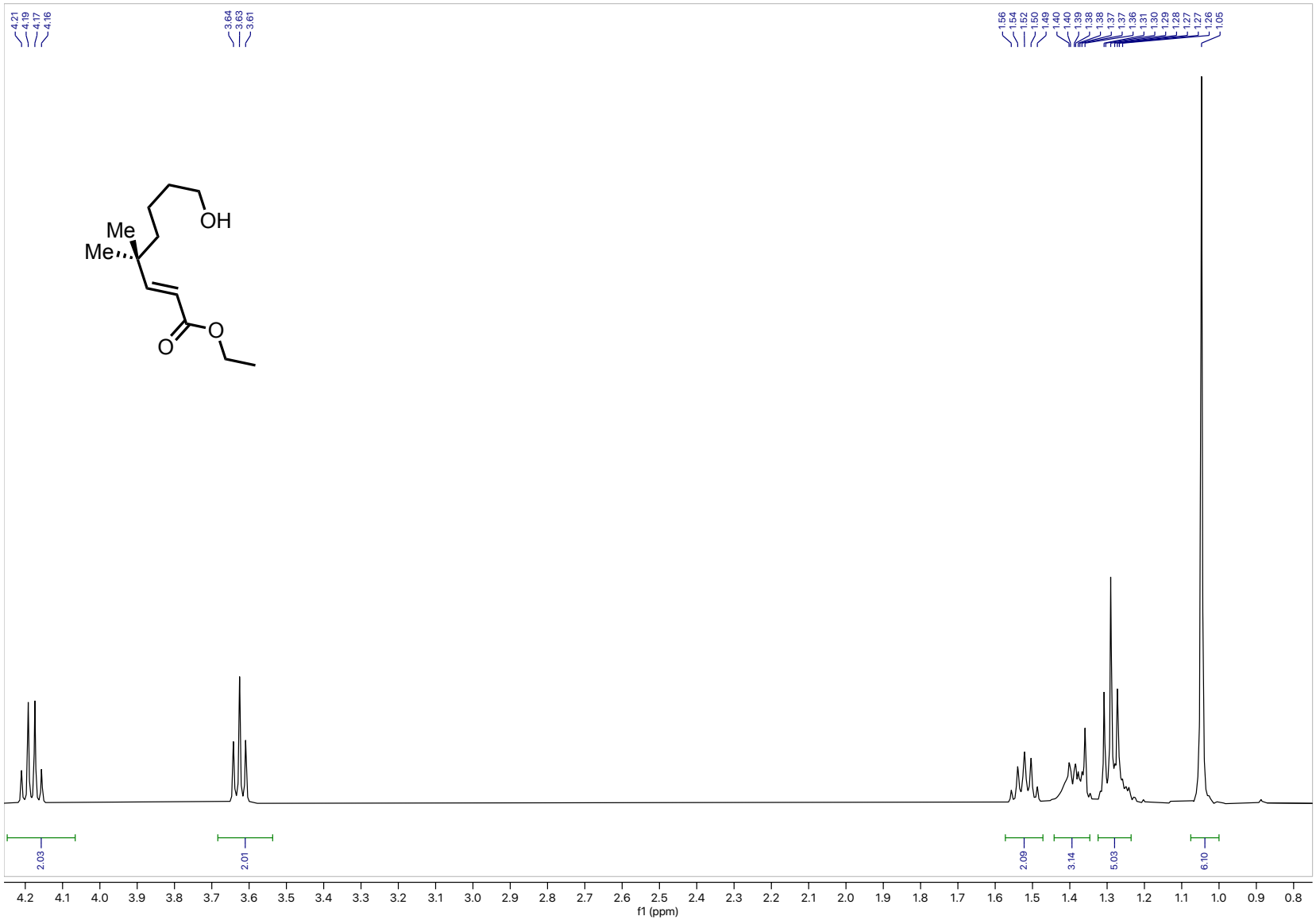

Figure A.10. ^{1}H NMR (400 MHz, $CDCl_3$) alcohol **1.73** (4.25 – 0.75 ppm inset)

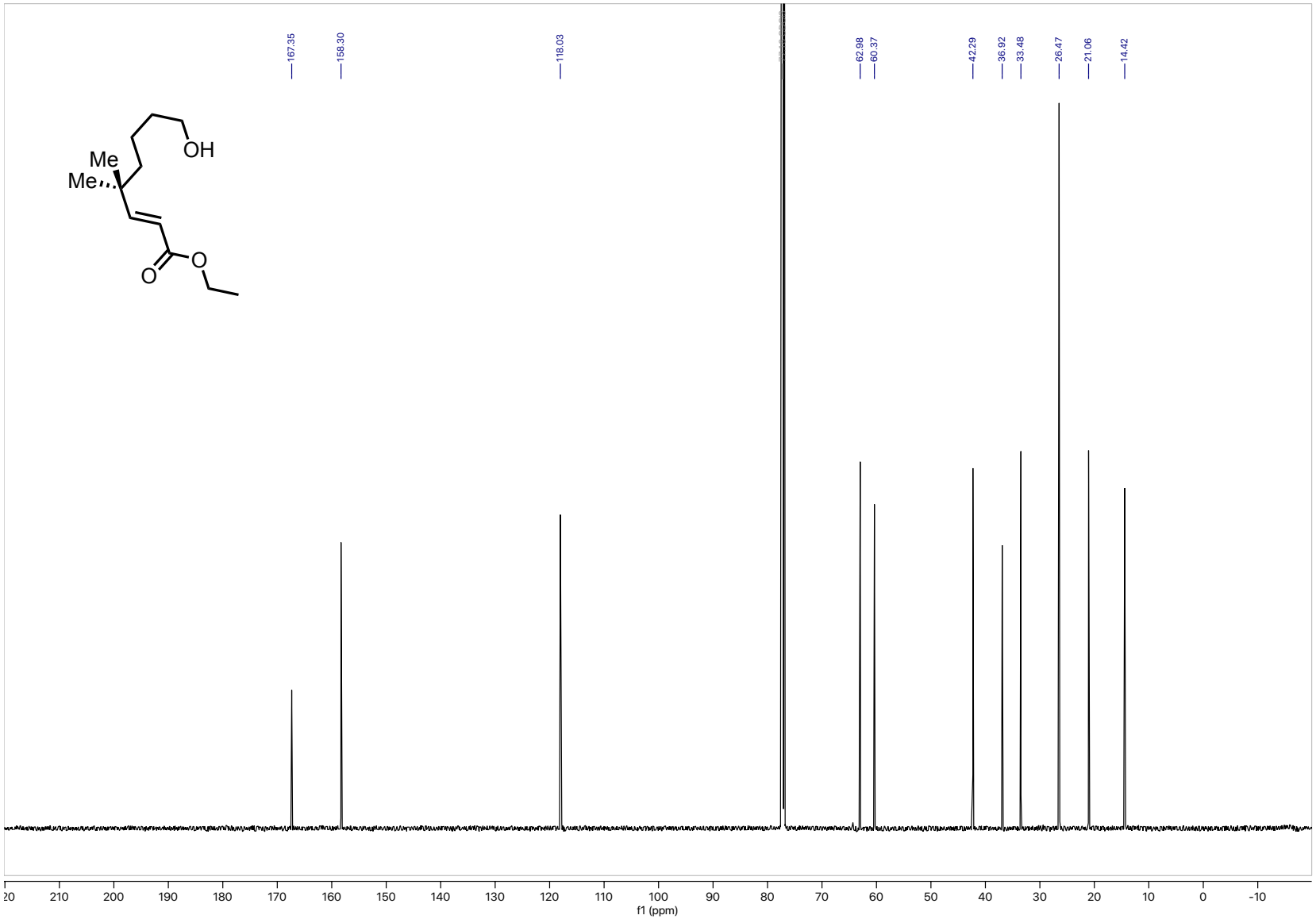

Figure A.11. ^{13}C NMR (151 MHz, $CDCl_3$) alcohol **1.73**

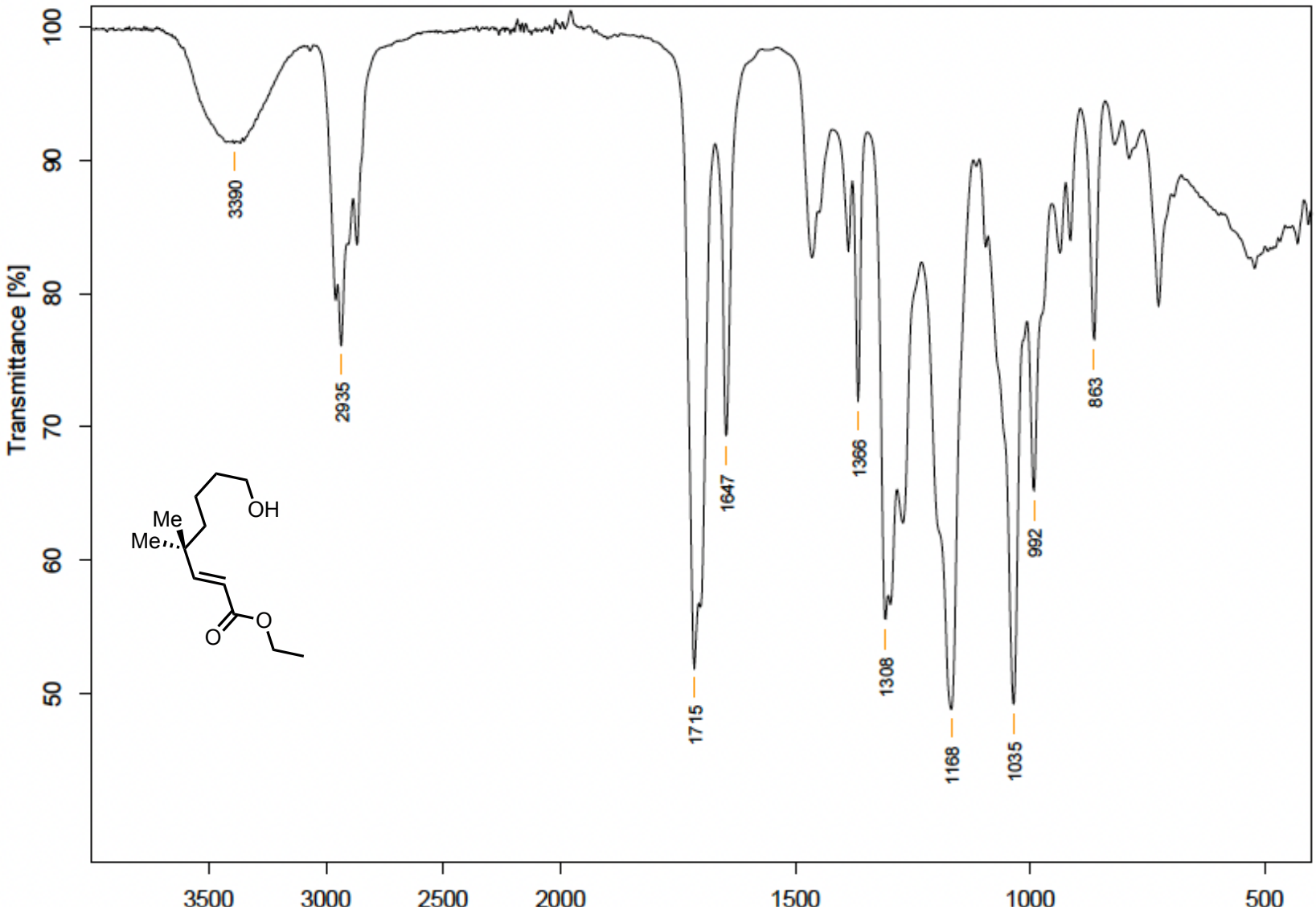

Figure A.12. FTIR (neat) alcohol **1.73**

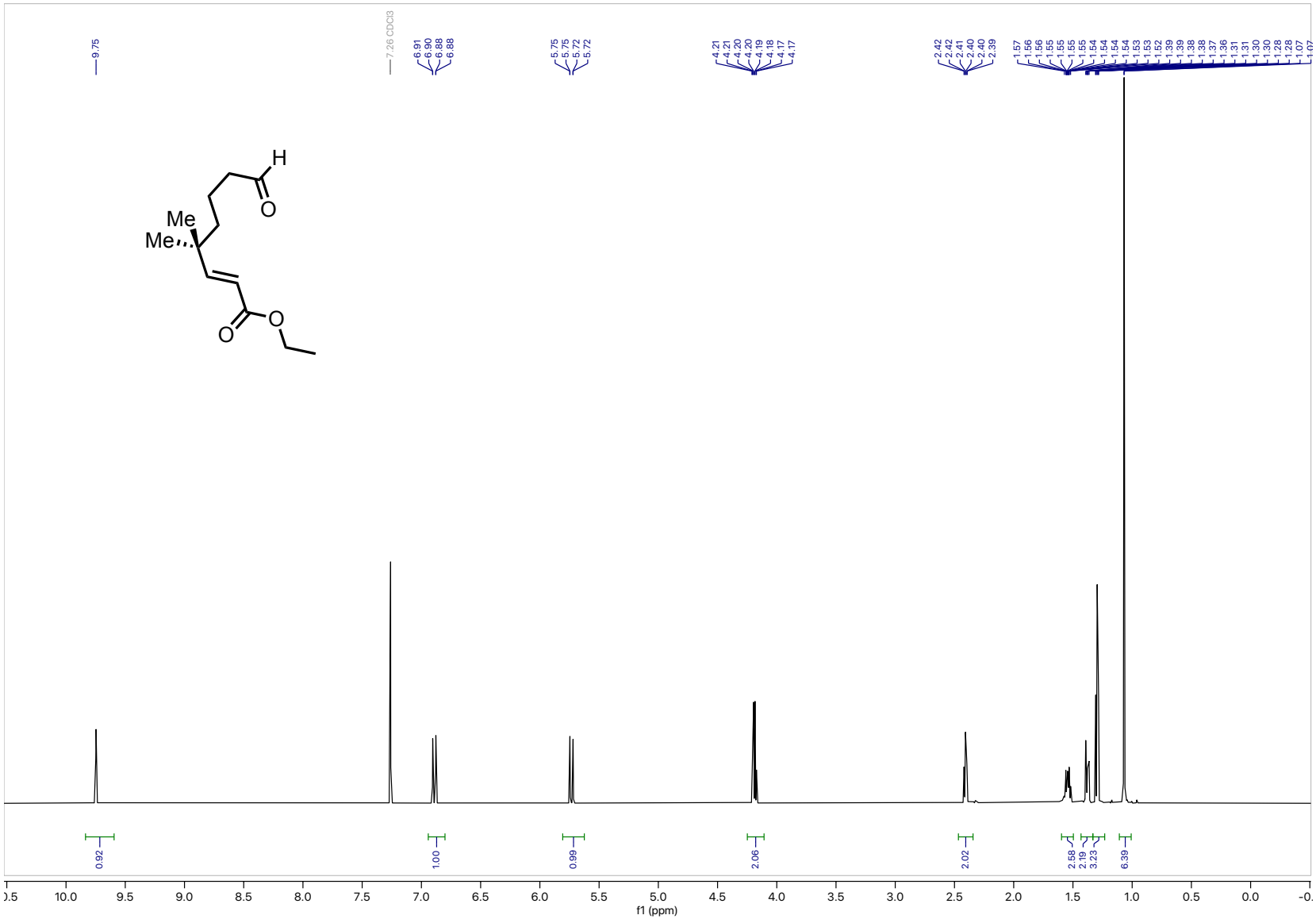

Figure A.13. ^{1}H NMR (600 MHz, $CDCl_3$) aldehyde **1.33**

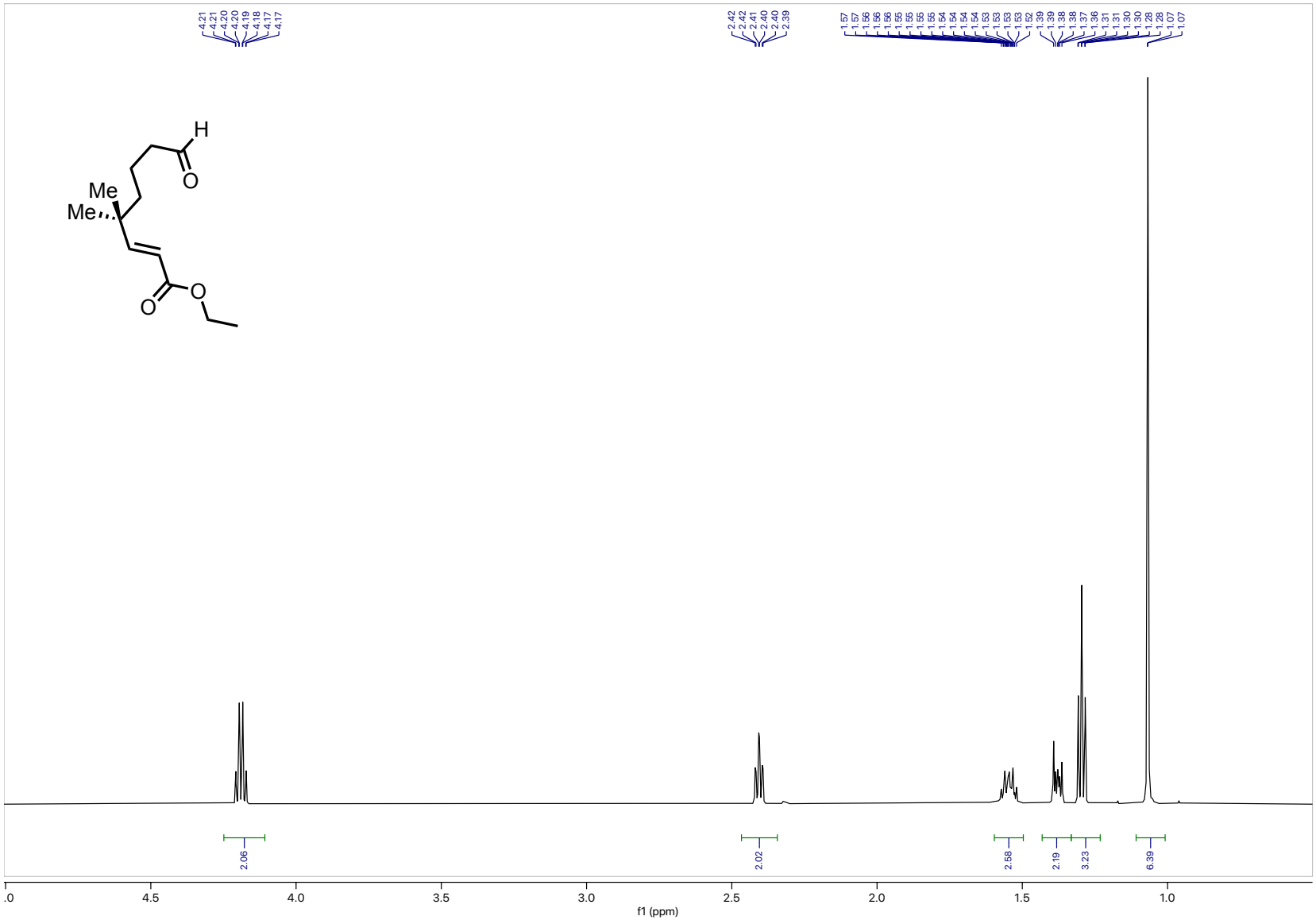

Figure A.14. ^{1}H NMR (600 MHz, $CDCl_3$) aldehyde **1.33** (5.0 – 0.5 ppm inset)

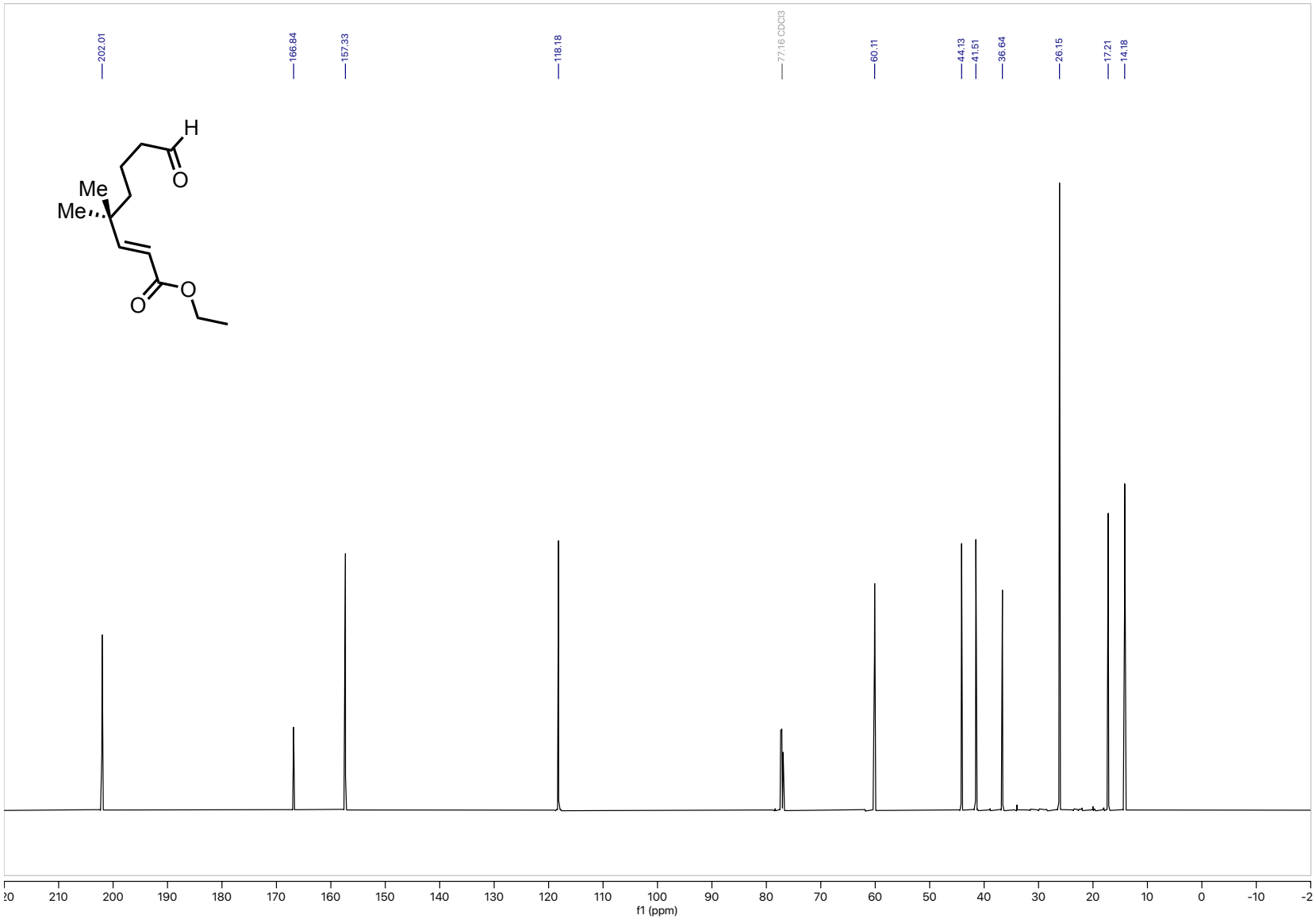

Figure A.15. ^{13}C NMR (151 MHz, $CDCl_3$) aldehyde **1.33**

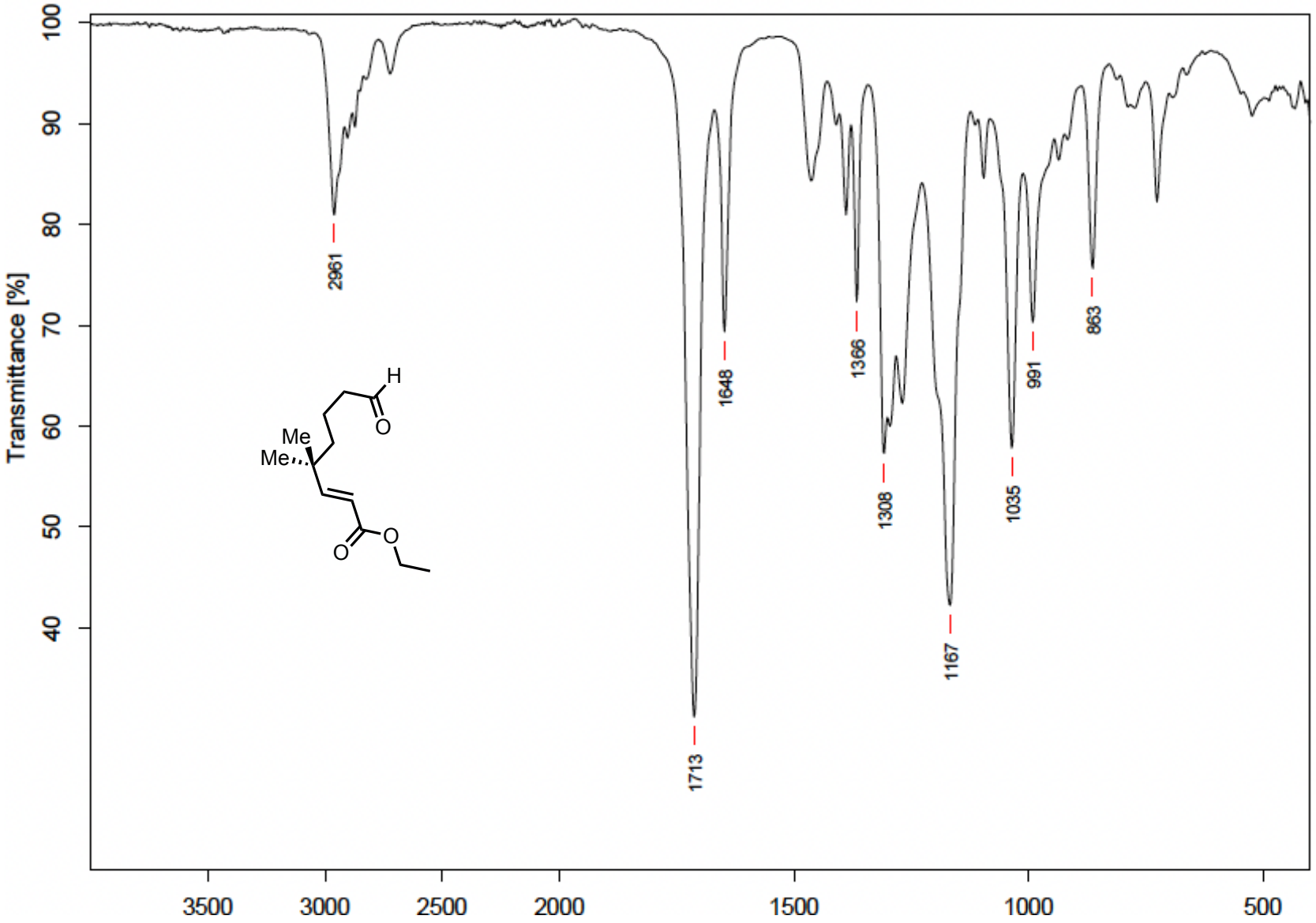

Figure A.16. FTIR (neat) aldehyde **1.33**

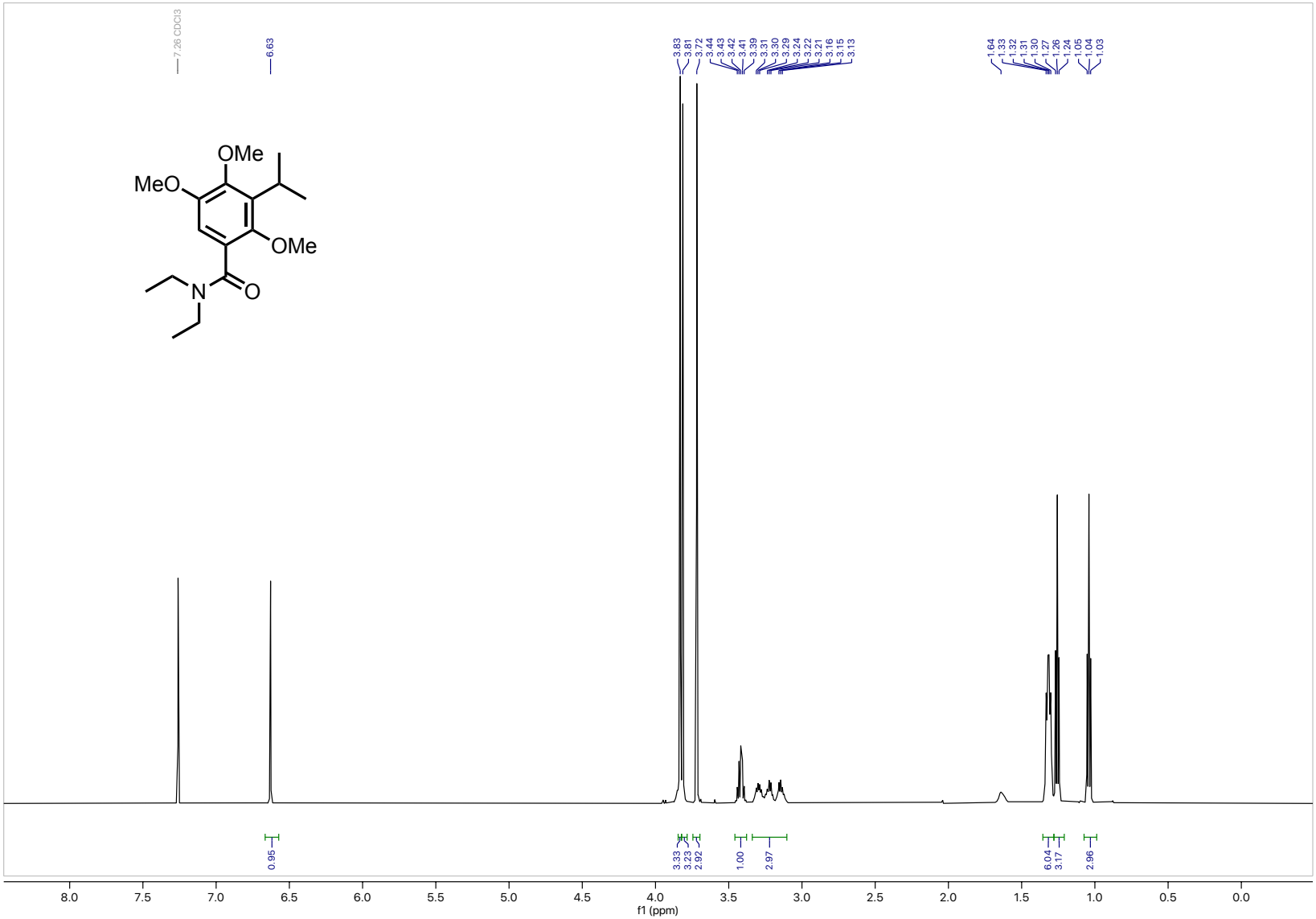

Figure A.17. ^{1}H NMR (600 MHz, $CDCl_3$) benzamide **1.34**

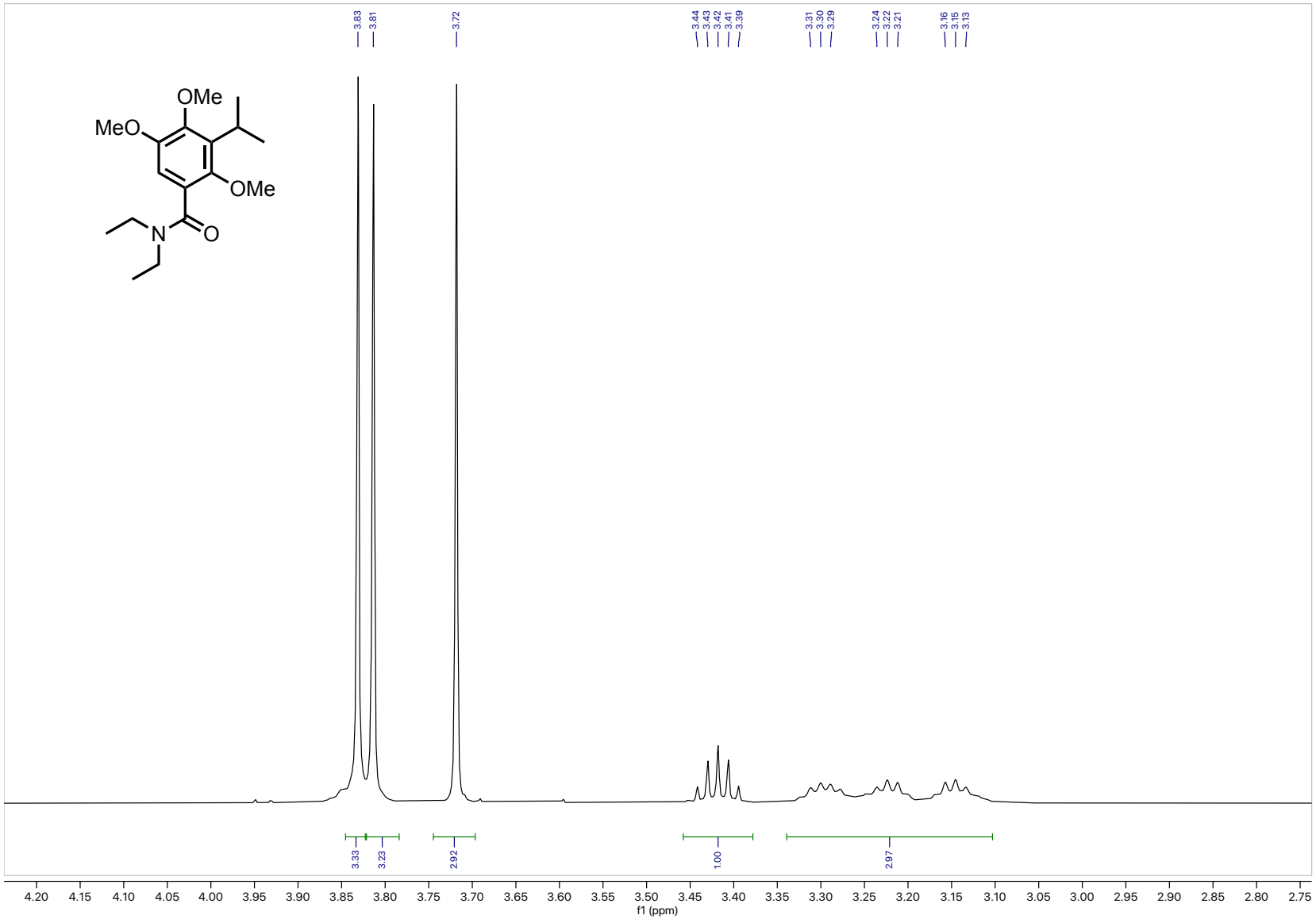

Figure A.18. ^{1}H NMR (600 MHz, $CDCl_3$) benzamide **1.34** (4.25 – 2.75 inset)

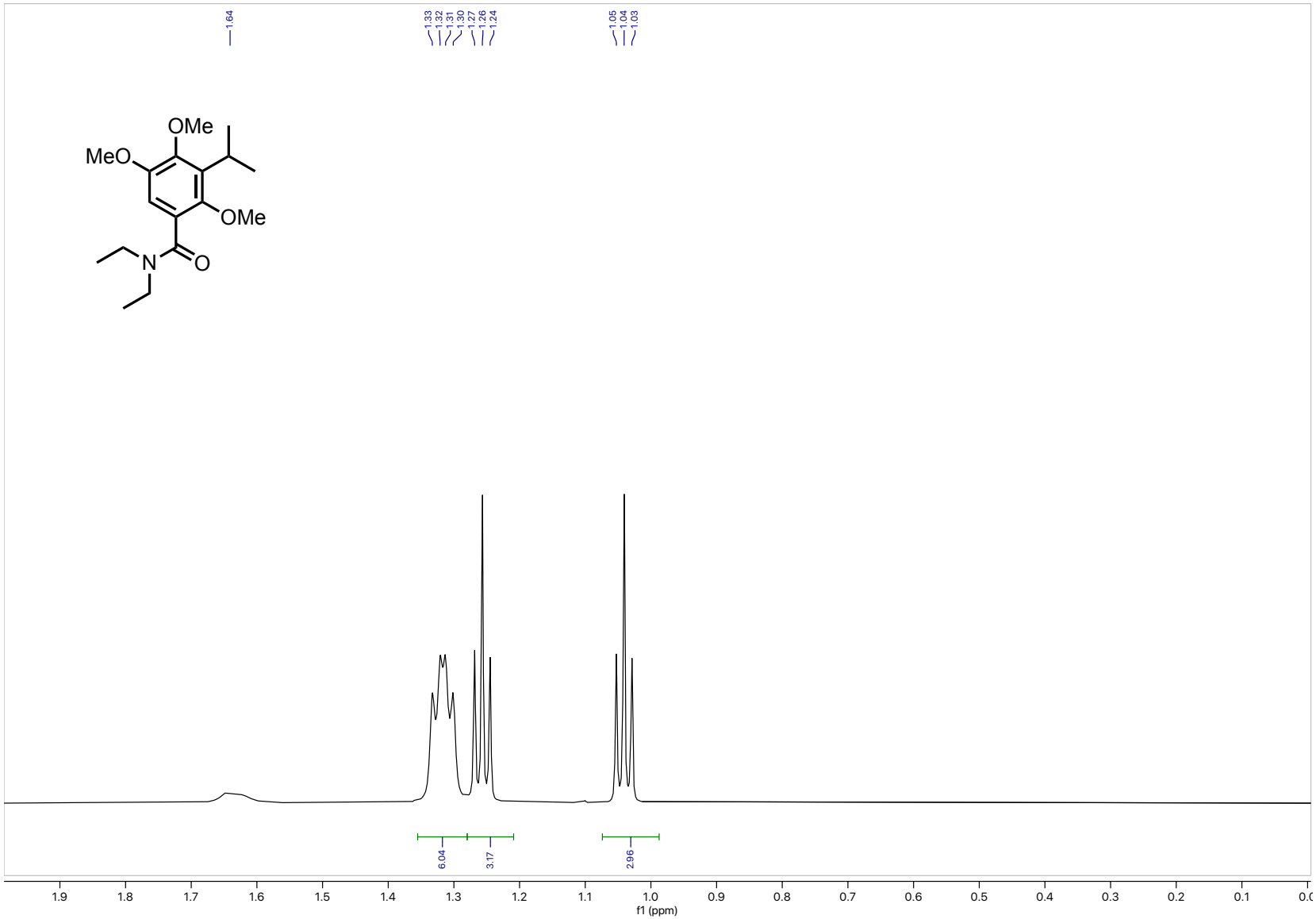

Figure A.19. ^{1}H NMR (600 MHz, $CDCl_3$) benzamide **1.34** (2.0 – 0 ppm inset)

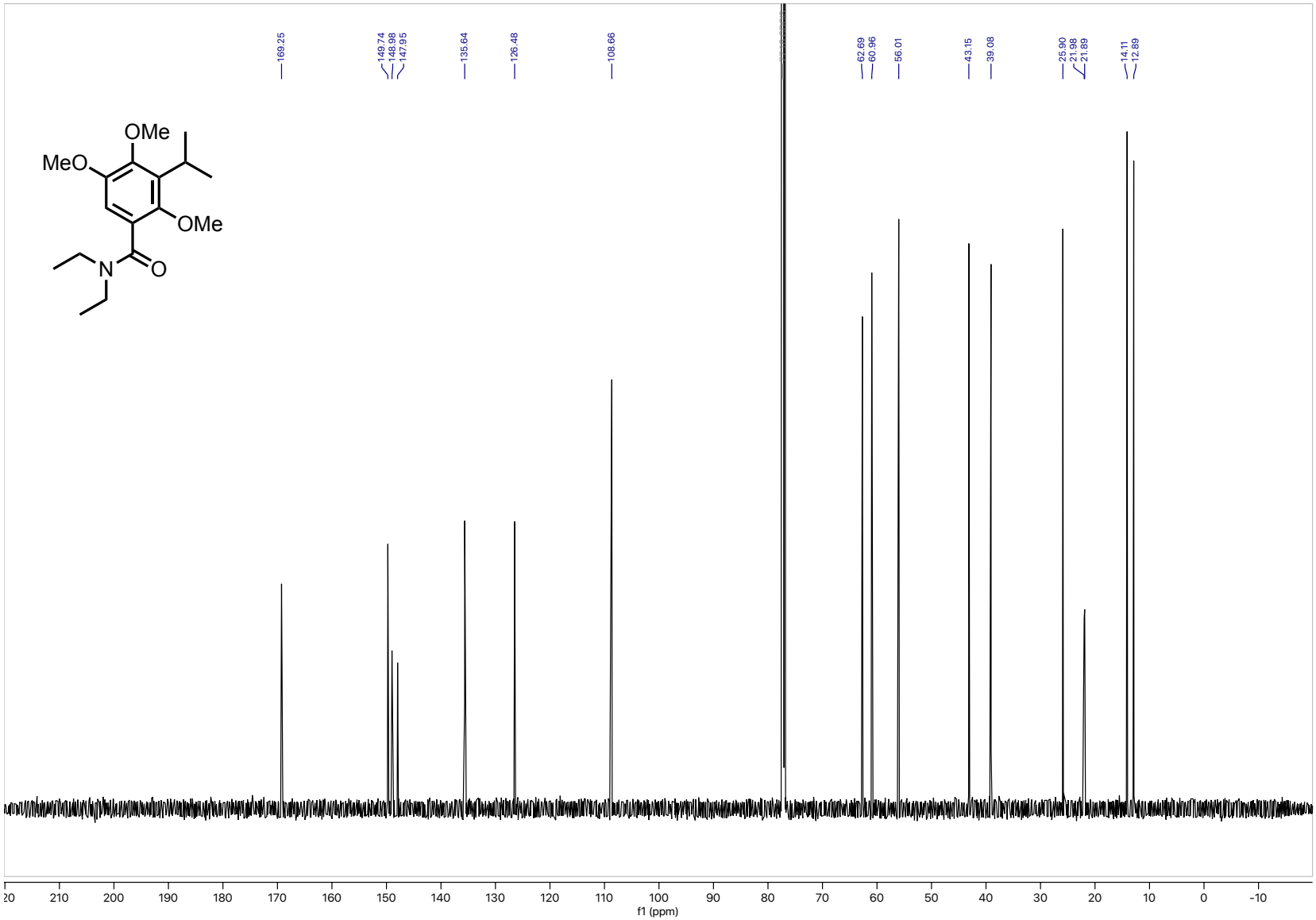

Figure A.20. ^{13}C NMR (151 MHz, $CDCl_3$) benzamide **1.34**

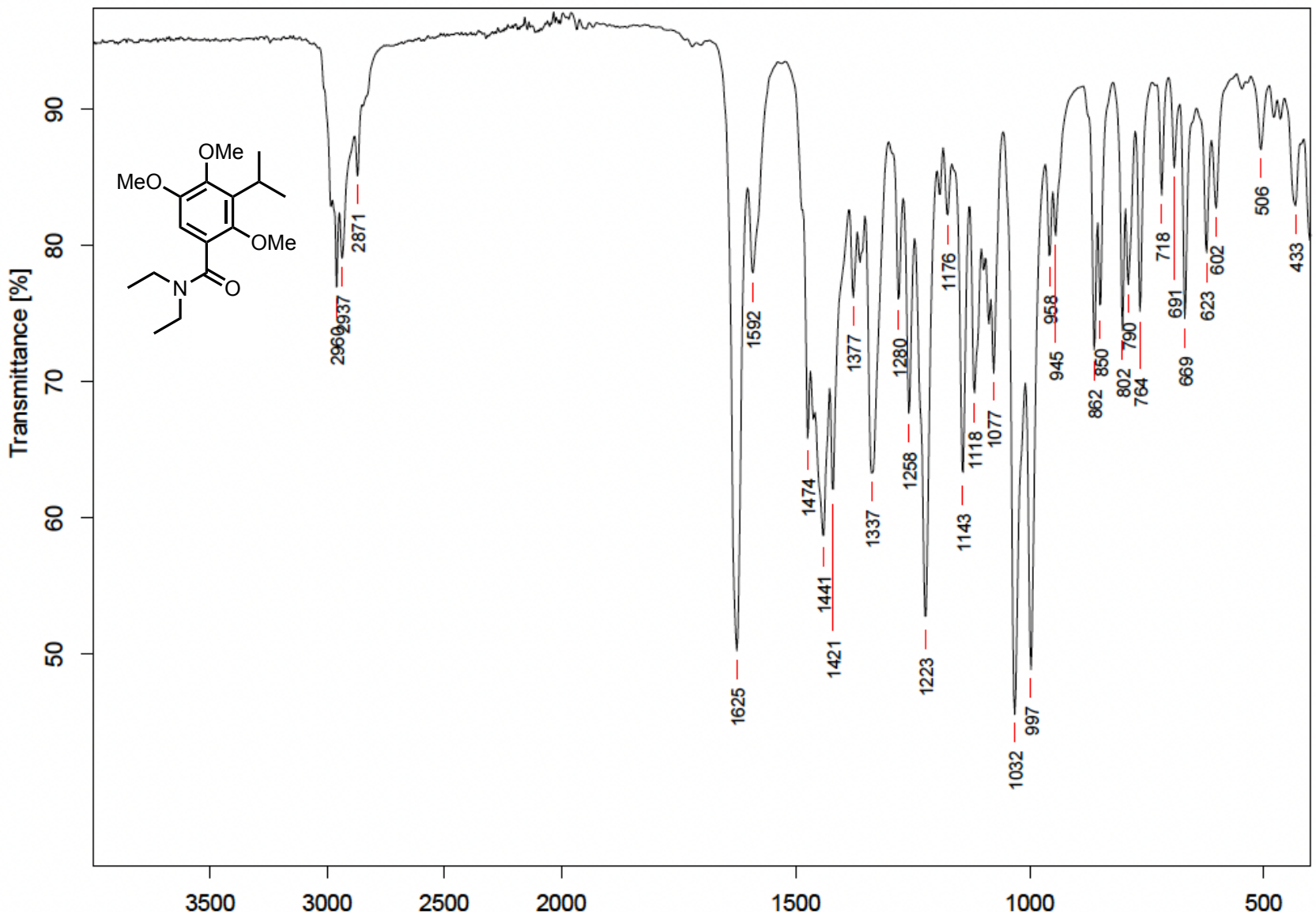

Figure A.21. FTIR (neat) benzamide **1.34**

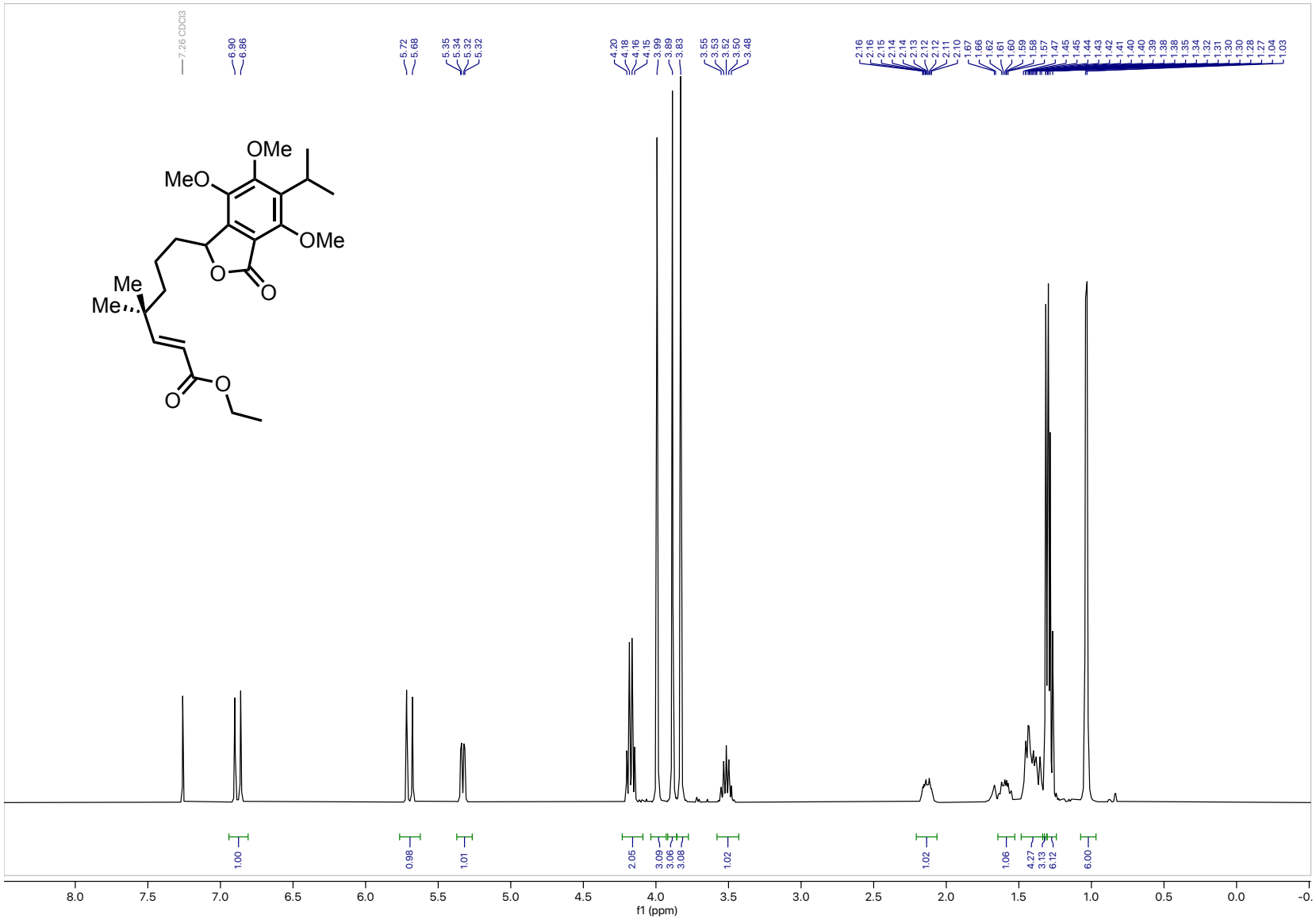

Figure A.22. ^{1}H NMR (600 MHz, $CDCl_3$) lactone **1.32**

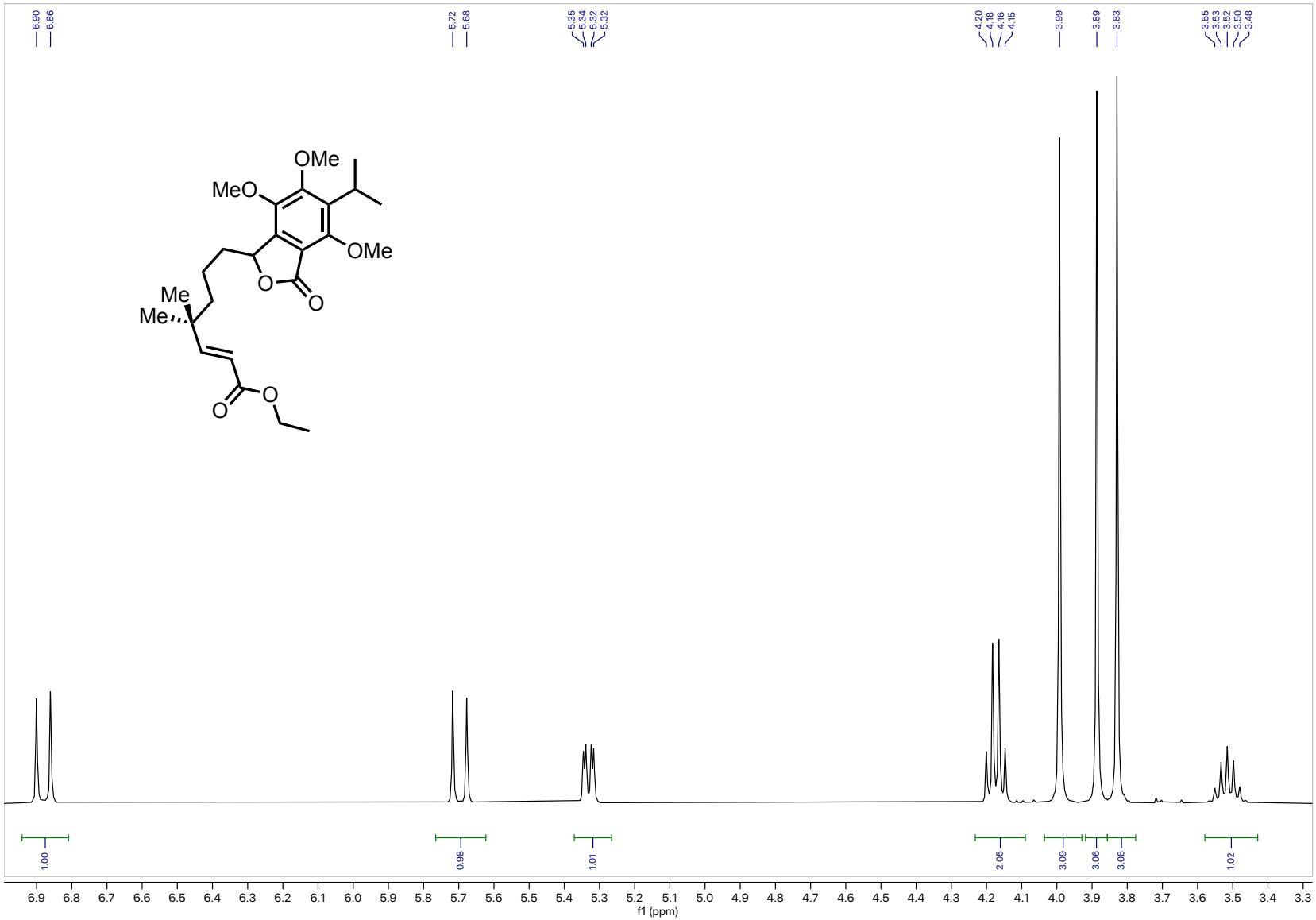

Figure A.23. ^{1}H NMR (600 MHz, $CDCl_3$) lactone **1.32** (7.0 – 3.25 ppm inset)

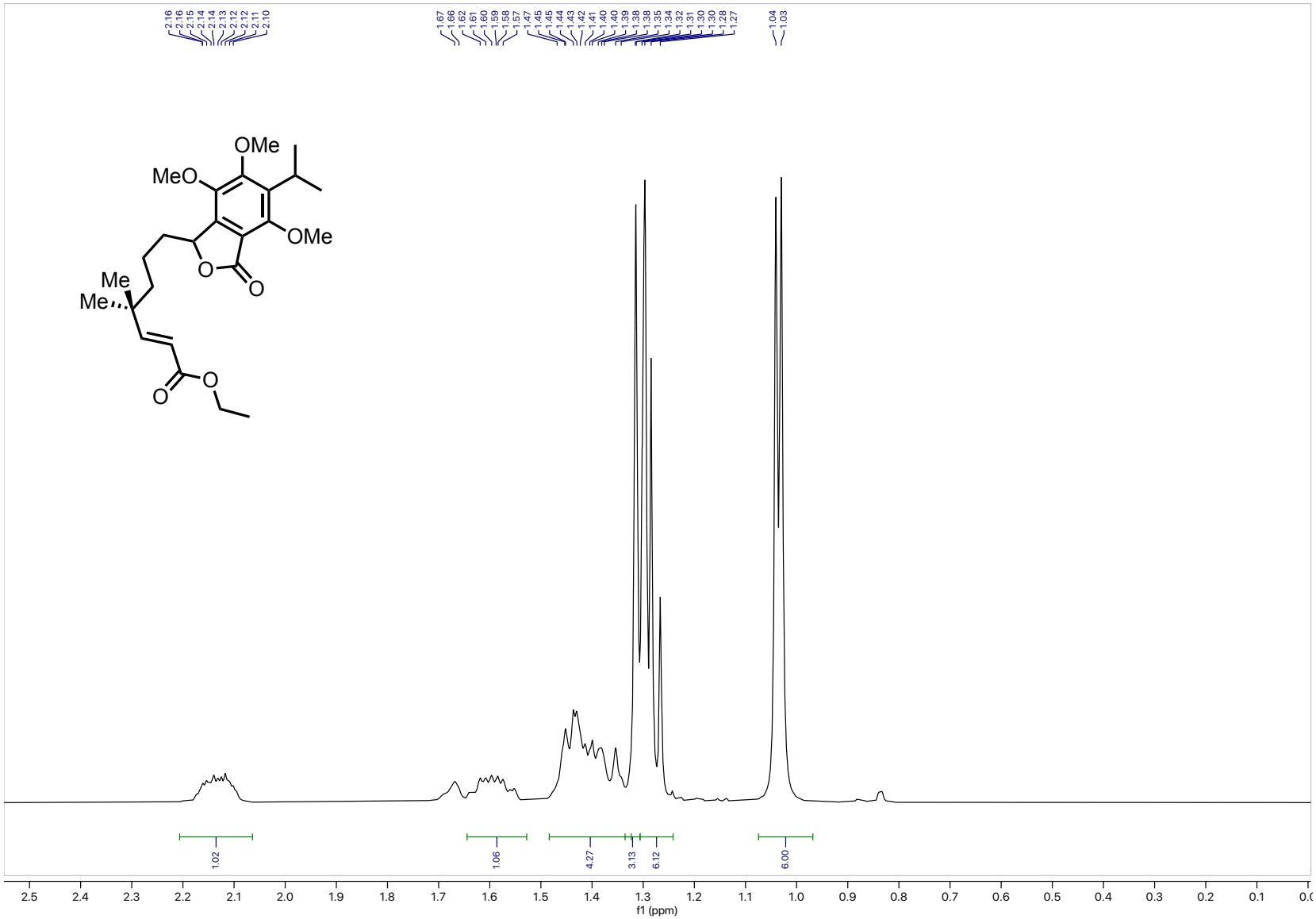

Figure A.24. ^{1}H NMR (600 MHz, $CDCl_3$) lactone **1.32** (2.5 – 0 ppm inset)

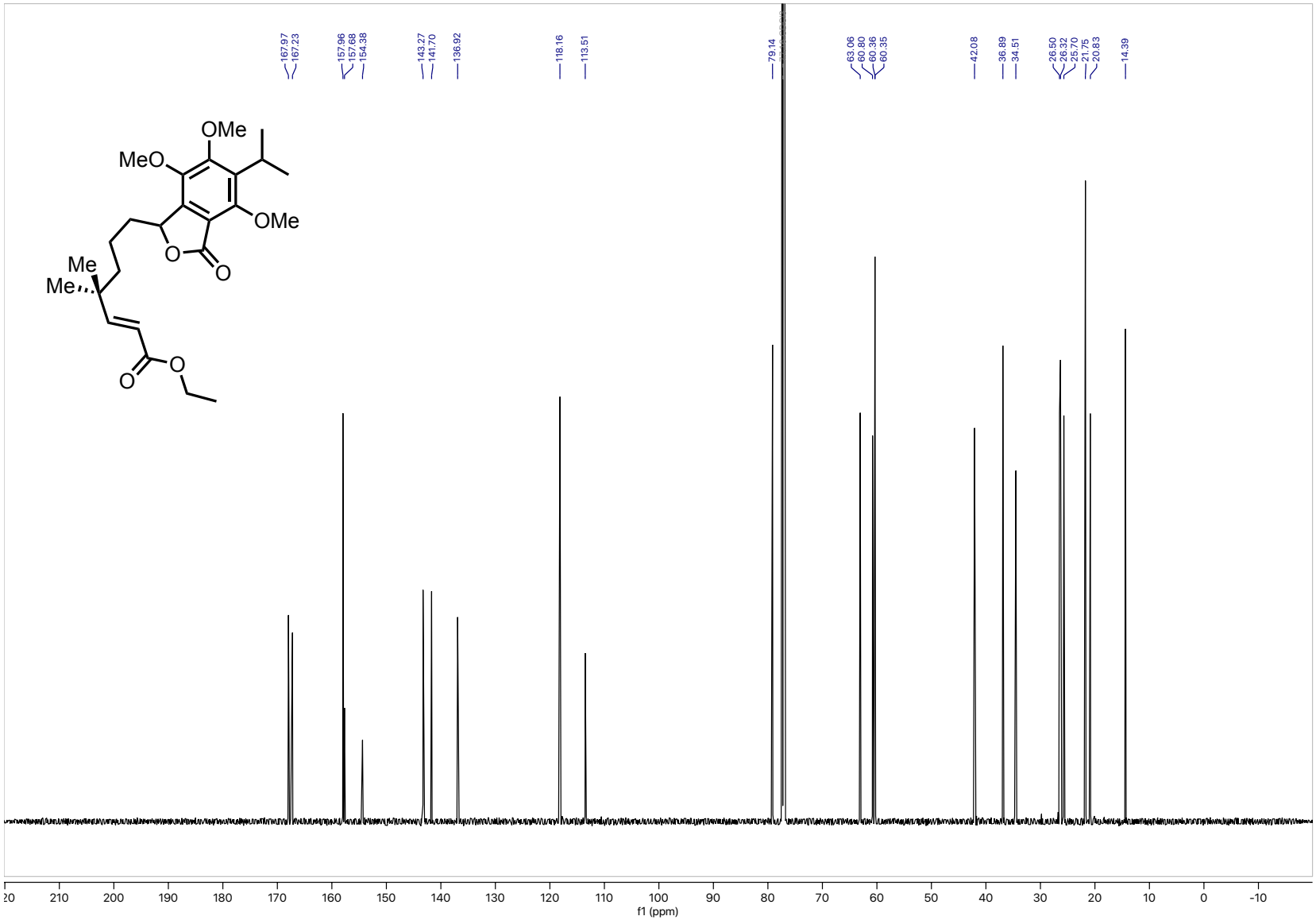

Figure A.25. ^{13}C NMR (151 MHz, $CDCl_3$) lactone **1.32**

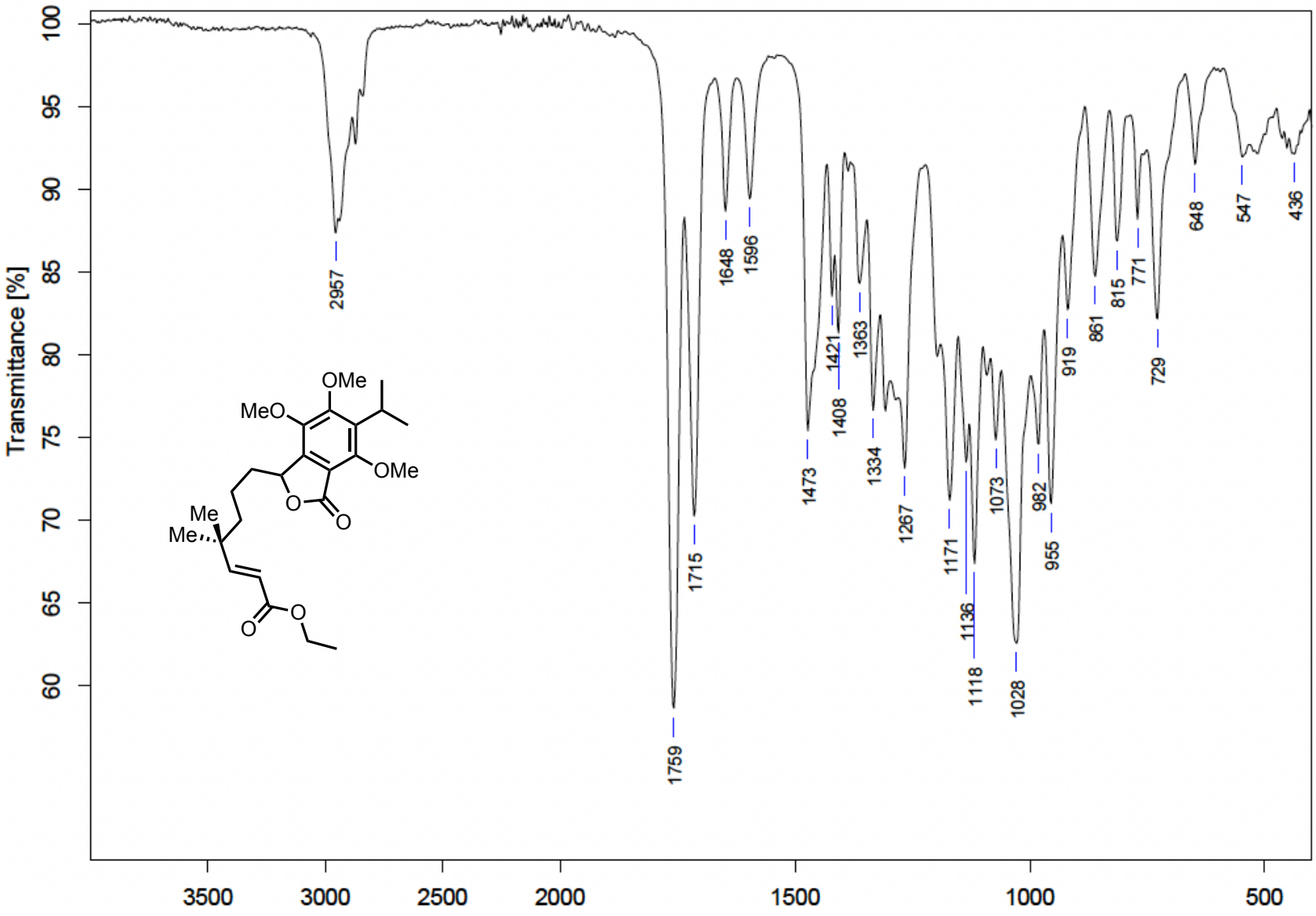

Figure A.26. FTIR (thin film) lactone **1.32**

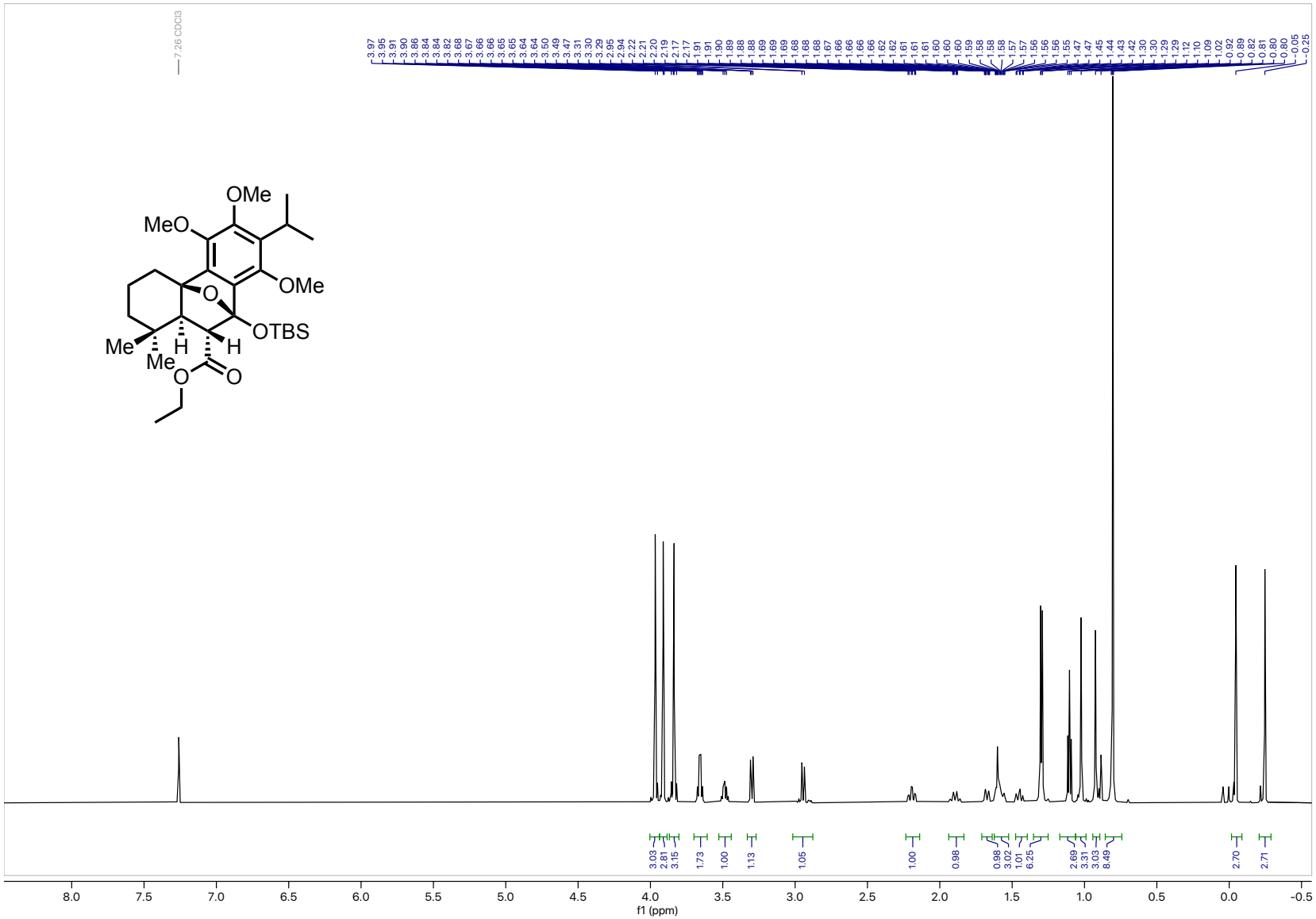

Figure A.27. ^{1}H NMR (600 MHz, $CDCl_3$) silyl acetal **1.30**

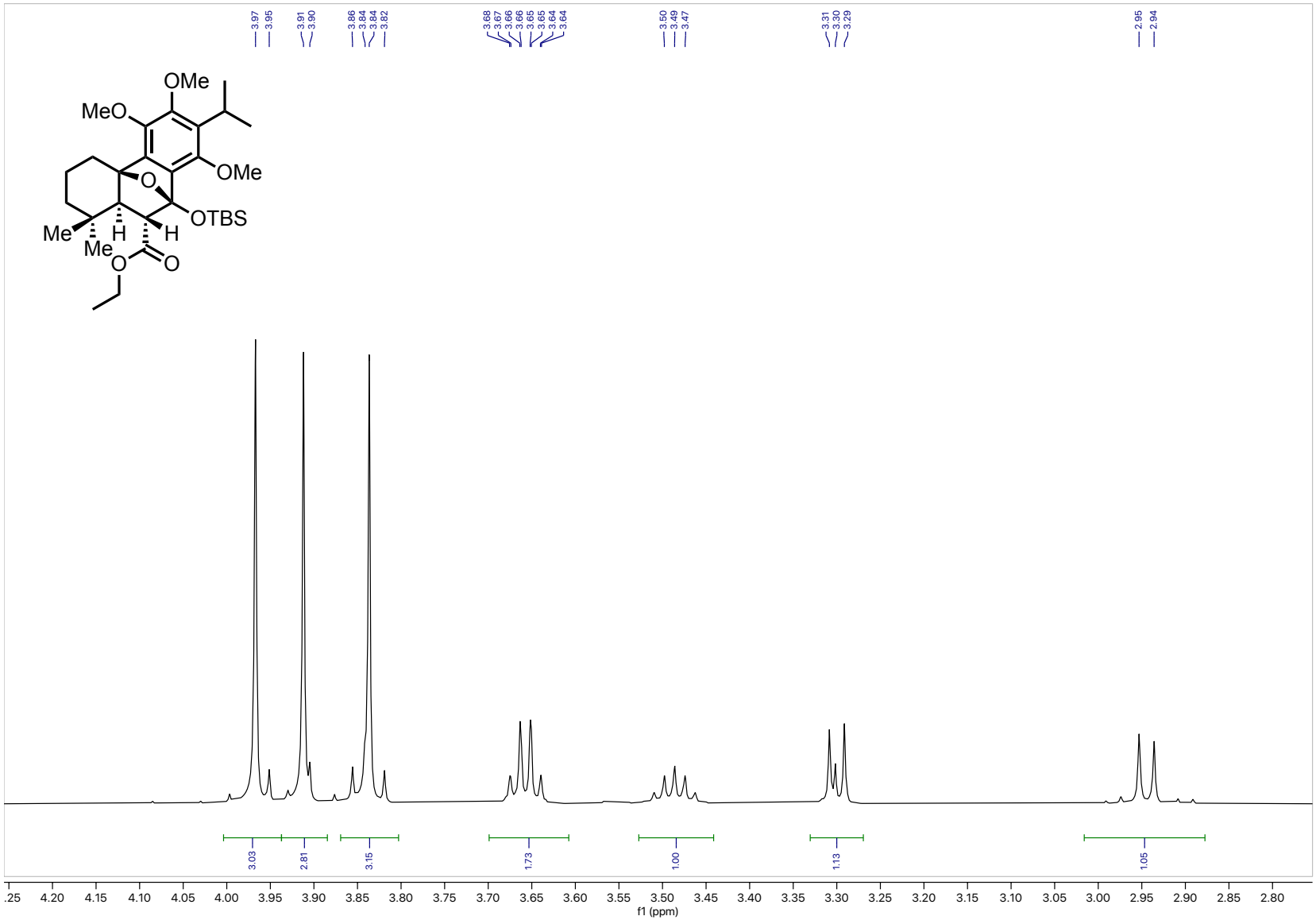

Figure A.28. ^{1}H NMR (600 MHz, $CDCl_3$) silyl acetal **1.30** (4.25 – 2.75 ppm inset)

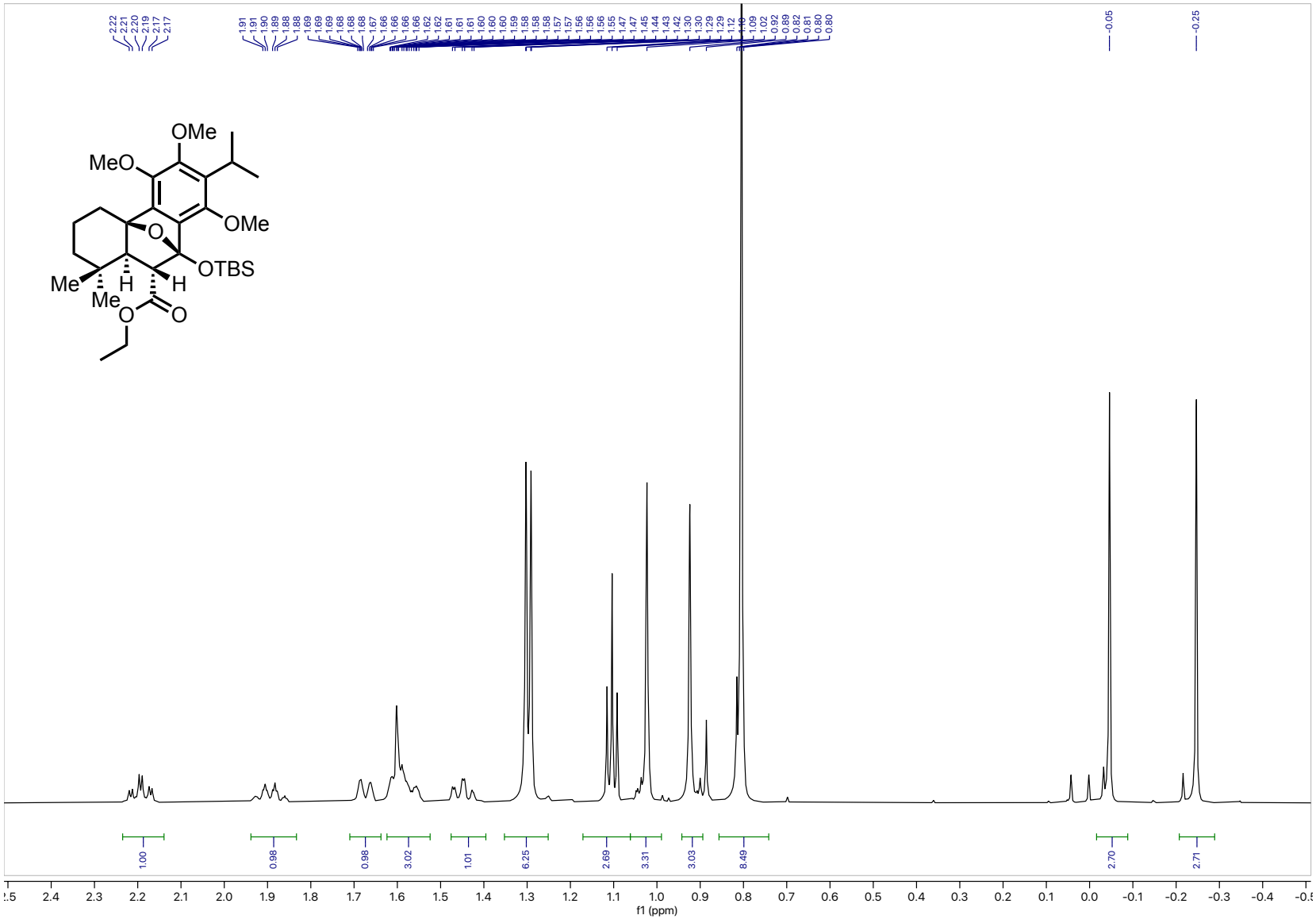

Figure A.29. ^{1}H NMR (600 MHz, $CDCl_3$) silyl acetal **1.30** (2.5 – -0.5 ppm inset)

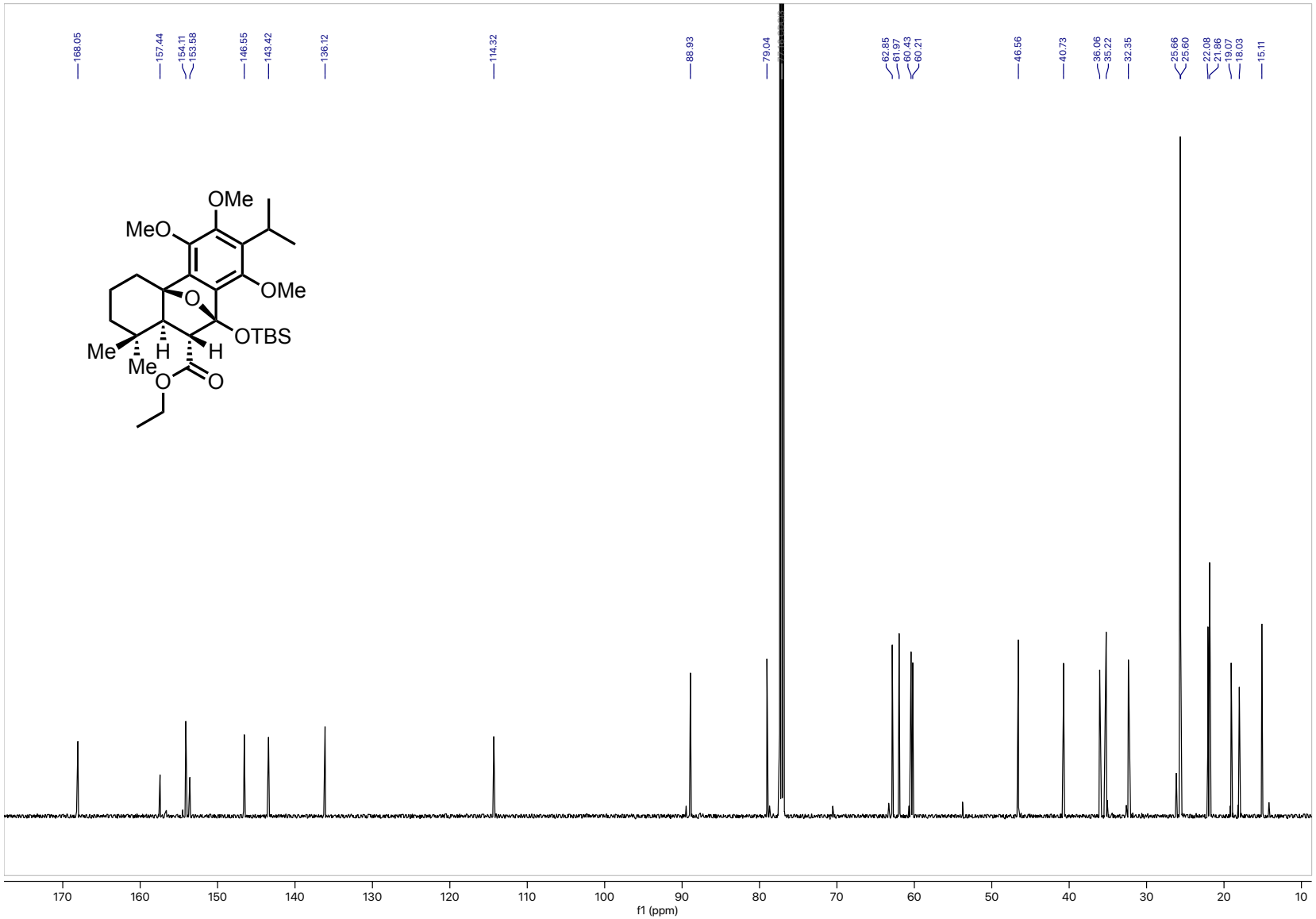

Figure A.30. ^{13}C NMR (151 MHz, $CDCl_3$) silyl acetal **1.30**

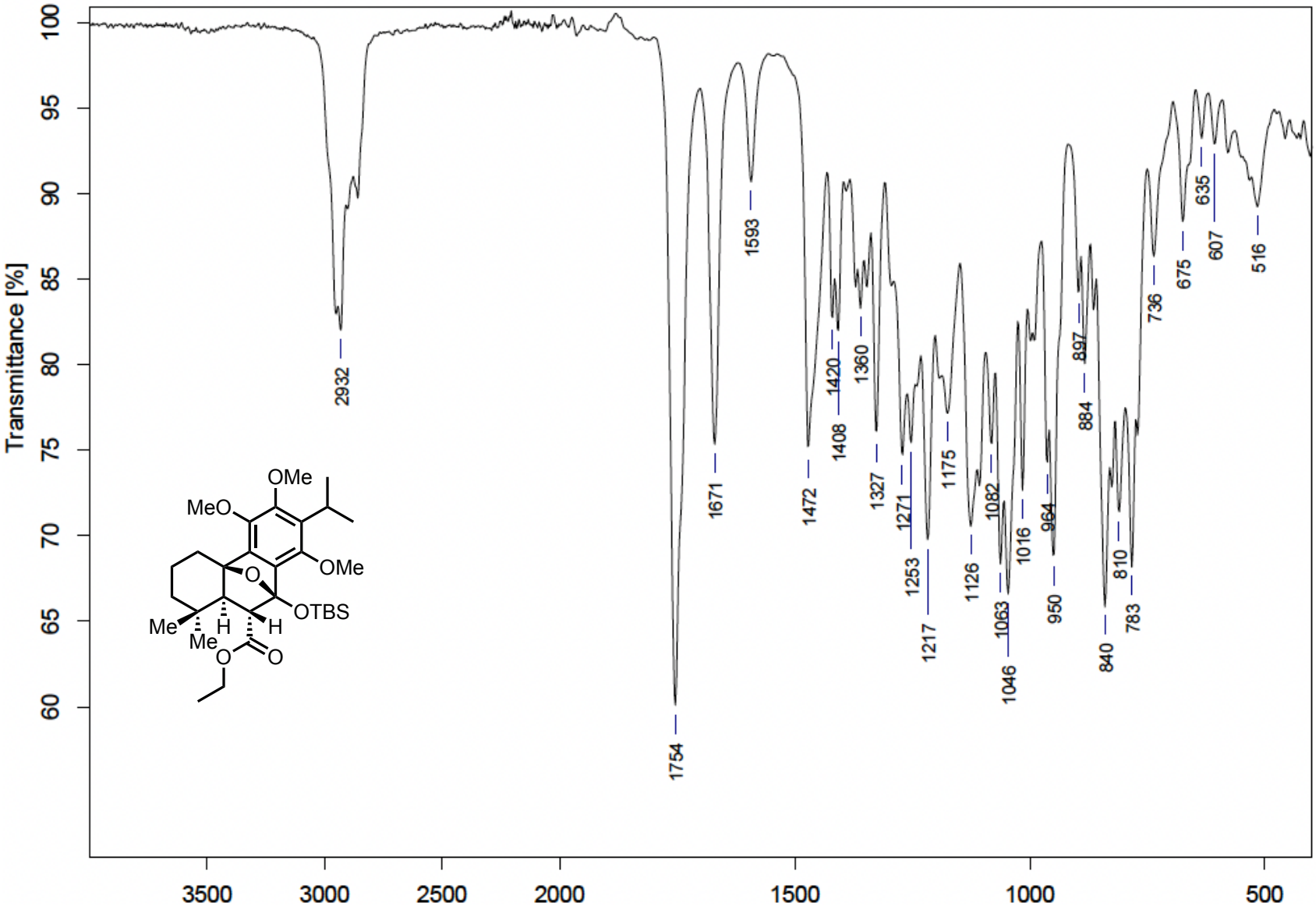

Figure A.31. FTIR (thin film) silyl acetal **1.30**

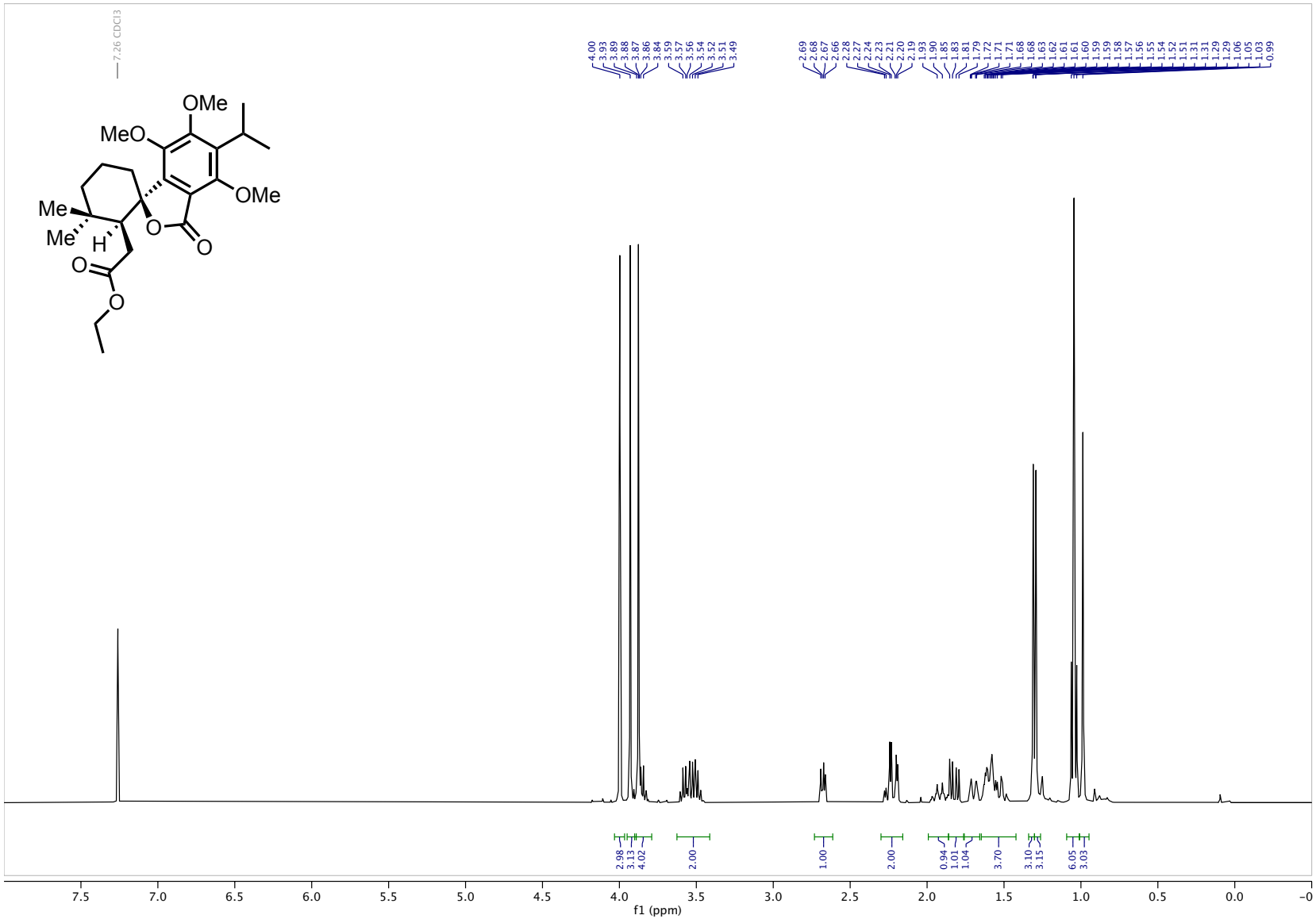

Figure A.32. ^{1}H NMR (400 MHz, $CDCl_3$) spirolactone **1.48**

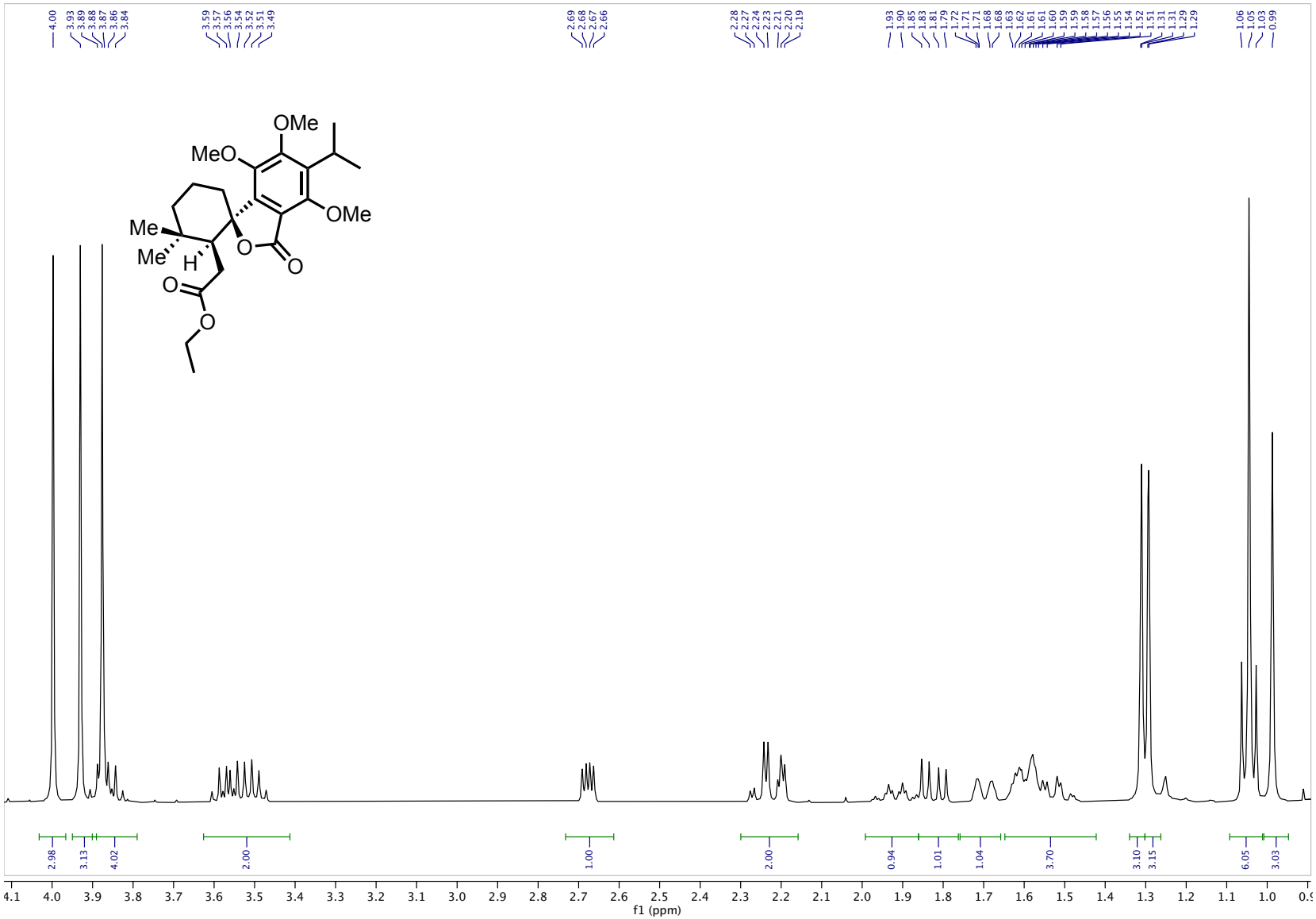

Figure A.33. ^{1}H NMR (400 MHz, $CDCl_3$) spirolactone **1.48** (4.1 – 0.9 ppm inset)

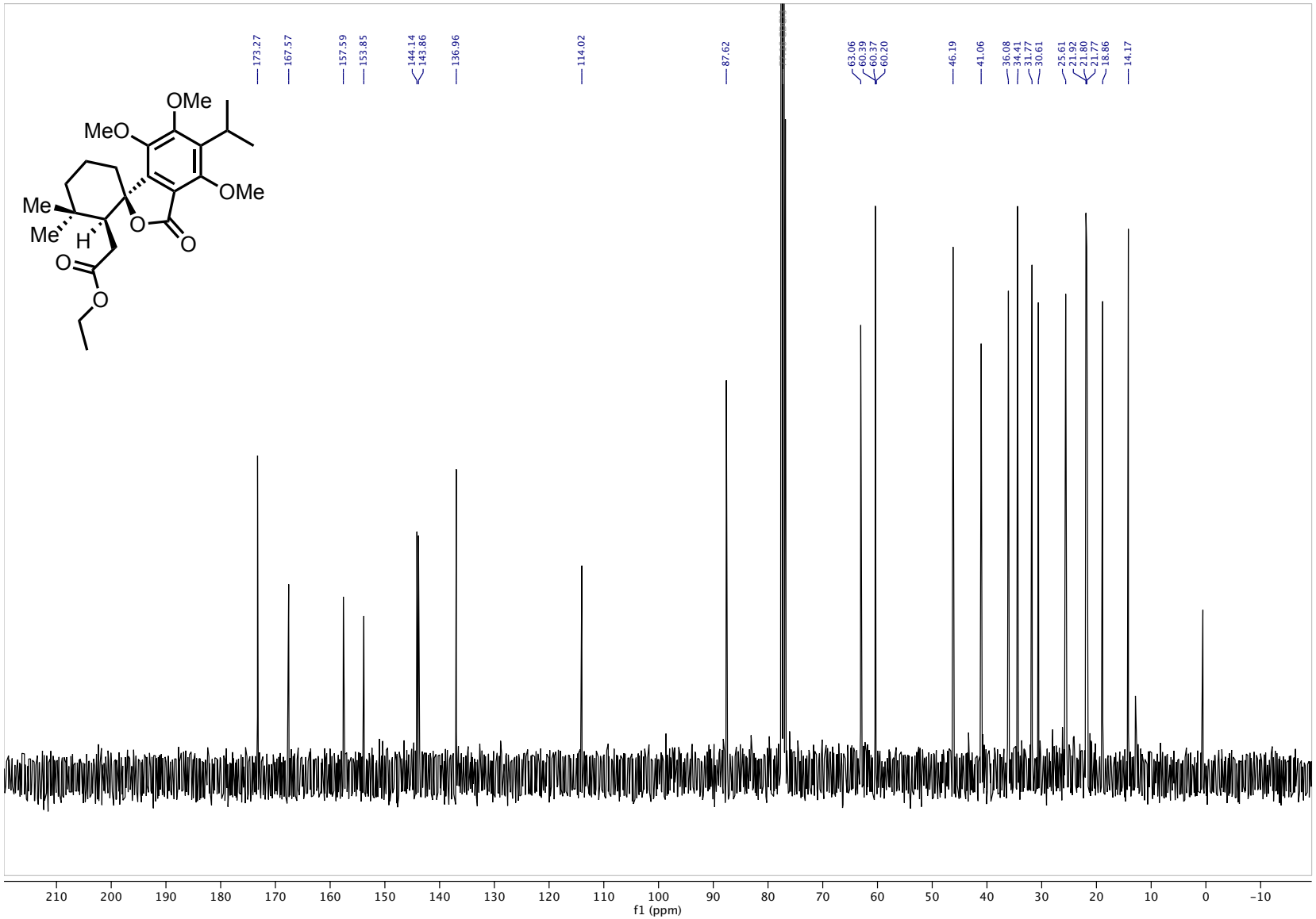

Figure A.34. ^{13}C NMR (101 MHz, $CDCl_3$) spirolactone **1.48**

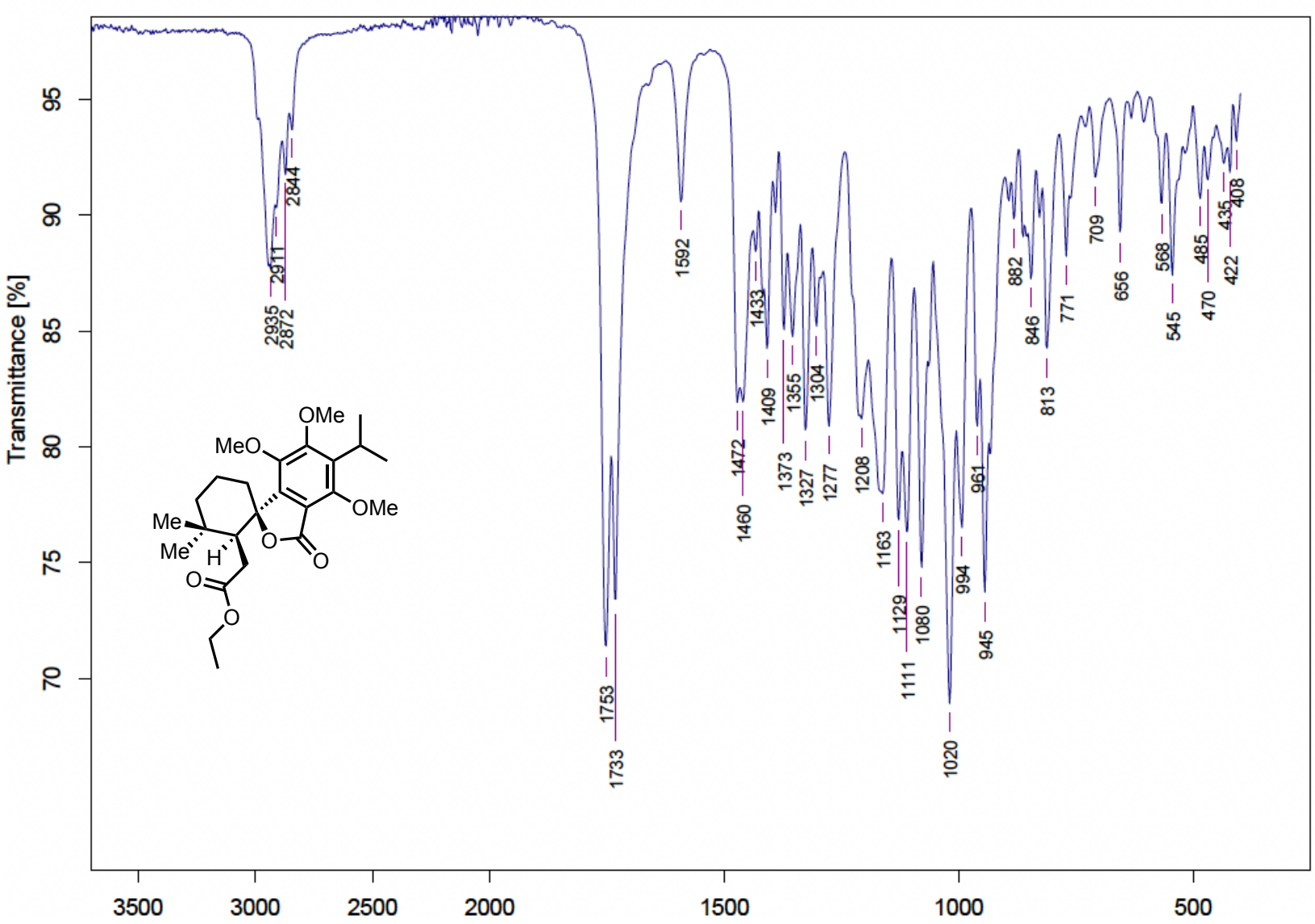

Figure A.35. FTIR (thin film) spirolactone **1.48**

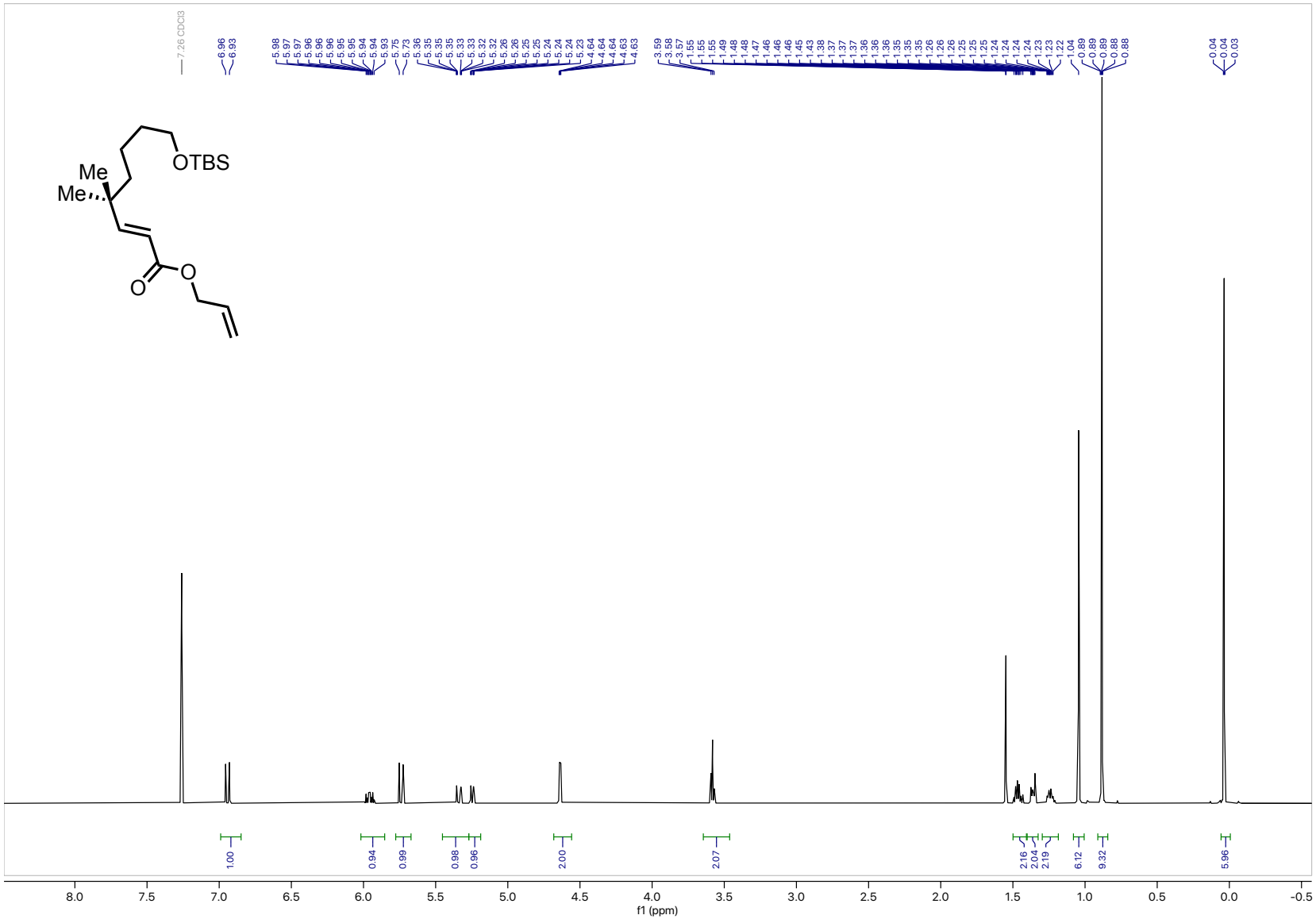

Figure A.36. ^{1}H NMR (400 MHz, $CDCl_3$) allyl ester **1.59**

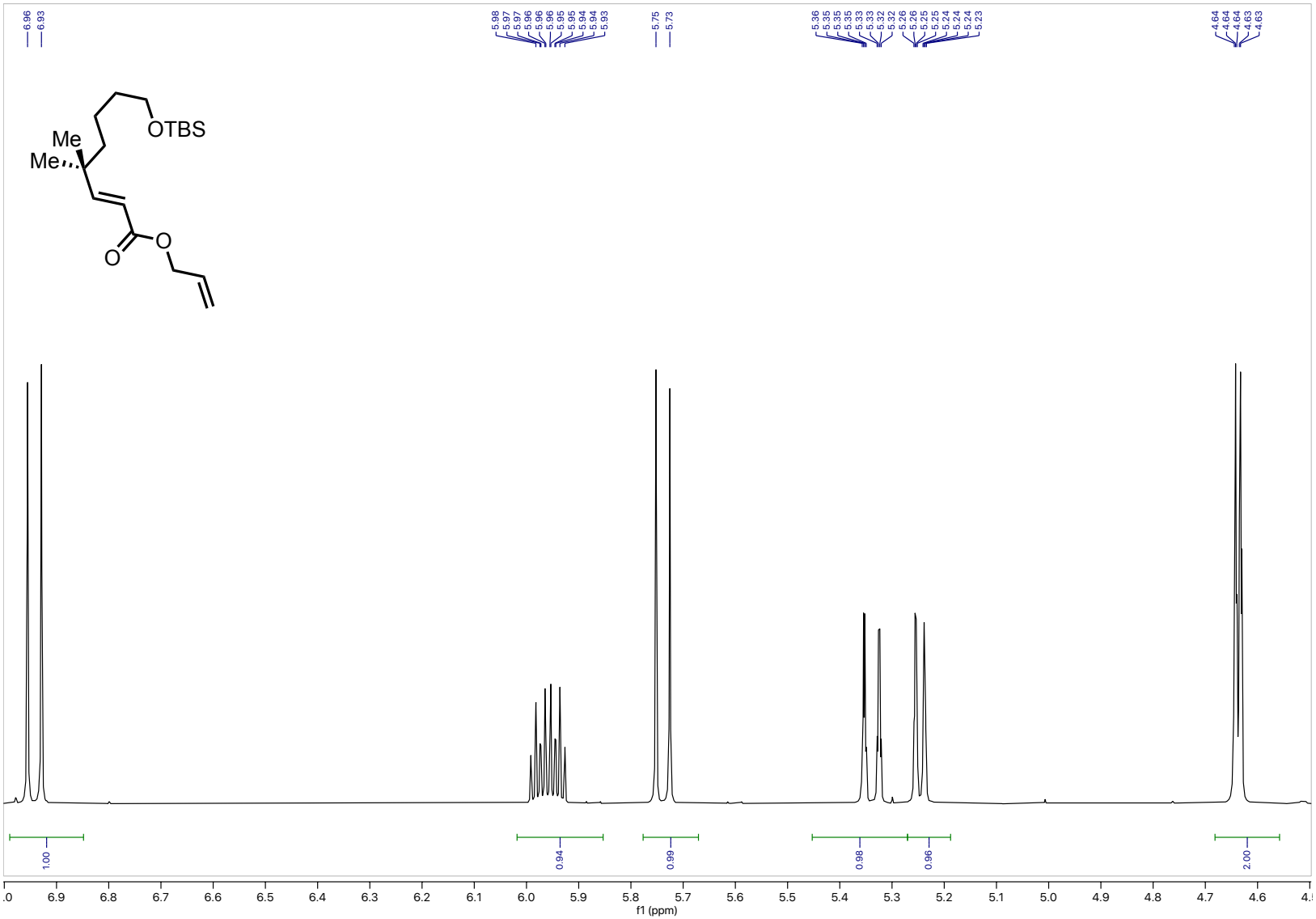

Figure A.37. ^{1}H NMR (400 MHz, $CDCl_3$) allyl ester **1.59** (7.5 – 4.0 ppm inset)

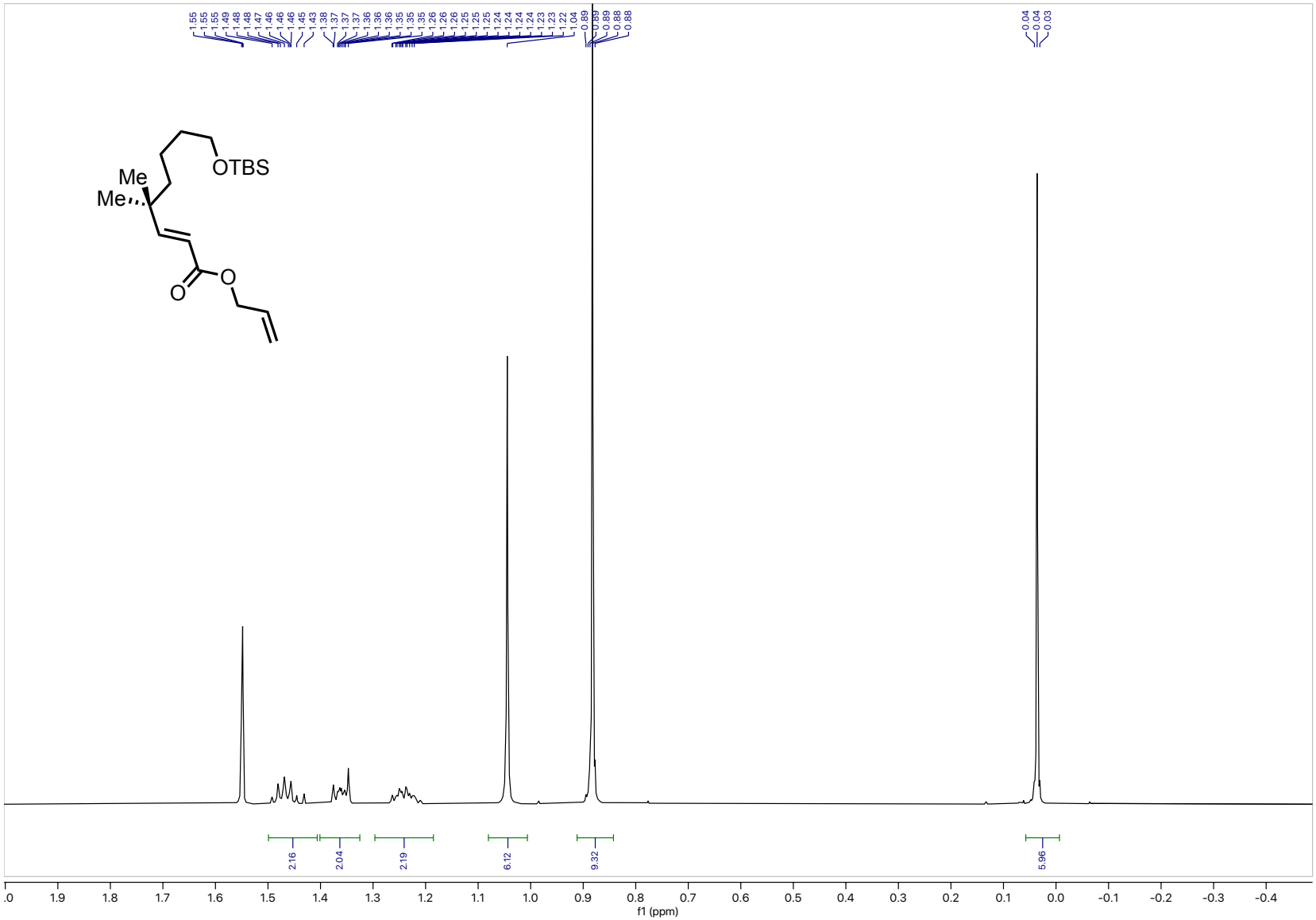

Figure A.38. ^{1}H NMR (400 MHz, $CDCl_3$) allyl ester **1.59** (2.0 – -0.5 ppm inset)

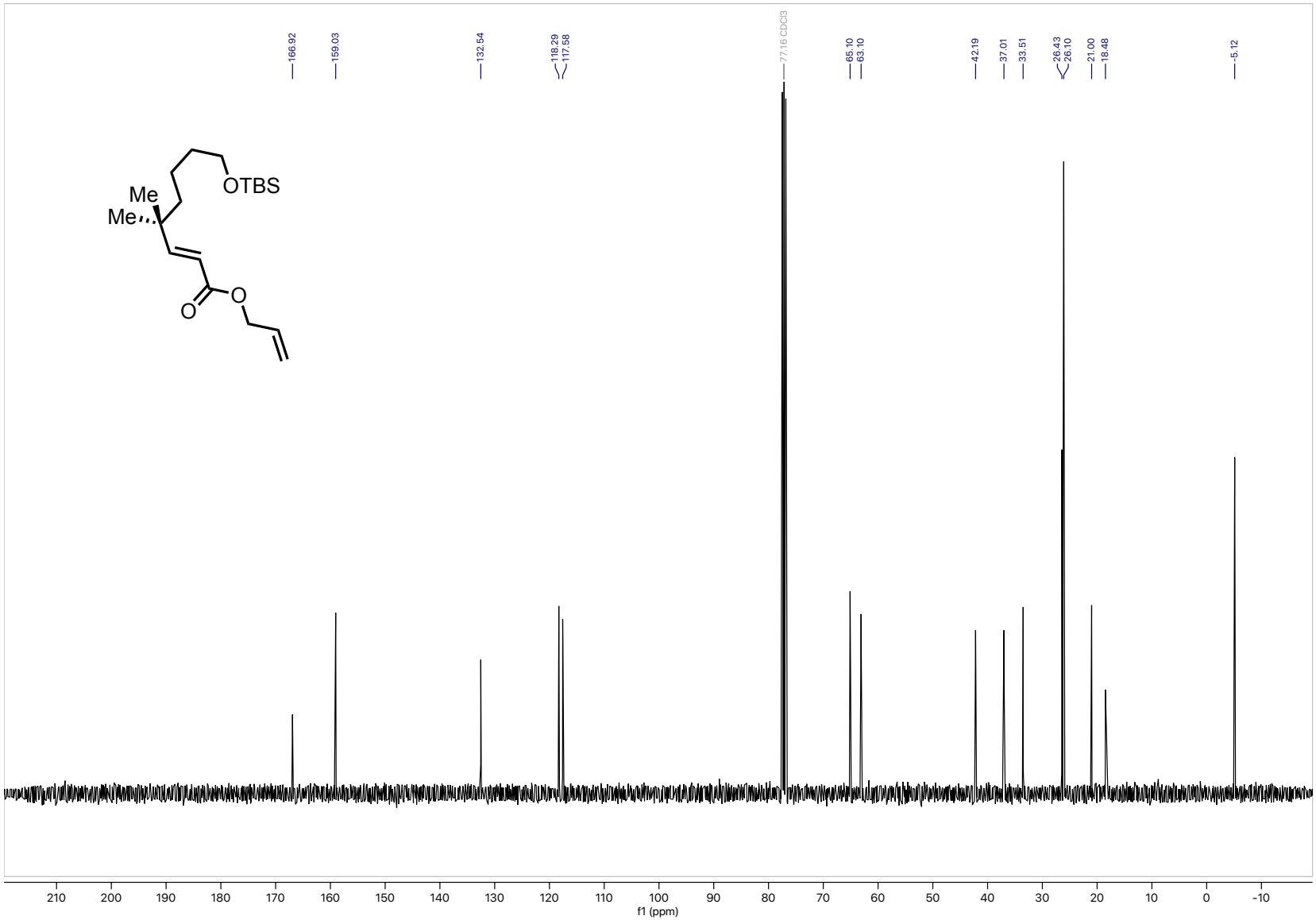

Figure A.39. ^{13}C NMR (151 MHz, $CDCl_3$) allyl ester **1.59**

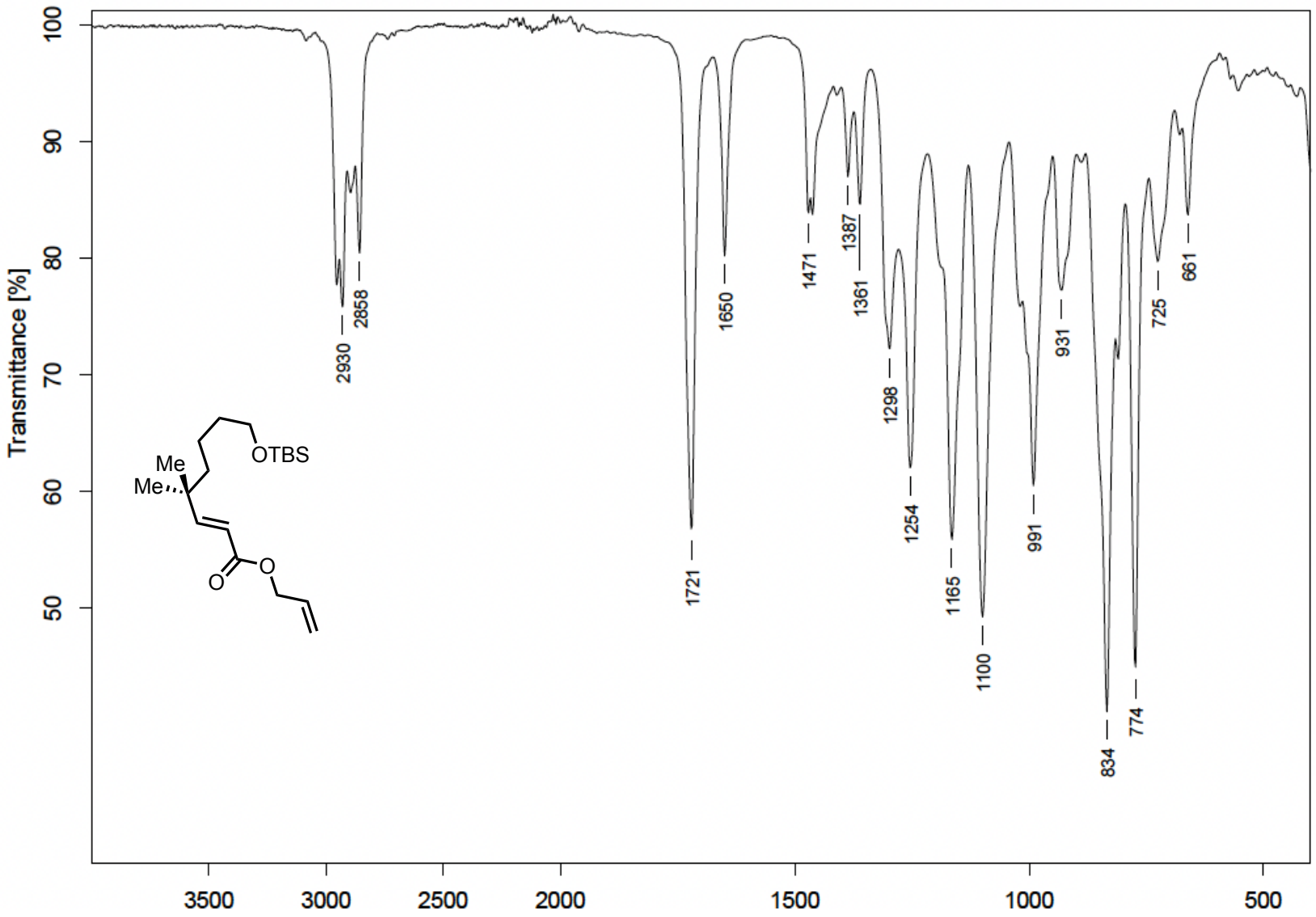

Figure A.40. FTIR (neat) allyl ester **1.59**

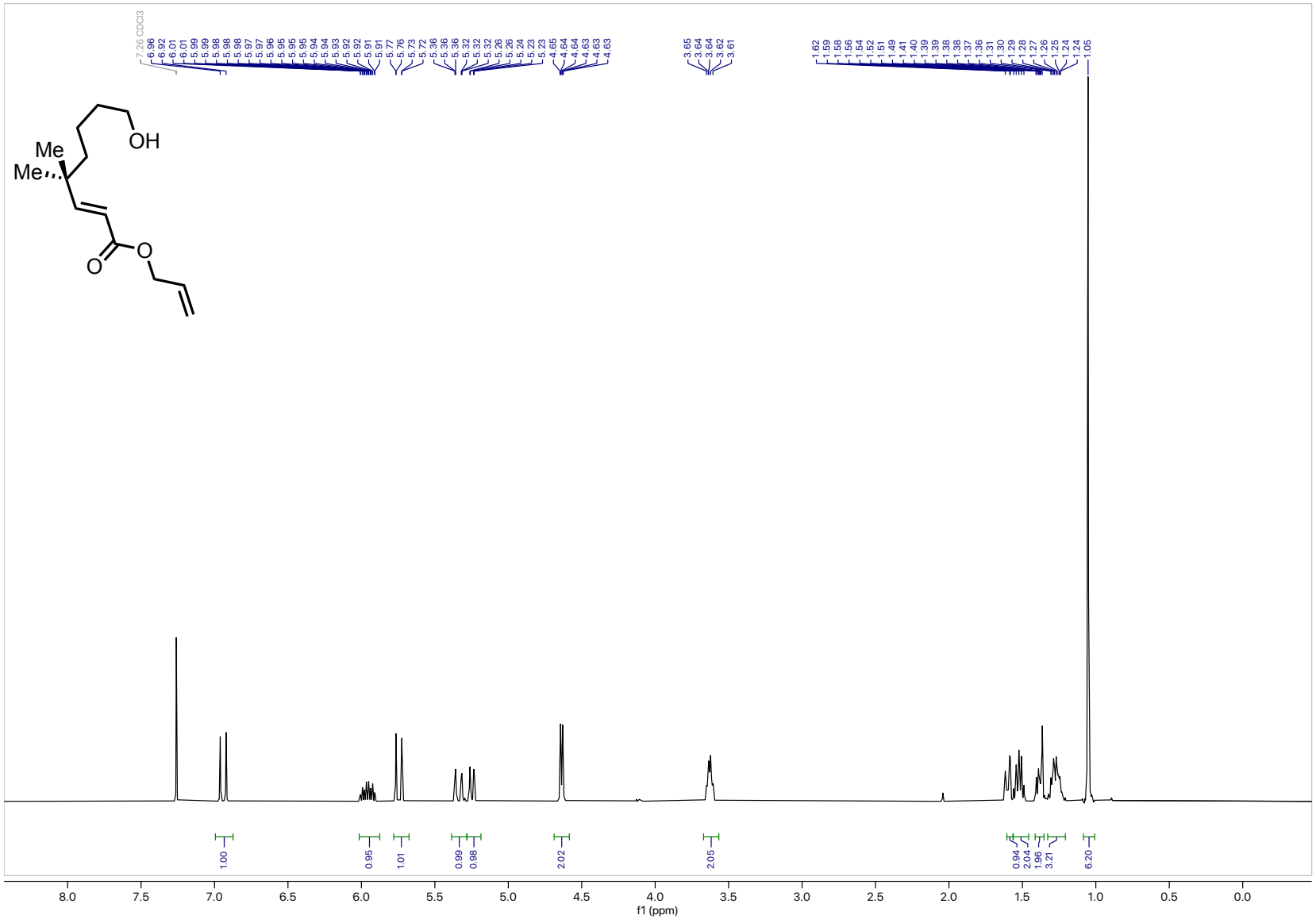

Figure A.41. ^{1}H NMR (400 MHz, $CDCl_3$) alcohol **1.74**

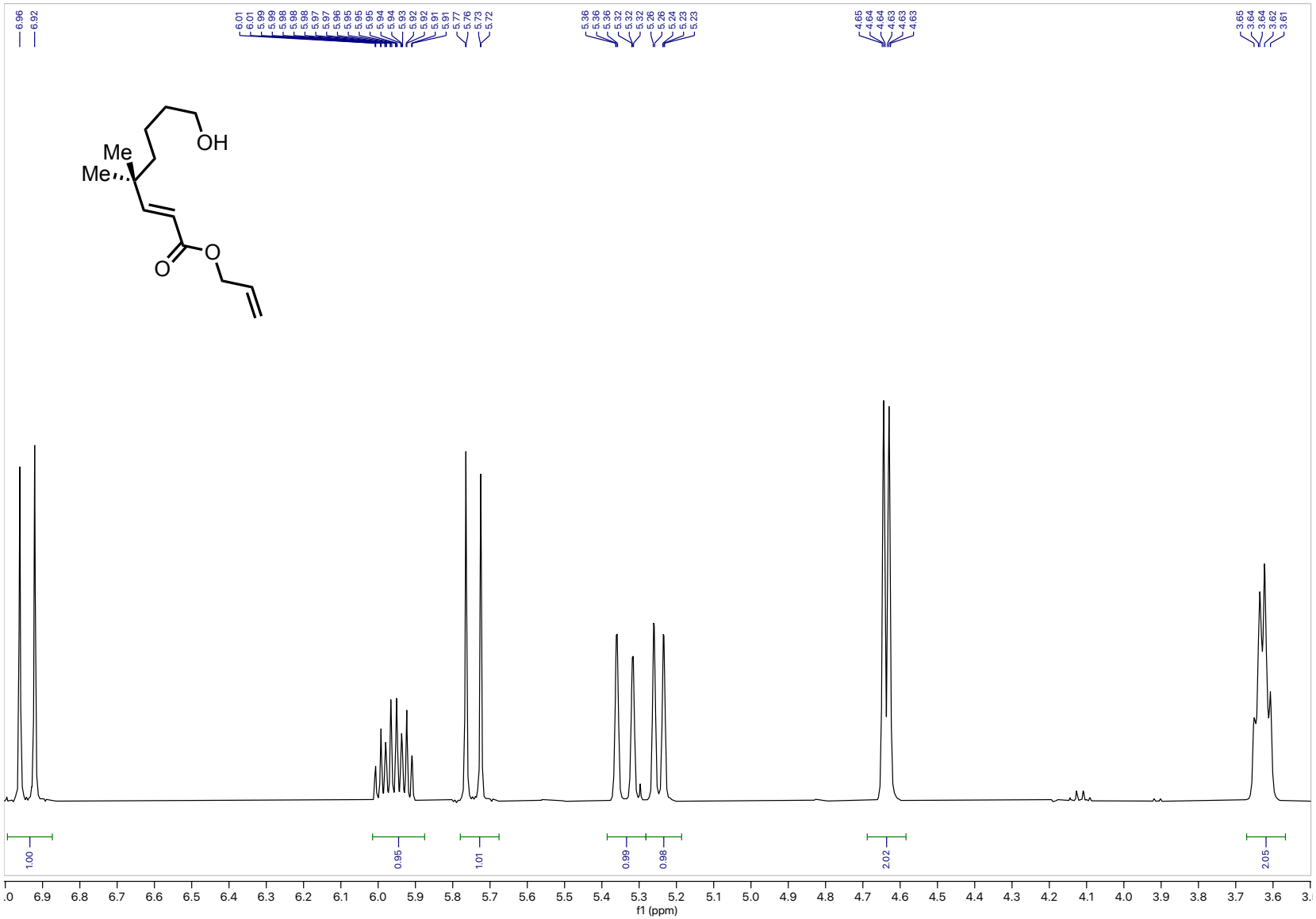

Figure A.42. ^{1}H NMR (400 MHz, $CDCl_3$) alcohol **1.74** (7.0 – 3.5 ppm inset)

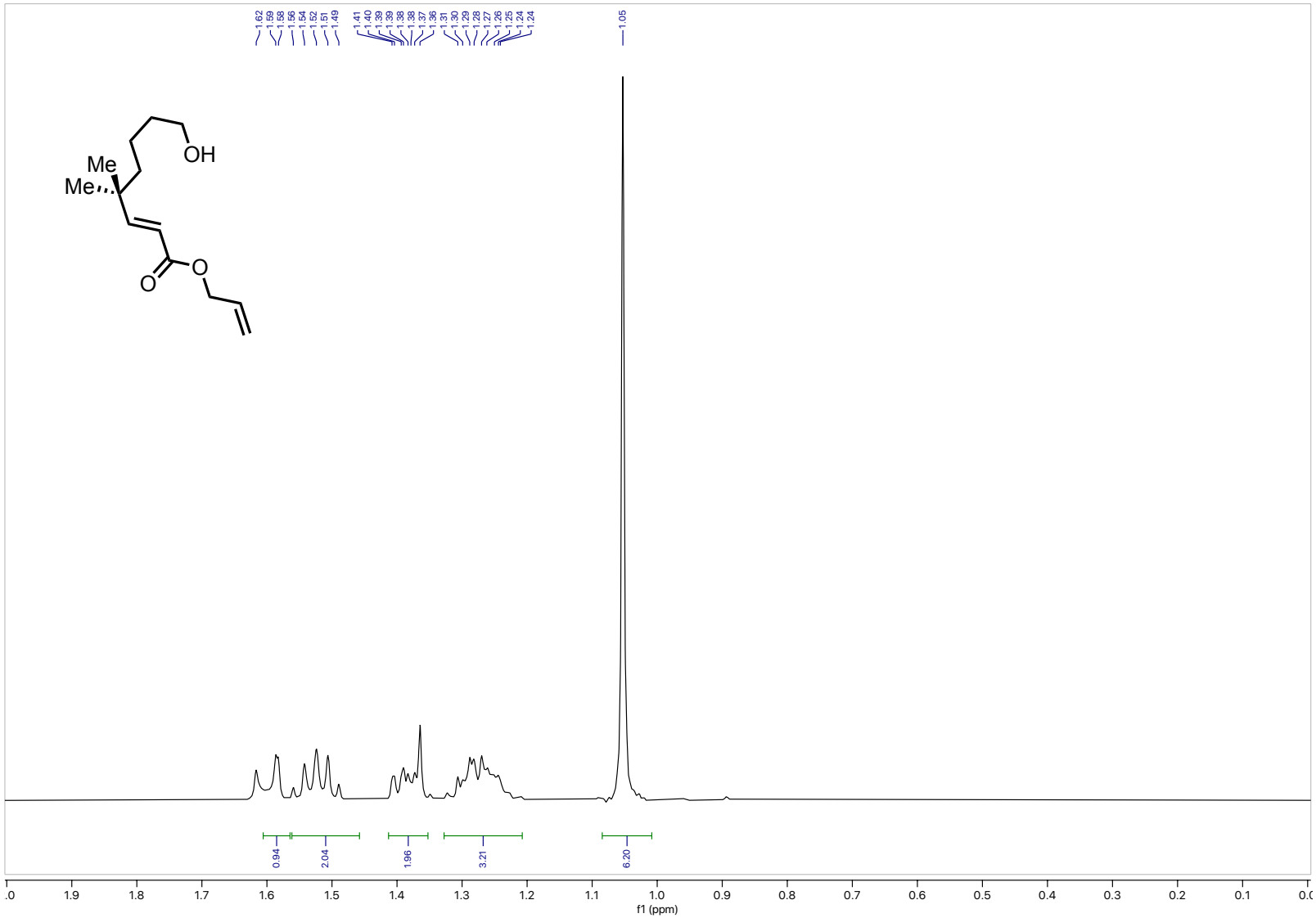

Figure A.43. ^{1}H NMR (400 MHz, $CDCl_3$) alcohol **1.74** (2.0 – 0 ppm inset)

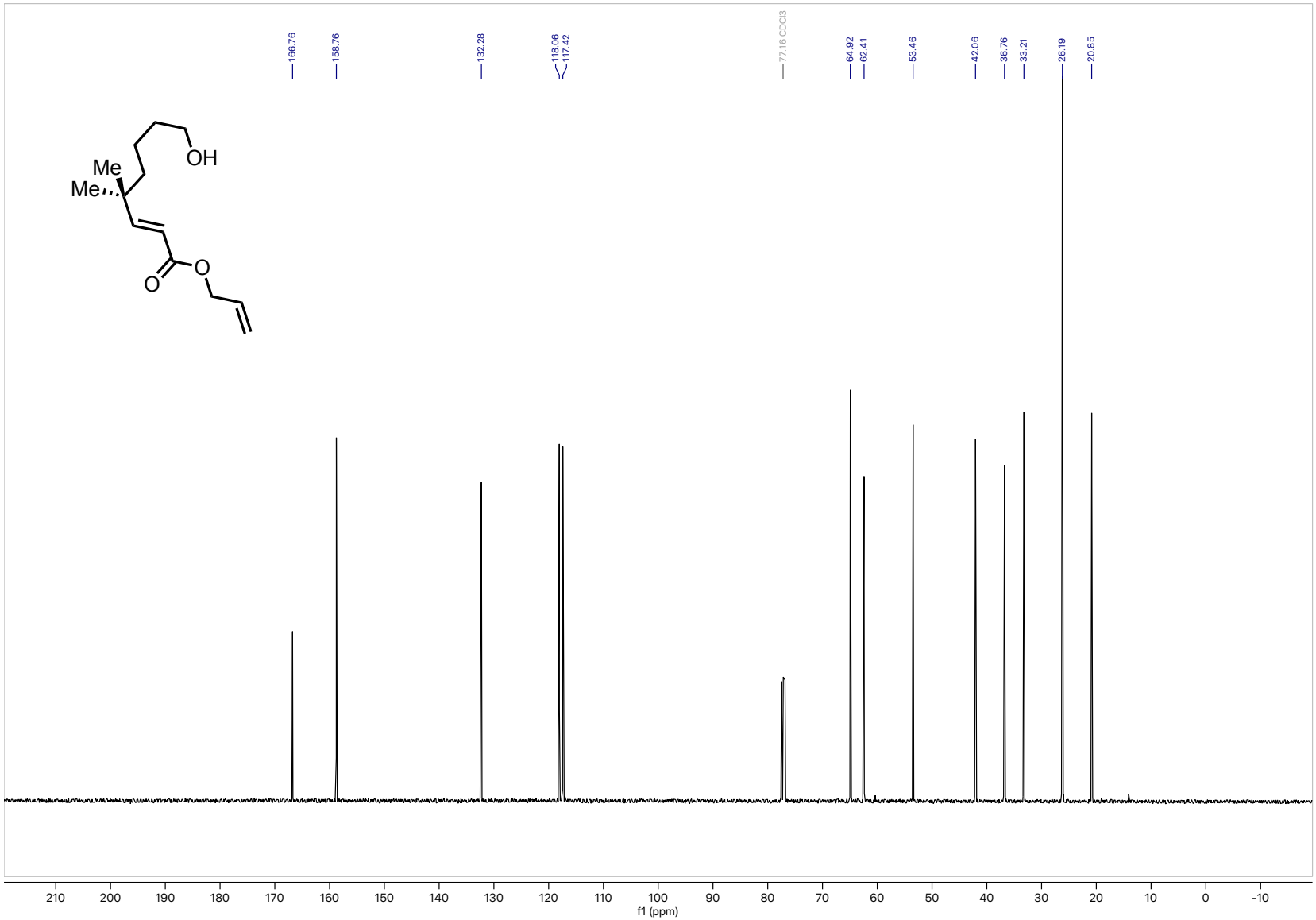

Figure A.44. ^{13}C NMR (101 MHz, $CDCl_3$) alcohol **1.74**

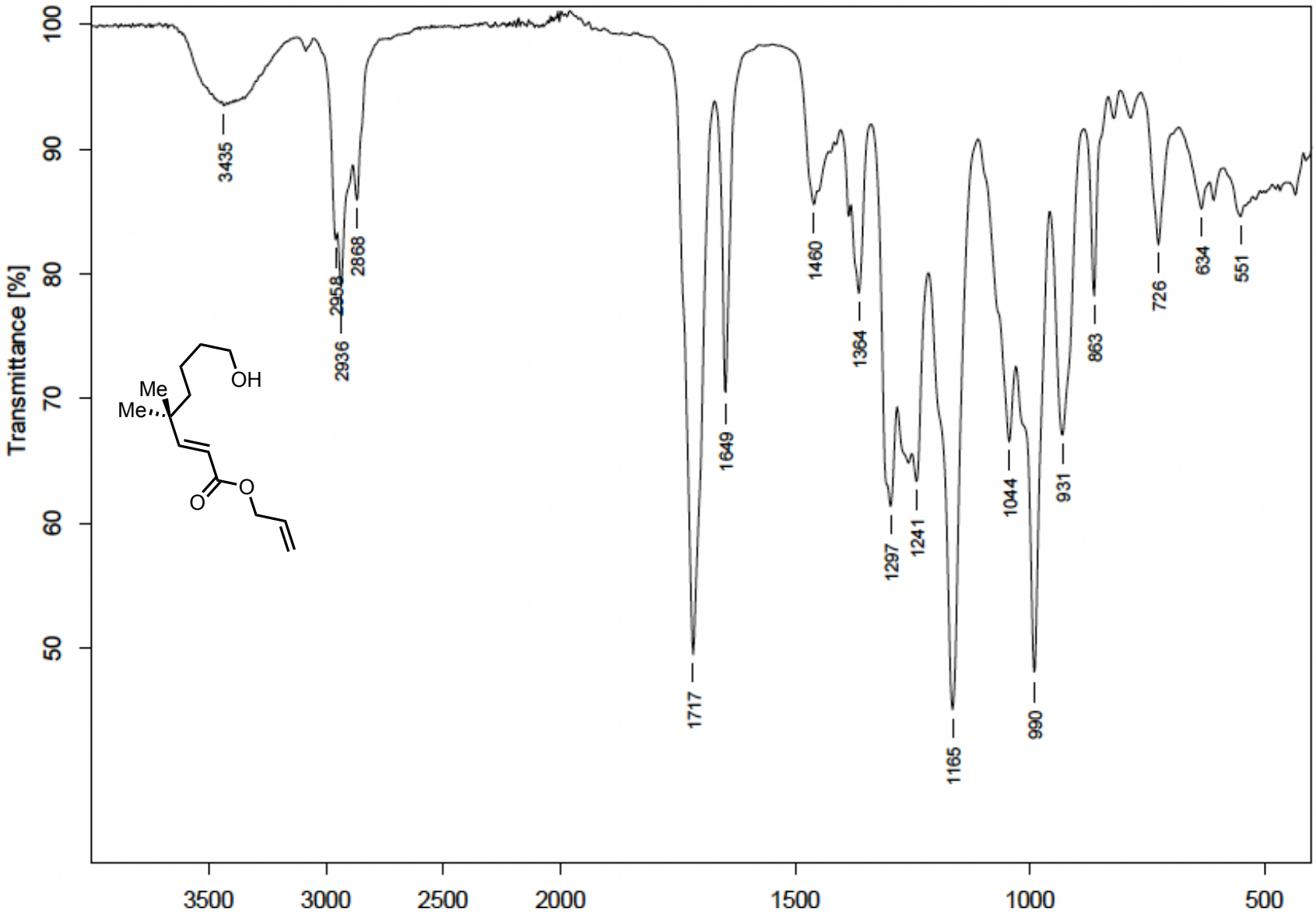

Figure A.45. FTIR (neat) alcohol **1.74**

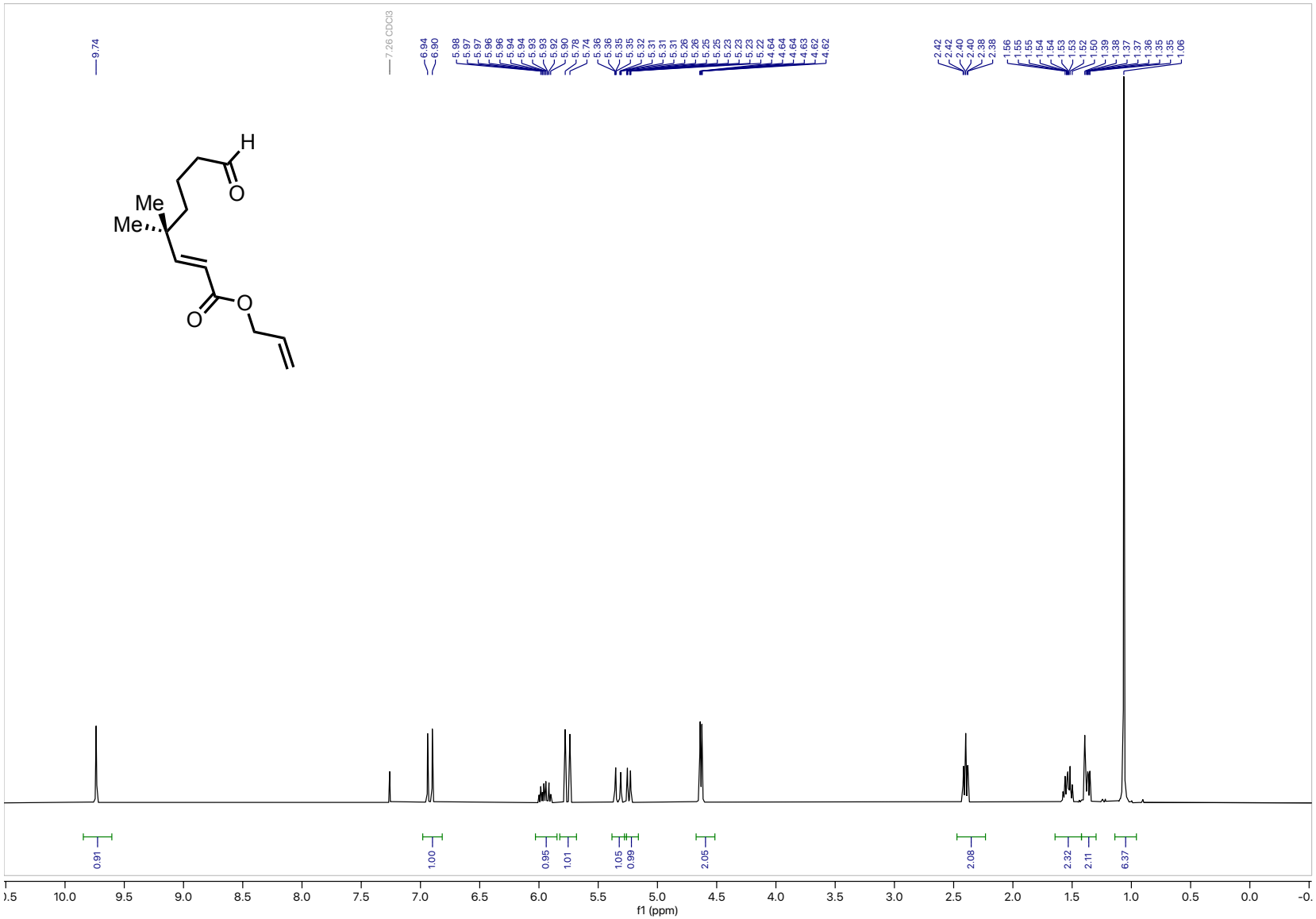

Figure A.46. ^{1}H NMR (400 MHz, $CDCl_3$) aldehyde **1.58**

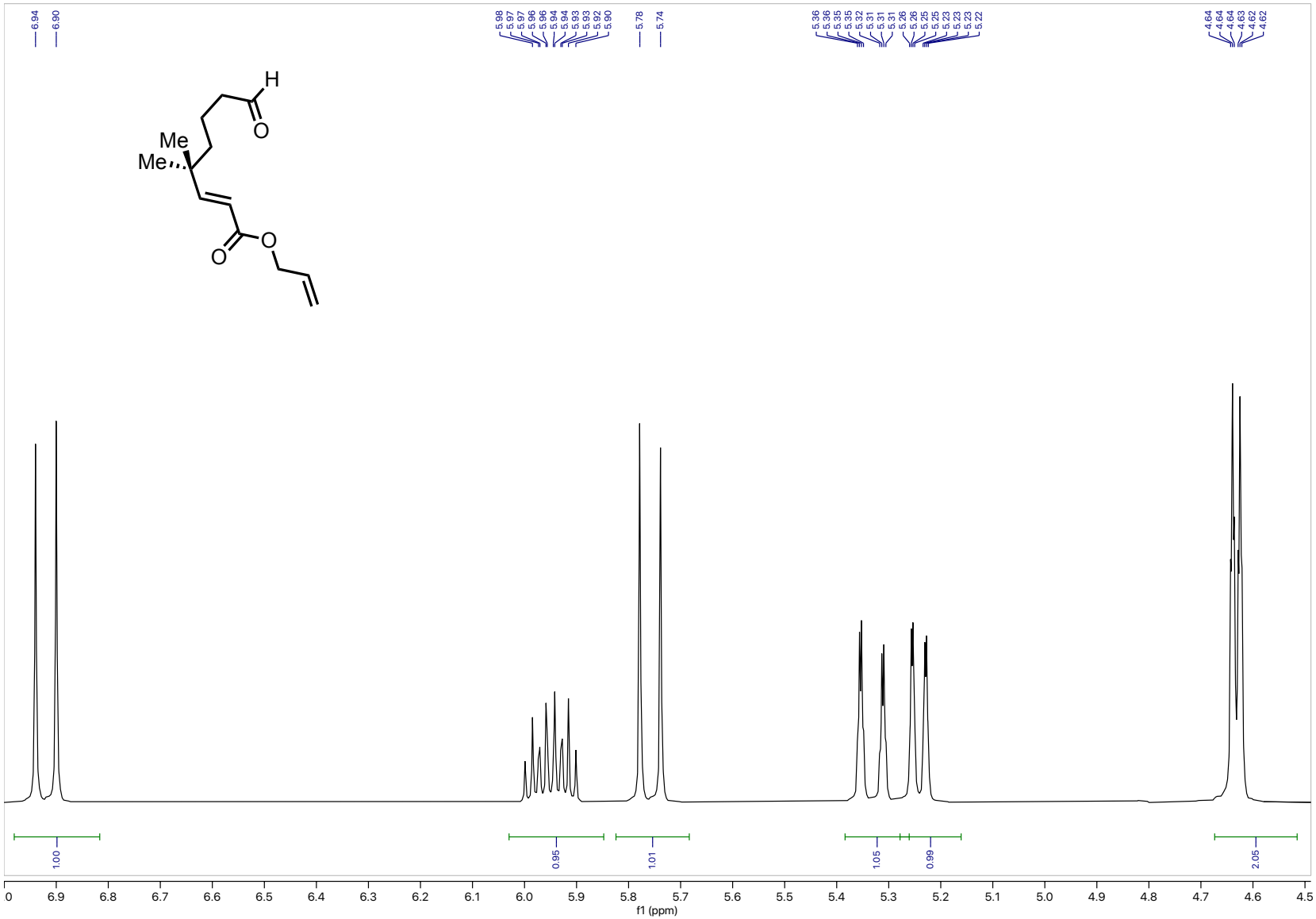

Figure A.47. ^{1}H NMR (400 MHz, $CDCl_3$) aldehyde **1.58** (7.0 – 4.5 ppm inset)

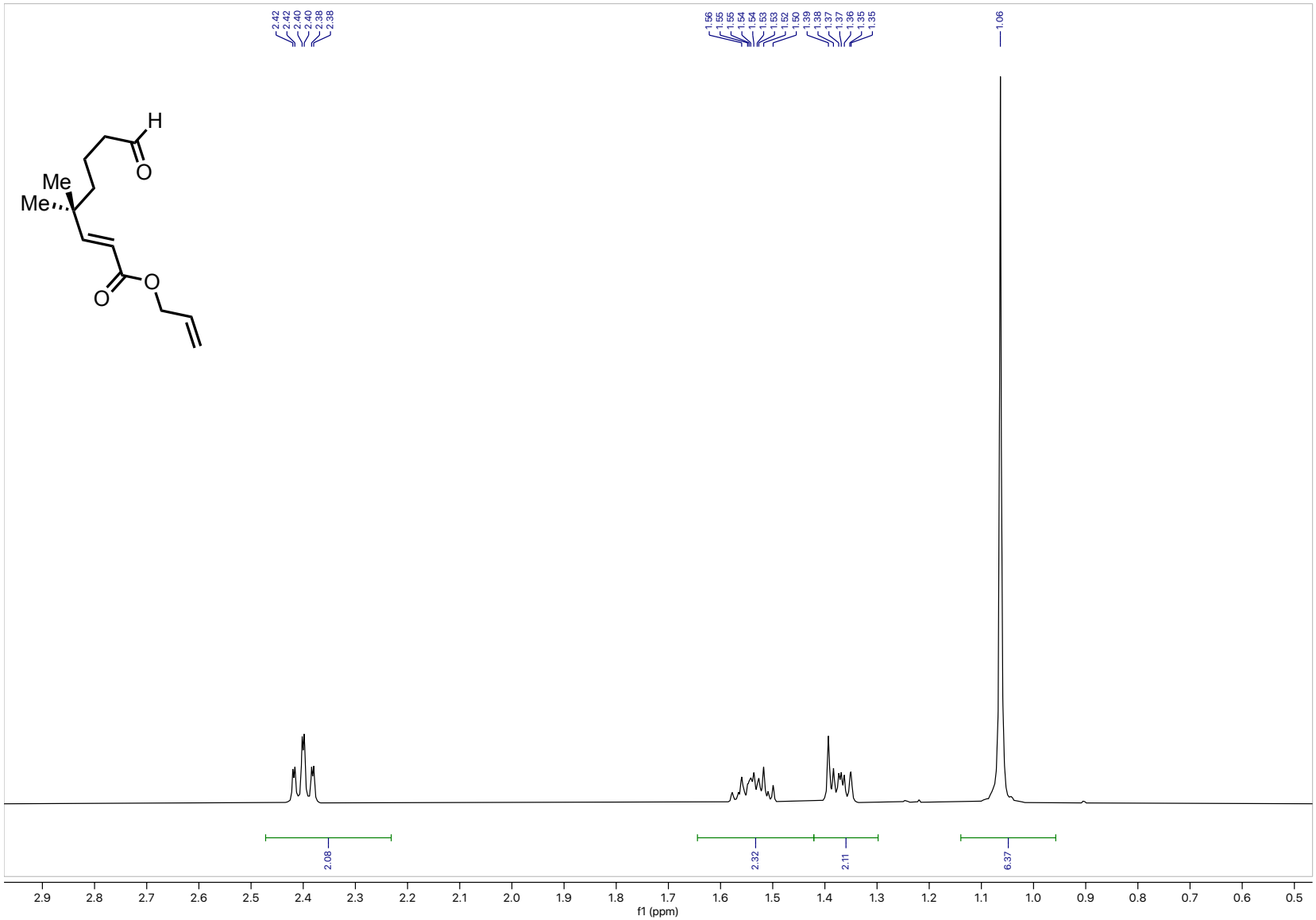

Figure A.48. ^{1}H NMR (400 MHz, $CDCl_3$) aldehyde **1.58** (3.0 – 0.5 ppm inset)

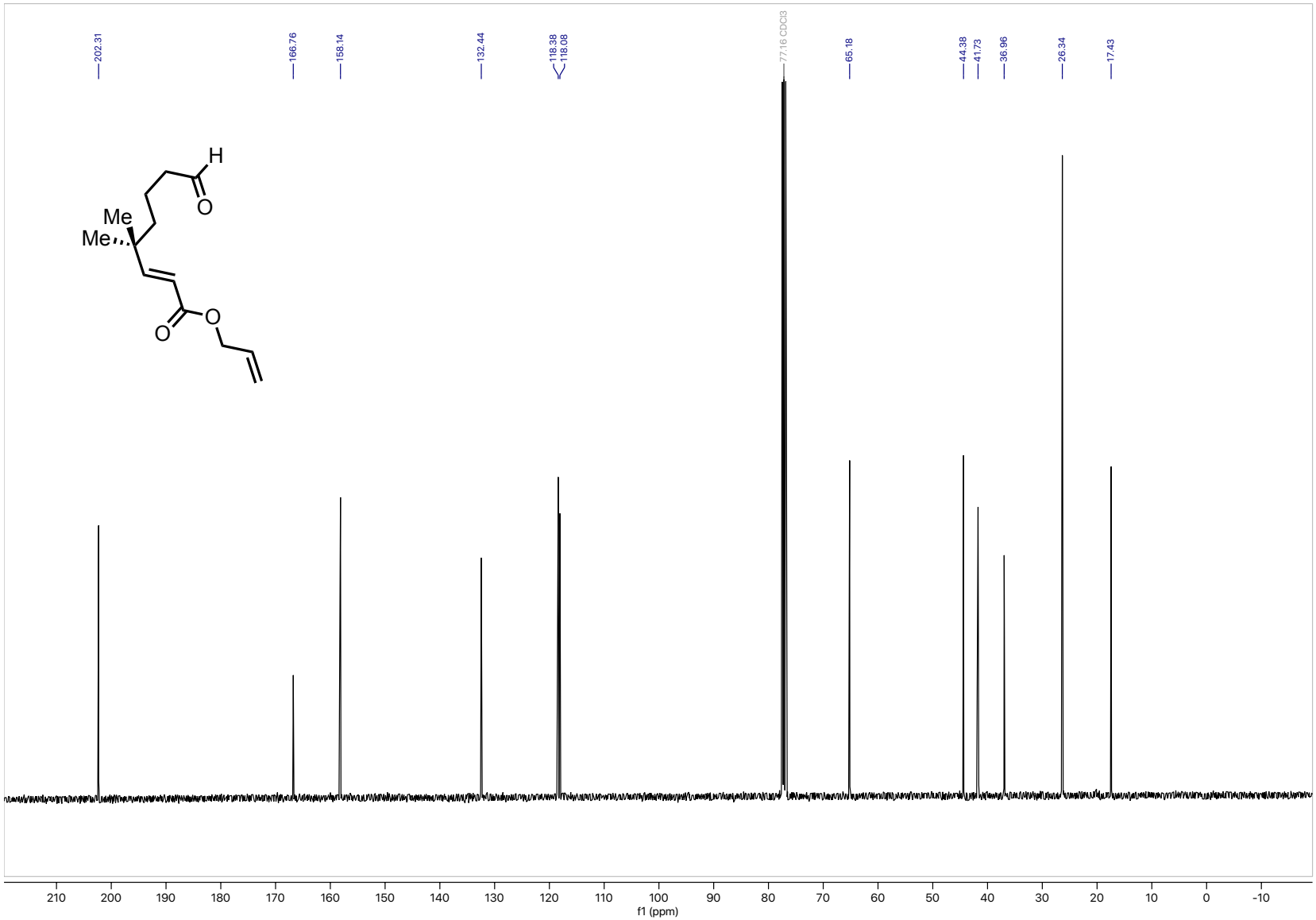

Figure A.49. ^{13}C NMR (101 MHz, $CDCl_3$) aldehyde **1.58**

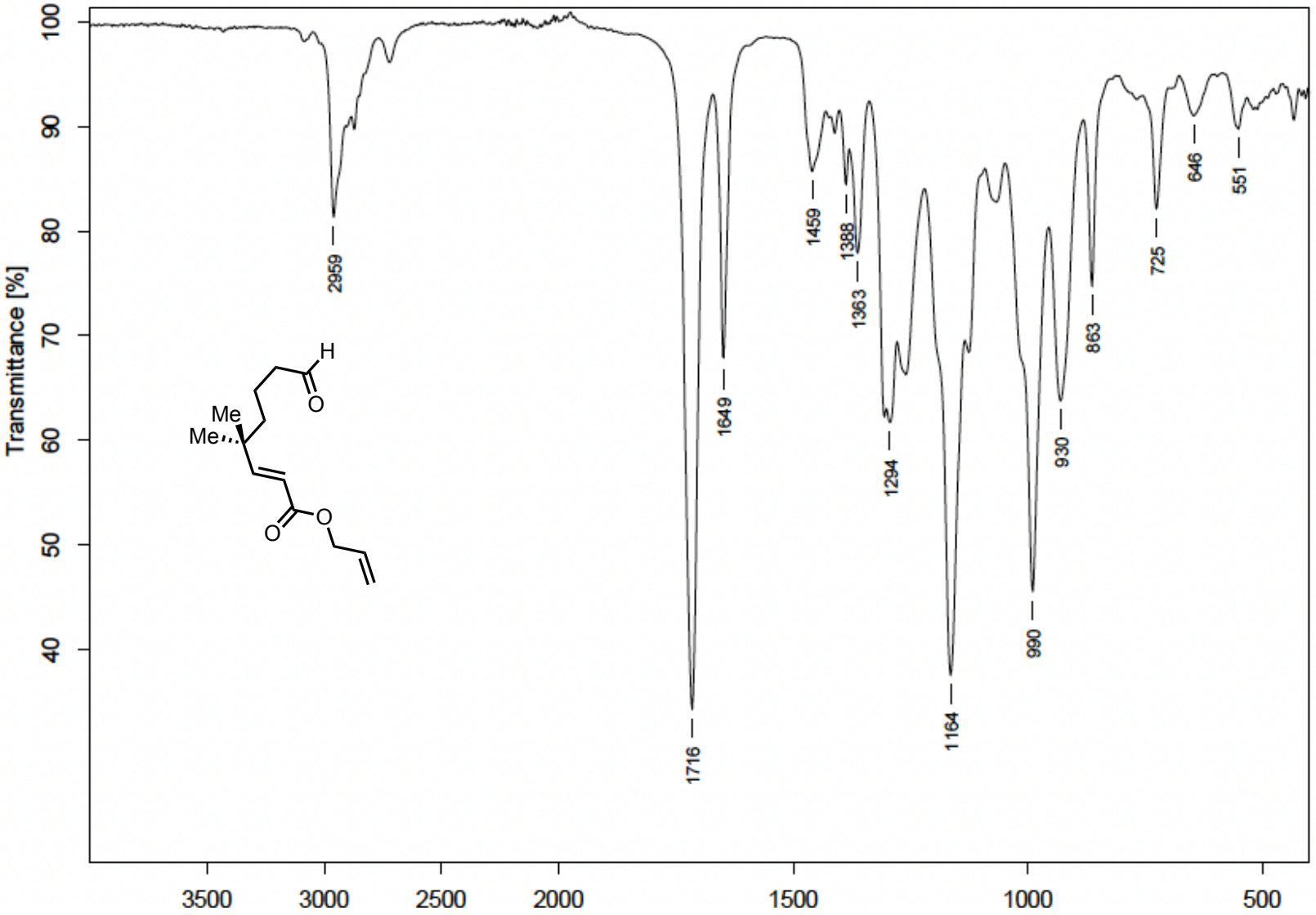

Figure A.50. FTIR (neat) aldehyde **1.58**

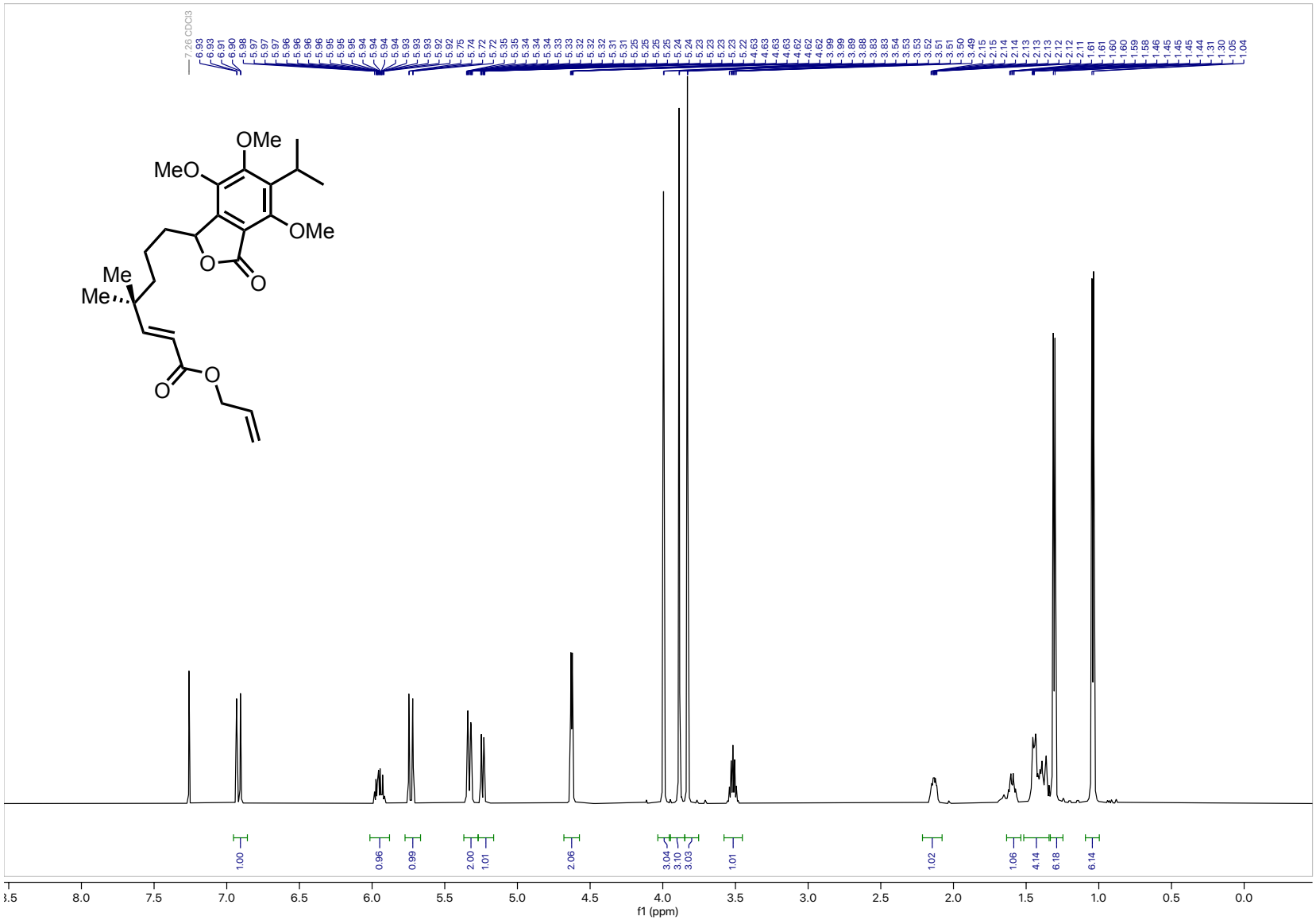

Figure A.51. ^{1}H NMR (600 MHz, $CDCl_3$) lactone **1.57**

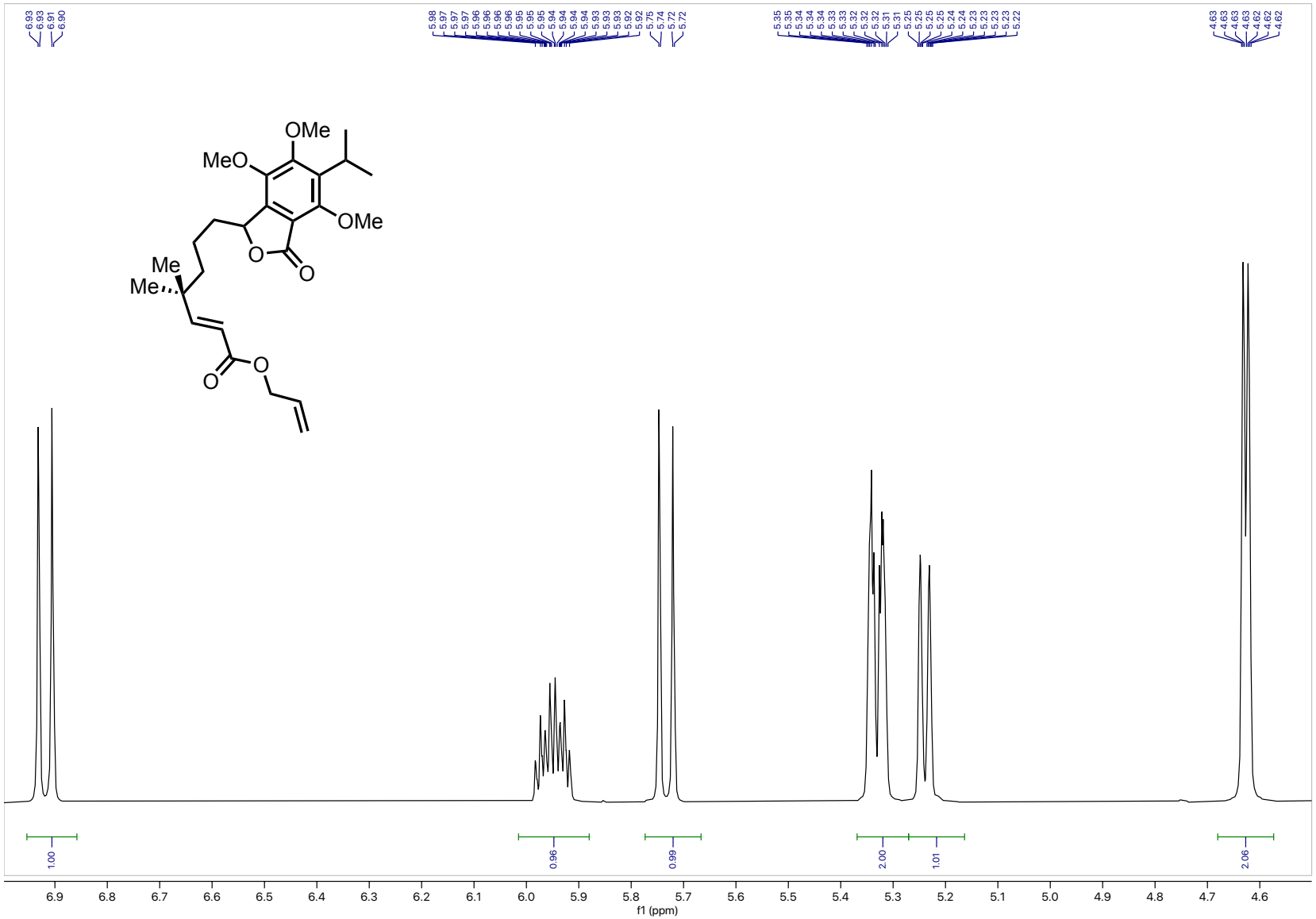

Figure A.52. ^{1}H NMR (600 MHz, $CDCl_3$) lactone **1.57** (7.0 – 4.5 ppm inset)

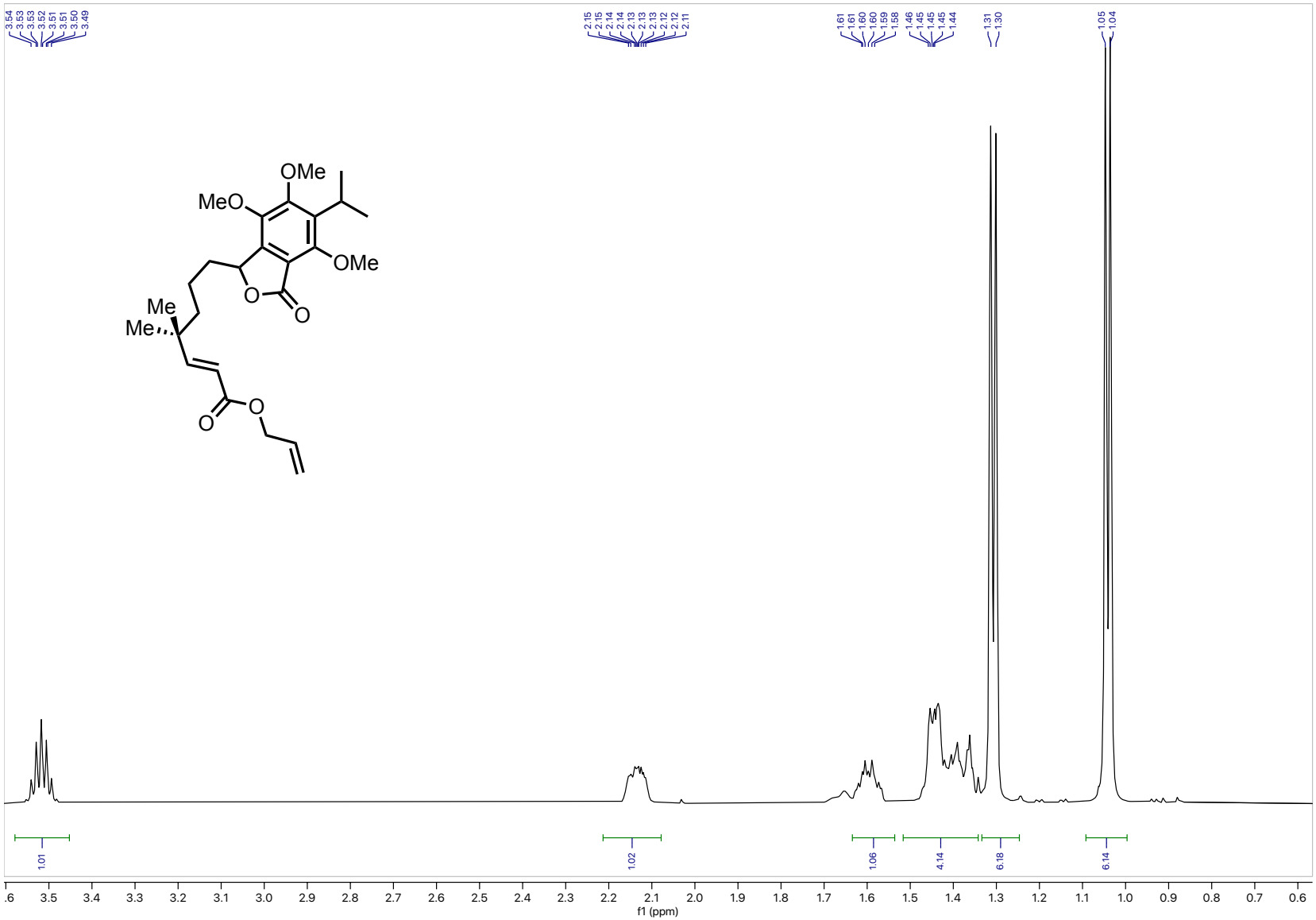

Figure A.53. ^{1}H NMR (600 MHz, $CDCl_3$) lactone **1.57** (3.6 – 0.5 ppm inset)

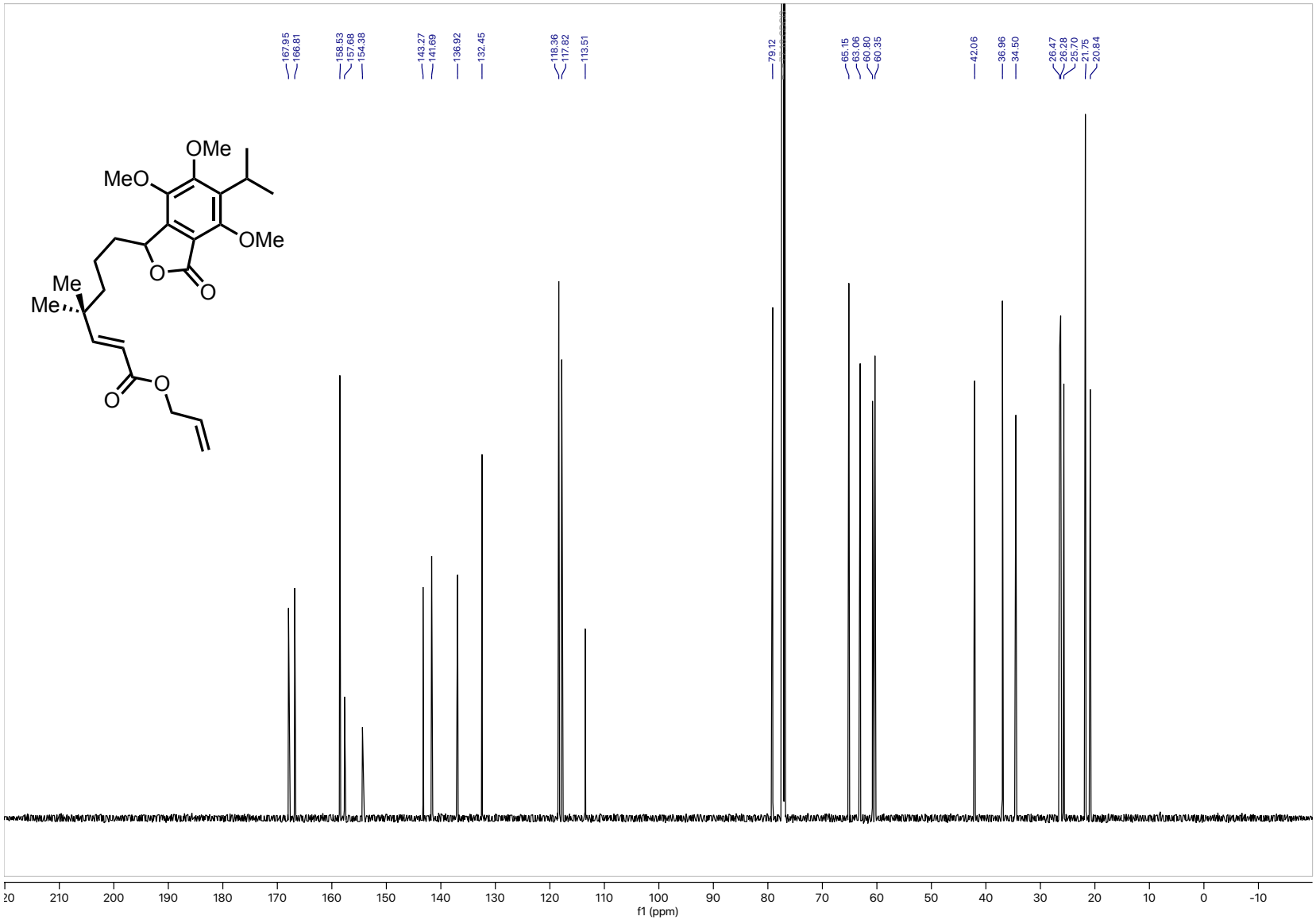

Figure A.54. ^{13}C NMR (151 MHz, $CDCl_3$) lactone **1.57**

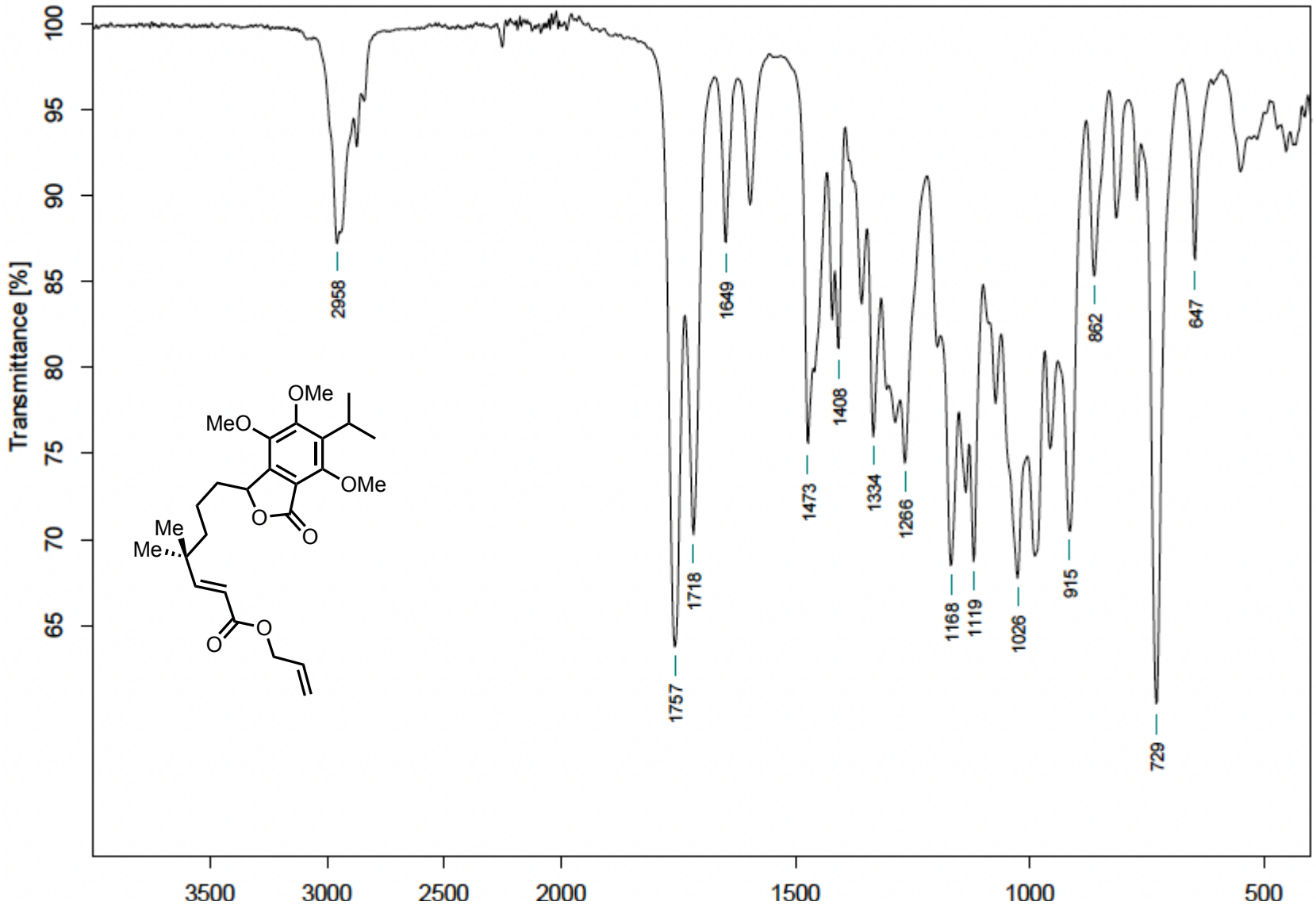

Figure A.55. FTIR (neat) lactone **1.57**

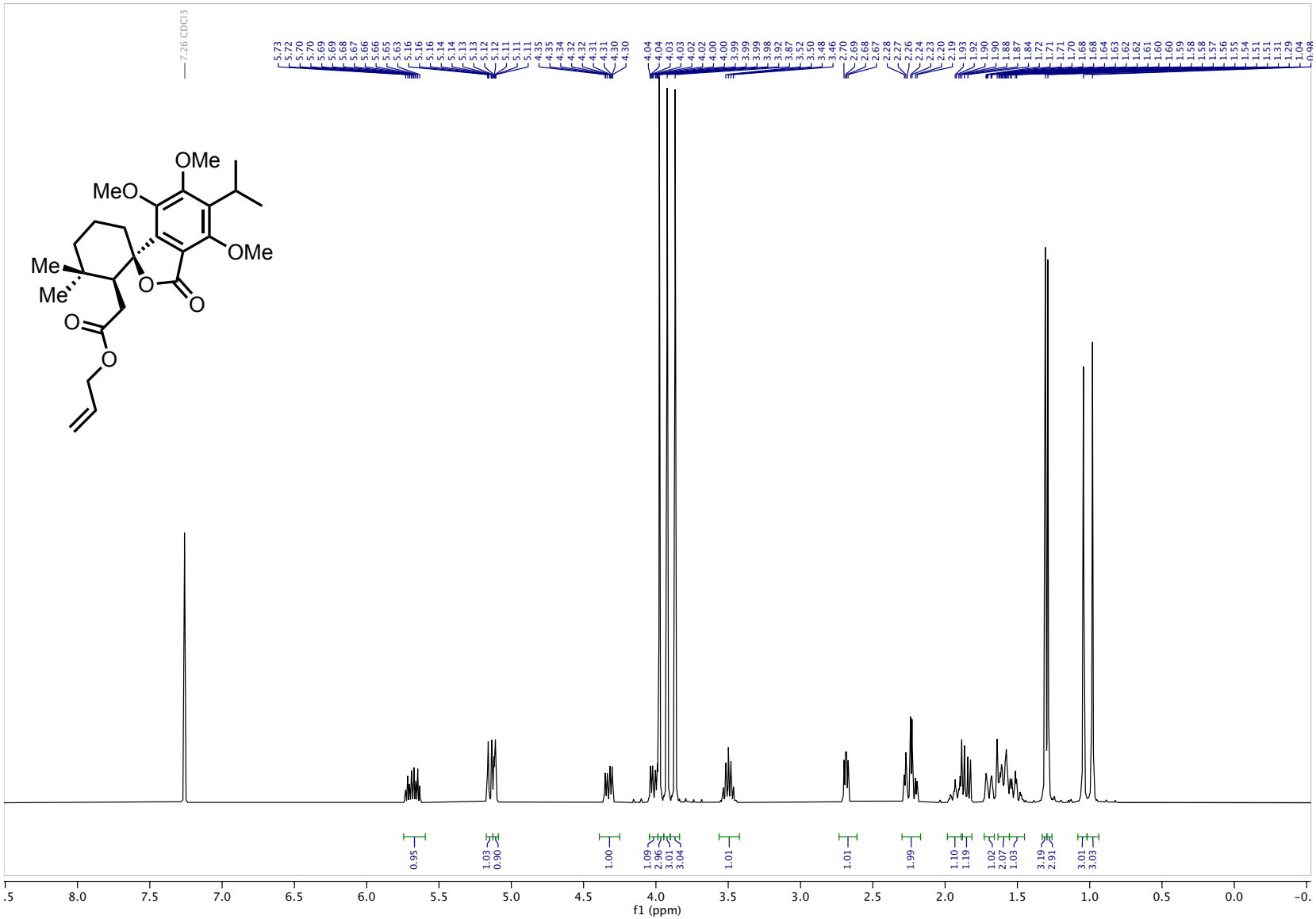

Figure A.56. ^{1}H NMR (400 MHz, $CDCl_3$) spirolactone **1.56**

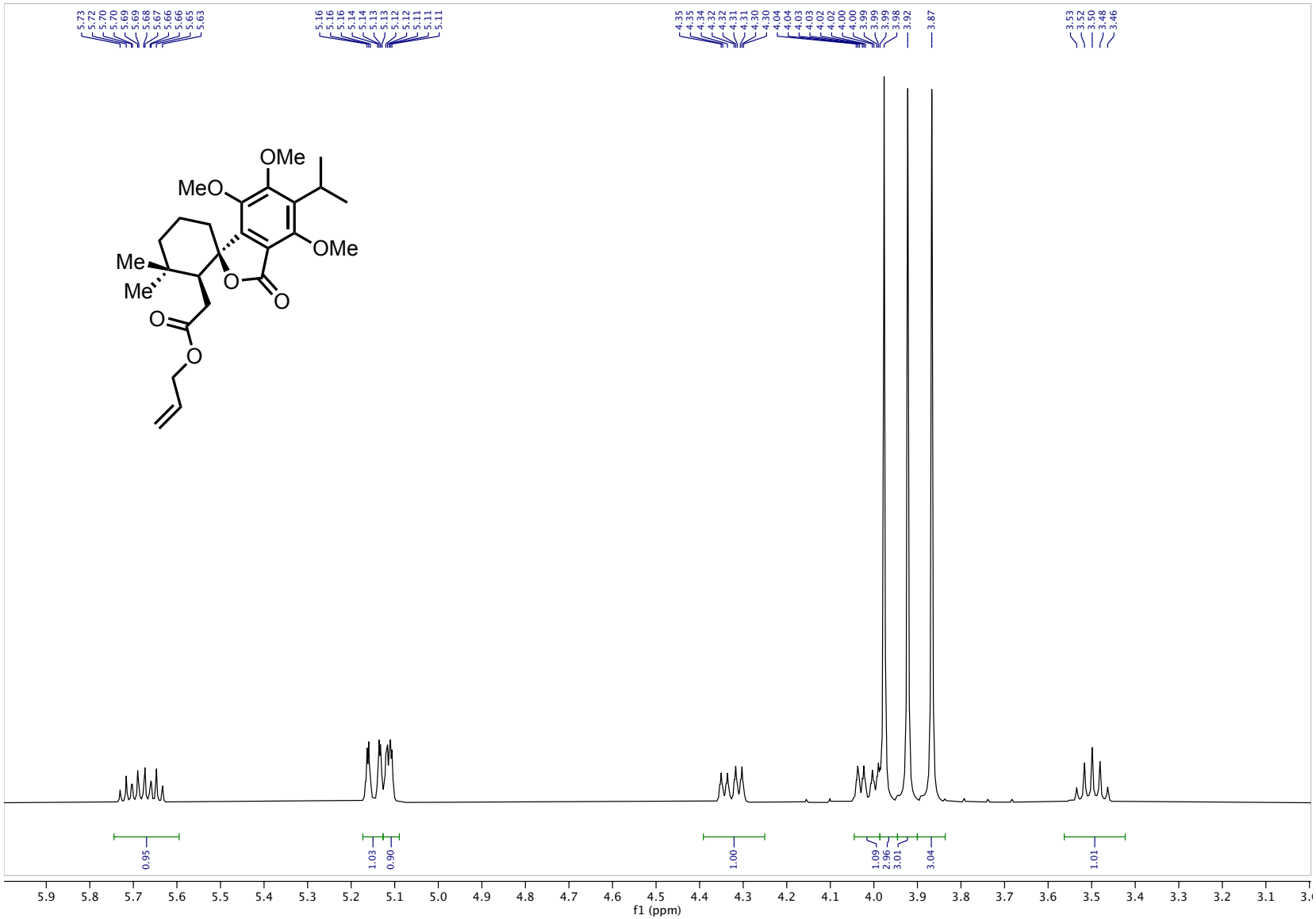

Figure A.57. ^{1}H NMR (400 MHz, $CDCl_3$) spirolactone **1.56** (6.0 – 3.0 ppm inset)

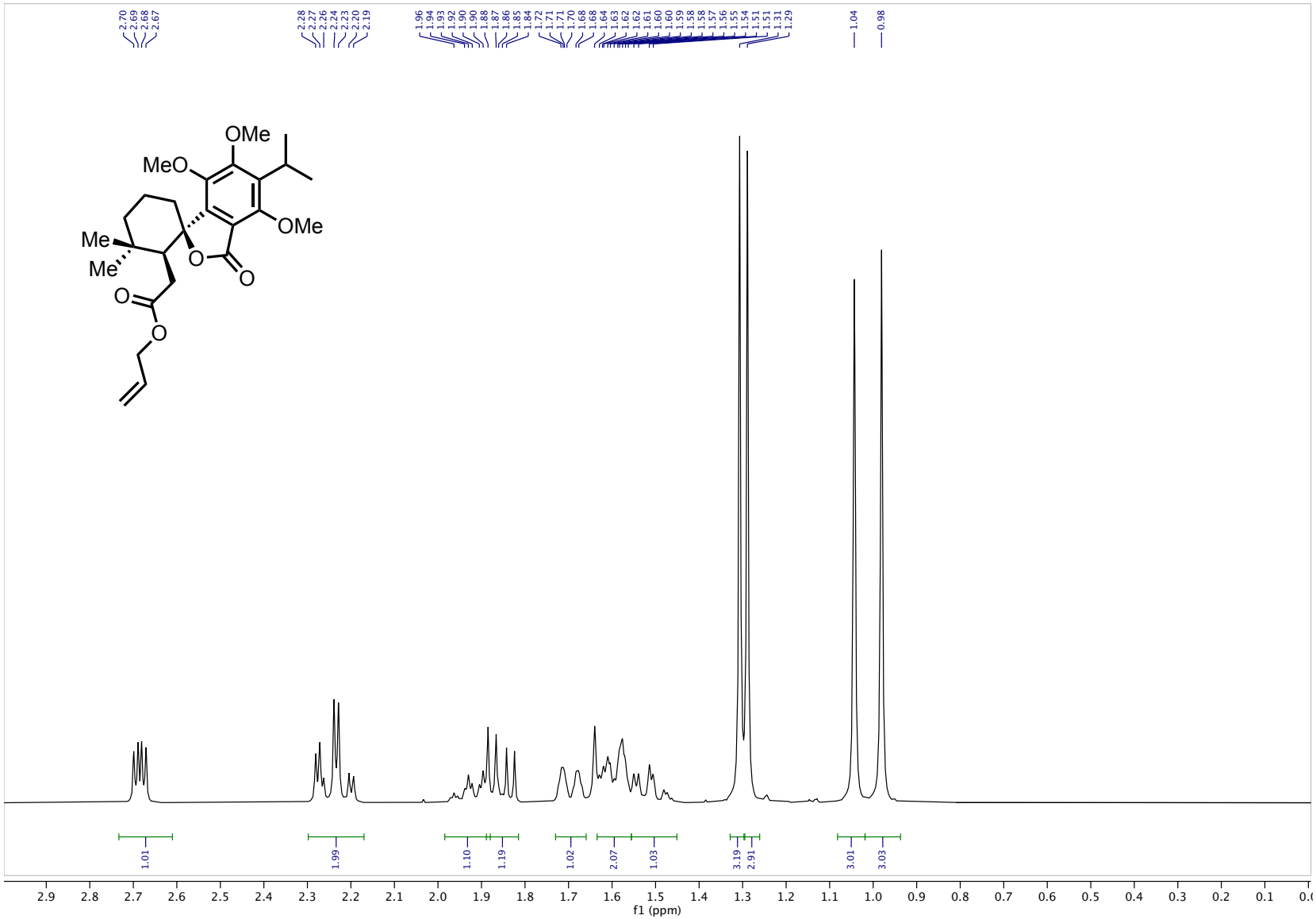

Figure A.58. ^{1}H NMR (400 MHz, $CDCl_3$) spirolactone **1.56** (3.0 – 0 ppm inset)

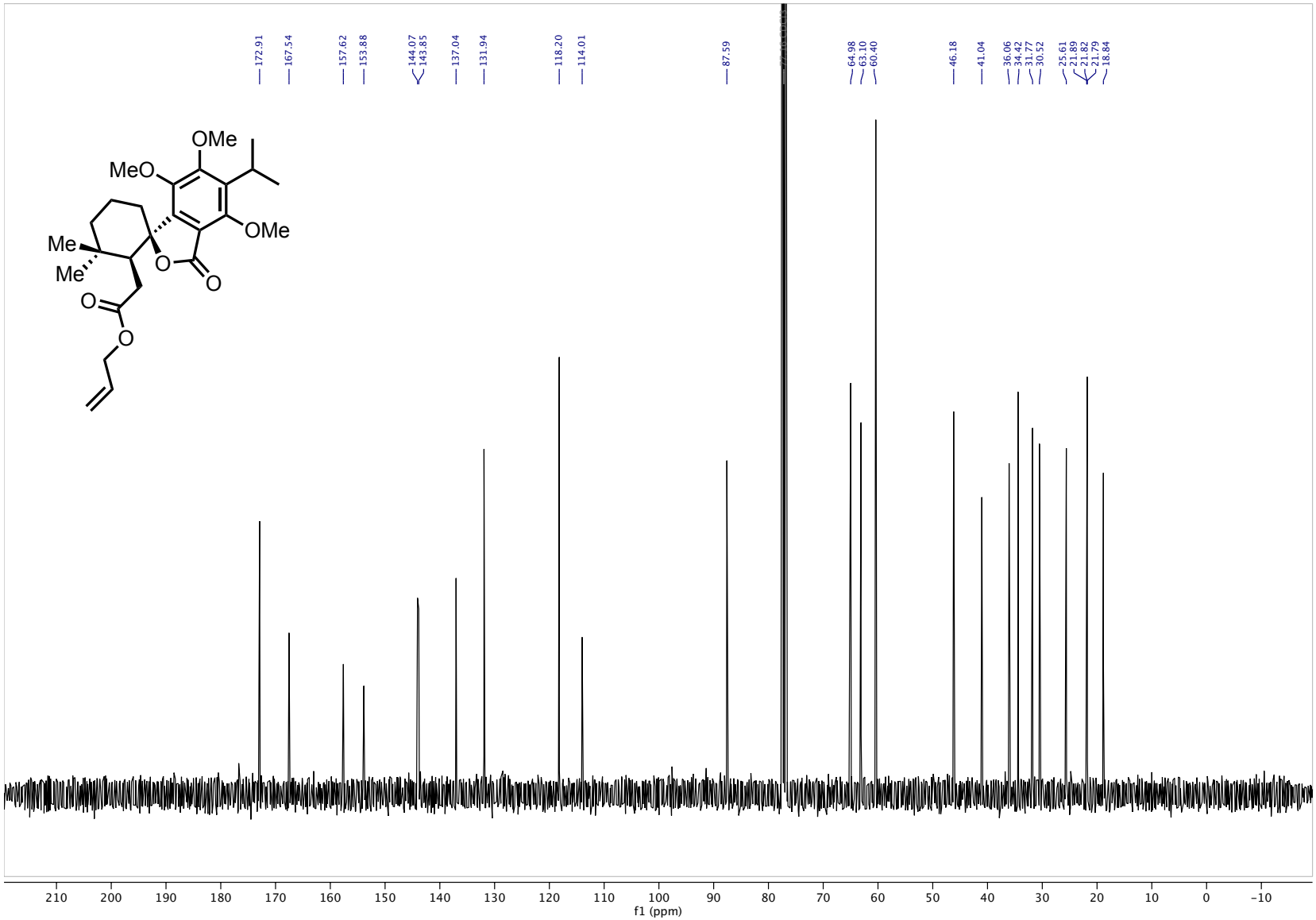

Figure A.59. ^{13}C NMR (101 MHz, $CDCl_3$) spirolactone **1.56**

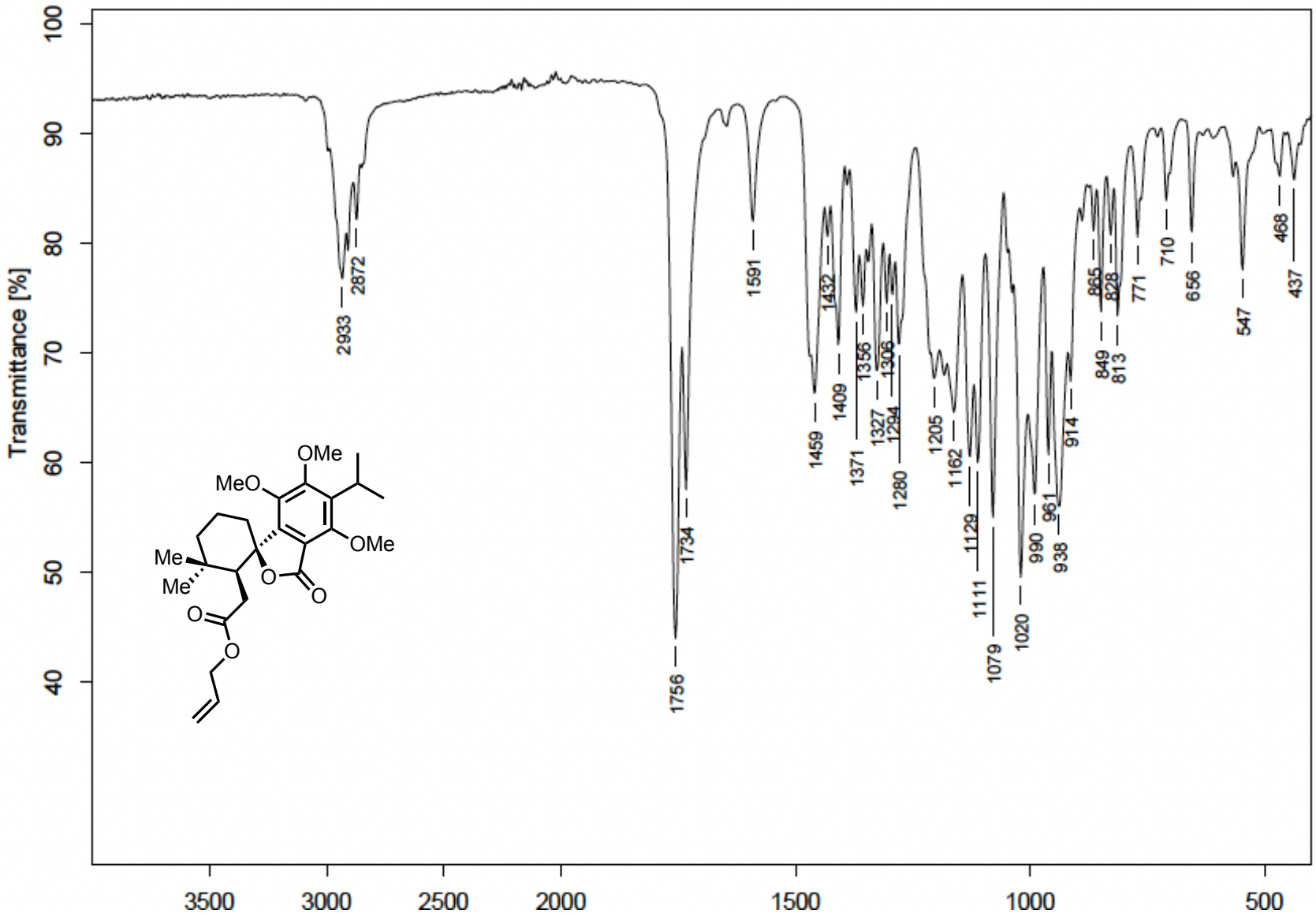

Figure A.60. FTIR (thin film) spirolactone **1.56**

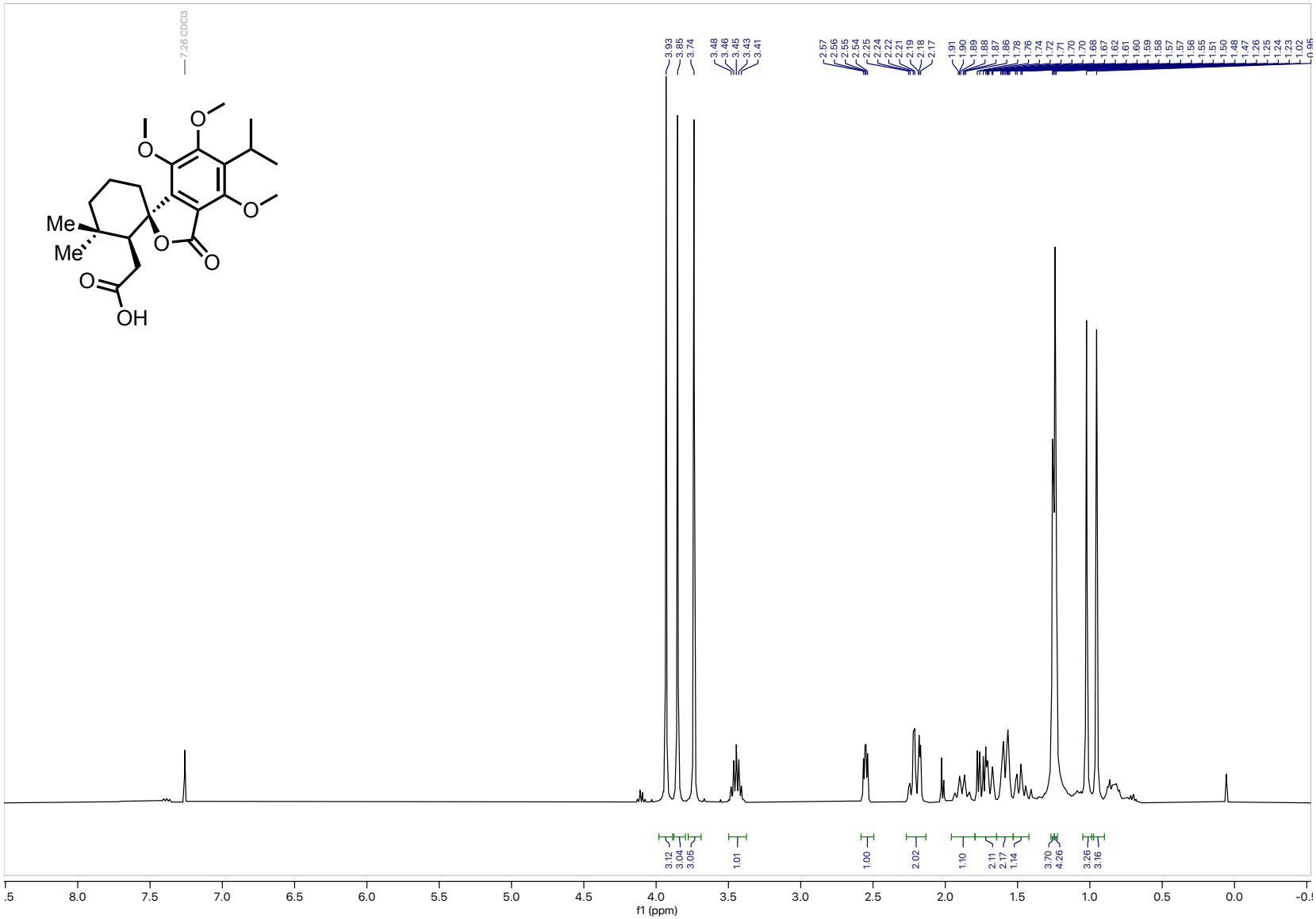

Figure A.61. ^{1}H NMR (400 MHz, $CDCl_3$) carboxylic acid **1.55**

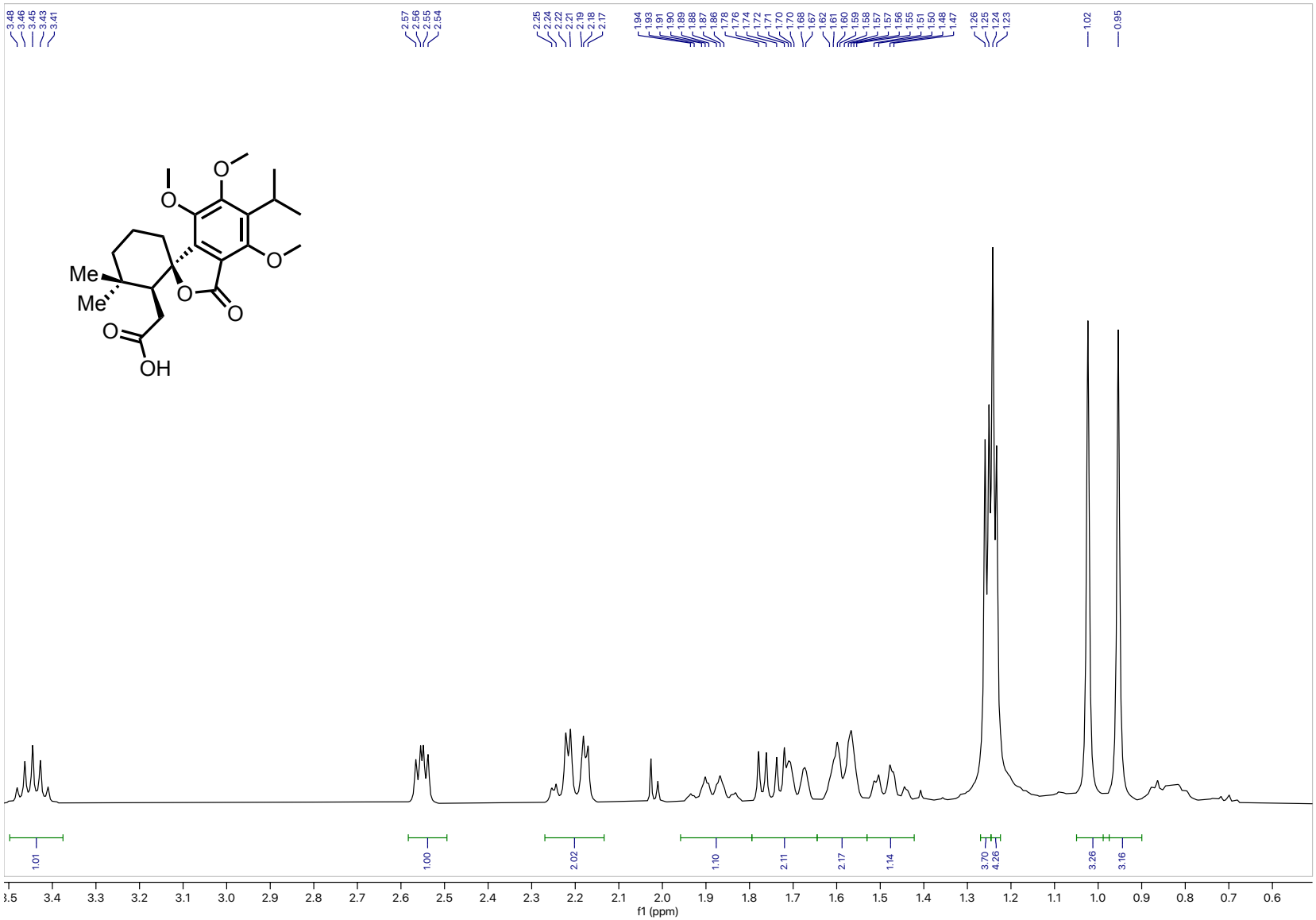

Figure A.62. ^{1}H NMR (400 MHz, $CDCl_3$) carboxylic acid **1.55** (3.5 – 0.5 ppm inset)

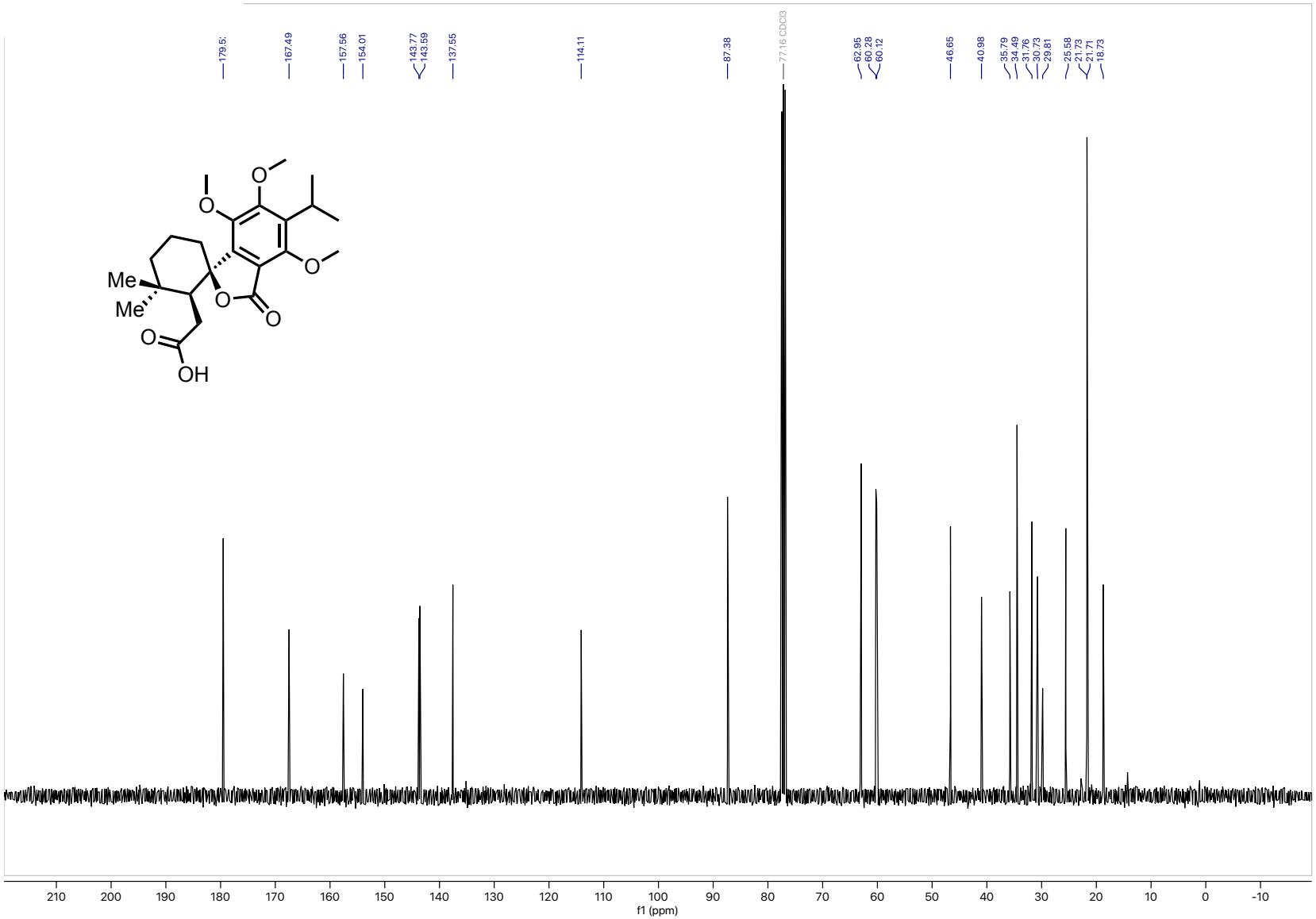

Figure A.63. ^{13}C NMR (101 MHz, $CDCl_3$) carboxylic acid **1.55**

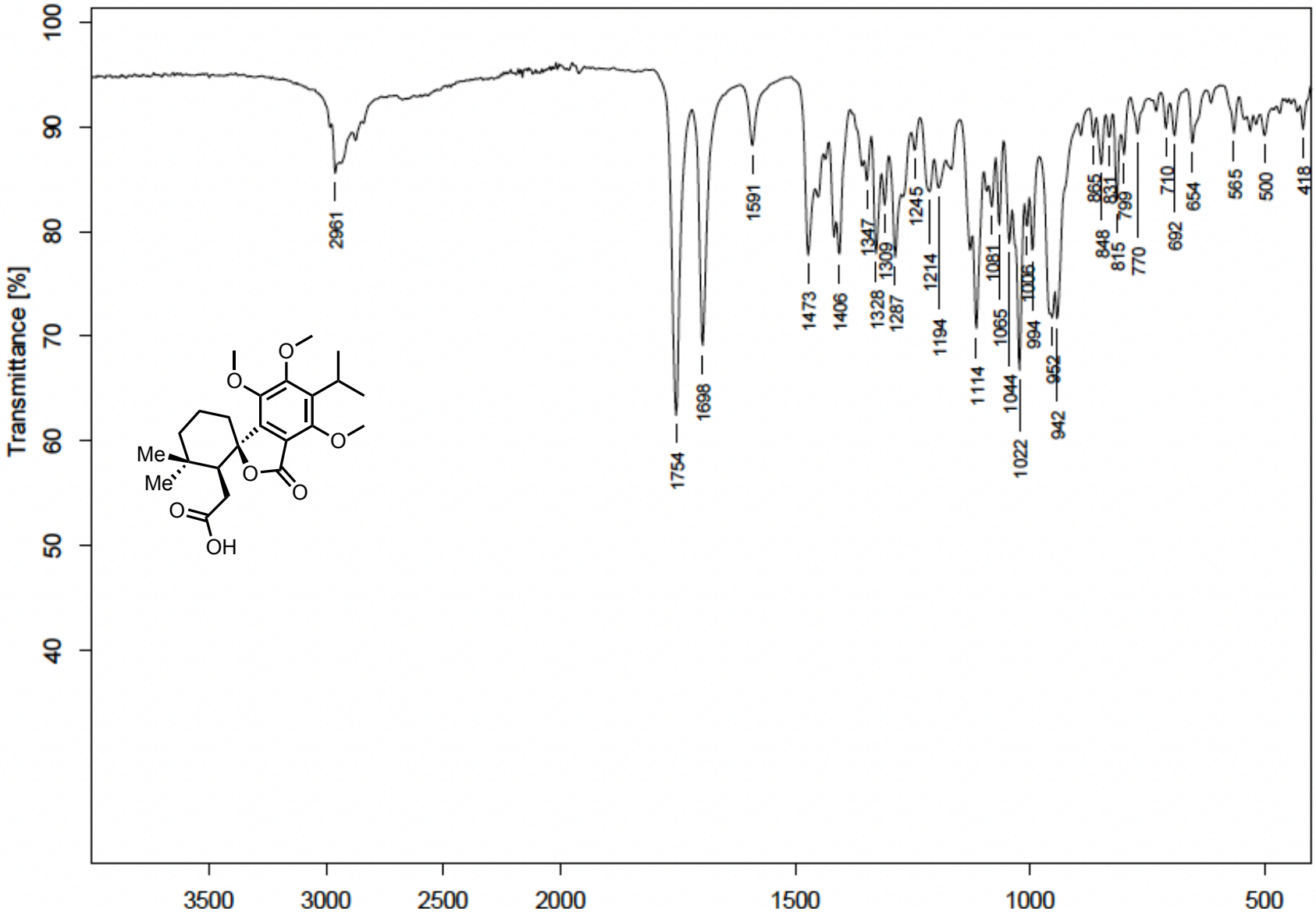

Figure A.64. FTIR (thin film) carboxylic acid **1.55**

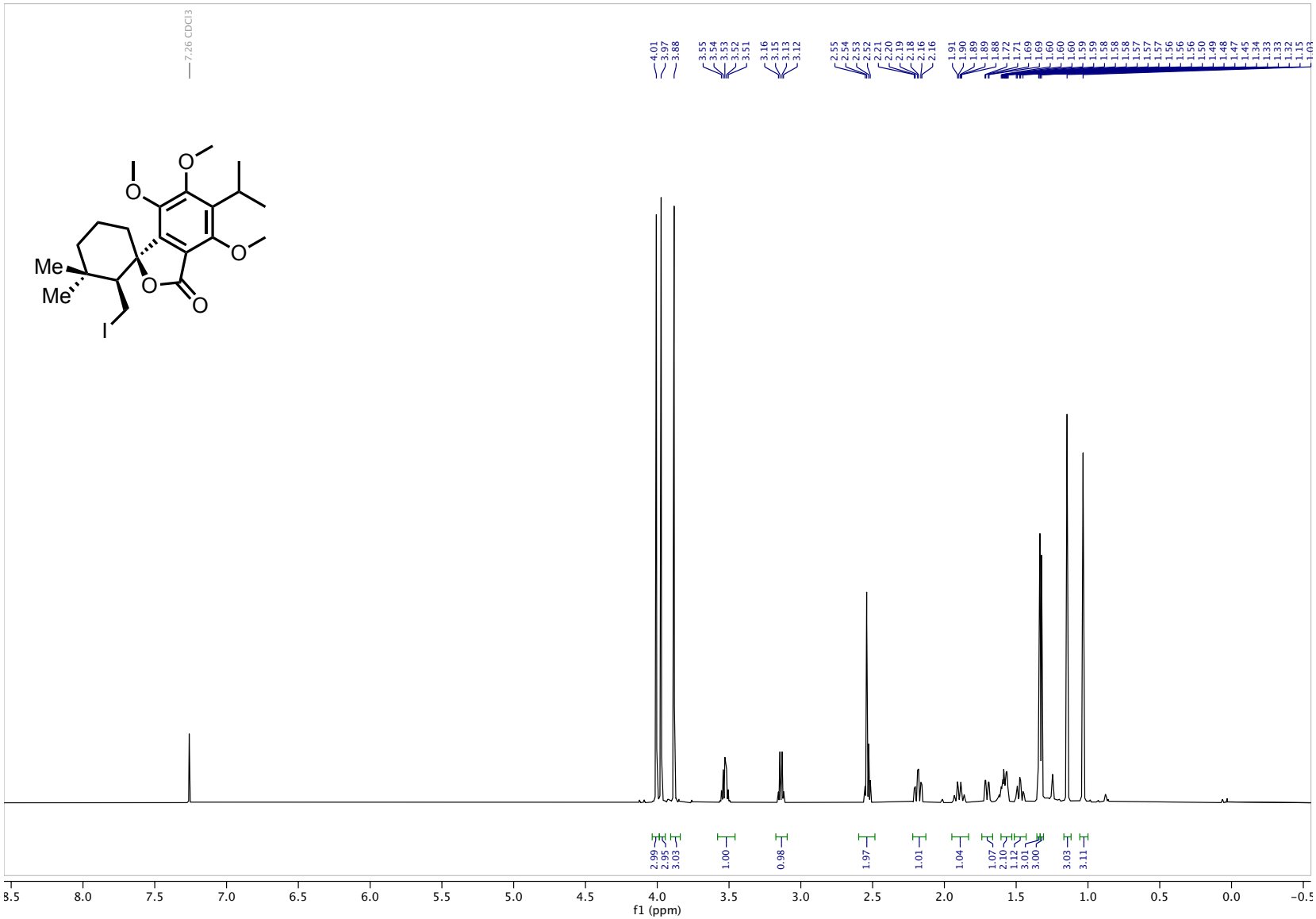

Figure A.65. ^{1}H NMR (600 MHz, $CDCl_3$) for iodide **1.54**

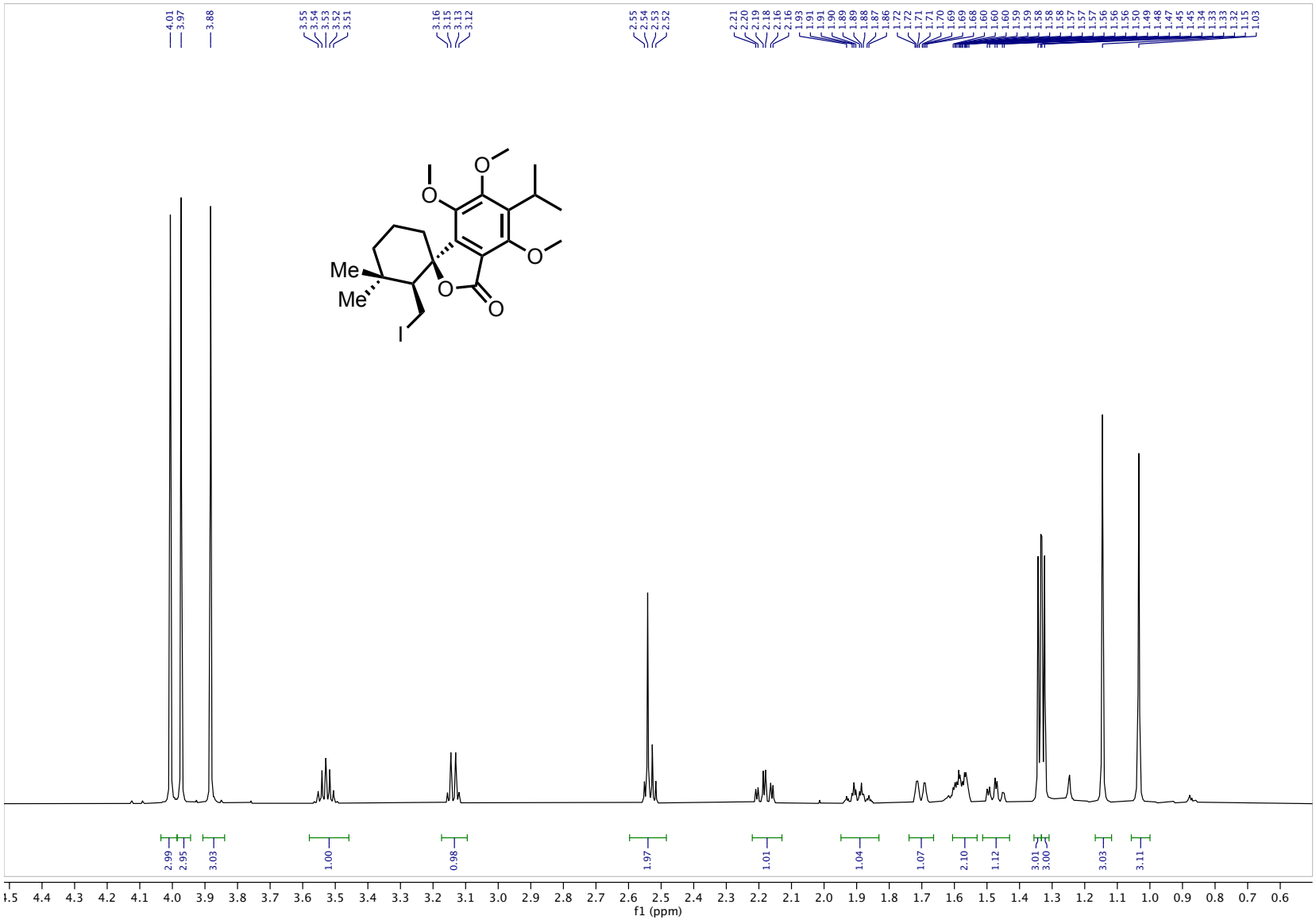

Figure A.66. ^{1}H NMR (600 MHz, $CDCl_3$) iodide **1.54** (4.5 – 0.5 ppm inset)

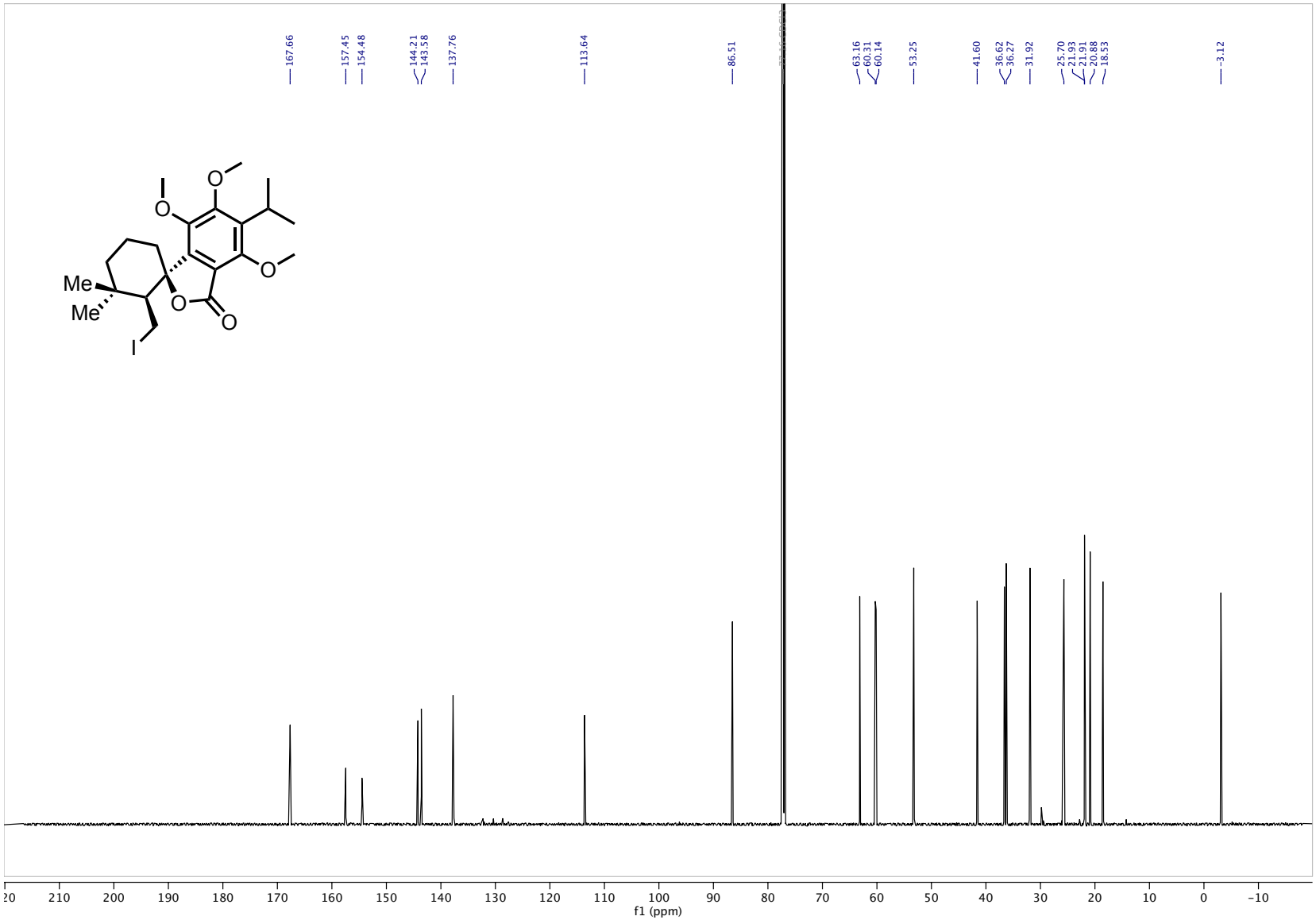

Figure A.67. ^{13}C NMR (151 MHz, $CDCl_3$) iodide **1.54**

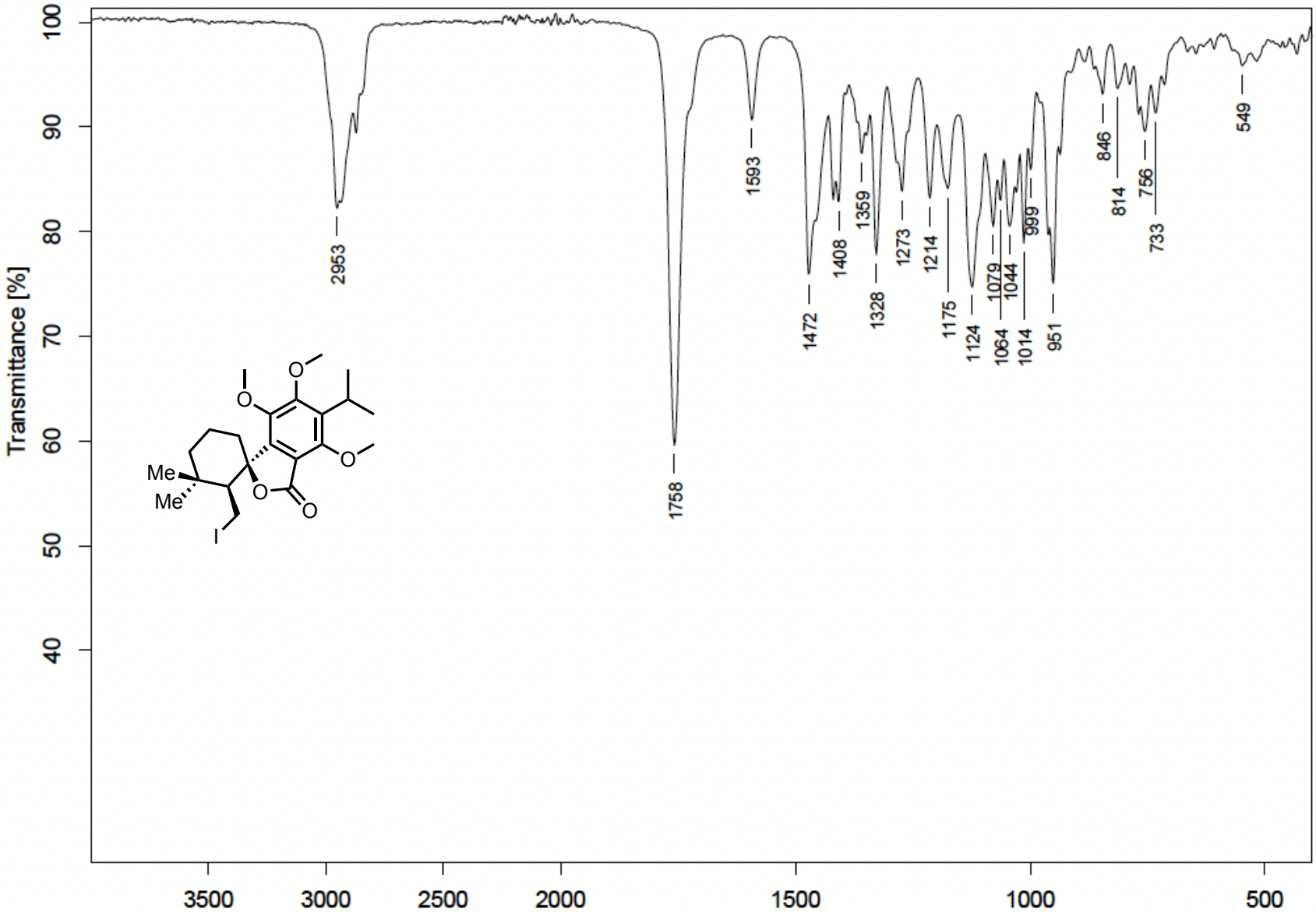

Figure A.68. FTIR (thin film) iodide **1.54**

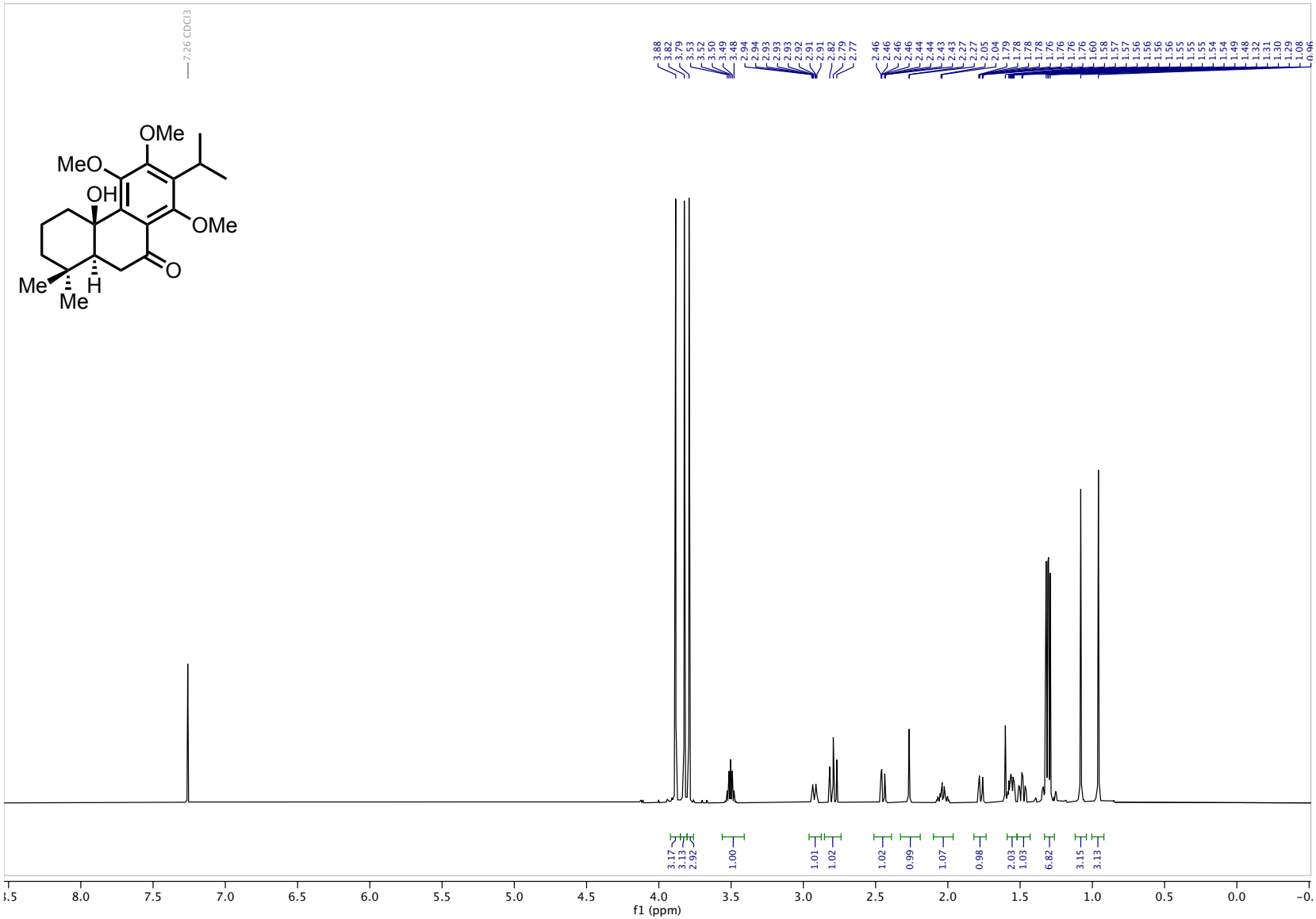

Figure A.69. ^{1}H NMR (600 MHz, $CDCl_3$) ketone **1.52**

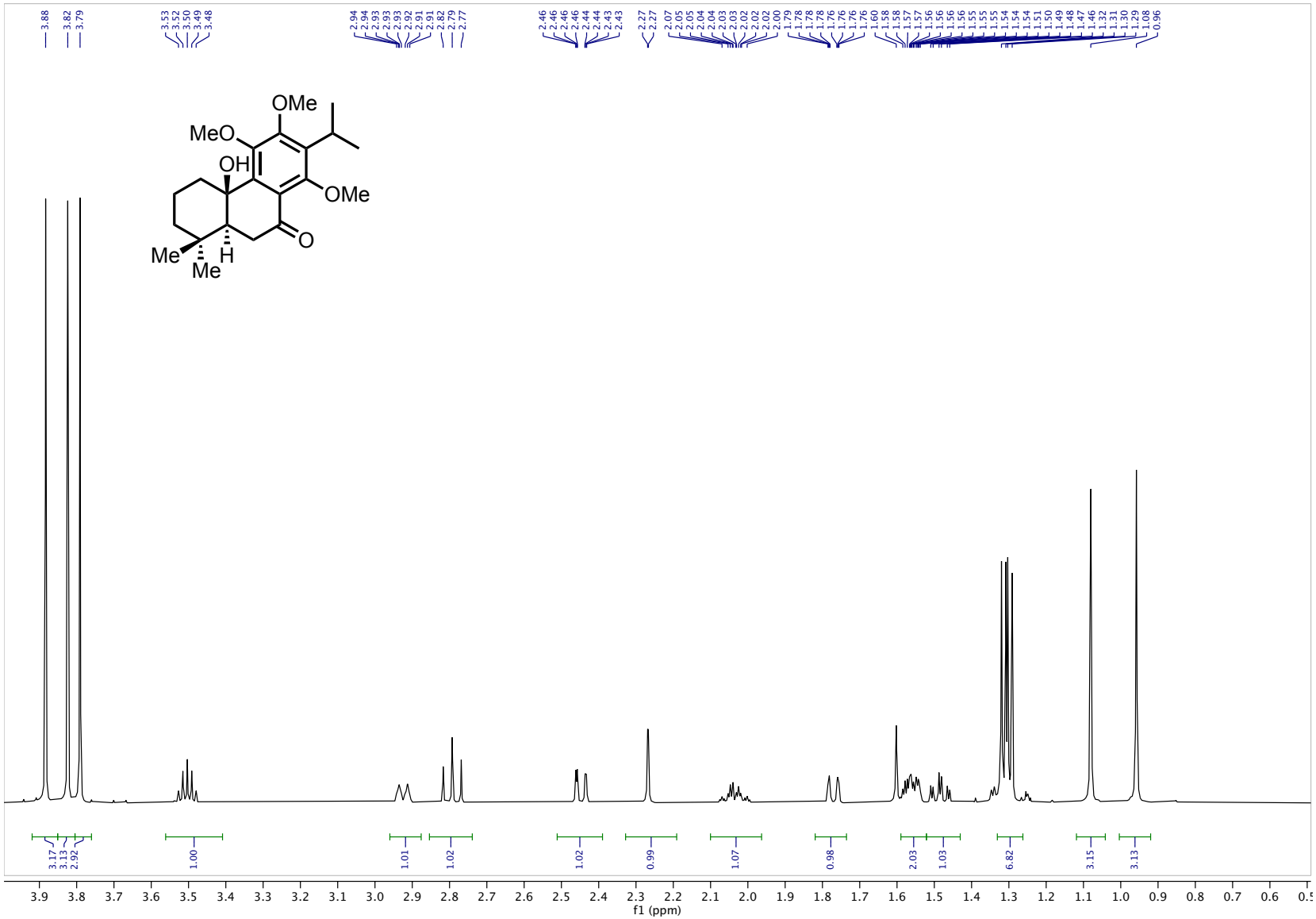

Figure A.70. ^{1}H NMR (600 MHz, $CDCl_3$) ketone **1.52** (4.0 – 0.5 ppm)

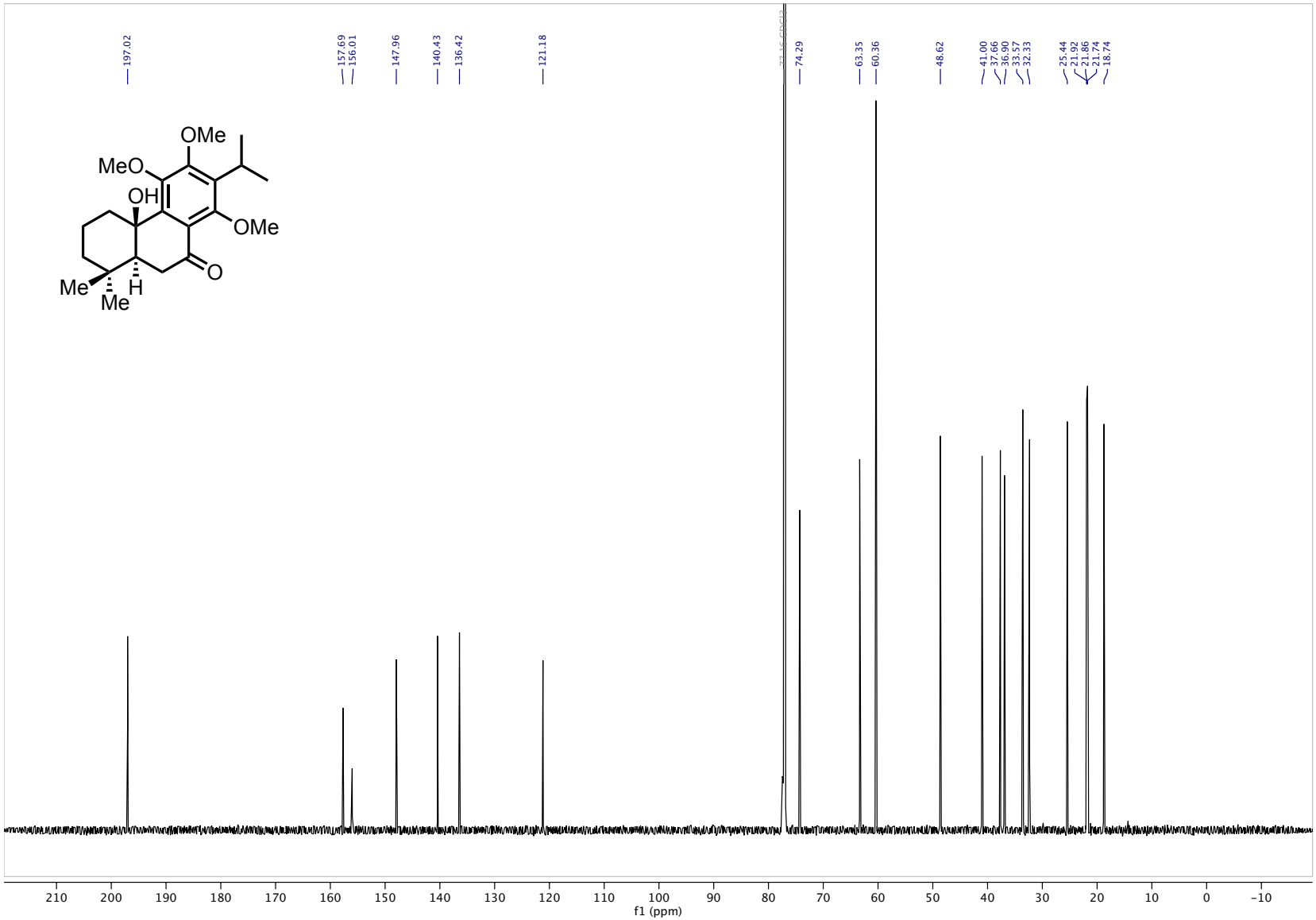

Figure A.71. ^{13}C NMR (151 MHz, $CDCl_3$) ketone **1.52**

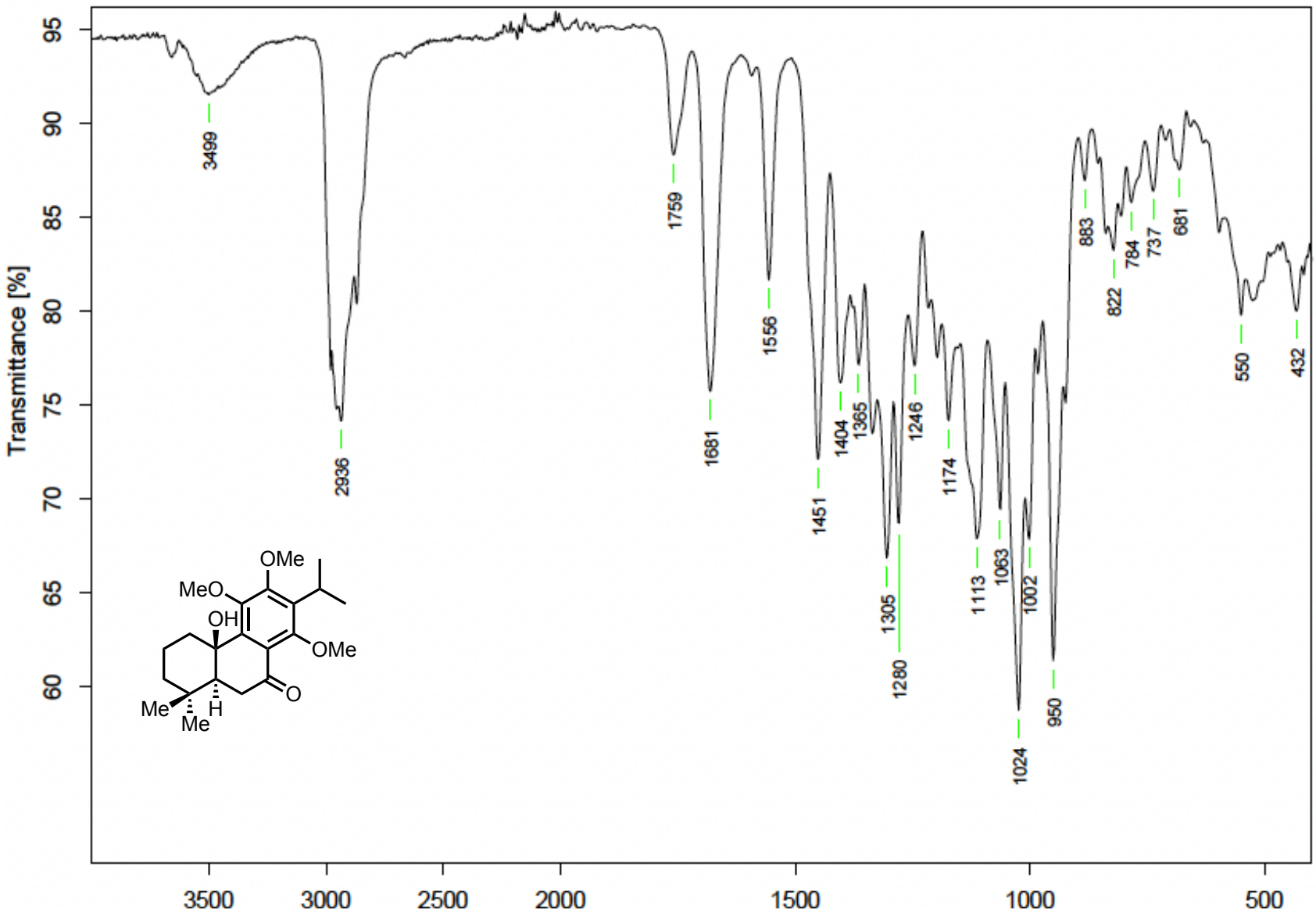

Figure A.72. FTIR (thin film) ketone **1.52**

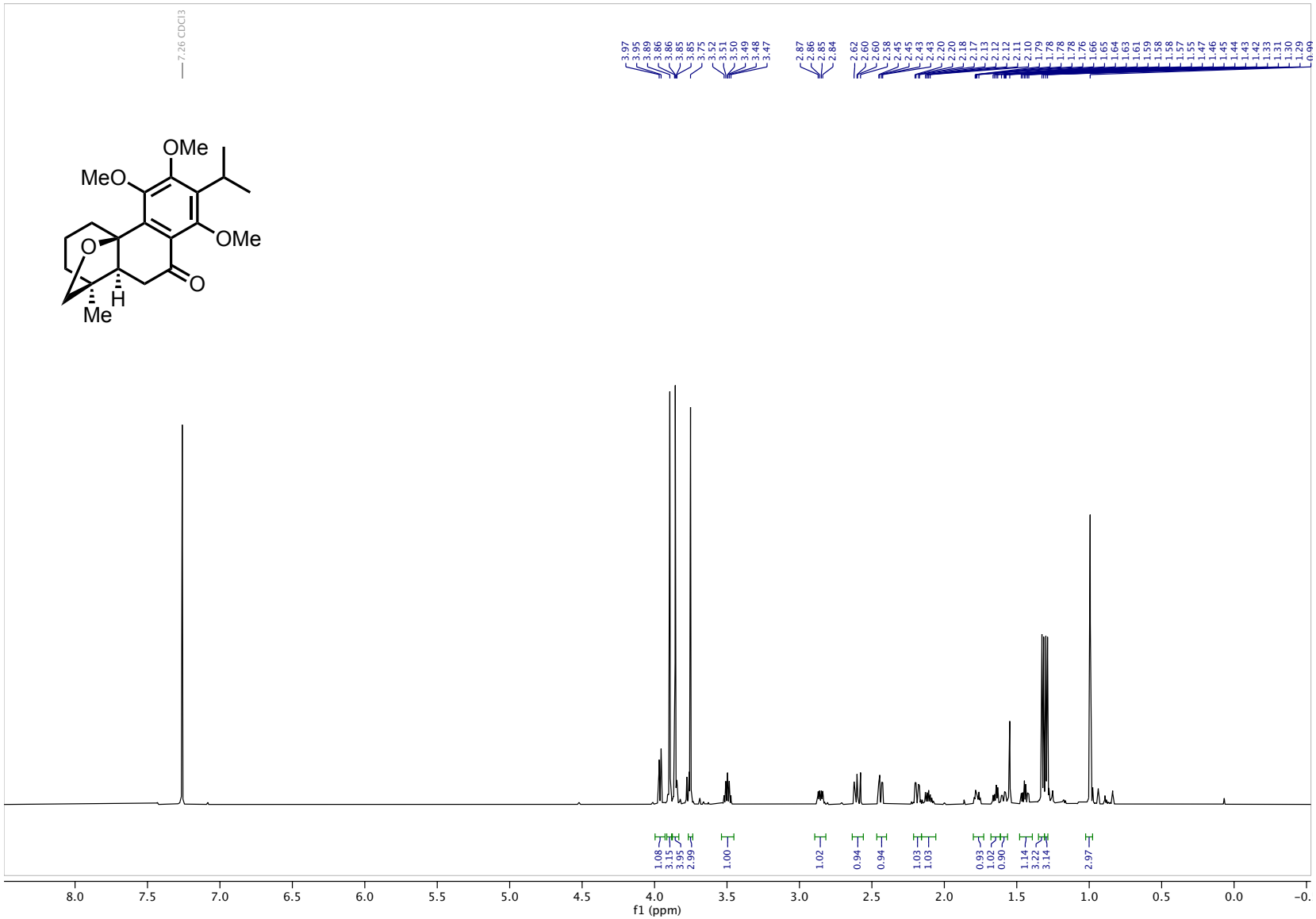

Figure A.73. ^{1}H NMR (600 MHz, $CDCl_3$) tetrahydrofuran **1.29**

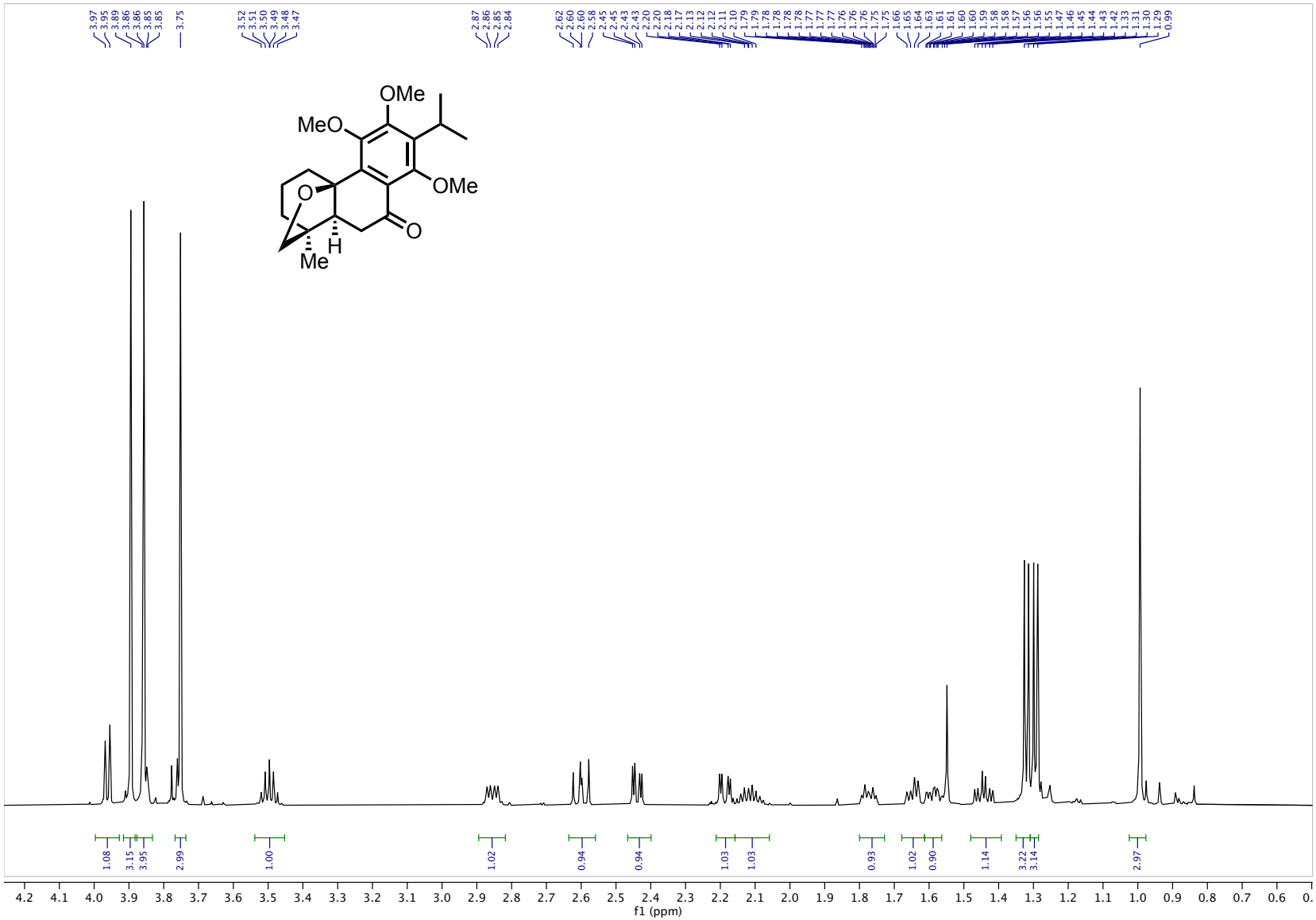

Figure A.74. ^{1}H NMR (600 MHz, $CDCl_3$) tetrahydrofuran **1.29** (4.25 – 0.5 ppm inset)

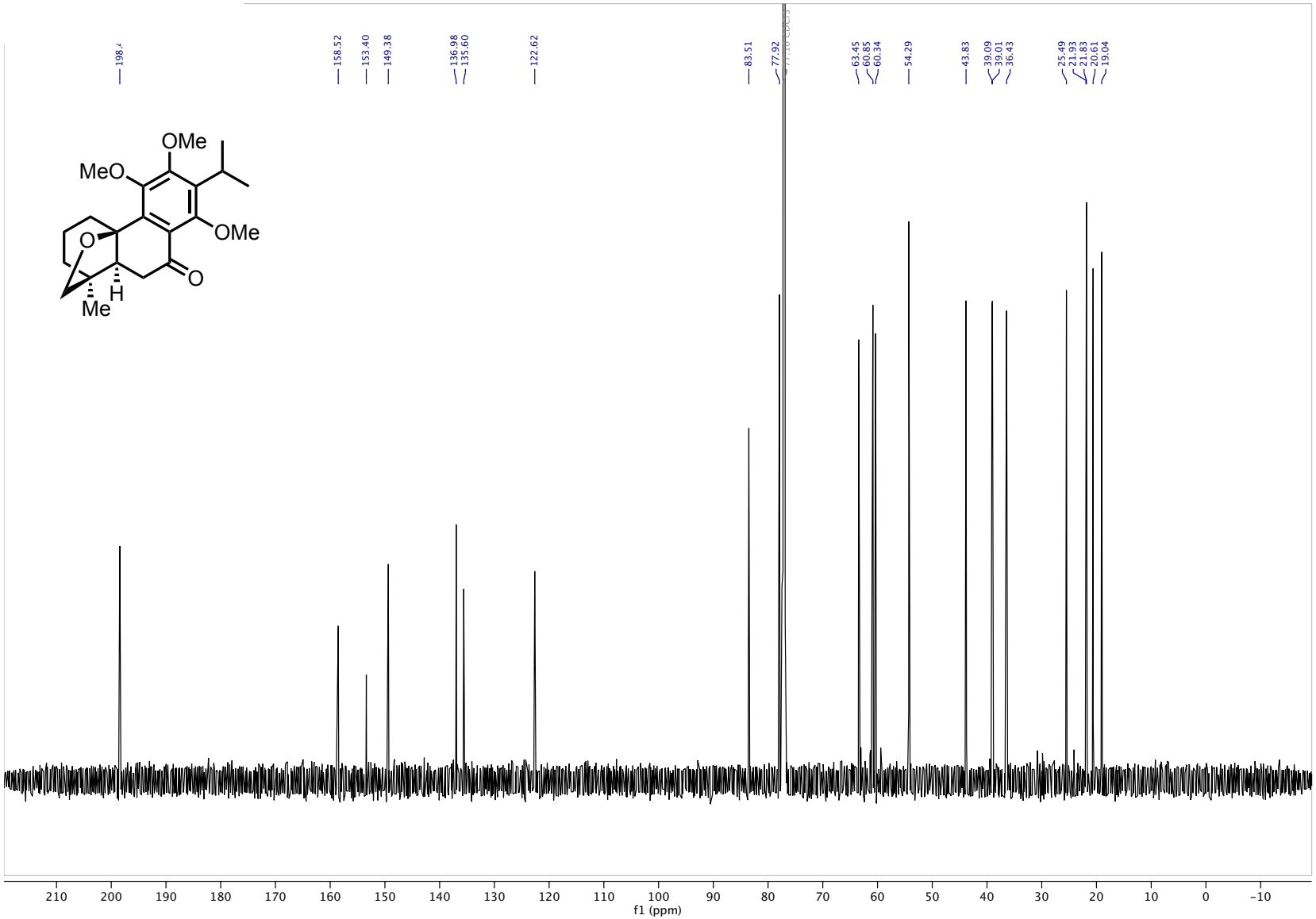

Figure A.75. ^{13}C NMR (151 MHz, $CDCl_3$) tetrahydrofuran **1.29**

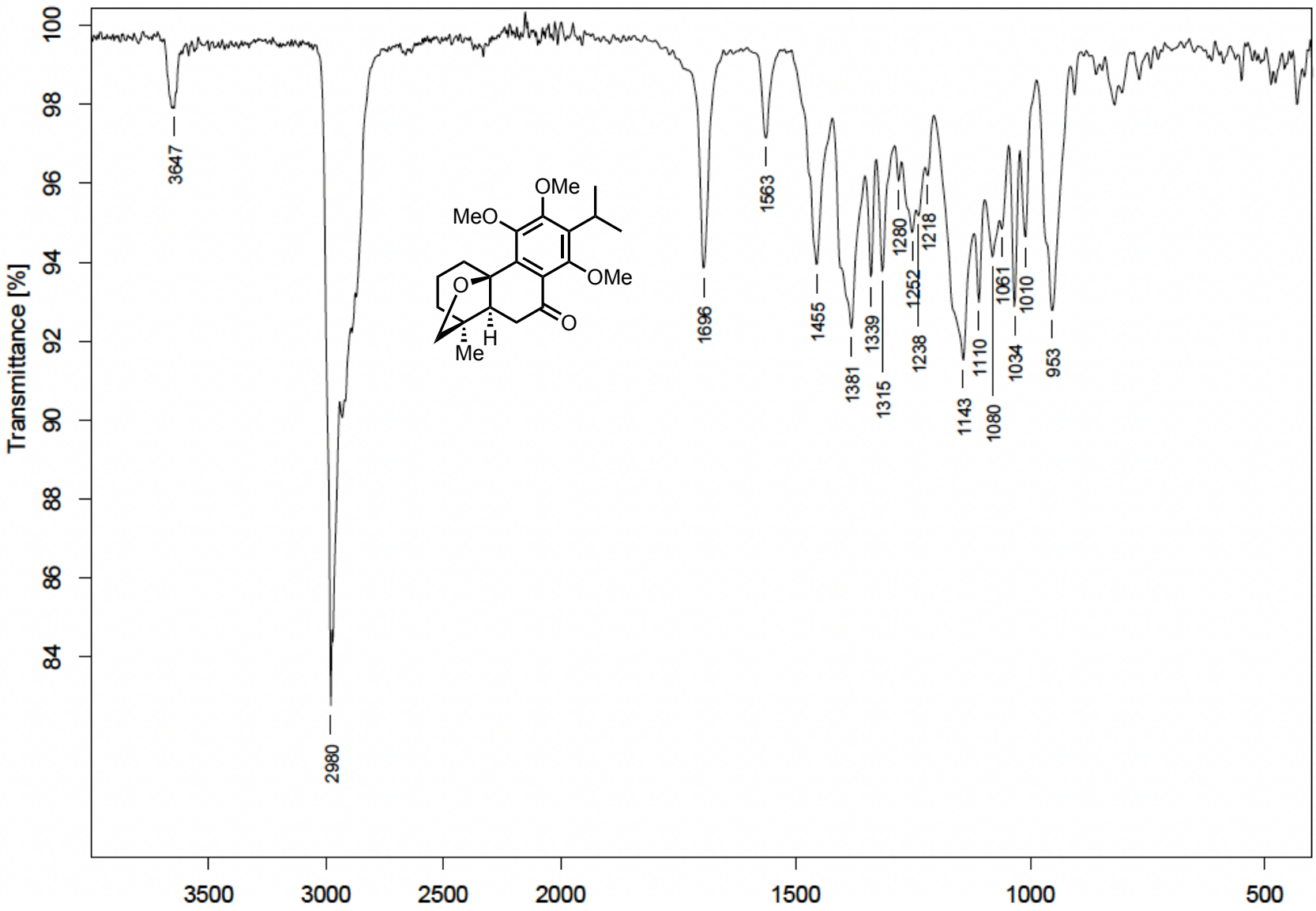

Figure A.76. FTIR (thin film) tetrahydrofuran **1.29**

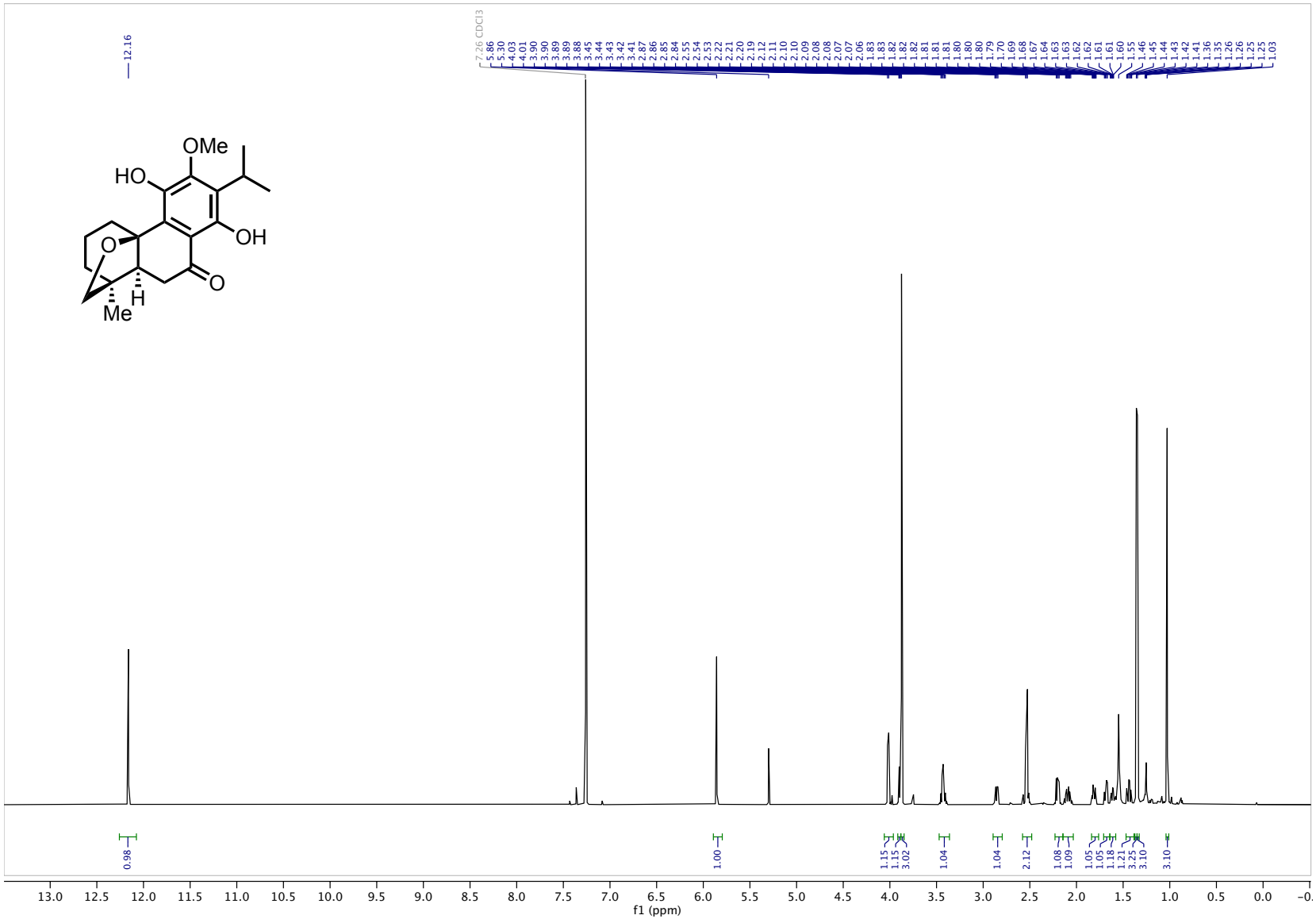

Figure A.77. ^{1}H NMR (600 MHz, $CDCl_3$) dracocephalone A **1.01**

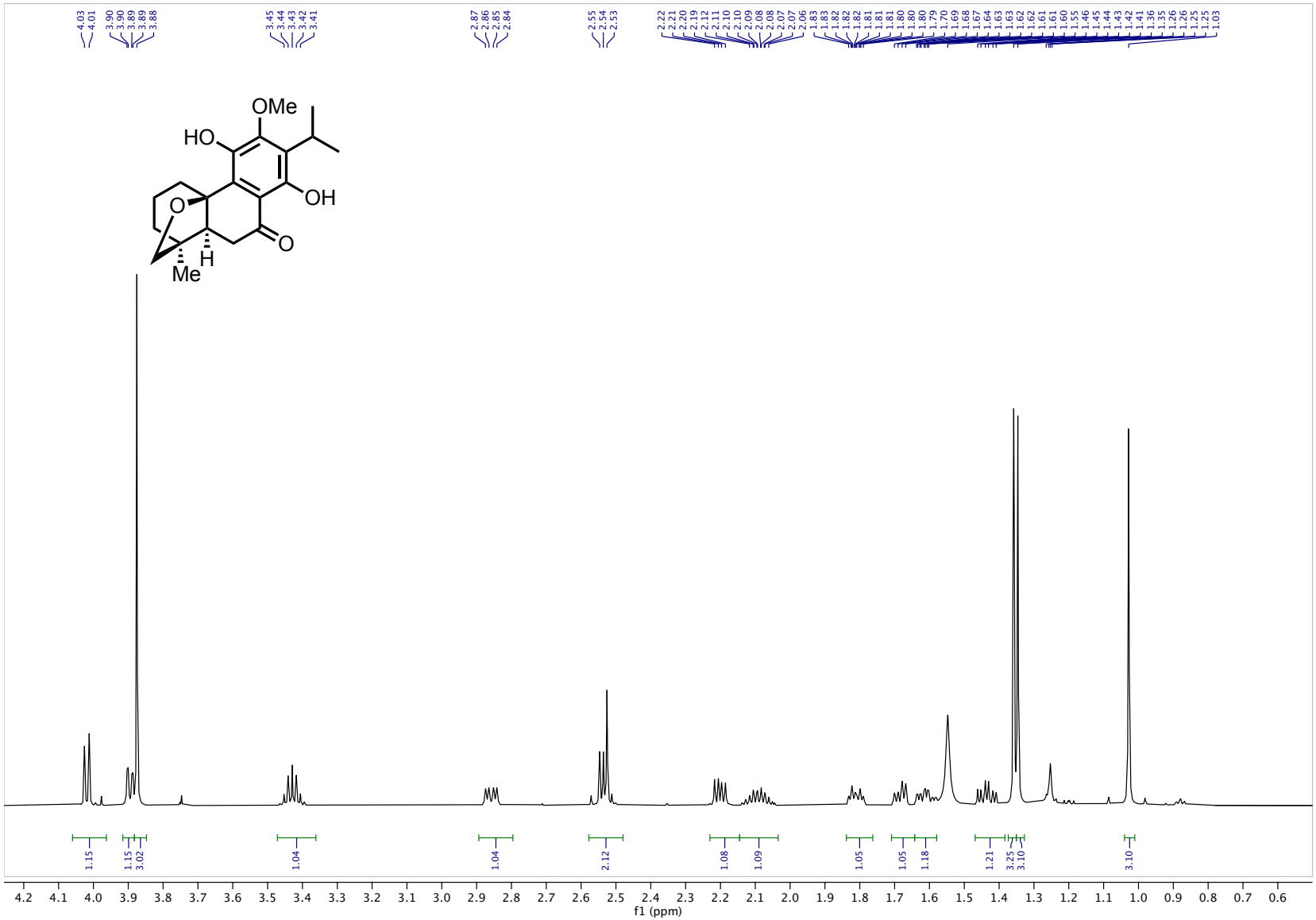

Figure A.78. ^{1}H NMR (600 MHz, $CDCl_3$) dracocephalone A **1.01** (4.25 – 0.5 ppm inset)

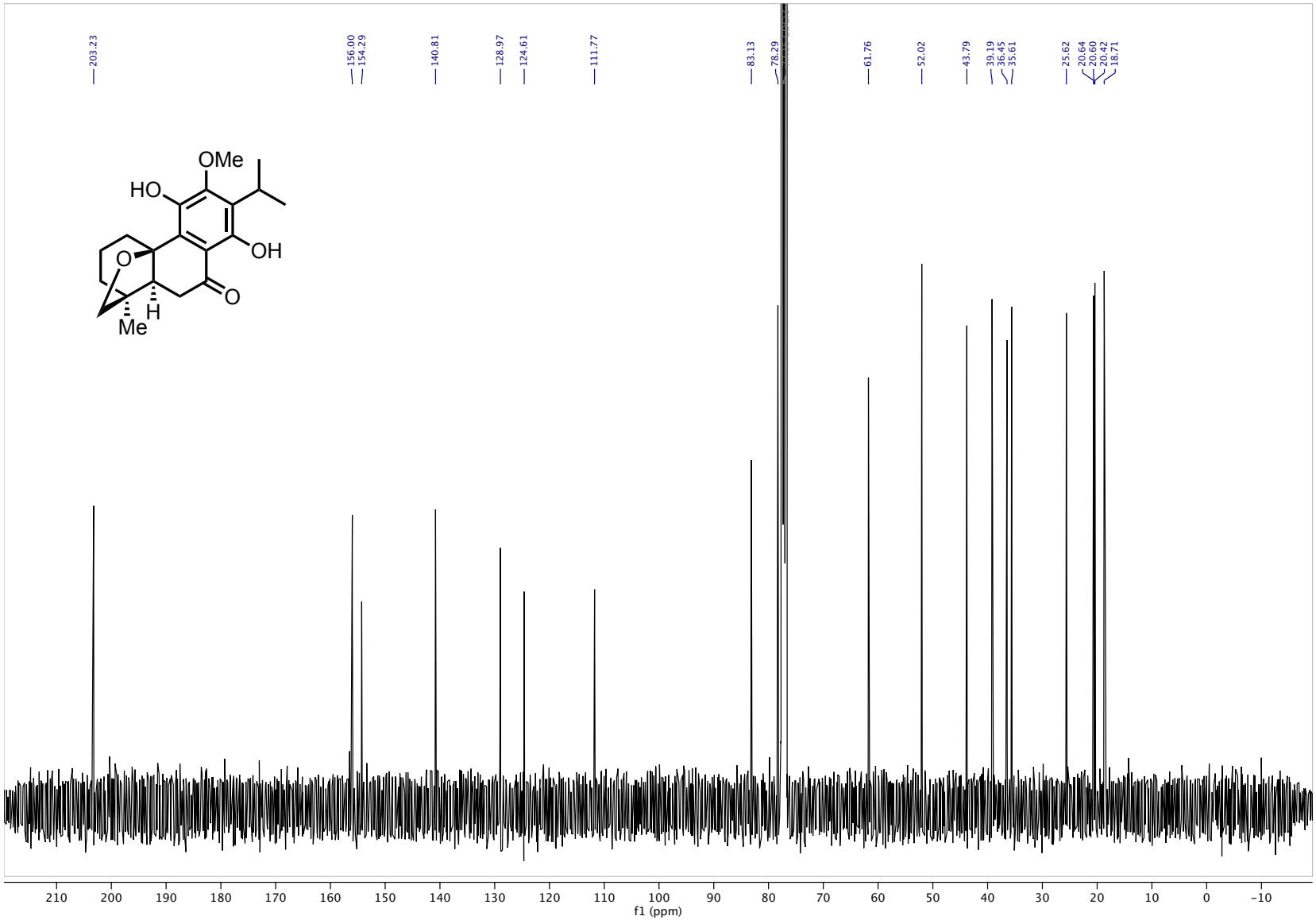

Figure A.79. ^{13}C NMR (151 MHz, $CDCl_3$) dracocephalone A **1.01**

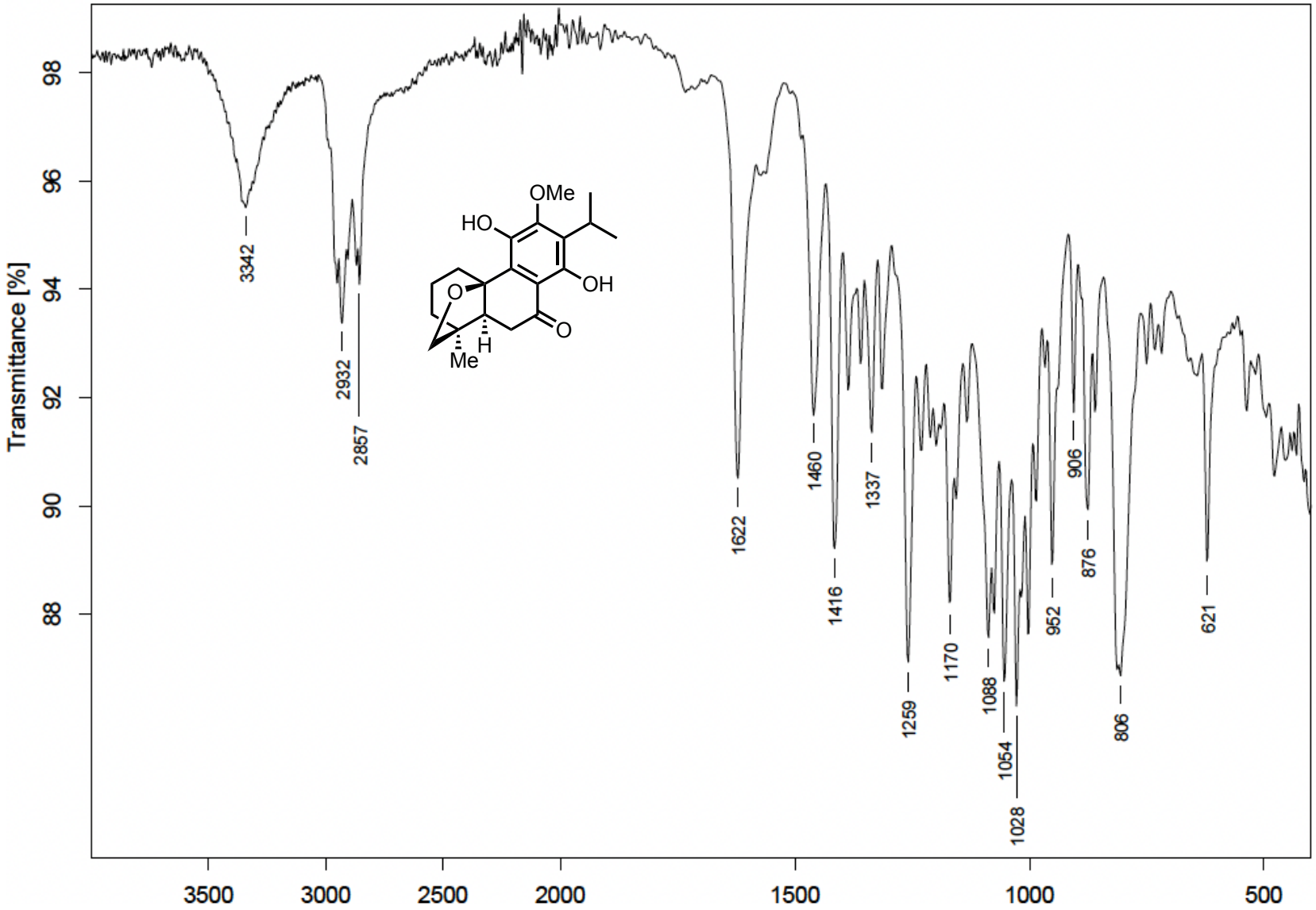

Figure A.80. FTIR (thin film) dracocephalone A **1.01**

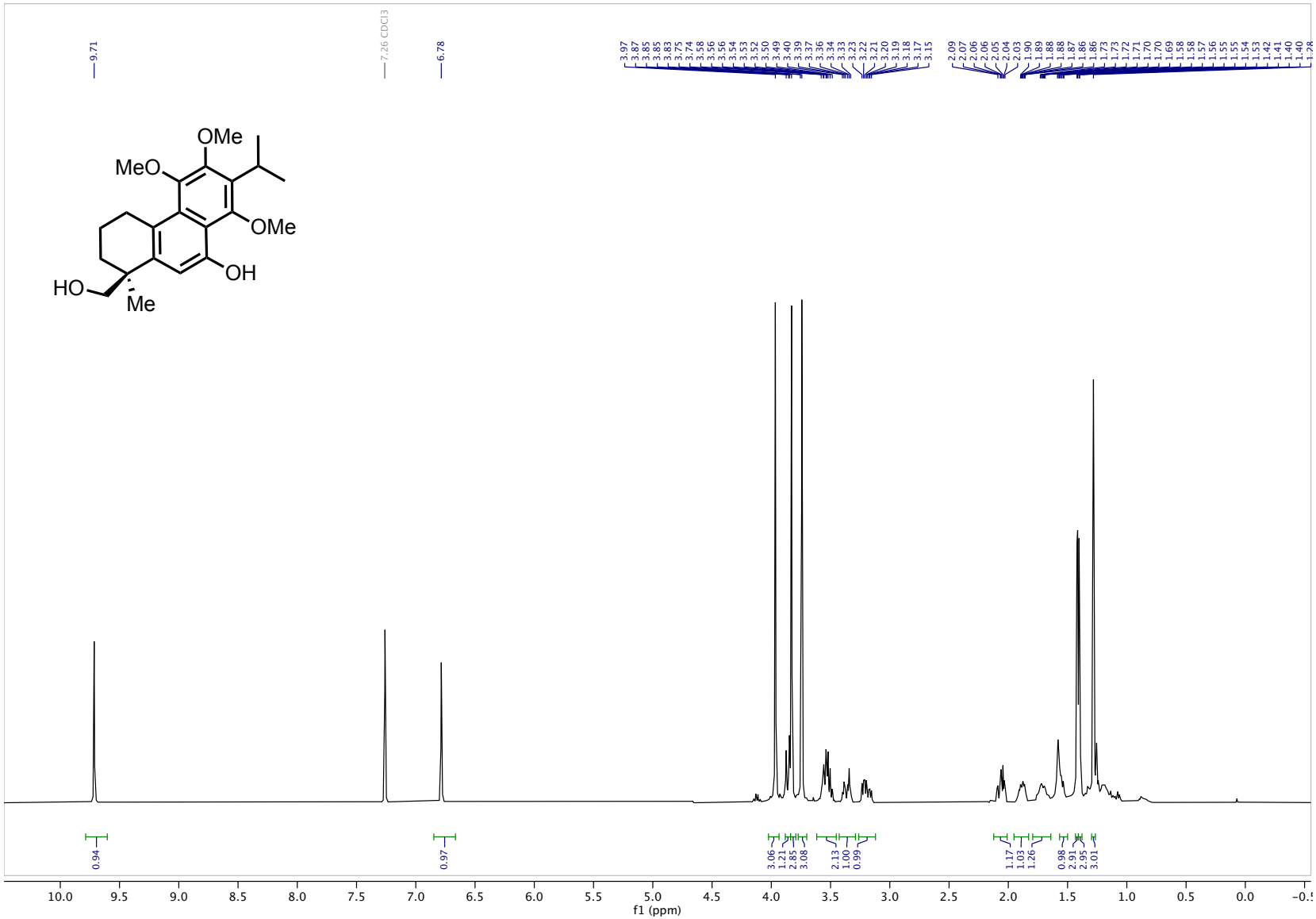

Figure A.81. ^{1}H NMR (400 MHz, $CDCl_3$) naphthol **1.66**

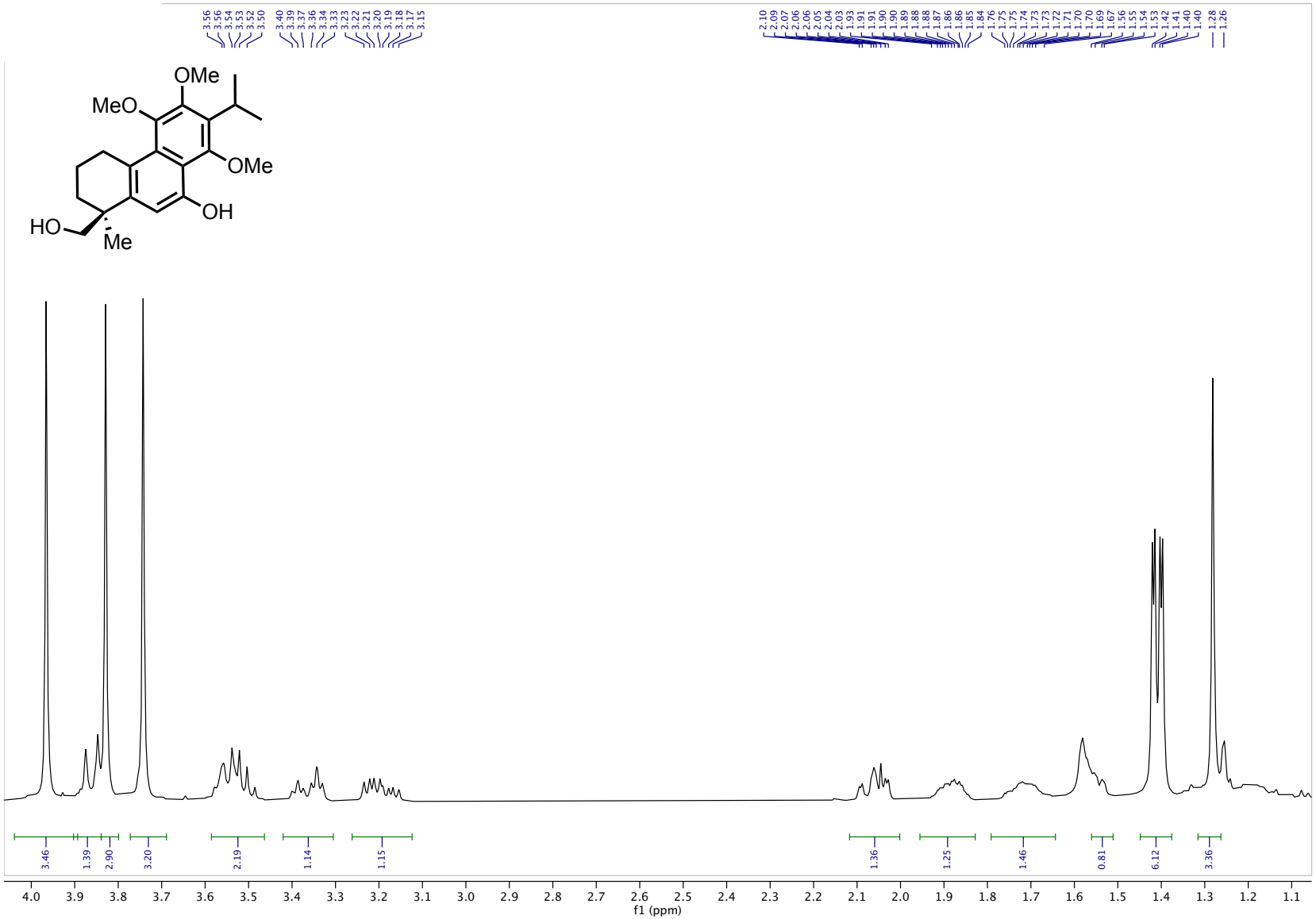

Figure A.82. ^{1}H NMR (400 MHz, $CDCl_3$) naphthol **1.66** (4.25 – 1.0 ppm inset)

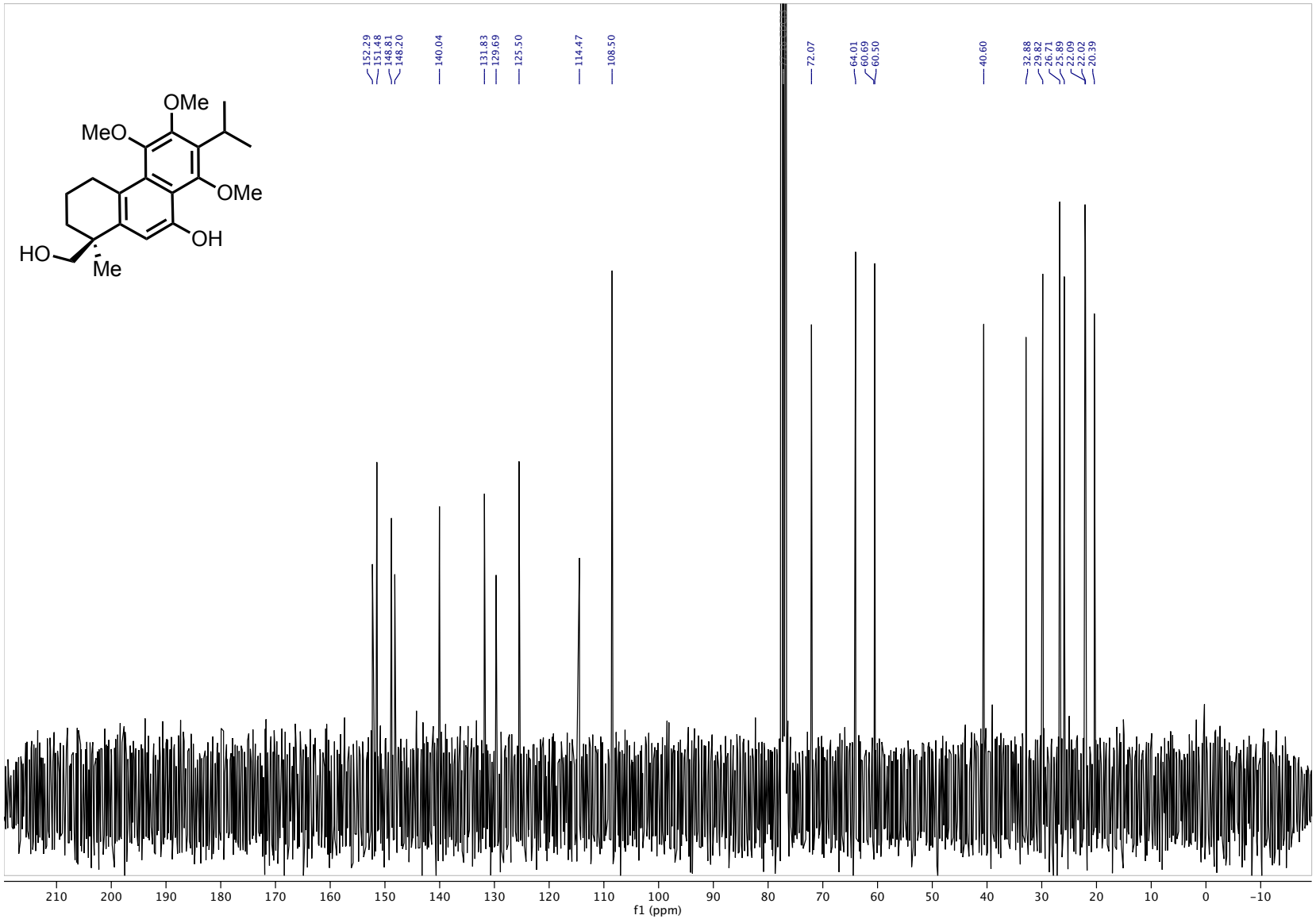

Figure A.83. ^{13}C NMR (101 MHz, $CDCl_3$) naphthol **1.66**

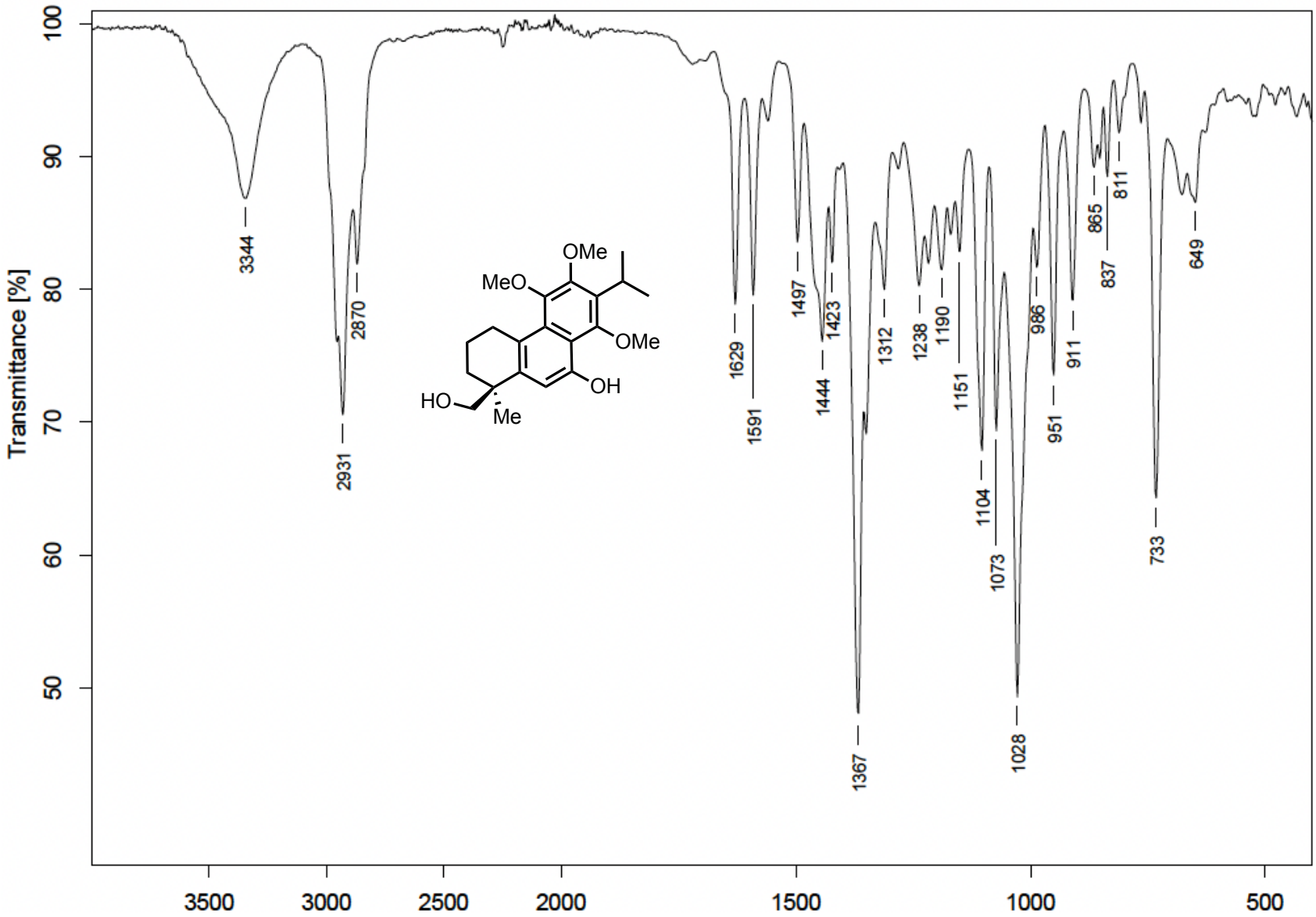

Figure A.84. FTIR (thin film) naphthol **1.66**

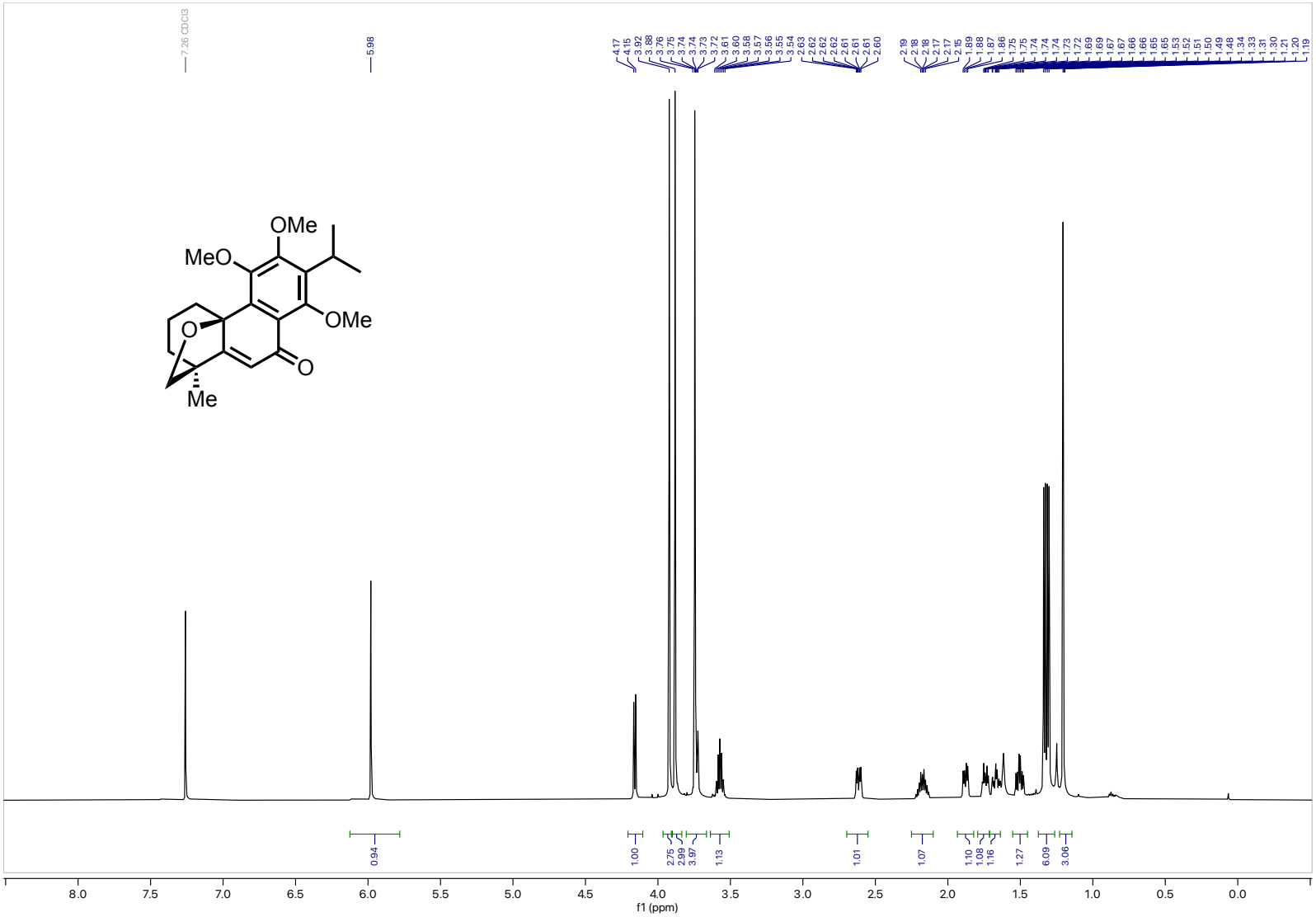

Figure A.85. ^{1}H NMR (400 MHz, $CDCl_3$) phenolic oxidation product **1.67**

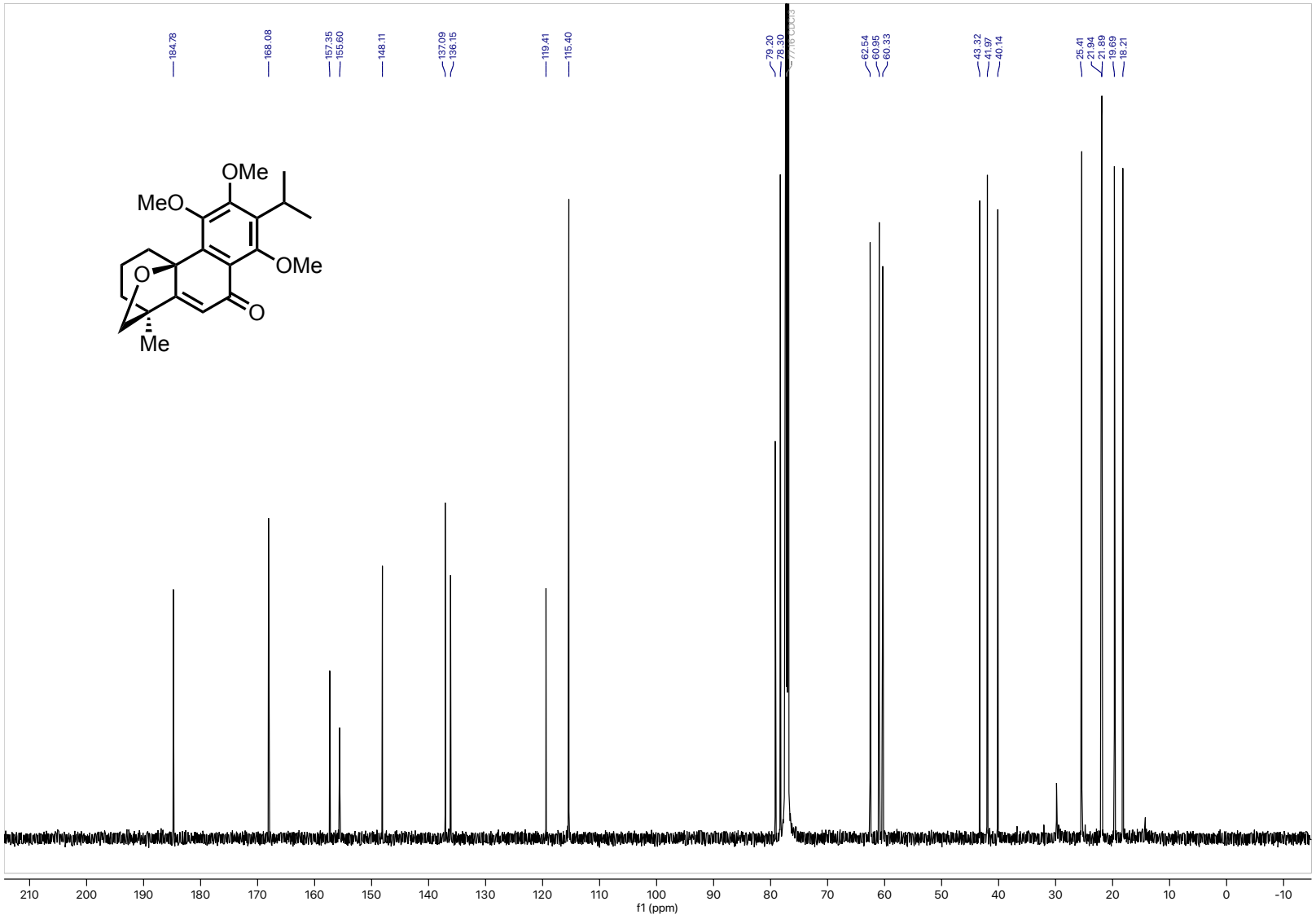

Figure A.86. ^{13}C NMR (101 MHz, $CDCl_3$) phenolic oxidation product **1.67**

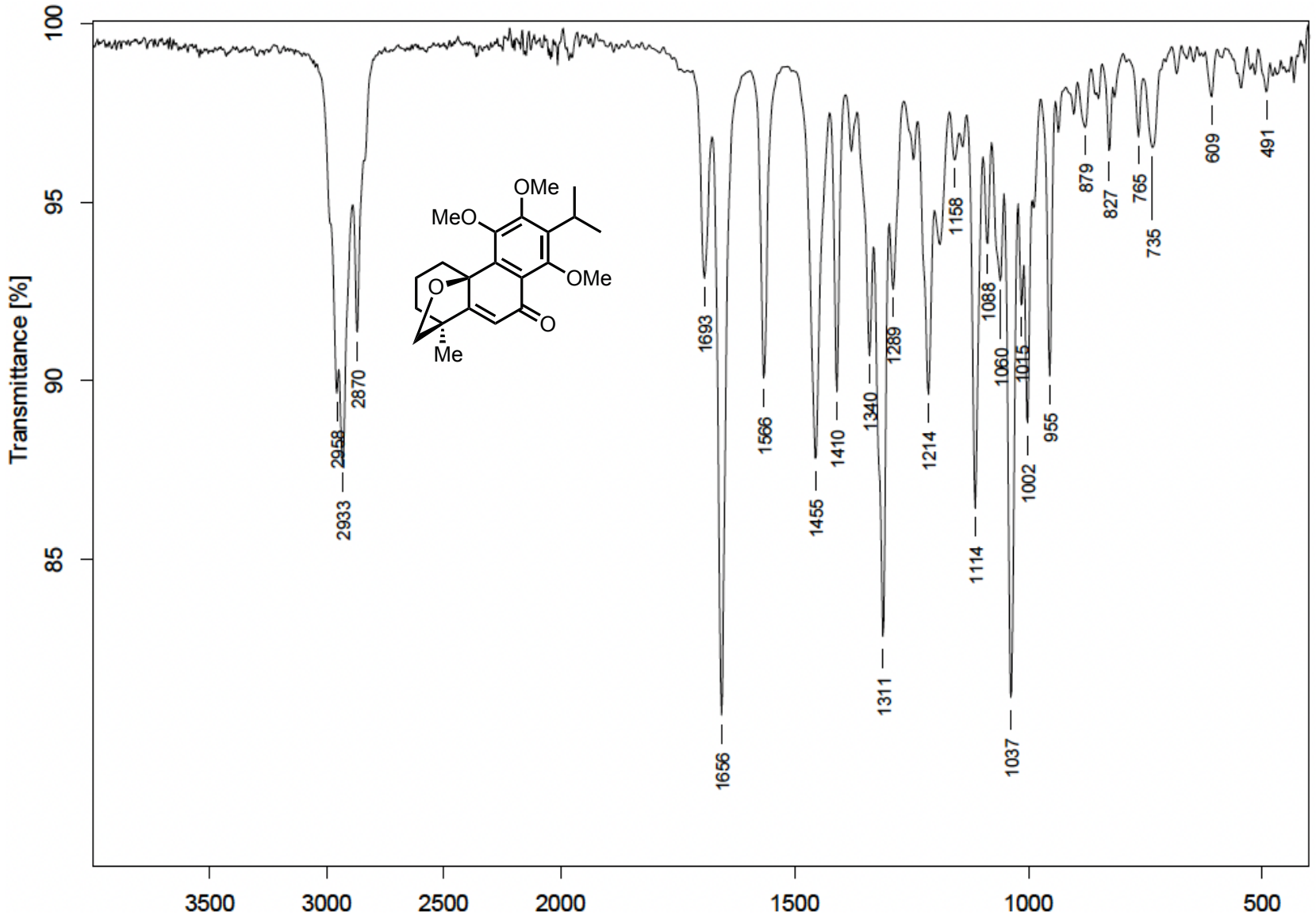

Figure A.87. FTIR (thin film) phenolic oxidation product **1.67**

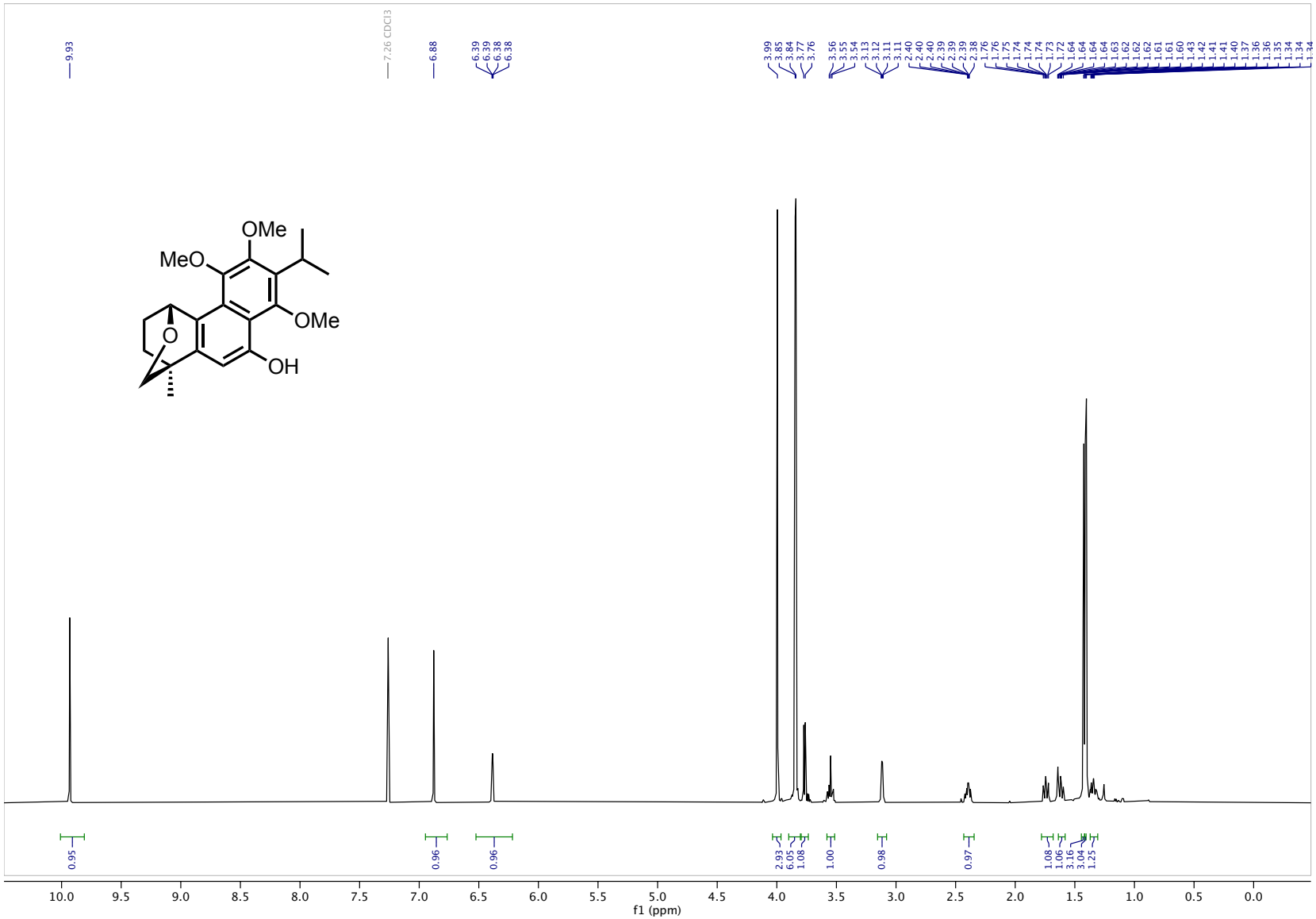

Figure A.88. ^{1}H NMR (600 MHz, $CDCl_3$) tetrahydropyran **1.64**

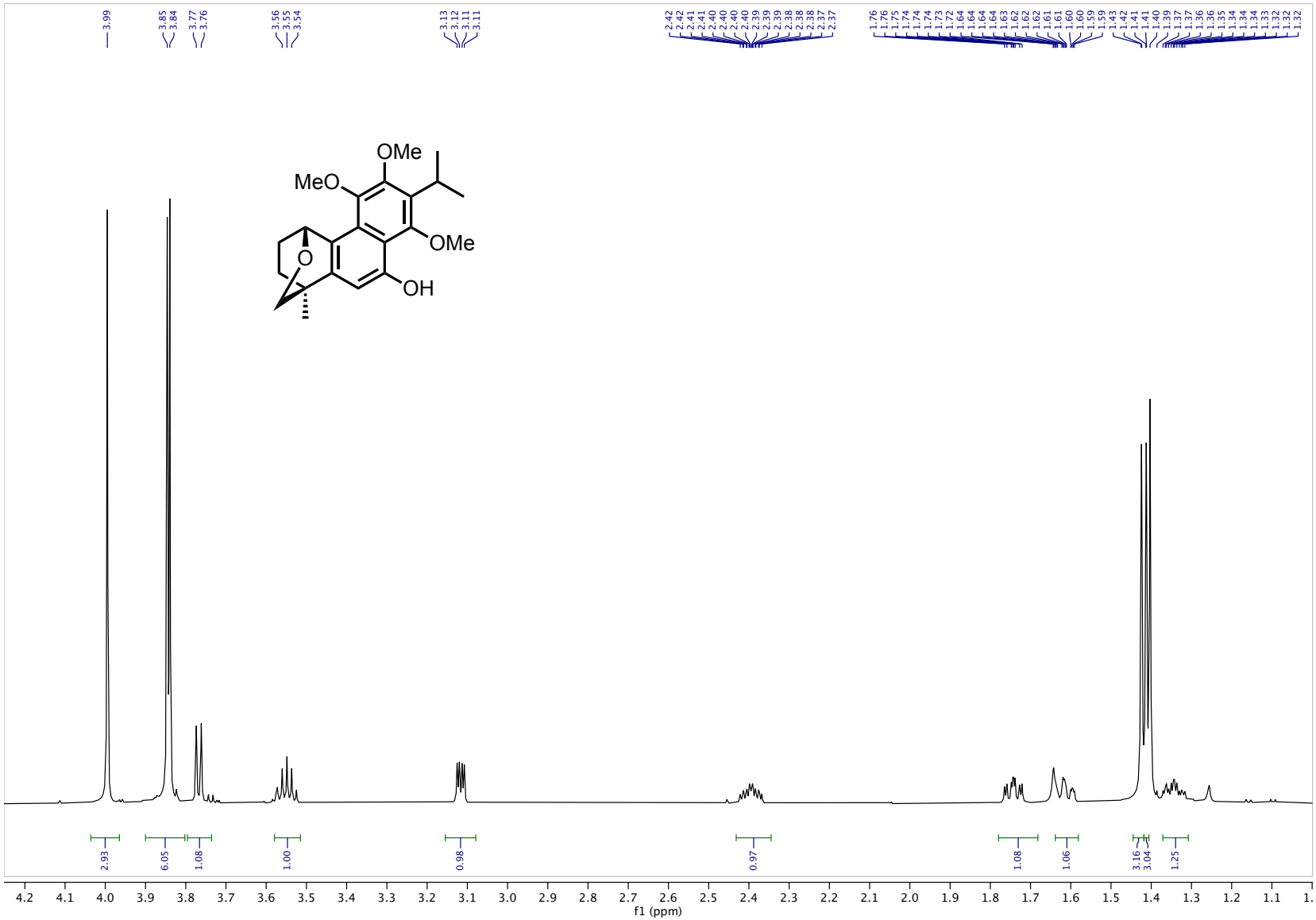

Figure A.89. ^{1}H NMR (600 MHz, $CDCl_3$) tetrahydropyran **1.64** (4.25 – 1.0 ppm inset)

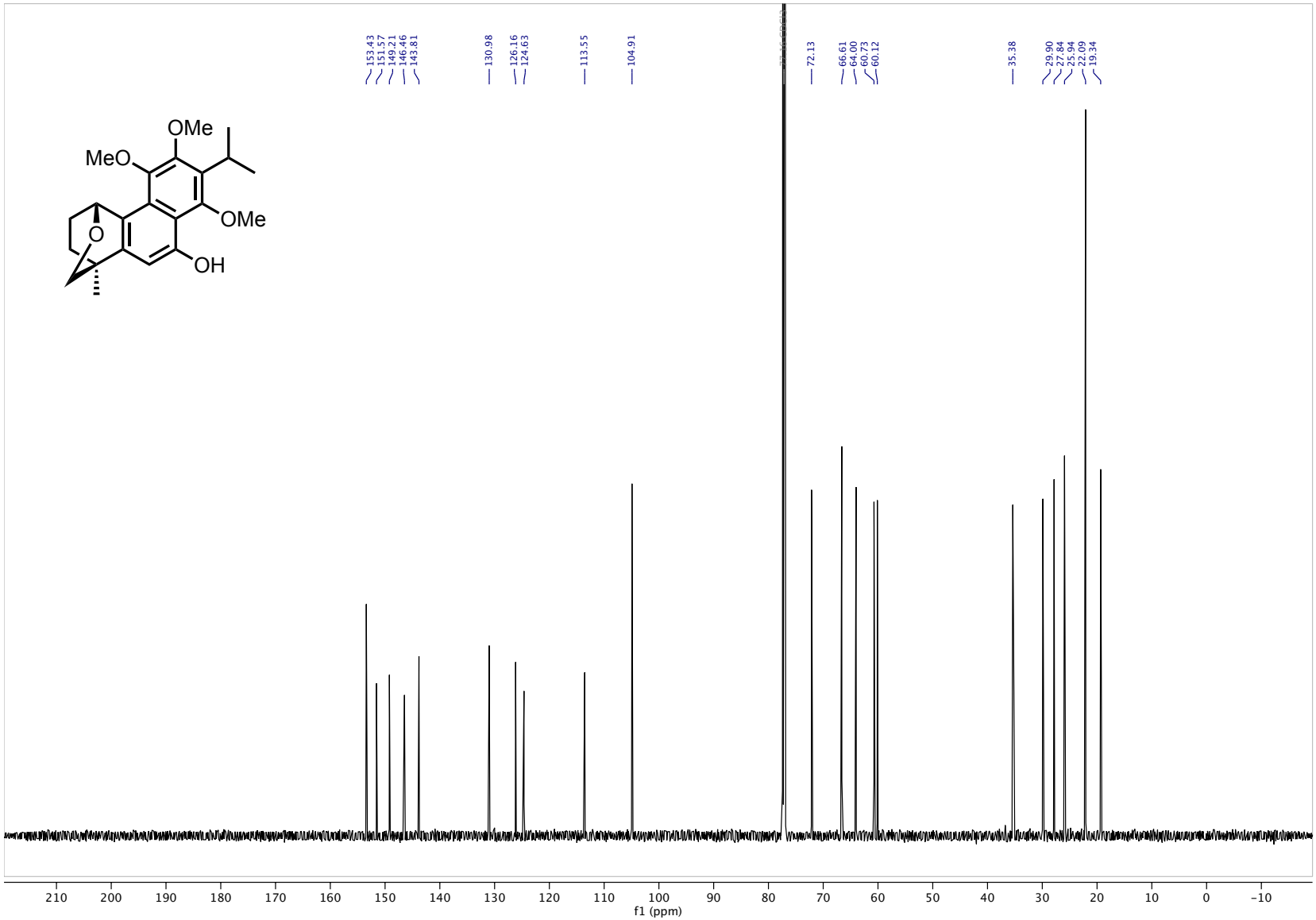

Figure A.90. ^{13}C NMR (151 MHz, $CDCl_3$) tetrahydropyran **1.64**

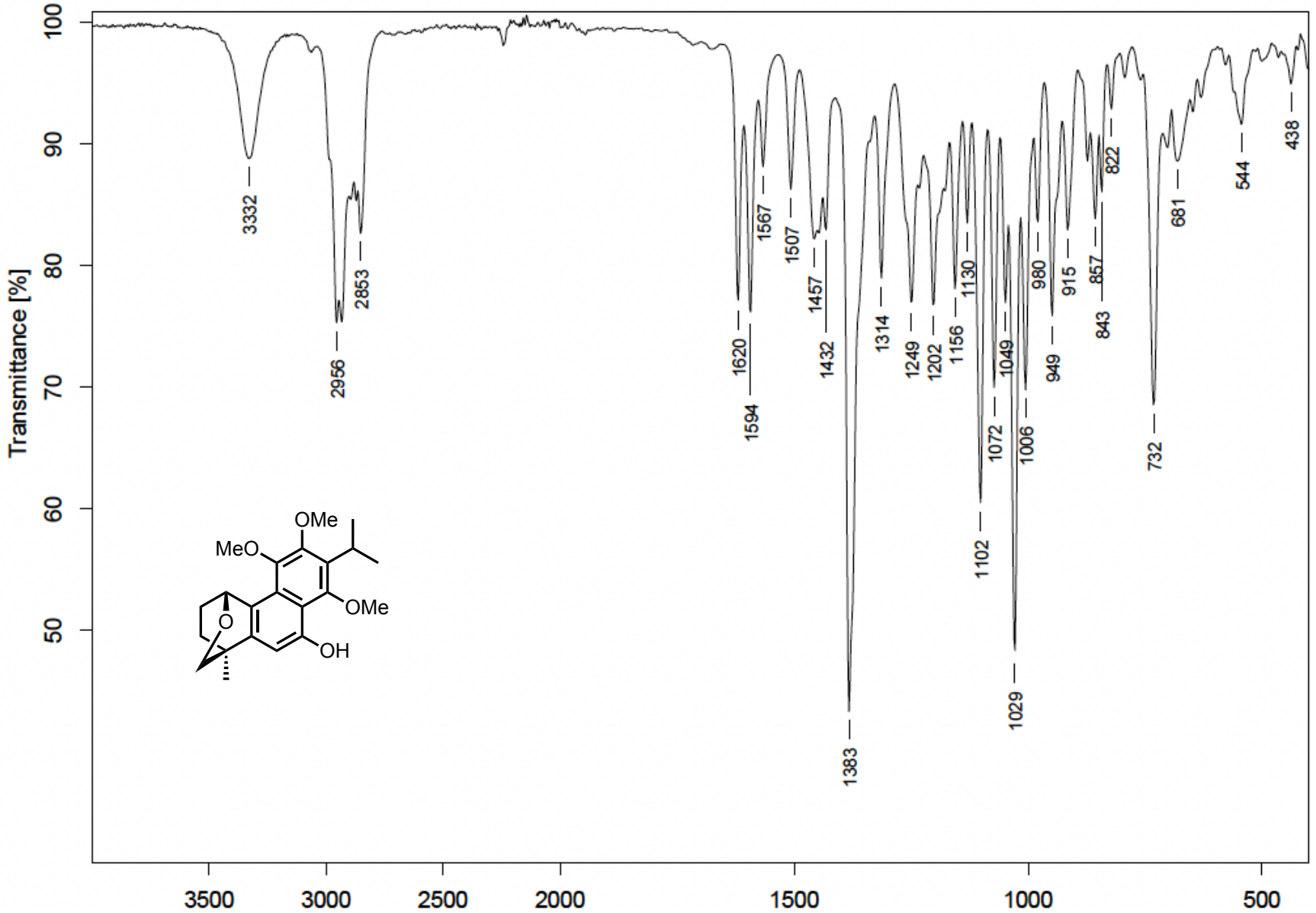

Figure A.91. FTIR (thin film) tetrahydropyran **1.64**

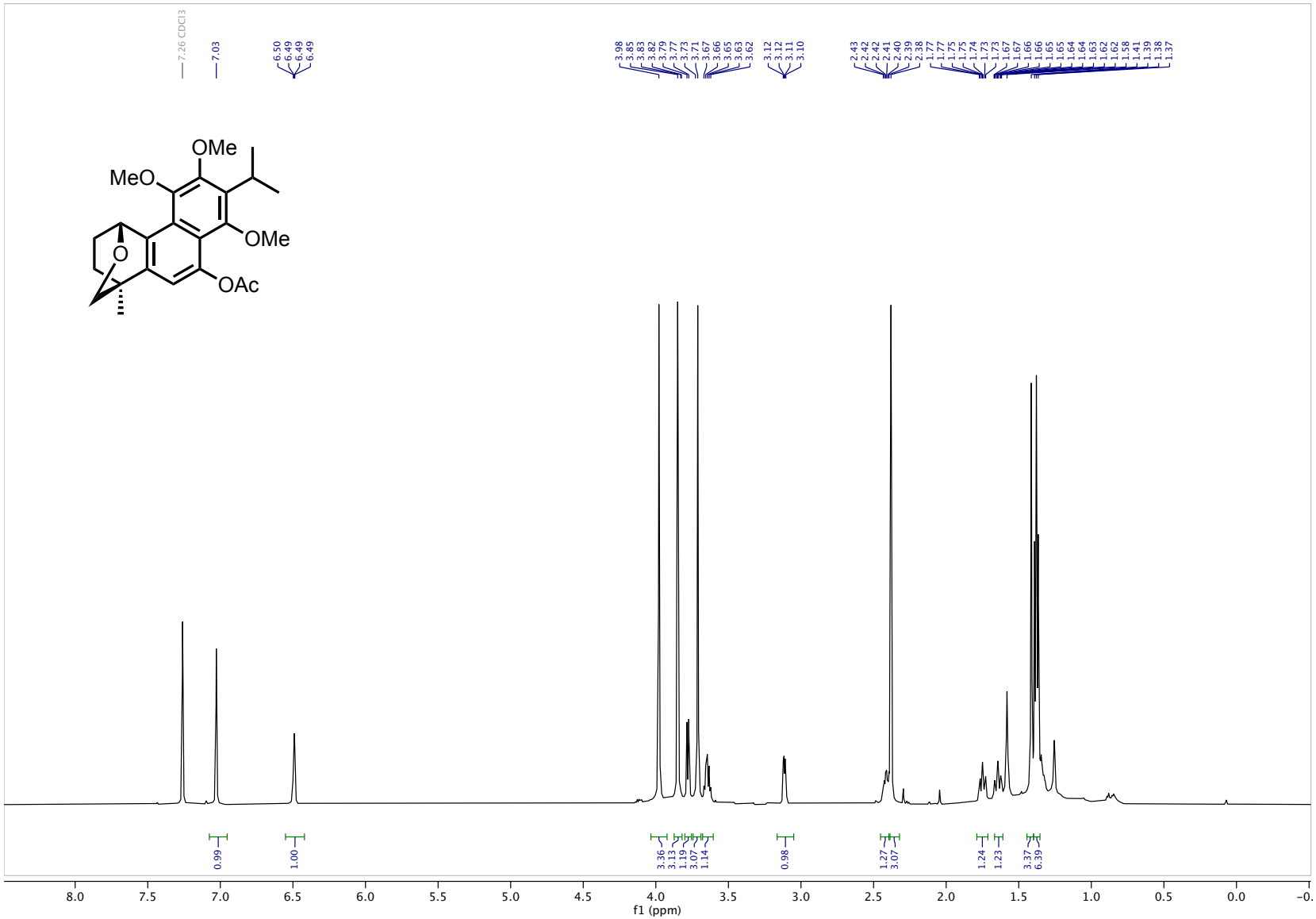

Figure A.92. ^{1}H NMR (600 MHz, $CDCl_3$) acetate **1.68**

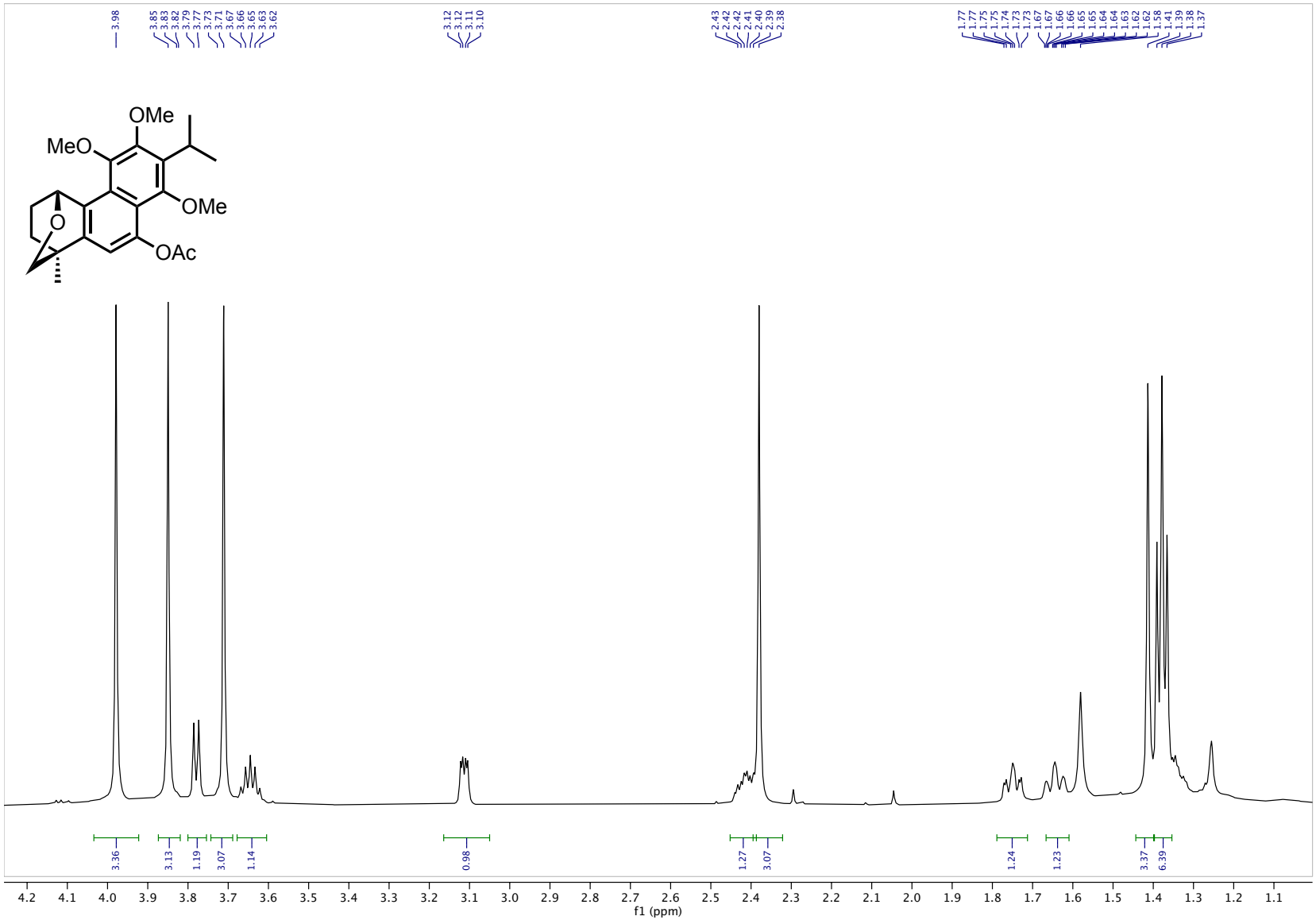

Figure A.93. ^{1}H NMR (600 MHz, $CDCl_3$) acetate **1.68** (4.25 – 1.0 ppm inset)

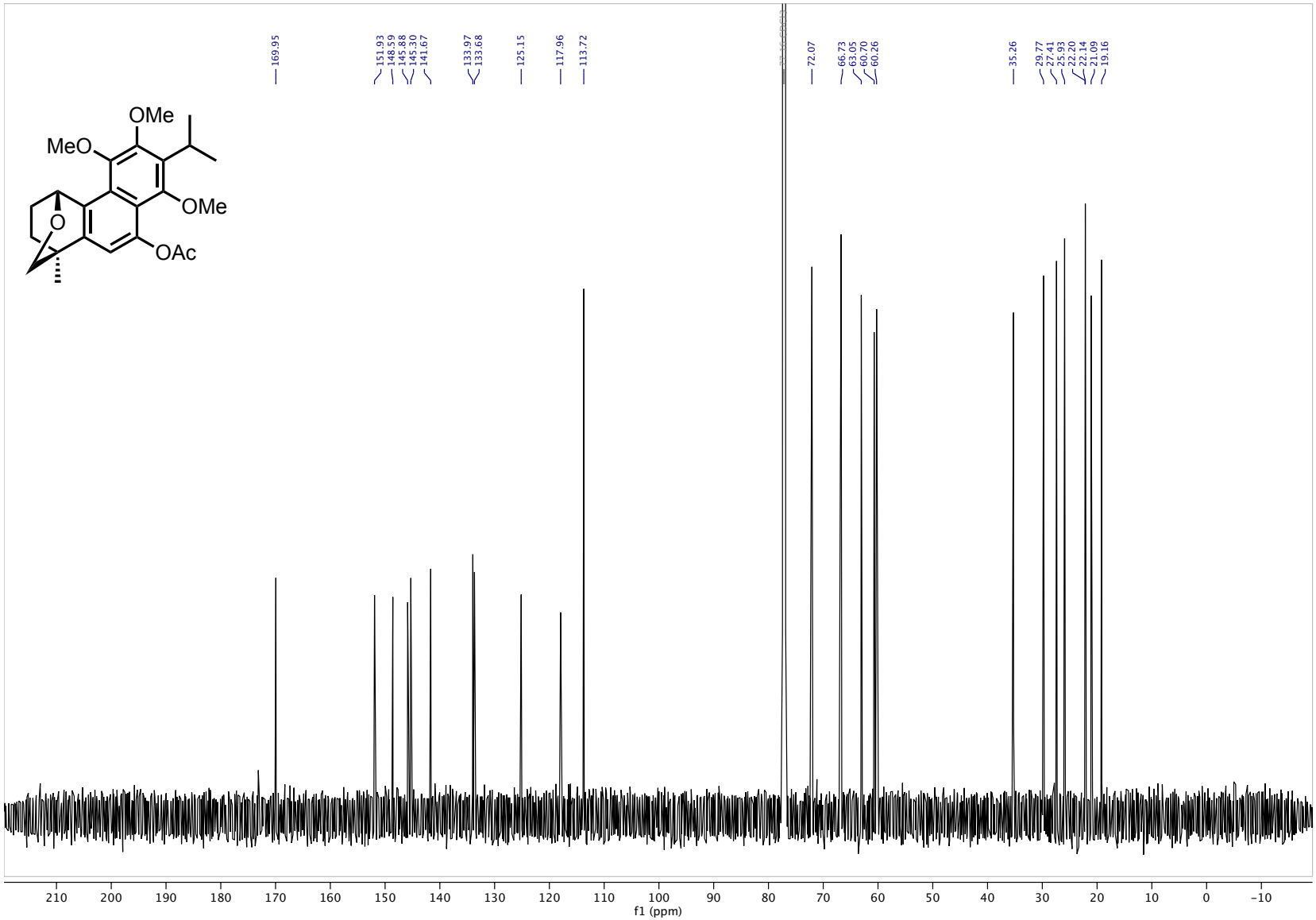

Figure A.94. ^{13}C NMR (151 MHz, $CDCl_3$) acetate **1.68**

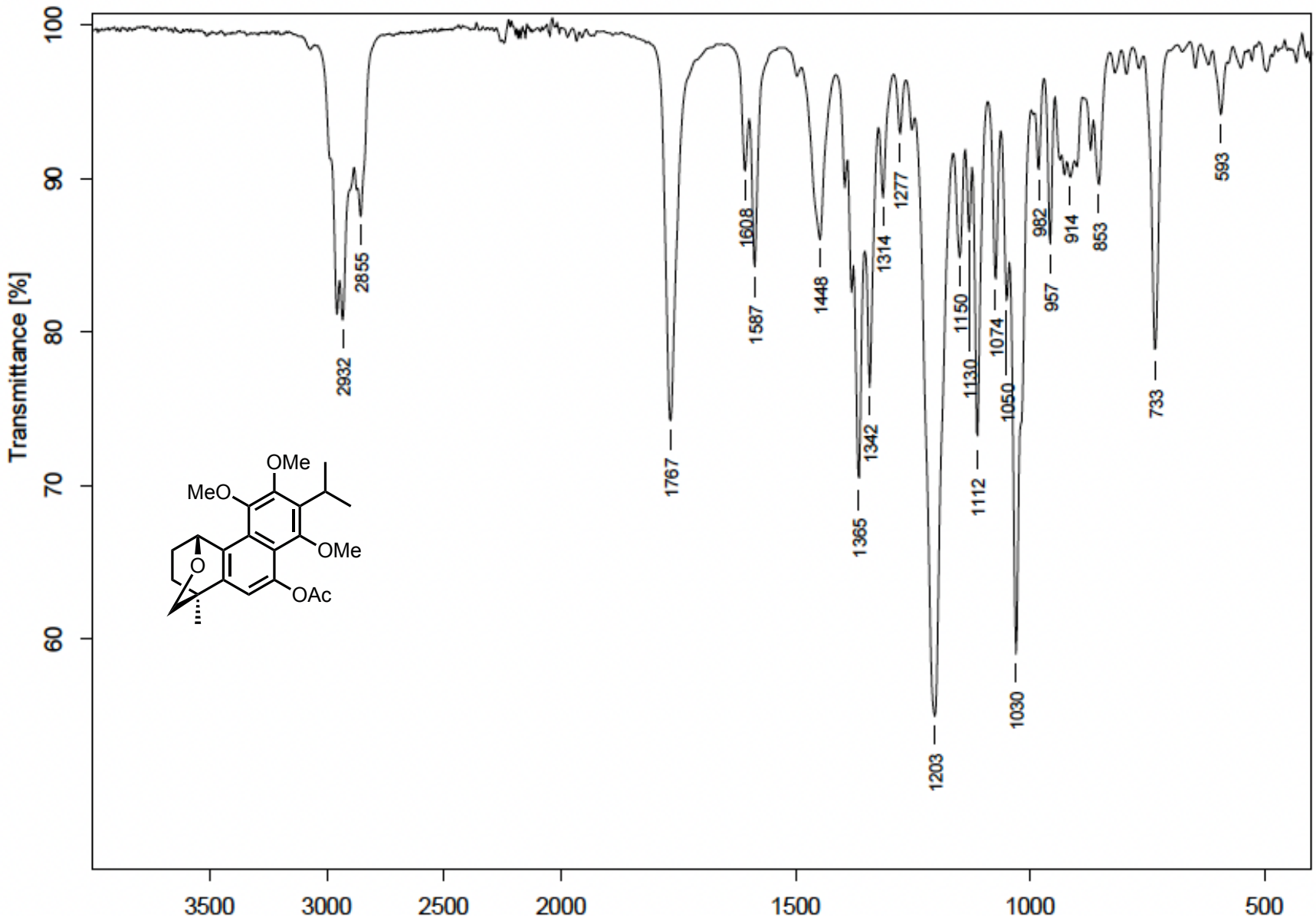

Figure A.95. FTIR (thin film) acetate **1.68**

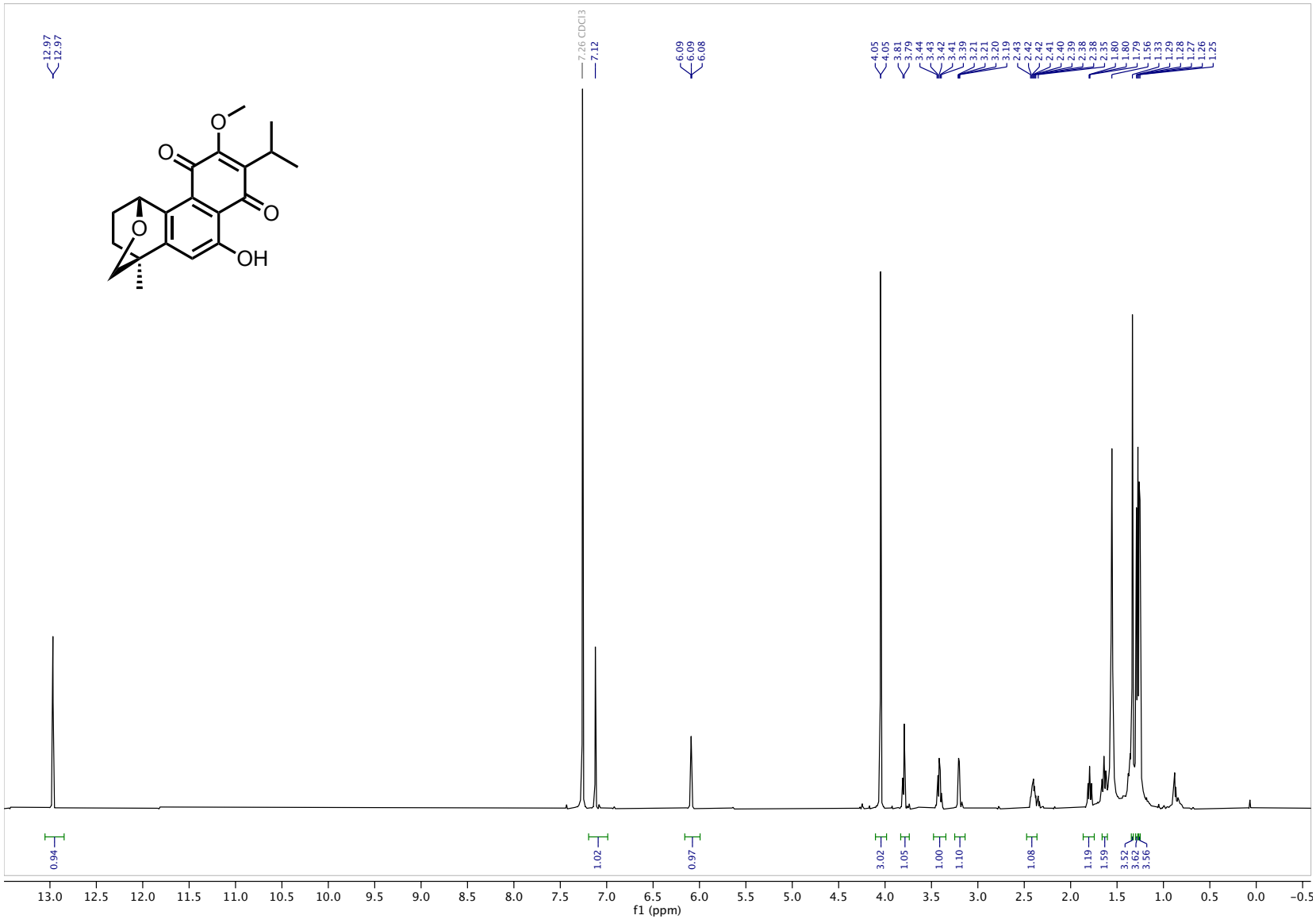

Figure A.96. ^{1}H NMR (600 MHz, $CDCl_3$) dracocequinone A **1.04**

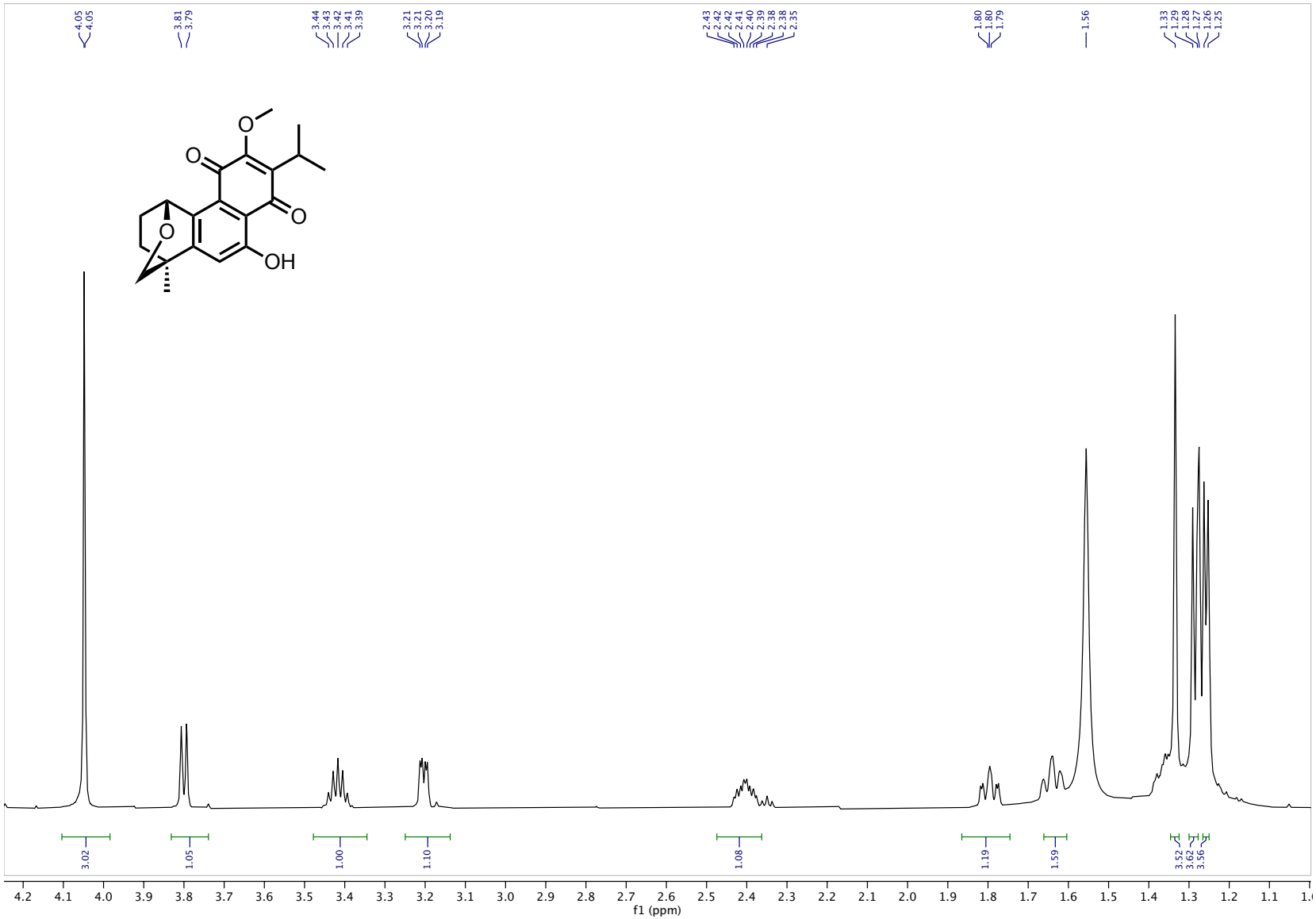

Figure A.97. ^{1}H NMR (600 MHz, $CDCl_3$) dracocequinone A **1.04** (4.25 – 1.0 ppm inset)

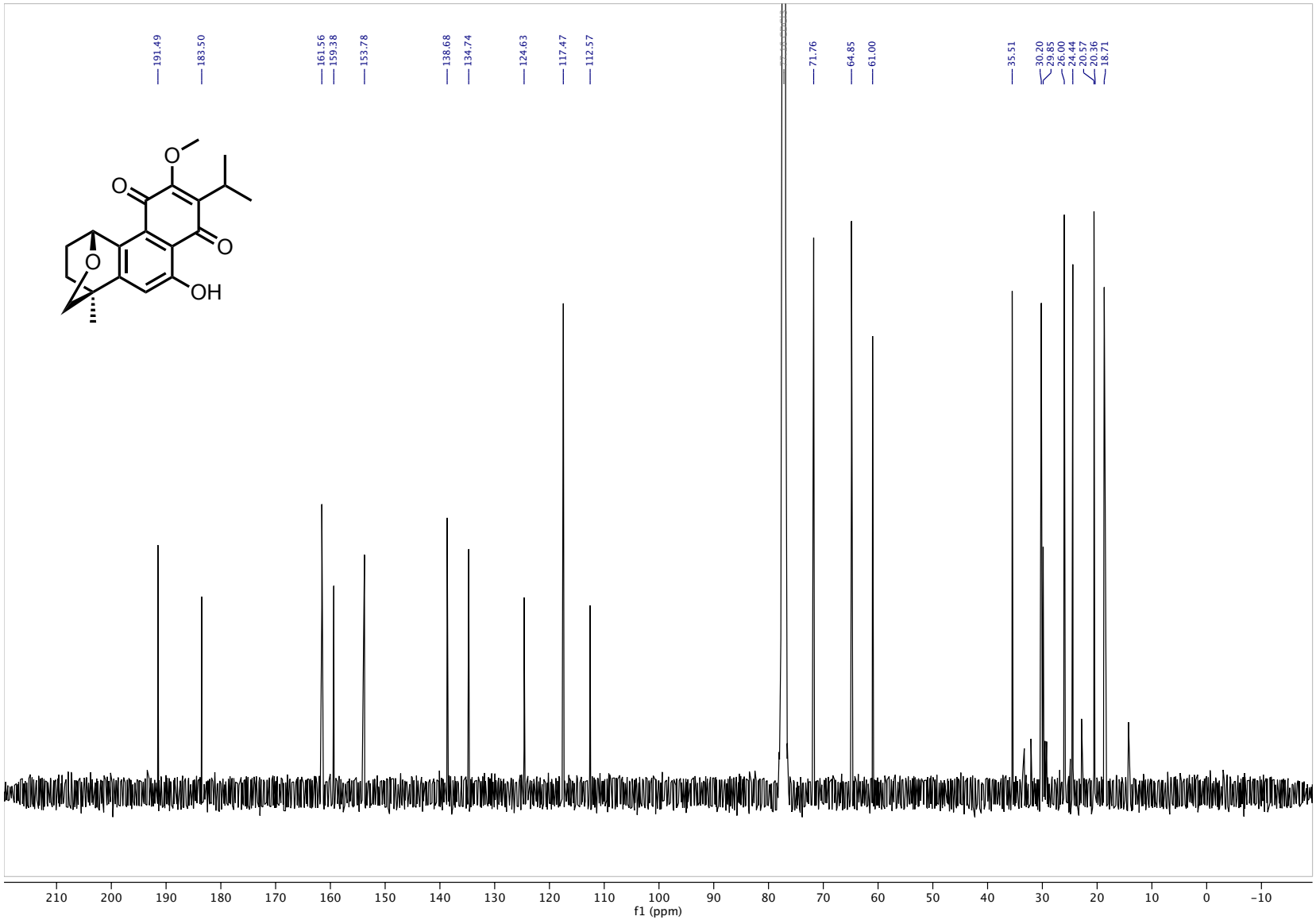

Figure A.98. ^{13}C NMR (151 MHz, $CDCl_3$) dracocequinone A **1.04**

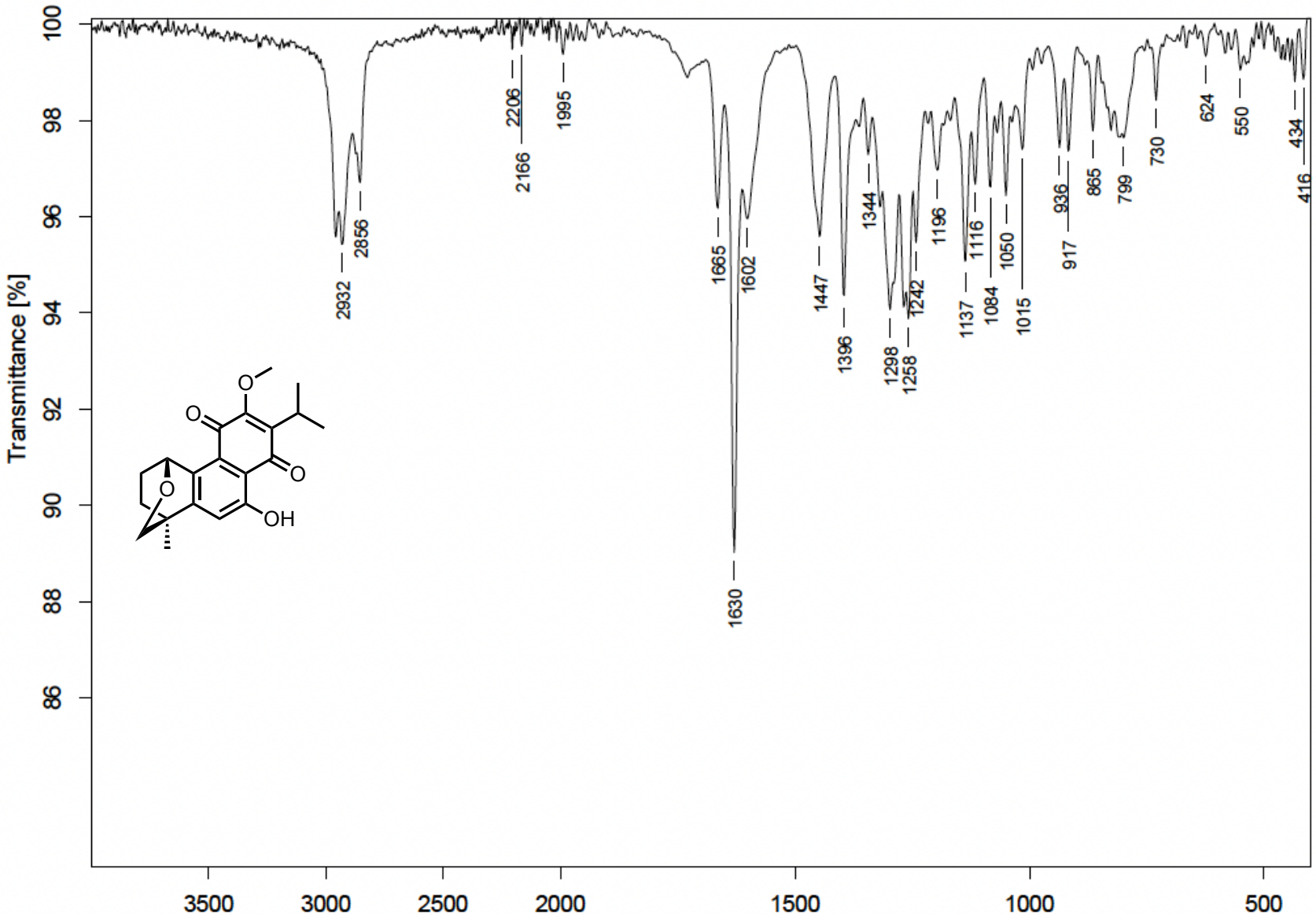

Figure A.99 FTIR (thin film) dracocequinone A **1.04**

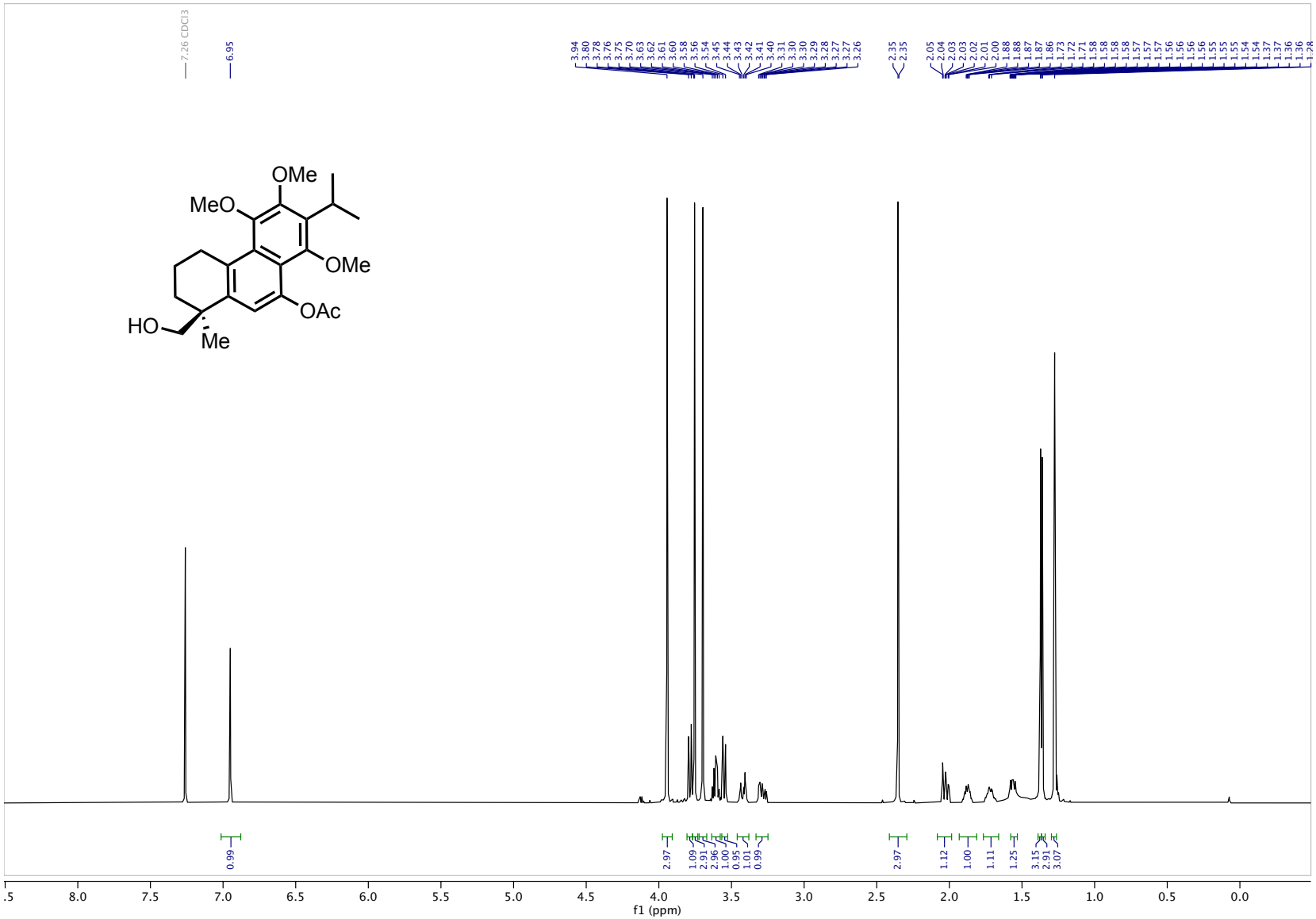

Figure A.100. ^{1}H NMR (600 MHz, $CDCl_3$) naphthol acetate **1.75**

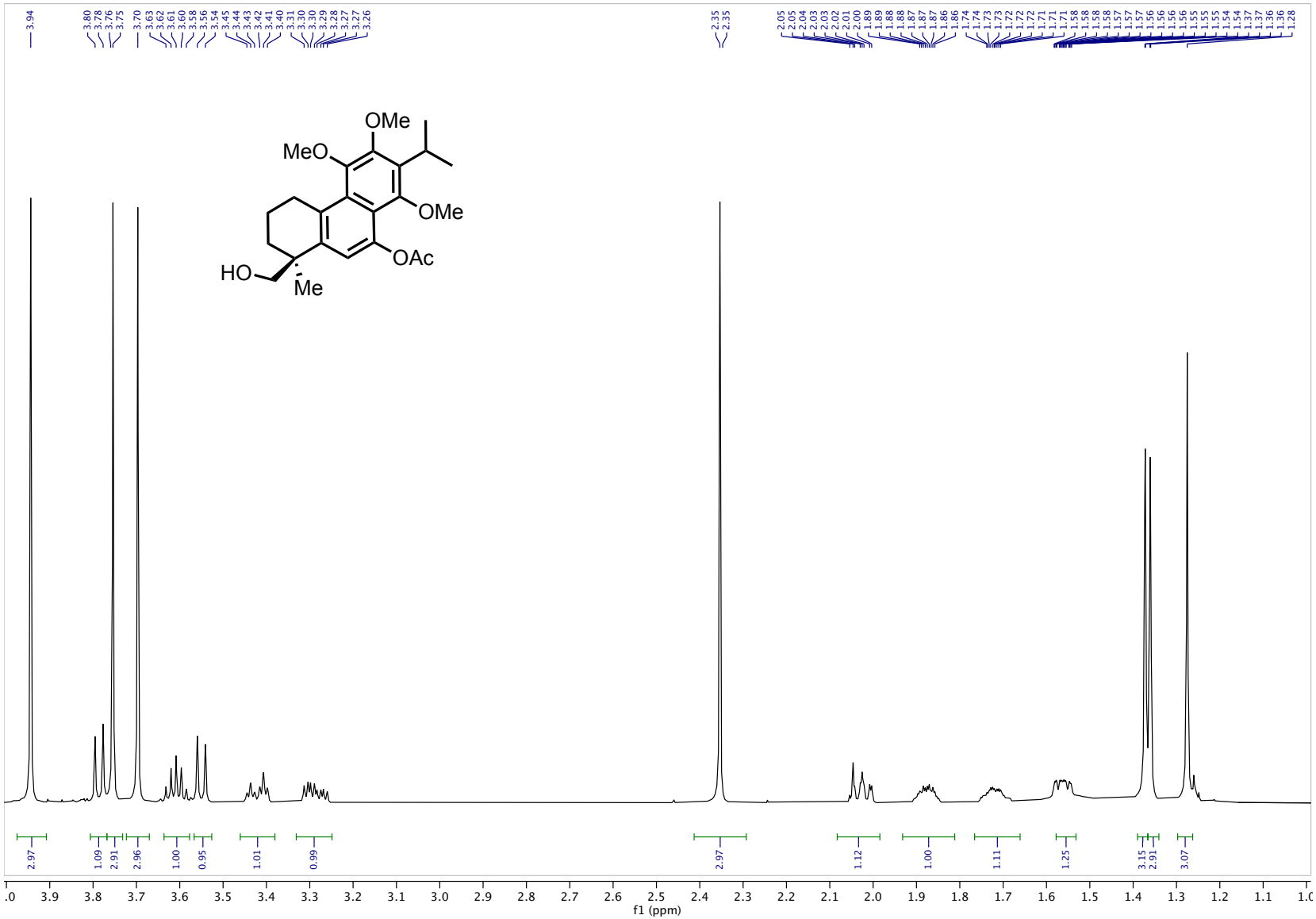

Figure A.101. ^{1}H NMR (600 MHz, $CDCl_3$) naphthol acetate **1.75** (4.0 – 1.0 ppm inset)

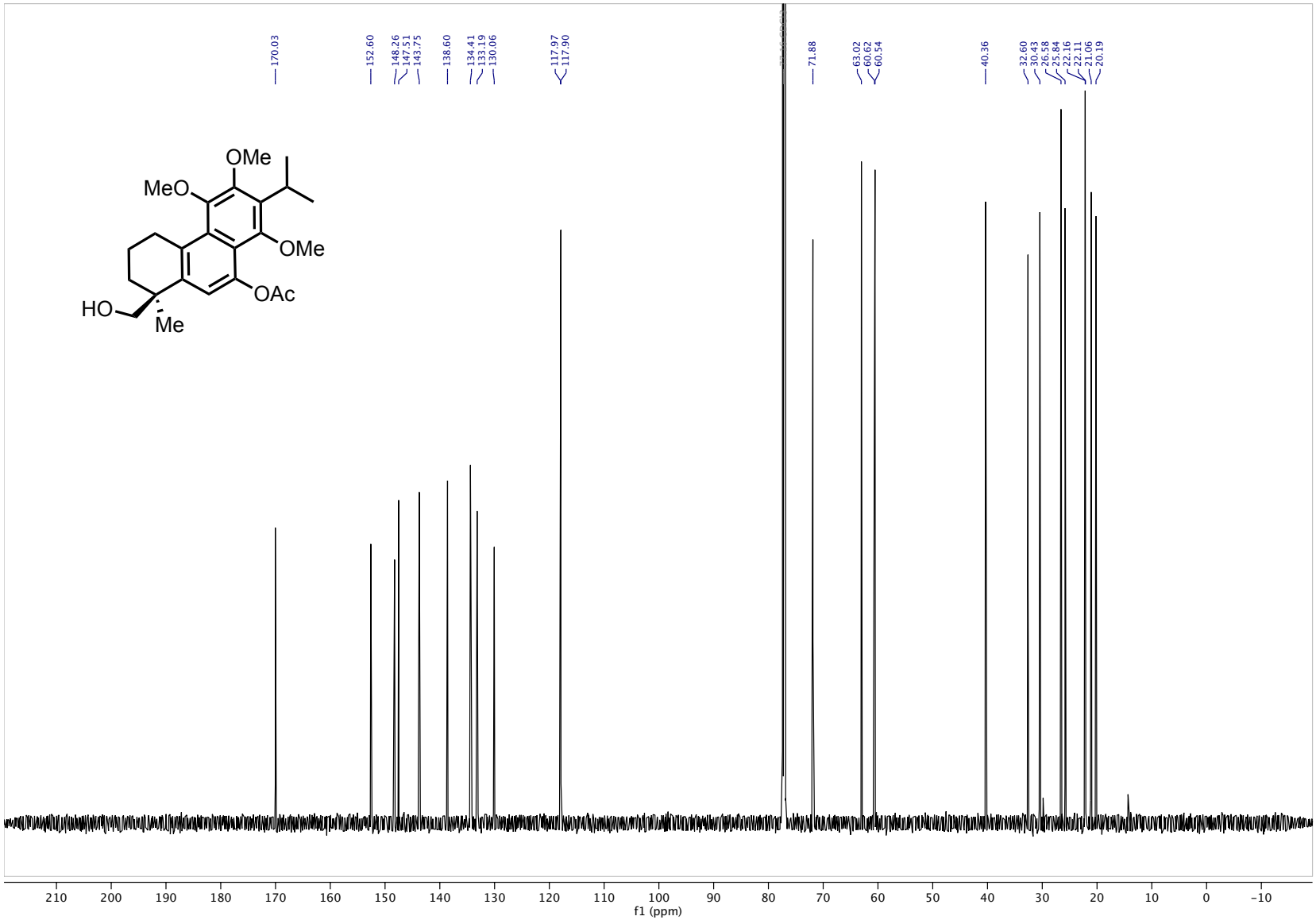

Figure A.102. ^{13}C NMR (151 MHz, $CDCl_3$) naphthol acetate **1.75**

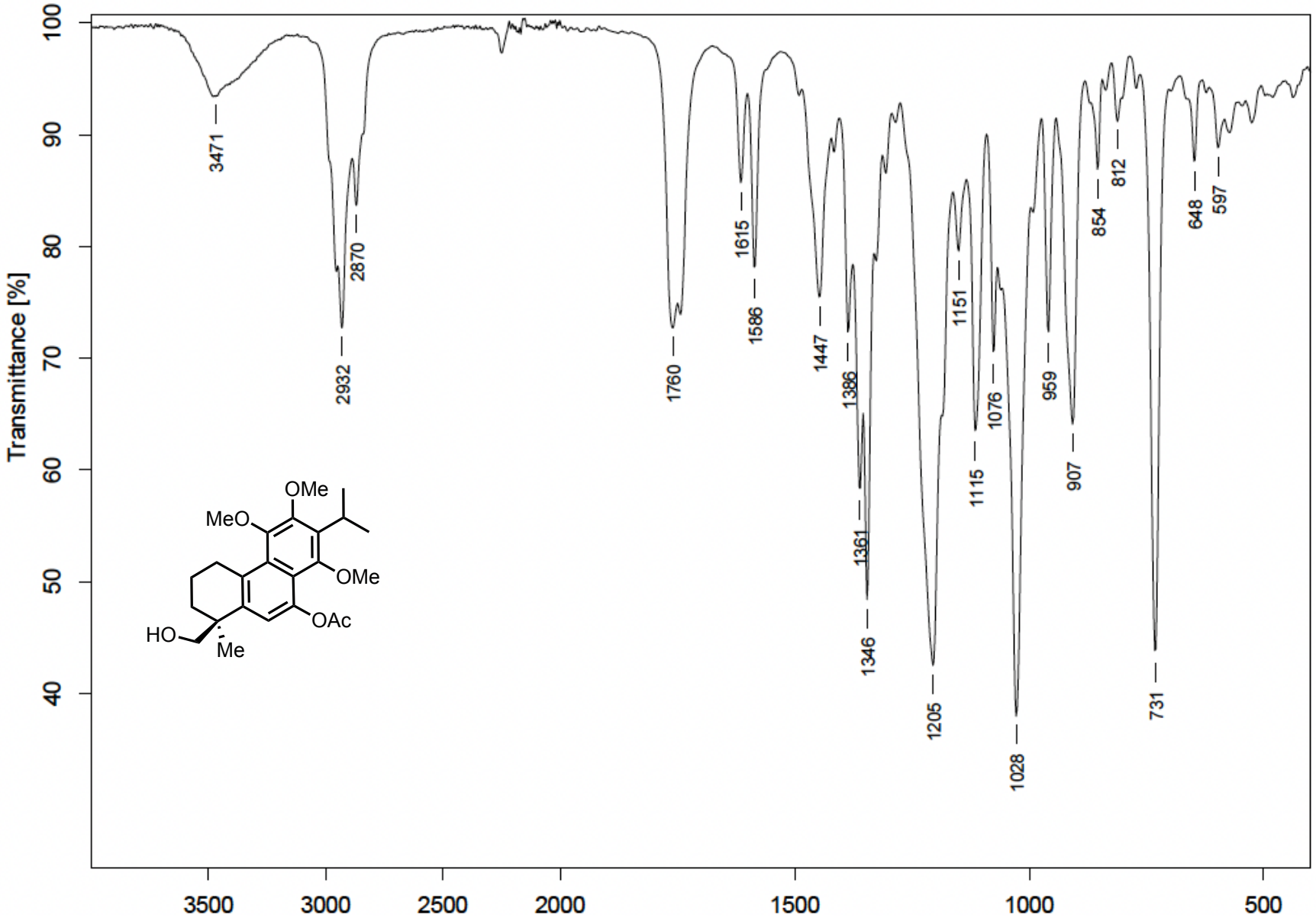

Figure A.103. FTIR (thin film) naphthol acetate **1.75**

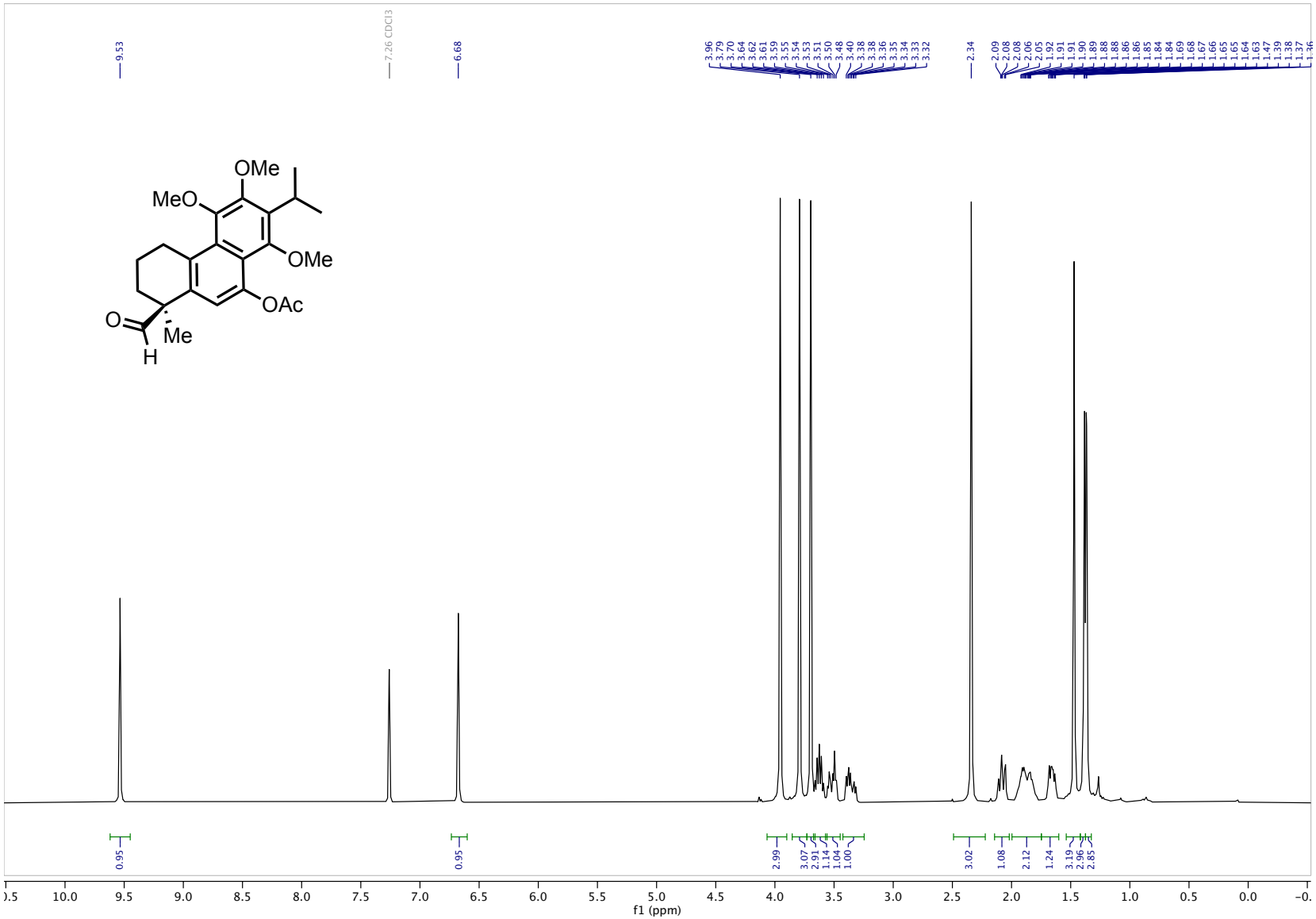

Figure A.104. ^{1}H NMR (400 MHz, $CDCl_3$) aldehyde **1.70**

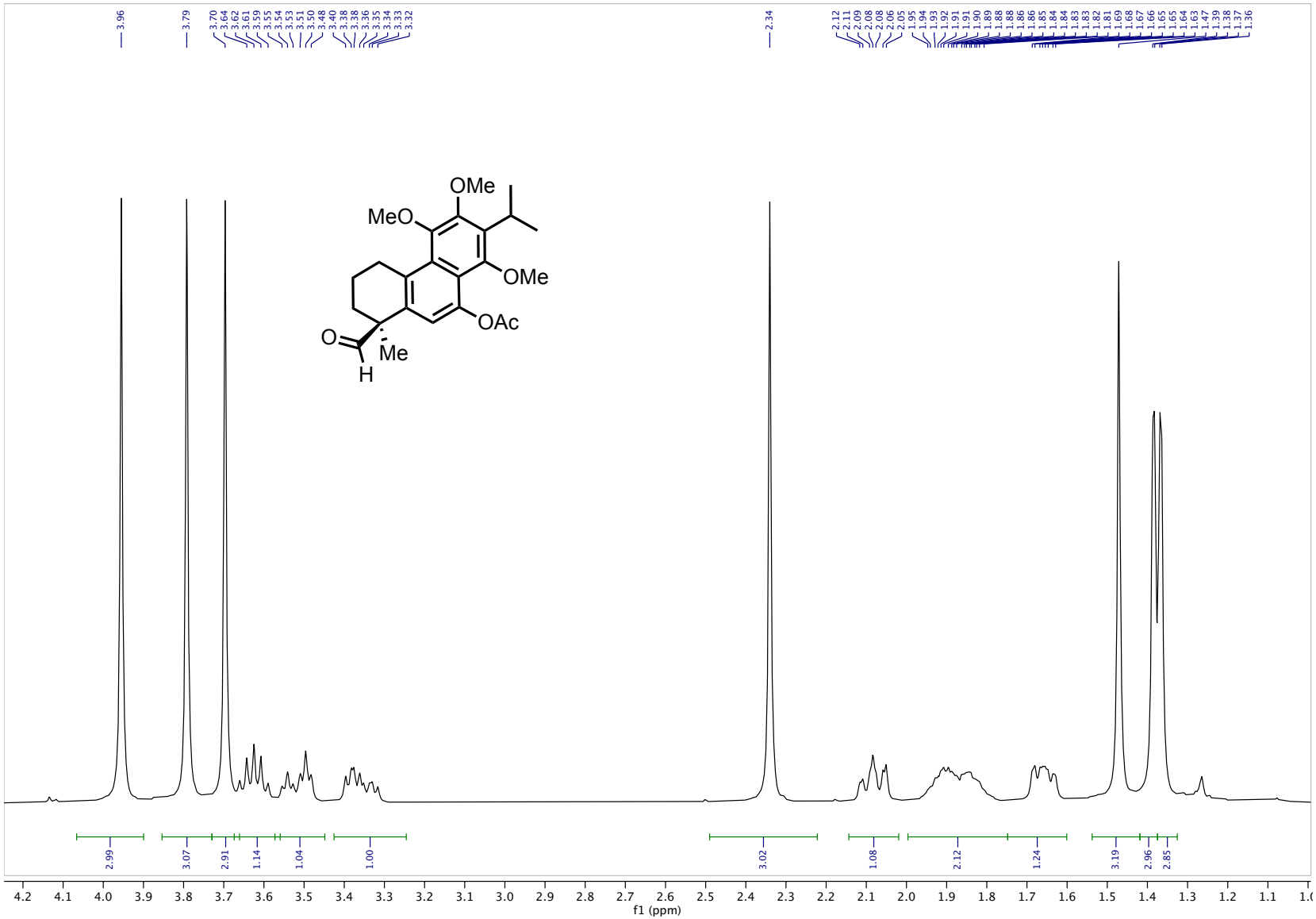

Figure A.105. ^{1}H NMR (400 MHz, $CDCl_3$) aldehyde **1.70** (4.25 – 1.0 ppm inset)

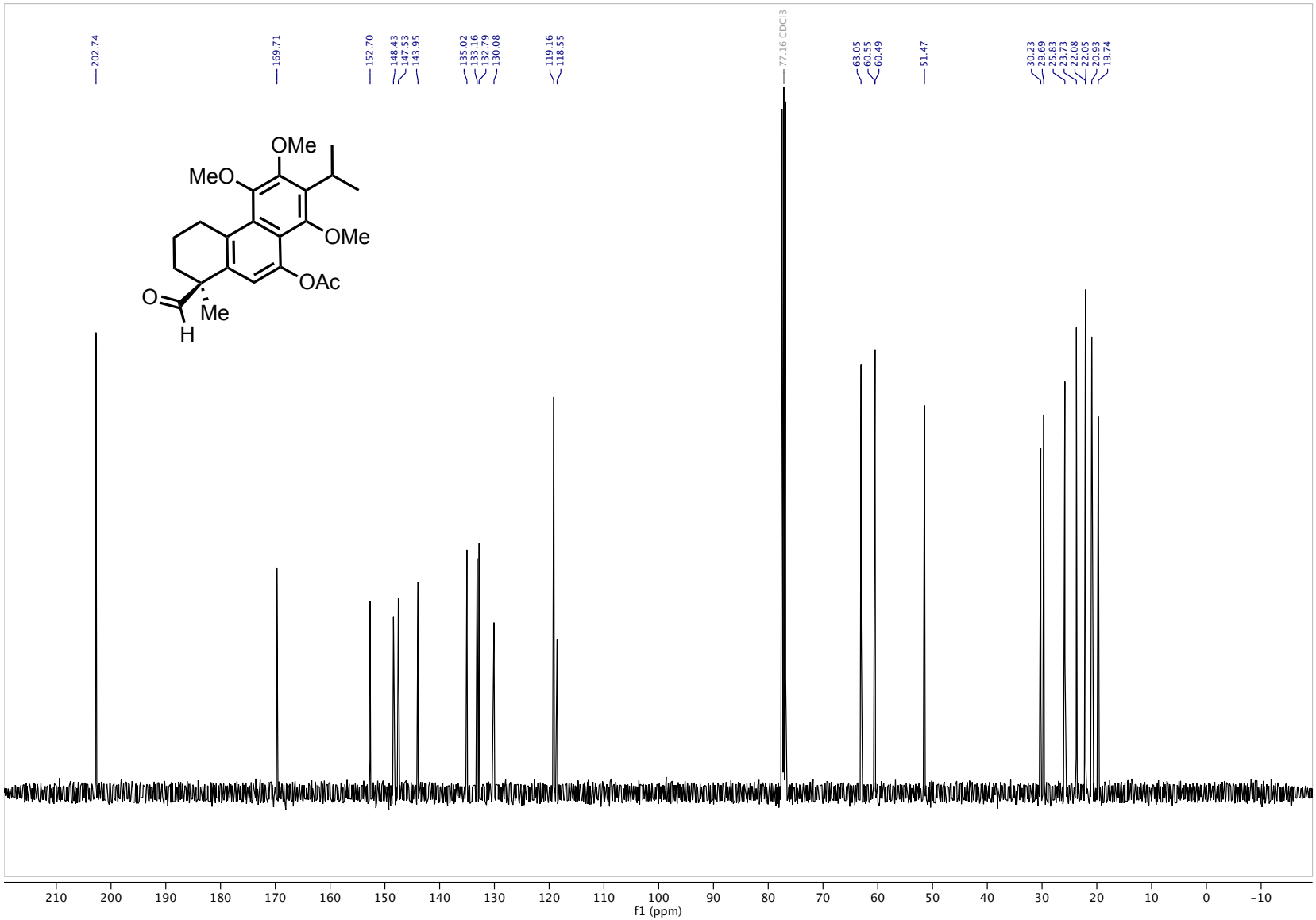

Figure A.106. ^{13}C NMR (101 MHz, $CDCl_3$) aldehyde **1.70**

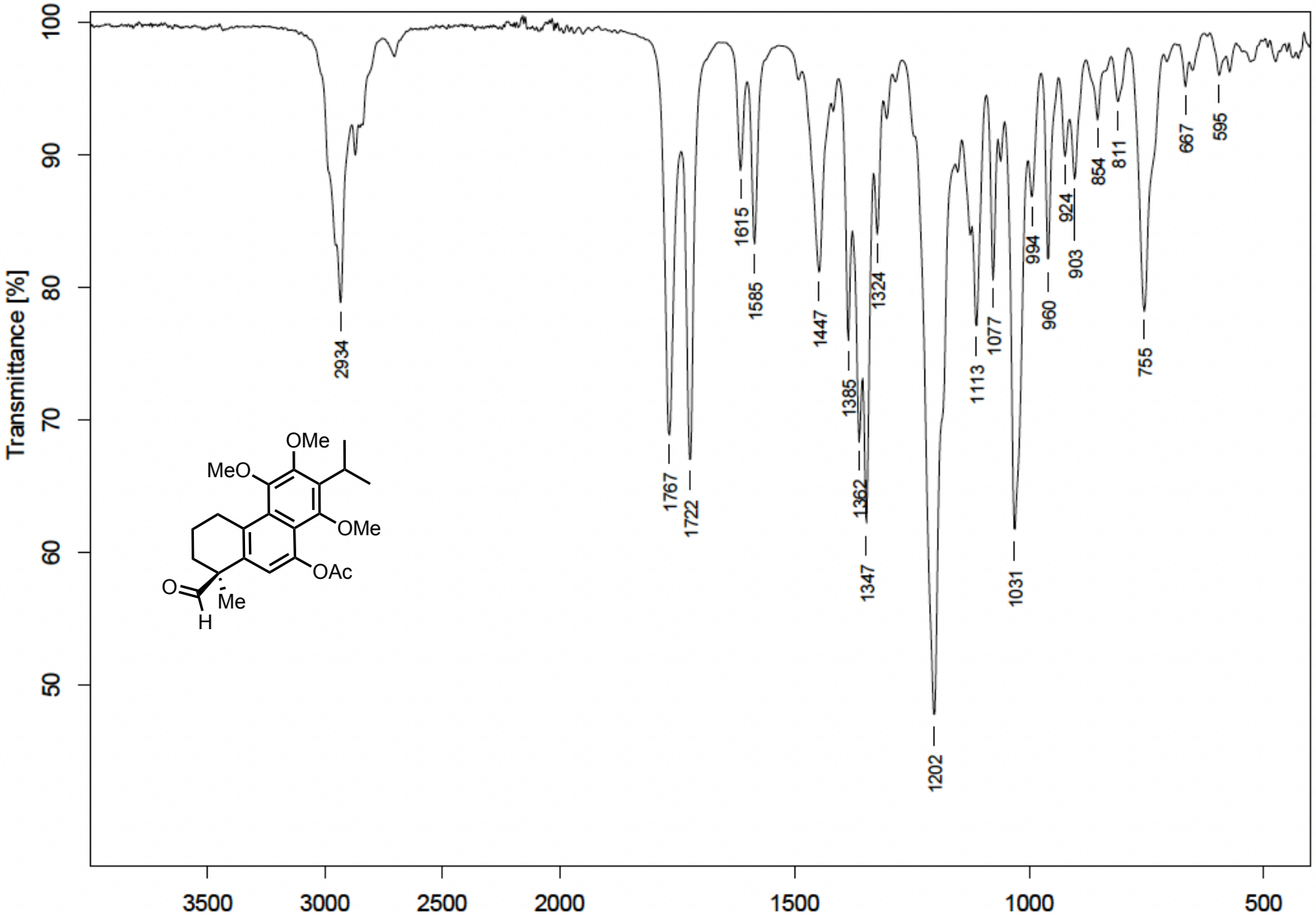

Figure A.107. FTIR (thin film) aldehyde **1.70**

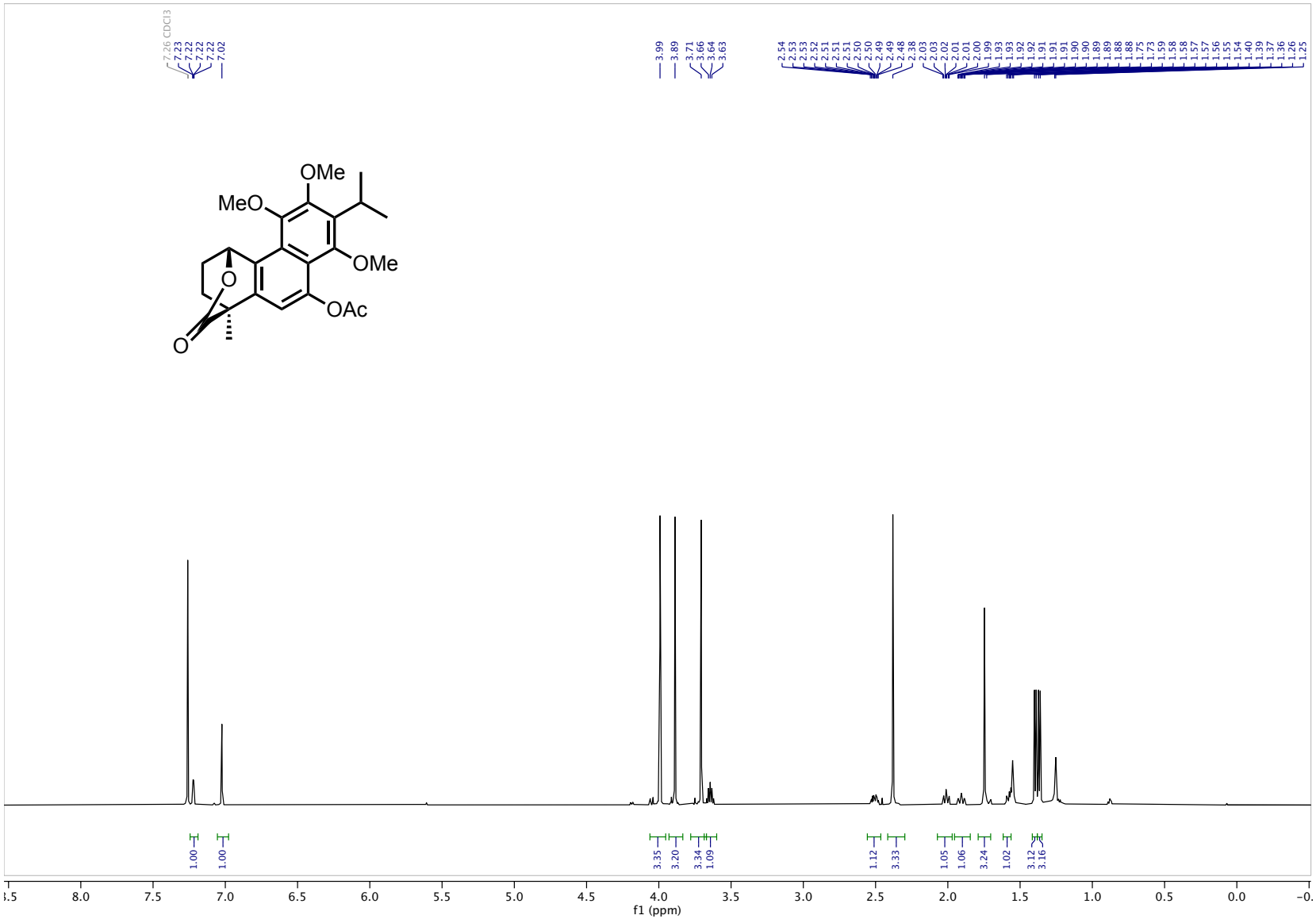

Figure A.108. ^{1}H NMR (600 MHz, $CDCl_3$) lactone **1.72**

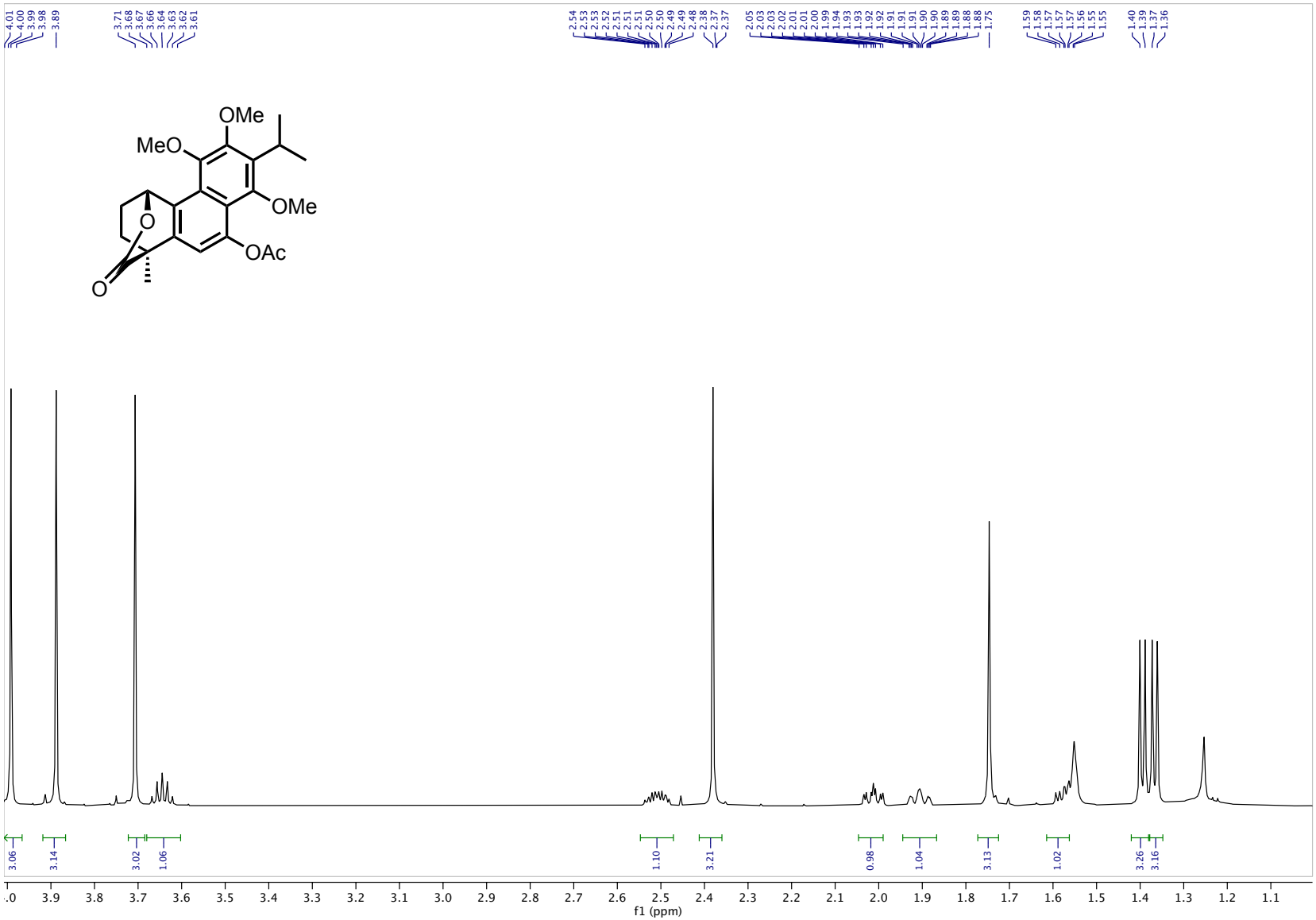

Figure A.109. ^{1}H NMR (600 MHz, $CDCl_3$) lactone **1.72** (4.0 – 1.0 ppm inset)

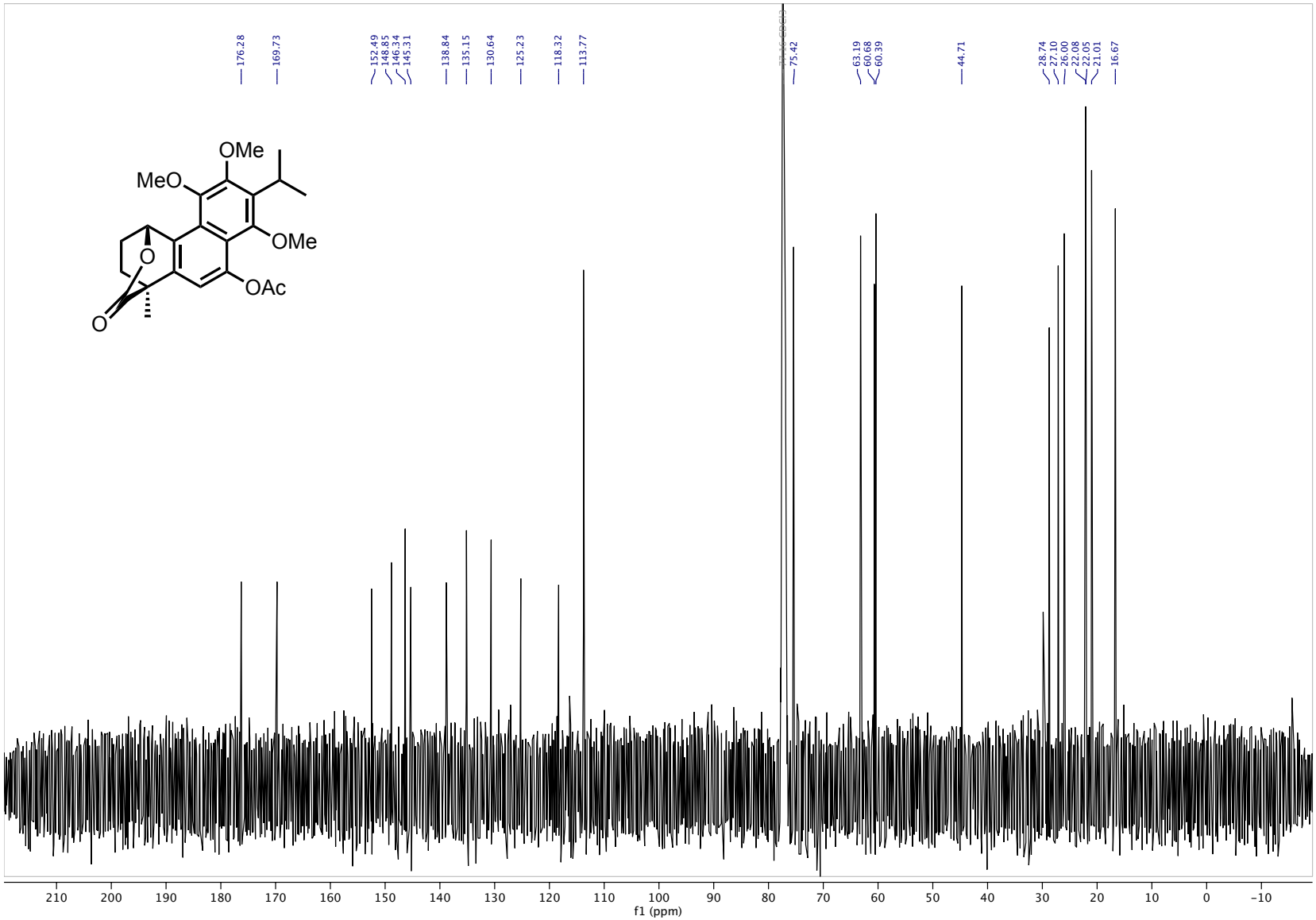

Figure A.110. ^{13}C NMR (151 MHz, $CDCl_3$) lactone **1.72**

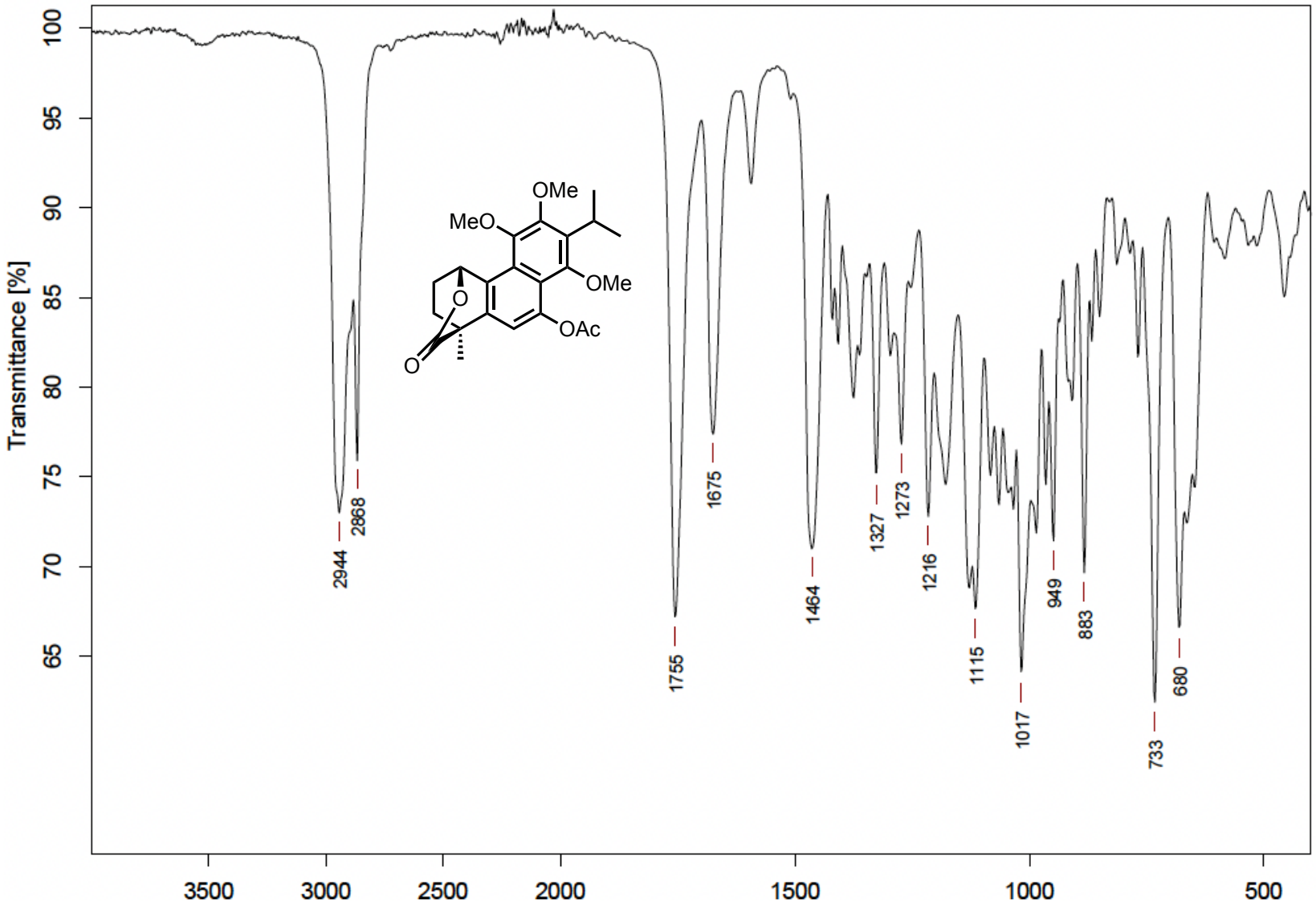

Figure A.111. FTIR (thin film) lactone **1.72**

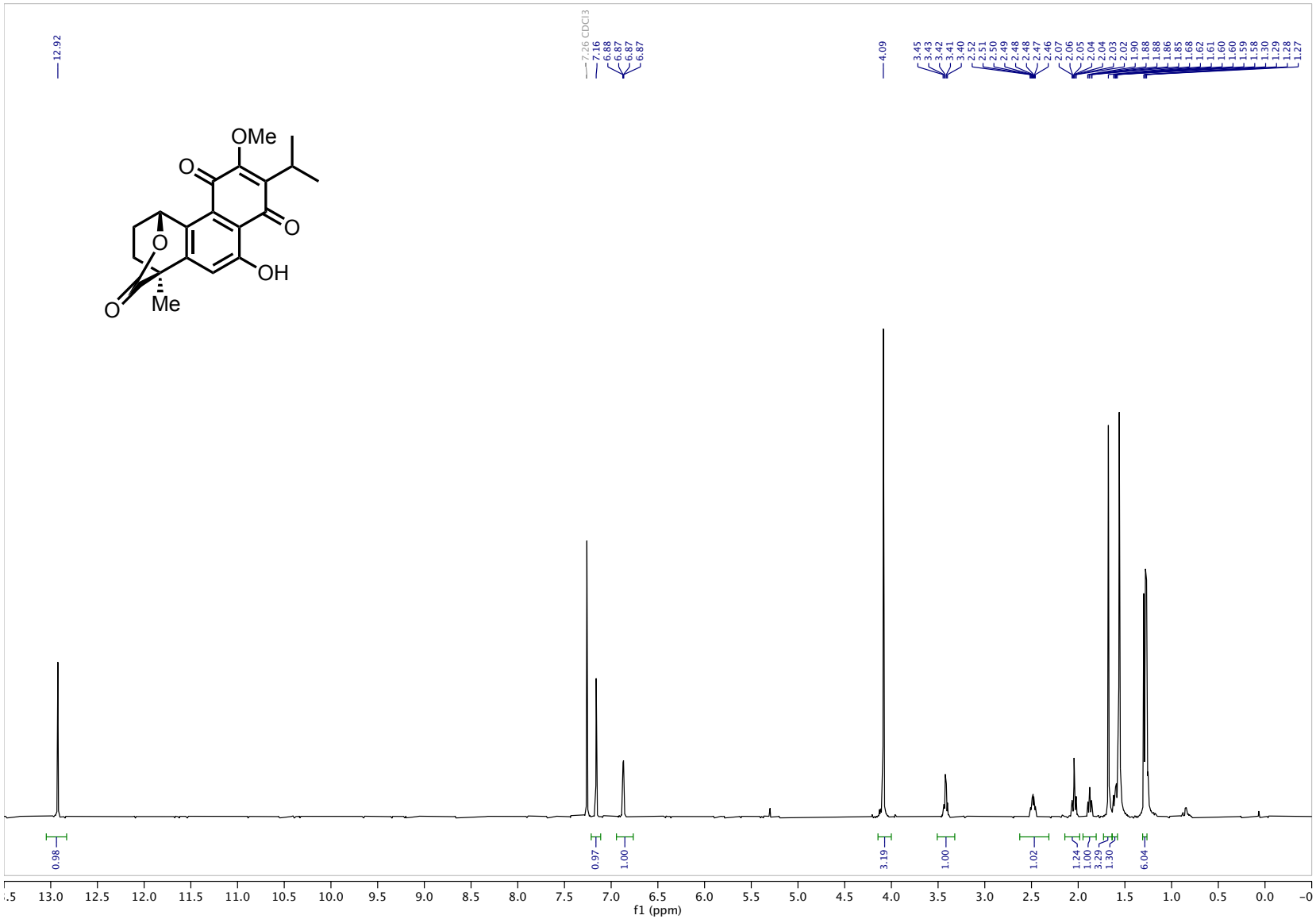

Figure A.112. ^{1}H NMR (600 MHz, $CDCl_3$) dracocequinone B **1.05**

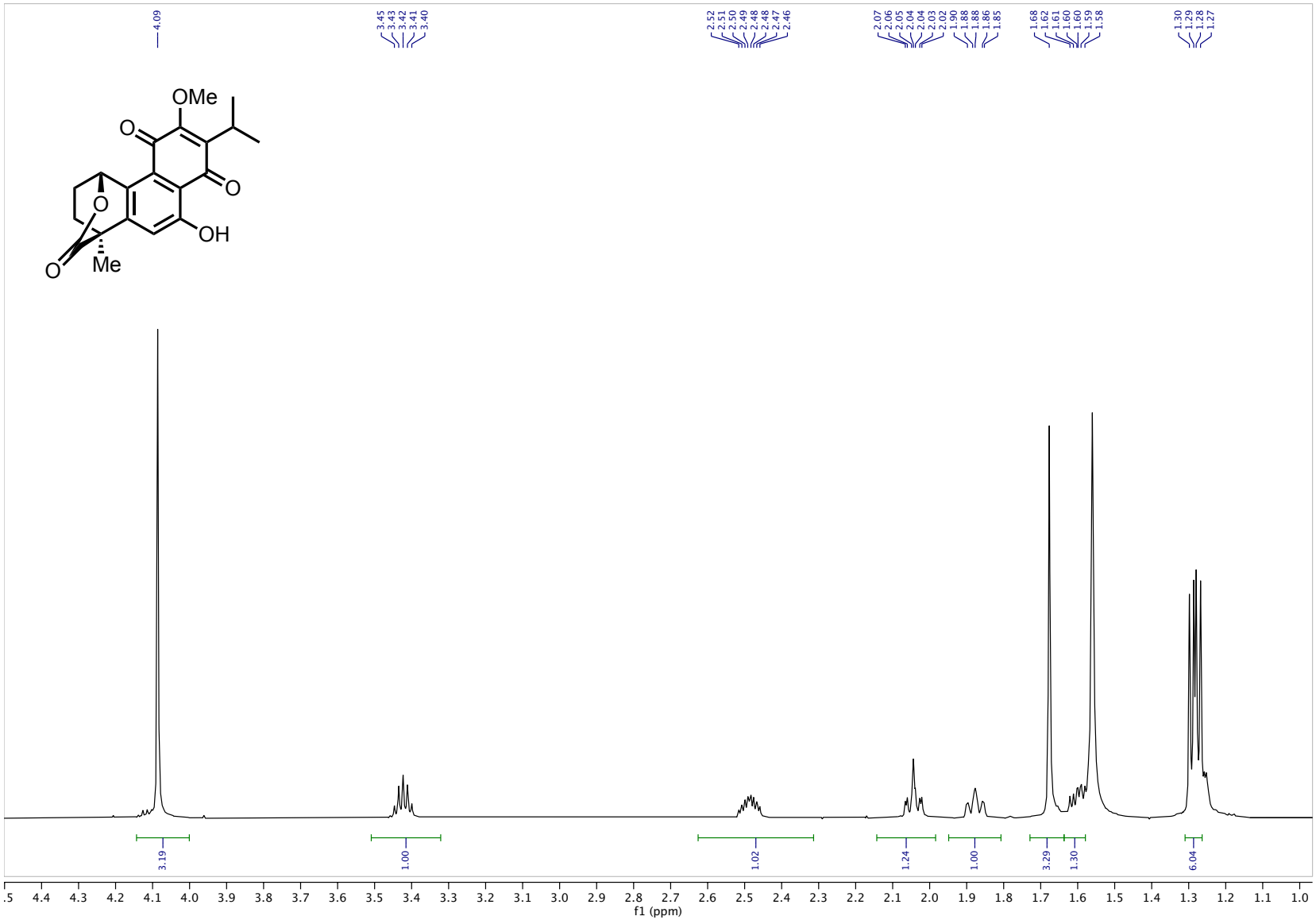

Figure A.113. ^{1}H NMR (600 MHz, $CDCl_3$) dracocequinone B **1.05** (4.5 – 1.0 ppm inset)

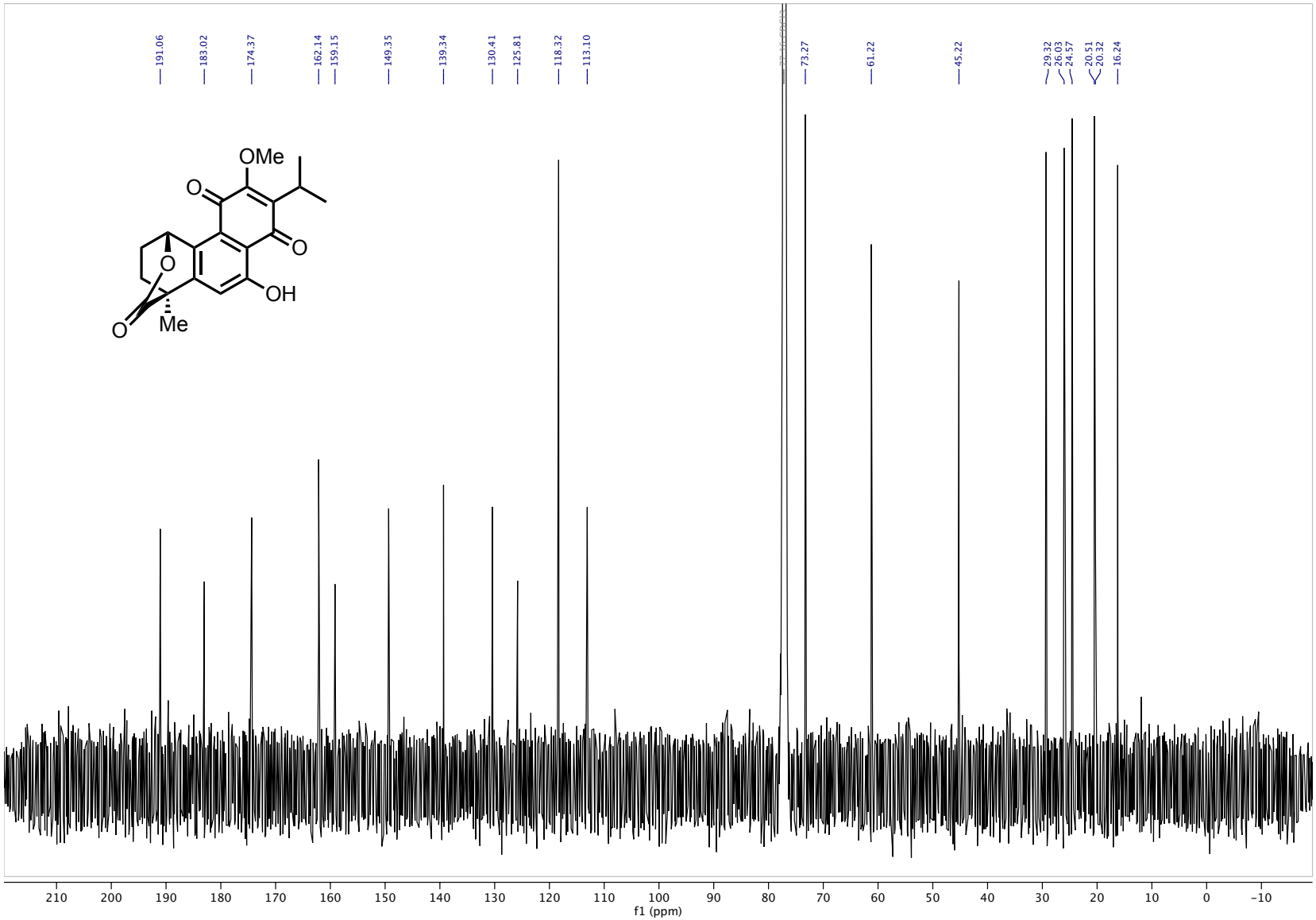

Figure A.114. ^{13}C NMR (151 MHz, $CDCl_3$) dracocequinone B **1.05**

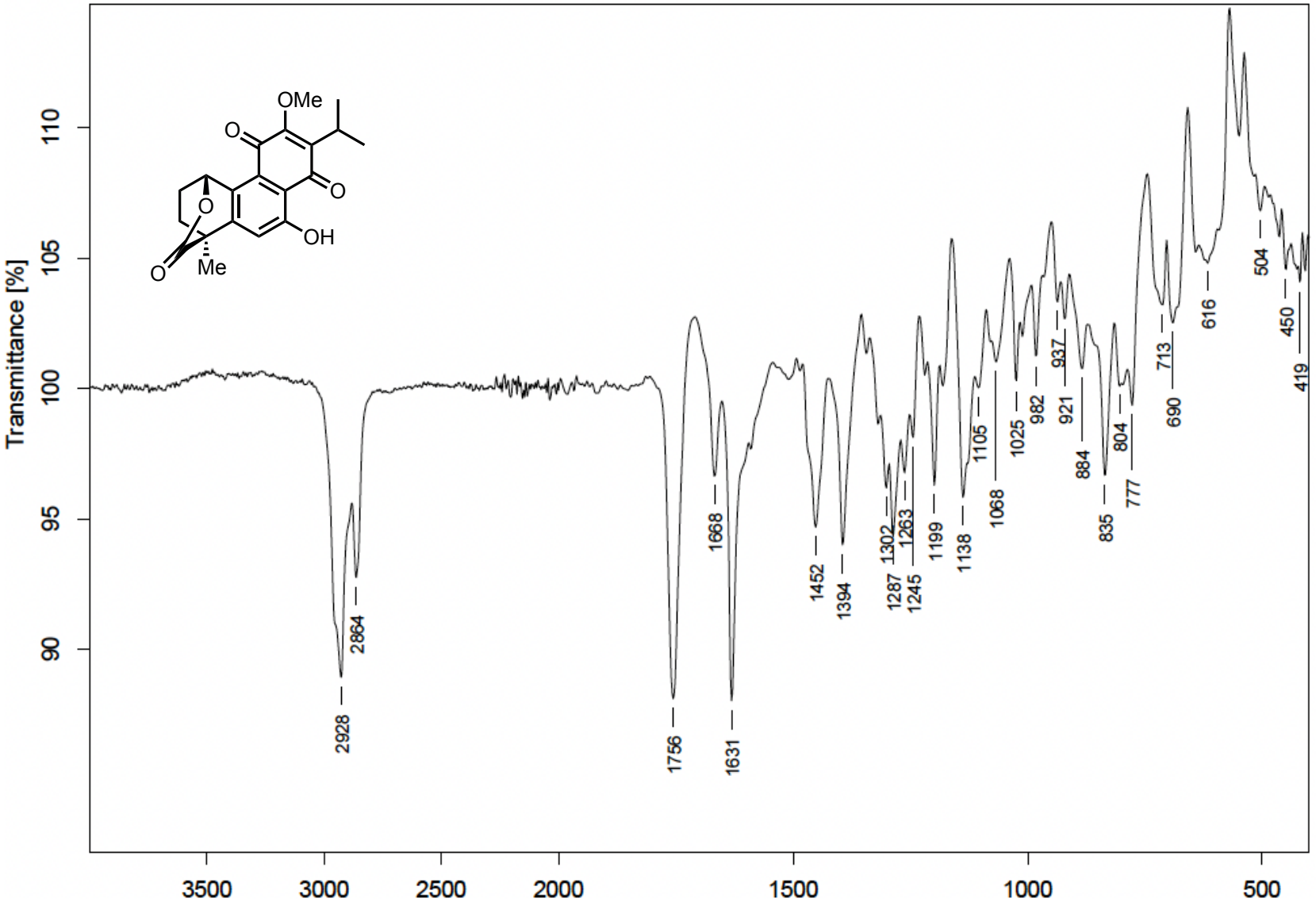

Figure A.115. FTIR (neat) dracocequinone B **1.05**

APPENDIX B

Spectral Data for Chapter Two

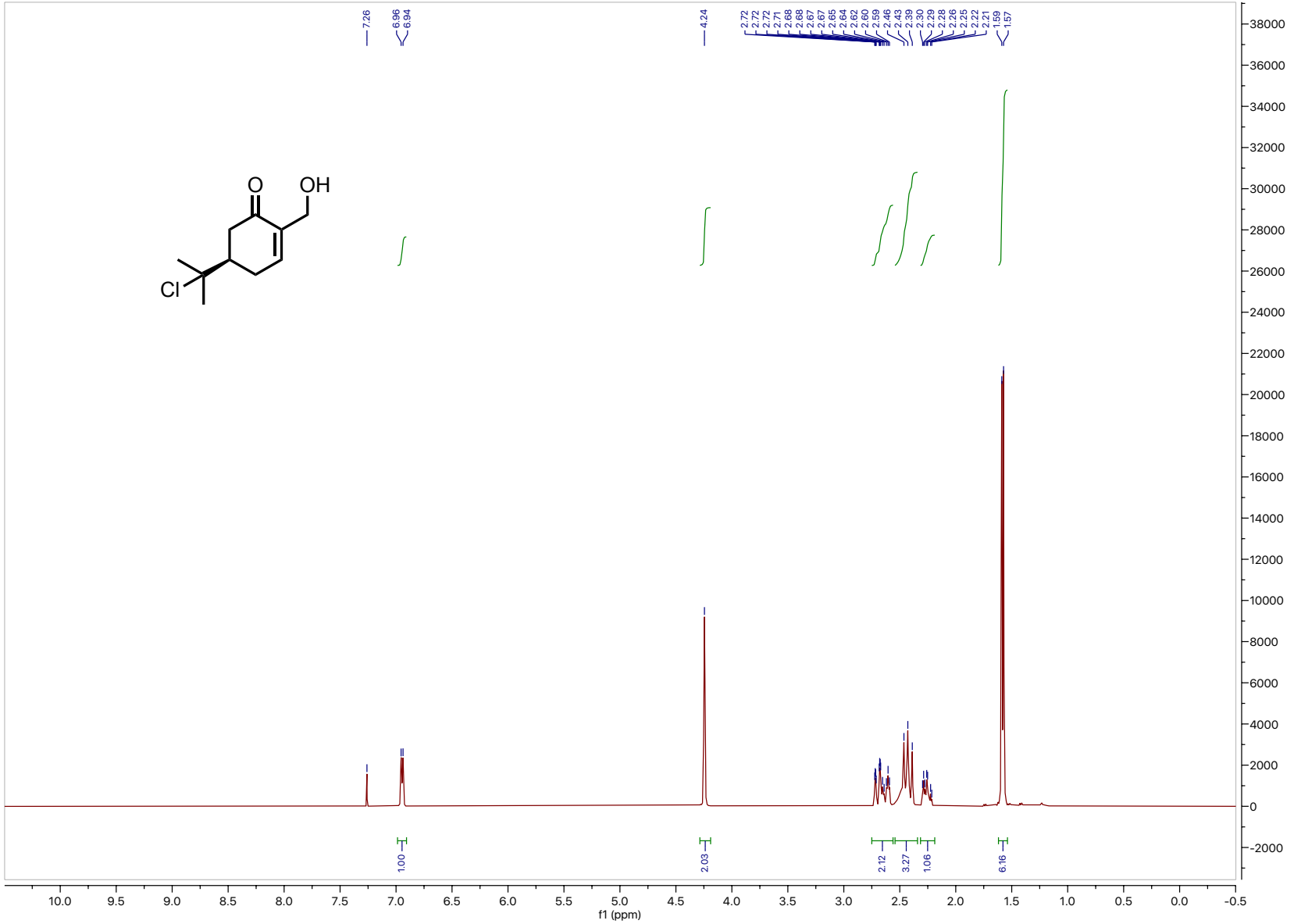

Figure B.01. ^{1}H NMR (400 MHz, $CDCl_3$) tertiary chloride **2.36**

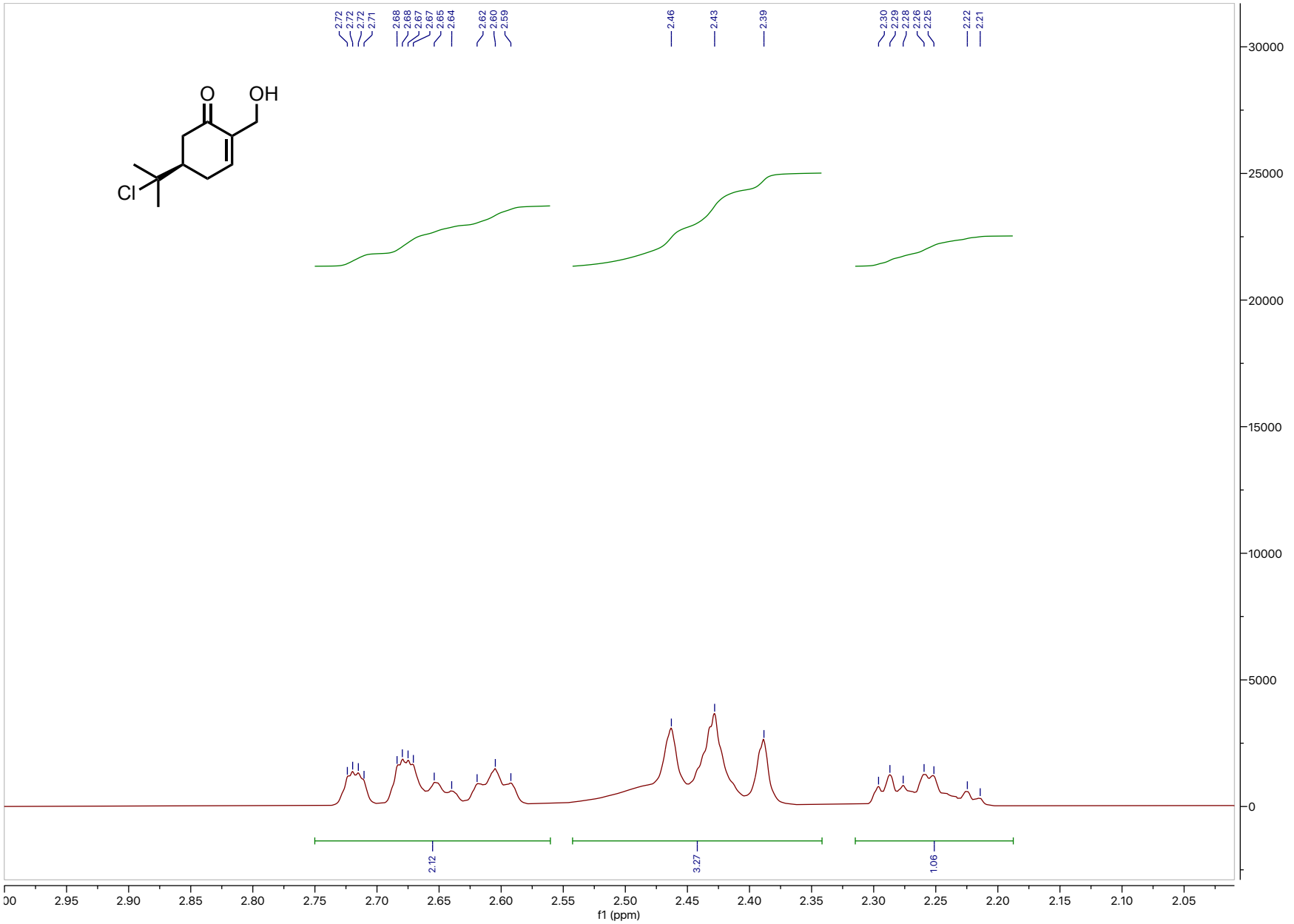

Figure B.02. ^{1}H NMR (400 MHz, $CDCl_3$) tertiary chloride **2.36** (3.0 – 2.0 ppm inset)

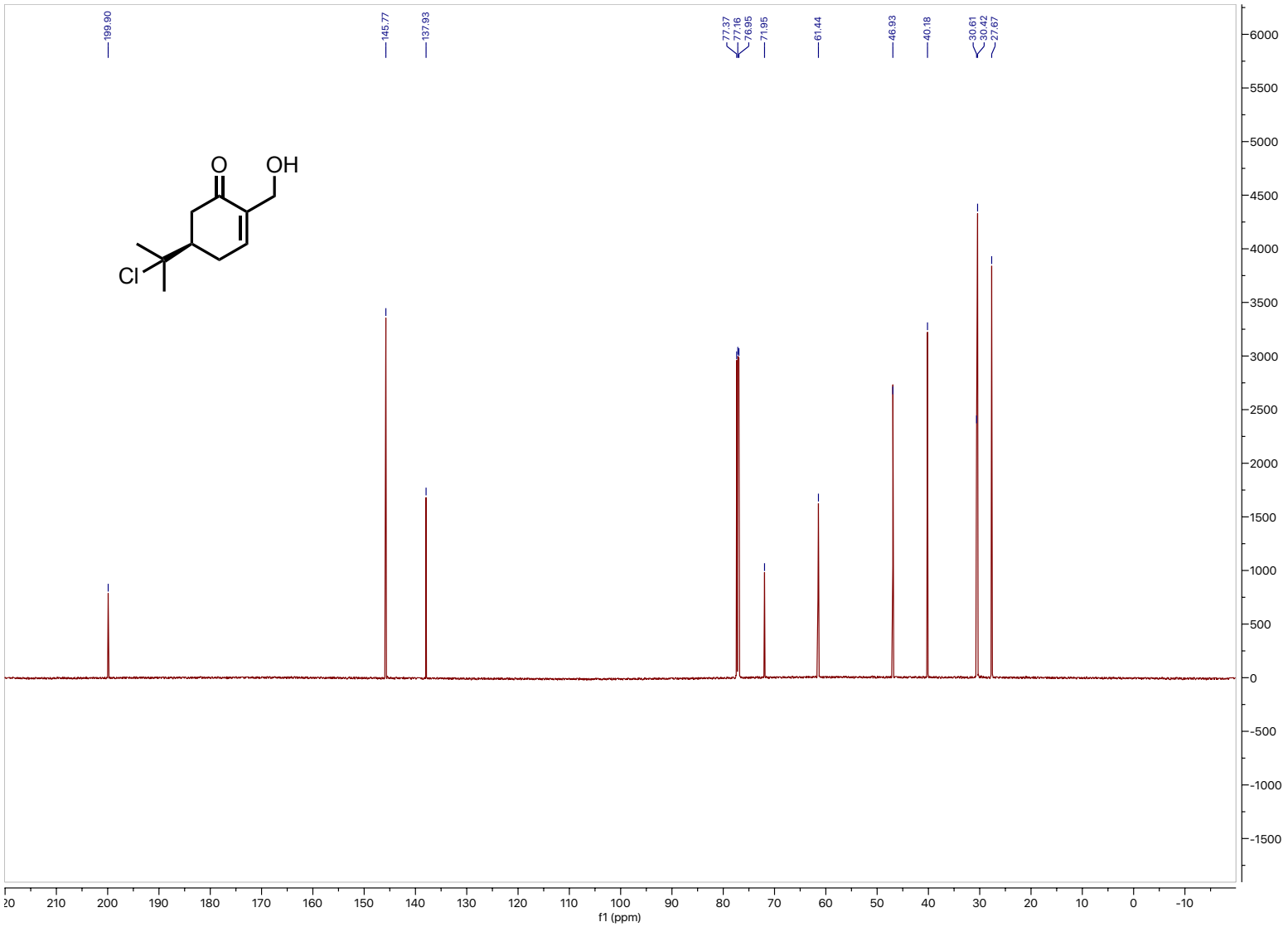

Figure B.03. ^{13}C NMR (151 MHz, $CDCl_3$) tertiary chloride **2.36**

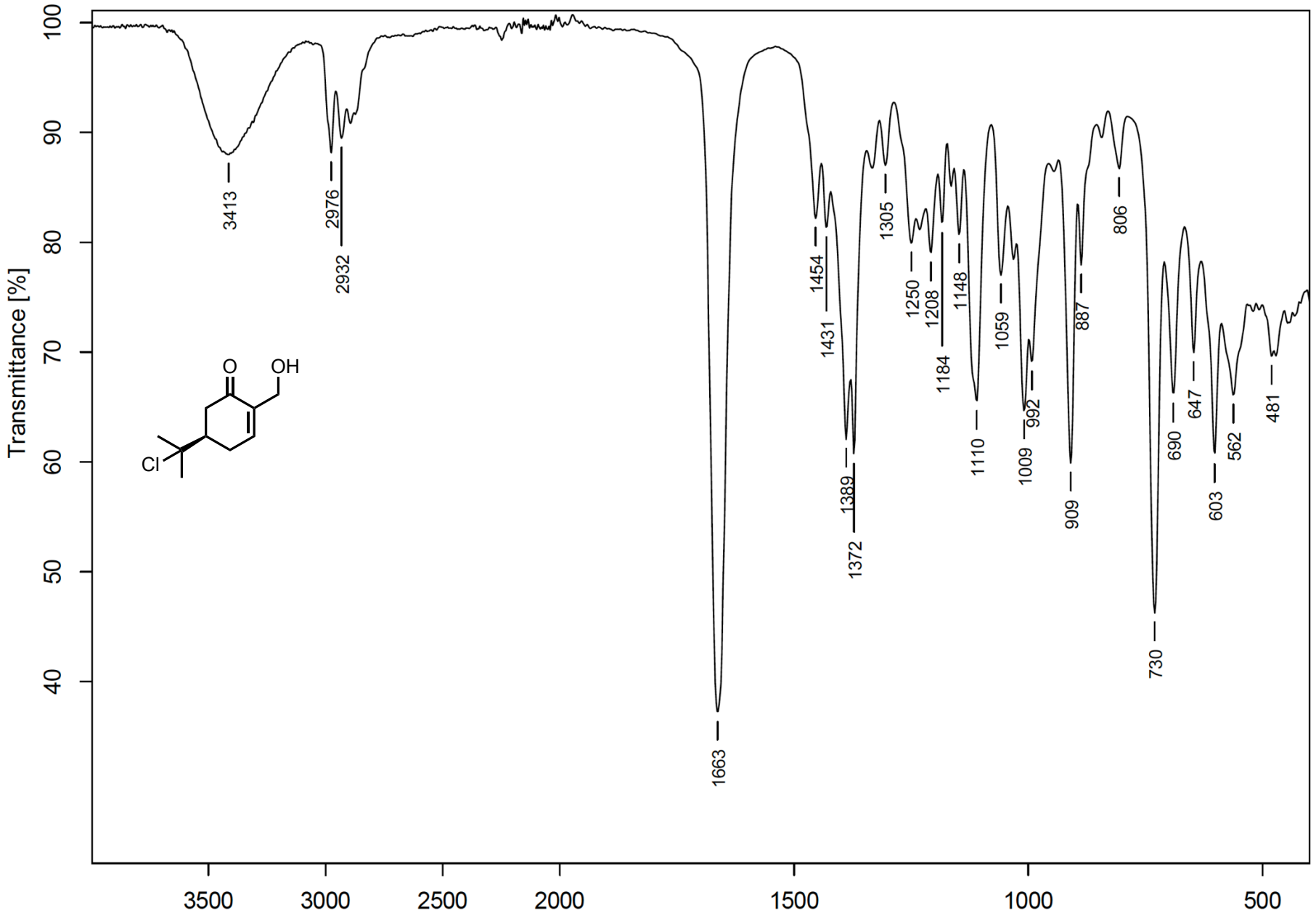

Figure B.04. FTIR (neat) tertiary chloride **2.36**

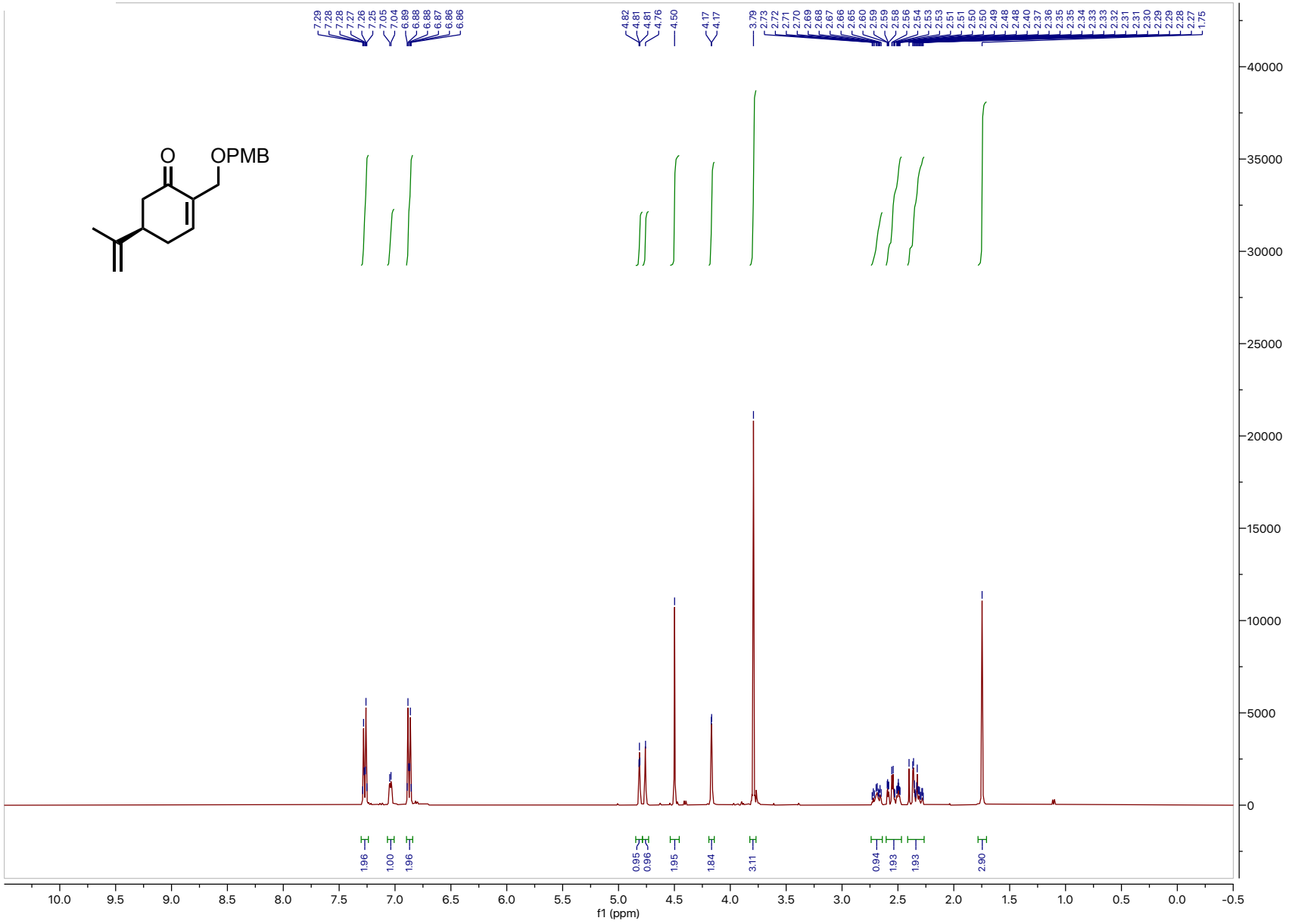

Figure B.05. ^{1}H NMR (400 MHz, $CDCl_3$) (*R*)-7-*para*-methoxybenzyloxycarvone **2.39**

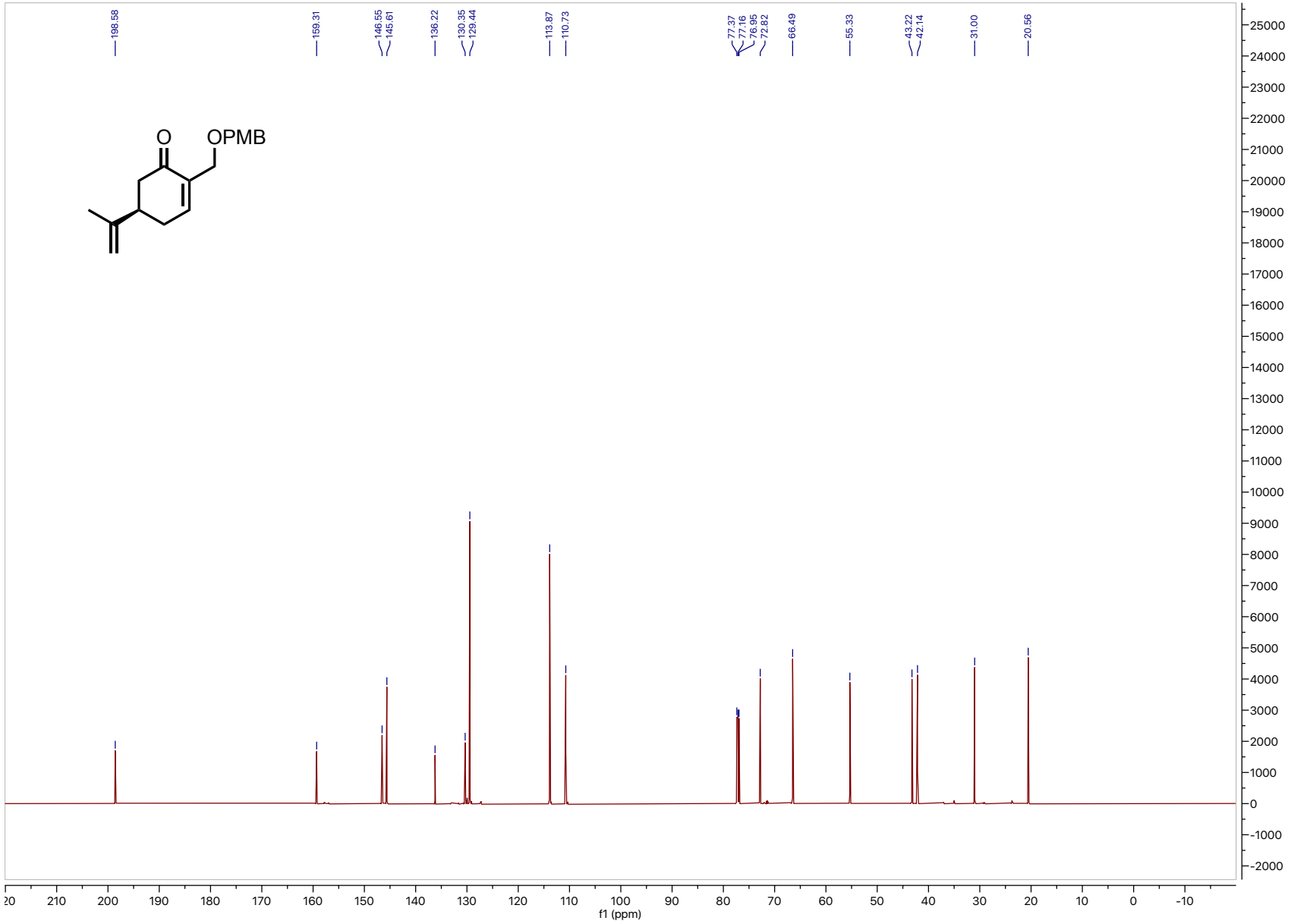

Figure B.06. ^{13}C NMR (151 MHz, $CDCl_3$) (*R*)-7-*para*-methoxybenzyloxycarvone **2.39**

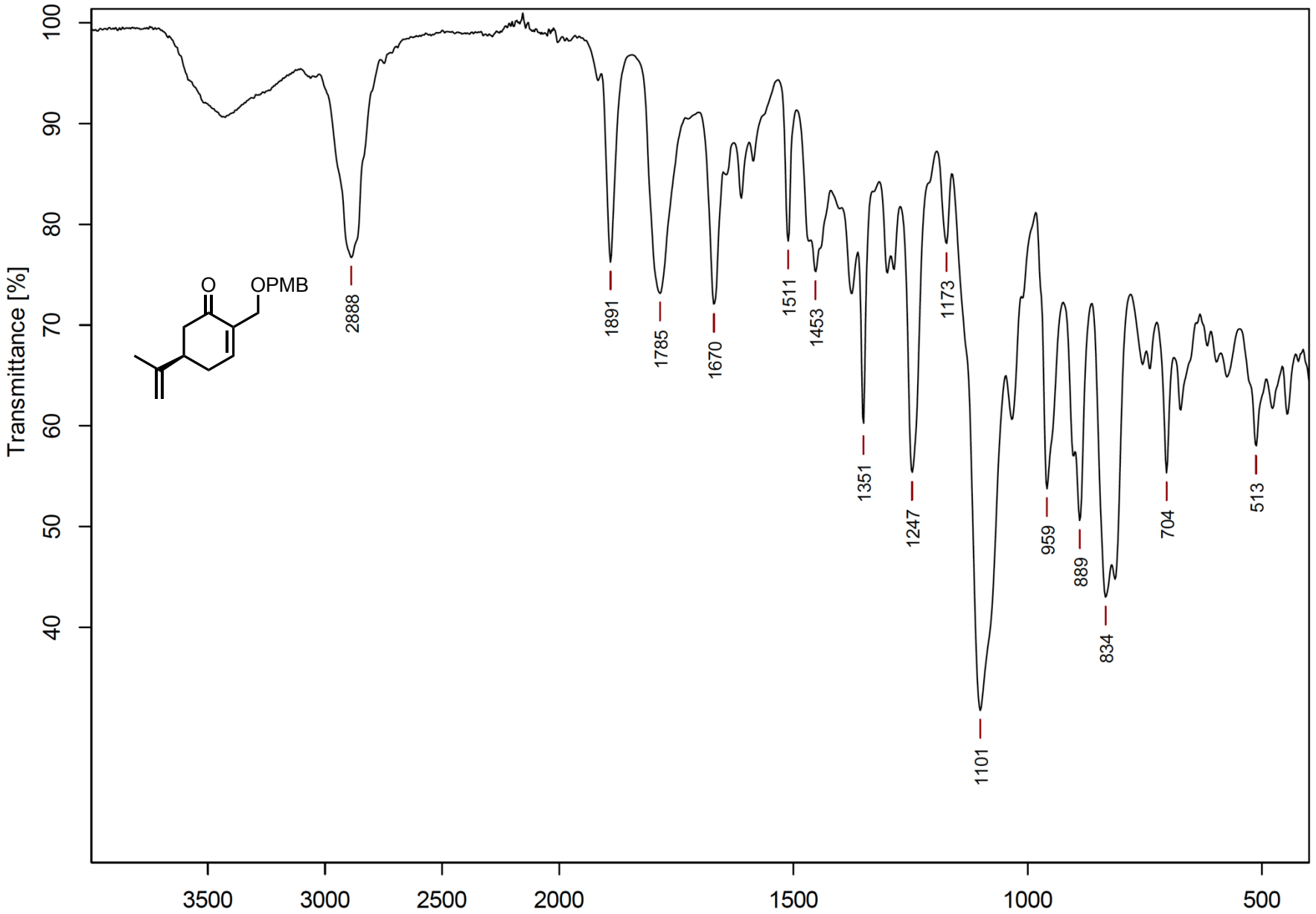

Figure B.07. FTIR (neat) (*R*)-7-*para*-methoxybenzyloxycarvone **2.39**

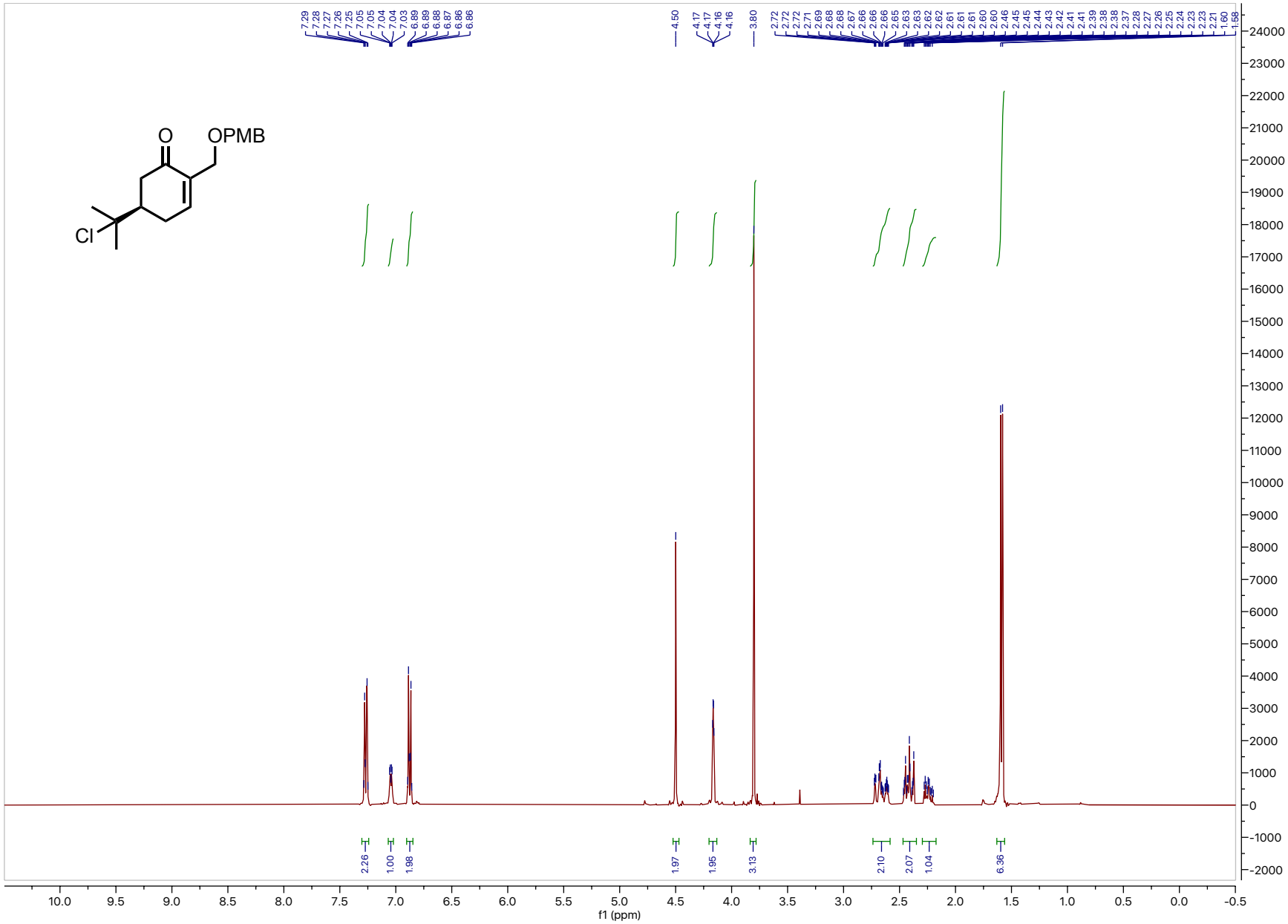

Figure B.08. ^{1}H NMR (400 MHz, $CDCl_3$) tertiary chloride **2.38**

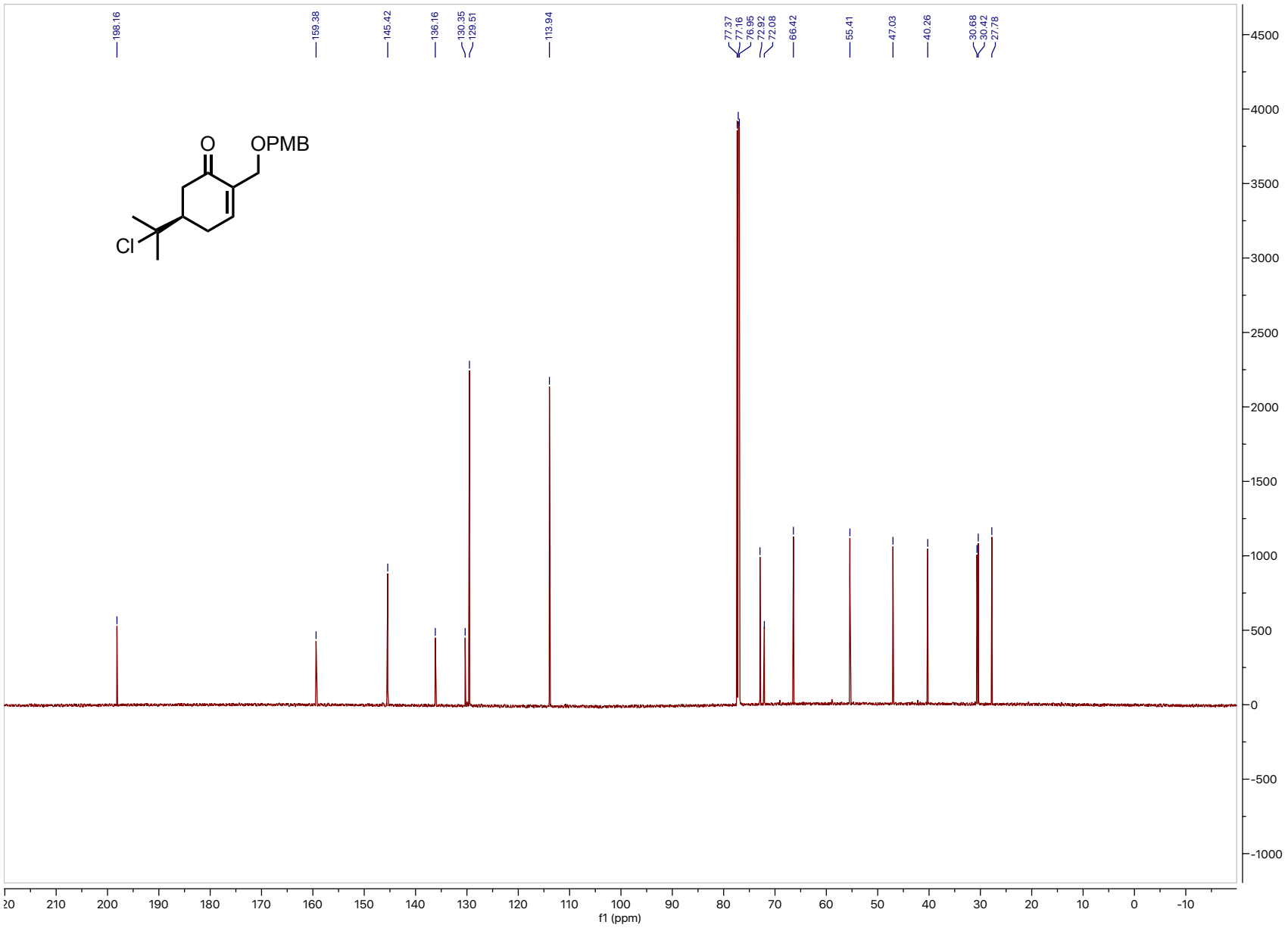

Figure B.09. ^{13}C NMR (151 MHz, $CDCl_3$) tertiary chloride **2.38**

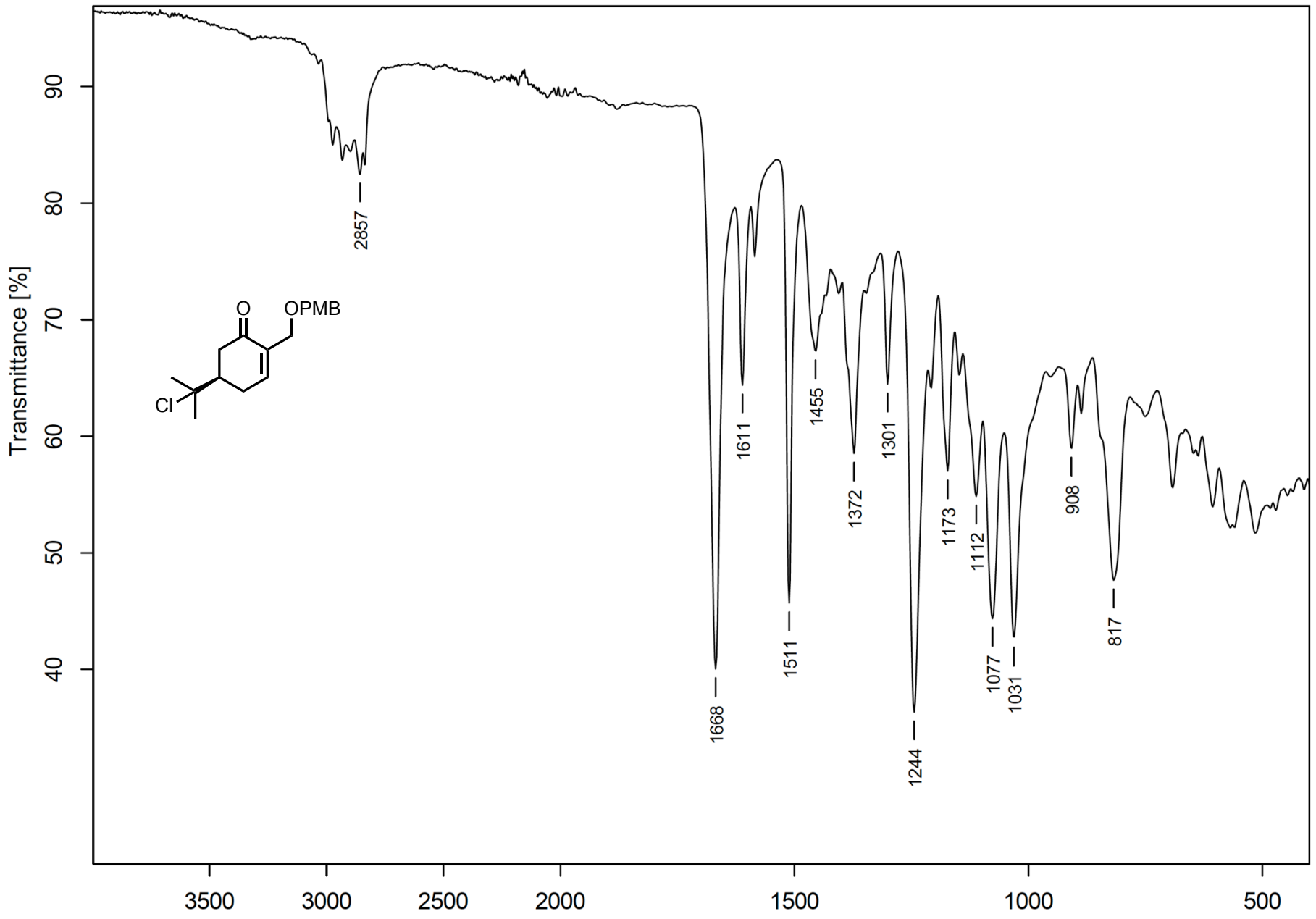

Figure B.10. FTIR (neat) tertiary chloride **2.38**

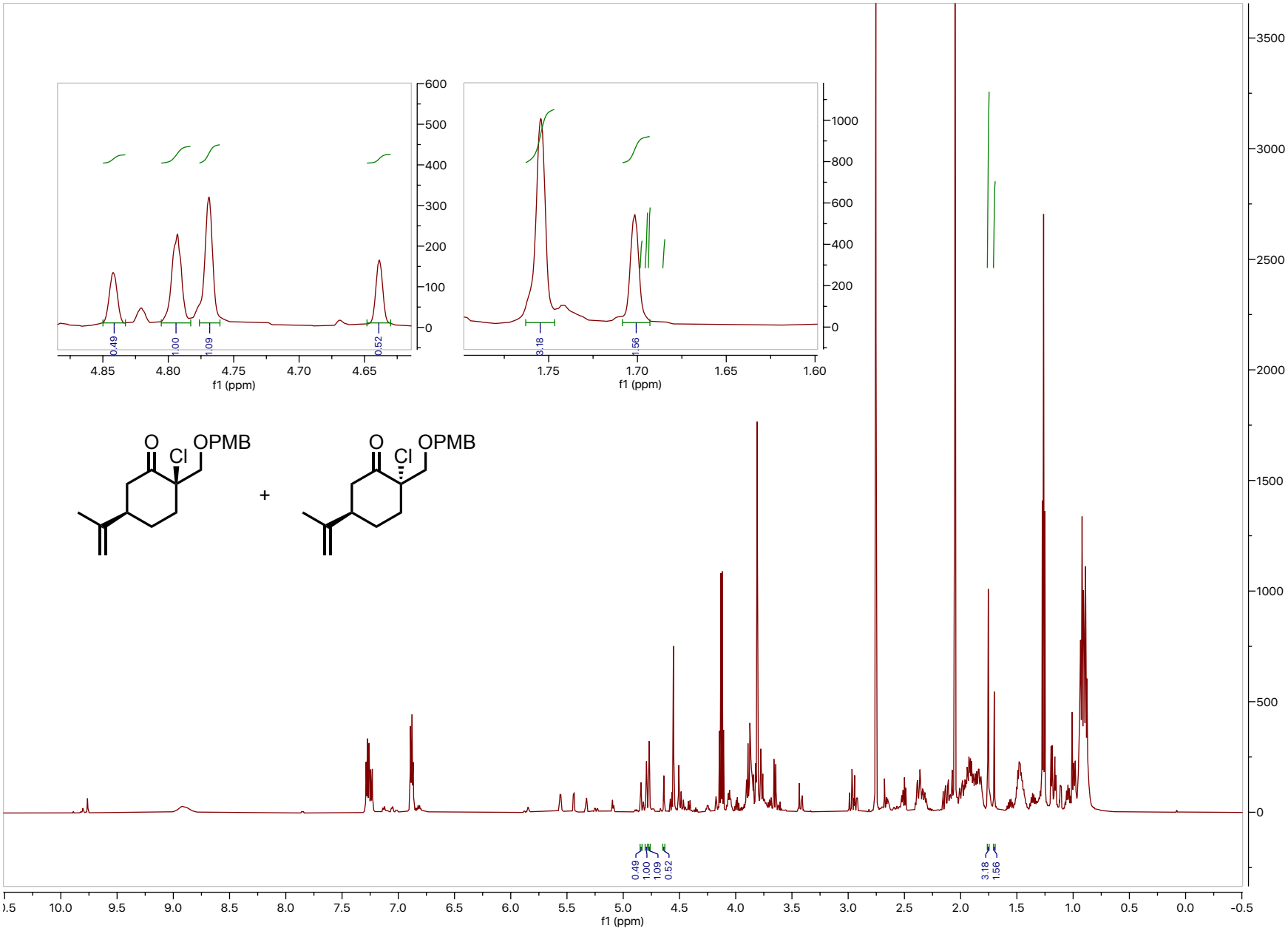

Figure B.11. Crude ^{1}H NMR (400 MHz, $CDCl_3$) chloroketone **2.14**

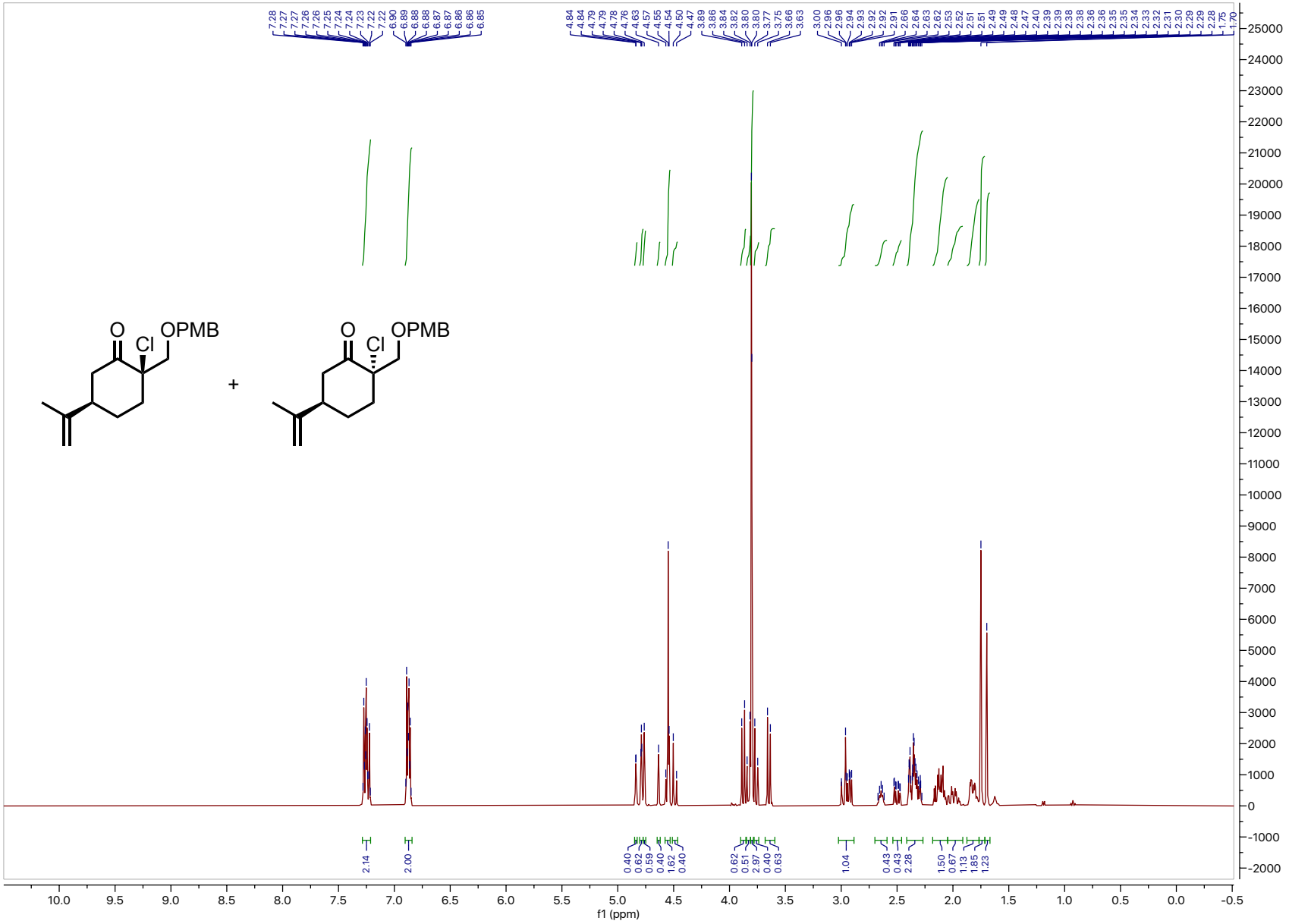

Figure B.12. ^{1}H NMR (400 MHz, $CDCl_3$) chloroketone **2.14**

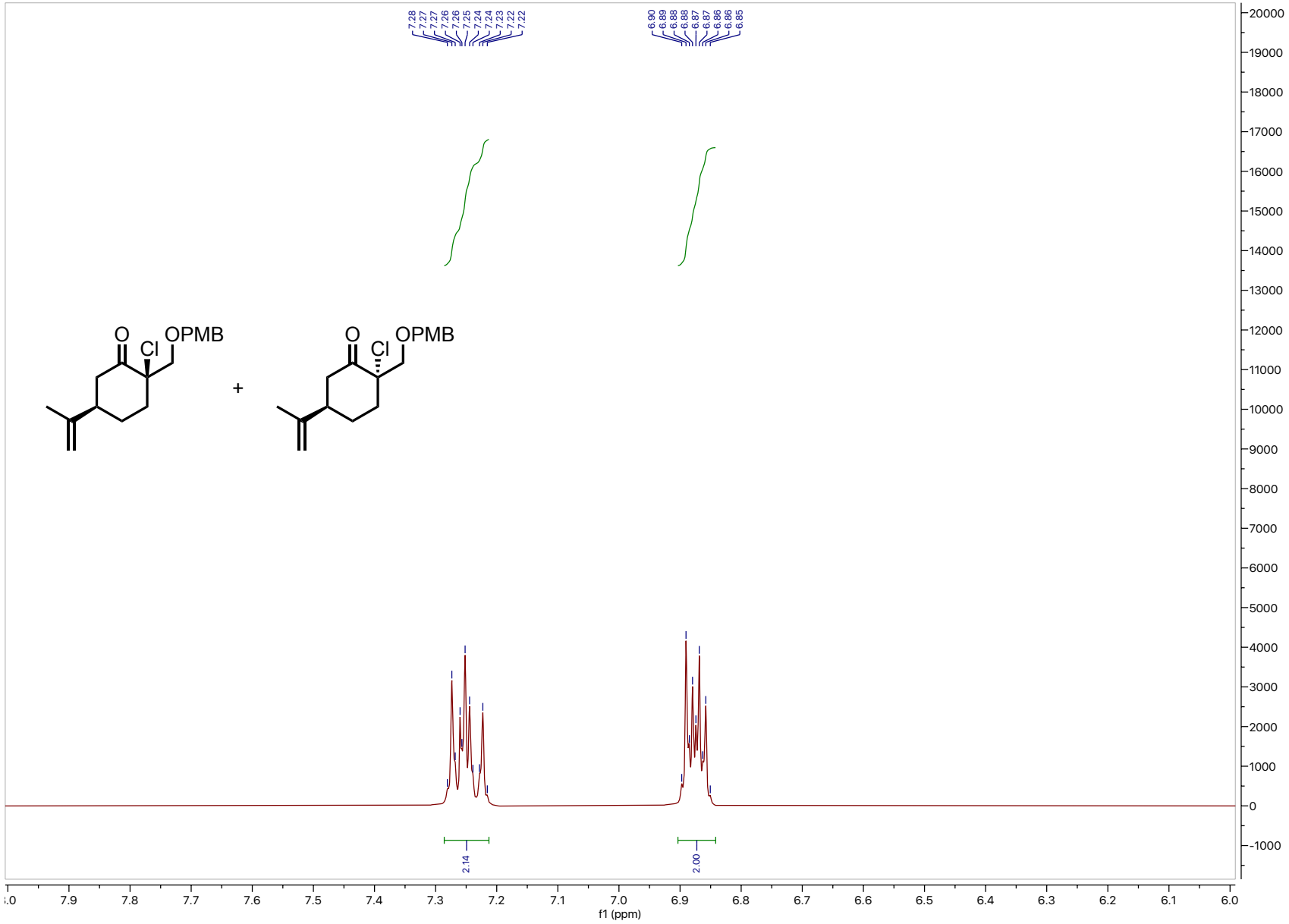

Figure B.13. ^{1}H NMR (400 MHz, $CDCl_3$) chloroketone **2.14** (8.0 – 6.0 ppm inset)

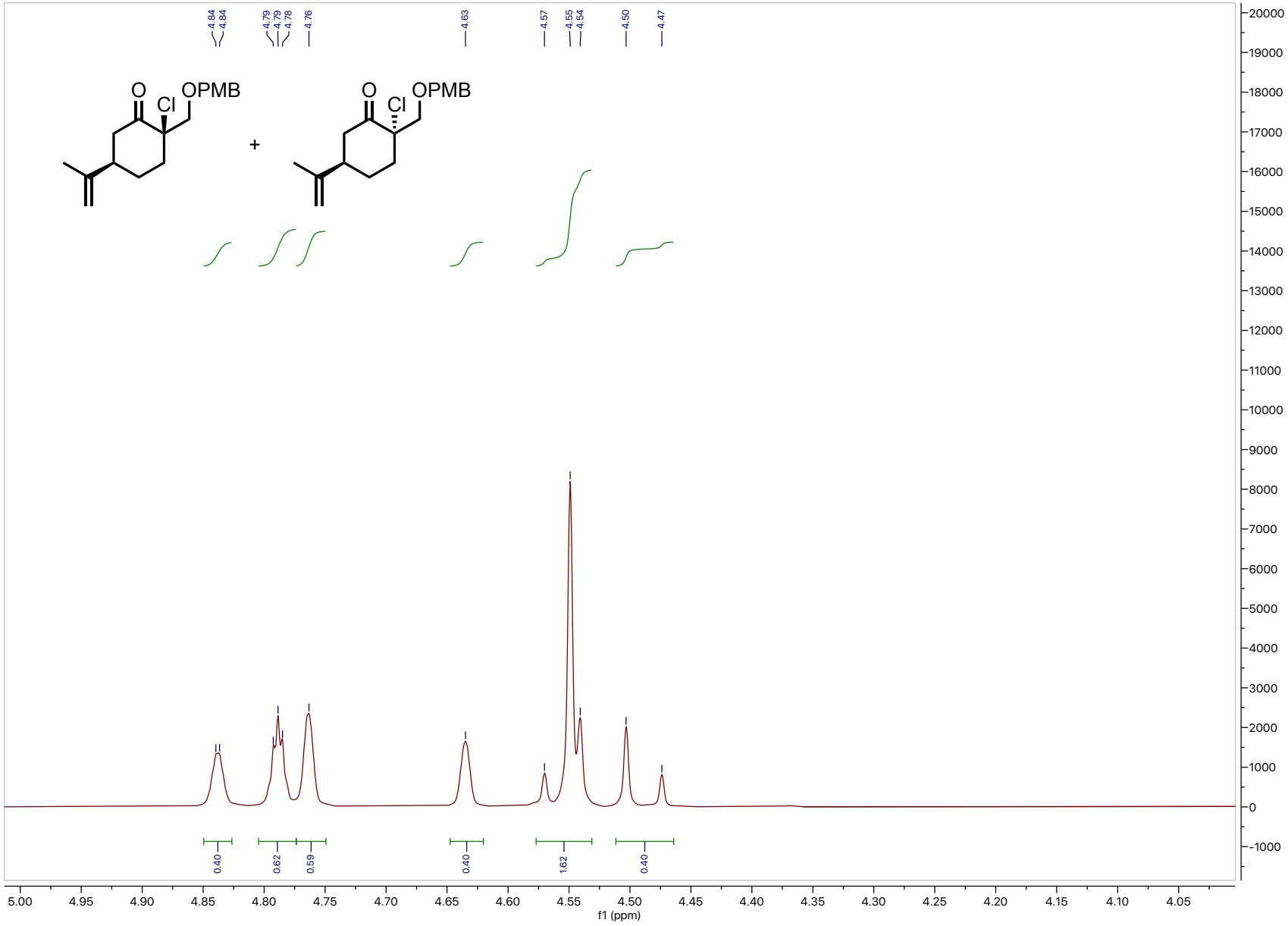

Figure B.14. ^{1}H NMR (400 MHz, $CDCl_3$) chloroketone **2.14** (5.0 – 4.0 ppm inset)

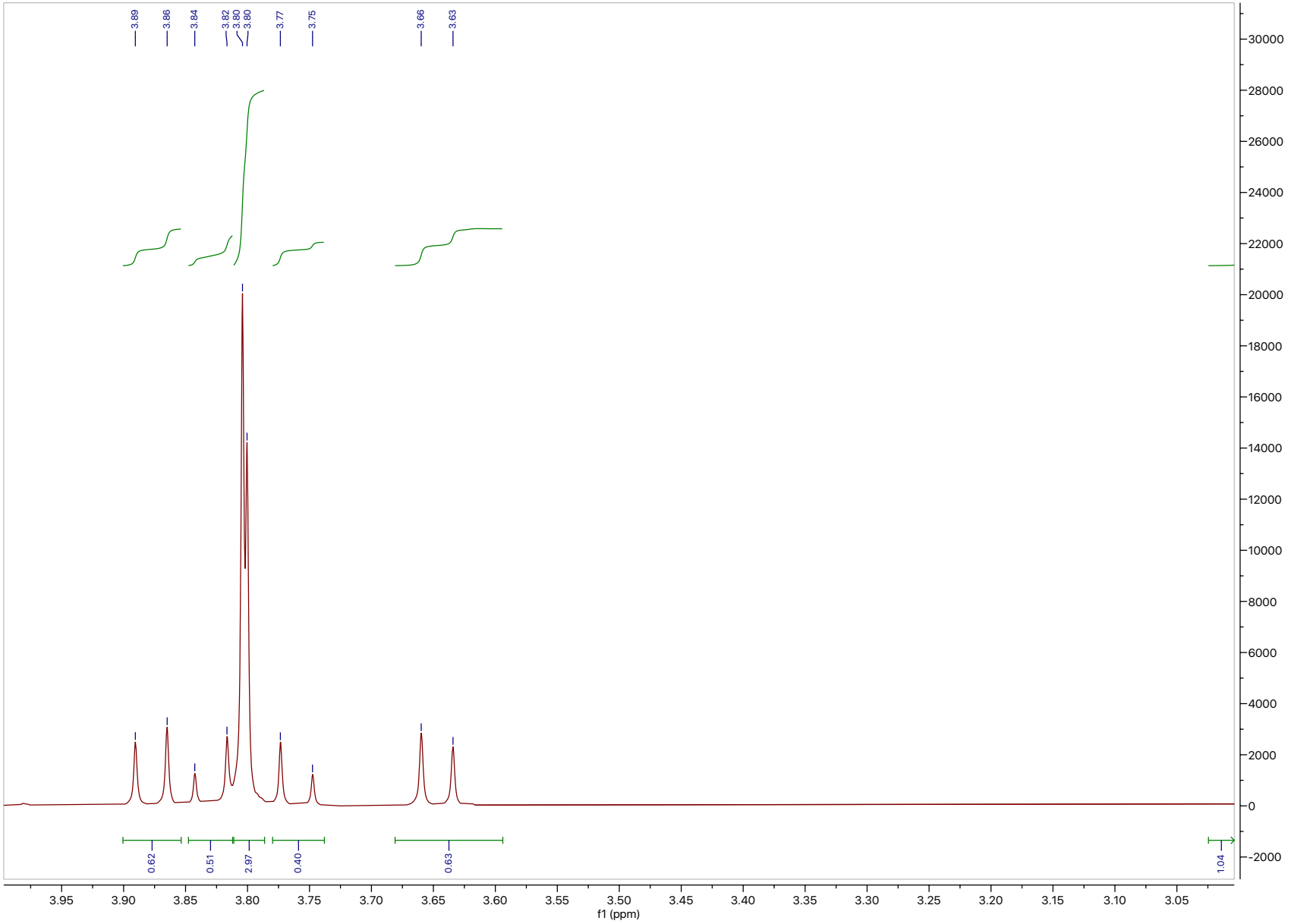

Figure B.15. ^{1}H NMR (400 MHz, $CDCl_3$) chloroketone **2.14** (4.0 – 3.0 ppm inset)

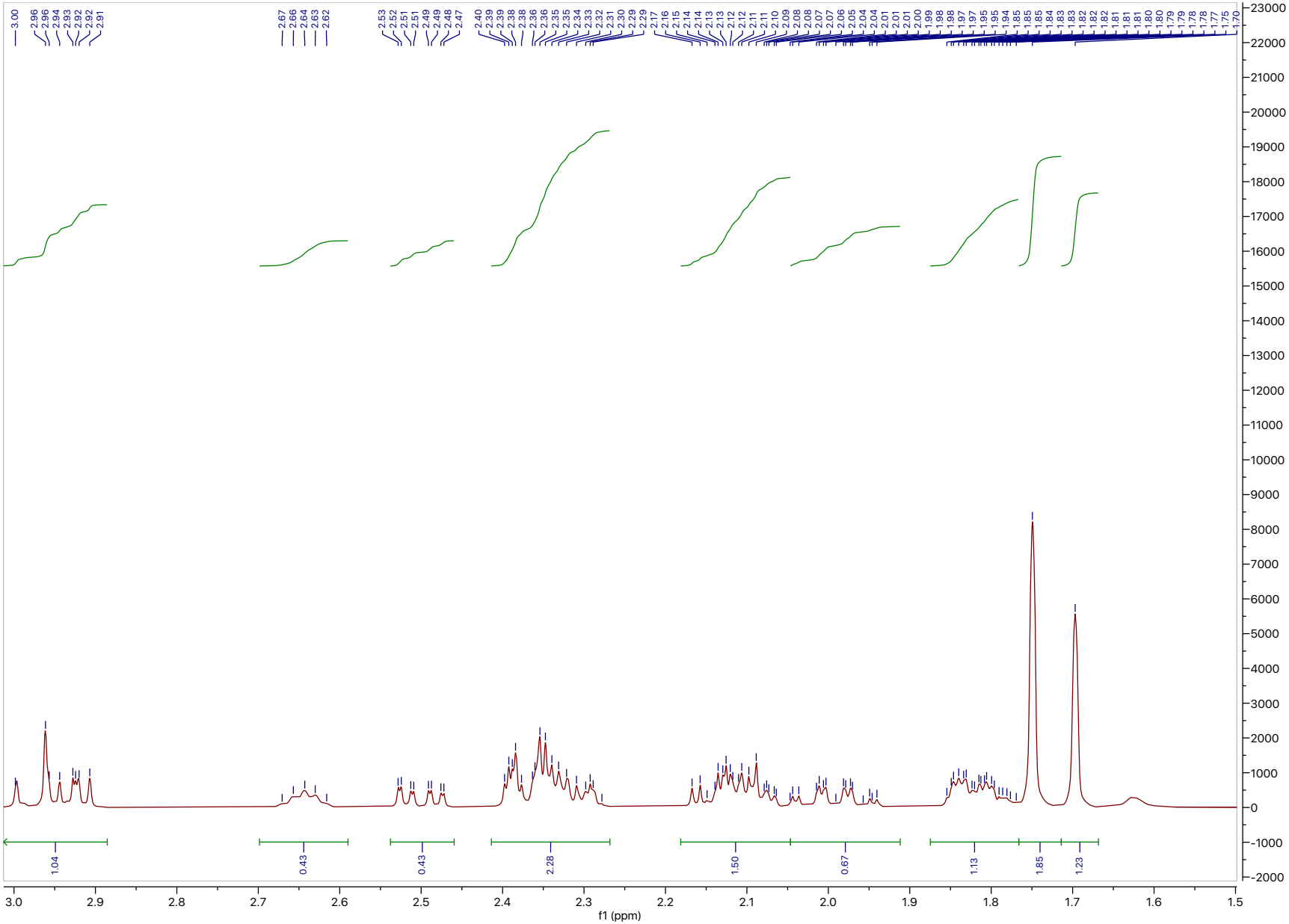

Figure B.16. ^{1}H NMR (400 MHz, $CDCl_3$) chloroketone **2.14** (3.0 – 1.5 ppm inset)

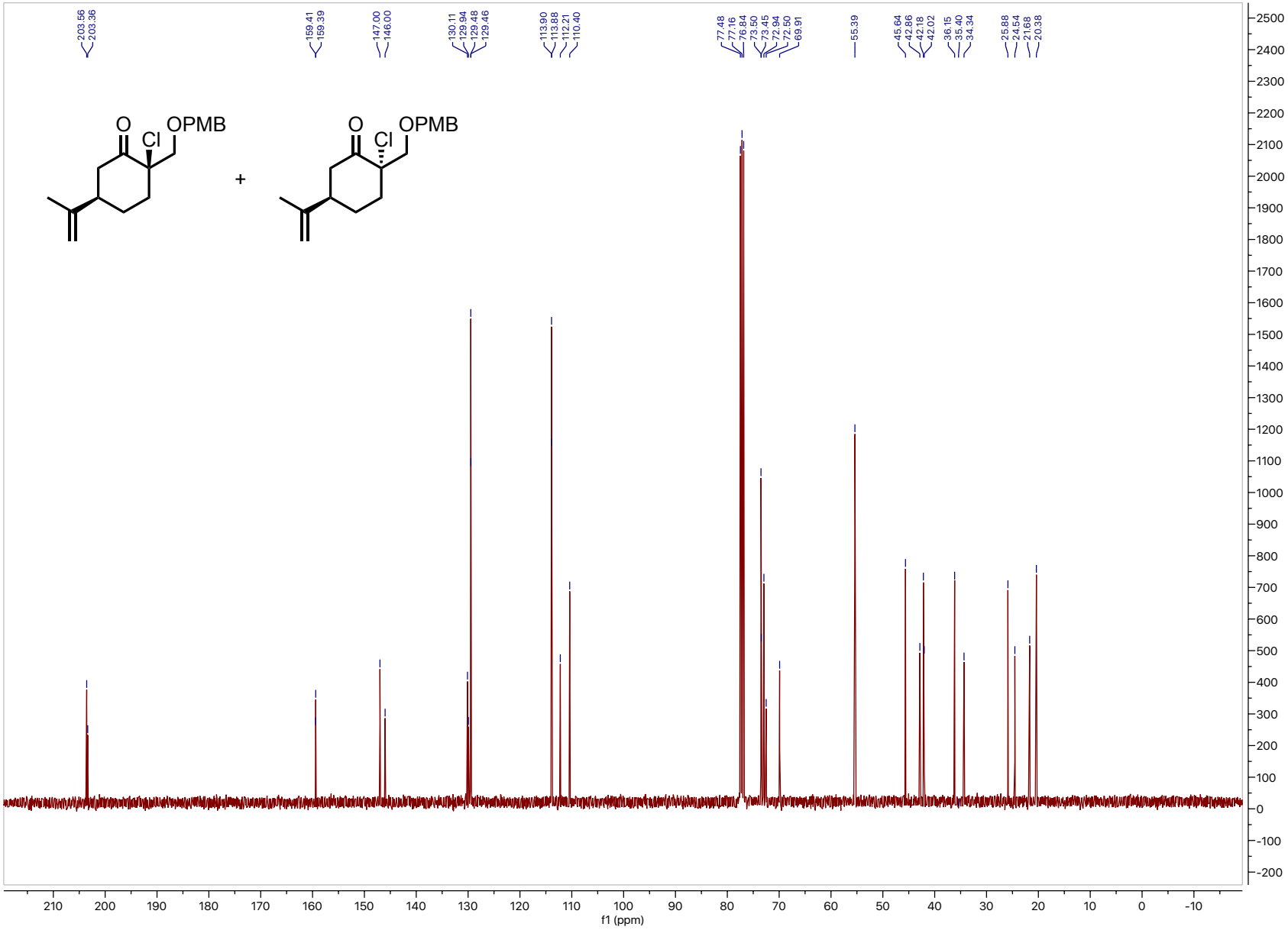

Figure B.17. ^{13}C NMR (101 MHz, $CDCl_3$) chloroketone **2.14**

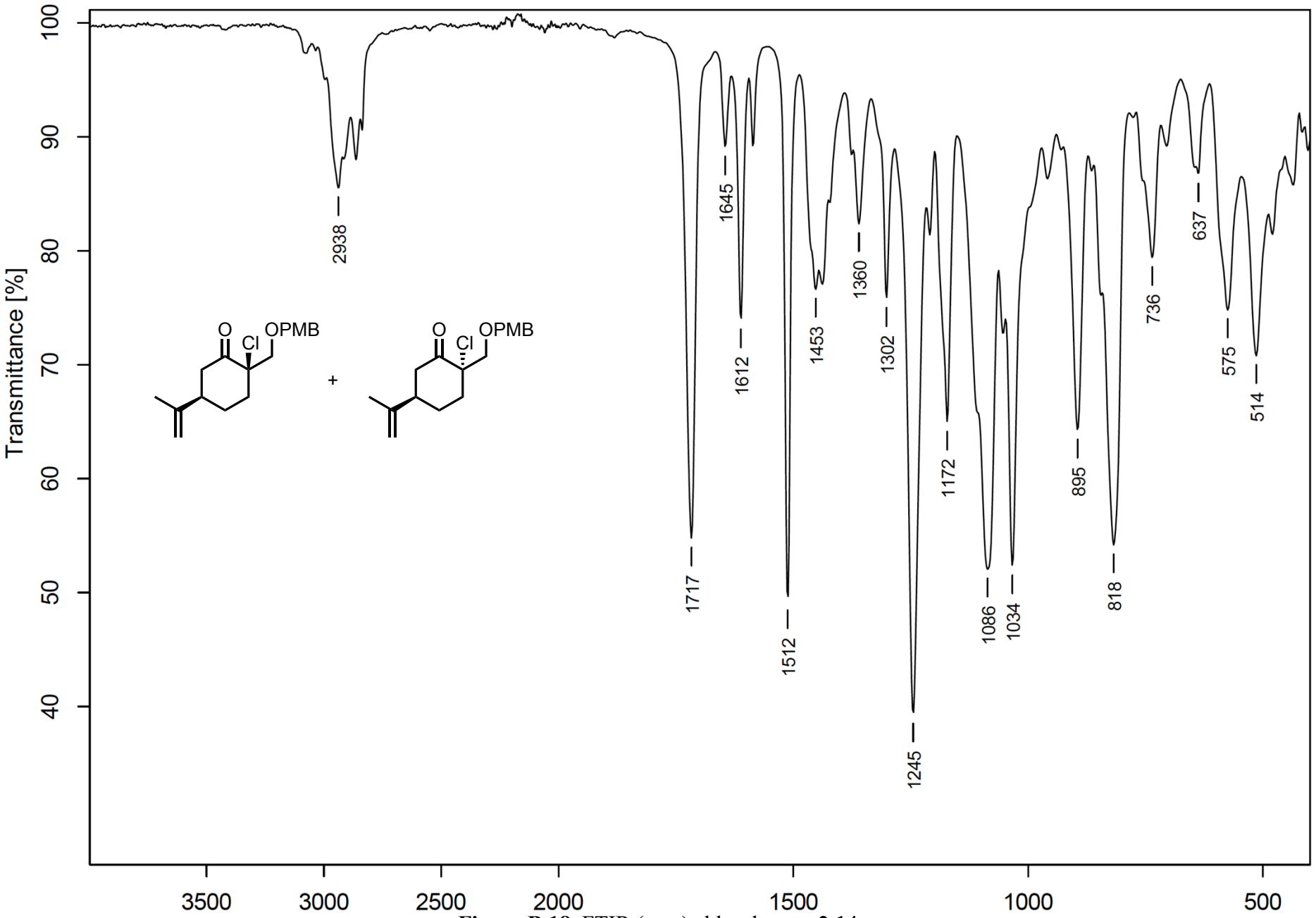

Figure B.18. FTIR (neat) chloroketone **2.14**

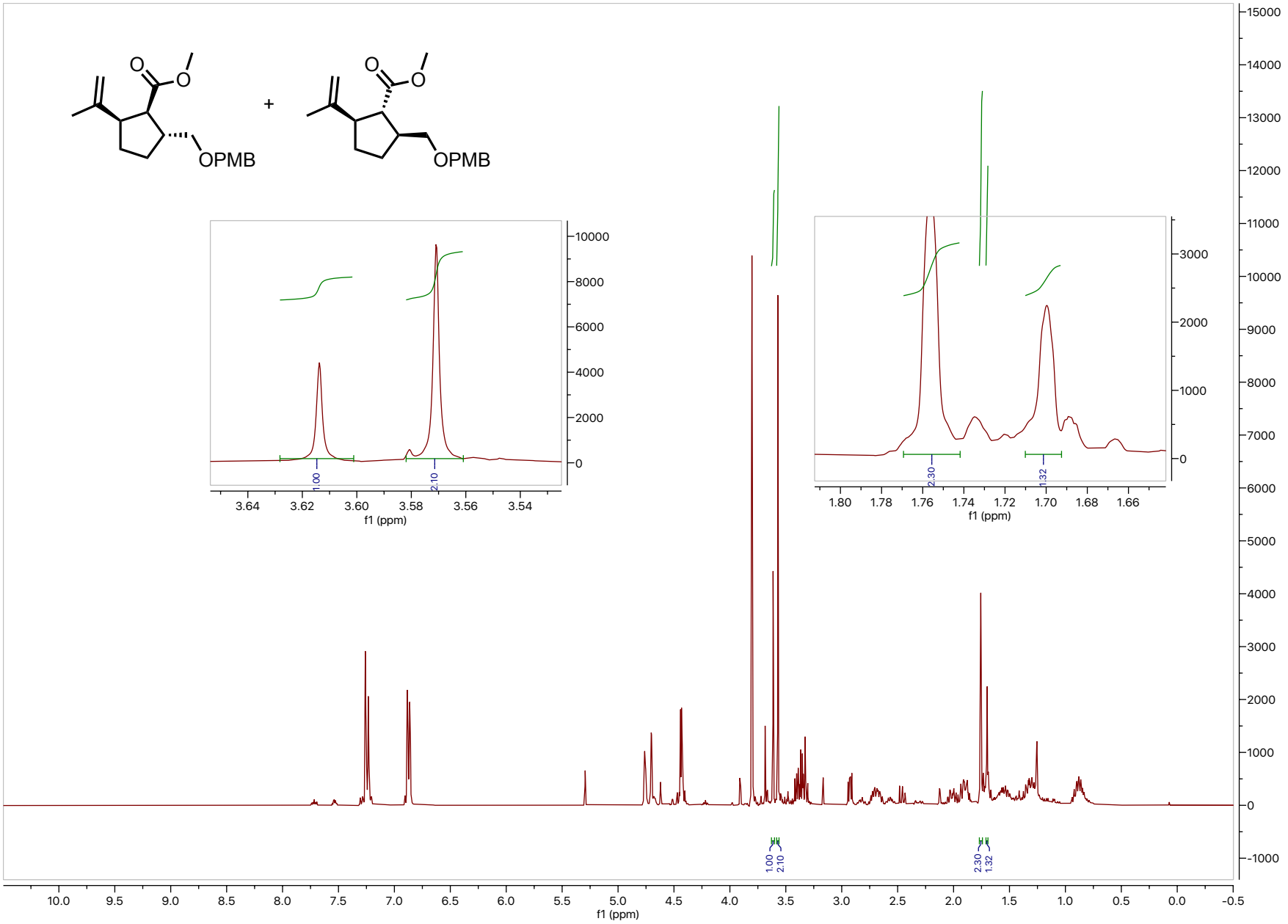

Figure B.19. Crude ^{1}H NMR (400 MHz, $CDCl_3$) methyl ester **2.13**

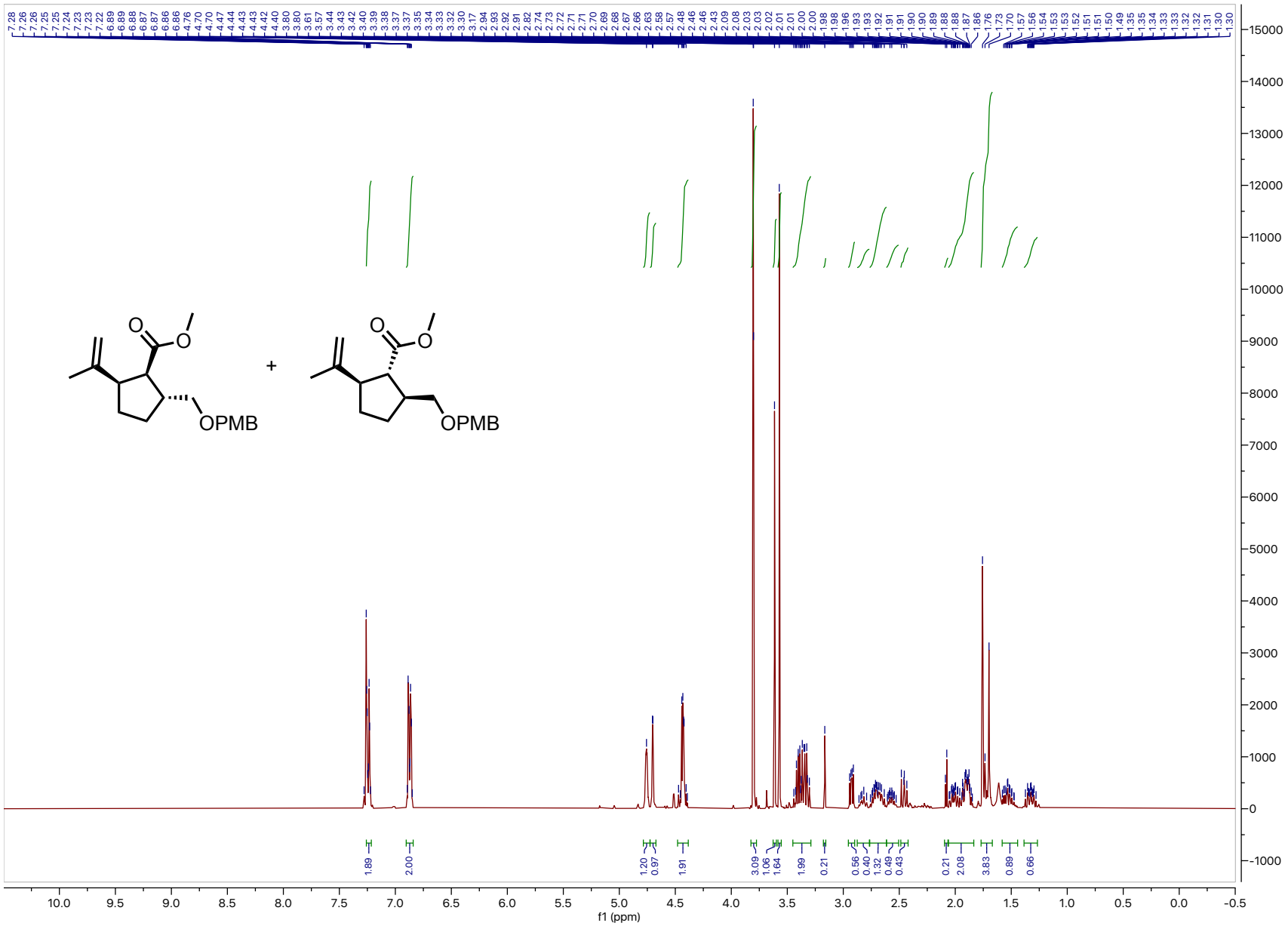

Figure B.20. ^{1}H NMR (400 MHz, $CDCl_3$) methyl ester **2.13**

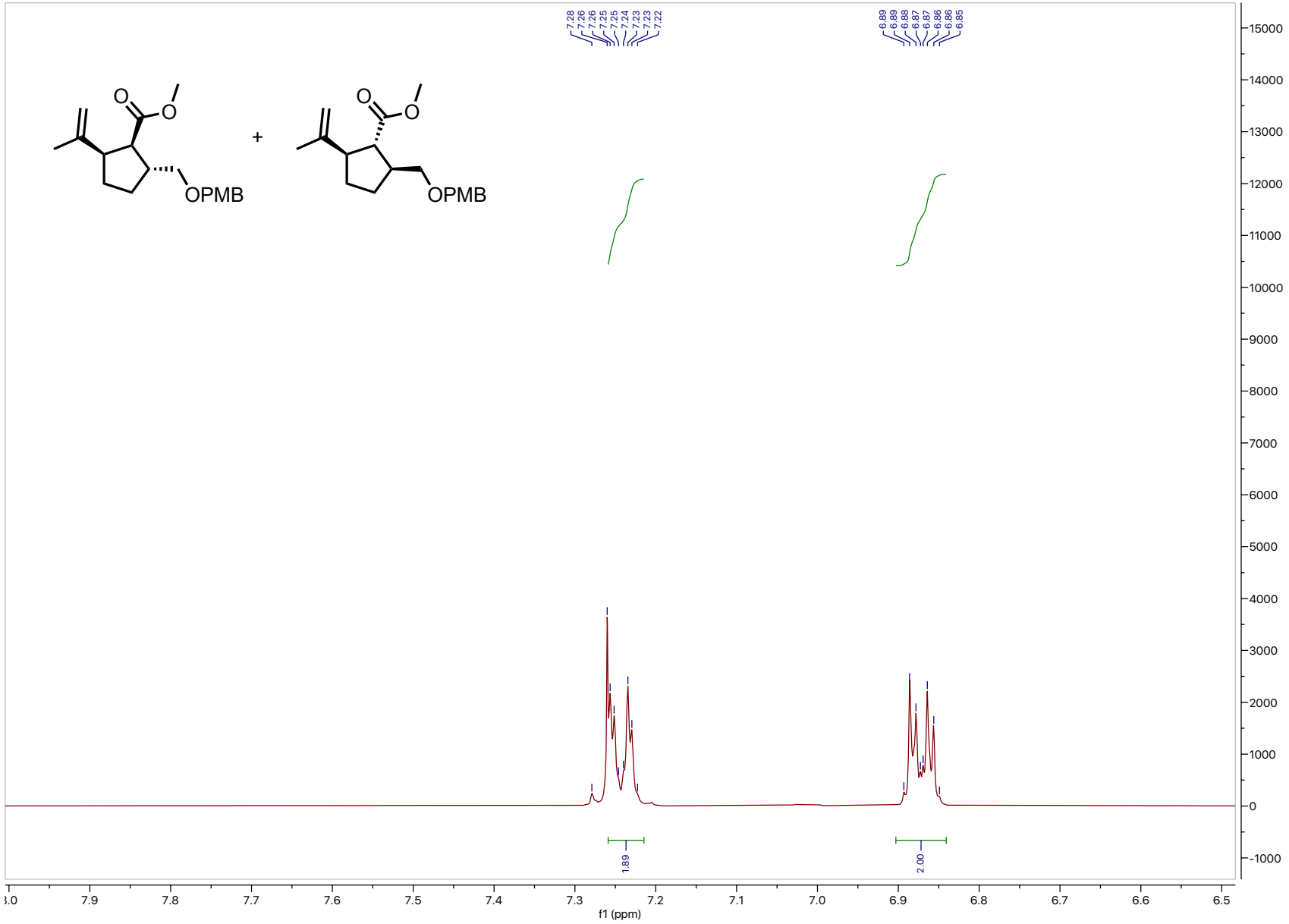

Figure B.21. ^{1}H NMR (400 MHz, $CDCl_3$) methyl ester **2.13** (8.0 – 6.5 ppm inset)

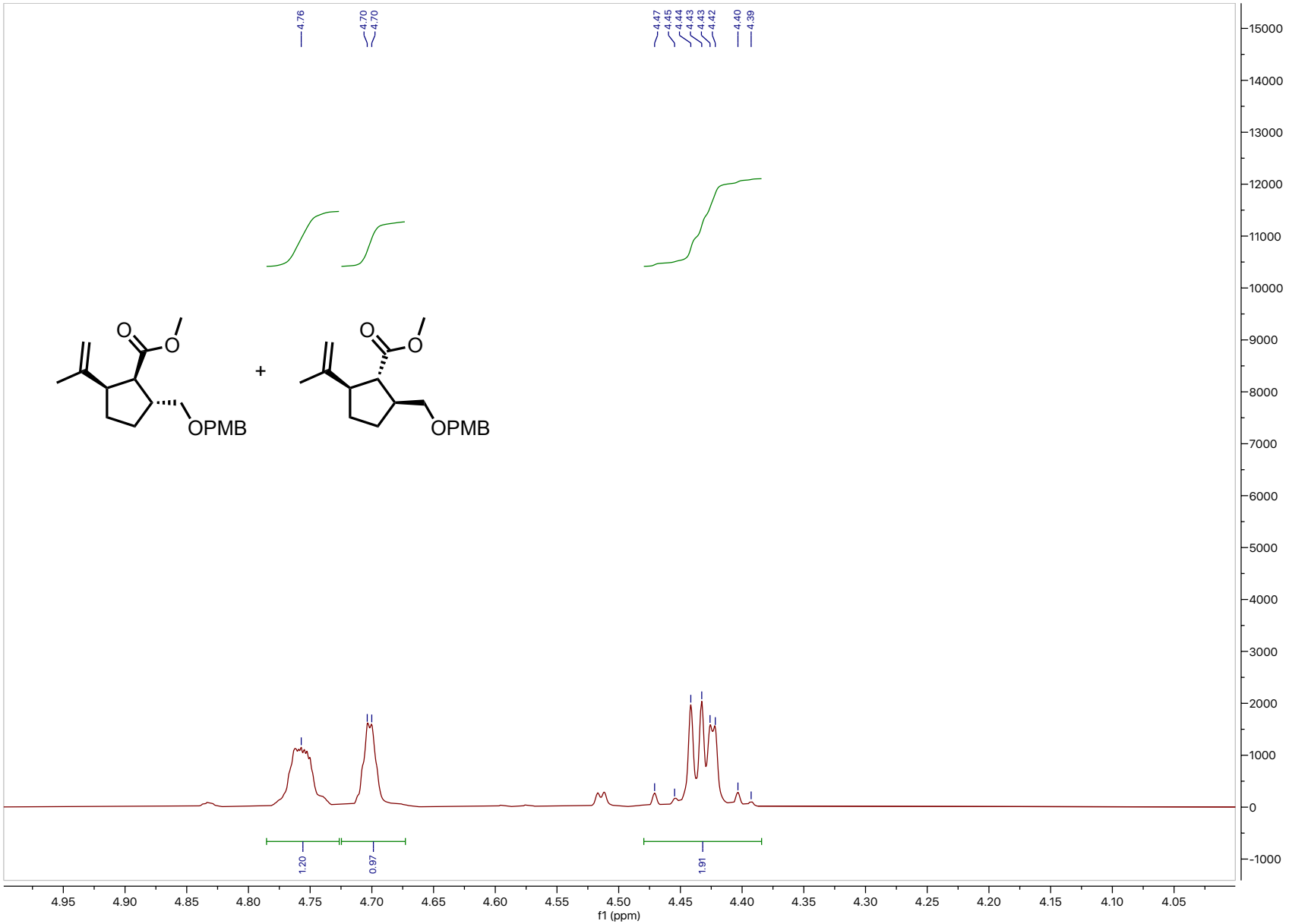

Figure B.22. ^{1}H NMR (400 MHz, $CDCl_3$) methyl ester **2.13** (5.0 – 4.0 ppm inset)

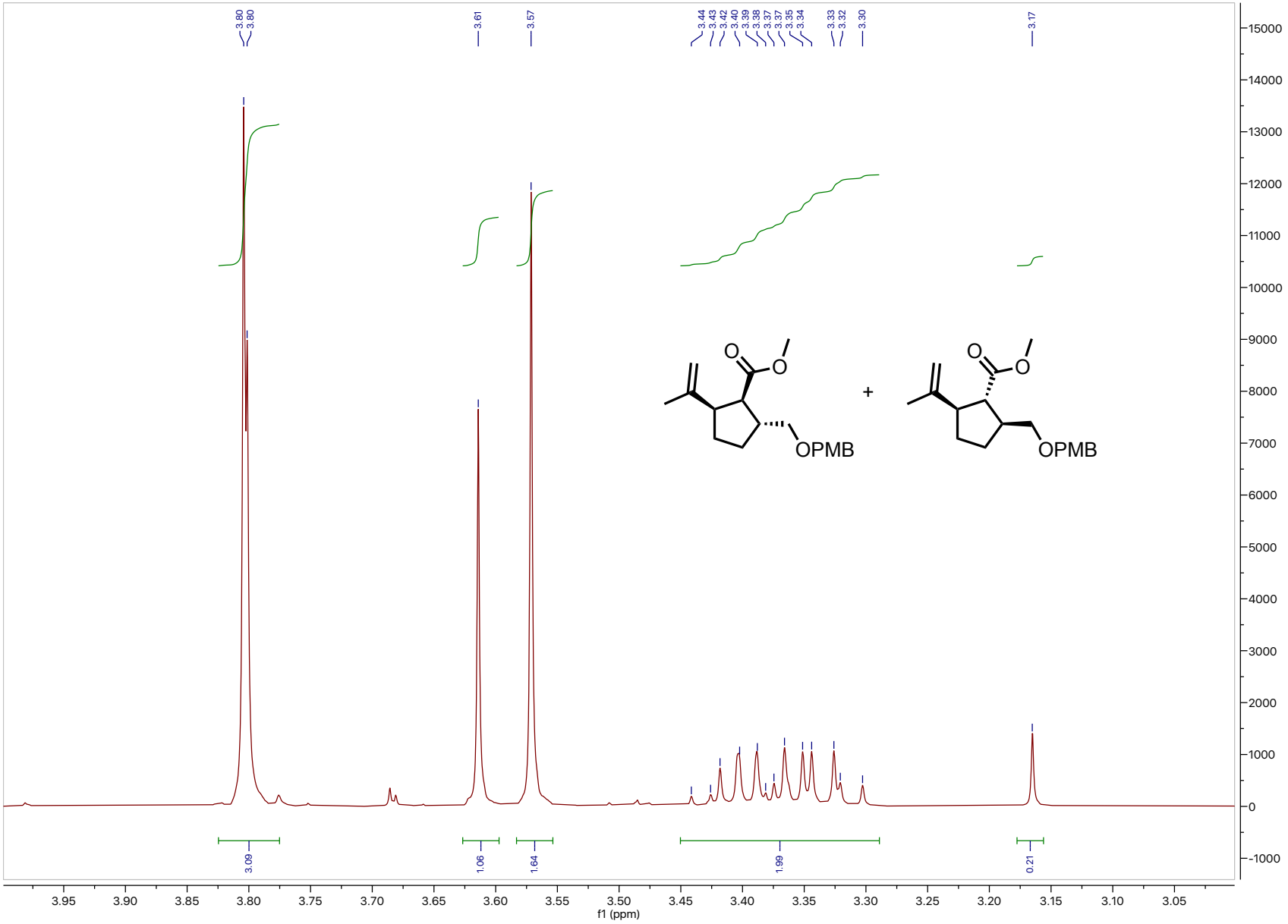

Figure B.23. ^{1}H NMR (400 MHz, $CDCl_3$) methyl ester **2.13** (4.0 – 3.0 ppm inset)

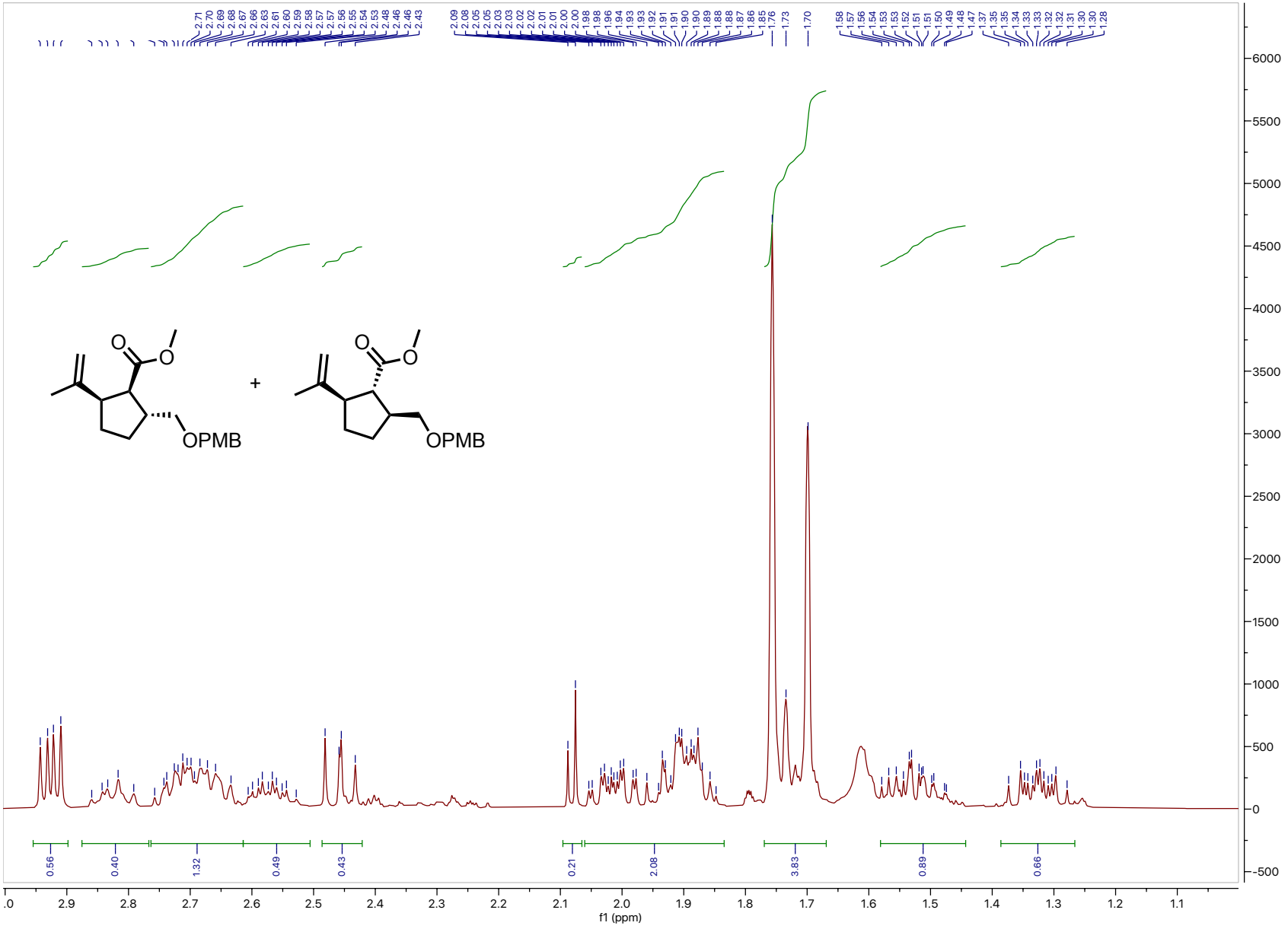

Figure B.24. ^{1}H NMR (400 MHz, $CDCl_3$) methyl ester **2.13** (3.0 – 1.0 ppm inset)

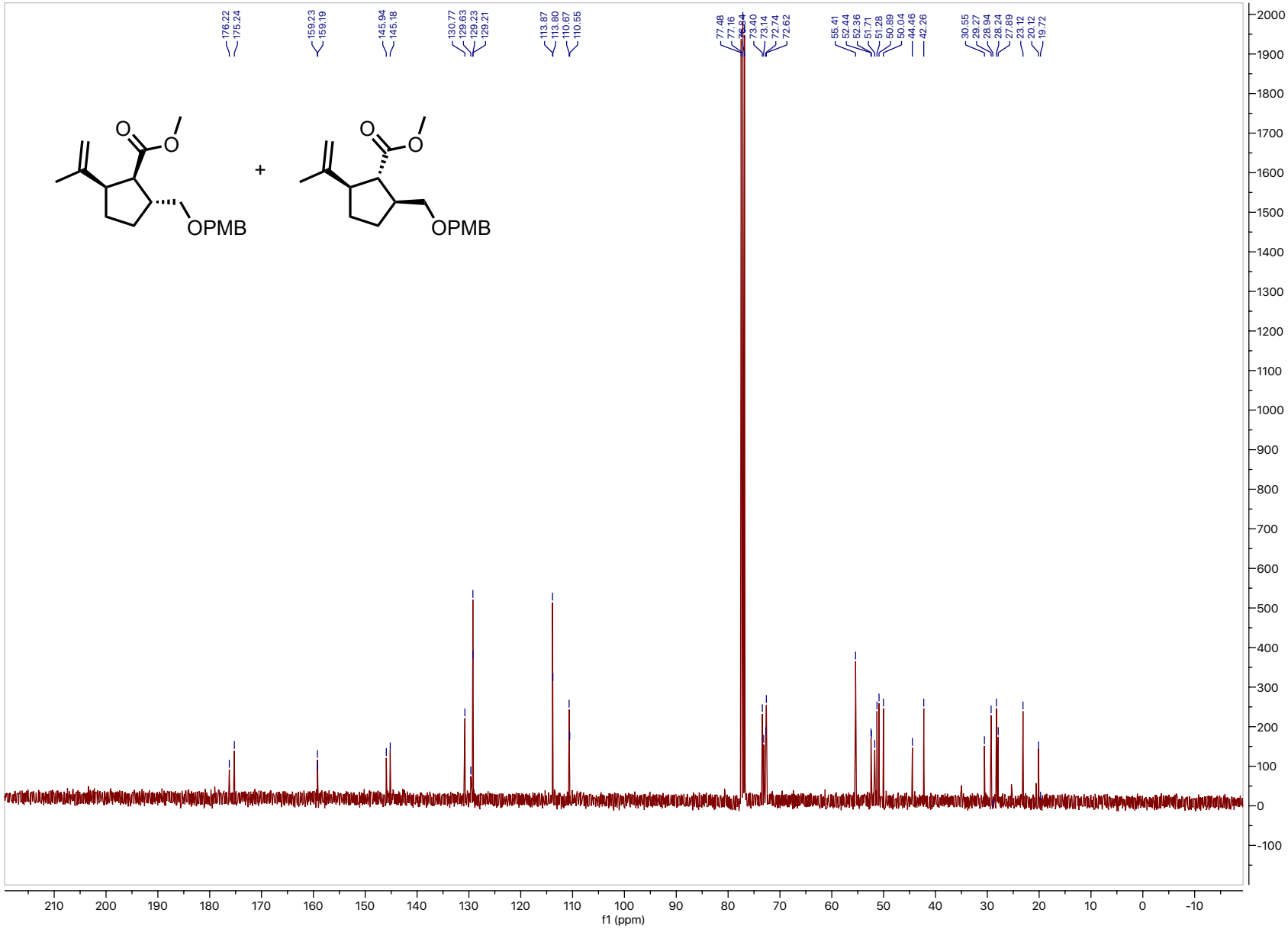

Figure B.25. ^{13}C NMR (101 MHz, $CDCl_3$) methyl ester **2.13**

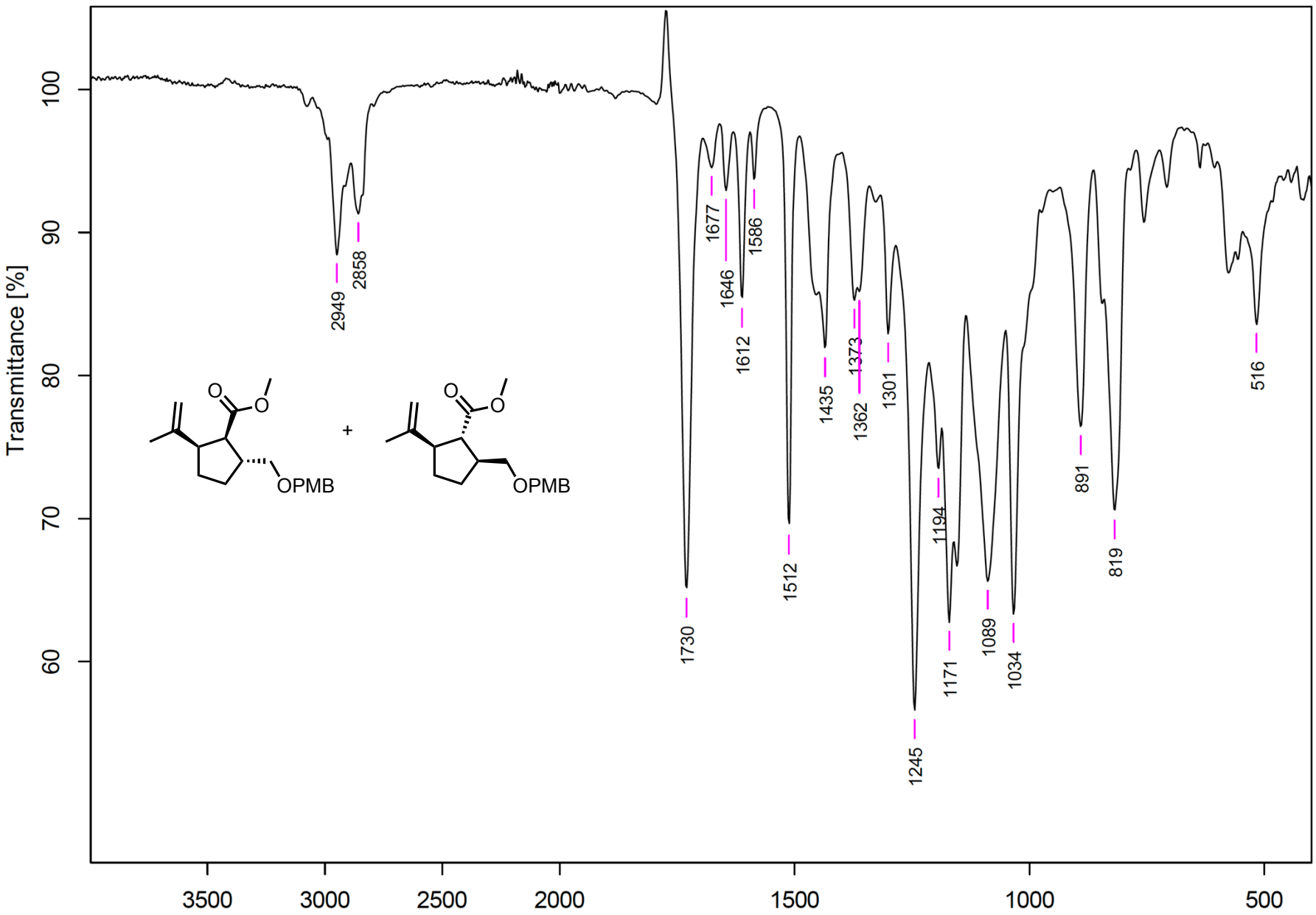

Figure B.26. FTIR (neat) methyl ester **2.13**

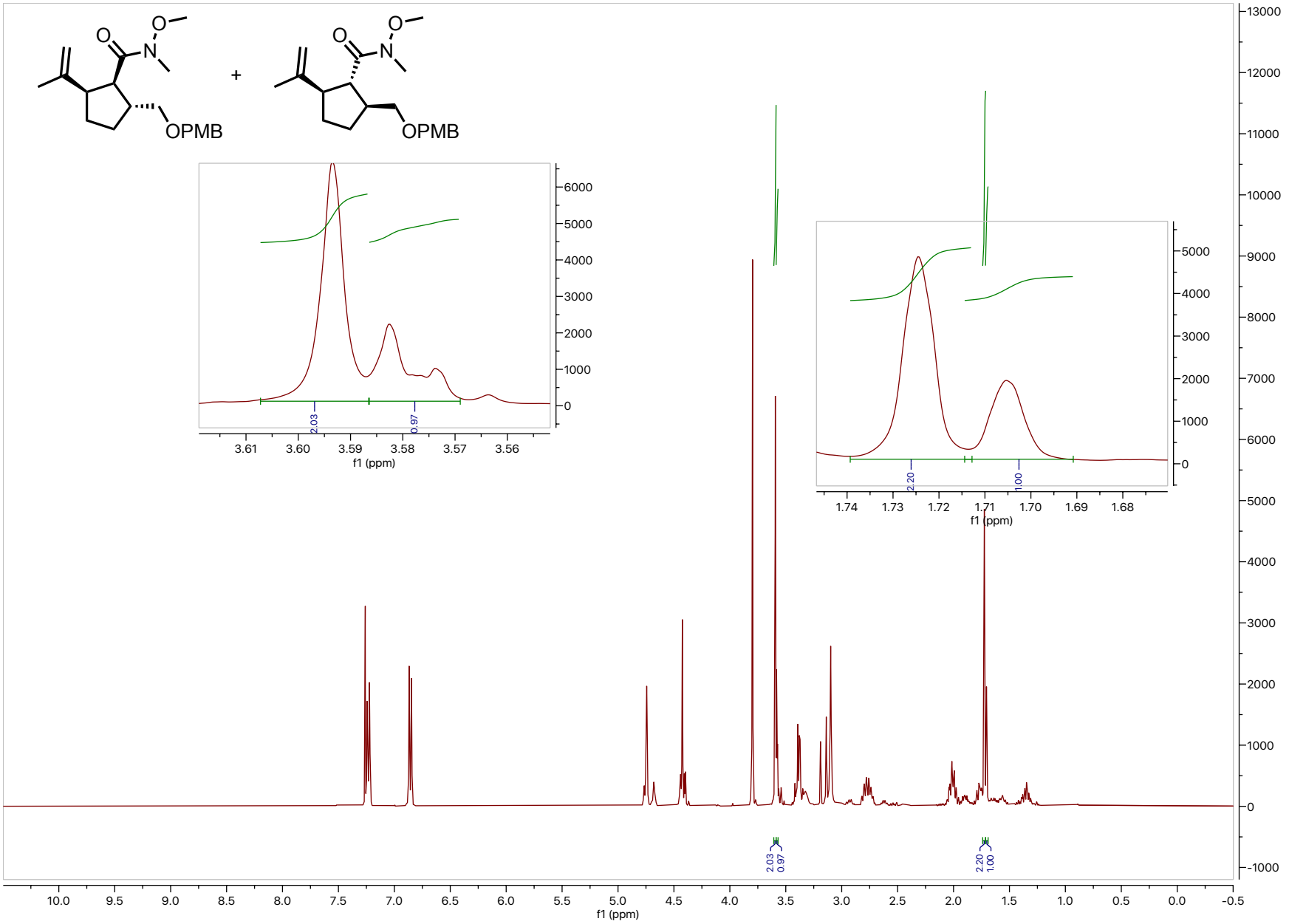

Figure B.27. Crude ^{1}H NMR (400 MHz, $CDCl_3$) amide **2.12**

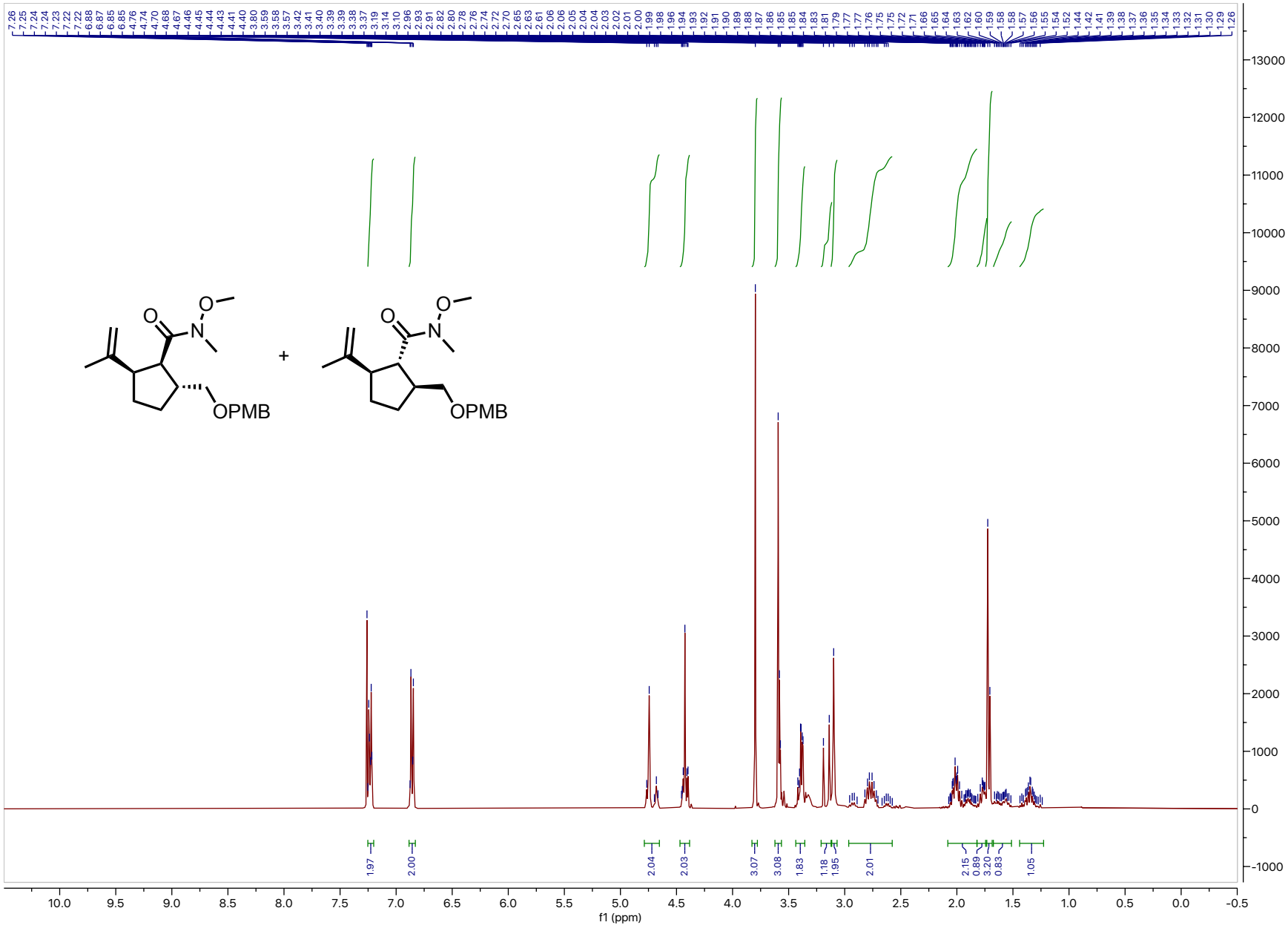

Figure B.28. ^{1}H NMR (400 MHz, $CDCl_3$) amide **2.12**

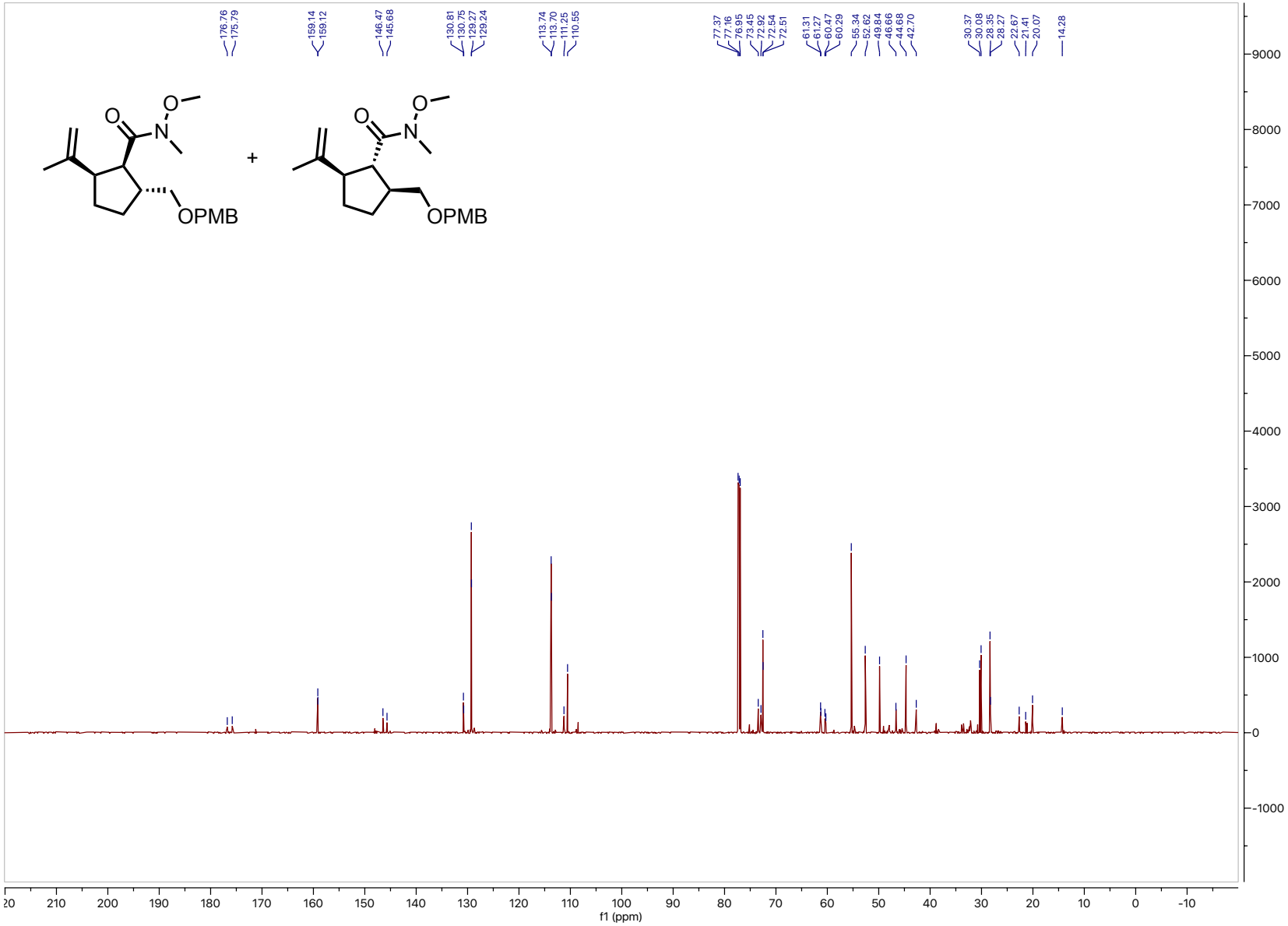

Figure B.29. ^{13}C NMR (151 MHz, $CDCl_3$) amide **2.12**

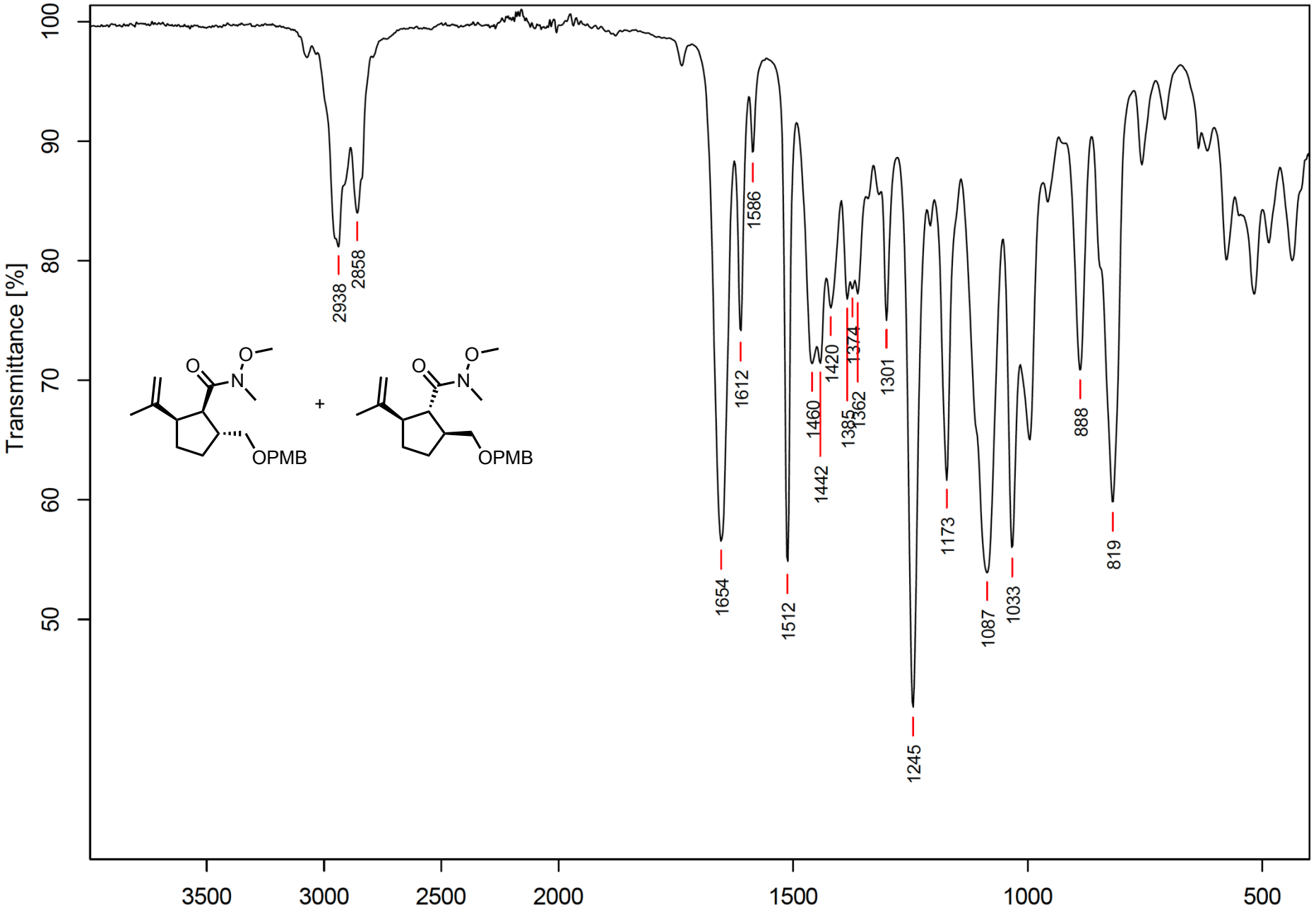

Figure B.30. FTIR (neat) amide **2.12**

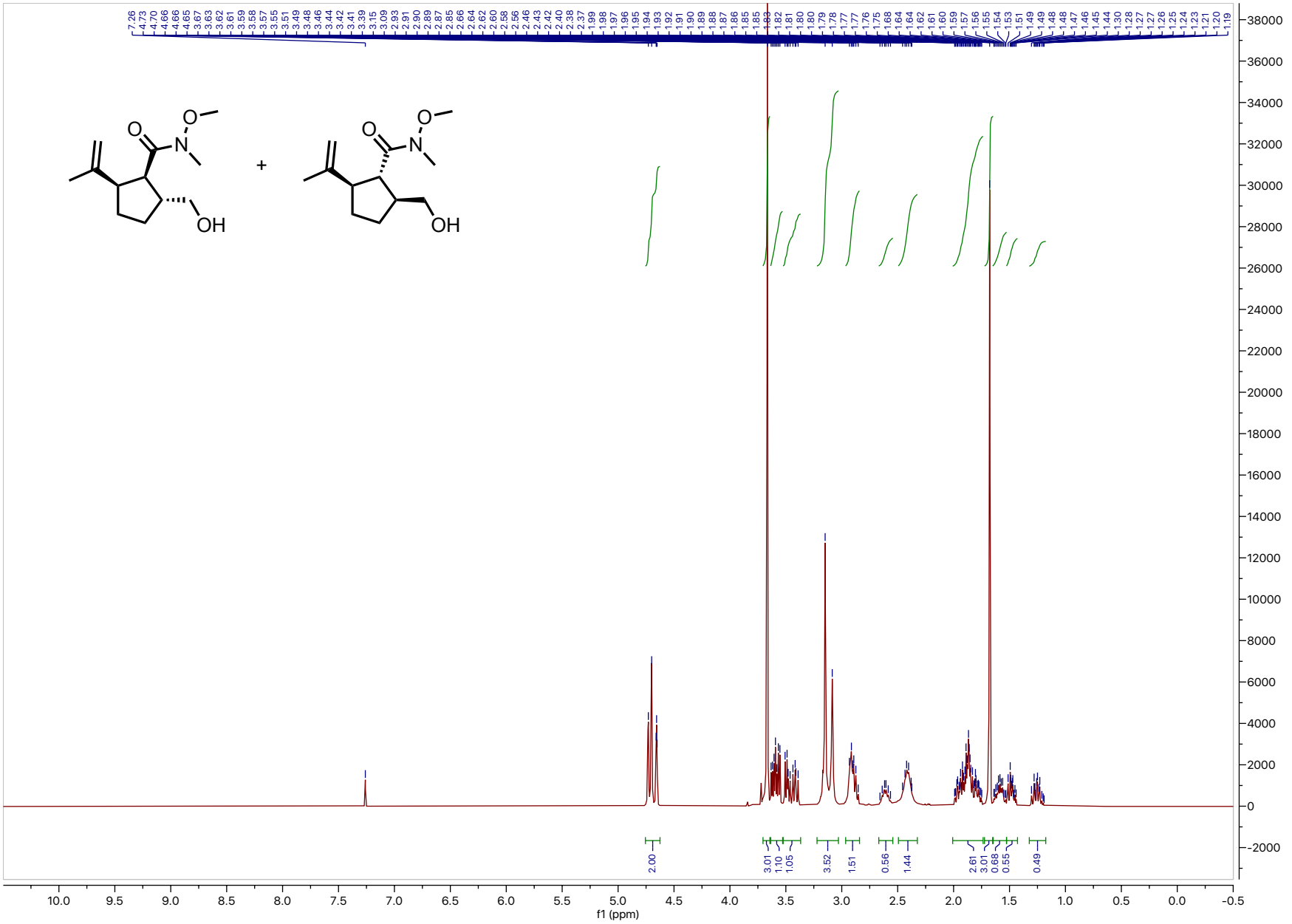

Figure B.31. ^{1}H NMR (400 MHz, $CDCl_3$) alcohol **2.49**

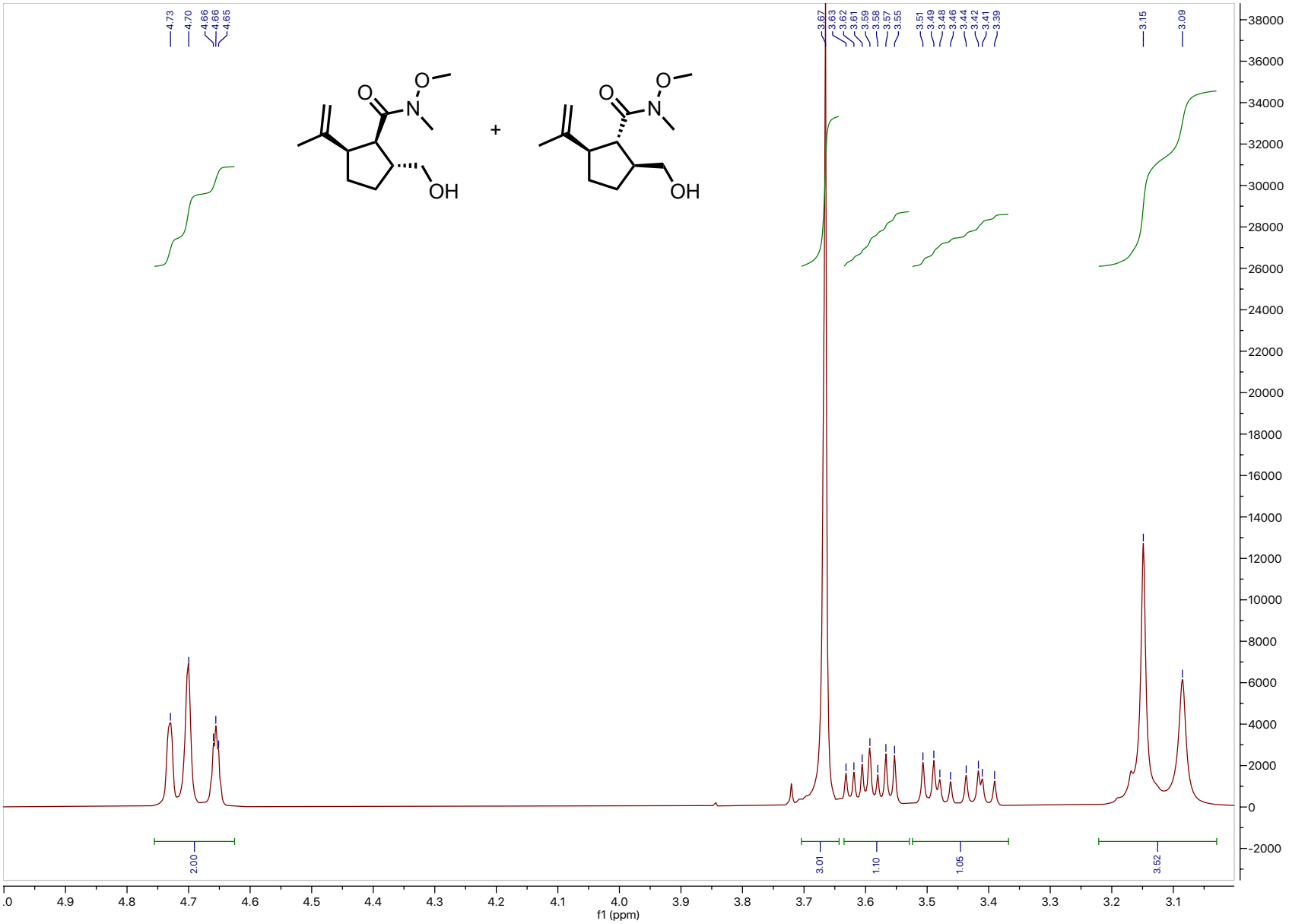

Figure B.32. ^{1}H NMR (400 MHz, $CDCl_3$) alcohol **2.49** (5.0 – 3.0 ppm inset)

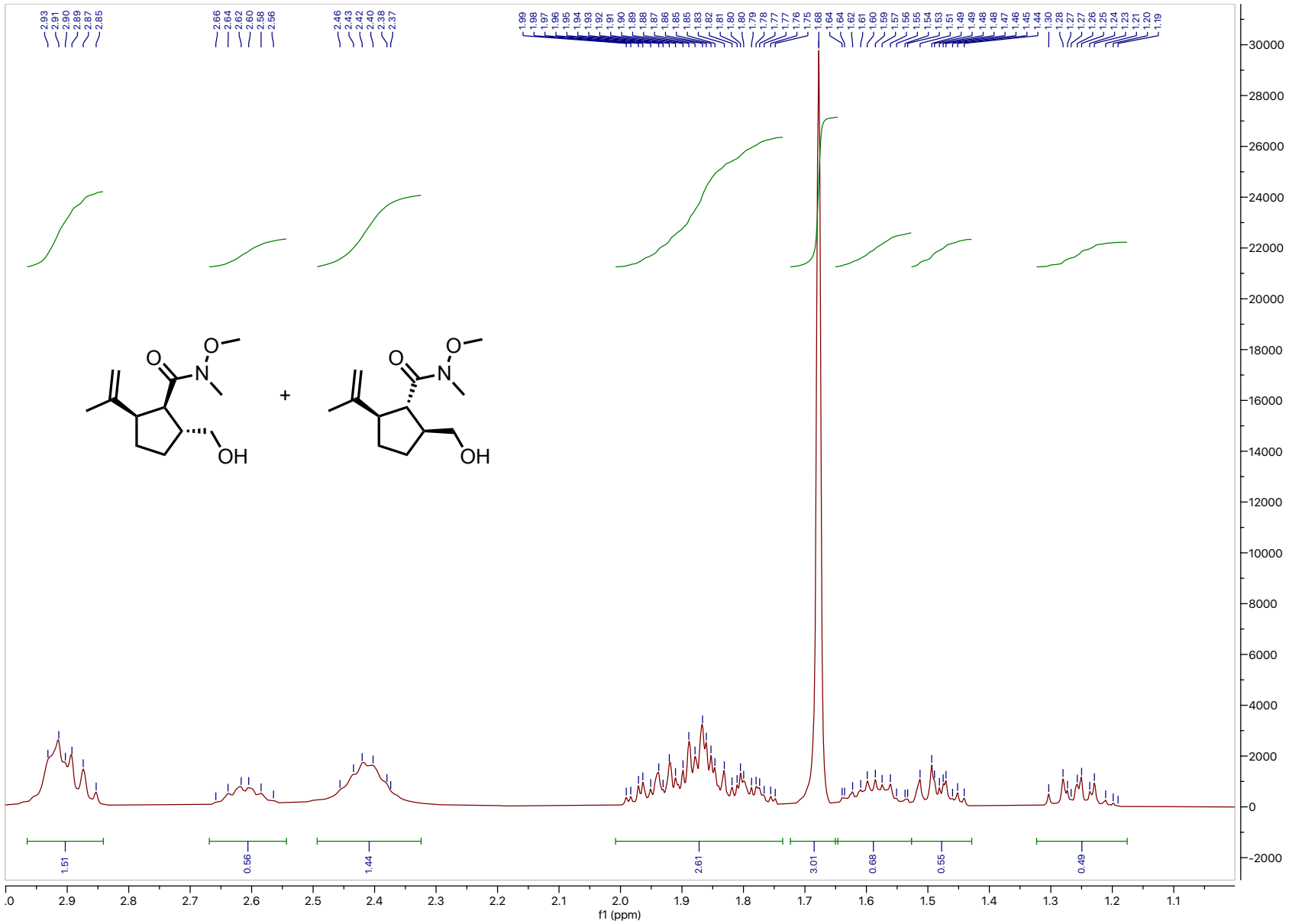

Figure B.33. ^{1}H NMR (400 MHz, $CDCl_3$) alcohol **2.49** (3.0 – 1.0 ppm inset)

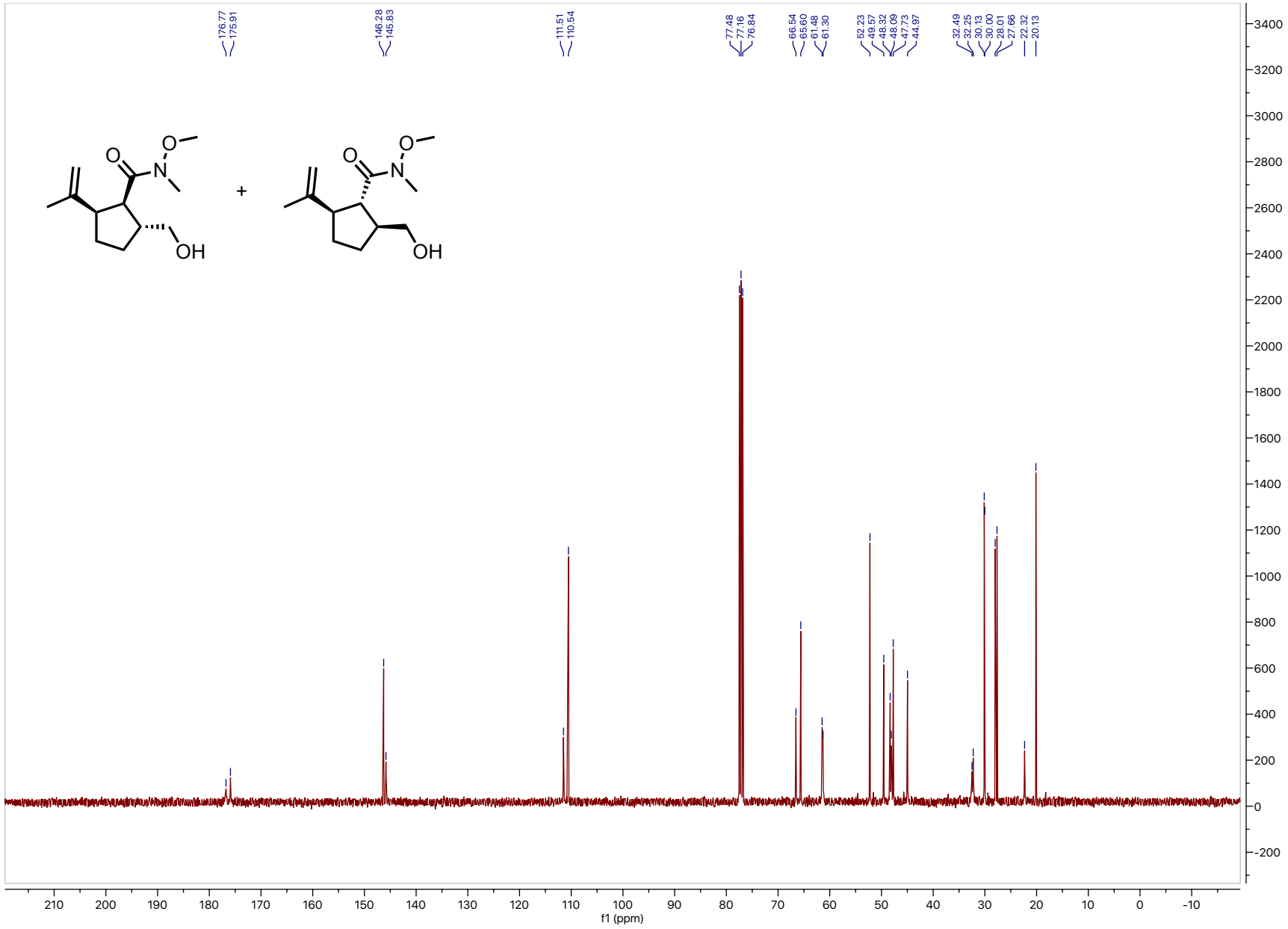

Figure B.34. ^{13}C NMR (101 MHz, $CDCl_3$) alcohol **2.49**

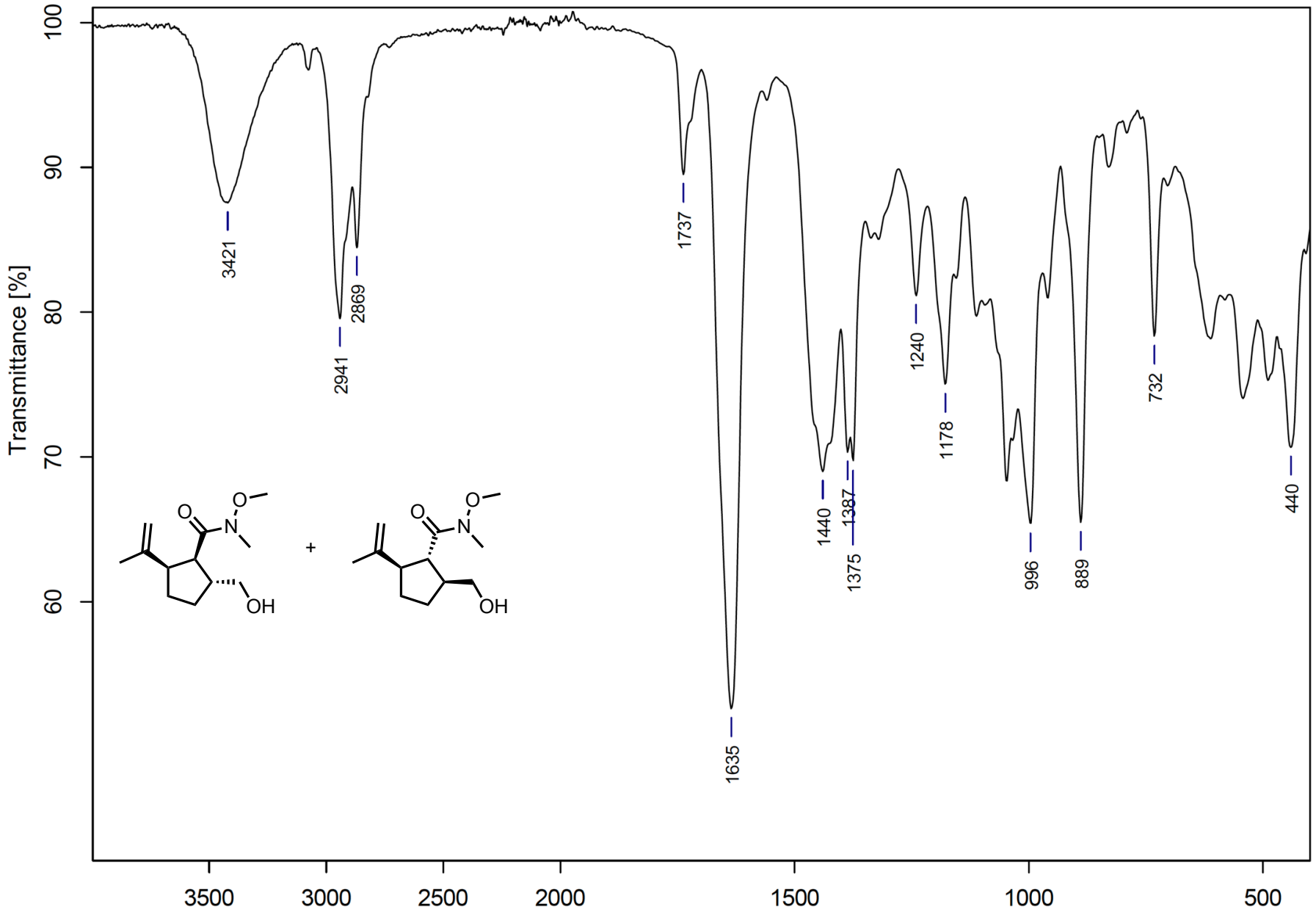

Figure B.35. FTIR (neat) alcohol **2.49**

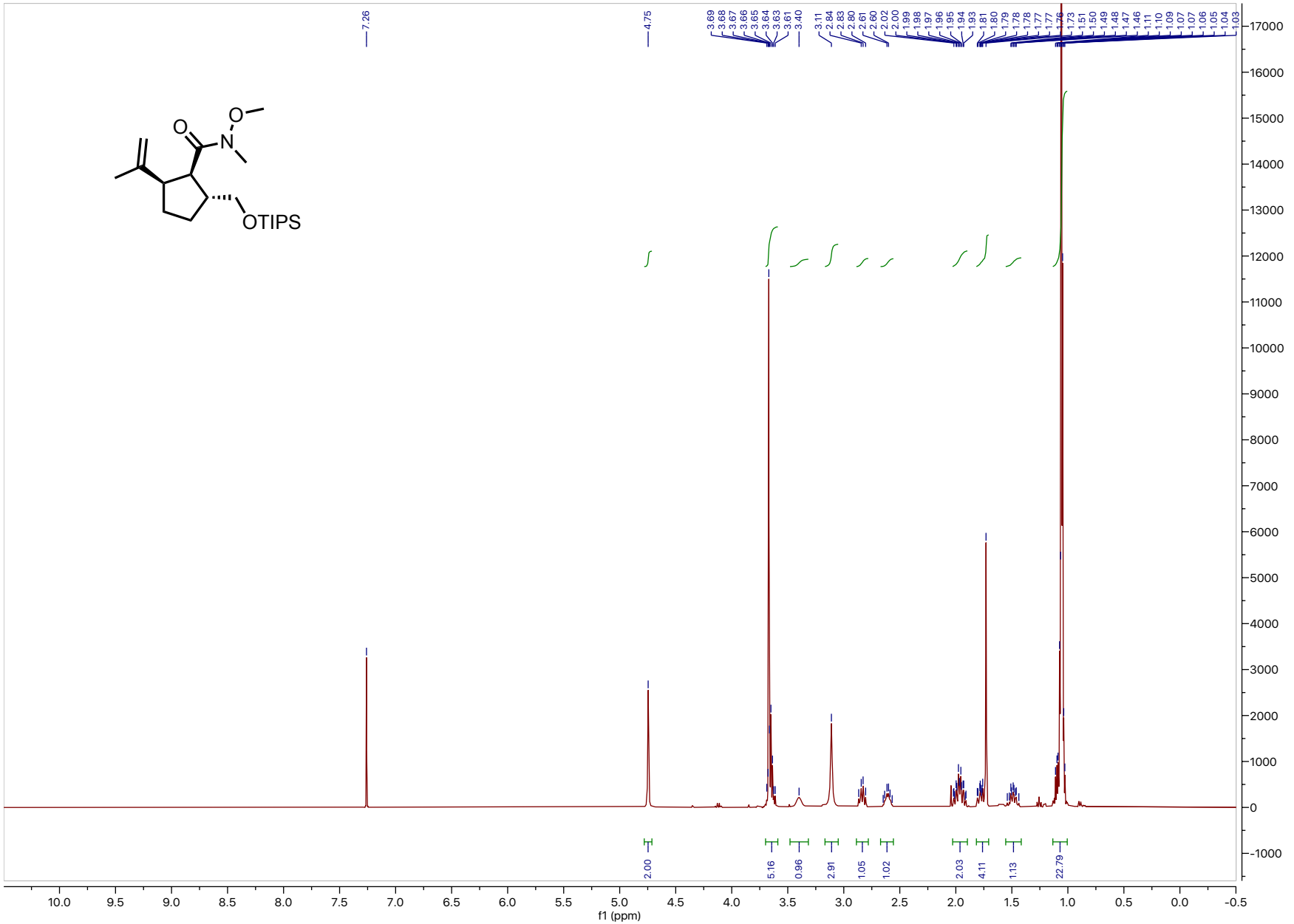

Figure B.36. ^{1}H NMR (400 MHz, $CDCl_3$) silyl ether **2.51**

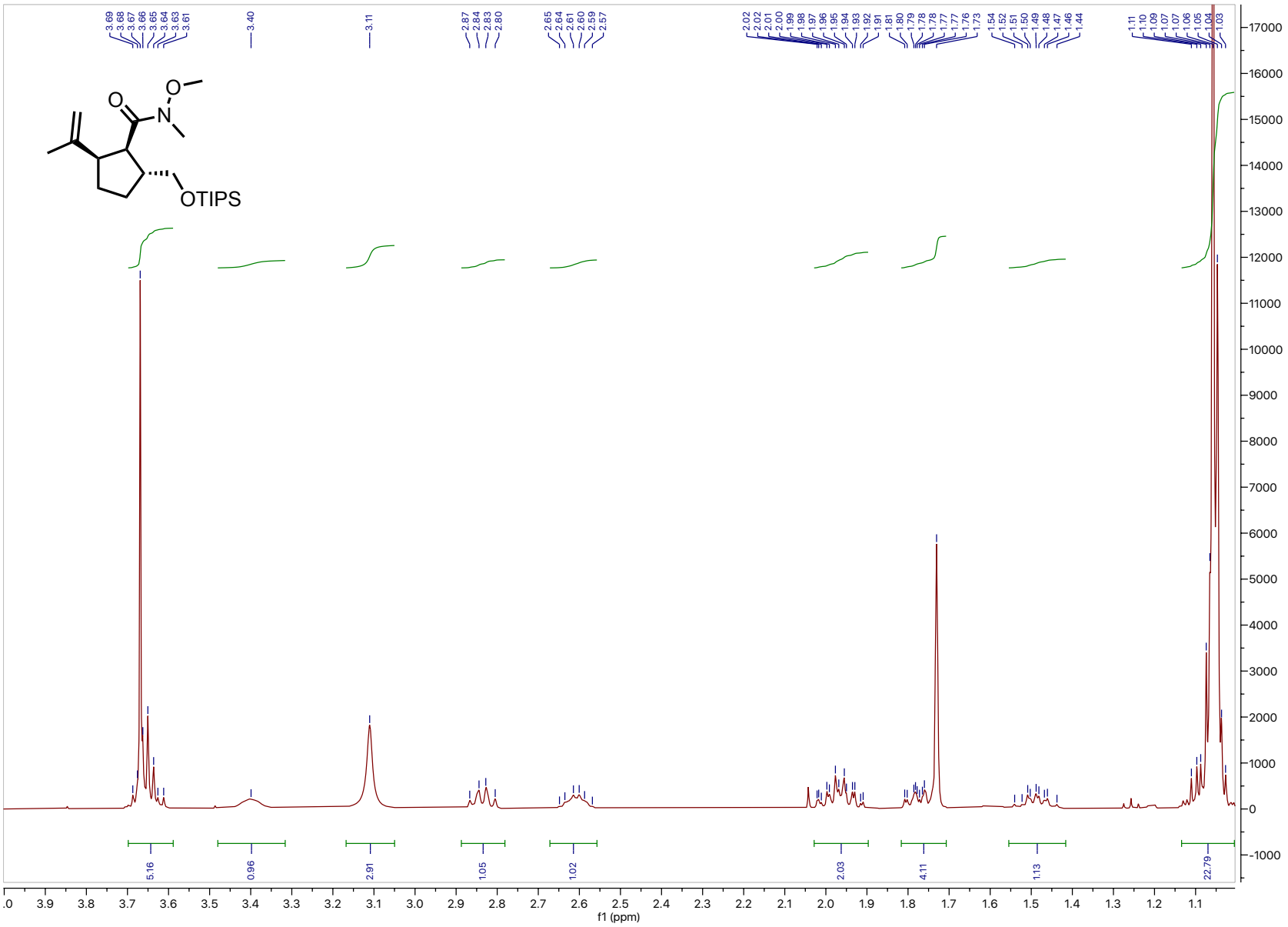

Figure B.37. ^{1}H NMR (400 MHz, $CDCl_3$) silyl ether **2.51** (4.0 – 1.0 ppm inset)

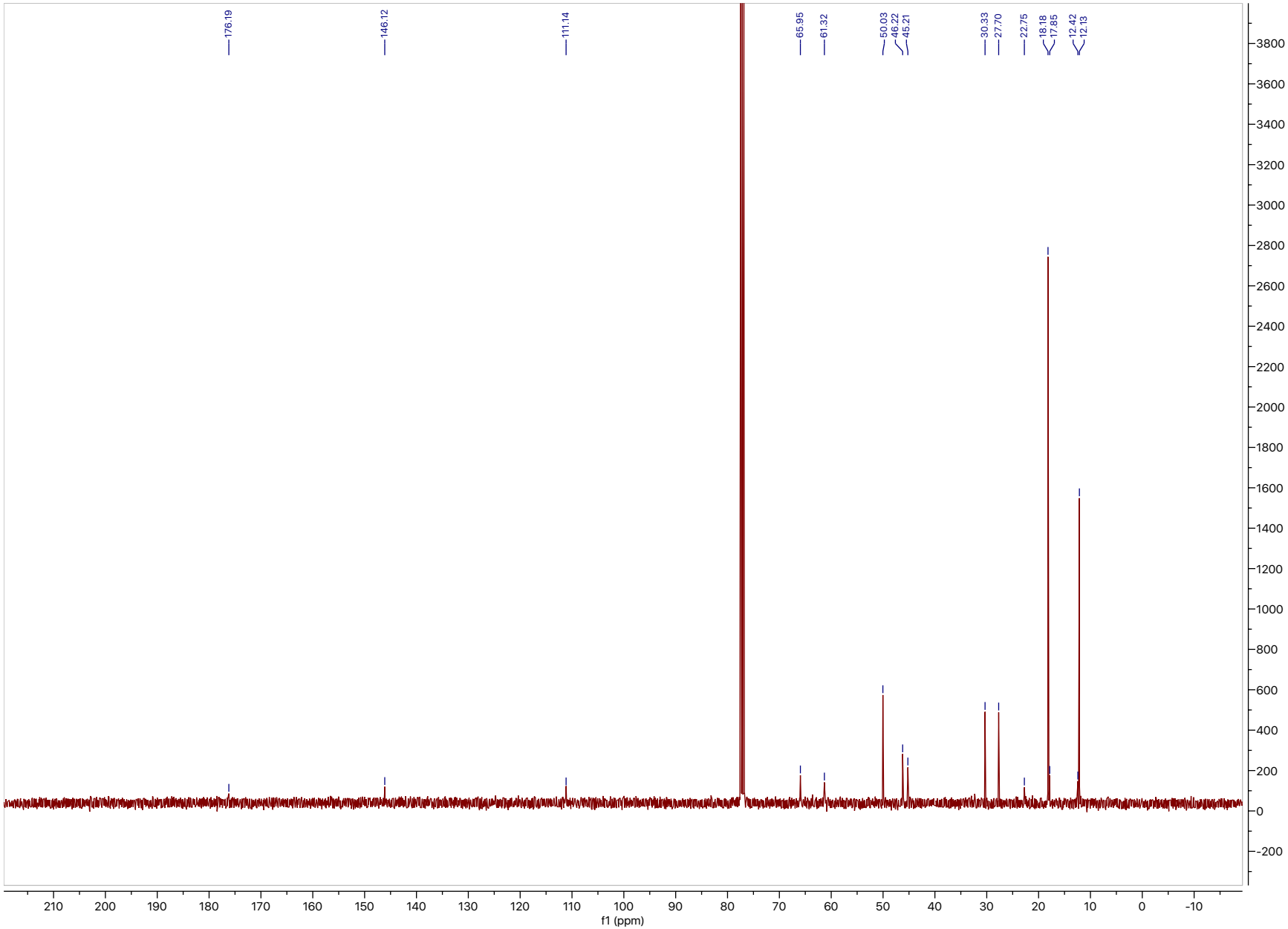

Figure B.38. ^{13}C NMR (101 MHz, $CDCl_3$) silyl ether **2.51**

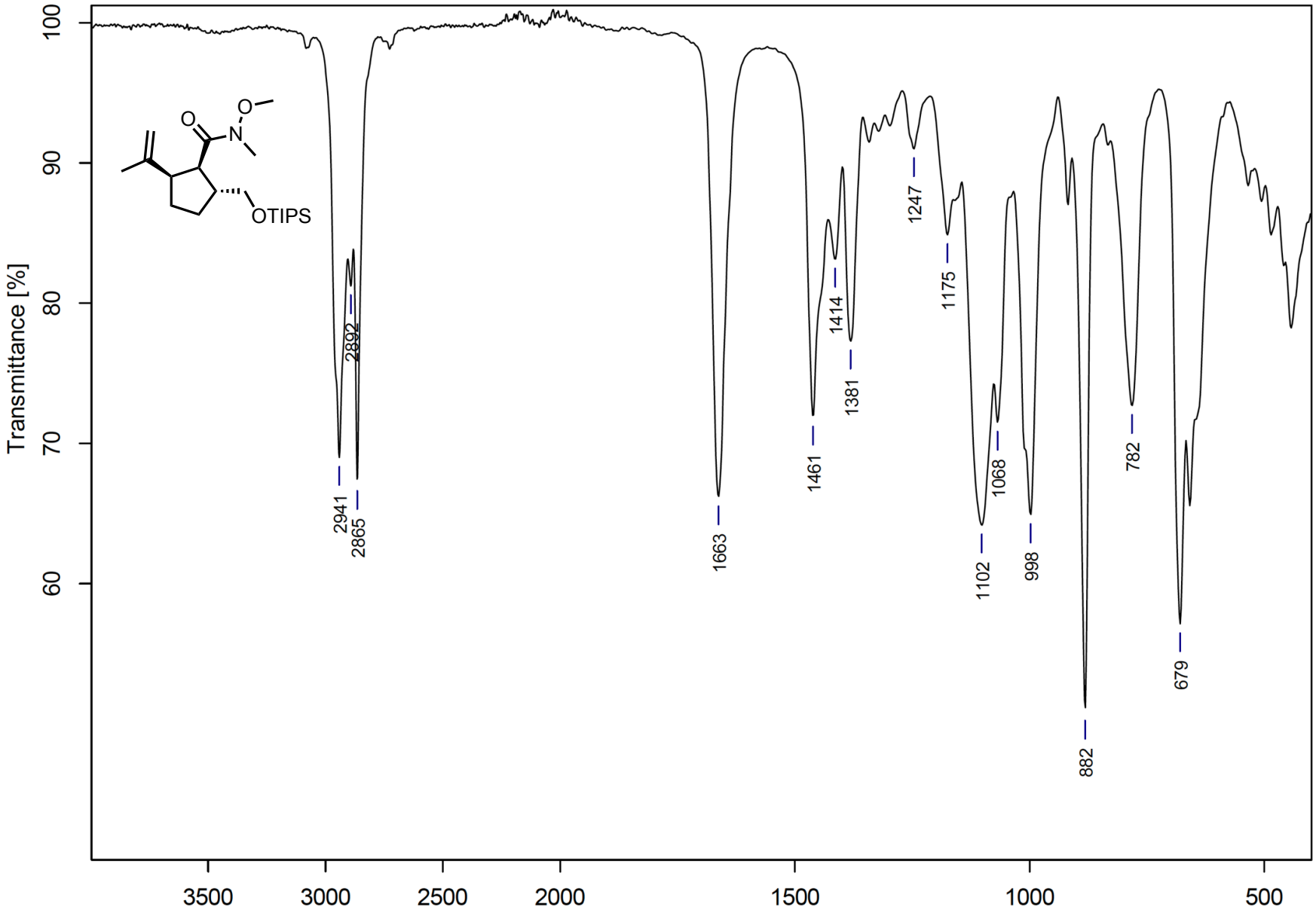

Figure B.39. FTIR (neat) silyl ether **2.51**

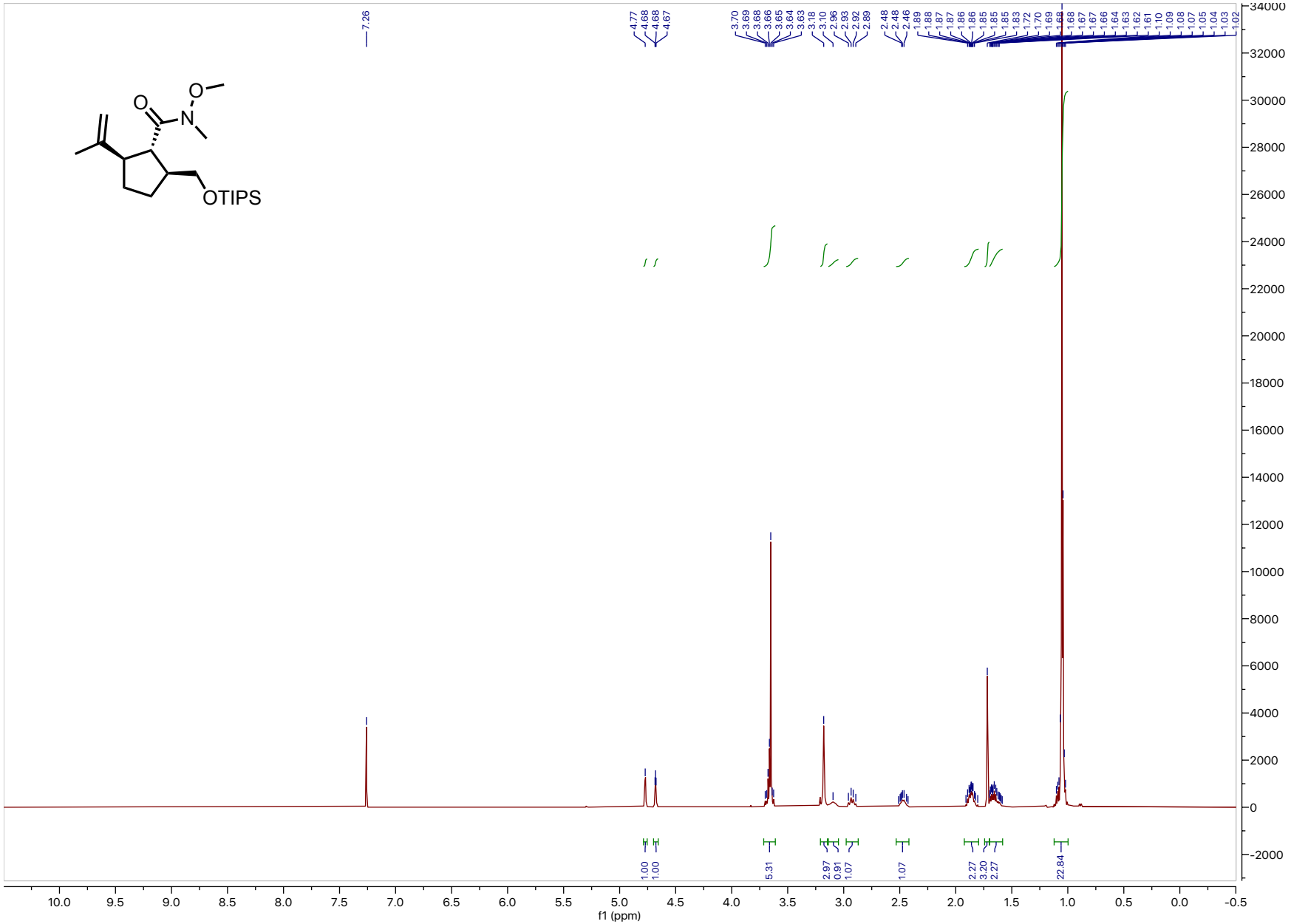

Figure B.40. ^{1}H NMR (400 MHz, $CDCl_3$) silyl ether **2.52**

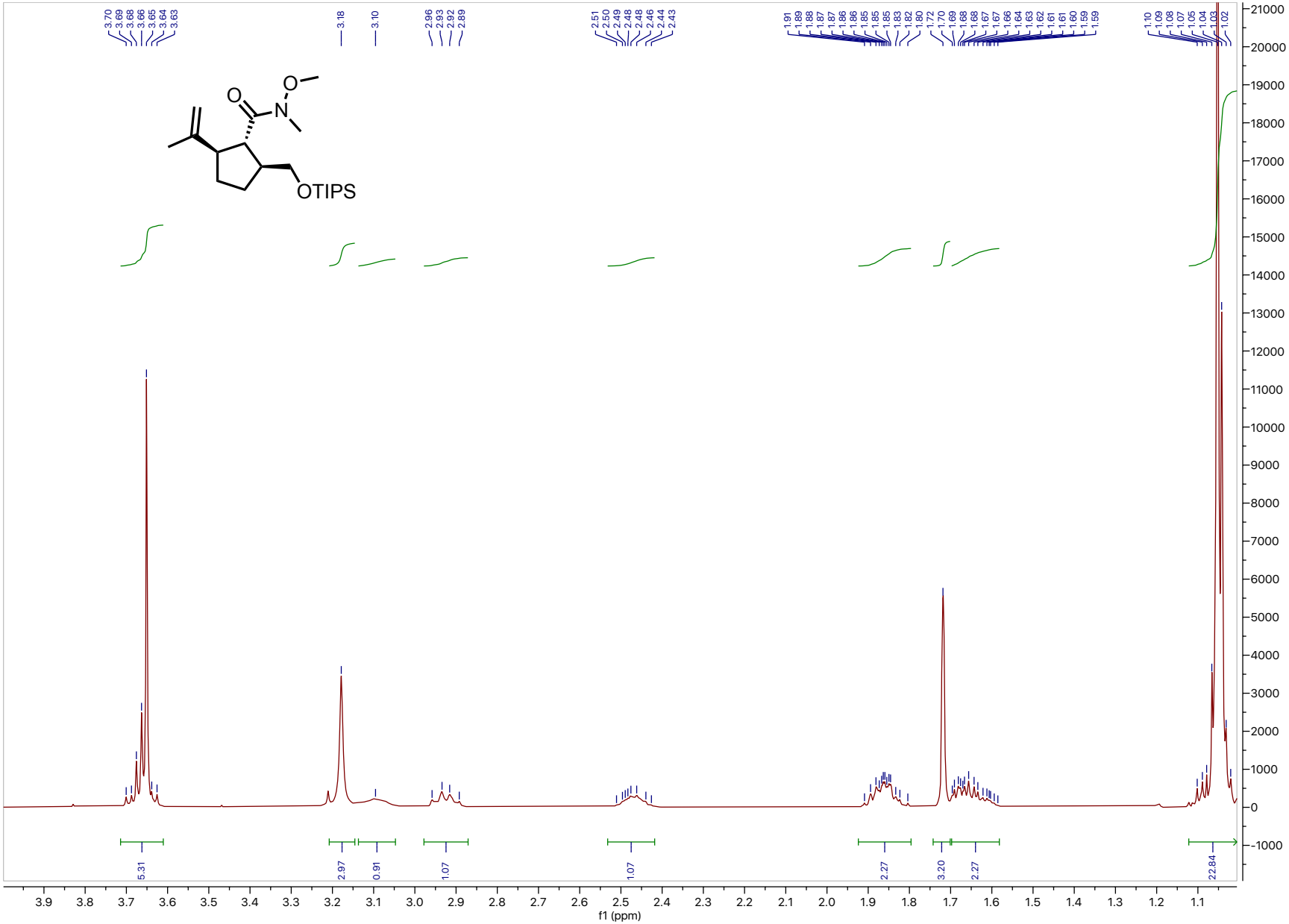

Figure B.41. ^{1}H NMR (400 MHz, $CDCl_3$) silyl ether **2.52** (4.0 – 1.0 ppm inset)

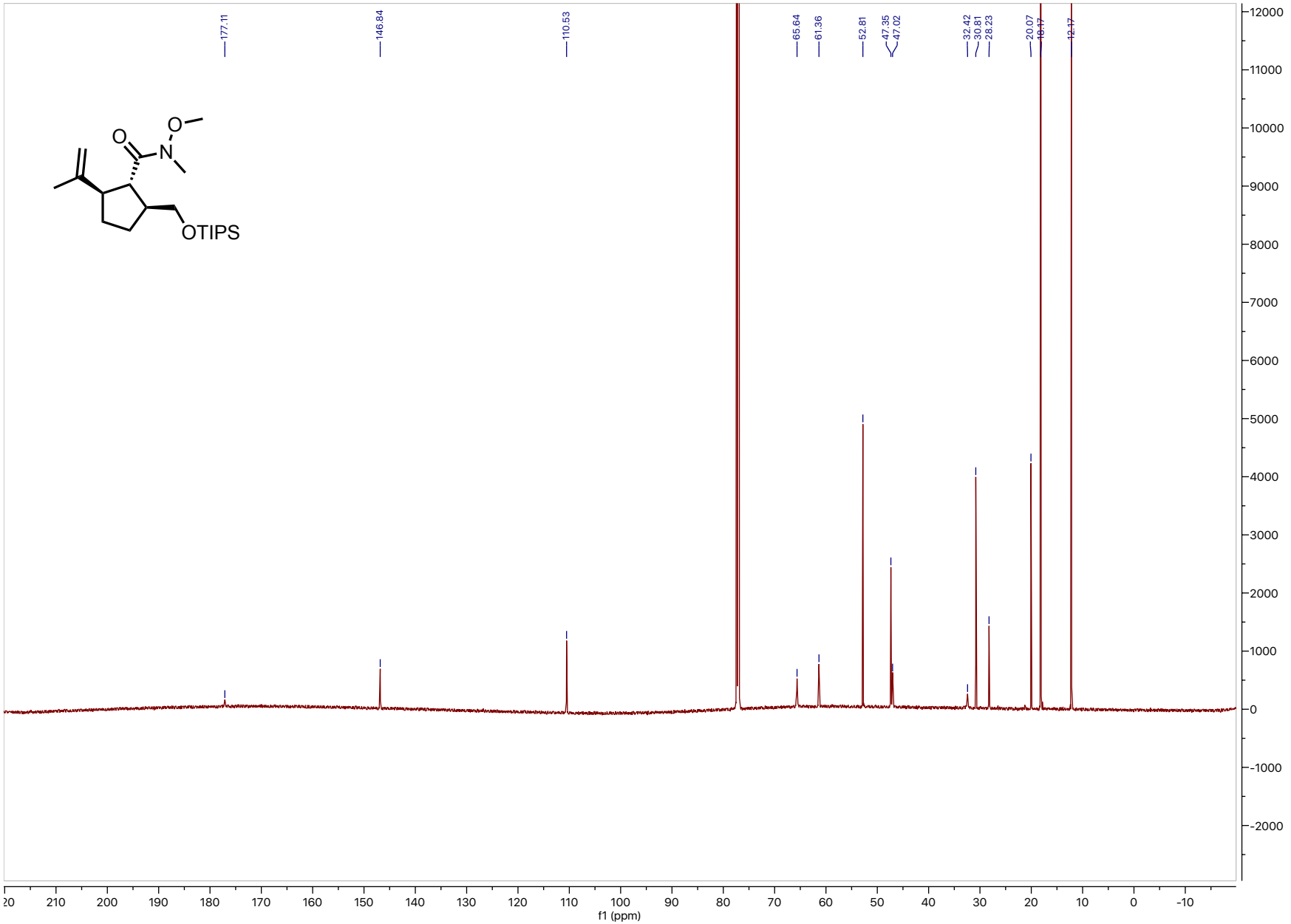

Figure B.42. ^{13}C NMR (101 MHz, $CDCl_3$) silyl ether **2.52**

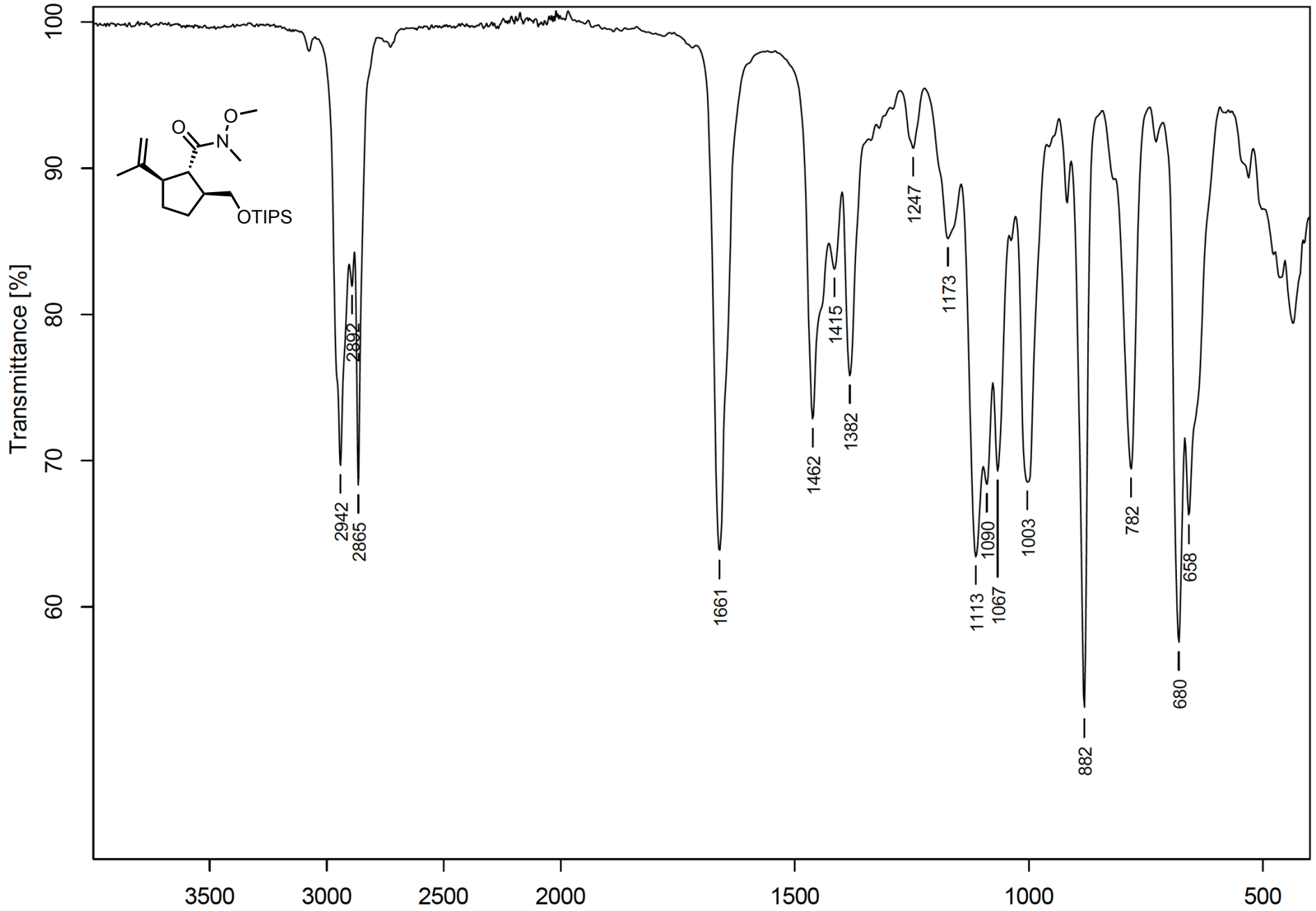

Figure B.43. FTIR (neat) silyl ether **2.52**

APPENDIX C

Spectral Data for Chapter Four

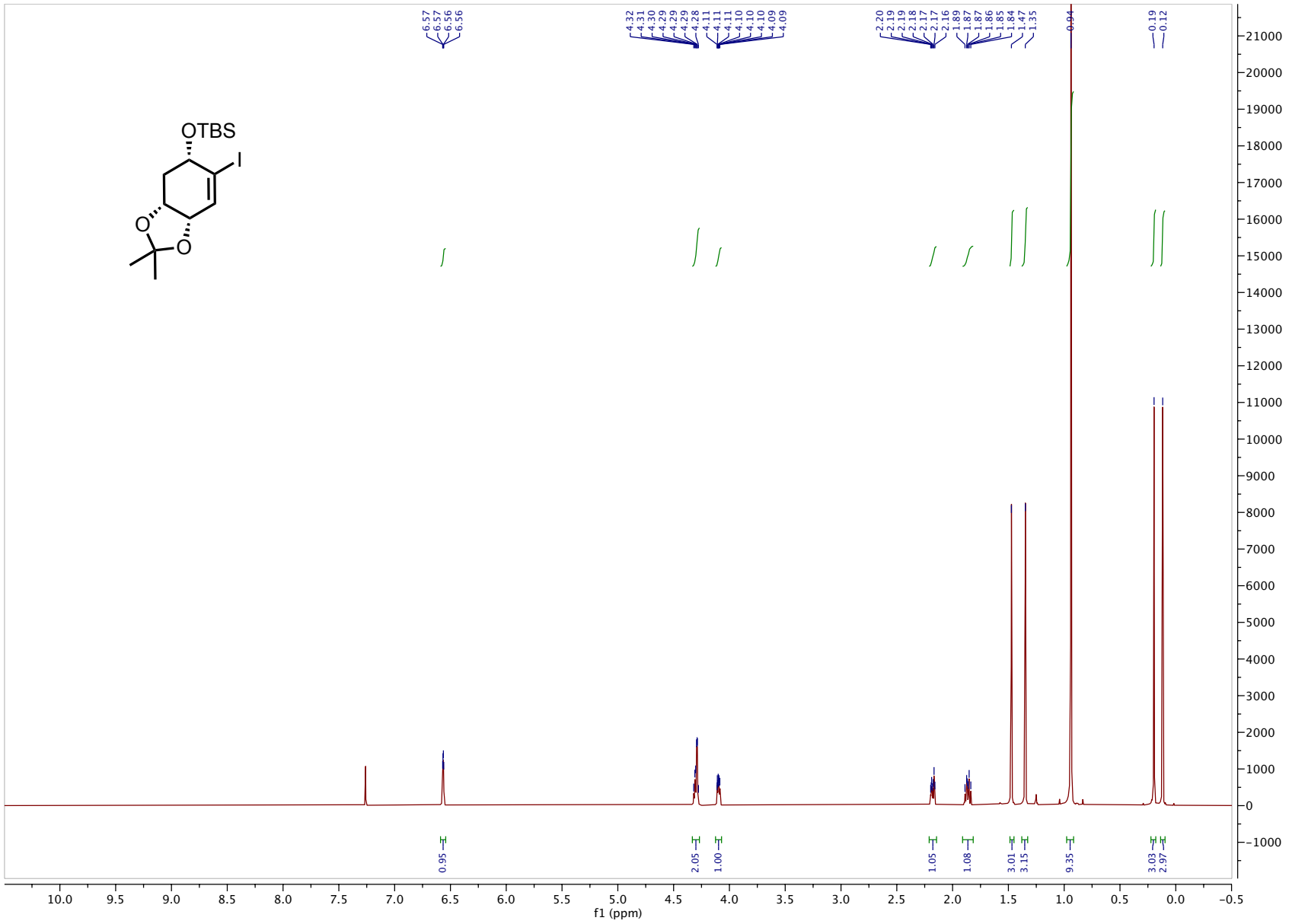

Figure C.01. ^{1}H NMR (600 MHz, $CDCl_3$) iodide **4.91**

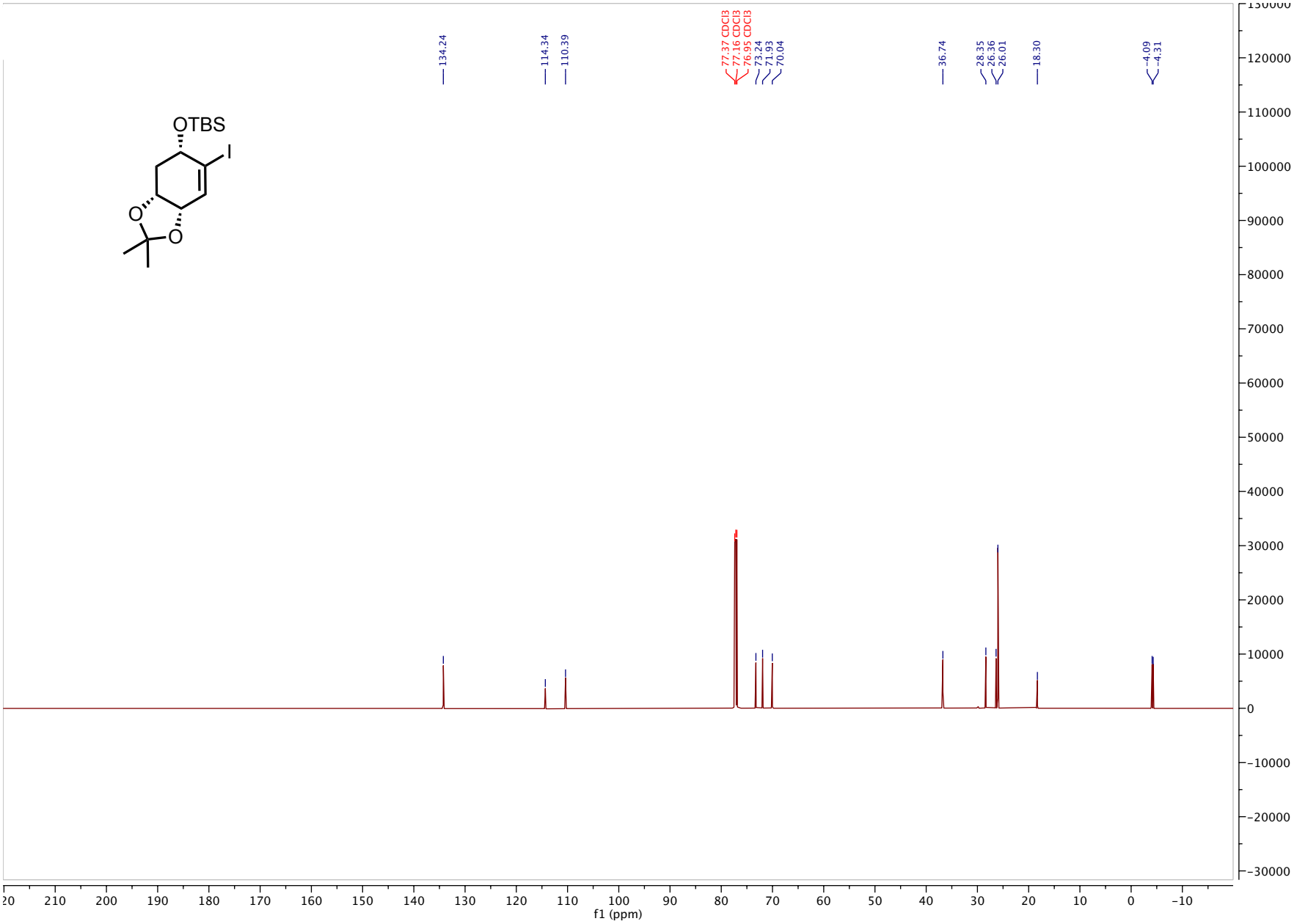

Figure C.02. ^{13}C NMR (151 MHz, $CDCl_3$) iodide **4.91**

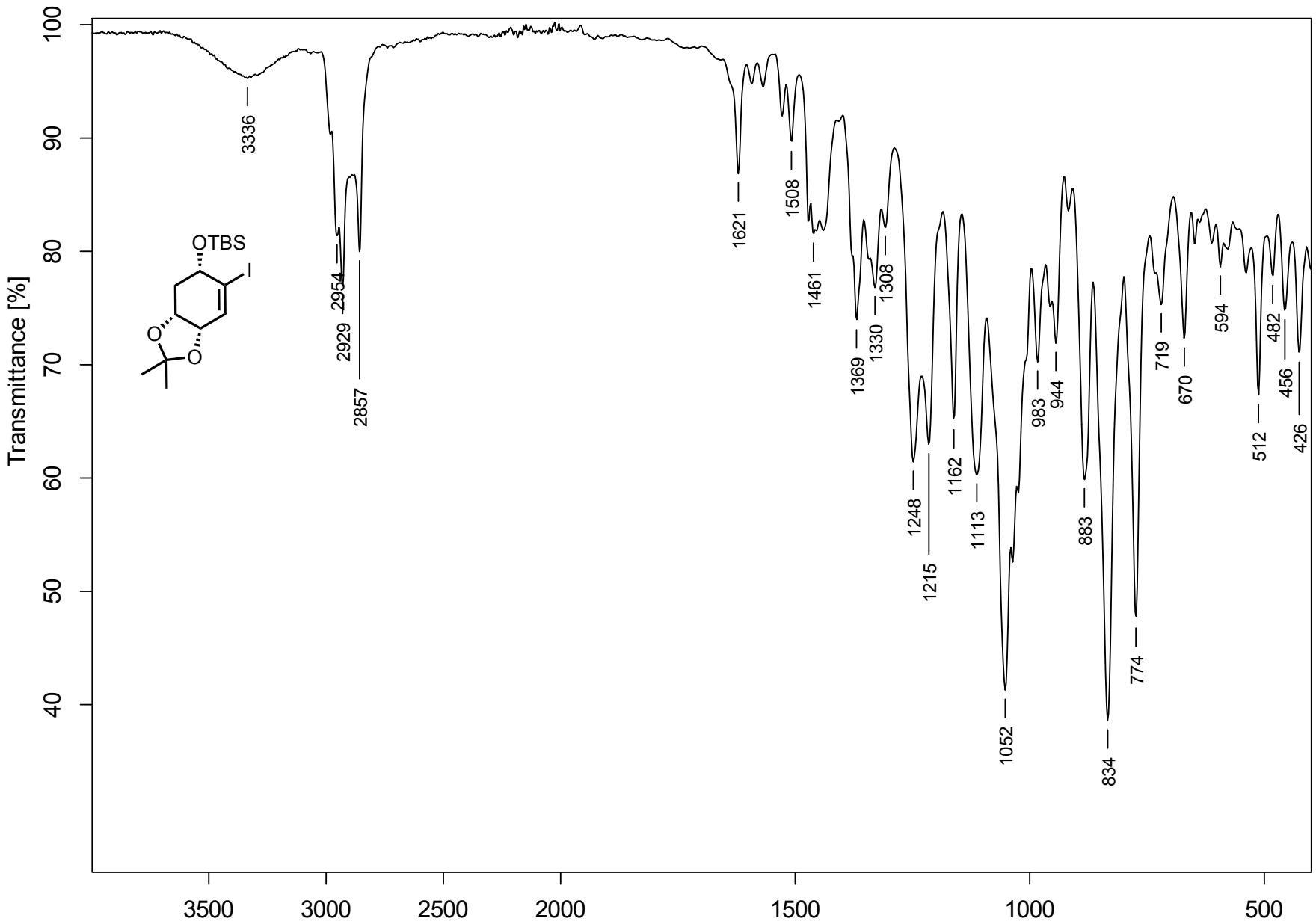

Figure C.03. FTIR (neat) iodide **4.91**

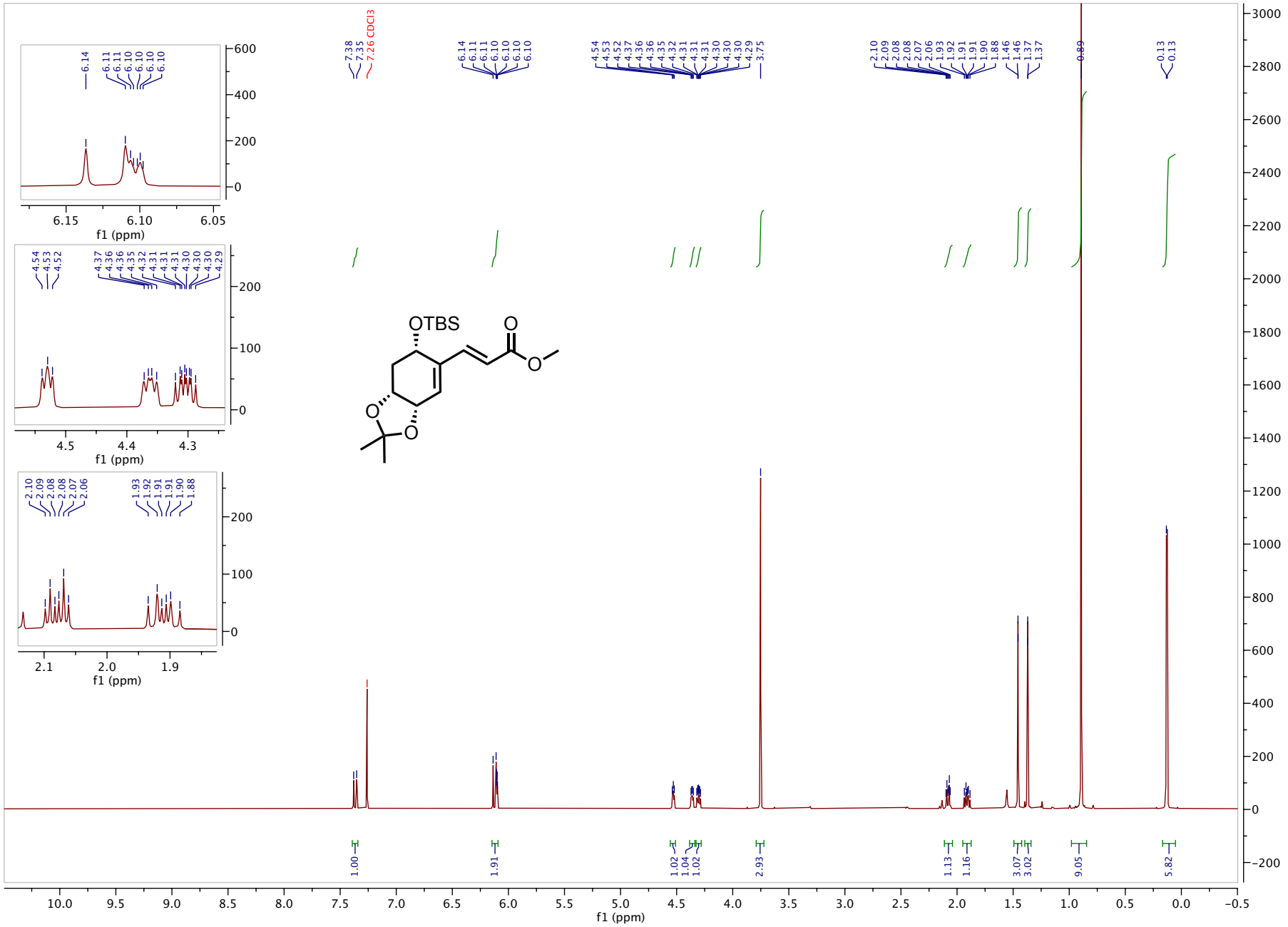

Figure C.04. ^{1}H NMR (600 MHz, $CDCl_3$) methyl ester **4.76**

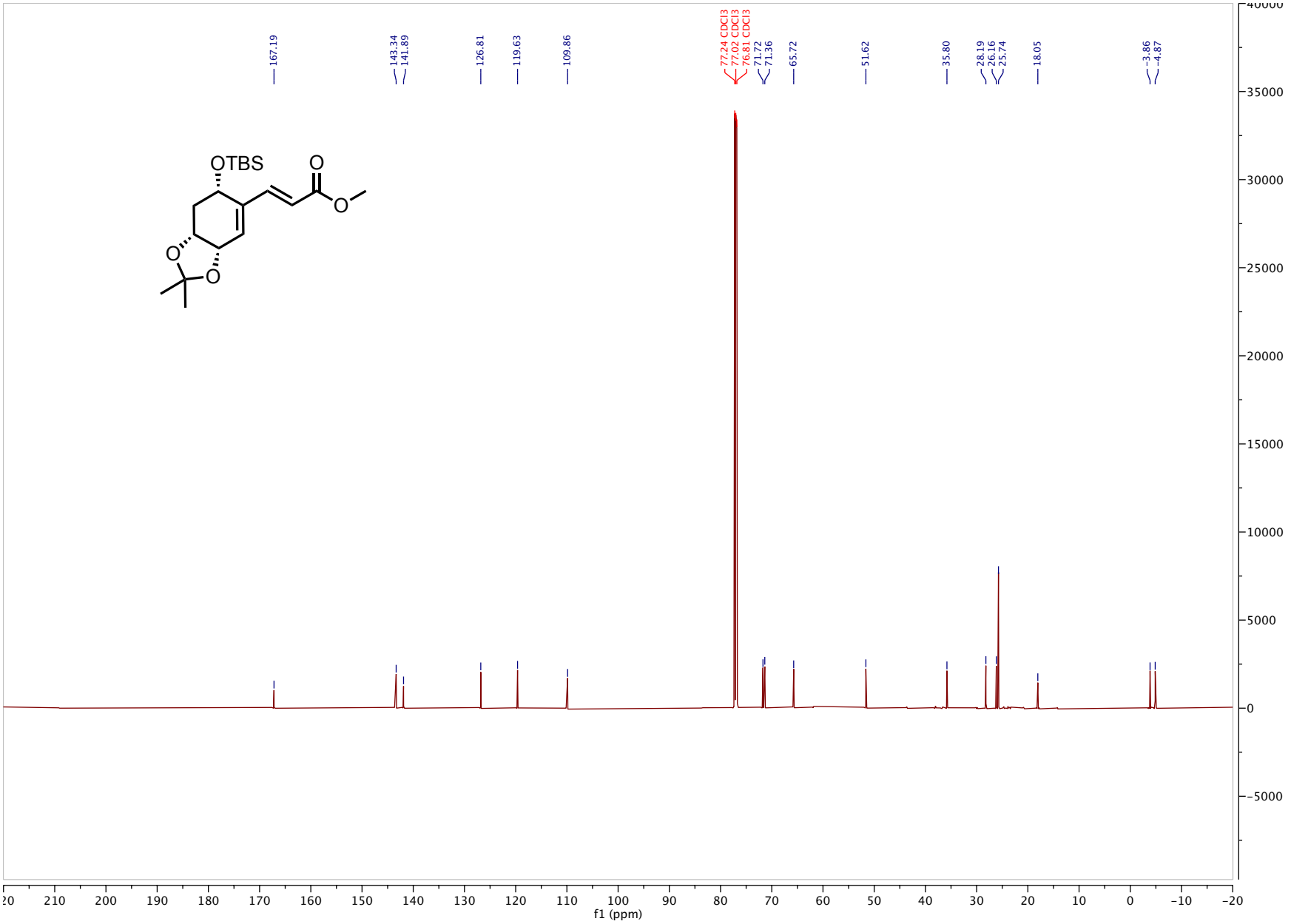

Figure C.05. ^{13}C NMR (151 MHz, $CDCl_3$) methyl ester **4.76**

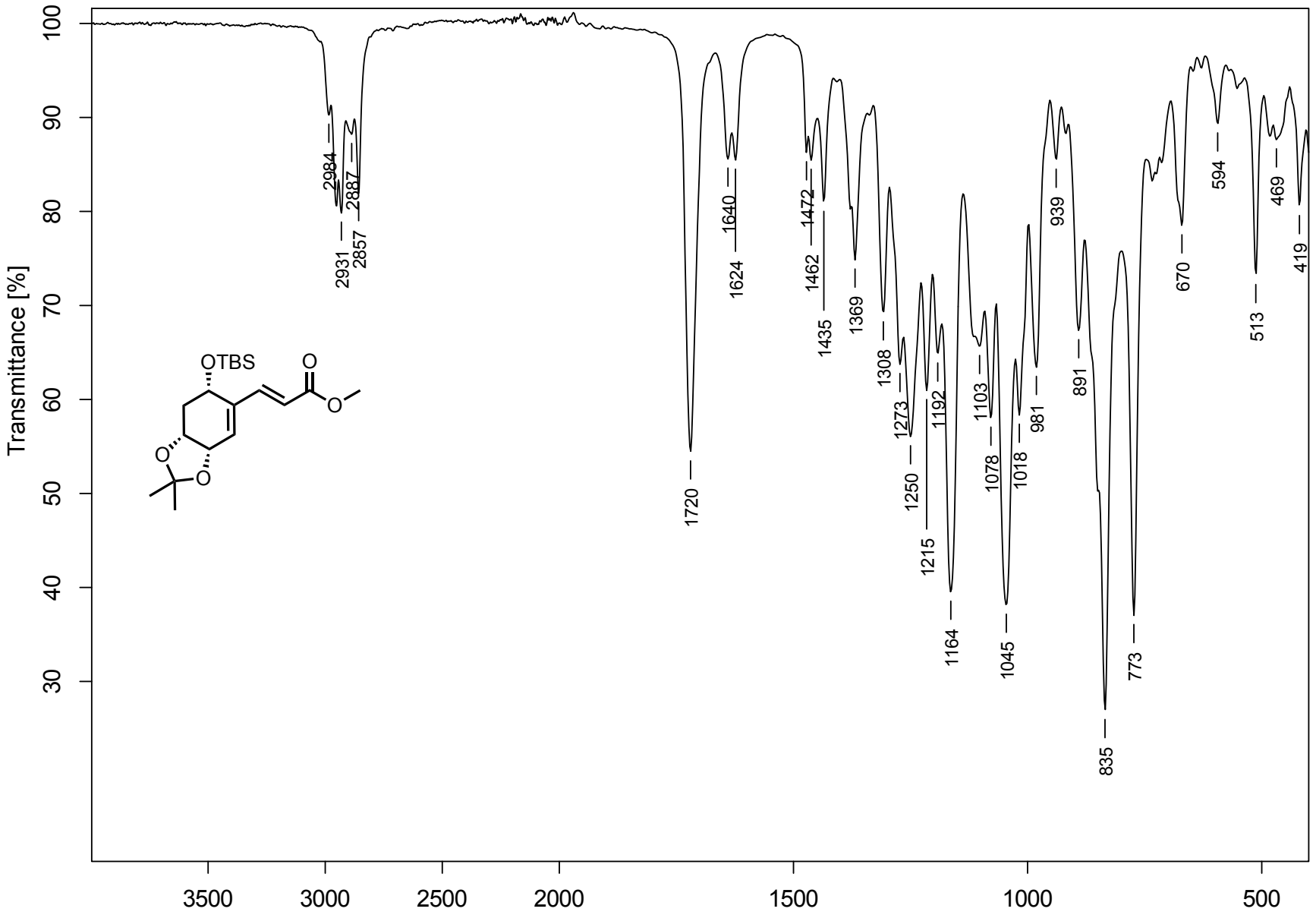

Figure C.06. FTIR (neat) methyl ester **4.76**

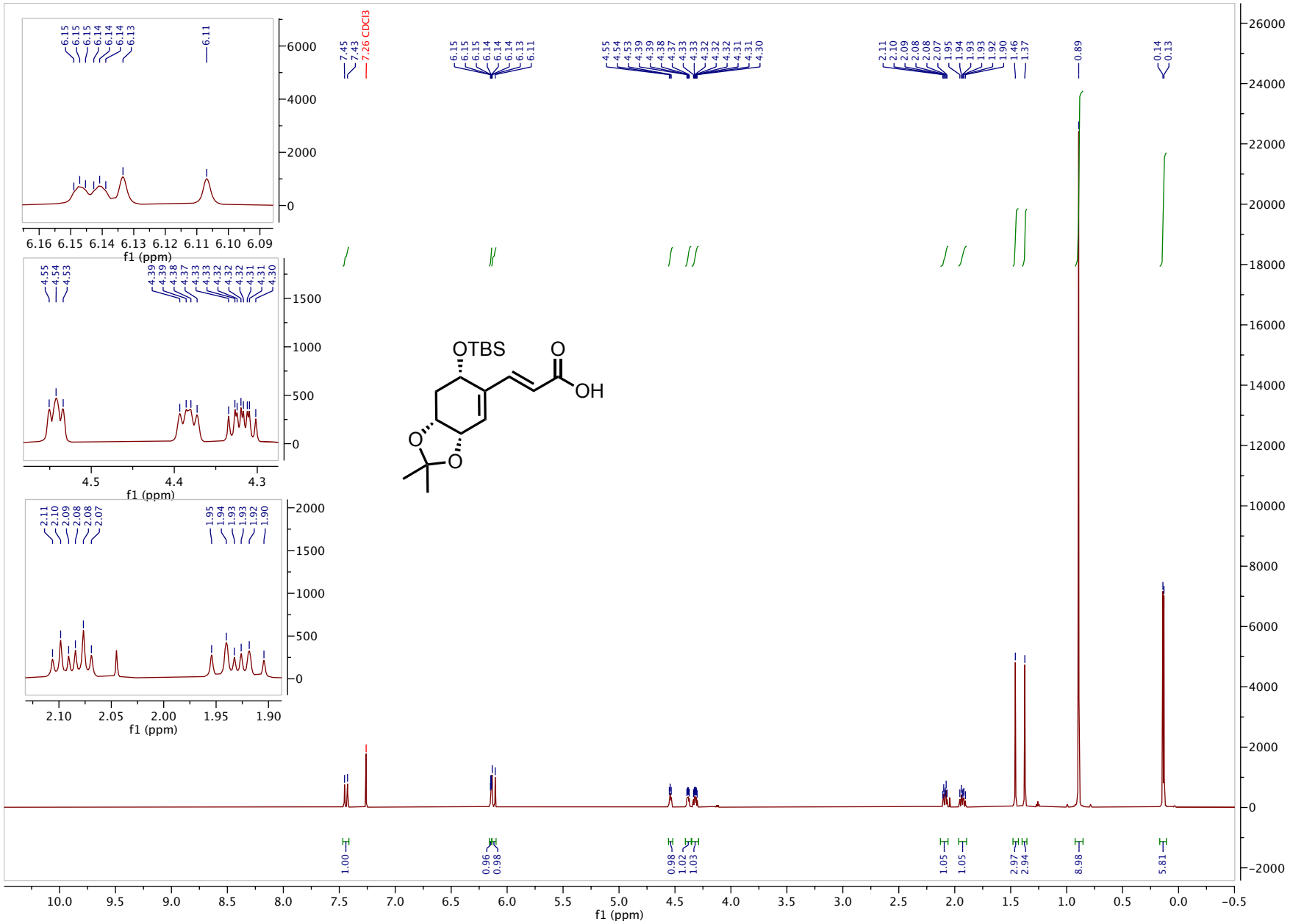

Figure C.07. ^{1}H NMR (600 MHz, $CDCl_3$) acid **4.92**

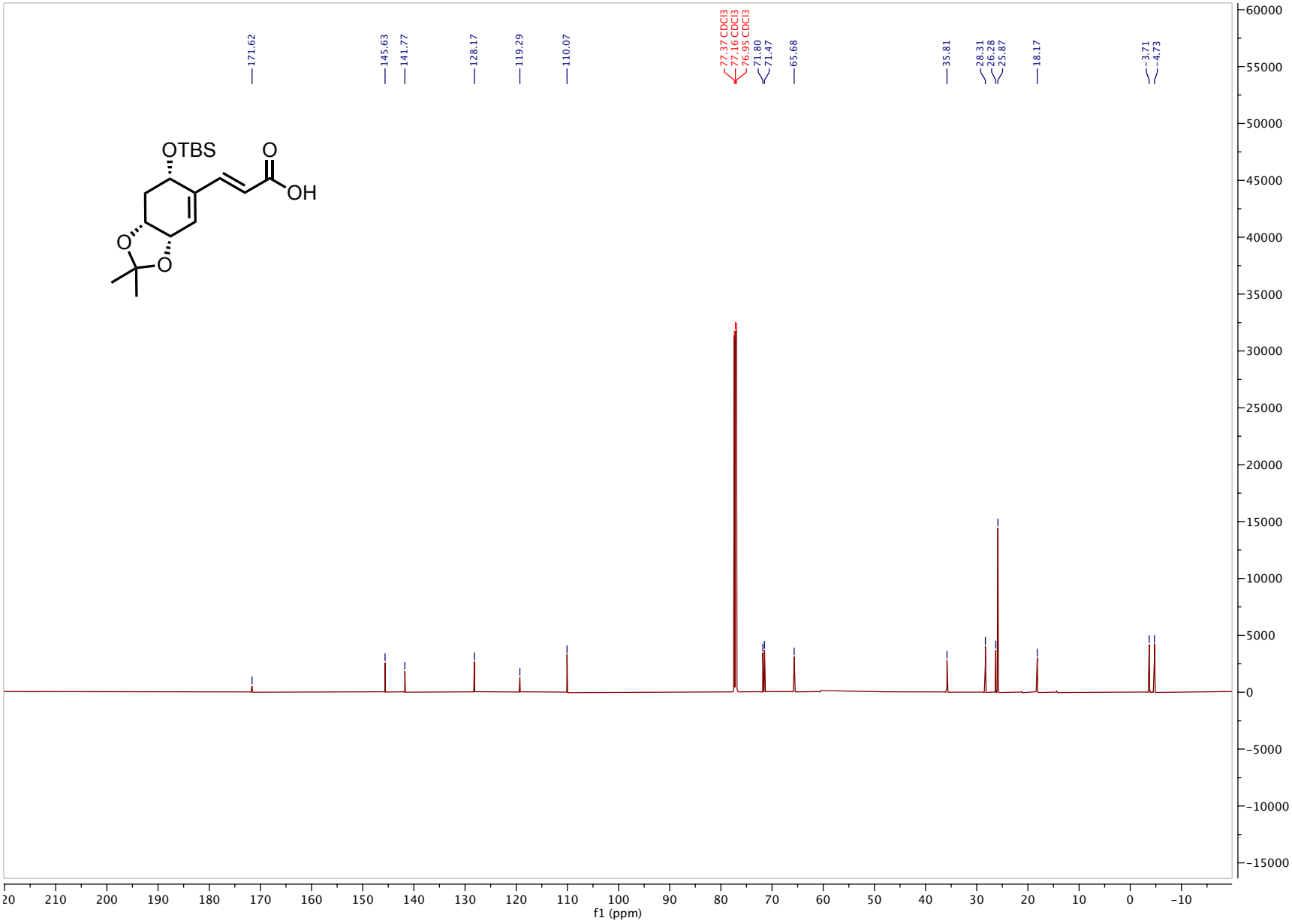

Figure C.08. ^{13}C NMR (151 MHz, $CDCl_3$) acid **4.92**

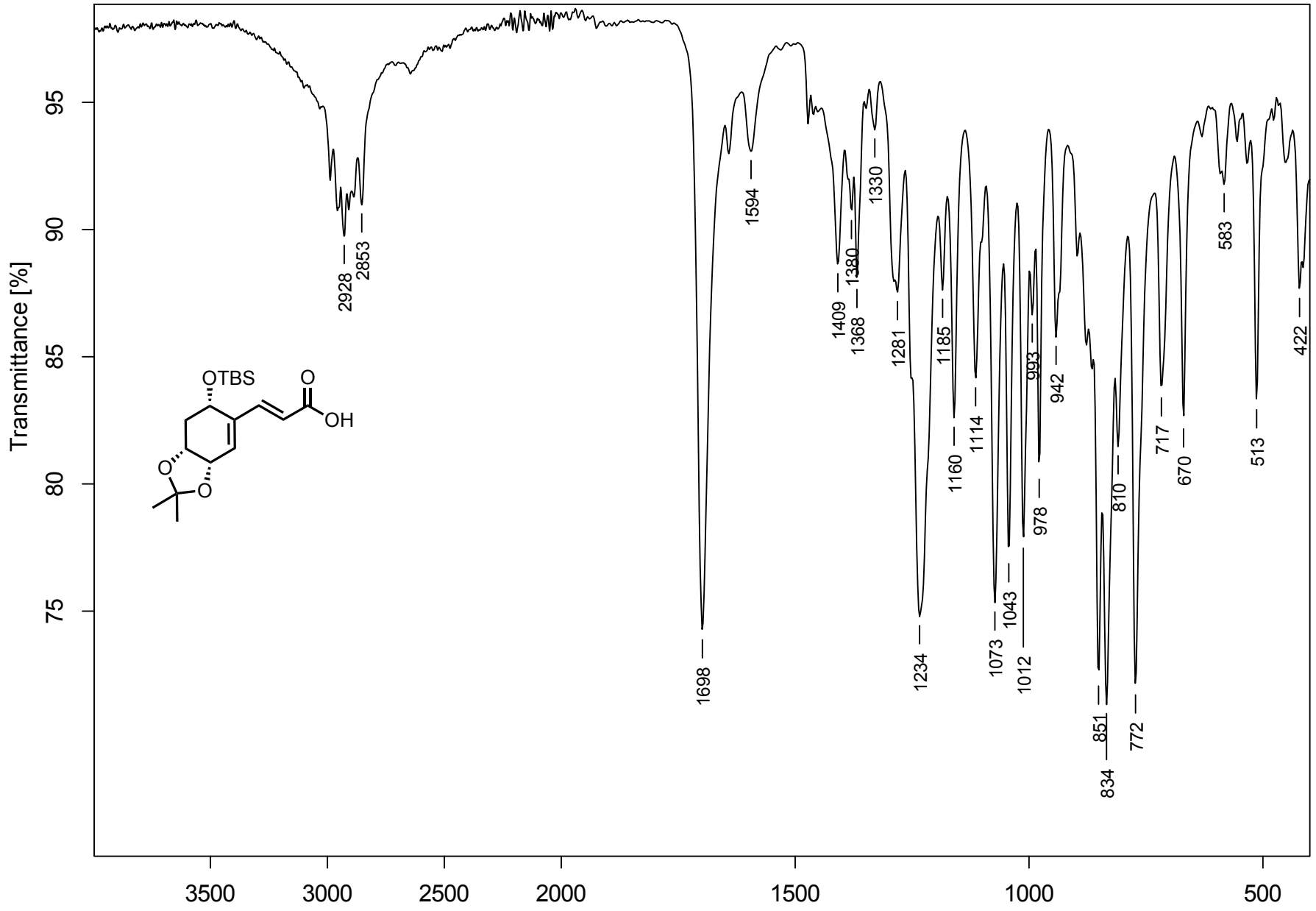

Figure C.09. FTIR (neat) acid **4.92**

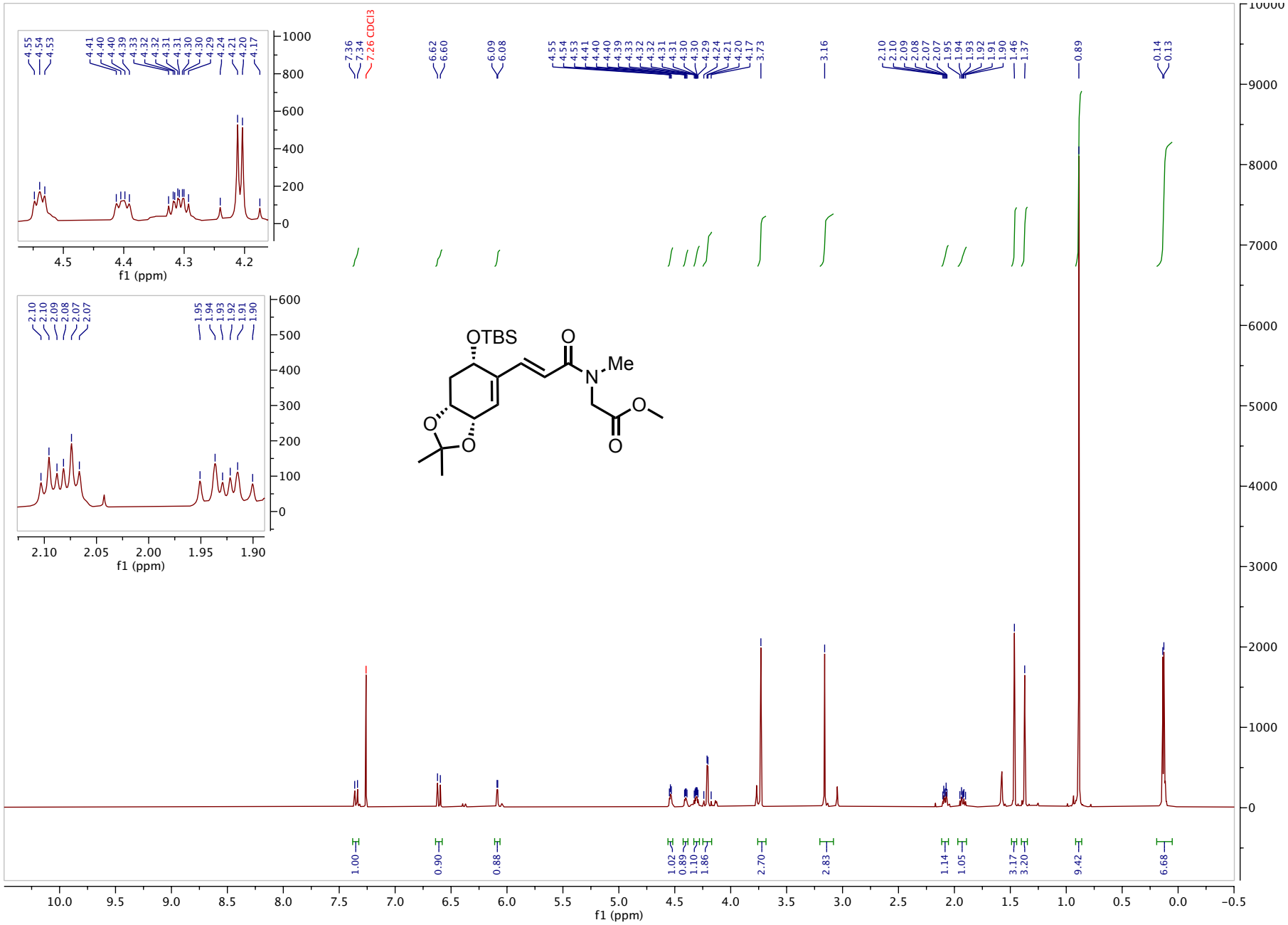

Figure C.10. ^{1}H NMR (600 MHz, $CDCl_3$) amide **4.74**

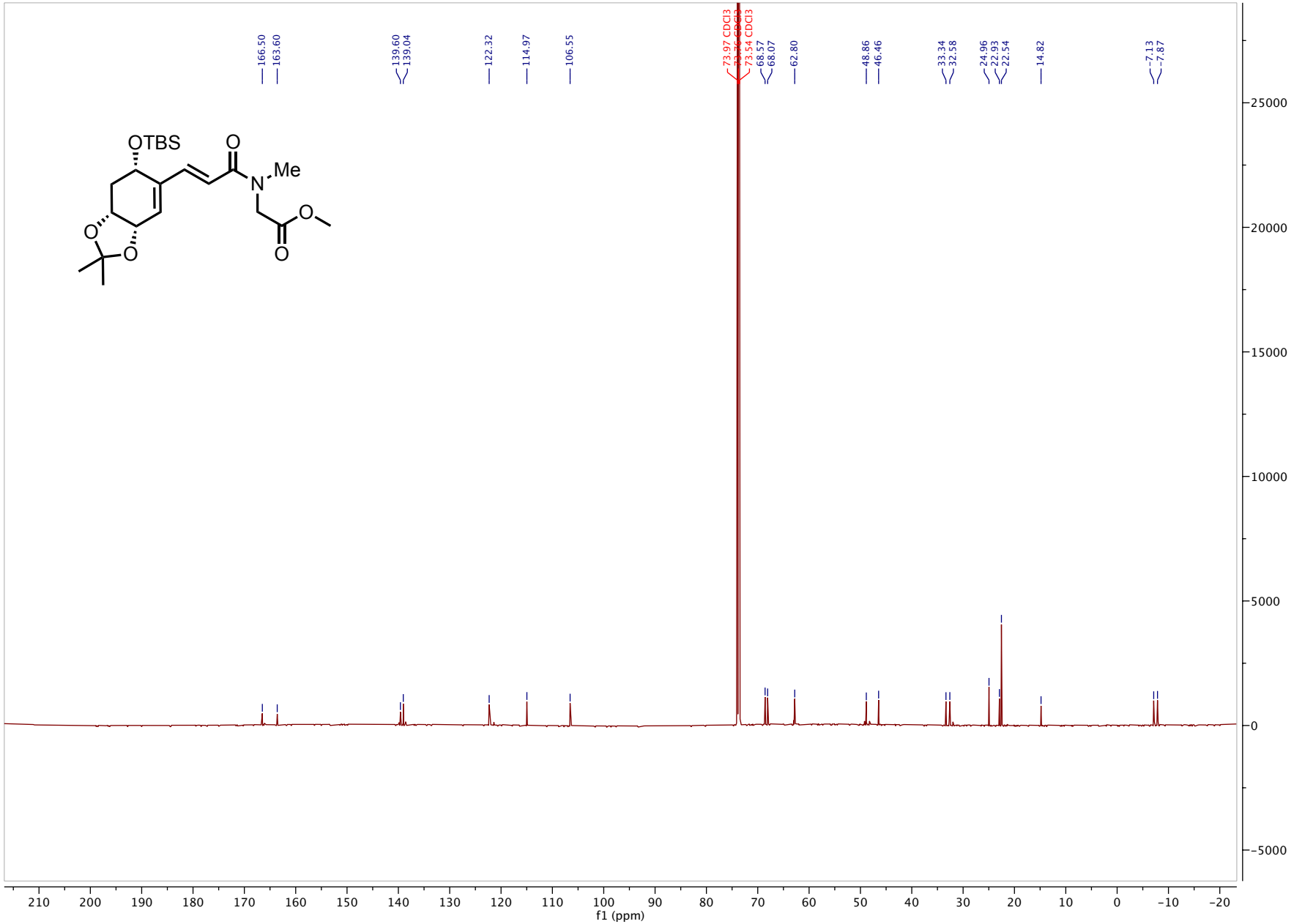

Figure C.11. ^{13}C NMR (151 MHz, $CDCl_3$) amide **4.74**

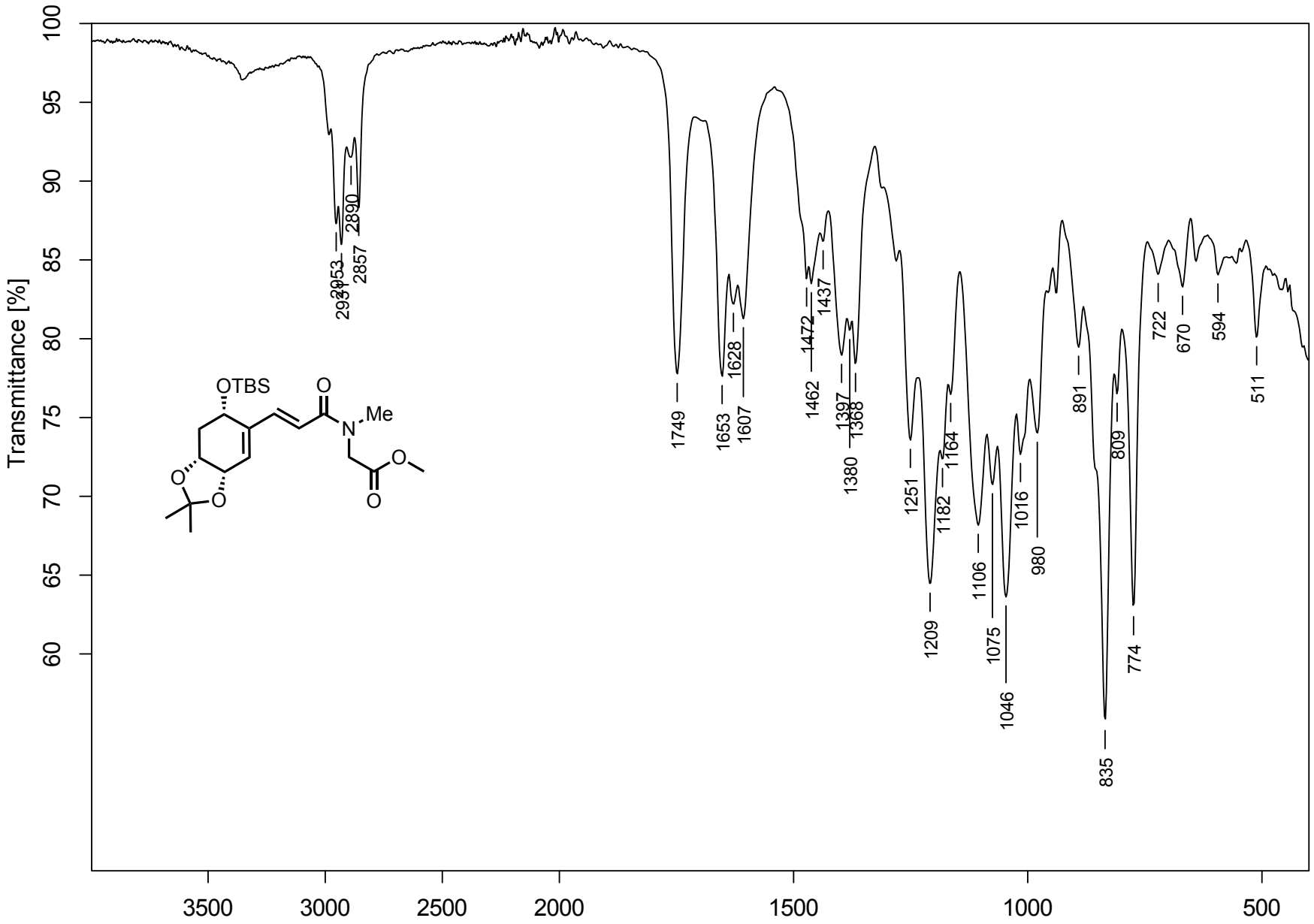

Figure C.12. FTIR (neat) amide **4.74**

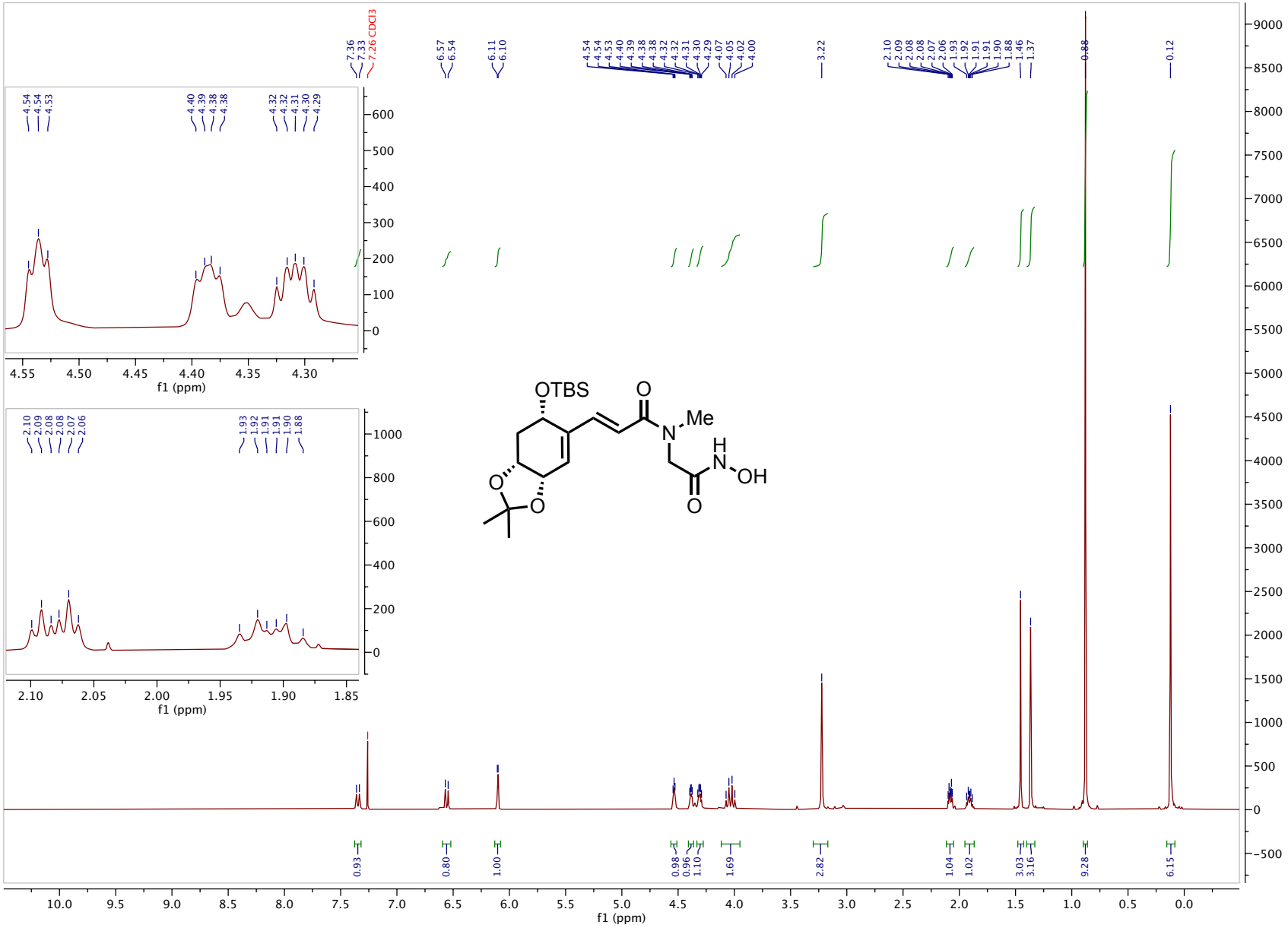

Figure C.13. ^{1}H NMR (600 MHz, $CDCl_3$) hydroxamic acid **4.73**

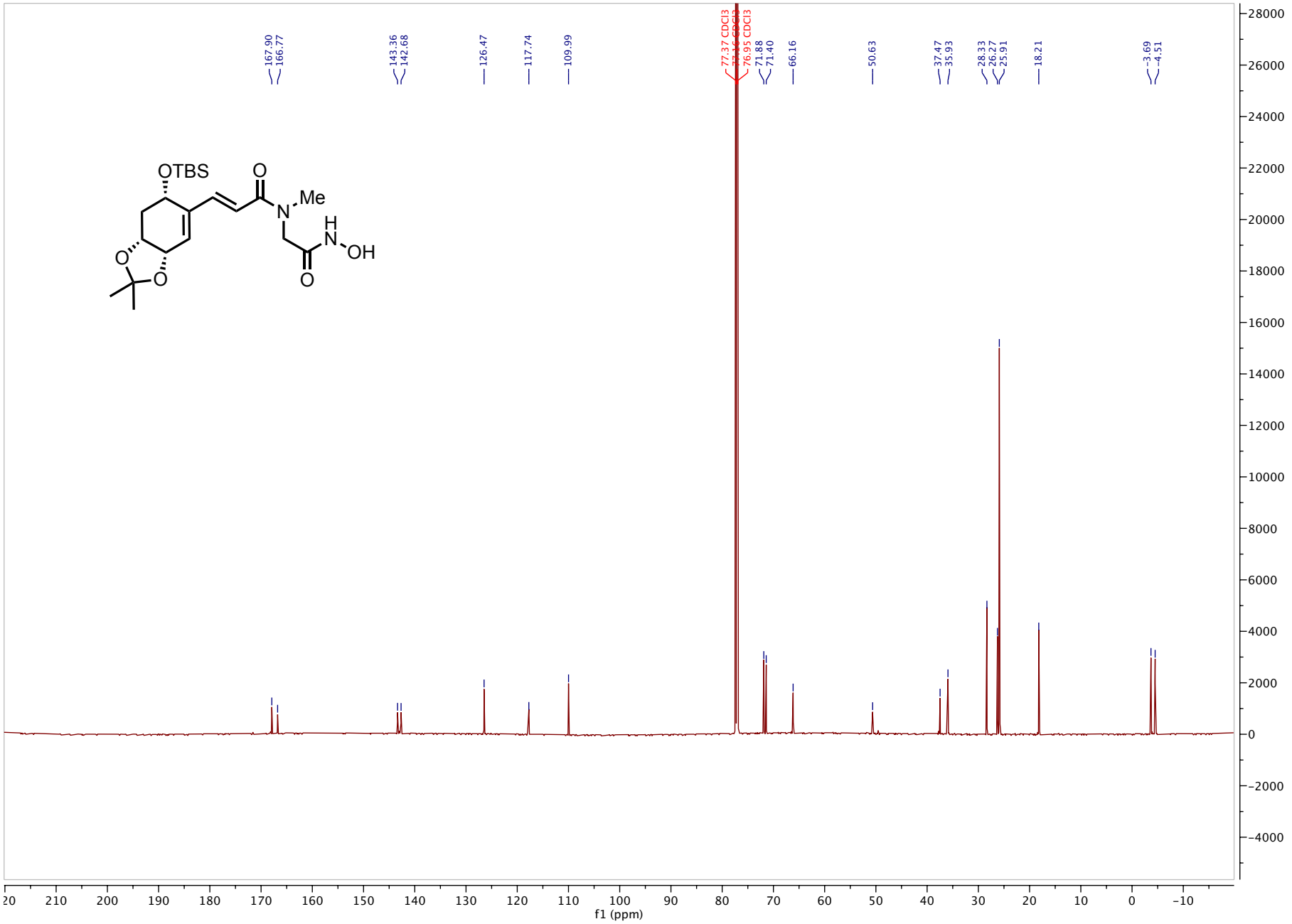

Figure C.14. ^{13}C NMR (151 MHz, $CDCl_3$) hydroxamic acid **4.73**

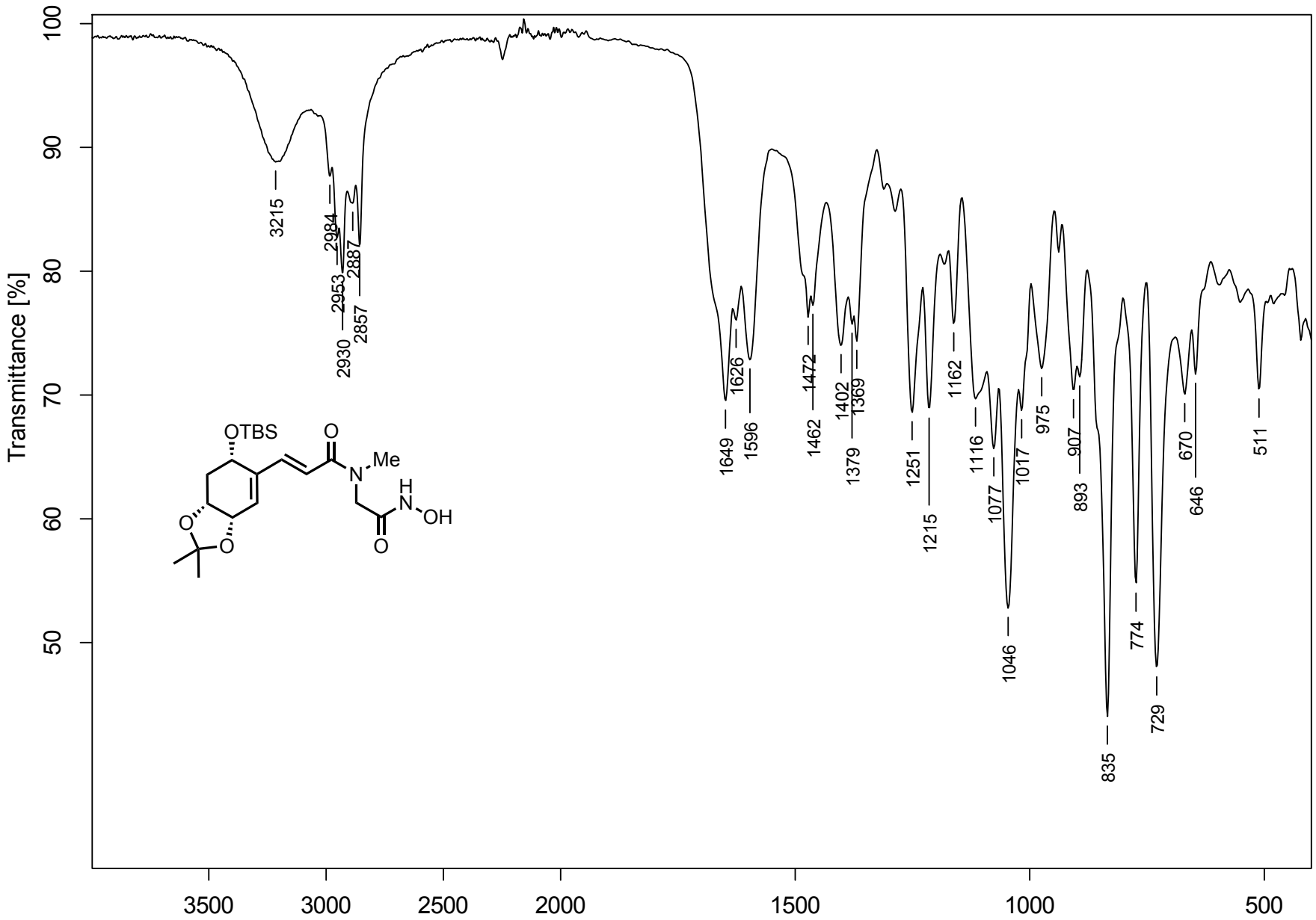

Figure C.15. FTIR (neat) hydroxamic acid **4.73**

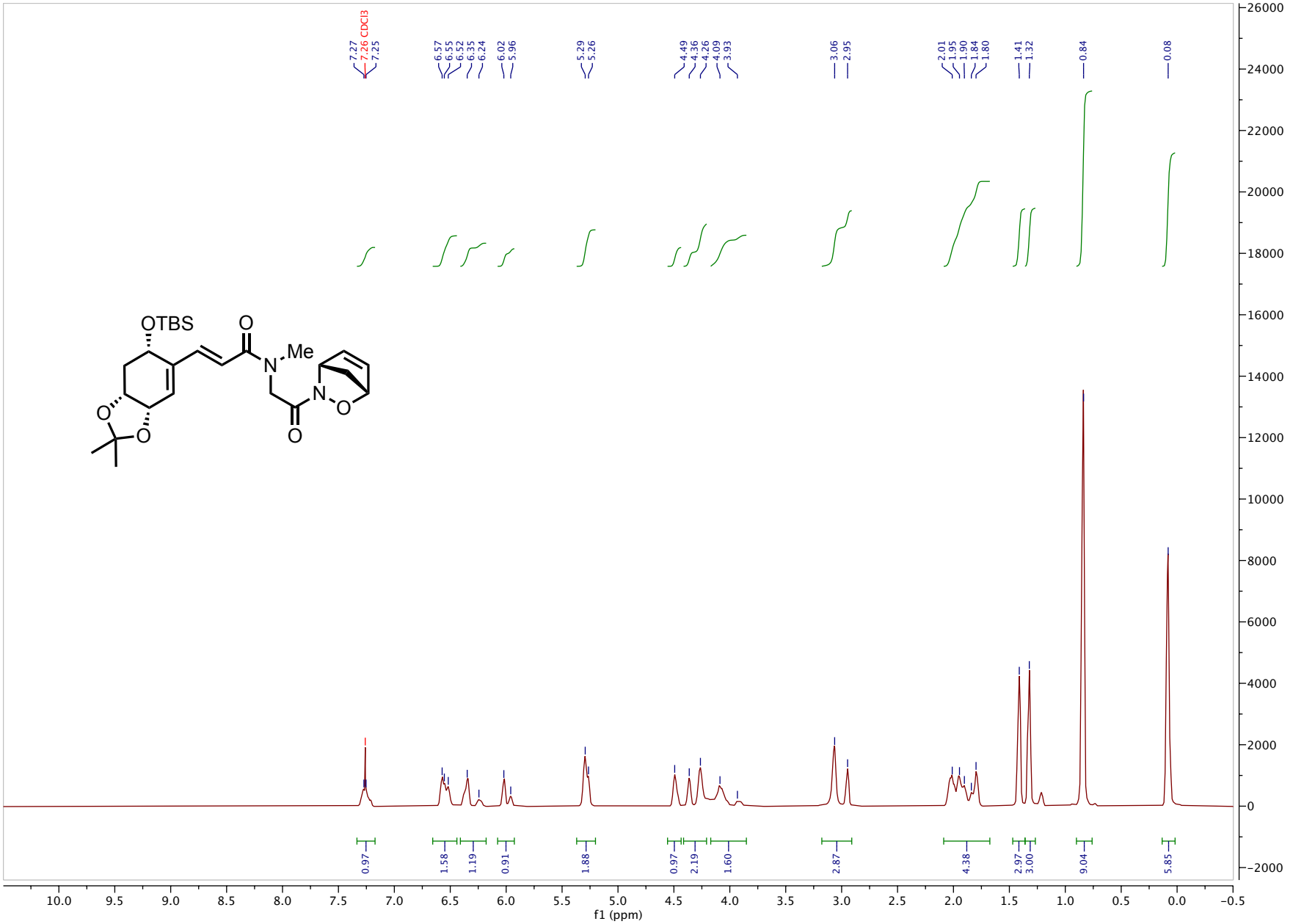

Figure C.16. ^{1}H NMR (600 MHz, $CDCl_3$) cyclopentadiene adduct **4.72**

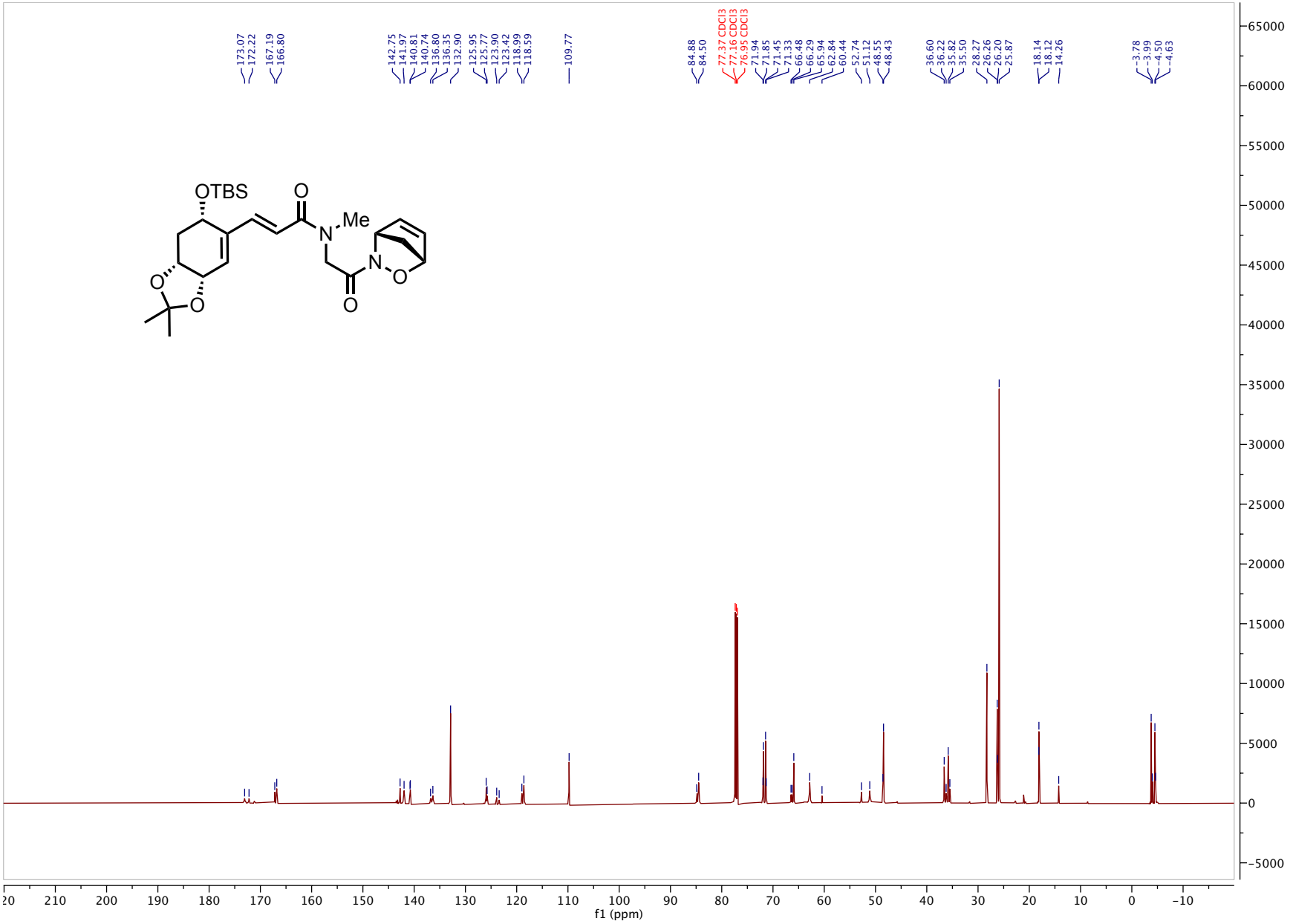

Figure C.17. ^{13}C NMR (151 MHz, $CDCl_3$) cyclopentadiene adduct **4.72**

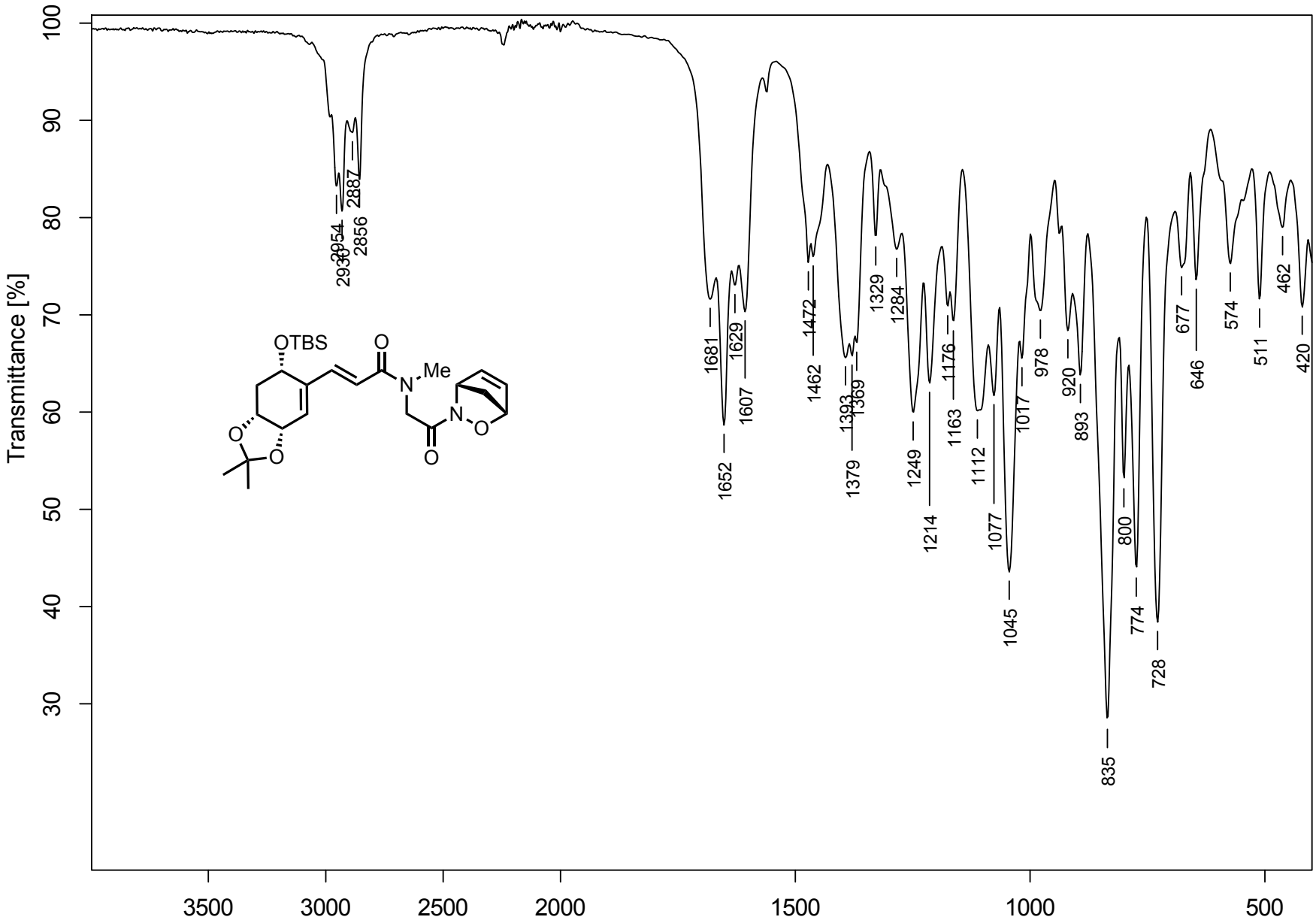

Figure C.18. FTIR (neat) cyclopentadiene adduct **4.72**

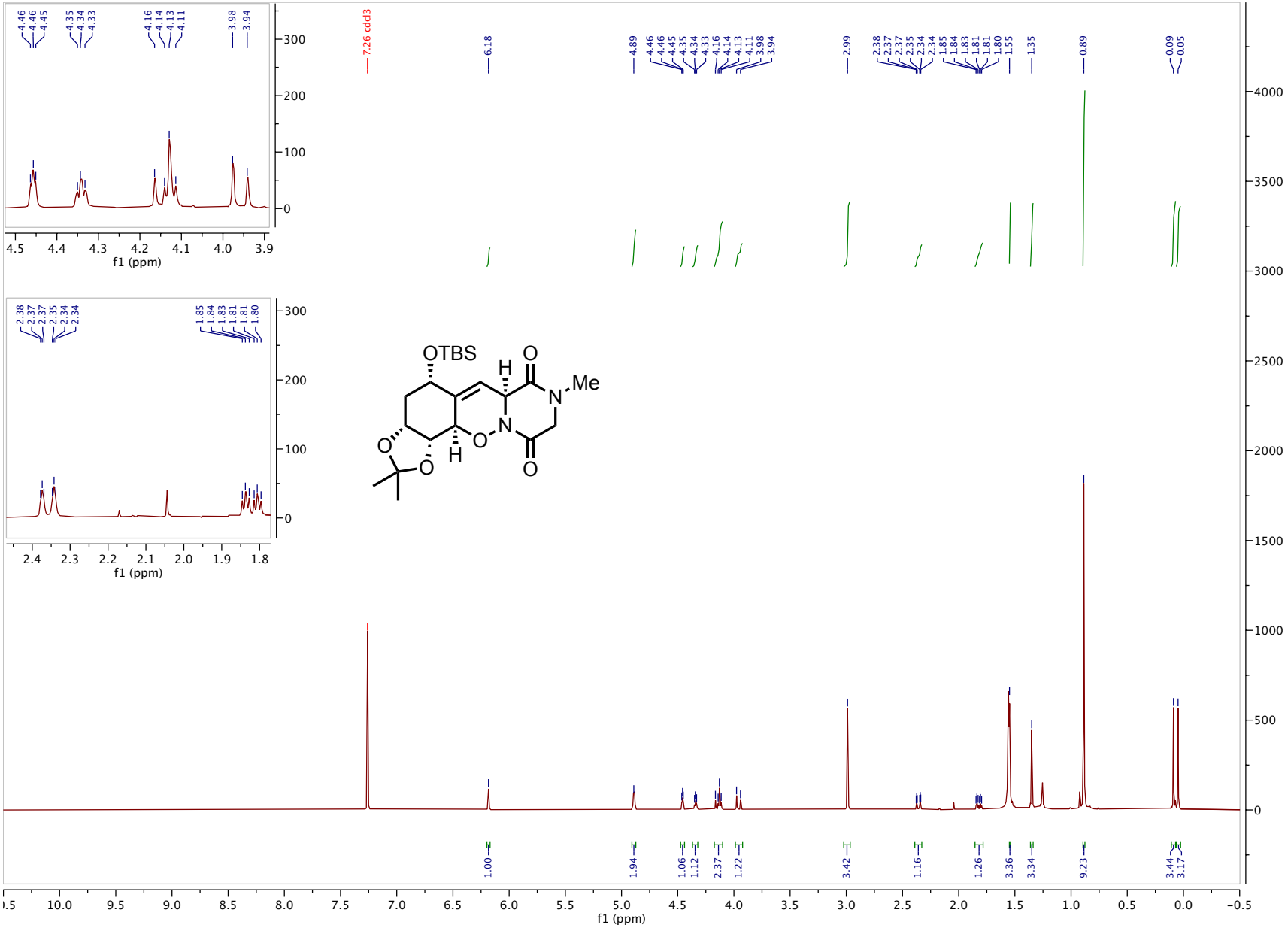

Figure C.19. ^{1}H NMR (500 MHz, $CDCl_3$) NDA cycloadduct **4.70**

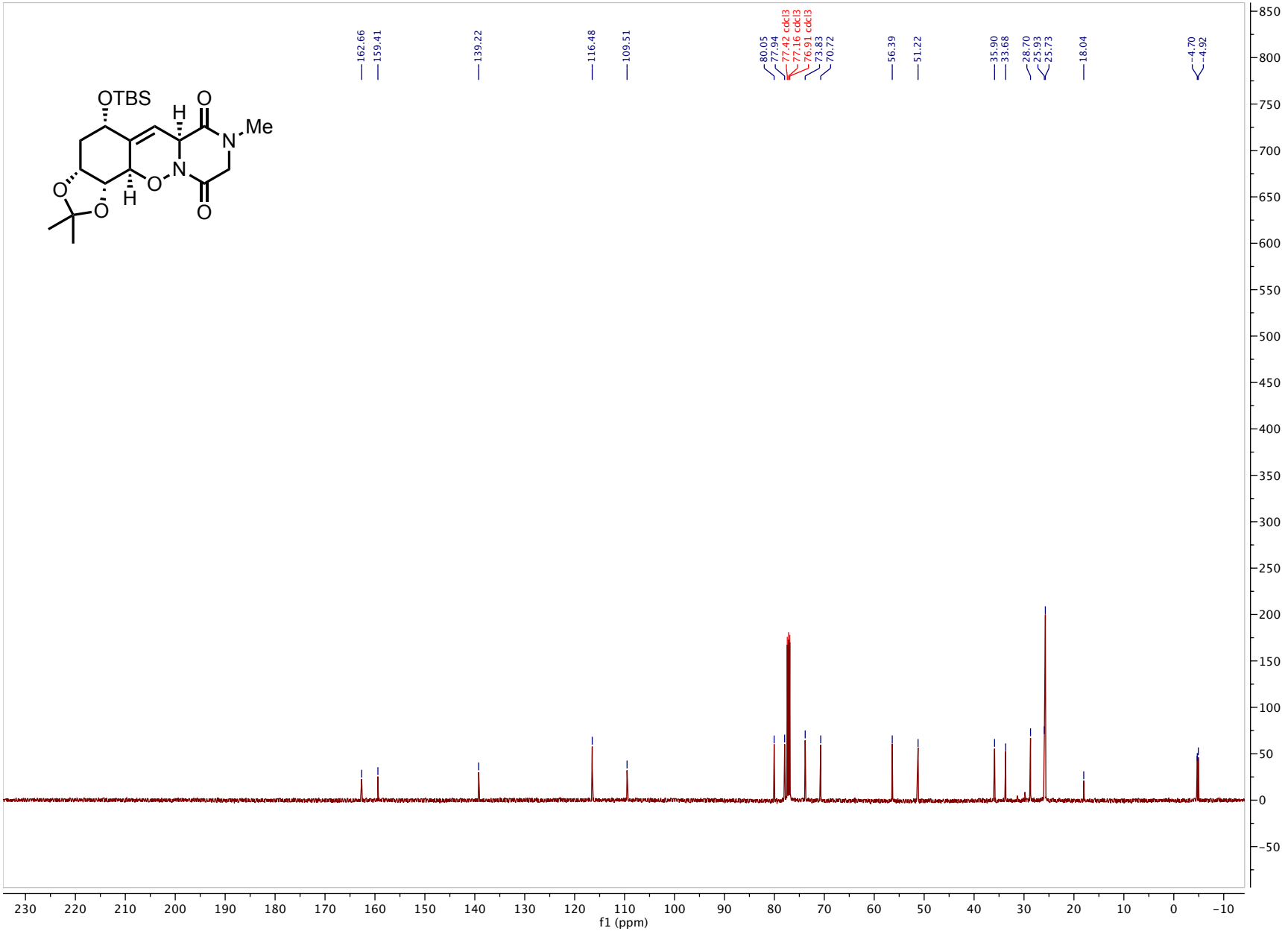

Figure C.20. ^{13}C NMR (126 MHz, $CDCl_3$) NDA cycloadduct **4.70**

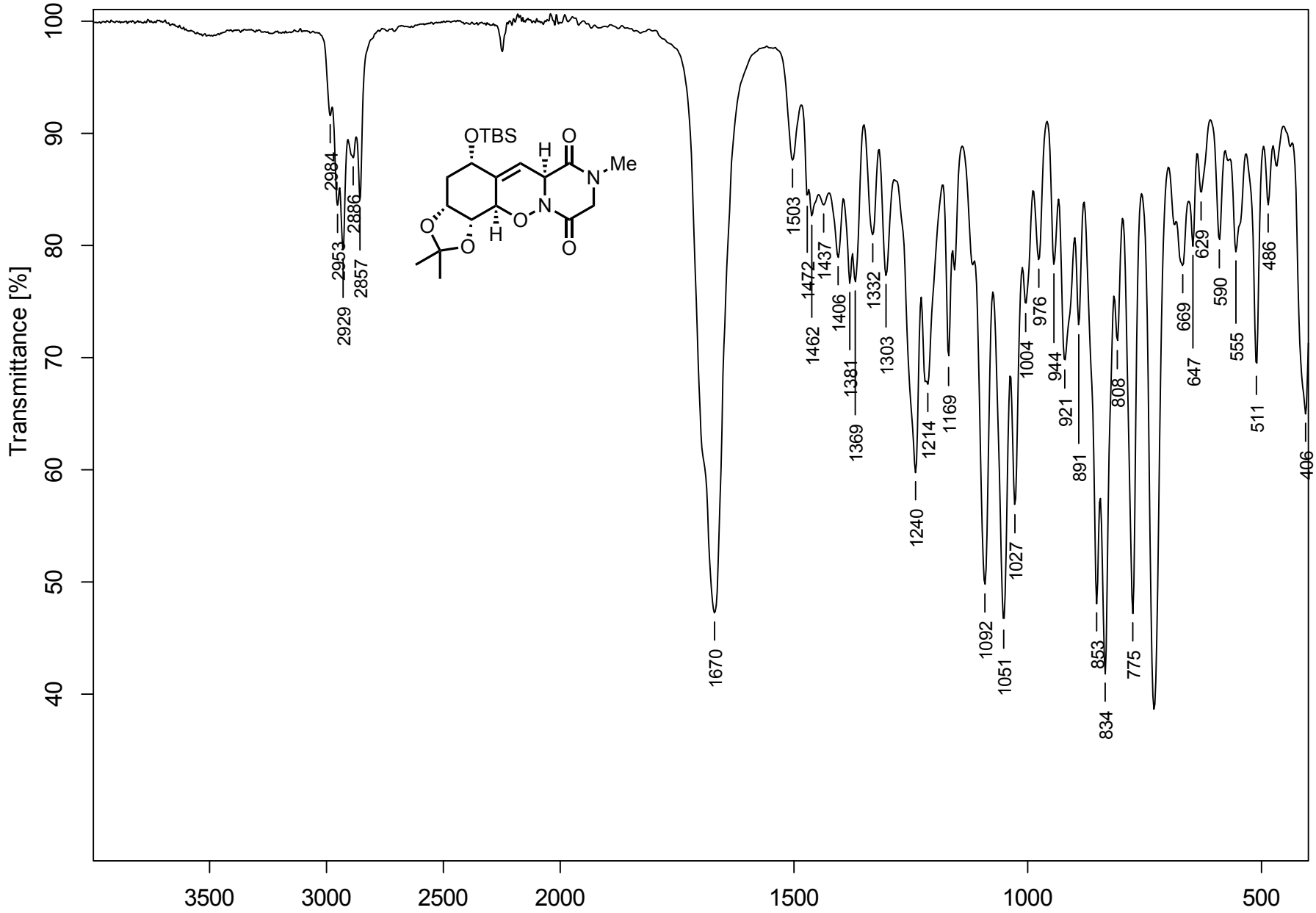

Figure C.21. FTIR (thin film) NDA cycloadduct **4.70**

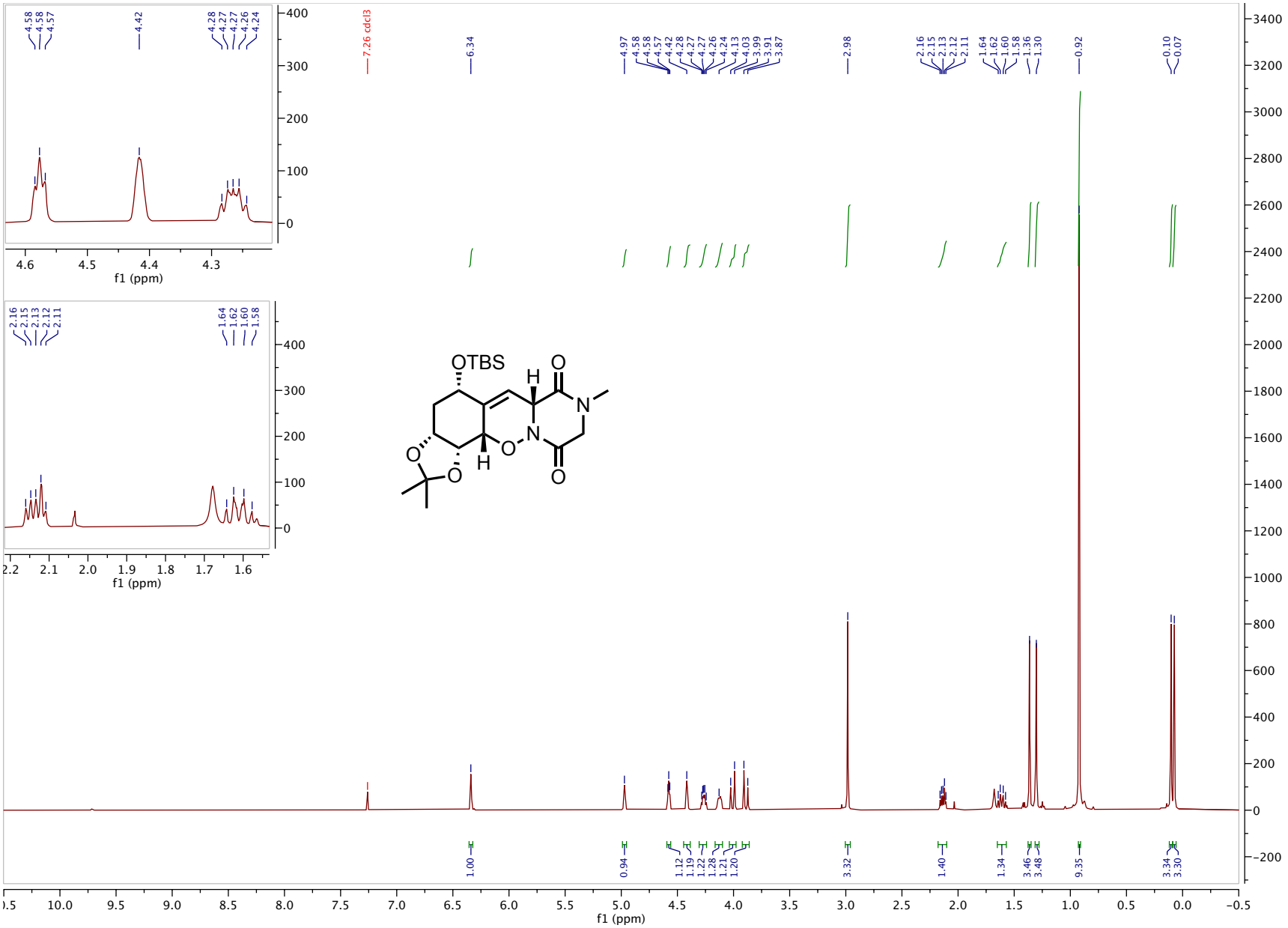

Figure C.22. ^{1}H NMR (500 MHz, $CDCl_3$) NDA cycloadduct **4.93**

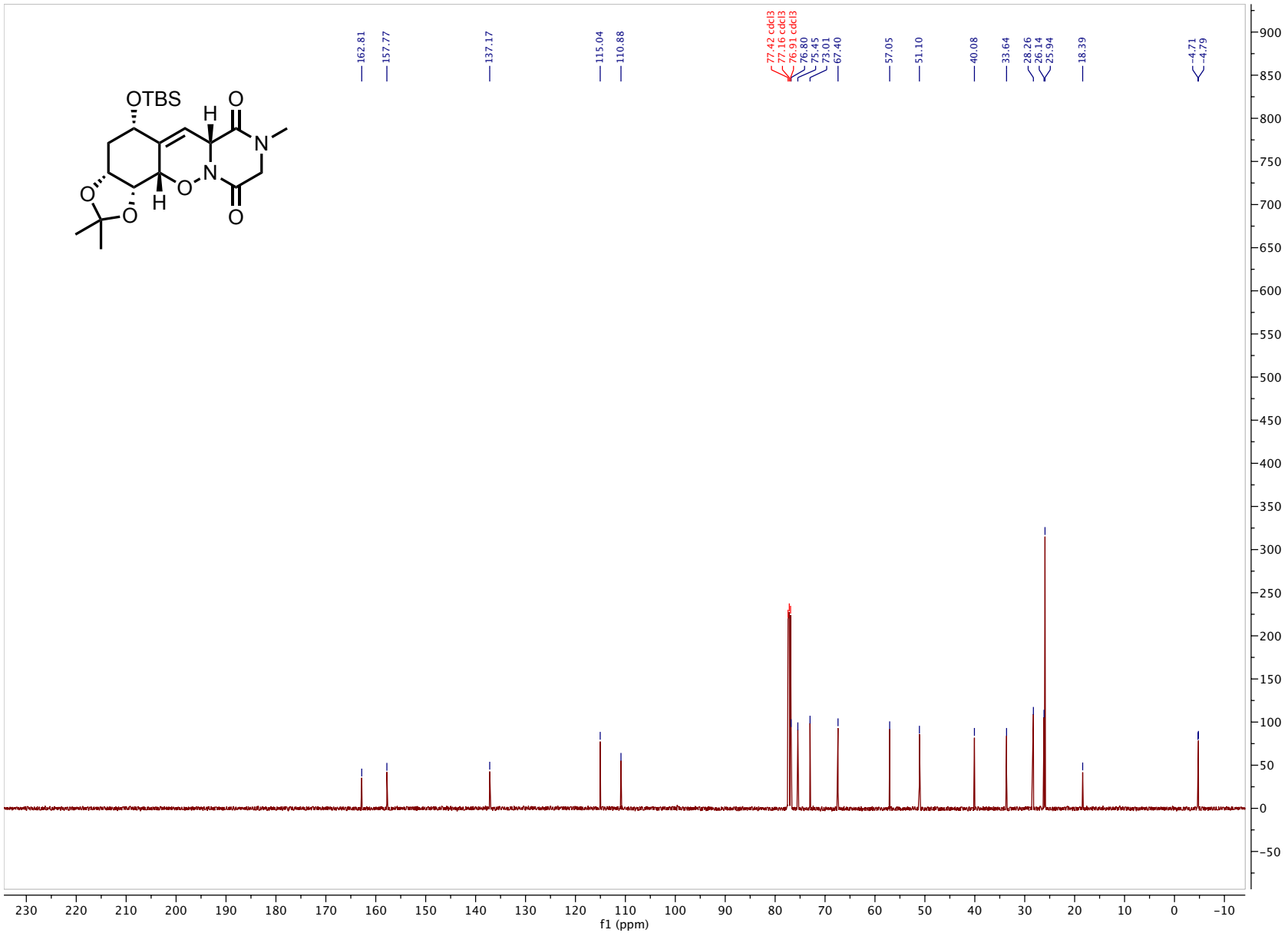

Figure C.23. ^{13}C NMR (126 MHz, $CDCl_3$) NDA cycloadduct **4.93**

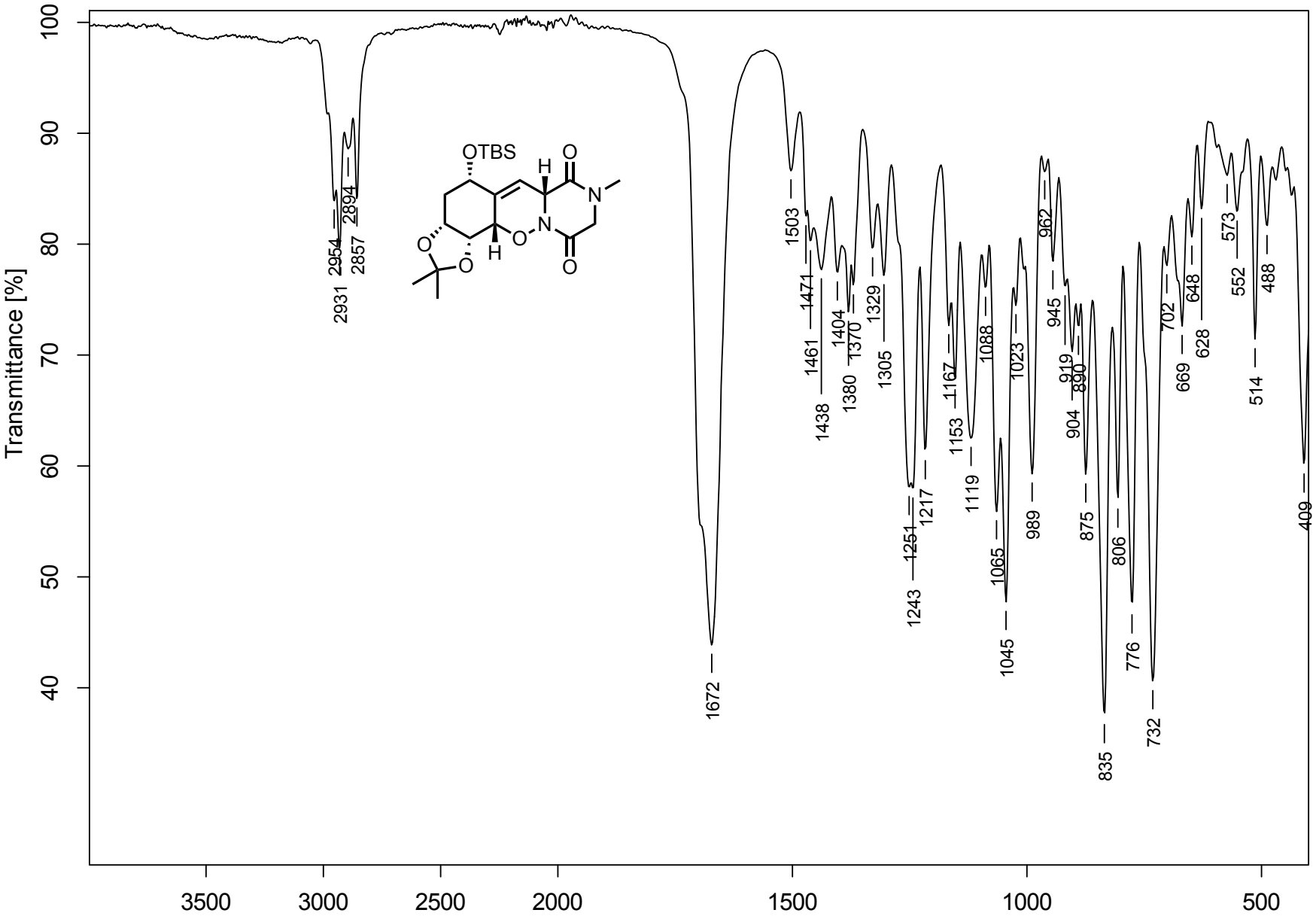

Figure C.24. FTIR (neat) NDA cycloadduct **4.93**

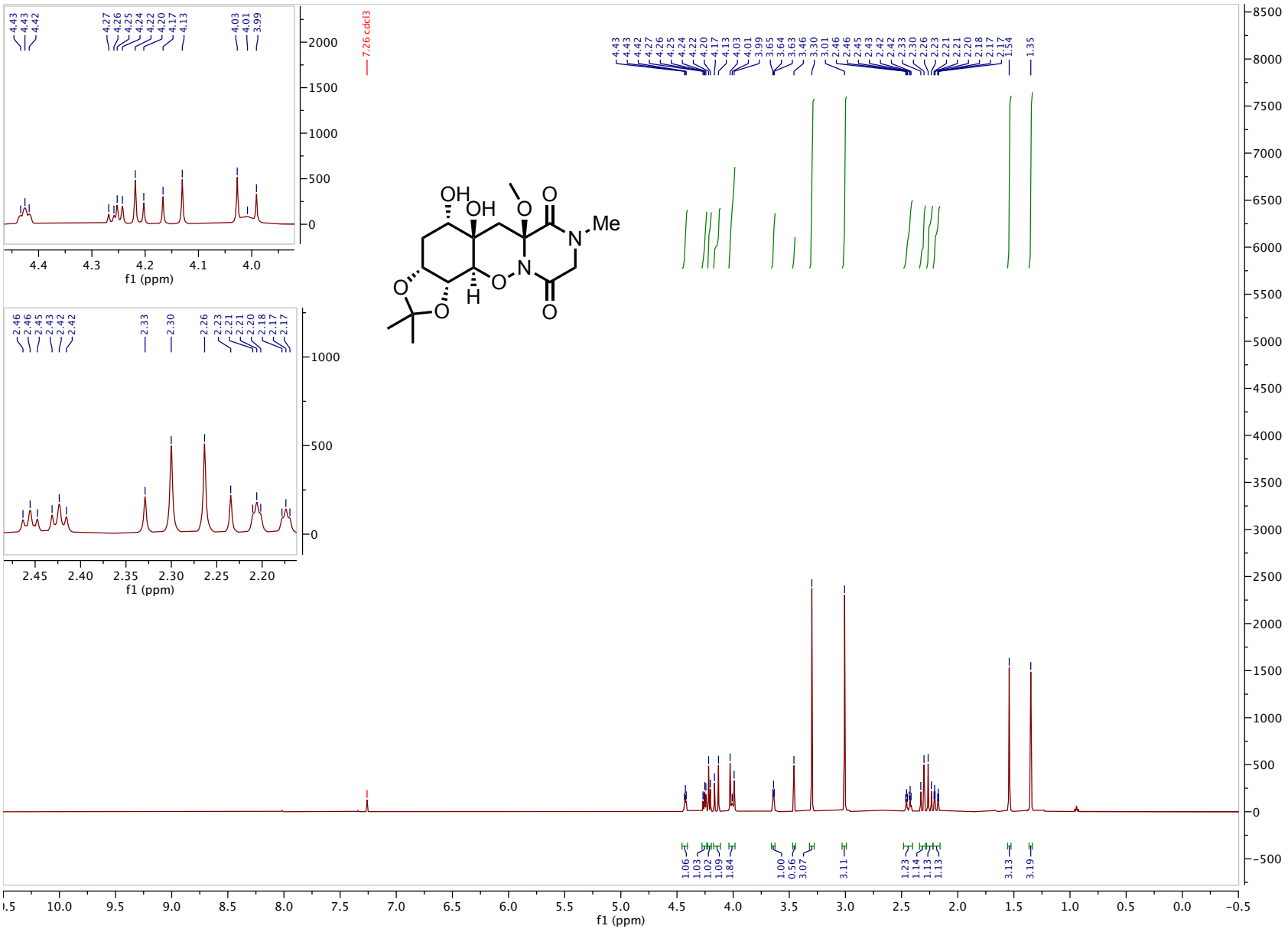

Figure C.25. ^{1}H NMR (500 MHz, $CDCl_3$) diol **4.97**

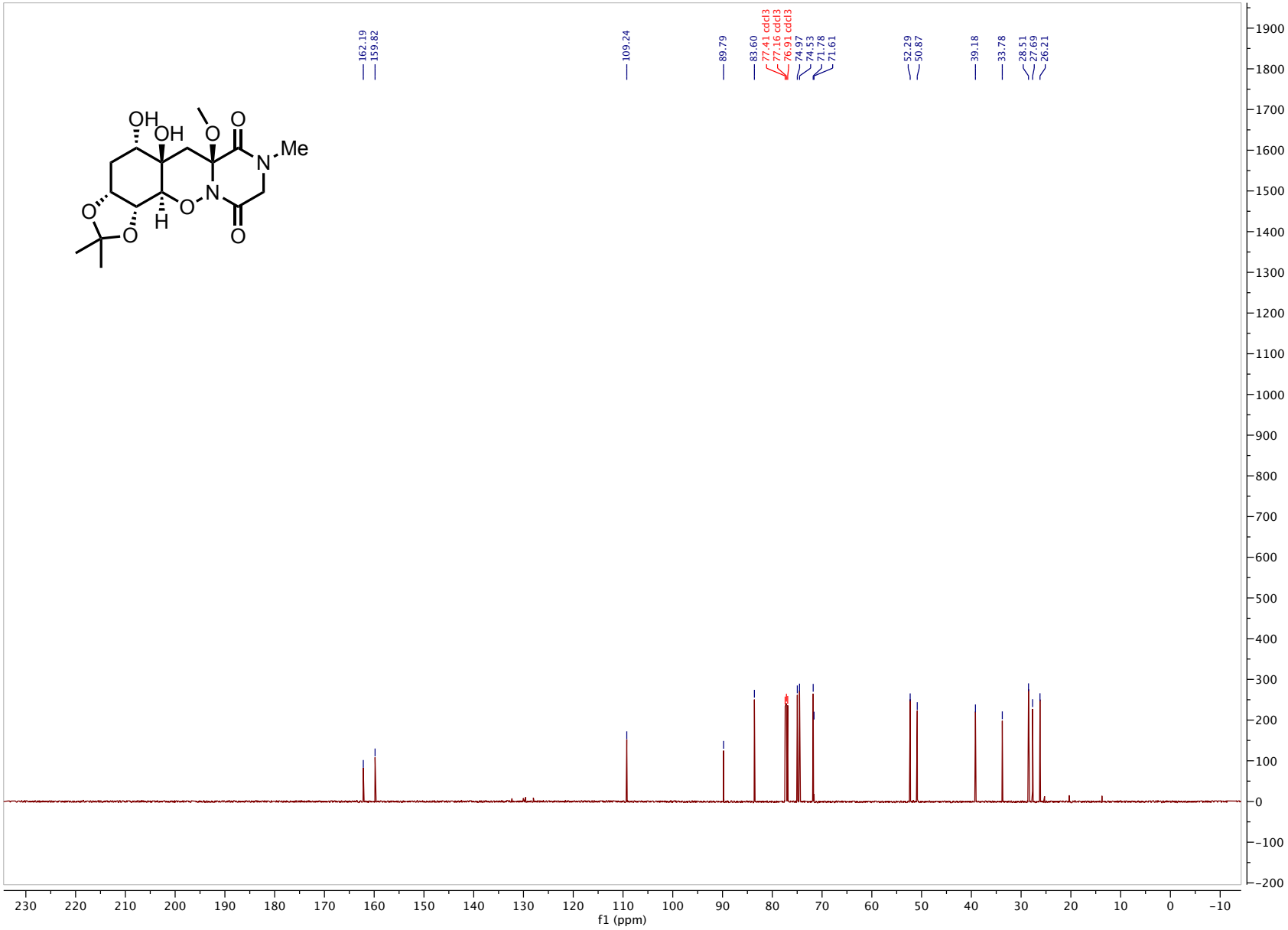

Figure C.26. ^{13}C NMR (126 MHz, $CDCl_3$) diol **4.97**

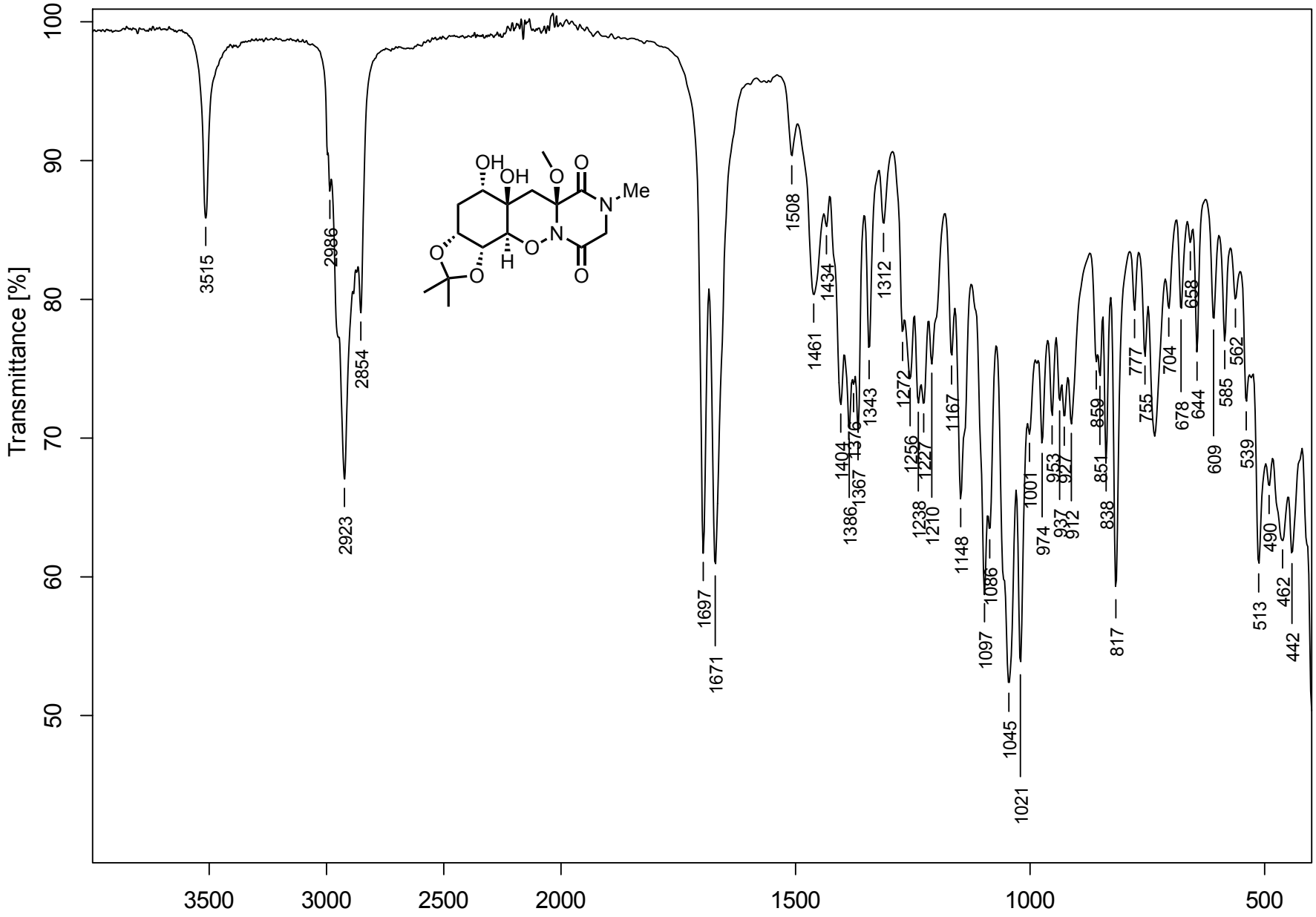

Figure C.27. FTIR (thin film) diol **4.97**

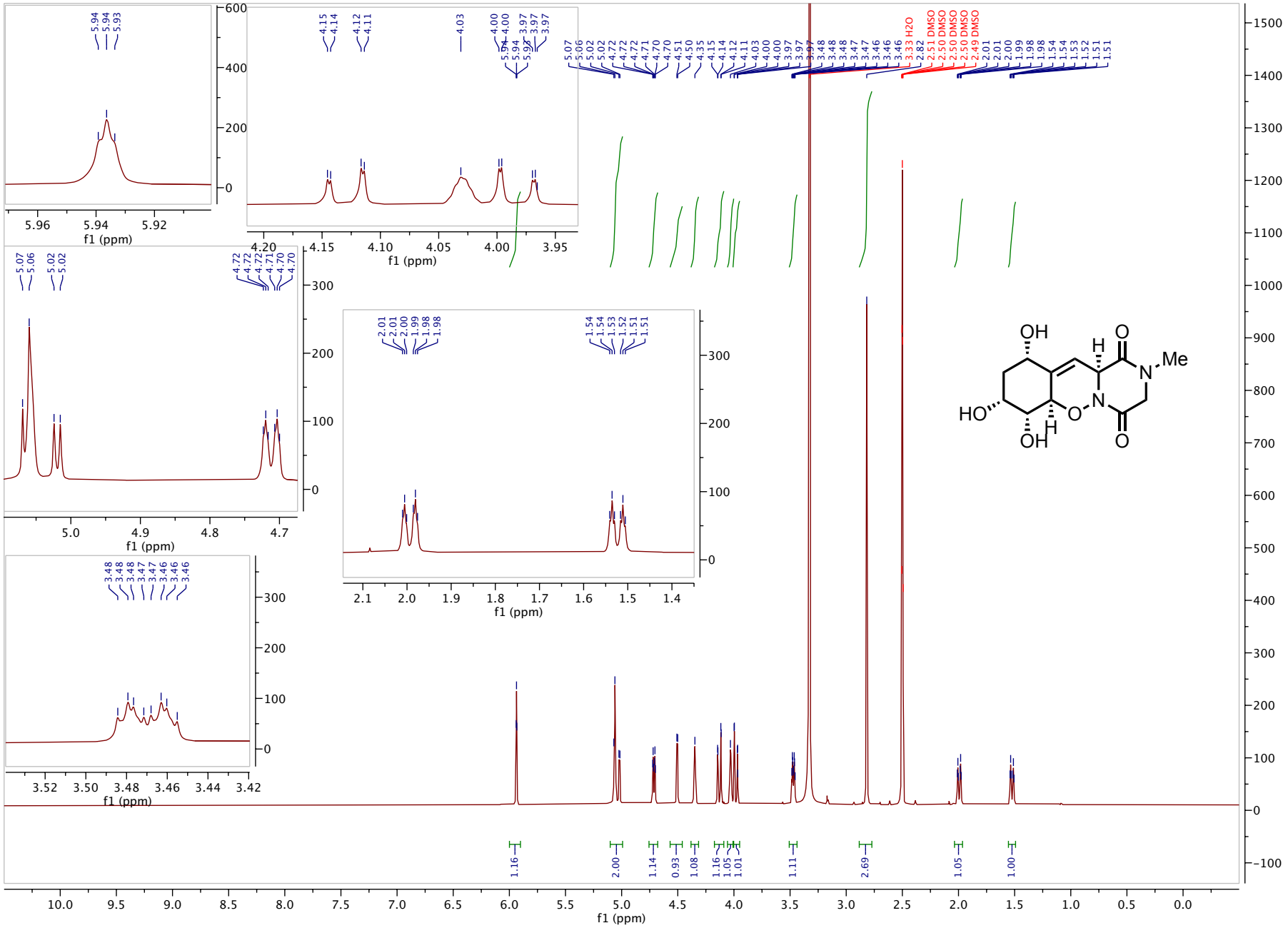

Figure C.28. ^{1}H NMR (600 MHz, DMSO) triol **4.98**

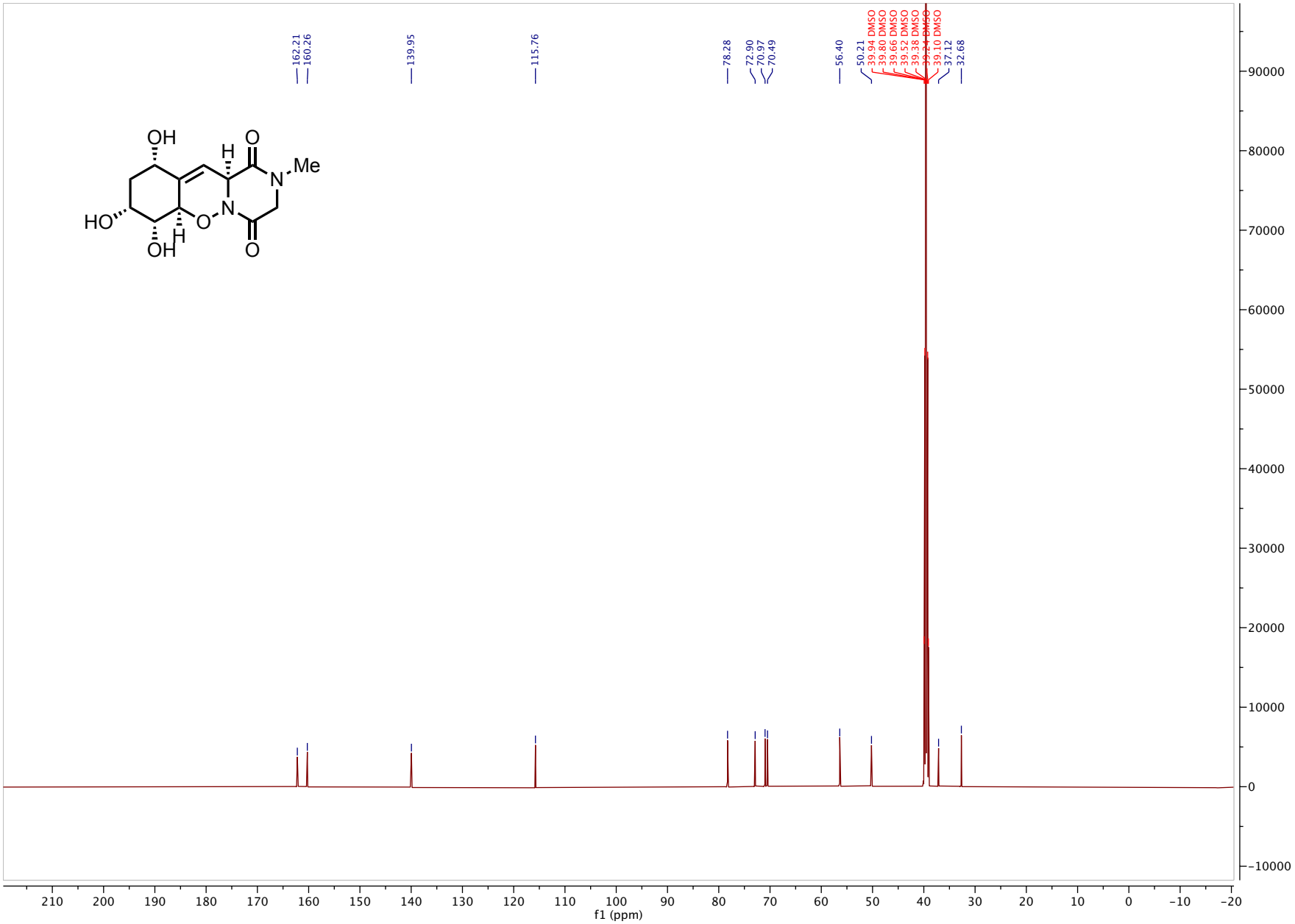

Figure C.29. ^{13}C NMR (151 MHz, DMSO) triol **4.98**

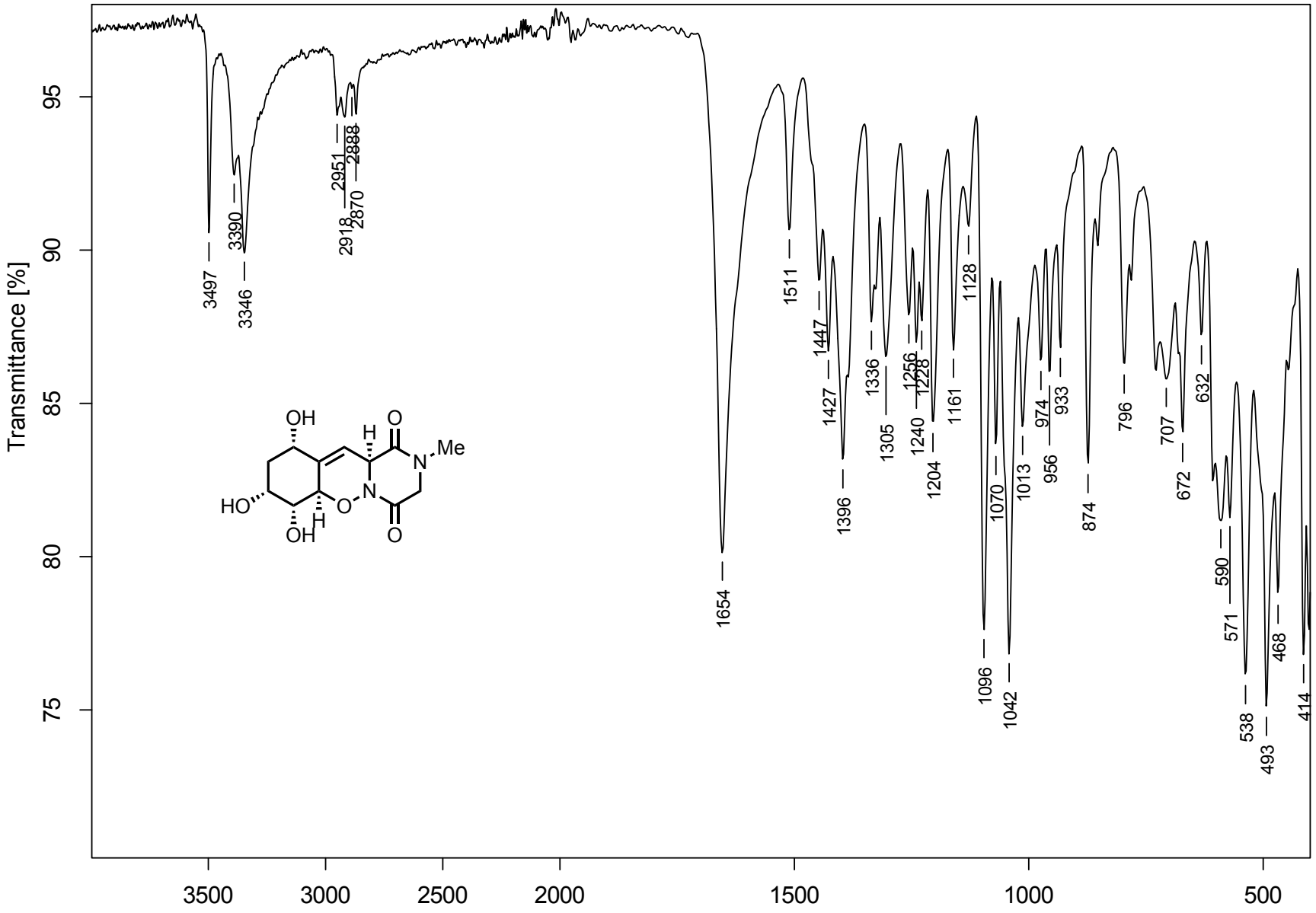

Figure C.30. FTIR (thin film) triol **4.98**

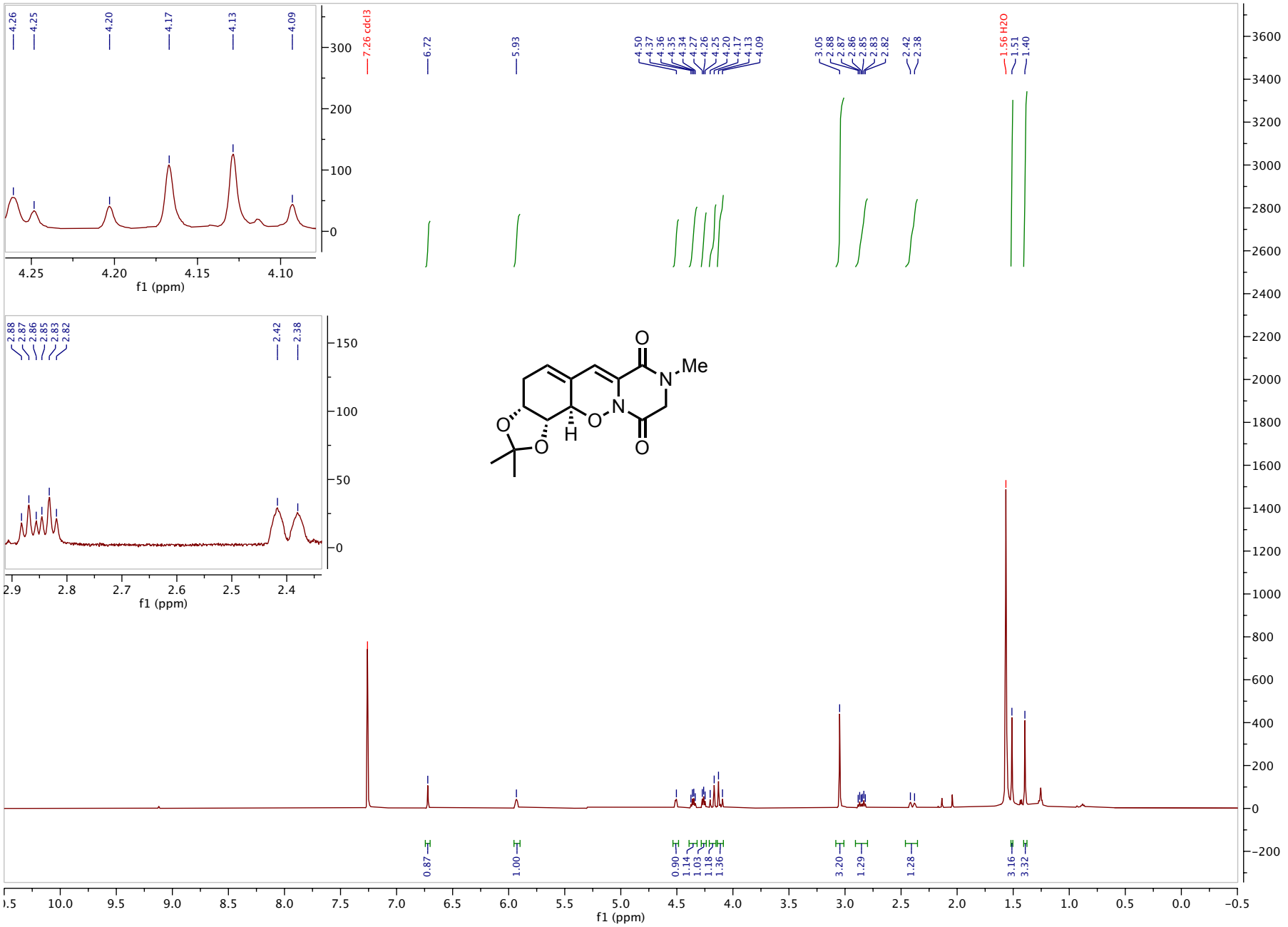

Figure C.31. ^{1}H NMR (500 MHz, $CDCl_3$) diene **4.105**

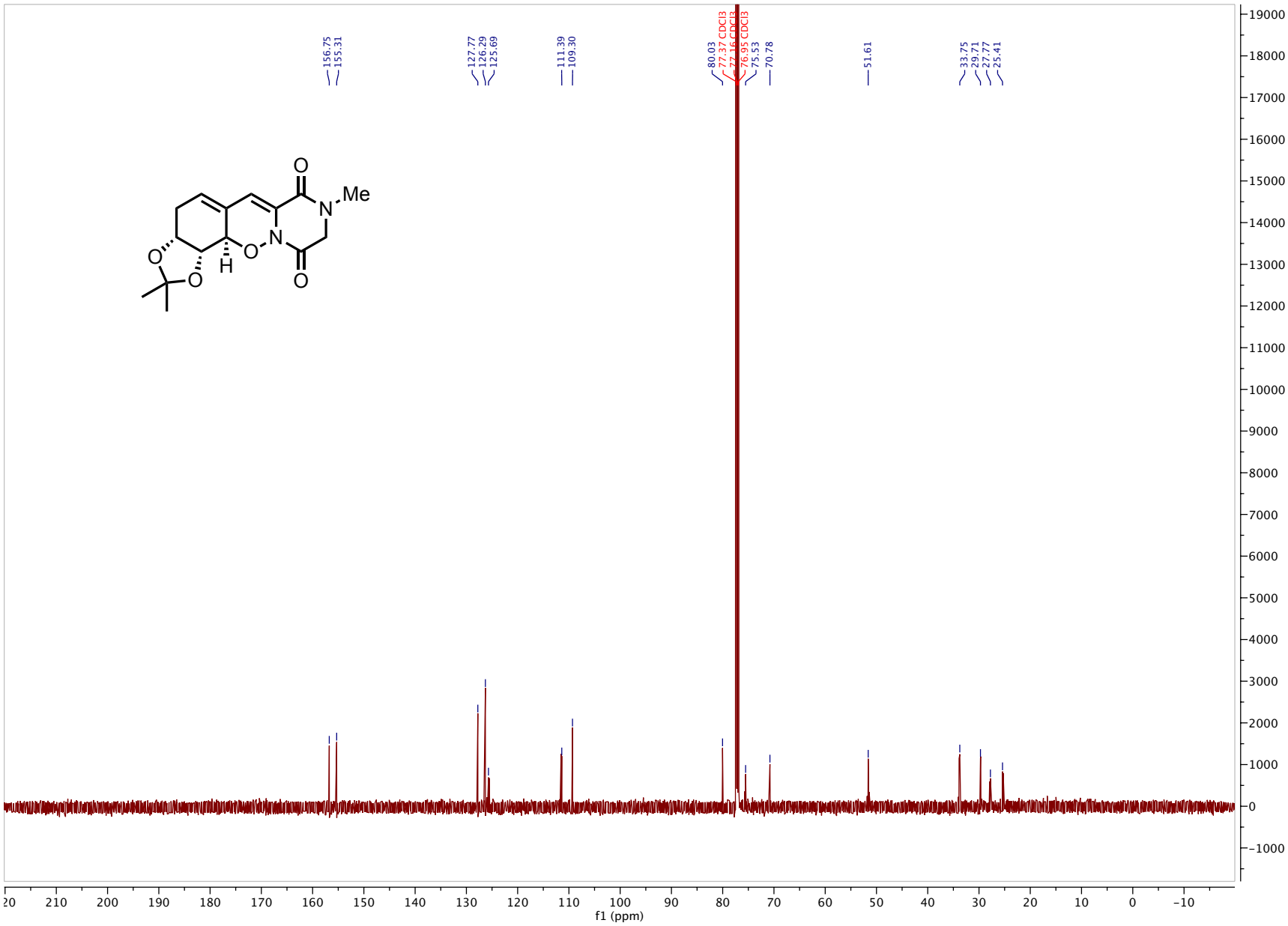

Figure C.32. ^{13}C NMR (126 MHz, $CDCl_3$) diene **4.105**

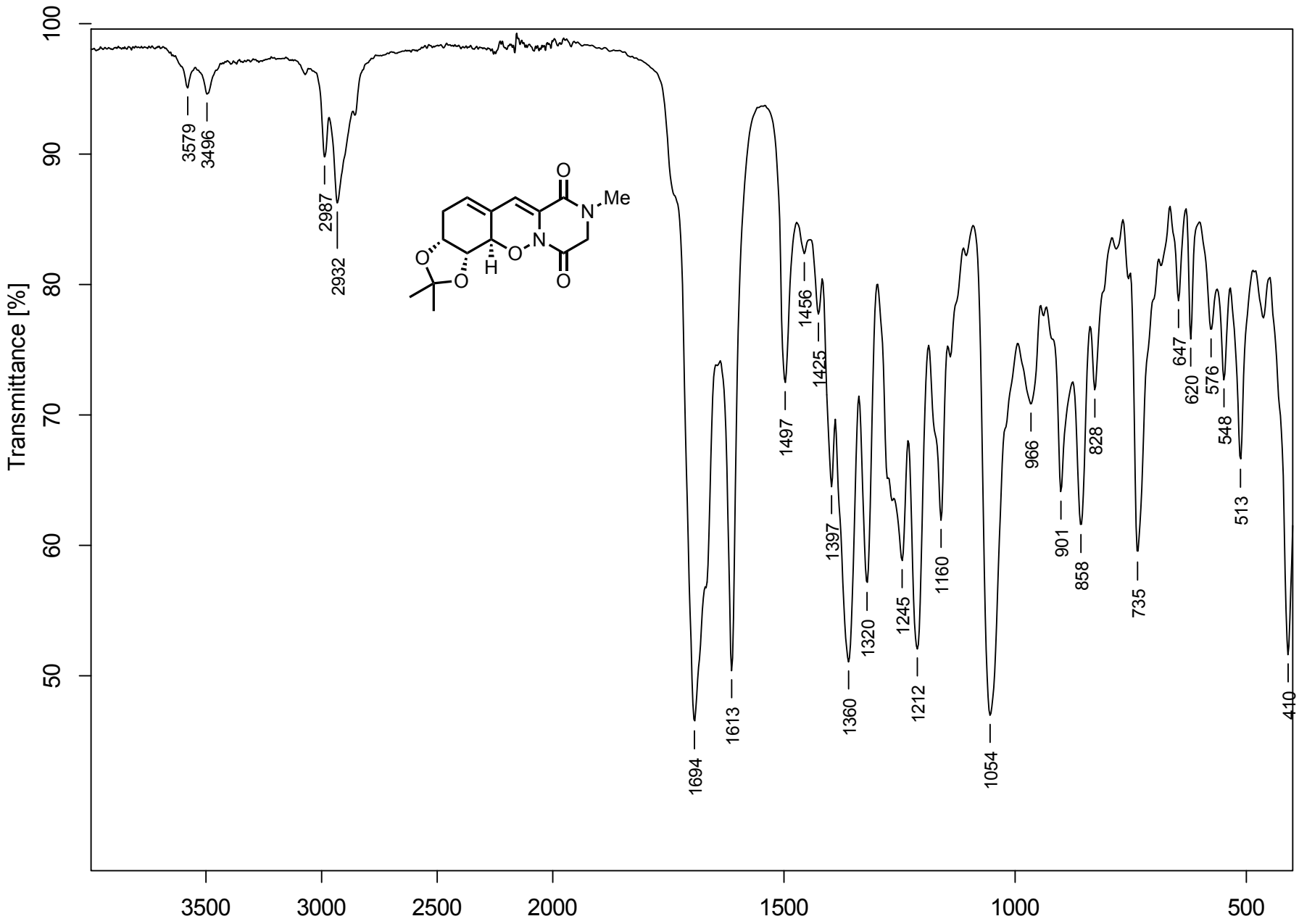

Figure C.33. FTIR (thin film) diene **4.105**

APPENDIX D

X-ray Crystallographic Data

*D.1. Crystal analysis of spirolactone **1.48***

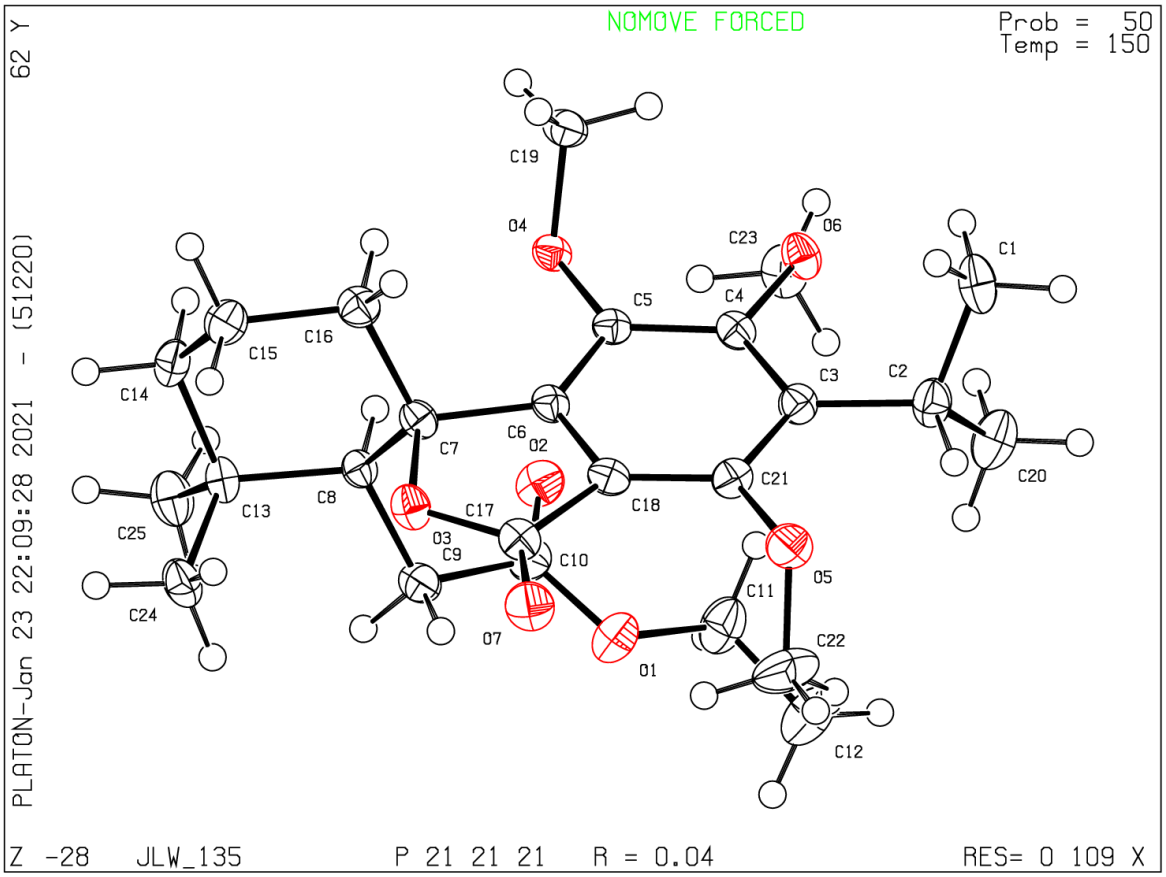

Figure D.1. ORTEP drawing of spirolactone **1.48**.

Table D.1. Crystal data and structure refinement for spirolactone **1.48** (JLW_135).

Identification code	JLW_135	
Empirical formula	C25 H36 O7	
Formula weight	448.54	
Temperature	150(2) K	
Wavelength	0.71073 Å	
Crystal system	Orthorhombic	
Space group	$P2_12_12_1$	
Unit cell dimensions	a = 7.8673(2) Å	α= 90°.
	b = 11.1377(3) Å	β= 90°.
	c = 27.4163(7) Å	γ = 90°.

Volume	2402.32(11) $Å^3$
Z	4
Density (calculated)	1.240 Mg/m^3
Absorption coefficient	0.089 mm^{-1}
F(000)	968
Crystal size	0.512 x 0.125 x 0.059 mm^3
Theta range for data collection	2.693 to 26.372°.
Index ranges	-9<=h<=9, -13<=k<=13, -34<=l<=34
Reflections collected	39849
Independent reflections	4886 [R(int) = 0.0395]
Completeness to theta = 25.242°	99.5 %
Absorption correction	Semi-empirical from equivalents
Max. and min. transmission	0.961 and 0.923
Refinement method	Full-matrix least-squares on F^2
Data / restraints / parameters	4886 / 0 / 297
Goodness-of-fit on F^2	1.086
Final R indices [I>2sigma(I)]	R1 = 0.0383, wR2 = 0.0999
R indices (all data)	R1 = 0.0394, wR2 = 0.1005
Absolute structure parameter	0.4(2)
Extinction coefficient	n/a
Largest diff. peak and hole	0.259 and -0.176 $e.Å^{-3}$

Table D.2. Atomic coordinates (x 10^4) and equivalent isotropic displacement parameters ($Å^2$x 10^3) for spirolactone **1.48** (JLW_135). U(eq) is defined as one third of the trace of the orthogonalized U^{ij} tensor.

	x	y	z	U(eq)
O(1)	4016(2)	7806(2)	3113(1)	30(1)
O(2)	2811(2)	7756(2)	3853(1)	28(1)
O(3)	7001(2)	4783(1)	3624(1)	22(1)
O(4)	5400(2)	7516(1)	4681(1)	19(1)
O(5)	9869(2)	7890(2)	3113(1)	29(1)
O(6)	6981(2)	9726(1)	4452(1)	23(1)
O(7)	8950(2)	5186(2)	3052(1)	30(1)

C(1)	10506(4)	10376(2)	4069(1)	34(1)
C(2)	9294(3)	10019(2)	3658(1)	26(1)
C(3)	8395(3)	8842(2)	3771(1)	21(1)
C(4)	7254(3)	8727(2)	4167(1)	19(1)
C(5)	6476(3)	7630(2)	4289(1)	18(1)
C(6)	6784(3)	6657(2)	3987(1)	18(1)
C(7)	6115(3)	5388(2)	4027(1)	19(1)
C(8)	4166(3)	5304(2)	3949(1)	18(1)
C(9)	3623(3)	5899(2)	3468(1)	24(1)
C(10)	3431(3)	7247(2)	3511(1)	23(1)
C(11)	3814(4)	9101(2)	3114(1)	34(1)
C(12)	4564(4)	9575(3)	2653(1)	45(1)
C(13)	3429(3)	4013(2)	4015(1)	22(1)
C(14)	4092(3)	3492(2)	4497(1)	25(1)
C(15)	6023(3)	3504(2)	4543(1)	27(1)
C(16)	6679(3)	4787(2)	4502(1)	23(1)
C(17)	8064(3)	5543(2)	3378(1)	22(1)
C(18)	7886(3)	6747(2)	3598(1)	20(1)
C(19)	6191(3)	7676(2)	5153(1)	26(1)
C(20)	8082(4)	11052(3)	3529(1)	39(1)
C(21)	8706(3)	7826(2)	3483(1)	20(1)
C(22)	9228(4)	7784(3)	2628(1)	45(1)
C(23)	5236(3)	10120(2)	4484(1)	30(1)
C(24)	3864(3)	3170(2)	3588(1)	28(1)
C(25)	1482(3)	4096(2)	4059(1)	31(1)

Table D.3. Bond lengths [Å] and angles [°] for spirolactone **1.48** (JLW_135).

O(1)-C(10)	1.339(3)
O(1)-C(11)	1.451(3)
O(2)-C(10)	1.200(3)
O(3)-C(17)	1.369(3)
O(3)-C(7)	1.470(3)
O(4)-C(5)	1.374(3)
O(4)-C(19)	1.449(3)

O(5)-C(21)	1.368(3)
O(5)-C(22)	1.428(3)
O(6)-C(4)	1.377(3)
O(6)-C(23)	1.443(3)
O(7)-C(17)	1.202(3)
C(1)-C(2)	1.527(4)
C(1)-H(1)	0.9800
C(1)-H(14)	0.9800
C(1)-H(15)	0.9800
C(2)-C(3)	1.522(3)
C(2)-C(20)	1.536(4)
C(2)-H(19)	1.0000
C(3)-C(21)	1.400(3)
C(3)-C(4)	1.414(3)
C(4)-C(5)	1.407(3)
C(5)-C(6)	1.384(3)
C(6)-C(18)	1.380(3)
C(6)-C(7)	1.512(3)
C(7)-C(16)	1.528(3)
C(7)-C(8)	1.551(3)
C(8)-C(9)	1.537(3)
C(8)-C(13)	1.561(3)
C(8)-H(34)	1.0000
C(9)-C(10)	1.514(3)
C(9)-H(6)	0.9900
C(9)-H(5)	0.9900
C(11)-C(12)	1.492(4)
C(11)-H(4)	0.9900
C(11)-H(35)	0.9900
C(12)-H(2)	0.9800
C(12)-H(36)	0.9800
C(12)-H(3)	0.9800
C(13)-C(14)	1.535(3)
C(13)-C(25)	1.539(3)
C(13)-C(24)	1.541(3)
C(14)-C(15)	1.525(4)

C(14)-H(8)	0.9900
C(14)-H(7)	0.9900
C(15)-C(16)	1.523(3)
C(15)-H(26)	0.9900
C(15)-H(27)	0.9900
C(16)-H(9)	0.9900
C(16)-H(10)	0.9900
C(17)-C(18)	1.476(3)
C(18)-C(21)	1.399(3)
C(19)-H(11)	0.9800
C(19)-H(12)	0.9800
C(19)-H(13)	0.9800
C(20)-H(17)	0.9800
C(20)-H(16)	0.9800
C(20)-H(18)	0.9800
C(22)-H(21)	0.9800
C(22)-H(22)	0.9800
C(22)-H(20)	0.9800
C(23)-H(25)	0.9800
C(23)-H(24)	0.9800
C(23)-H(23)	0.9800
C(24)-H(29)	0.9800
C(24)-H(28)	0.9800
C(24)-H(30)	0.9800
C(25)-H(33)	0.9800
C(25)-H(32)	0.9800
C(25)-H(31)	0.9800

C(10)-O(1)-C(11)	115.0(2)
C(17)-O(3)-C(7)	112.15(17)
C(5)-O(4)-C(19)	115.09(17)
C(21)-O(5)-C(22)	116.8(2)
C(4)-O(6)-C(23)	115.33(18)
C(2)-C(1)-H(1)	109.5
C(2)-C(1)-H(14)	109.5
H(1)-C(1)-H(14)	109.5

C(2)-C(1)-H(15)	109.5
H(1)-C(1)-H(15)	109.5
H(14)-C(1)-H(15)	109.5
C(3)-C(2)-C(1)	111.4(2)
C(3)-C(2)-C(20)	113.8(2)
C(1)-C(2)-C(20)	111.3(2)
C(3)-C(2)-H(19)	106.6
C(1)-C(2)-H(19)	106.6
C(20)-C(2)-H(19)	106.6
C(21)-C(3)-C(4)	118.0(2)
C(21)-C(3)-C(2)	120.1(2)
C(4)-C(3)-C(2)	121.9(2)
O(6)-C(4)-C(5)	119.89(19)
O(6)-C(4)-C(3)	117.5(2)
C(5)-C(4)-C(3)	122.5(2)
O(4)-C(5)-C(6)	120.2(2)
O(4)-C(5)-C(4)	122.3(2)
C(6)-C(5)-C(4)	117.5(2)
C(18)-C(6)-C(5)	121.1(2)
C(18)-C(6)-C(7)	110.03(19)
C(5)-C(6)-C(7)	128.9(2)
O(3)-C(7)-C(6)	102.07(17)
O(3)-C(7)-C(16)	107.53(18)
C(6)-C(7)-C(16)	111.74(18)
O(3)-C(7)-C(8)	109.70(17)
C(6)-C(7)-C(8)	112.97(18)
C(16)-C(7)-C(8)	112.20(19)
C(9)-C(8)-C(7)	111.56(18)
C(9)-C(8)-C(13)	113.17(19)
C(7)-C(8)-C(13)	113.99(18)
C(9)-C(8)-H(34)	105.8
C(7)-C(8)-H(34)	105.8
C(13)-C(8)-H(34)	105.8
C(10)-C(9)-C(8)	112.83(19)
C(10)-C(9)-H(6)	109.0
C(8)-C(9)-H(6)	109.0

C(10)-C(9)-H(5)	109.0
C(8)-C(9)-H(5)	109.0
H(6)-C(9)-H(5)	107.8
O(2)-C(10)-O(1)	123.9(2)
O(2)-C(10)-C(9)	124.8(2)
O(1)-C(10)-C(9)	111.3(2)
O(1)-C(11)-C(12)	107.8(2)
O(1)-C(11)-H(4)	110.1
C(12)-C(11)-H(4)	110.1
O(1)-C(11)-H(35)	110.1
C(12)-C(11)-H(35)	110.1
H(4)-C(11)-H(35)	108.5
C(11)-C(12)-H(2)	109.5
C(11)-C(12)-H(36)	109.5
H(2)-C(12)-H(36)	109.5
C(11)-C(12)-H(3)	109.5
H(2)-C(12)-H(3)	109.5
H(36)-C(12)-H(3)	109.5
C(14)-C(13)-C(25)	107.0(2)
C(14)-C(13)-C(24)	110.44(19)
C(25)-C(13)-C(24)	108.5(2)
C(14)-C(13)-C(8)	108.81(19)
C(25)-C(13)-C(8)	108.89(19)
C(24)-C(13)-C(8)	112.97(19)
C(15)-C(14)-C(13)	113.9(2)
C(15)-C(14)-H(8)	108.8
C(13)-C(14)-H(8)	108.8
C(15)-C(14)-H(7)	108.8
C(13)-C(14)-H(7)	108.8
H(8)-C(14)-H(7)	107.7
C(16)-C(15)-C(14)	109.8(2)
C(16)-C(15)-H(26)	109.7
C(14)-C(15)-H(26)	109.7
C(16)-C(15)-H(27)	109.7
C(14)-C(15)-H(27)	109.7
H(26)-C(15)-H(27)	108.2

C(15)-C(16)-C(7)	112.09(19)
C(15)-C(16)-H(9)	109.2
C(7)-C(16)-H(9)	109.2
C(15)-C(16)-H(10)	109.2
C(7)-C(16)-H(10)	109.2
H(9)-C(16)-H(10)	107.9
O(7)-C(17)-O(3)	121.1(2)
O(7)-C(17)-C(18)	131.2(2)
O(3)-C(17)-C(18)	107.64(19)
C(6)-C(18)-C(21)	121.7(2)
C(6)-C(18)-C(17)	108.0(2)
C(21)-C(18)-C(17)	130.2(2)
O(4)-C(19)-H(11)	109.5
O(4)-C(19)-H(12)	109.5
H(11)-C(19)-H(12)	109.5
O(4)-C(19)-H(13)	109.5
H(11)-C(19)-H(13)	109.5
H(12)-C(19)-H(13)	109.5
C(2)-C(20)-H(17)	109.5
C(2)-C(20)-H(16)	109.5
H(17)-C(20)-H(16)	109.5
C(2)-C(20)-H(18)	109.5
H(17)-C(20)-H(18)	109.5
H(16)-C(20)-H(18)	109.5
O(5)-C(21)-C(18)	121.3(2)
O(5)-C(21)-C(3)	119.5(2)
C(18)-C(21)-C(3)	119.2(2)
O(5)-C(22)-H(21)	109.5
O(5)-C(22)-H(22)	109.5
H(21)-C(22)-H(22)	109.5
O(5)-C(22)-H(20)	109.5
H(21)-C(22)-H(20)	109.5
H(22)-C(22)-H(20)	109.5
O(6)-C(23)-H(25)	109.5
O(6)-C(23)-H(24)	109.5
H(25)-C(23)-H(24)	109.5

O(6)-C(23)-H(23)	109.5
H(25)-C(23)-H(23)	109.5
H(24)-C(23)-H(23)	109.5
C(13)-C(24)-H(29)	109.5
C(13)-C(24)-H(28)	109.5
H(29)-C(24)-H(28)	109.5
C(13)-C(24)-H(30)	109.5
H(29)-C(24)-H(30)	109.5
H(28)-C(24)-H(30)	109.5
C(13)-C(25)-H(33)	109.5
C(13)-C(25)-H(32)	109.5
H(33)-C(25)-H(32)	109.5
C(13)-C(25)-H(31)	109.5
H(33)-C(25)-H(31)	109.5
H(32)-C(25)-H(31)	109.5

Symmetry transformations used to generate equivalent atoms:

Table D.4. Anisotropic displacement parameters ($Å^2 x\ 10^3$) for spirolactone **1.48** (JLW_135). The anisotropic displacement factor exponent takes the form: $-2p^2[\ h^2\ a^{*2}U^{11} + ...\ + 2\ h\ k\ a^*\ b^*\ U^{12}\ ]$.

	U^{11}	U^{22}	U^{33}	U^{23}	U^{13}	U^{12}
O(1)	32(1)	29(1)	29(1)	7(1)	6(1)	4(1)
O(2)	30(1)	26(1)	27(1)	1(1)	2(1)	7(1)
O(3)	21(1)	19(1)	27(1)	-4(1)	5(1)	1(1)
O(4)	16(1)	24(1)	18(1)	-2(1)	1(1)	-3(1)
O(5)	26(1)	36(1)	24(1)	-5(1)	9(1)	-6(1)
O(6)	22(1)	18(1)	30(1)	-5(1)	3(1)	0(1)
O(7)	30(1)	30(1)	29(1)	-7(1)	10(1)	2(1)
C(1)	29(1)	26(1)	48(2)	0(1)	3(1)	-10(1)
C(2)	28(1)	22(1)	29(1)	1(1)	8(1)	-2(1)
C(3)	18(1)	22(1)	22(1)	0(1)	0(1)	-1(1)
C(4)	17(1)	19(1)	22(1)	-2(1)	-2(1)	2(1)
C(5)	13(1)	21(1)	18(1)	-1(1)	-1(1)	0(1)

C(6)	14(1)	20(1)	21(1)	0(1)	-3(1)	-1(1)
C(7)	18(1)	18(1)	21(1)	-4(1)	1(1)	1(1)
C(8)	17(1)	16(1)	20(1)	-1(1)	-1(1)	0(1)
C(9)	25(1)	23(1)	23(1)	-3(1)	-3(1)	0(1)
C(10)	17(1)	27(1)	26(1)	5(1)	-4(1)	1(1)
C(11)	38(2)	27(1)	38(1)	6(1)	10(1)	5(1)
C(12)	52(2)	42(2)	40(2)	16(1)	5(1)	2(2)
C(13)	20(1)	16(1)	29(1)	0(1)	1(1)	-2(1)
C(14)	29(1)	19(1)	28(1)	5(1)	4(1)	-2(1)
C(15)	31(1)	22(1)	28(1)	4(1)	-3(1)	3(1)
C(16)	22(1)	23(1)	25(1)	0(1)	-4(1)	2(1)
C(17)	18(1)	22(1)	25(1)	-1(1)	-1(1)	2(1)
C(18)	17(1)	23(1)	20(1)	-3(1)	-2(1)	2(1)
C(19)	28(1)	30(1)	20(1)	-4(1)	-1(1)	-6(1)
C(20)	44(2)	29(1)	44(2)	12(1)	3(1)	1(1)
C(21)	15(1)	25(1)	21(1)	2(1)	1(1)	1(1)
C(22)	46(2)	67(2)	22(1)	4(1)	6(1)	2(2)
C(23)	28(1)	24(1)	37(1)	-3(1)	8(1)	6(1)
C(24)	31(1)	19(1)	33(1)	-6(1)	2(1)	-4(1)
C(25)	22(1)	28(1)	42(1)	-1(1)	1(1)	-3(1)

Table D.5. Hydrogen coordinates (x 10^4) and isotropic displacement parameters (Å^{2}x 10^3) for spirolactone **1.48** (JLW_135).

	x	y	z	U(eq)
H(1)	9849	10576	4361	52
H(14)	11173	11076	3968	52
H(15)	11272	9705	4140	52
H(19)	10012	9873	3363	32
H(34)	3645	5800	4214	21
H(6)	4480	5717	3214	28
H(5)	2527	5550	3361	28
H(4)	4403	9453	3399	41

H(35)	2594	9314	3133	41
H(2)	5785	9399	2646	67
H(36)	4390	10445	2636	67
H(3)	4011	9191	2373	67
H(8)	3601	3957	4771	30
H(7)	3687	2654	4528	30
H(26)	6362	3160	4861	32
H(27)	6530	3004	4282	32
H(9)	7936	4781	4517	28
H(10)	6255	5261	4782	28
H(11)	7111	7091	5193	39
H(12)	5341	7555	5410	39
H(13)	6654	8490	5177	39
H(17)	7358	10811	3255	59
H(16)	8745	11762	3437	59
H(18)	7370	11242	3812	59
H(21)	8482	7082	2606	67
H(22)	10179	7691	2400	67
H(20)	8583	8509	2544	67
H(25)	4917	10526	4180	44
H(24)	5112	10677	4758	44
H(23)	4496	9423	4535	44
H(29)	5101	3102	3557	42
H(28)	3392	3498	3285	42
H(30)	3376	2375	3649	42
H(33)	995	4306	3742	46
H(32)	1183	4714	4299	46
H(31)	1028	3320	4166	46

Table D.6. Torsion angles [°] for spirolactone **1.48** (JLW_135).

C(1)-C(2)-C(3)-C(21)	-114.4(3)
C(20)-C(2)-C(3)-C(21)	118.8(2)
C(1)-C(2)-C(3)-C(4)	64.7(3)
C(20)-C(2)-C(3)-C(4)	-62.2(3)

C(23)-O(6)-C(4)-C(5)	-61.2(3)
C(23)-O(6)-C(4)-C(3)	122.0(2)
C(21)-C(3)-C(4)-O(6)	178.9(2)
C(2)-C(3)-C(4)-O(6)	-0.2(3)
C(21)-C(3)-C(4)-C(5)	2.1(3)
C(2)-C(3)-C(4)-C(5)	-176.9(2)
C(19)-O(4)-C(5)-C(6)	115.9(2)
C(19)-O(4)-C(5)-C(4)	-66.3(3)
O(6)-C(4)-C(5)-O(4)	1.7(3)
C(3)-C(4)-C(5)-O(4)	178.4(2)
O(6)-C(4)-C(5)-C(6)	179.59(19)
C(3)-C(4)-C(5)-C(6)	-3.8(3)
O(4)-C(5)-C(6)-C(18)	-178.72(19)
C(4)-C(5)-C(6)-C(18)	3.4(3)
O(4)-C(5)-C(6)-C(7)	-1.6(3)
C(4)-C(5)-C(6)-C(7)	-179.5(2)
C(17)-O(3)-C(7)-C(6)	0.7(2)
C(17)-O(3)-C(7)-C(16)	-117.0(2)
C(17)-O(3)-C(7)-C(8)	120.77(19)
C(18)-C(6)-C(7)-O(3)	1.3(2)
C(5)-C(6)-C(7)-O(3)	-176.0(2)
C(18)-C(6)-C(7)-C(16)	115.9(2)
C(5)-C(6)-C(7)-C(16)	-61.4(3)
C(18)-C(6)-C(7)-C(8)	-116.4(2)
C(5)-C(6)-C(7)-C(8)	66.2(3)
O(3)-C(7)-C(8)-C(9)	-59.8(2)
C(6)-C(7)-C(8)-C(9)	53.3(2)
C(16)-C(7)-C(8)-C(9)	-179.29(18)
O(3)-C(7)-C(8)-C(13)	69.9(2)
C(6)-C(7)-C(8)-C(13)	-176.99(18)
C(16)-C(7)-C(8)-C(13)	-49.6(3)
C(7)-C(8)-C(9)-C(10)	-82.3(2)
C(13)-C(8)-C(9)-C(10)	147.5(2)
C(11)-O(1)-C(10)-O(2)	-1.4(3)
C(11)-O(1)-C(10)-C(9)	177.4(2)
C(8)-C(9)-C(10)-O(2)	-40.5(3)

C(8)-C(9)-C(10)-O(1)	140.7(2)
C(10)-O(1)-C(11)-C(12)	178.7(2)
C(9)-C(8)-C(13)-C(14)	178.26(19)
C(7)-C(8)-C(13)-C(14)	49.4(2)
C(9)-C(8)-C(13)-C(25)	-65.4(3)
C(7)-C(8)-C(13)-C(25)	165.71(19)
C(9)-C(8)-C(13)-C(24)	55.2(3)
C(7)-C(8)-C(13)-C(24)	-73.7(2)
C(25)-C(13)-C(14)-C(15)	-172.3(2)
C(24)-C(13)-C(14)-C(15)	69.8(3)
C(8)-C(13)-C(14)-C(15)	-54.7(3)
C(13)-C(14)-C(15)-C(16)	59.1(3)
C(14)-C(15)-C(16)-C(7)	-56.4(3)
O(3)-C(7)-C(16)-C(15)	-68.3(2)
C(6)-C(7)-C(16)-C(15)	-179.5(2)
C(8)-C(7)-C(16)-C(15)	52.4(3)
C(7)-O(3)-C(17)-O(7)	176.5(2)
C(7)-O(3)-C(17)-C(18)	-2.4(2)
C(5)-C(6)-C(18)-C(21)	-1.4(3)
C(7)-C(6)-C(18)-C(21)	-179.0(2)
C(5)-C(6)-C(18)-C(17)	174.9(2)
C(7)-C(6)-C(18)-C(17)	-2.7(2)
O(7)-C(17)-C(18)-C(6)	-175.5(3)
O(3)-C(17)-C(18)-C(6)	3.2(2)
O(7)-C(17)-C(18)-C(21)	0.4(4)
O(3)-C(17)-C(18)-C(21)	179.1(2)
C(22)-O(5)-C(21)-C(18)	70.1(3)
C(22)-O(5)-C(21)-C(3)	-113.3(3)
C(6)-C(18)-C(21)-O(5)	176.3(2)
C(17)-C(18)-C(21)-O(5)	0.9(4)
C(6)-C(18)-C(21)-C(3)	-0.3(3)
C(17)-C(18)-C(21)-C(3)	-175.7(2)
C(4)-C(3)-C(21)-O(5)	-176.7(2)
C(2)-C(3)-C(21)-O(5)	2.4(3)
C(4)-C(3)-C(21)-C(18)	-0.1(3)
C(2)-C(3)-C(21)-C(18)	179.0(2)

Symmetry transformations used to generate equivalent atoms.

*D.2. Crystal analysis of spirolactone **1.56***

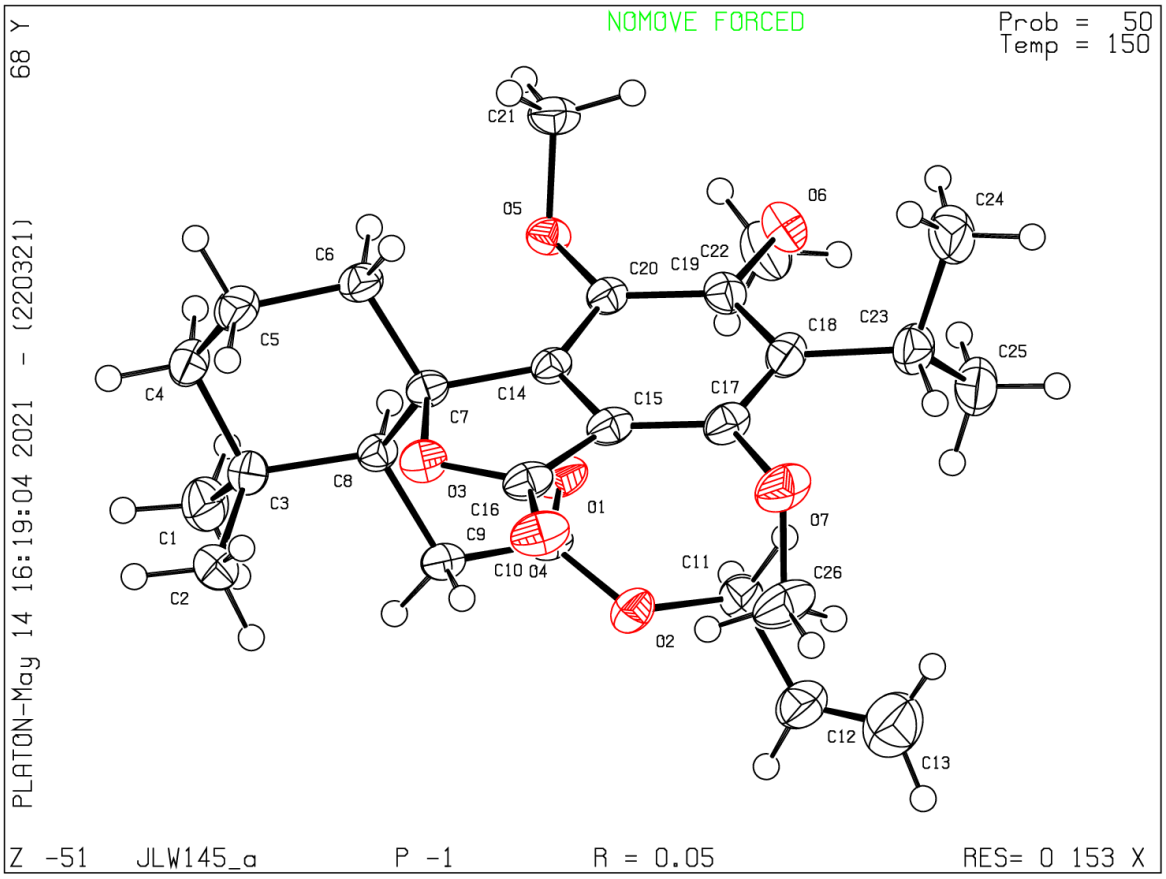

Figure D.2. ORTEP drawing of spirolactone **1.56**.

Table D.7. Crystal data and structure refinement for spirolactone **1.56** (JLW145_a).

Identification code	JLW145_a	
Empirical formula	C26 H36 O7	
Formula weight	460.55	
Temperature	150(2) K	
Wavelength	0.71073 Å	
Crystal system	Triclinic	
Space group	P-1	
Unit cell dimensions	a = 7.6106(6) Å	α = 105.970(3)°.
	b = 11.6336(10) Å	β = 101.564(3)°.
	c = 15.0933(12) Å	γ = 103.630(3)°.
Volume	1197.19(17) Å^3	

Z	2
Density (calculated)	1.278 Mg/m^3
Absorption coefficient	0.092 mm^{-1}
F(000)	496
Crystal size	0.617 x 0.292 x 0.194 mm^3
Theta range for data collection	2.776 to 26.621°.
Index ranges	-9<=h<=9, -14<=k<=14, -19<=l<=19
Reflections collected	34894
Independent reflections	4958 [R(int) = 0.0323]
Completeness to theta = 25.242°	99.5 %
Refinement method	Full-matrix least-squares on F^2
Data / restraints / parameters	4958 / 0 / 305
Goodness-of-fit on F^2	1.081
Final R indices [I>2sigma(I)]	R1 = 0.0519, wR2 = 0.1415
R indices (all data)	R1 = 0.0562, wR2 = 0.1453
Extinction coefficient	n/a
Largest diff. peak and hole	0.506 and -0.449 $e.Å^{-3}$

Table D.8. Atomic coordinates (x 10^4) and equivalent isotropic displacement parameters ($Å^2$x 10^3) for spirolactone **1.56** (JLW145_a). U(eq) is defined as one third of the trace of the orthogonalized U^{ij} tensor.

	x	y	z	U(eq)
O(1)	3390(2)	5013(1)	2750(1)	33(1)
O(2)	4269(2)	5290(1)	1466(1)	29(1)
O(3)	6899(2)	2424(1)	1624(1)	27(1)
O(4)	8826(2)	3200(1)	844(1)	34(1)
O(5)	6500(2)	4827(1)	4353(1)	24(1)
O(6)	8637(2)	7326(1)	4721(1)	33(1)
O(7)	10240(2)	6084(1)	1766(1)	40(1)
C(1)	949(3)	1006(2)	1880(2)	39(1)
C(2)	2958(3)	439(2)	818(1)	36(1)
C(3)	2993(2)	1137(2)	1848(1)	28(1)
C(4)	3833(3)	519(2)	2540(1)	32(1)
C(5)	5954(3)	762(2)	2733(1)	33(1)

C(6)	6968(2)	2169(2)	3162(1)	27(1)
C(7)	6297(2)	2854(2)	2493(1)	22(1)
C(8)	4126(2)	2566(2)	2210(1)	22(1)
C(9)	3475(2)	3226(2)	1506(1)	25(1)
C(10)	3700(2)	4590(2)	1994(1)	24(1)
C(11)	4609(3)	6634(2)	1884(1)	30(1)
C(12)	4295(4)	7143(2)	1092(2)	46(1)
C(13)	5442(4)	7956(2)	926(2)	60(1)
C(14)	7346(2)	4244(2)	2884(1)	22(1)
C(15)	8311(2)	4559(2)	2255(1)	25(1)
C(16)	8104(2)	3392(2)	1491(1)	27(1)
C(17)	9352(2)	5794(2)	2423(1)	28(1)
C(18)	9488(2)	6734(2)	3264(1)	29(1)
C(19)	8512(2)	6393(2)	3901(1)	26(1)
C(20)	7464(2)	5146(2)	3731(1)	22(1)
C(21)	7684(3)	4975(2)	5278(1)	32(1)
C(22)	6857(3)	7466(2)	4846(2)	40(1)
C(23)	10686(3)	8077(2)	3464(2)	36(1)
C(24)	12427(3)	8481(2)	4307(2)	52(1)
C(25)	9614(3)	9024(2)	3554(2)	45(1)
C(26)	9011(3)	6044(2)	912(2)	45(1)

Table D.9. Bond lengths [Å] and angles [°] for spirolactone **1.56** (JLW145_a).

O(1)-C(10)	1.205(2)
O(2)-C(10)	1.348(2)
O(2)-C(11)	1.452(2)
O(3)-C(16)	1.364(2)
O(3)-C(7)	1.4717(18)
O(4)-C(16)	1.207(2)
O(5)-C(20)	1.3773(19)
O(5)-C(21)	1.443(2)
O(6)-C(19)	1.373(2)
O(6)-C(22)	1.444(2)
O(7)-C(17)	1.379(2)

O(7)-C(26)	1.415(2)
C(1)-C(3)	1.539(3)
C(2)-C(3)	1.535(2)
C(3)-C(4)	1.542(2)
C(3)-C(8)	1.563(2)
C(4)-C(5)	1.523(3)
C(5)-C(6)	1.522(2)
C(6)-C(7)	1.531(2)
C(7)-C(14)	1.510(2)
C(7)-C(8)	1.550(2)
C(8)-C(9)	1.543(2)
C(9)-C(10)	1.505(2)
C(11)-C(12)	1.476(3)
C(12)-C(13)	1.245(4)
C(14)-C(20)	1.384(2)
C(14)-C(15)	1.386(2)
C(15)-C(17)	1.392(2)
C(15)-C(16)	1.471(2)
C(17)-C(18)	1.396(3)
C(18)-C(19)	1.411(2)
C(18)-C(23)	1.524(2)
C(19)-C(20)	1.404(2)
C(23)-C(25)	1.511(3)
C(23)-C(24)	1.516(3)

C(10)-O(2)-C(11)	116.12(13)
C(16)-O(3)-C(7)	111.82(13)
C(20)-O(5)-C(21)	114.65(12)
C(19)-O(6)-C(22)	115.23(13)
C(17)-O(7)-C(26)	114.47(14)
C(2)-C(3)-C(1)	108.47(15)
C(2)-C(3)-C(4)	110.00(15)
C(1)-C(3)-C(4)	107.21(15)
C(2)-C(3)-C(8)	113.13(14)
C(1)-C(3)-C(8)	108.54(14)
C(4)-C(3)-C(8)	109.31(14)

C(5)-C(4)-C(3)	114.23(14)
C(6)-C(5)-C(4)	109.83(14)
C(5)-C(6)-C(7)	111.20(14)
O(3)-C(7)-C(14)	102.41(12)
O(3)-C(7)-C(6)	106.88(12)
C(14)-C(7)-C(6)	112.12(13)
O(3)-C(7)-C(8)	109.58(12)
C(14)-C(7)-C(8)	112.91(13)
C(6)-C(7)-C(8)	112.29(13)
C(9)-C(8)-C(7)	111.39(13)
C(9)-C(8)-C(3)	112.31(13)
C(7)-C(8)-C(3)	114.35(13)
C(10)-C(9)-C(8)	113.40(13)
O(1)-C(10)-O(2)	123.62(16)
O(1)-C(10)-C(9)	125.26(15)
O(2)-C(10)-C(9)	111.11(14)
O(2)-C(11)-C(12)	108.11(15)
C(13)-C(12)-C(11)	128.1(2)
C(20)-C(14)-C(15)	120.71(15)
C(20)-C(14)-C(7)	129.84(14)
C(15)-C(14)-C(7)	109.44(14)
C(14)-C(15)-C(17)	121.66(16)
C(14)-C(15)-C(16)	108.08(15)
C(17)-C(15)-C(16)	130.14(15)
O(4)-C(16)-O(3)	120.78(16)
O(4)-C(16)-C(15)	131.25(17)
O(3)-C(16)-C(15)	107.94(13)
O(7)-C(17)-C(15)	120.31(16)
O(7)-C(17)-C(18)	120.37(16)
C(15)-C(17)-C(18)	119.31(15)
C(17)-C(18)-C(19)	118.14(15)
C(17)-C(18)-C(23)	119.23(16)
C(19)-C(18)-C(23)	122.63(17)
O(6)-C(19)-C(20)	119.82(15)
O(6)-C(19)-C(18)	117.70(15)
C(20)-C(19)-C(18)	122.48(16)

O(5)-C(20)-C(14)	120.37(14)
O(5)-C(20)-C(19)	121.95(14)
C(14)-C(20)-C(19)	117.60(15)
C(25)-C(23)-C(24)	112.43(19)
C(25)-C(23)-C(18)	114.57(16)
C(24)-C(23)-C(18)	111.29(16)

Symmetry transformations used to generate equivalent atoms:

Table D.10. Anisotropic displacement parameters ($Å^2 x\ 10^3$) for spirolactone **1.56** (JLW145_a). The anisotropic displacement factor exponent takes the form: $-2p^2[\ h^2\ a^{*2}U^{11} + ...\ + 2\ h\ k\ a^*\ b^*\ U^{12}\ ]$.

	U^{11}	U^{22}	U^{33}	U^{23}	U^{13}	U^{12}
O(1)	44(1)	40(1)	26(1)	16(1)	15(1)	23(1)
O(2)	34(1)	30(1)	29(1)	15(1)	15(1)	12(1)
O(3)	28(1)	32(1)	25(1)	10(1)	13(1)	12(1)
O(4)	34(1)	52(1)	30(1)	20(1)	18(1)	22(1)
O(5)	21(1)	32(1)	21(1)	10(1)	7(1)	6(1)
O(6)	28(1)	28(1)	34(1)	3(1)	6(1)	5(1)
O(7)	29(1)	59(1)	42(1)	32(1)	16(1)	8(1)
C(1)	29(1)	39(1)	47(1)	18(1)	10(1)	2(1)
C(2)	42(1)	30(1)	29(1)	6(1)	5(1)	4(1)
C(3)	28(1)	27(1)	29(1)	11(1)	8(1)	5(1)
C(4)	38(1)	26(1)	34(1)	14(1)	11(1)	7(1)
C(5)	40(1)	28(1)	33(1)	14(1)	9(1)	14(1)
C(6)	29(1)	29(1)	26(1)	13(1)	5(1)	12(1)
C(7)	24(1)	26(1)	20(1)	9(1)	9(1)	10(1)
C(8)	22(1)	26(1)	22(1)	10(1)	7(1)	7(1)
C(9)	24(1)	31(1)	22(1)	12(1)	6(1)	9(1)
C(10)	21(1)	34(1)	23(1)	15(1)	6(1)	12(1)
C(11)	30(1)	29(1)	31(1)	11(1)	7(1)	9(1)
C(12)	66(2)	36(1)	37(1)	17(1)	8(1)	19(1)
C(13)	84(2)	50(1)	54(2)	20(1)	29(1)	24(1)
C(14)	18(1)	26(1)	23(1)	12(1)	6(1)	9(1)

C(15)	20(1)	35(1)	26(1)	16(1)	8(1)	11(1)
C(16)	22(1)	39(1)	27(1)	17(1)	9(1)	15(1)
C(17)	20(1)	38(1)	32(1)	21(1)	10(1)	8(1)
C(18)	19(1)	31(1)	39(1)	19(1)	5(1)	6(1)
C(19)	20(1)	26(1)	29(1)	9(1)	3(1)	8(1)
C(20)	18(1)	27(1)	23(1)	12(1)	6(1)	8(1)
C(21)	29(1)	44(1)	22(1)	13(1)	6(1)	9(1)
C(22)	37(1)	34(1)	45(1)	2(1)	15(1)	12(1)
C(23)	29(1)	32(1)	45(1)	19(1)	7(1)	2(1)
C(24)	31(1)	40(1)	71(2)	24(1)	-9(1)	-2(1)
C(25)	37(1)	31(1)	64(1)	22(1)	2(1)	5(1)
C(26)	46(1)	66(1)	42(1)	35(1)	22(1)	22(1)

Table D.11. Hydrogen coordinates (x 10^4) and isotropic displacement parameters ($Å^2$x 10^3) for spirolactone **1.56** (JLW145_a).

	x	y	z	U(eq)
H(1A)	346	1348	1420	59
H(1B)	949	1471	2529	59
H(1C)	250	117	1712	59
H(2A)	4251	503	788	54
H(2B)	2378	817	380	54
H(2C)	2224	-447	629	54
H(4A)	3556	836	3160	38
H(4B)	3199	-399	2269	38
H(5A)	6392	343	3184	39
H(5B)	6248	408	2125	39
H(6A)	8343	2321	3276	33
H(6B)	6731	2510	3789	33
H(8)	3815	2956	2813	27
H(9A)	4212	3165	1033	30
H(9B)	2132	2780	1150	30
H(11A)	5920	7044	2304	36

H(11B)	3739	6795	2277	36
H(12)	3065	6809	655	55
H(13A)	6695	8327	1337	73
H(13B)	5063	8207	388	73
H(21A)	8306	4321	5207	48
H(21B)	6910	4901	5718	48
H(21C)	8639	5805	5538	48
H(22A)	5860	6995	4241	60
H(22B)	6940	8358	5030	60
H(22C)	6566	7142	5351	60
H(23)	11155	8061	2889	43
H(24A)	12054	8574	4902	78
H(24B)	13272	9286	4352	78
H(24C)	13080	7844	4214	78
H(25A)	8553	8751	2976	68
H(25B)	10457	9846	3629	68
H(25C)	9139	9091	4118	68
H(26A)	7964	5257	660	67
H(26B)	9702	6088	434	67
H(26C)	8515	6758	1050	67

D.3. Crystal analysis of dracocephalone A ***1.01***

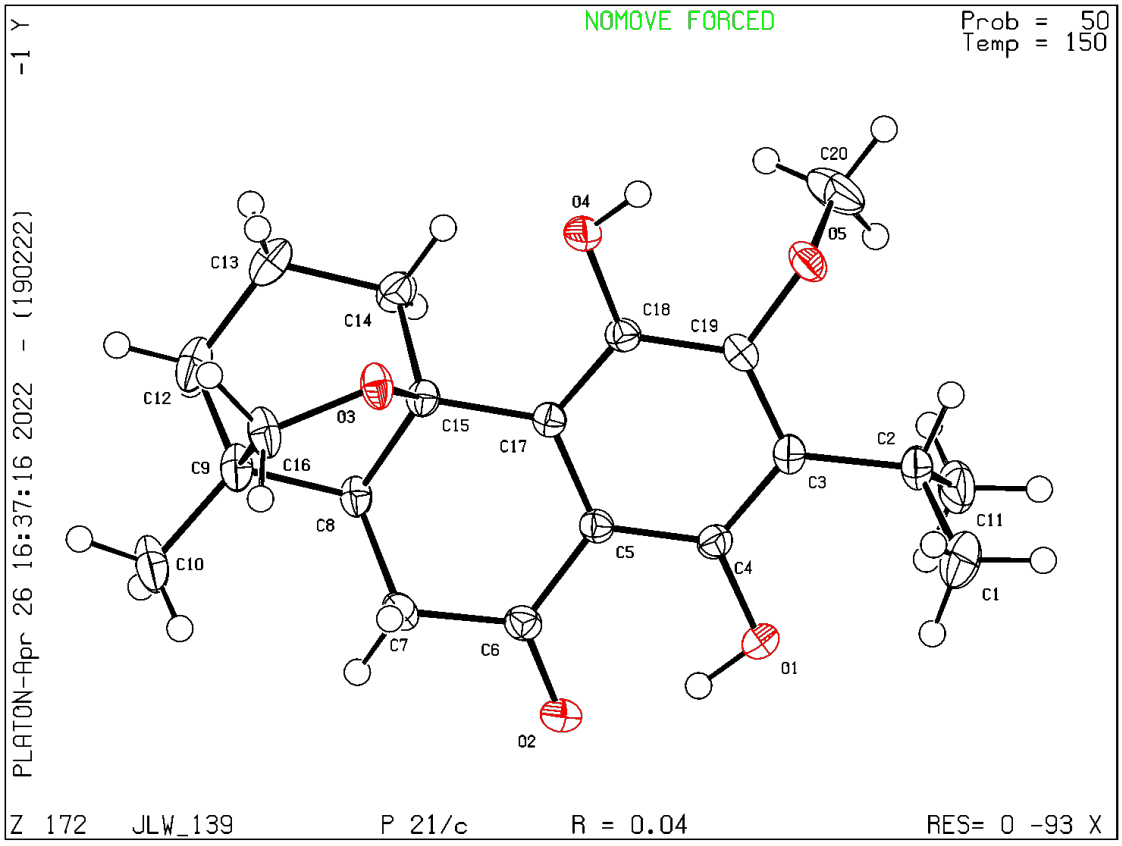

Figure D.3. ORTEP drawing of dracocephalone A **1.01**.

Table D.12. Crystal data and structure refinement for dracocephalone A **1.01** (JLW_139).

Identification code	JLW_139	
Empirical formula	C20 H26 O5	
Formula weight	346.41	
Temperature	150(2) K	
Wavelength	0.71073 Å	
Crystal system	Monoclinic	
Space group	$P2_1/c$	
Unit cell dimensions	a = 13.0936(3) Å	α = 90°.
	b = 9.3686(2) Å	β = 111.012(10)°.
	c = 15.7215(4) Å	γ = 90°.
Volume	1800.30(7) $Å^3$	

Z	4
Density (calculated)	1.278 Mg/m^3
Absorption coefficient	0.091 mm^{-1}
F(000)	744
Crystal size	0.491 x 0.435 x 0.423 mm^3
Theta range for data collection	2.788 to 26.369°.
Index ranges	-15<=h<=16, -11<=k<=11, -19<=l<=19
Reflections collected	33380
Independent reflections	3642 [R(int) = 0.0240]
Completeness to theta = 25.242°	98.6 %
Absorption correction	Semi-empirical from equivalents
Max. and min. transmission	0.922 and 0.916
Refinement method	Full-matrix least-squares on F^2
Data / restraints / parameters	3642 / 0 / 238
Goodness-of-fit on F^2	1.079
Final R indices [I>2sigma(I)]	R1 = 0.0368, wR2 = 0.0978
R indices (all data)	R1 = 0.0378, wR2 = 0.0986
Extinction coefficient	n/a
Largest diff. peak and hole	0.307 and -0.170 $e.Å^{-3}$

Table D.13. Atomic coordinates (x 10^4) and equivalent isotropic displacement parameters ($Å^2$x 10^3) for dracocephalone A **1.01** (JLW_139). U(eq) is defined as one third of the trace of the orthogonalized U^{ij} tensor.

	x	y	z	U(eq)
O(1)	1681(1)	5935(1)	5495(1)	26(1)
O(2)	3412(1)	5725(1)	5142(1)	25(1)
O(3)	5794(1)	8335(1)	7898(1)	21(1)
O(4)	4185(1)	7971(1)	8891(1)	23(1)
O(5)	2004(1)	7737(1)	8413(1)	24(1)
C(1)	-76(1)	7640(2)	5854(1)	43(1)
C(2)	554(1)	6705(1)	6673(1)	26(1)
C(3)	1786(1)	6827(1)	6926(1)	19(1)
C(4)	2314(1)	6431(1)	6327(1)	18(1)
C(5)	3463(1)	6515(1)	6587(1)	17(1)
C(6)	3957(1)	6209(1)	5907(1)	19(1)
C(7)	5131(1)	6600(1)	6131(1)	22(1)
C(8)	5807(1)	6197(1)	7114(1)	19(1)
C(9)	6982(1)	6799(1)	7463(1)	24(1)
C(10)	7582(1)	6687(1)	6795(1)	34(1)
C(11)	178(1)	5144(2)	6527(1)	35(1)
C(12)	7625(1)	6035(1)	8364(1)	31(1)
C(13)	7115(1)	6271(1)	9085(1)	32(1)
C(14)	5869(1)	6066(1)	8707(1)	24(1)
C(15)	5368(1)	6885(1)	7798(1)	17(1)
C(16)	6759(1)	8347(1)	7658(1)	25(1)
C(17)	4126(1)	6969(1)	7477(1)	16(1)
C(18)	3600(1)	7423(1)	8052(1)	17(1)
C(19)	2452(1)	7310(1)	7778(1)	18(1)
C(20)	1921(1)	6574(2)	8983(1)	40(1)

Table D.14. Bond lengths [Å] and angles [°] for dracocephalone A **1.01** (JLW_139).

O(1)-C(4)	1.3549(13)
O(1)-H(1A)	0.92(2)
O(2)-C(6)	1.2440(13)
O(3)-C(16)	1.4426(12)
O(3)-C(15)	1.4560(12)
O(4)-C(18)	1.3658(12)
O(4)-H(4A)	0.871(18)
O(5)-C(19)	1.3858(12)
O(5)-C(20)	1.4391(15)
C(1)-C(2)	1.5311(18)
C(1)-H(1)	0.9800
C(1)-H(5)	0.9800
C(1)-H(4)	0.9800
C(2)-C(3)	1.5210(14)
C(2)-C(11)	1.5335(18)
C(2)-H(22)	1.0000
C(3)-C(19)	1.3854(15)
C(3)-C(4)	1.4043(14)
C(4)-C(5)	1.4115(14)
C(5)-C(17)	1.4221(14)
C(5)-C(6)	1.4626(14)
C(6)-C(7)	1.4943(14)
C(7)-C(8)	1.5268(15)
C(7)-H(21)	0.9900
C(7)-H(20)	0.9900
C(8)-C(15)	1.5322(14)
C(8)-C(9)	1.5426(14)
C(8)-H(6)	1.0000
C(9)-C(10)	1.5244(16)
C(9)-C(16)	1.5314(15)
C(9)-C(12)	1.5405(17)
C(10)-H(2)	0.9800
C(10)-H(8)	0.9800
C(10)-H(7)	0.9800

C(11)-H(3)	0.9800
C(11)-H(24)	0.9800
C(11)-H(23)	0.9800
C(12)-C(13)	1.5243(18)
C(12)-H(19)	0.9900
C(12)-H(9)	0.9900
C(13)-C(14)	1.5345(15)
C(13)-H(10)	0.9900
C(13)-H(18)	0.9900
C(14)-C(15)	1.5459(14)
C(14)-H(12)	0.9900
C(14)-H(11)	0.9900
C(15)-C(17)	1.5221(13)
C(16)-H(14)	0.9900
C(16)-H(13)	0.9900
C(17)-C(18)	1.3856(14)
C(18)-C(19)	1.4108(14)
C(20)-H(17)	0.9800
C(20)-H(15)	0.9800
C(20)-H(16)	0.9800

C(4)-O(1)-H(1A)	103.8(12)
C(16)-O(3)-C(15)	108.48(7)
C(18)-O(4)-H(4A)	109.5(11)
C(19)-O(5)-C(20)	112.11(9)
C(2)-C(1)-H(1)	109.5
C(2)-C(1)-H(5)	109.5
H(1)-C(1)-H(5)	109.5
C(2)-C(1)-H(4)	109.5
H(1)-C(1)-H(4)	109.5
H(5)-C(1)-H(4)	109.5
C(3)-C(2)-C(1)	112.28(10)
C(3)-C(2)-C(11)	111.37(9)
C(1)-C(2)-C(11)	111.85(11)
C(3)-C(2)-H(22)	107.0
C(1)-C(2)-H(22)	107.0

C(11)-C(2)-H(22)	107.0
C(19)-C(3)-C(4)	116.37(9)
C(19)-C(3)-C(2)	121.25(9)
C(4)-C(3)-C(2)	122.36(9)
O(1)-C(4)-C(3)	117.40(9)
O(1)-C(4)-C(5)	121.21(9)
C(3)-C(4)-C(5)	121.37(9)
C(4)-C(5)-C(17)	120.85(9)
C(4)-C(5)-C(6)	118.82(9)
C(17)-C(5)-C(6)	120.23(9)
O(2)-C(6)-C(5)	121.85(9)
O(2)-C(6)-C(7)	120.15(9)
C(5)-C(6)-C(7)	117.85(9)
C(6)-C(7)-C(8)	110.61(8)
C(6)-C(7)-H(21)	109.5
C(8)-C(7)-H(21)	109.5
C(6)-C(7)-H(20)	109.5
C(8)-C(7)-H(20)	109.5
H(21)-C(7)-H(20)	108.1
C(7)-C(8)-C(15)	112.24(8)
C(7)-C(8)-C(9)	114.31(9)
C(15)-C(8)-C(9)	99.99(8)
C(7)-C(8)-H(6)	110.0
C(15)-C(8)-H(6)	110.0
C(9)-C(8)-H(6)	110.0
C(10)-C(9)-C(16)	112.62(10)
C(10)-C(9)-C(12)	110.77(10)
C(16)-C(9)-C(12)	109.67(10)
C(10)-C(9)-C(8)	115.12(9)
C(16)-C(9)-C(8)	100.42(8)
C(12)-C(9)-C(8)	107.69(9)
C(9)-C(10)-H(2)	109.5
C(9)-C(10)-H(8)	109.5
H(2)-C(10)-H(8)	109.5
C(9)-C(10)-H(7)	109.5
H(2)-C(10)-H(7)	109.5

H(8)-C(10)-H(7)	109.5
C(2)-C(11)-H(3)	109.5
C(2)-C(11)-H(24)	109.5
H(3)-C(11)-H(24)	109.5
C(2)-C(11)-H(23)	109.5
H(3)-C(11)-H(23)	109.5
H(24)-C(11)-H(23)	109.5
C(13)-C(12)-C(9)	112.07(9)
C(13)-C(12)-H(19)	109.2
C(9)-C(12)-H(19)	109.2
C(13)-C(12)-H(9)	109.2
C(9)-C(12)-H(9)	109.2
H(19)-C(12)-H(9)	107.9
C(12)-C(13)-C(14)	112.47(10)
C(12)-C(13)-H(10)	109.1
C(14)-C(13)-H(10)	109.1
C(12)-C(13)-H(18)	109.1
C(14)-C(13)-H(18)	109.1
H(10)-C(13)-H(18)	107.8
C(13)-C(14)-C(15)	109.65(9)
C(13)-C(14)-H(12)	109.7
C(15)-C(14)-H(12)	109.7
C(13)-C(14)-H(11)	109.7
C(15)-C(14)-H(11)	109.7
H(12)-C(14)-H(11)	108.2
O(3)-C(15)-C(17)	108.08(8)
O(3)-C(15)-C(8)	104.02(8)
C(17)-C(15)-C(8)	114.49(8)
O(3)-C(15)-C(14)	110.12(8)
C(17)-C(15)-C(14)	112.42(8)
C(8)-C(15)-C(14)	107.37(8)
O(3)-C(16)-C(9)	106.99(8)
O(3)-C(16)-H(14)	110.3
C(9)-C(16)-H(14)	110.3
O(3)-C(16)-H(13)	110.3
C(9)-C(16)-H(13)	110.3

H(14)-C(16)-H(13)	108.6
C(18)-C(17)-C(5)	117.59(9)
C(18)-C(17)-C(15)	121.44(9)
C(5)-C(17)-C(15)	120.90(9)
O(4)-C(18)-C(17)	120.50(9)
O(4)-C(18)-C(19)	119.39(9)
C(17)-C(18)-C(19)	120.10(9)
C(3)-C(19)-O(5)	120.55(9)
C(3)-C(19)-C(18)	123.51(9)
O(5)-C(19)-C(18)	115.94(9)
O(5)-C(20)-H(17)	109.5
O(5)-C(20)-H(15)	109.5
H(17)-C(20)-H(15)	109.5
O(5)-C(20)-H(16)	109.5
H(17)-C(20)-H(16)	109.5
H(15)-C(20)-H(16)	109.5

Symmetry transformations used to generate equivalent atoms:

Table D.15. Anisotropic displacement parameters ($Å^2 x\ 10^3$) for dracocephalone A **1.01** (JLW_139). The anisotropic displacement factor exponent takes the form: $-2p^2[\ h^2\ a^{*2}U^{11} + ... + 2\ h\ k\ a^*\ b^*\ U^{12}\ ]$.

	U^{11}	U^{22}	U^{33}	U^{23}	U^{13}	U^{12}
O(1)	19(1)	40(1)	18(1)	-4(1)	4(1)	-3(1)
O(2)	25(1)	34(1)	16(1)	-2(1)	8(1)	-2(1)
O(3)	17(1)	16(1)	32(1)	-5(1)	12(1)	-3(1)
O(4)	21(1)	31(1)	18(1)	-7(1)	8(1)	-4(1)
O(5)	24(1)	28(1)	26(1)	-6(1)	16(1)	-3(1)
C(1)	22(1)	58(1)	44(1)	7(1)	5(1)	13(1)
C(2)	15(1)	36(1)	28(1)	-4(1)	9(1)	0(1)
C(3)	15(1)	20(1)	23(1)	2(1)	7(1)	1(1)
C(4)	17(1)	20(1)	16(1)	2(1)	5(1)	0(1)
C(5)	17(1)	17(1)	16(1)	2(1)	7(1)	0(1)
C(6)	21(1)	20(1)	18(1)	2(1)	8(1)	2(1)

C(7)	21(1)	27(1)	22(1)	-1(1)	12(1)	-1(1)
C(8)	15(1)	17(1)	25(1)	-2(1)	8(1)	0(1)
C(9)	16(1)	22(1)	34(1)	-6(1)	10(1)	-1(1)
C(10)	21(1)	37(1)	51(1)	-12(1)	21(1)	-4(1)
C(11)	22(1)	44(1)	42(1)	-12(1)	15(1)	-11(1)
C(12)	16(1)	28(1)	41(1)	-5(1)	3(1)	2(1)
C(13)	21(1)	36(1)	28(1)	2(1)	-2(1)	3(1)
C(14)	21(1)	26(1)	22(1)	4(1)	4(1)	1(1)
C(15)	16(1)	15(1)	20(1)	-1(1)	6(1)	-1(1)
C(16)	19(1)	21(1)	40(1)	-5(1)	16(1)	-4(1)
C(17)	17(1)	14(1)	18(1)	2(1)	6(1)	-1(1)
C(18)	19(1)	17(1)	16(1)	0(1)	7(1)	-2(1)
C(19)	20(1)	17(1)	21(1)	0(1)	12(1)	0(1)
C(20)	57(1)	39(1)	38(1)	-5(1)	34(1)	-16(1)

Table D.16. Hydrogen bonds for dracocephalone A **1.01** (JLW_139) [Å and °].

D-H...A	d(D-H)	d(H...A)	d(D...A)	<(DHA)
O(4)-H(4A)...O(5)	0.871(18)	2.217(17)	2.6882(11)	113.7(13)
O(4)-H(4A)...O(2)#1	0.871(18)	1.992(18)	2.7943(11)	152.6(15)
O(1)-H(1A)...O(2)	0.92(2)	1.667(19)	2.5276(11)	154.0(18)

Symmetry transformations used to generate equivalent atoms:
#1 x,-y+3/2,z+1/2

*D.4. Crystal analysis of acetate **1.68***

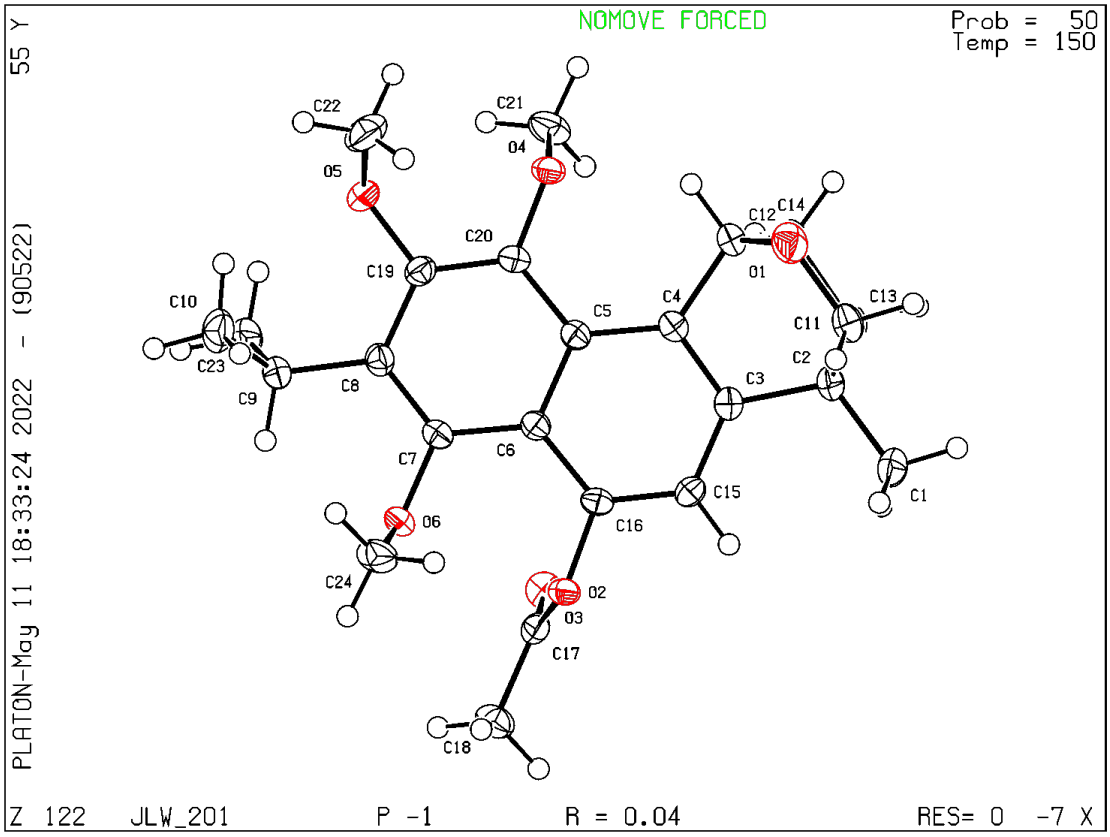

Figure D.4. ORTEP drawing of acetate **1.68**.

Table D.17. Crystal data and structure refinement for acetate **1.68** (JLW_201).

Identification code	JLW_201	
Empirical formula	C24 H30 O6	
Formula weight	414.48	
Temperature	150(2) K	
Wavelength	0.71073 Å	
Crystal system	Triclinic	
Space group	P-1	
Unit cell dimensions	a = 5.7424(3) Å	α = 77.909(2)°.
	b = 12.0461(6) Å	β = 83.352(2)°.
	c = 15.5779(8) Å	γ = 86.832(2)°.
Volume	1046.06(9) $Å^3$	
Z	2	
Density (calculated)	1.316 Mg/m^3	

Absorption coefficient	0.094 mm^{-1}
F(000)	444
Crystal size	0.158 x 0.114 x 0.068 mm^3
Theta range for data collection	3.447 to 25.682°.
Index ranges	-7<=h<=6, -14<=k<=14, -18<=l<=18
Reflections collected	24369
Independent reflections	3880 [R(int) = 0.0287]
Completeness to theta = 25.242°	98.4 %
Absorption correction	None
Refinement method	Full-matrix least-squares on F^2
Data / restraints / parameters	3880 / 0 / 278
Goodness-of-fit on F^2	1.061
Final R indices [I>2sigma(I)]	R1 = 0.0448, wR2 = 0.1324
R indices (all data)	R1 = 0.0480, wR2 = 0.1352
Extinction coefficient	n/a
Largest diff. peak and hole	0.311 and -0.204 e.$Å^{-3}$

Table D.18. Atomic coordinates (x 10^4) and equivalent isotropic displacement parameters ($Å^2$x 10^3) for acetate **1.68** (JLW_201). U(eq) is defined as one third of the trace of the orthogonalized U^{ij} tensor.

	x	y	z	U(eq)
O(1)	2300(2)	8451(1)	9686(1)	33(1)
O(2)	7584(2)	8734(1)	5961(1)	21(1)
O(3)	4819(2)	8611(1)	5074(1)	29(1)
O(4)	1845(2)	5559(1)	8960(1)	23(1)
O(5)	3766(2)	3886(1)	8138(1)	26(1)
O(6)	7984(2)	6579(1)	5901(1)	23(1)
C(1)	2855(3)	11139(1)	7933(1)	30(1)
C(2)	2222(3)	9916(1)	8333(1)	22(1)
C(3)	3457(2)	9038(1)	7858(1)	19(1)
C(4)	2936(3)	7929(1)	8255(1)	20(1)
C(5)	3920(2)	7010(1)	7864(1)	19(1)
C(6)	5507(2)	7257(1)	7067(1)	19(1)
C(7)	6458(2)	6340(1)	6666(1)	20(1)

C(8)	5890(3)	5224(1)	7001(1)	22(1)
C(9)	6805(3)	4293(1)	6514(1)	26(1)
C(10)	8265(3)	3358(1)	7056(1)	35(1)
C(11)	2849(3)	9609(1)	9286(1)	26(1)
C(12)	1263(3)	7889(1)	9089(1)	26(1)
C(13)	-432(3)	9748(1)	8374(1)	25(1)
C(14)	-1000(3)	8535(1)	8835(1)	26(1)
C(15)	4982(2)	9284(1)	7082(1)	20(1)
C(16)	5973(2)	8420(1)	6707(1)	19(1)
C(17)	6814(3)	8752(1)	5163(1)	21(1)
C(18)	8789(3)	9000(2)	4446(1)	32(1)
C(19)	4362(3)	4997(1)	7798(1)	21(1)
C(20)	3384(3)	5850(1)	8203(1)	20(1)
C(21)	-453(3)	5317(2)	8785(1)	32(1)
C(22)	4331(4)	3418(2)	9020(1)	39(1)
C(23)	4813(3)	3789(1)	6158(1)	32(1)
C(24)	10390(3)	6554(2)	6068(1)	33(1)

Table D.19. Bond lengths [Å] and angles [°] for acetate **1.68** (JLW_201).

O(1)-C(11)	1.440(2)
O(1)-C(12)	1.455(2)
O(2)-C(17)	1.3627(18)
O(2)-C(16)	1.3984(17)
O(3)-C(17)	1.1949(19)
O(4)-C(20)	1.3835(17)
O(4)-C(21)	1.4350(19)
O(5)-C(19)	1.3778(18)
O(5)-C(22)	1.439(2)
O(6)-C(7)	1.3838(17)
O(6)-C(24)	1.432(2)
C(1)-C(2)	1.521(2)
C(1)-H(1)	0.9800
C(1)-H(6)	0.9800
C(1)-H(5)	0.9800

C(2)-C(3)	1.514(2)
C(2)-C(11)	1.533(2)
C(2)-C(13)	1.541(2)
C(3)-C(4)	1.383(2)
C(3)-C(15)	1.397(2)
C(4)-C(5)	1.431(2)
C(4)-C(12)	1.518(2)
C(5)-C(20)	1.424(2)
C(5)-C(6)	1.440(2)
C(6)-C(16)	1.424(2)
C(6)-C(7)	1.431(2)
C(7)-C(8)	1.379(2)
C(8)-C(19)	1.421(2)
C(8)-C(9)	1.520(2)
C(9)-C(10)	1.532(2)
C(9)-C(23)	1.532(2)
C(9)-H(24)	1.0000
C(10)-H(26)	0.9800
C(10)-H(25)	0.9800
C(10)-H(2)	0.9800
C(11)-H(3)	0.9900
C(11)-H(30)	0.9900
C(12)-C(14)	1.526(2)
C(12)-H(4)	1.0000
C(13)-C(14)	1.522(2)
C(13)-H(7)	0.9900
C(13)-H(8)	0.9900
C(14)-H(10)	0.9900
C(14)-H(9)	0.9900
C(15)-C(16)	1.363(2)
C(15)-H(11)	0.9500
C(17)-C(18)	1.492(2)
C(18)-H(14)	0.9800
C(18)-H(12)	0.9800
C(18)-H(13)	0.9800
C(19)-C(20)	1.377(2)

C(21)-H(17)	0.9800
C(21)-H(15)	0.9800
C(21)-H(16)	0.9800
C(22)-H(20)	0.9800
C(22)-H(19)	0.9800
C(22)-H(18)	0.9800
C(23)-H(22)	0.9800
C(23)-H(23)	0.9800
C(23)-H(21)	0.9800
C(24)-H(29)	0.9800
C(24)-H(28)	0.9800
C(24)-H(27)	0.9800

C(11)-O(1)-C(12)	111.95(11)
C(17)-O(2)-C(16)	116.83(11)
C(20)-O(4)-C(21)	113.22(11)
C(19)-O(5)-C(22)	116.22(12)
C(7)-O(6)-C(24)	112.92(11)
C(2)-C(1)-H(1)	109.5
C(2)-C(1)-H(6)	109.5
H(1)-C(1)-H(6)	109.5
C(2)-C(1)-H(5)	109.5
H(1)-C(1)-H(5)	109.5
H(6)-C(1)-H(5)	109.5
C(3)-C(2)-C(1)	115.05(13)
C(3)-C(2)-C(11)	106.73(12)
C(1)-C(2)-C(11)	109.40(12)
C(3)-C(2)-C(13)	106.93(12)
C(1)-C(2)-C(13)	111.57(13)
C(11)-C(2)-C(13)	106.73(12)
C(4)-C(3)-C(15)	120.93(13)
C(4)-C(3)-C(2)	114.15(13)
C(15)-C(3)-C(2)	124.92(13)
C(3)-C(4)-C(5)	120.31(13)
C(3)-C(4)-C(12)	110.68(13)
C(5)-C(4)-C(12)	129.00(14)

C(20)-C(5)-C(4)	123.94(13)
C(20)-C(5)-C(6)	117.00(13)
C(4)-C(5)-C(6)	119.05(13)
C(16)-C(6)-C(7)	123.79(13)
C(16)-C(6)-C(5)	117.10(13)
C(7)-C(6)-C(5)	119.07(13)
C(8)-C(7)-O(6)	118.13(13)
C(8)-C(7)-C(6)	122.88(13)
O(6)-C(7)-C(6)	118.98(13)
C(7)-C(8)-C(19)	117.13(13)
C(7)-C(8)-C(9)	120.81(13)
C(19)-C(8)-C(9)	122.02(13)
C(8)-C(9)-C(10)	113.72(14)
C(8)-C(9)-C(23)	111.34(13)
C(10)-C(9)-C(23)	111.04(13)
C(8)-C(9)-H(24)	106.8
C(10)-C(9)-H(24)	106.8
C(23)-C(9)-H(24)	106.8
C(9)-C(10)-H(26)	109.5
C(9)-C(10)-H(25)	109.5
H(26)-C(10)-H(25)	109.5
C(9)-C(10)-H(2)	109.5
H(26)-C(10)-H(2)	109.5
H(25)-C(10)-H(2)	109.5
O(1)-C(11)-C(2)	111.15(12)
O(1)-C(11)-H(3)	109.4
C(2)-C(11)-H(3)	109.4
O(1)-C(11)-H(30)	109.4
C(2)-C(11)-H(30)	109.4
H(3)-C(11)-H(30)	108.0
O(1)-C(12)-C(4)	109.27(13)
O(1)-C(12)-C(14)	108.65(12)
C(4)-C(12)-C(14)	108.23(13)
O(1)-C(12)-H(4)	110.2
C(4)-C(12)-H(4)	110.2
C(14)-C(12)-H(4)	110.2

C(14)-C(13)-C(2)	109.59(12)
C(14)-C(13)-H(7)	109.8
C(2)-C(13)-H(7)	109.8
C(14)-C(13)-H(8)	109.8
C(2)-C(13)-H(8)	109.8
H(7)-C(13)-H(8)	108.2
C(13)-C(14)-C(12)	109.14(12)
C(13)-C(14)-H(10)	109.9
C(12)-C(14)-H(10)	109.9
C(13)-C(14)-H(9)	109.9
C(12)-C(14)-H(9)	109.9
H(10)-C(14)-H(9)	108.3
C(16)-C(15)-C(3)	119.70(13)
C(16)-C(15)-H(11)	120.2
C(3)-C(15)-H(11)	120.2
C(15)-C(16)-O(2)	116.06(13)
C(15)-C(16)-C(6)	122.90(13)
O(2)-C(16)-C(6)	120.98(12)
O(3)-C(17)-O(2)	123.18(14)
O(3)-C(17)-C(18)	126.68(14)
O(2)-C(17)-C(18)	110.12(13)
C(17)-C(18)-H(14)	109.5
C(17)-C(18)-H(12)	109.5
H(14)-C(18)-H(12)	109.5
C(17)-C(18)-H(13)	109.5
H(14)-C(18)-H(13)	109.5
H(12)-C(18)-H(13)	109.5
C(20)-C(19)-O(5)	120.00(13)
C(20)-C(19)-C(8)	122.07(13)
O(5)-C(19)-C(8)	117.83(13)
C(19)-C(20)-O(4)	118.40(13)
C(19)-C(20)-C(5)	121.78(13)
O(4)-C(20)-C(5)	119.82(13)
O(4)-C(21)-H(17)	109.5
O(4)-C(21)-H(15)	109.5
H(17)-C(21)-H(15)	109.5

O(4)-C(21)-H(16)	109.5
H(17)-C(21)-H(16)	109.5
H(15)-C(21)-H(16)	109.5
O(5)-C(22)-H(20)	109.5
O(5)-C(22)-H(19)	109.5
H(20)-C(22)-H(19)	109.5
O(5)-C(22)-H(18)	109.5
H(20)-C(22)-H(18)	109.5
H(19)-C(22)-H(18)	109.5
C(9)-C(23)-H(22)	109.5
C(9)-C(23)-H(23)	109.5
H(22)-C(23)-H(23)	109.5
C(9)-C(23)-H(21)	109.5
H(22)-C(23)-H(21)	109.5
H(23)-C(23)-H(21)	109.5
O(6)-C(24)-H(29)	109.5
O(6)-C(24)-H(28)	109.5
H(29)-C(24)-H(28)	109.5
O(6)-C(24)-H(27)	109.5
H(29)-C(24)-H(27)	109.5
H(28)-C(24)-H(27)	109.5

Symmetry transformations used to generate equivalent atoms:

Table D.20. Anisotropic displacement parameters ($Å^2 x\ 10^3$) for acetate **1.68** (JLW_201). The anisotropic displacement factor exponent takes the form: $-2p^2[\ h^2\ a^{*2}U^{11} + ...\ + 2\ h\ k\ a^*\ b^*\ U^{12}\ ]$

	U^{11}	U^{22}	U^{33}	U^{23}	U^{13}	U^{12}
O(1)	45(1)	33(1)	22(1)	-8(1)	-5(1)	5(1)
O(2)	21(1)	22(1)	19(1)	-3(1)	2(1)	-5(1)
O(3)	27(1)	31(1)	28(1)	-6(1)	-5(1)	0(1)
O(4)	24(1)	24(1)	19(1)	-3(1)	3(1)	-6(1)
O(5)	34(1)	18(1)	26(1)	-3(1)	1(1)	-5(1)
O(6)	22(1)	24(1)	21(1)	-5(1)	4(1)	1(1)

C(1)	34(1)	22(1)	35(1)	-12(1)	-1(1)	-1(1)
C(2)	22(1)	22(1)	23(1)	-10(1)	-2(1)	1(1)
C(3)	18(1)	21(1)	21(1)	-7(1)	-6(1)	1(1)
C(4)	19(1)	22(1)	20(1)	-6(1)	-1(1)	0(1)
C(5)	18(1)	21(1)	19(1)	-4(1)	-1(1)	0(1)
C(6)	16(1)	21(1)	19(1)	-4(1)	-2(1)	0(1)
C(7)	17(1)	23(1)	18(1)	-4(1)	0(1)	0(1)
C(8)	19(1)	21(1)	24(1)	-7(1)	-1(1)	1(1)
C(9)	26(1)	21(1)	29(1)	-8(1)	6(1)	0(1)
C(10)	30(1)	26(1)	49(1)	-12(1)	-2(1)	6(1)
C(11)	25(1)	30(1)	25(1)	-13(1)	-4(1)	3(1)
C(12)	29(1)	23(1)	24(1)	-8(1)	5(1)	1(1)
C(13)	22(1)	26(1)	28(1)	-10(1)	-4(1)	4(1)
C(14)	17(1)	28(1)	34(1)	-12(1)	4(1)	-1(1)
C(15)	20(1)	18(1)	22(1)	-3(1)	-4(1)	-2(1)
C(16)	16(1)	23(1)	17(1)	-3(1)	-1(1)	-3(1)
C(17)	26(1)	16(1)	22(1)	-3(1)	-2(1)	1(1)
C(18)	34(1)	37(1)	22(1)	-5(1)	3(1)	-2(1)
C(19)	21(1)	18(1)	24(1)	-3(1)	-2(1)	-3(1)
C(20)	20(1)	22(1)	18(1)	-3(1)	1(1)	-3(1)
C(21)	24(1)	43(1)	29(1)	-10(1)	5(1)	-10(1)
C(22)	58(1)	23(1)	33(1)	2(1)	-7(1)	-7(1)
C(23)	36(1)	29(1)	33(1)	-14(1)	1(1)	-1(1)
C(24)	20(1)	37(1)	36(1)	1(1)	5(1)	3(1)

Table D.21. Hydrogen coordinates (x 10^4) and isotropic displacement parameters ($Å^2$x 10^3) for acetate **1.68** (JLW_201).

	x	y	z	U(eq)
H(1)	4540	11224	7941	45
H(6)	1970	11646	8277	45
H(5)	2465	11334	7322	45
H(24)	7869	4660	5989	31

H(26)	9512	3702	7282	53
H(25)	8965	2842	6680	53
H(2)	7254	2932	7552	53
H(3)	4544	9716	9291	31
H(30)	1966	10125	9635	31
H(4)	927	7084	9380	31
H(7)	-1312	10288	8700	30
H(8)	-909	9900	7768	30
H(10)	-1749	8157	8437	31
H(9)	-2108	8540	9371	31
H(11)	5326	10049	6815	24
H(14)	8743	8491	4034	47
H(12)	10283	8883	4704	47
H(13)	8637	9790	4129	47
H(17)	-1086	5972	8384	48
H(15)	-1485	5163	9341	48
H(16)	-356	4651	8512	48
H(20)	5272	3955	9215	58
H(19)	5227	2700	9027	58
H(18)	2880	3280	9419	58
H(22)	3700	3437	6652	48
H(23)	5463	3214	5828	48
H(21)	4003	4394	5767	48
H(29)	10621	7147	6392	50
H(28)	11395	6688	5506	50
H(27)	10799	5810	6420	50

Table D.22. Torsion angles [°] for acetate **1.68** (JLW_201).

C(1)-C(2)-C(3)-C(4)	177.29(13)
C(11)-C(2)-C(3)-C(4)	55.72(16)
C(13)-C(2)-C(3)-C(4)	-58.21(16)
C(1)-C(2)-C(3)-C(15)	-3.4(2)
C(11)-C(2)-C(3)-C(15)	-124.99(15)
C(13)-C(2)-C(3)-C(15)	121.08(15)

C(15)-C(3)-C(4)-C(5)	-1.2(2)
C(2)-C(3)-C(4)-C(5)	178.07(12)
C(15)-C(3)-C(4)-C(12)	179.57(13)
C(2)-C(3)-C(4)-C(12)	-1.11(18)
C(3)-C(4)-C(5)-C(20)	-176.67(13)
C(12)-C(4)-C(5)-C(20)	2.3(2)
C(3)-C(4)-C(5)-C(6)	1.7(2)
C(12)-C(4)-C(5)-C(6)	-179.29(13)
C(20)-C(5)-C(6)-C(16)	177.56(12)
C(4)-C(5)-C(6)-C(16)	-0.9(2)
C(20)-C(5)-C(6)-C(7)	-0.4(2)
C(4)-C(5)-C(6)-C(7)	-178.84(12)
C(24)-O(6)-C(7)-C(8)	-90.62(16)
C(24)-O(6)-C(7)-C(6)	90.48(16)
C(16)-C(6)-C(7)-C(8)	-176.56(13)
C(5)-C(6)-C(7)-C(8)	1.2(2)
C(16)-C(6)-C(7)-O(6)	2.3(2)
C(5)-C(6)-C(7)-O(6)	-179.94(12)
O(6)-C(7)-C(8)-C(19)	178.60(12)
C(6)-C(7)-C(8)-C(19)	-2.5(2)
O(6)-C(7)-C(8)-C(9)	-3.5(2)
C(6)-C(7)-C(8)-C(9)	175.40(13)
C(7)-C(8)-C(9)-C(10)	121.25(16)
C(19)-C(8)-C(9)-C(10)	-60.92(19)
C(7)-C(8)-C(9)-C(23)	-112.41(16)
C(19)-C(8)-C(9)-C(23)	65.43(19)
C(12)-O(1)-C(11)-C(2)	-1.06(17)
C(3)-C(2)-C(11)-O(1)	-54.24(16)
C(1)-C(2)-C(11)-O(1)	-179.32(12)
C(13)-C(2)-C(11)-O(1)	59.83(15)
C(11)-O(1)-C(12)-C(4)	57.75(16)
C(11)-O(1)-C(12)-C(14)	-60.14(16)
C(3)-C(4)-C(12)-O(1)	-57.32(16)
C(5)-C(4)-C(12)-O(1)	123.59(16)
C(3)-C(4)-C(12)-C(14)	60.83(16)
C(5)-C(4)-C(12)-C(14)	-118.26(16)

C(3)-C(2)-C(13)-C(14)	57.27(16)
C(1)-C(2)-C(13)-C(14)	-176.14(12)
C(11)-C(2)-C(13)-C(14)	-56.67(15)
C(2)-C(13)-C(14)-C(12)	-0.92(17)
O(1)-C(12)-C(14)-C(13)	60.56(16)
C(4)-C(12)-C(14)-C(13)	-57.99(16)
C(4)-C(3)-C(15)-C(16)	0.0(2)
C(2)-C(3)-C(15)-C(16)	-179.24(13)
C(3)-C(15)-C(16)-O(2)	-176.35(11)
C(3)-C(15)-C(16)-C(6)	0.8(2)
C(17)-O(2)-C(16)-C(15)	-102.58(15)
C(17)-O(2)-C(16)-C(6)	80.22(16)
C(7)-C(6)-C(16)-C(15)	177.50(13)
C(5)-C(6)-C(16)-C(15)	-0.3(2)
C(7)-C(6)-C(16)-O(2)	-5.5(2)
C(5)-C(6)-C(16)-O(2)	176.69(12)
C(16)-O(2)-C(17)-O(3)	6.6(2)
C(16)-O(2)-C(17)-C(18)	-174.94(12)
C(22)-O(5)-C(19)-C(20)	-61.55(19)
C(22)-O(5)-C(19)-C(8)	121.95(16)
C(7)-C(8)-C(19)-C(20)	3.2(2)
C(9)-C(8)-C(19)-C(20)	-174.73(14)
C(7)-C(8)-C(19)-O(5)	179.60(12)
C(9)-C(8)-C(19)-O(5)	1.7(2)
O(5)-C(19)-C(20)-O(4)	1.3(2)
C(8)-C(19)-C(20)-O(4)	177.62(12)
O(5)-C(19)-C(20)-C(5)	-178.84(13)
C(8)-C(19)-C(20)-C(5)	-2.5(2)
C(21)-O(4)-C(20)-C(19)	-77.62(17)
C(21)-O(4)-C(20)-C(5)	102.49(16)
C(4)-C(5)-C(20)-C(19)	179.41(14)
C(6)-C(5)-C(20)-C(19)	1.0(2)
C(4)-C(5)-C(20)-O(4)	-0.7(2)
C(6)-C(5)-C(20)-O(4)	-179.10(12)

*D.5. Crystal analysis of diol **4.97***

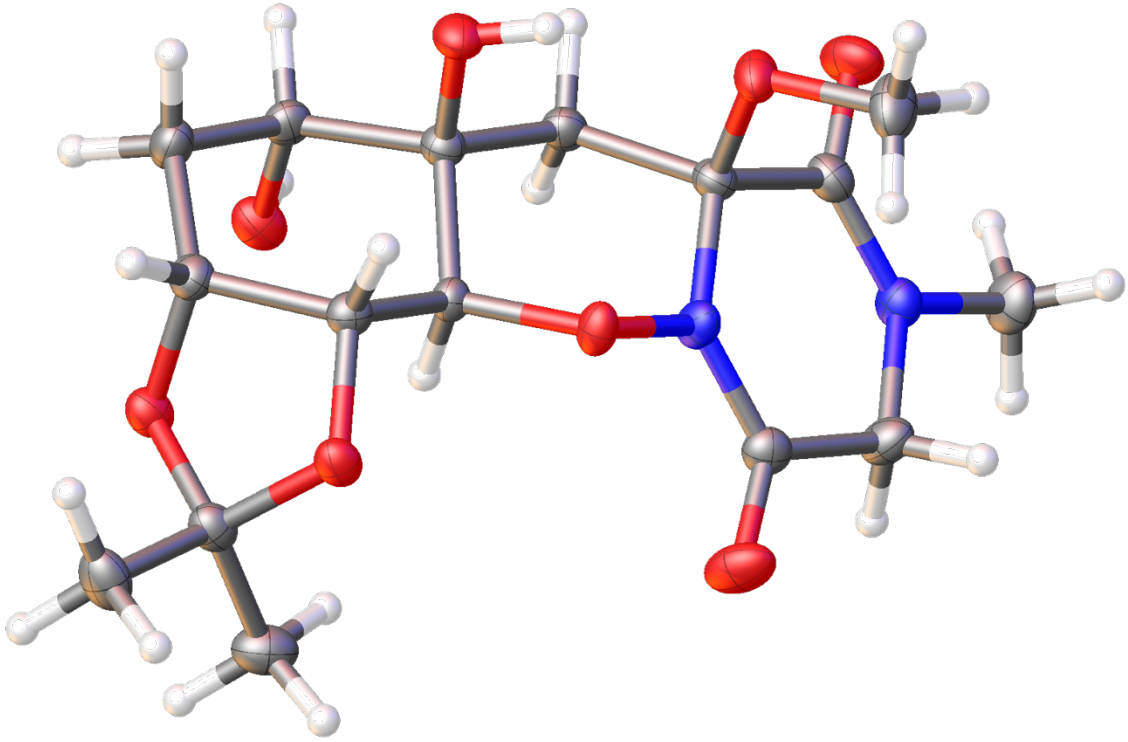

Figure D.5. ORTEP drawing of diol **4.97**

Table D.23. Crystal data and structure refinement for diol **4.97** (JLW_259).

Identification code	JLW_259	
Empirical formula	C16 H24 N2 O8	
Formula weight	372.37	
Temperature	161(2) K	
Wavelength	0.71073 Å	
Crystal system	Orthorhombic	
Space group	P 21 21 21	
Unit cell dimensions	a = 7.12660(10) Å	α = 90°.
	b = 11.9753(3) Å	β = 90°.
	c = 19.8321(5) Å	γ = 90°.
Volume	1692.53(6) $Å^3$	
Z	4	
Density (calculated)	1.461 Mg/m^3	
Absorption coefficient	0.118 mm^{-1}	

F(000)	792
Crystal size	0.408 x 0.143 x 0.104 mm^3
Theta range for data collection	3.037 to 25.677°.
Index ranges	-8<=h<=7, -14<=k<=14, -24<=l<=24
Reflections collected	15130
Independent reflections	3189 [R(int) = 0.0309]
Completeness to theta = 25.242°	98.5 %
Absorption correction	Semi-empirical from equivalents
Max. and min. transmission	0.922 and 0.911
Refinement method	Full-matrix least-squares on F^2
Data / restraints / parameters	3189 / 0 / 241
Goodness-of-fit on F^2	1.095
Final R indices [I>2sigma(I)]	R1 = 0.0280, wR2 = 0.0662
R indices (all data)	R1 = 0.0310, wR2 = 0.0692
Absolute structure parameter	-0.1(3)
Extinction coefficient	n/a
Largest diff. peak and hole	0.213 and -0.148 $e.Å^{-3}$

Table D.24. Atomic coordinates (x 10^4) and equivalent isotropic displacement parameters ($Å^2$x 10^3) for **diol 4.97** (JLW_259). U(eq) is defined as one third of the trace of the orthogonalized U^{ij} tensor.

	x	y	z	U(eq)
O(1)	-1111(2)	2359(1)	5881(1)	24(1)
O(2)	446(2)	4489(1)	7068(1)	24(1)
O(3)	4404(2)	1891(1)	6966(1)	21(1)
O(4)	1709(2)	914(1)	6725(1)	21(1)
O(5)	3961(2)	4048(1)	6339(1)	20(1)
O(6)	6350(2)	3837(1)	5314(1)	33(1)
O(7)	2207(2)	6126(1)	6297(1)	23(1)
O(8)	632(2)	6709(1)	5027(1)	31(1)
N(1)	3750(2)	4656(1)	5739(1)	20(1)
N(2)	3263(2)	5927(1)	4599(1)	21(1)
C(1)	-1033(3)	3010(2)	6484(1)	20(1)
C(2)	-737(3)	2235(2)	7090(1)	23(1)
C(3)	1243(3)	1792(2)	7189(1)	20(1)
C(4)	2828(3)	2608(2)	7043(1)	18(1)
C(5)	2428(3)	3262(2)	6403(1)	16(1)
C(6)	553(3)	3880(2)	6447(1)	18(1)
C(7)	358(3)	4670(2)	5839(1)	20(1)
C(8)	2122(3)	5385(2)	5738(1)	18(1)
C(9)	1968(3)	6072(2)	5078(1)	21(1)
C(10)	4955(3)	5261(2)	4664(1)	24(1)
C(11)	5073(3)	4508(2)	5266(1)	21(1)
C(12)	3796(4)	6851(2)	6298(1)	32(1)
C(13)	3165(3)	6589(2)	3978(1)	29(1)
C(14)	3714(3)	814(2)	6748(1)	21(1)
C(15)	4302(3)	-45(2)	7268(1)	29(1)
C(16)	4439(3)	563(2)	6047(1)	30(1)

Table D.25. Bond lengths [Å] and angles [°] for diol **4.97** (JLW_259).

O(1)-C(1)	1.428(2)
O(2)-C(6)	1.433(2)
O(3)-C(4)	1.422(2)
O(3)-C(14)	1.446(2)
O(4)-C(14)	1.434(2)
O(4)-C(3)	1.437(2)
O(5)-N(1)	1.404(2)
O(5)-C(5)	1.447(2)
O(6)-C(11)	1.218(3)
O(7)-C(8)	1.421(2)
O(7)-C(12)	1.427(3)
O(8)-C(9)	1.224(3)
N(1)-C(11)	1.341(3)
N(1)-C(8)	1.452(3)
N(2)-C(9)	1.335(3)
N(2)-C(10)	1.452(3)
N(2)-C(13)	1.468(3)
C(1)-C(2)	1.534(3)
C(1)-C(6)	1.539(3)
C(2)-C(3)	1.520(3)
C(3)-C(4)	1.522(3)
C(4)-C(5)	1.517(3)
C(5)-C(6)	1.530(3)
C(6)-C(7)	1.538(3)
C(7)-C(8)	1.535(3)
C(8)-C(9)	1.550(3)
C(10)-C(11)	1.498(3)
C(14)-C(16)	1.514(3)
C(14)-C(15)	1.514(3)
C(4)-O(3)-C(14)	107.54(14)
C(14)-O(4)-C(3)	105.67(15)
N(1)-O(5)-C(5)	109.35(13)
C(8)-O(7)-C(12)	114.48(16)

C(11)-N(1)-O(5)	116.69(16)
C(11)-N(1)-C(8)	129.81(17)
O(5)-N(1)-C(8)	113.48(15)
C(9)-N(2)-C(10)	125.66(17)
C(9)-N(2)-C(13)	119.60(17)
C(10)-N(2)-C(13)	114.26(17)
O(1)-C(1)-C(2)	109.35(16)
O(1)-C(1)-C(6)	111.02(16)
C(2)-C(1)-C(6)	110.23(16)
C(3)-C(2)-C(1)	116.13(17)
O(4)-C(3)-C(2)	112.79(17)
O(4)-C(3)-C(4)	100.11(15)
C(2)-C(3)-C(4)	116.09(17)
O(3)-C(4)-C(5)	111.74(15)
O(3)-C(4)-C(3)	102.68(15)
C(5)-C(4)-C(3)	110.60(16)
O(5)-C(5)-C(4)	105.52(15)
O(5)-C(5)-C(6)	110.46(15)
C(4)-C(5)-C(6)	111.53(16)
O(2)-C(6)-C(5)	109.95(15)
O(2)-C(6)-C(7)	110.84(15)
C(5)-C(6)-C(7)	109.42(16)
O(2)-C(6)-C(1)	105.31(15)
C(5)-C(6)-C(1)	108.45(16)
C(7)-C(6)-C(1)	112.77(16)
C(8)-C(7)-C(6)	111.80(17)
O(7)-C(8)-N(1)	109.93(16)
O(7)-C(8)-C(7)	106.33(16)
N(1)-C(8)-C(7)	108.58(15)
O(7)-C(8)-C(9)	109.34(15)
N(1)-C(8)-C(9)	112.13(16)
C(7)-C(8)-C(9)	110.38(16)
O(8)-C(9)-N(2)	124.07(19)
O(8)-C(9)-C(8)	117.09(18)
N(2)-C(9)-C(8)	118.83(17)
N(2)-C(10)-C(11)	116.59(17)

O(6)-C(11)-N(1)	123.88(19)
O(6)-C(11)-C(10)	120.09(18)
N(1)-C(11)-C(10)	116.00(18)
O(4)-C(14)-O(3)	105.93(16)
O(4)-C(14)-C(16)	109.04(17)
O(3)-C(14)-C(16)	109.53(17)
O(4)-C(14)-C(15)	110.77(18)
O(3)-C(14)-C(15)	107.99(16)
C(16)-C(14)-C(15)	113.31(18)

Symmetry transformations used to generate equivalent atoms:

Table D.26. Anisotropic displacement parameters ($Å^2 x\ 10^3$) for diol **4.97** (JLW_259). The anisotropic displacement factor exponent takes the form: $-2p^2[\ h^2\ a^{*2}U^{11} + ...\ + 2\ h\ k\ a^*\ b^*\ U^{12}\ ]$.

	U^{11}	U^{22}	U^{33}	U^{23}	U^{13}	U^{12}
O(1)	23(1)	22(1)	27(1)	-1(1)	-7(1)	2(1)
O(2)	28(1)	21(1)	22(1)	-4(1)	4(1)	1(1)
O(3)	17(1)	19(1)	26(1)	2(1)	-4(1)	1(1)
O(4)	20(1)	19(1)	25(1)	-1(1)	-4(1)	-1(1)
O(5)	18(1)	22(1)	20(1)	7(1)	-2(1)	-2(1)
O(6)	26(1)	45(1)	29(1)	7(1)	2(1)	15(1)
O(7)	28(1)	20(1)	21(1)	-2(1)	4(1)	-6(1)
O(8)	33(1)	29(1)	31(1)	7(1)	3(1)	14(1)
N(1)	20(1)	21(1)	19(1)	8(1)	2(1)	3(1)
N(2)	22(1)	22(1)	19(1)	4(1)	-1(1)	1(1)
C(1)	15(1)	22(1)	24(1)	1(1)	-1(1)	1(1)
C(2)	19(1)	23(1)	28(1)	5(1)	3(1)	-1(1)
C(3)	21(1)	20(1)	18(1)	1(1)	1(1)	0(1)
C(4)	17(1)	20(1)	18(1)	-1(1)	-1(1)	0(1)
C(5)	16(1)	16(1)	17(1)	1(1)	0(1)	-2(1)
C(6)	19(1)	18(1)	18(1)	-1(1)	0(1)	1(1)
C(7)	17(1)	18(1)	23(1)	1(1)	0(1)	2(1)
C(8)	19(1)	16(1)	19(1)	-1(1)	1(1)	2(1)
C(9)	25(1)	17(1)	22(1)	1(1)	-2(1)	1(1)
C(10)	21(1)	30(1)	21(1)	4(1)	3(1)	4(1)
C(11)	17(1)	23(1)	21(1)	0(1)	-3(1)	1(1)
C(12)	39(1)	28(1)	29(1)	-2(1)	1(1)	-13(1)
C(13)	31(1)	32(1)	24(1)	11(1)	0(1)	0(1)
C(14)	20(1)	19(1)	25(1)	0(1)	-4(1)	1(1)
C(15)	29(1)	23(1)	36(1)	6(1)	-9(1)	1(1)
C(16)	28(1)	33(1)	29(1)	-7(1)	-2(1)	6(1)

Table D.27. Hydrogen coordinates (x 10^4) and isotropic displacement parameters ($Å^2$x 10^3) for diol **4.97** (JLW_259).

	x	y	z	U(eq)
H(1)	-1911	2633	5618	36
H(2)	1078	5078	7036	35
H(1A)	-2255	3409	6540	24
H(2A)	-1107	2644	7503	28
H(2B)	-1596	1590	7043	28
H(3)	1376	1506	7661	24
H(4)	3017	3125	7432	22
H(5)	2418	2745	6007	20
H(7A)	126	4223	5427	23
H(7B)	-737	5165	5909	23
H(10A)	6044	5774	4675	29
H(10B)	5080	4795	4254	29
H(12A)	4947	6407	6264	48
H(12B)	3815	7283	6717	48
H(12C)	3716	7362	5913	48
H(13A)	1854	6779	3882	43
H(13B)	3680	6154	3602	43
H(13C)	3896	7276	4033	43
H(15A)	3702	126	7700	44
H(15B)	5669	-26	7322	44
H(15C)	3916	-790	7117	44
H(16A)	4074	-196	5918	45
H(16B)	5811	626	6043	45
H(16C)	3903	1098	5727	45

D.6. Crystal analysis of triol ***4.98***

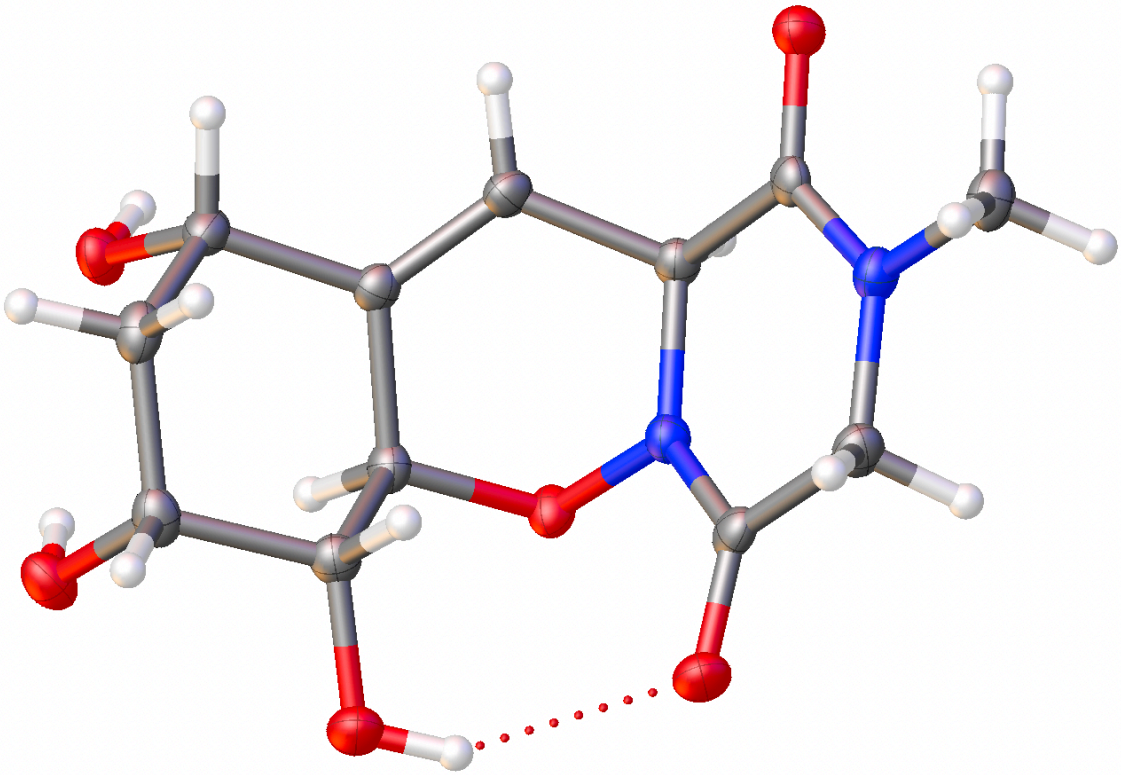

Figure D.6. ORTEP drawing of triol **4.98**

Table D.28. Crystal data and structure refinement for triol **4.98** (JLW_246).

Identification code	JLW_246	
Empirical formula	C12 H16 N2 O6	
Formula weight	284.27	
Temperature	150(2) K	
Wavelength	0.71073 Å	
Crystal system	Monoclinic	
Space group	P 21	
Unit cell dimensions	a = 6.62220(10) Å	α = 90°.
	b = 10.2749(2) Å	β = 105.314(10)°.
	c = 9.3080(2) Å	γ = 90°.
Volume	610.85(2) $Å^3$	
Z	2	
Density (calculated)	1.546 Mg/m^3	

Absorption coefficient	0.125 mm^{-1}
F(000)	300
Crystal size	0.390 x 0.294 x 0.138 mm^3
Theta range for data collection	3.013 to 25.697°.
Index ranges	-8<=h<=6, -12<=k<=12, -11<=l<=11
Reflections collected	8136
Independent reflections	2243 [R(int) = 0.0279]
Completeness to theta = 25.242°	96.7 %
Absorption correction	None
Max. and min. transmission	0.887 and 0.859
Refinement method	Full-matrix least-squares on F^2
Data / restraints / parameters	2243 / 1 / 185
Goodness-of-fit on F^2	1.092
Final R indices [I>2sigma(I)]	R1 = 0.0246, wR2 = 0.0632
R indices (all data)	R1 = 0.0251, wR2 = 0.0638
Absolute structure parameter	0.4(2)
Extinction coefficient	n/a
Largest diff. peak and hole	0.196 and -0.127 e.$Å^{-3}$

Table D.29. Atomic coordinates (x 10^4) and equivalent isotropic displacement parameters ($Å^2$x 10^3) for triol **4.97** (JLW_246). U(eq) is defined as one third of the trace of the orthogonalized U^{ij} tensor.

	x	y	z	U(eq)
O(1)	4295(2)	3626(1)	1435(2)	22(1)
O(2)	7116(2)	5751(1)	7976(2)	21(1)
O(3)	3343(2)	6304(2)	8910(2)	25(1)
O(4)	-106(2)	6662(2)	6354(2)	25(1)
O(5)	2295(2)	6998(1)	4230(1)	19(1)
O(6)	-1668(2)	6252(2)	3167(2)	25(1)
N(1)	1715(2)	6048(2)	3116(2)	17(1)
N(2)	835(3)	4040(2)	1094(2)	19(1)
C(1)	3498(3)	5397(2)	2795(2)	17(1)
C(2)	4923(3)	4922(2)	4245(2)	18(1)
C(3)	4737(3)	5347(2)	5550(2)	16(1)
C(4)	5884(3)	4777(2)	7032(2)	19(1)
C(5)	4290(3)	4268(2)	7827(2)	22(1)
C(6)	2592(3)	5266(2)	7896(2)	21(1)
C(7)	1518(3)	5762(2)	6319(2)	19(1)
C(8)	3167(3)	6371(2)	5658(2)	17(1)
C(9)	-326(3)	5728(2)	2675(2)	18(1)
C(10)	-895(3)	4699(2)	1488(2)	22(1)
C(11)	2873(3)	4260(2)	1708(2)	17(1)
C(12)	193(3)	2996(2)	-4(2)	22(1)

Table D.30. Bond lengths [Å] and angles [°] for triol **4.98** (JLW_246).

O(1)-C(11)	1.226(2)
O(2)-C(4)	1.436(2)
O(3)-C(6)	1.424(2)
O(4)-C(7)	1.426(2)
O(5)-N(1)	1.402(2)
O(5)-C(8)	1.453(2)
O(6)-C(9)	1.228(2)
N(1)-C(9)	1.346(3)
N(1)-C(1)	1.454(2)
N(2)-C(11)	1.338(2)
N(2)-C(10)	1.459(3)
N(2)-C(12)	1.465(2)
C(1)-C(2)	1.508(3)
C(1)-C(11)	1.529(3)
C(2)-C(3)	1.327(3)
C(3)-C(8)	1.501(3)
C(3)-C(4)	1.507(2)
C(4)-C(5)	1.532(3)
C(5)-C(6)	1.535(3)
C(6)-C(7)	1.539(3)
C(7)-C(8)	1.522(2)
C(9)-C(10)	1.503(3)

N(1)-O(5)-C(8)	109.44(13)
C(9)-N(1)-O(5)	116.90(15)
C(9)-N(1)-C(1)	128.97(16)
O(5)-N(1)-C(1)	113.19(14)
C(11)-N(2)-C(10)	125.78(16)
C(11)-N(2)-C(12)	119.73(17)
C(10)-N(2)-C(12)	114.35(16)
N(1)-C(1)-C(2)	108.38(15)
N(1)-C(1)-C(11)	113.25(15)
C(2)-C(1)-C(11)	109.96(15)
C(3)-C(2)-C(1)	121.66(18)

C(2)-C(3)-C(8)	121.70(17)
C(2)-C(3)-C(4)	124.34(17)
C(8)-C(3)-C(4)	113.68(15)
O(2)-C(4)-C(3)	110.91(15)
O(2)-C(4)-C(5)	107.16(15)
C(3)-C(4)-C(5)	109.27(15)
C(4)-C(5)-C(6)	113.44(17)
O(3)-C(6)-C(5)	113.39(16)
O(3)-C(6)-C(7)	112.08(17)
C(5)-C(6)-C(7)	109.89(16)
O(4)-C(7)-C(8)	111.64(16)
O(4)-C(7)-C(6)	110.76(15)
C(8)-C(7)-C(6)	108.76(15)
O(5)-C(8)-C(3)	111.38(14)
O(5)-C(8)-C(7)	113.45(15)
C(3)-C(8)-C(7)	108.81(15)
O(6)-C(9)-N(1)	123.16(18)
O(6)-C(9)-C(10)	121.14(17)
N(1)-C(9)-C(10)	115.67(16)
N(2)-C(10)-C(9)	116.71(16)
O(1)-C(11)-N(2)	124.40(18)
O(1)-C(11)-C(1)	117.04(17)
N(2)-C(11)-C(1)	118.54(16)

Symmetry transformations used to generate equivalent atoms:

Table D.31. Anisotropic displacement parameters ($Å^2 x\ 10^3$) for triol **4.98** (JLW_246). The anisotropic displacement factor exponent takes the form: $-2p^2[\ h^2\ a^{*2}U^{11} + ... + 2\ h\ k\ a^*\ b^*\ U^{12}\ ]$.

	U^{11}	U^{22}	U^{33}	U^{23}	U^{13}	U^{12}
O(1)	19(1)	26(1)	20(1)	-2(1)	5(1)	1(1)
O(2)	19(1)	28(1)	17(1)	-6(1)	4(1)	-4(1)
O(3)	24(1)	31(1)	22(1)	-6(1)	10(1)	-3(1)
O(4)	20(1)	34(1)	24(1)	0(1)	8(1)	5(1)
O(5)	22(1)	16(1)	17(1)	0(1)	3(1)	1(1)
O(6)	17(1)	32(1)	26(1)	0(1)	6(1)	4(1)
N(1)	17(1)	19(1)	15(1)	-1(1)	3(1)	-1(1)
N(2)	18(1)	21(1)	16(1)	0(1)	2(1)	-2(1)
C(1)	15(1)	21(1)	16(1)	0(1)	4(1)	-1(1)
C(2)	13(1)	21(1)	19(1)	-1(1)	3(1)	0(1)
C(3)	14(1)	18(1)	17(1)	0(1)	3(1)	-1(1)
C(4)	19(1)	19(1)	17(1)	-2(1)	2(1)	3(1)
C(5)	26(1)	21(1)	17(1)	2(1)	2(1)	-3(1)
C(6)	21(1)	26(1)	17(1)	0(1)	6(1)	-6(1)
C(7)	16(1)	21(1)	19(1)	0(1)	5(1)	-2(1)
C(8)	19(1)	17(1)	14(1)	1(1)	4(1)	-1(1)
C(9)	16(1)	23(1)	16(1)	7(1)	3(1)	2(1)
C(10)	16(1)	28(1)	20(1)	1(1)	4(1)	-1(1)
C(11)	19(1)	20(1)	12(1)	3(1)	4(1)	-1(1)
C(12)	23(1)	22(1)	19(1)	0(1)	1(1)	-4(1)

Table D.32. Hydrogen coordinates (x 10^4) and isotropic displacement parameters (Å^{2}x 10^3) for triol **4.98** (JLW_246).

	x	y	z	U(eq)
H(2)	7952	6088	7544	32
H(3)	4420	6626	8736	37
H(4)	-792	6836	5480	38
H(1)	4281	6047	2351	21
H(2A)	5981	4304	4222	22
H(4A)	6807	4049	6878	23
H(5A)	5040	4011	8854	26
H(5B)	3609	3480	7303	26
H(6)	1504	4795	8263	25
H(7)	885	5003	5688	22
H(8)	3916	7052	6369	20
H(10A)	-1753	4031	1820	26
H(10B)	-1789	5105	576	26
H(12A)	1437	2599	-203	33
H(12B)	-701	3356	-930	33
H(12C)	-588	2335	387	33

APPENDIX E

DFT Calculations

E.1. Computational Methods

Energy calculations were carried out using Density Functional Theory using the Gaussian16 software package and were visualized in GaussView 6.1.1.[1] Initial minimized geometries were generated using the Molecular Operating Environment (MOE) software package and the lowest energy geometry was used in all cases for further calculations.[2] The minimum energy geometries obtained were further optimized in Gaussian16 using the B3LYP functional with a 6-31+G(d,p) basis set for all atoms, with no dispersion correction, in the gas phase. The lowest energy optimized geometry obtained was then used for subsequent frequency calculations. Frequency calculations were carried out on optimized structures to determine energetic minima with no imaginary frequencies. Calculated single-point electronic energies were obtained using the 6-31+G(d,p) basis set, and the calculated free energies (in hartrees) are reported uncorrected. The difference in energies of compared structures was converted to kcal/mol for comparison purposes.

E.2. References

1) Frisch, M. J.; Trucks, G. W.; Schlegel, H. B.; Scuseria, G. E.; Robb, M. A.; Cheeseman, J. R.; Scalmani, G.; Barone, V.; Petersson, G. A.; Nakatsuji, H.; Li, X.; Caricato, M.; Marenich, A. V.; Bloino, J.; Janesko, B. G.; Gomperts, R.; Mennucci, B.; Hratchian, H. P.; Ortiz, J. V.; Izmaylov, A. F.; Sonnenberg, J. L.; Williams-Young, D.; Ding, F.; Lipparini, F.; Egidi, F.; Goings, J.; Peng, B.; Petrone, A.; Henderson, T.; Ranasinghe, D.; Zakrzewski, V. G.; Gao, J.; Rega, N.; Zheng, G.; Liang, W.; Hada, M.; Ehara, M.; Toyota, K.; Fukuda, R.; Hasegawa, J.; Ishida, M.; Nakajima, T.; Honda, Y.; Kitao, O.; Nakai, H.; Vreven, T.; Throssell, K.; Montgomery, J. A., Jr.; Peralta, J. E.; Ogliaro, F.; Bearpark, M. J.; Heyd, J. J.; Brothers, E. N.; Kudin, K. N.; Staroverov, V. N.; Keith, T. A.; Kobayashi, R.; Normand, J.; Raghavachari, K.; Rendell, A. P.; Burant, J. C.; Iyengar, S. S.; Tomasi, J.; Cossi, M.; Millam, J. M.; Klene, M.; Adamo, C.; Cammi, R.; Ochterski, J. W.; Martin, R. L.; Morokuma, K.; Farkas, O.; Foresman, J. B.; Fox, D. J. Gaussian 16, Revision A.03, Gaussian, Inc.: Wallingford CT, **2016**.

2) *Molecular Operating Environment (MOE)*, 2022.02 Chemical Computing Group ULC, 1010 Sherbooke St. West, Suite #910, Montreal, QC, Canada, H3A 2R7, **2022**.

E.3. XYZ coordinates and free energies (hartrees) of calculated structures of spirolactone ***1.56***

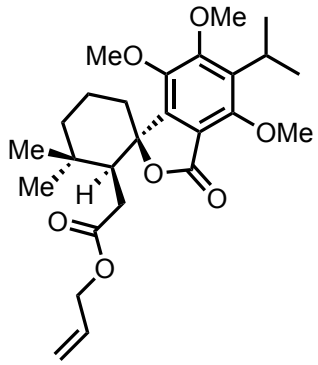

Uncorrected single-point electronic energy (B3LYP/6-311+G(d,p)) = **-1539.0407956**

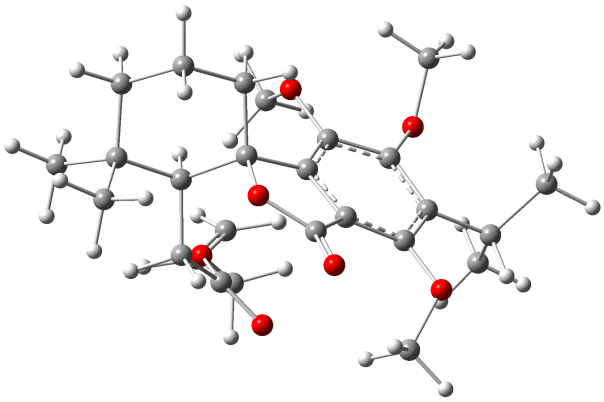

O	0.66578	3.69758	-1.22086
C	0.67931	2.65518	-0.60966
O	1.85248	2.1558	-0.09179
C	1.64478	0.92632	0.66163
C	2.10164	1.18272	2.10899
C	3.61586	1.33645	2.23534
C	4.30915	0.09726	1.66923
C	3.99575	-0.16928	0.17506
C	4.67073	0.91204	-0.69811
C	4.61444	-1.54011	-0.17507
C	2.4353	-0.2318	-0.03841
C	2.08322	-0.32824	-1.54748
C	0.76801	-0.96482	-1.94968
O	0.65846	-2.23768	-1.49006
C	-0.52076	-2.95833	-1.93581
C	-0.34518	-4.39866	-1.57296

C	-1.25387	-5.11514	-0.91213
O	-0.065	-0.45586	-2.66989
C	0.13998	0.74437	0.59516
C	-0.41023	1.73151	-0.22339
C	-1.78985	1.76774	-0.48997
O	-2.36895	2.64645	-1.34746
C	-1.79085	2.8183	-2.65782
C	-2.64456	0.86988	0.19442
C	-4.14513	0.90041	-0.0879
C	-4.99113	1.33268	1.12461
C	-4.65028	-0.4274	-0.68559
C	-2.06868	-0.04192	1.10185
O	-2.90195	-0.88792	1.8043
C	-2.89897	-0.7051	3.22981
C	-0.6692	-0.1672	1.26115
O	-0.11224	-1.07838	2.13545
C	-0.30833	-2.47015	1.82804
H	1.57661	2.07332	2.47026
H	1.76242	0.33658	2.71512
H	3.94711	2.24061	1.71341
H	3.88344	1.46793	3.29019
H	3.99785	-0.77823	2.25754
H	5.3969	0.17622	1.78706
H	4.57494	0.68608	-1.76456
H	5.74237	0.95199	-0.47314
H	4.24672	1.90407	-0.53554
H	5.68672	-1.53313	0.04912
H	4.51257	-1.79494	-1.23452
H	4.15702	-2.34611	0.40961
H	2.09645	-1.14859	0.45731
H	2.84927	-0.93399	-2.04142
H	2.10808	0.65858	-2.00938
H	-1.41028	-2.52289	-1.47047
H	-0.6119	-2.8211	-3.01897
H	0.57758	-4.86362	-1.91649
H	-1.109	-6.17182	-0.71028
H	-2.18315	-4.67347	-0.56059
H	-1.32436	1.88709	-2.993
H	-1.05084	3.61798	-2.64437
H	-2.62435	3.07347	-3.31604
H	-4.27703	1.66881	-0.85233
H	-4.99752	0.56988	1.90659
H	-6.02861	1.49792	0.81351
H	-4.61958	2.26846	1.55425
H	-4.08693	-0.68976	-1.58716
H	-5.70559	-0.33535	-0.96607

H	-4.55787	-1.24742	0.03071
H	-3.24092	0.30321	3.48815
H	-1.9054	-0.87486	3.65171
H	-3.60331	-1.43811	3.62734
H	-1.37122	-2.71188	1.74939
H	0.13431	-3.02271	2.65912
H	0.20169	-2.73445	0.89849

*E.4. XYZ coordinates and free energies (hartrees) of calculated structures of theoretical diastereomer of spirolactone **1.63***

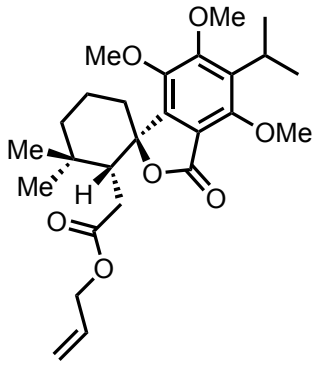

Uncorrected single-point electronic energy (B3LYP/6-311+G(d,p)) = **-1539.0312986**

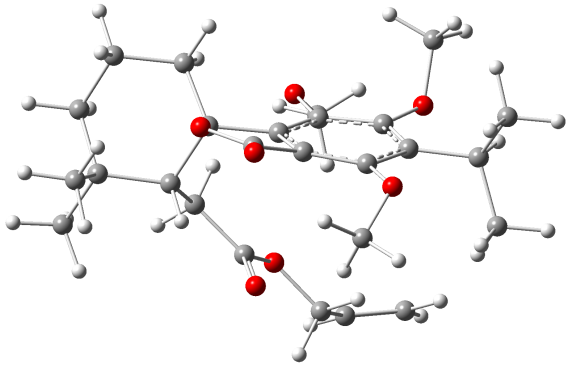

O	0.82046	3.6915	-1.18609
C	0.82909	2.63571	-0.59483
O	1.972	2.16184	-0.01395
C	1.78547	0.84033	0.58021
C	2.36827	0.88071	2.00064
C	3.89214	1.02645	2.0269
C	4.55688	-0.07069	1.18982
C	4.09812	-0.06944	-0.28723
C	4.59472	1.21181	-1.00104
C	4.7778	-1.2492	-1.01685
C	2.52444	-0.16792	-0.38104
C	1.95465	-1.5956	-0.23685
C	0.83421	-1.87558	-1.22631
O	0.16926	-3.00845	-0.89322
C	-0.894	-3.39926	-1.80204
C	-1.43917	-4.70847	-1.32721
C	-2.72401	-4.91608	-1.04254
O	0.57138	-1.22515	-2.21509

C	0.26168	0.70437	0.57179
C	-0.26677	1.69687	-0.26305
C	-1.6455	1.80412	-0.5076
O	-2.20012	2.68367	-1.38344
C	-1.60401	2.83593	-2.68471
C	-2.53304	0.99397	0.23537
C	-4.04881	1.09147	0.08102
C	-4.5227	0.67473	-1.32559
C	-4.60145	2.47564	0.4746
C	-1.9837	0.08814	1.16185
O	-2.83527	-0.65499	1.95724
C	-2.97917	-0.13252	3.28428
C	-0.5916	-0.12273	1.30222
O	-0.06857	-1.00698	2.21698
C	-0.60087	-2.34083	2.31338
H	1.88436	1.70189	2.54036
H	2.07524	-0.04431	2.50583
H	4.17948	2.01603	1.65635
H	4.24056	0.96972	3.06475
H	4.32621	-1.0489	1.63732
H	5.64885	0.03224	1.22498
H	4.33848	1.17617	-2.06579
H	5.68611	1.27759	-0.92497
H	4.16366	2.12583	-0.59737
H	5.84924	-1.04727	-1.11765
H	4.37363	-1.38634	-2.02641
H	4.68629	-2.19781	-0.47816
H	2.25275	0.15463	-1.3912
H	1.5984	-1.81049	0.77154
H	2.71333	-2.35338	-0.44831
H	-1.66038	-2.6187	-1.81825
H	-0.47202	-3.47352	-2.81071
H	-0.71916	-5.52095	-1.24291
H	-3.08929	-5.89076	-0.73432
H	-3.46019	-4.1194	-1.11533
H	-0.76986	3.53568	-2.64745
H	-2.39988	3.21653	-3.32817
H	-1.26095	1.86597	-3.06109
H	-4.46511	0.36253	0.781
H	-4.18692	1.38136	-2.087
H	-4.14782	-0.3196	-1.58973
H	-5.61739	0.63842	-1.35398
H	-4.30987	2.74369	1.49575
H	-5.69628	2.46745	0.43114
H	-4.23597	3.25532	-0.19672
H	-3.67017	-0.79902	3.80424

H	-2.01711	-0.11592	3.80898
H	-3.39705	0.88068	3.26356
H	-0.87188	-2.73196	1.33135
H	-1.46611	-2.38129	2.97669
H	0.20795	-2.94512	2.73118

APPENDIX F

References

F.1. Chapter 1 References

[1] Uchiyama, N.; Kiuchi, F.; Ito, M.; Honda, G.; Takeda, Y.; Khodzhimatov, O. K.; Ashurmetov, O. A. *J. Nat. Prod.* **2003**, *66*, 1, 128-131.

[2] Uchiyama, N.; Kiuchi, F.; Ito, M.; Honda, G.; Takeda, Y.; Khodzhimatov, O. K.; Ashurmetov, O. A. *Tetrahedron* **2006**, *62*, 18, 4355-4359.

[3] Previous total syntheses of komaroviquinone and cyclocoulterone:
(a) Sengupta, S.; Drew, M. G. B.; Mukhopadhyay, R.; Achari, B.; Banerjee, A. K. *J. Org. Chem.* **2005**, *70*, 7694-7700.
(b) Majetich, G.; Li, Y.; Zou, G. *Heterocycles*, **2007**, *73*, 217-225.
(c) Suto, Y.; Kaneko, K.; Yamagiwa, N.; Iwasaki, G. *Tetrahedron Lett.* **2010**, *51*, 6329-6330.
(d) Thommen, C.; Neuburger, M.; Gademann, K. *Chem. Eur. J.* **2016**, *22*, 1-9.
(e) Oh, C. H.; Piao, L.; Jung, J.; Kim, J. *Asian J. Org. Chem.* **2016**, *5*, 1237-1241.
(f) Ahmad, A.; Burtoloso, A. C. B. *Org. Lett.* **2019**, *21*, 6079-6083.

[4] Mills, R. J.; Snieckus, V. *J. Org. Chem.* **1989**, *54*, 4386-4390.

[5] Ciesielski, J.; Canterbury, D. P.; Frontier, A. J. *Org. Lett.* **2009**, *11*, 4374-4377.

[6] Carreño, M. C.; Ruano, J. L. G.; Toledo, M. A.; Urbano, A. *Tetrahedon: Asymmetry.* **1997**, *8*, 913-921.

[7] Maier, M. E.; Bayer A. *Eur. J. Org. Chem*. **2006**, 4034-4043.

[8] Schneider, F.; Samarin, K.; Zanella, S.; Gaich, T. *Science,* **2020**, *367*, 676-681.

[9] Krasovskiy, A.; Kopp, F.; Knochel, P. *Angew. Chem. Int. Ed.* **2006**, *118*, 511-515.

[10] Ihara, M.; Toyota, M.; Abe, M.; Ishida, Y.; Fukumoto, K.; Kametani, T. *J. Chem. Soc. Perkin Trans. 1.* **1986**, 1543-1549.

[11] Caine, D.; Collison, R. F. *Synlett*, **1995**, 503-504.

[12] Nakhla, M. C.; Wood, J. L. *J. Am. Chem. Soc.* **2017**, *139*, 18504-18507.

[13] Beemelmanns, C.; Gross, S.; Reissig, H.-U. *Chem. Eur. J.* **2013**, *19*, 17801-17808.

[14] Haider, M.; Sennari, G.; Eggert, A.; Sarpong, R. *J. Am. Chem. Soc.* **2021**, *143*, 2710-2715.

[15] Deng, J.; Zhou, S.; Zhang, W.; Li, J.; Li, R.; Li, A. *J. Am. Chem. Soc.* **2014**, *136*, 8185-8188.

[16] Ramadayl, F. D.; Kiemle, D. J. LaLonde, R. T. *J. Org. Chem.* **1999**, *64*, 4607-4609.

[17] Hardman, C.; Ho, S.; Shimizu, A.; Luu-Nguyen, Q.; Sloane, J.L.; Soliman, M. S. A.; Marsden, M. D.; Zack, J. A.; Wender, P. A. *Nature Communications* **2020**, *11* (1879), 1-11.

F.2. Chapter 2 References

[1] Zhou, H.; Guoruoluo, Y.; Tuo, Y.; Zhou, J.; Zhang, H.; Wang, W.; Xiang, M.; Aisa, H. A.; Yao, G. *Org. Lett.* **2019**, *21*, 549-553.

[2] Lee, E.; Yoon, C. H. *J. Chem. Soc., Chem. Commun*, **1994**, 479-481.

[3] Lakshmi, R.; Bateman, T. D.; McIntosh, M. C. *J. Org. Chem.* **2005**, *70*, 5313-5315.

[4] Egoshi, Y.; Kondo, R.; Yoshimoto, Y.; Sugiyama, Usuki, T. *Tetrahedron Lett.* **2013**, *54*, 7029-7030.

[5] Xing, X.; O'Connor, N. R.; Stoltz, B. M. *Angew. Chem. Ent. Ed.* **2015**, *54*, 11186-11190.

[6] Nwoye, E. O.; Dudley, G. B. *Chem. Commun.* **2007**, 1436-1437.

[7] Reisman, S. E.; Ready, J. M.; Weiss, M. M.; Hasuoka, A.; Hirata, M.; Tamaki, K.; Ovaska, T. V.; Smith, C. J.; Wood, J. L. *J. Am. Chem. Soc.* **2008**, *130*, 2087-2100.

[8] Boukouvalas, J.; Albert, V. *Tetrahedron Lett.* **2012**, *53*, 3027-3029.

[9] Maity, S.; Manna, S.; Rana, S.; Naveen, T.; Mallick, A.; Maiti, D. *J. Am. Chem. Soc.* **2013**, *135*, 3355-3358.

F.3. Chapter 3 References

[1] Borthwick, A. D. *Chem. Rev.* **2012**, *112*, 3641-3716.

[2] Isolation of (-)-haenamindole :
(a) Kim, J. W.; Ko, S.-K.; Son, S.; Shin, K.-S.; Ryoo, I.-J. Hong, Y.-S.; Oh, H.; Hwang, B. Y.; Hirota, H.; Takahashi, S.; Kim, B. Y.; Osada, H.; Jang, J.-H.; Ahn, J. S. *Bioorg. Med. Chem. Lett*. **2015**, *25*, 5398-5401.
(b) Song, F.; He, H.; Ma, R.; Xiao, X.; Wei, Q.; Wang, Q.; Ji, Z.; Dai, H.; Zhang, L.; Capon, R. J. *Tetrahedron Lett.* **2016**, *57*, 3851-3852.
(c) Hwang, I. H., Che, Y.; Swenson, D. C.; Gloer, J. B.; Wicklow, D. T.; Peterson, S. W.; Dowd, P. F. *J. Antibiot*, **2016**, *69*, 631-636.

[3] Li, J.; Hu, Y.; Hao, X.; Tan, J.; Li, F.; Qiao, X.; Chen, S.; Xiao, C.; Chen, M.; Peng, Z.; Gan, M. *J. Nat. Prod.* **2019**, *82*, 1391-1395.

[4] Pham, T. L.; Sae-Lao, P.; Toh, H. H. M.; Csókás, D.; Bates, R. W. *J. Org. Chem.* **2022**, *87*, 16111-16114.

[5] Shimizu, H.; Yoshimura, A.; Noguchi, K.; Nemekin, V. N.; Zhdankin, V. V.; Saito, A. *Beilstein. J. Org. Chem.* **2018**, *14*, 531-536.

[6] Vogt, P. F.; Miller, M. J. *Tetrahedron* **1998**, *54*, 1317-1348.

[7] Miloserdov, F. M.; Kirillova, M. S.; Muratore, M. E.; Echavarren, A. M. *J. Am. Chem. Soc.* **2018**, *140*, 5393-5400.

[8] Zacharie, B.; Connolly, T. P.; Penney, C. L. *J. Org. Chem.* **1995**, *60*, 7072-7074.

F.4. Chapter 4 References

[1] Miknis, G. F.; Williams, R. M. *J. Am. Chem. Soc.* **1993**, *115*, 536-547.

[2] Tsunematsu, Y.; Maeda, N.; Sato, M.; Hara, K.; Hashimoto, H.; Watanabe, K.; Hertweck, C. *J. Am. Chem. Soc.* **2021**, *143*, 206-213.

[3] Stipanovic, R. D.; Howell, C. R. *J. Antiobiot.* **1982**, 1326-1330.

[4] Seephonkai, P.; Kongsaeree, P.; Prabpai, S.; Isaka, M.; Thebtaranonth, Y. *Org. Lett.* **2006**, *8*,
3073-3075.

[5] Fan, J.; Ran, H.; Wei, P.-L. Li, Y.; Liu, H.; Li, S.-M.; Hu, Y.; Yin, W.-B. *Angew. Chem. Int. Ed.* **2023**, *62*, e202217212.

[6] Miyamoto, C.; Yokose, K.; Furumai, T.; Maruyama, H. B. *J. Antiobiot.* **1982**, 1326-1330.

[7] Isolation of *N*-methylpretrichodermamide B and pretrichodermamide C:
(a) Orfali, R. S.; Aly, A. H.; Ebrahim, W.; Abdel-Aziz, M. S.; Müller, W. E. G.; Lin, W.; Daletos, G.; Proksch, P. *Phytochem. Lett.* **2015**, *11*, 168-172.
(b) Liu, Y.; Li, X.-M.; Meng, L.-H.; Jiang, W.-L., Xu, G.-M.; Huang, C.-G.; Wang, B.-G. *J. Nat. Prod.* **2015**, *78*, 1294-1299.

[8] Nakano, H.; Hara, M.; Meshiro, T.; Ando, K.; Saito, Y.; Morimoto, S. Japan Patent Kokai 1990–218686 (1990.08.31).

[9] Krasovskiy, A.; Kopp, F.; Knochel, P. *Angew. Chem. Int. Ed.* **2006**, *118*, 511-515.

[10] Wu, Z.; Williams, L. J.; Danishefsky, S. J. *Angew. Chem. Int. Ed.* **2000**, *39*, 3866-3868.

[11] Cowper, N. G. W.; Hesse, M. J.; Chan, K. M.; Reisman, S. E. *Chem. Sci.* **2020**, *11*, 11897-11901.
[12] Gayler, K. M.; Lambert, K. M.; Wood, J. L. *Tetrahedron* **2019**, *75*, 3154-3159.

[13] Sheradsky, T.; Silcoff, E. R. *Molecules* **1998**, *3*, 80-87.

[14] Hong, A.-W.; Cheng, T.-H.; Raghukumar, V.; Sha, C.-K. *J. Org. Chem.* **2008**, *73*, 7580-7585.

[15] Shimizu, H.; Yoshimura, A.; Noguchi, K.; Nemykin, V. N.; Zhdankin, V. V.; Saito, A. *Beilstein J. Org. Chem.* **2018**, *14*, 531-536.

[16] Hodges, T. R.; Benjamin, N. M.; Martin, S. F. *Tetrahedron* **2018**, *74*, 3329-3338.

[17] Roush, W. R.; Bennett, C. E. *J. Am. Chem. Soc.* **2000**, *122*, 6124-6125.

ABOUT THE AUTHOR

Taehwan (Tae) Hwang was born on August 26th, 1992 in Seoul, Korea to Insoo Hwang and Yunsook Choi as their first child. Growing up in Seoul with his younger brother Ilhwan, they transferred schools twice. First, they transferred from Yeokchon Elementary School to Nokbeon Elementary School when Tae was a third grader when his family moved to a different town in Seoul. Thereafter, he attended Sunjung Junior High School for 1.5 years until his family decided to immigrate to the U.S. Thereafter, he transferred once more to Plum Grove Junior High School in Rolling Meadows, Illinois. He then attended Fremd High School.

With a vague idea of pursuing a career in pharmacy, he began his undergraduate studies at University of Illinois at Urbana-Champaign majoring in Chemistry. However, his uncertainty in finding his career path lasted all the way until his junior year. Without further hesitation, he decided to apply to research laboratories he found interesting. In the midst of anxious time, he was extremely fortunate to work with Dr. Daeshik Kang in the laboratory of Professor John A. Rogers where he worked in the field of material science. Even though he had learned a tremendous amount of knowledge and laboratory techniques in microfabrication with a peer-reviewed publication, his interest was not in the field of material science. Nonetheless, he grew a passion for research through this experience.

In looking for more opportunities in research, Tae began to work under the direction of Professor David Sarlah. Under his brief tutelage, he started to develop his interest in organic chemistry and natural products. Initially, he was captivated by natural

products being isolated from plants all around the world that turned into pharmaceutical drugs. This, coupled with his long affections for pharmacy, urged him to apply to the Ph.D. program in pharmacognosy at University of Illinois at Chicago after graduating with a B.S. in chemistry. However, he found out that they were not interested in isolating natural products from plants. He then went back to Professor Sarlah and started to work seriously in the field of organic synthesis.

After being exposed to organic synthesis, he wanted to assure himself that organic synthesis was the career path he was looking for. With intention of confirming this career path, he applied to scientist positions in pharmaceutical industry and he accepted a research associate position in medicinal chemistry at Gilead Sciences in Foster City, California. During his professional career, he highly enjoyed working with great colleagues and mentors towards the same goal in finding the drug analogues that could save millions of lives. Shortly after he realized that he was not sufficiently equipped with synthetic knowledge to be able to contribute to the endeavor independently. Therefore, he decided to apply to graduate school and study organic synthesis in depth.

After getting married to his wife, Yerim, Tae joined Professor John L. Wood's laboratory at Baylor University in Waco, Texas to start his graduate studies in the total synthesis of natural products. Tae received his Ph.D. in chemistry in May of 2023 and moved to Cambridge, MA to begin his postdoctoral studies in the laboratory of Professor Alison E. Wendlandt at the Massachusetts Institute of Technology.